

Evolution of a Sandur:  
Sixty Years of Change, Skeiðarársandur, Iceland

Volume 1 of 1

David J. Blauvelt

Doctor of Philosophy

School of Geography, Politics and Sociology

University of Newcastle

January 8<sup>th</sup>, 2013

## Abstract

Glaciers are a major component of the global climate system, adjusting to changes in climate over a range of timescales. Knowledge of the dynamics of contemporary glaciated landscapes will allow accurate reconstruction of glacier margin fluctuations within the landform and sedimentary record as well as predictions of the response of ice-marginal landscapes to future glacier margin fluctuations. Existing models of ice-marginal, proglacial landscape evolution focus primarily on landforms generated in response to single, relatively short-lived, high-magnitude large-scale events such as glacier surges or glacier outburst floods (jökulhlaups). Observations of these events have frequently been restricted to short time windows (days to several years) or inferred from stratigraphic sections and are therefore subject to misinterpretation. Relatively little research has been undertaken on the development of ice-marginal and proglacial landscapes over decadal time-scales ( $10^1$ - $10^2$  years).

This study examines the controls on the evolution of the ice-marginal landscape of Skeiðarárjökull over a decadal timescale. Skeiðarárjökull is a temperate, surge-type, piedmont outlet glacier located in south-east Iceland. Skeiðarárjökull, and its outwash plain Skeiðarársandur, have been subject to numerous surges and jökulhlaups and post-depositional modification due to the melt out of buried glacier ice, providing a valuable modern process-form analogue for landscape evolution at Pleistocene ice sheet margins. Digital Elevation Models (DEMs) were extracted from the aerial photographs taken at intervals over the past six decades to quantify the rate of landscape change over decadal time periods. This data, when combined with observations from aerial photographs of numerous suites of large-scale sub- and englacial features exposed by the glacier's recession permits models of the long-term response of proglacial regions to surges, jökulhlaups and glacier margin recession to be tested. This study developed a holistic model to describe the interdependence of glacier margin fluctuations, jökulhlaups and post-depositional modification and their impact on sandur evolution.



## Dedication

*“When the geomorphologist is required to interpret the origins of deposits and landforms many thousands of years after their formation and after they have been subjected to modifications by weathering and mass movement it is like asking someone to work out the plot of a 1000-page detective novel from the last five pages.”(Price, 1969)*

This volume is dedicated to my parents for their constant support, to Julie and Andy for giving me a place to land stateside, to Gareth Owens for inspiring me throughout these many years, and to Scott James for helping me to finish it.

## Acknowledgements

Special thanks go to the Andy's: Dr. Andy Russell, Dr. Andy Large, and Andy Gregory for their constant support, advice and help with fieldwork. Special thanks for assistance with data collection and camaraderie: Dr. Matthew Burke, Dr. John Woodward, Dr. Meredith Williams and the many Earthwatch teams through the years. Thanks to NERC for funding and the folks at the Vegagerðin (The Icelandic Road Administration (ICERA) for aerial photographs. Fieldwork was conducted throughout 2006 – 2007 and made possible by Earthwatch's Icelandic Glaciers project. DGPS equipment was provided by the University of Newcastle's Geography and Geomatics department. Thanks in particular go to Dr. Meredith Williams for software and to Dr. Pauline Miller for a crash course in SocetSet 5.4 and to Bjarney Guðbjörnsdóttir at Loftmyndir for digging through mounds of historical photographs and camera certificates to find the images that made these 3-D models possible. A very big thank you goes to the folks of BAE Systems who let me use their SocetGXP training labs in Virginia including Darren Stelle, Brian Roberts, Mike Servati and Veronica Acker. I'm very indebted to Dr. Andy Russell for providing feedback and revisions from 'across the pond' over these last several years and to Keith Luter for proof-reading. Special thanks to my father, Thomas Blauvelt, for exercising his Librarian superpowers and sorting out my references after EndNote imploded.

This project began on my first Earthwatch expedition to Iceland in 2002 so thanks go to Drs Russell, Tweed, Roberts, Fay, Fleischer and Tim Harris. It has also been made possible with the support of wonderful people that I have met and worked with along the way. Special thanks therefore go to friends and co-workers in several places: in San Diego thanks to Daniela Garza, J. Tessier, Debbie Turner, Jason Thacker, Catherine Marshall, Lisa Tucker, Brian Cox, Marc Aragon, Dan Jackson, James Biddle, Jessica Oppen, Simcha Benami, Ron Mosher, Rob Kriebel, and Crystal Nicholls. In Newcastle, Steve Blenkinsop, Rebecca Payne, Chris Leach, John Amos and Charlotte Thompson. In Washington D.C., thanks to Julie Christie, Andy Hanes, Roger Welborn, Lee Finewood, Eric Andersen, Rachael Harbes, Donnie Kenneth, Charlie Chapin, Heather Howard, Greg Kelsey, Brian Hemmerly, Justin Wilcox, Justin Binder, Dawn Granger and Cynthia Kancler. In New York, thanks to Dalma Tanzos, Mary Theodore, Erin Loope, and of course, my brother Timothy.

# Contents

<b>Title page .....</b>	<b>i</b>
<b>Abstract .....</b>	<b>ii</b>
<b>Dedication .....</b>	<b>iii</b>
<b>Acknowledgements .....</b>	<b>iv</b>
<b>Contents .....</b>	<b>v</b>
<b>List of figures .....</b>	<b>xi</b>
<b>List of tables .....</b>	<b>xxvii</b>
<b>Chapter 1            Introduction, aims and rationale .....</b>	<b>1</b>
1.1 Introduction.....	1
1.2 Rationale .....	3
1.3 Summary .....	8
1.4 Overall research aims.....	8
1.5 Research approach .....	9
1.6 Site Selection: Skeiðarárjökull, Iceland.....	10
1.6.1 Skeiðarárjökull: introduction .....	10
1.6.2 Skeiðarárjökull: location.....	11
1.6.3 Large-scale processes at Skeiðarárjökull: glacier margin fluctuations.....	17
1.1.1 Large-scale processes at Skeiðarárjökull: jökulhlaups .....	19
1.1.2 Large-scale processes at Skeiðarárjökull: post-depositional modification.....	20
1.6.4 Summary .....	20
1.7 Thesis structure .....	21
<b>Chapter 2            Literature review: context of the research .....</b>	<b>23</b>
2.1 Dynamics of glacier margins: controls on drainage and sedimentation regimes in response to margin fluctuations, floods and secondary modification.....	23
2.1.1 Introduction.....	23
2.2 Glacier margin fluctuations.....	23
2.2.1 Introduction.....	23
2.2.2 Glacier advance and surges.....	26

2.2.3	Surges: diagnostic landforms and landsystem models.....	29
2.2.4	Retreat .....	31
2.2.5	Summary .....	35
2.3	Jökulhlaups: mechanics and related landforms.....	36
2.3.1	Introduction to jökulhlaups .....	36
2.3.2	Jökulhlaups: initiation and internal controls .....	37
2.3.3	Jökulhlaups: routing.....	39
2.3.4	Jökulhlaups: landforms and controls .....	41
2.3.5	Jökulhlaups: summary .....	46
2.4	Post-depositional modification: buried ice, collapse areas and en/subglacial meltout features .....	47
2.4.1	Introduction.....	47
2.4.2	Emplacement.....	51
2.4.3	Meltout: primary and secondary .....	52
2.4.4	Quantification of melt rate .....	54
2.4.5	Summary of buried ice.....	54
2.5	Summary of large-scale processes .....	55

### **Chapter 3                      Literature review: large-scale processes and landforms at Skeiðarársandur      57**

3.1	Introduction.....	57
3.2	Margin fluctuations at Skeiðarárjökull: surges and retreat .....	57
3.2.1	Introduction.....	57
3.2.2	Surges.....	58
3.2.3	Glacier Margin Retreat: 20 <sup>th</sup> century to present.....	62
3.2.4	Eastern Skeiðarárjökull .....	63
3.2.5	Central Skeiðarárjökull .....	65
3.2.6	Western Skeiðarárjökull.....	66
3.2.7	Summary of fluctuations at Skeiðarárjökull .....	68
3.3	Jökulhlaups at Skeiðarárjökull.....	68
3.3.1	Introduction.....	68
3.3.2	Glacier recession and jökulhlaups at Skeiðarárjökull: 1934-2009 .....	69
3.3.3	November 1996 jökulhlaup.....	71
3.3.4	November 1996 jökulhlaup: controls on floodwater routing.....	73
3.3.5	1996 jökulhlaup: proglacial controls .....	75
3.3.6	November 1996 jökulhlaups: landforms and persistence .....	79
3.3.7	Grænalón jökulhlaups .....	82
3.3.8	Summary of jökulhlaups at Skeiðarárjökull .....	85

3.4	Post-depositional modification of proglacial outwash at Skeiðarárjökull .....	86
3.4.1	Introduction .....	86
3.4.2	Emplacement mechanisms: surges and floods.....	88
3.4.3	Summary: post-depositional modification at Skeiðarárjökull .....	89
3.5	Summary of large-scale landsystem models and hypotheses .....	90
3.6	Guide to large-scale processes and landforms commonly found at Skeiðarárjökull .....	93
<b>Chapter 4</b>	<b>Principles of photogrammetry and field methods.....</b>	<b>99</b>
4.1	Introduction to Photogrammetry .....	99
4.2	Principles of photogrammetry: How does it work? .....	101
4.2.1	Background .....	101
4.2.2	Analytical photogrammetry .....	101
4.2.3	Aerial photography basics.....	102
4.2.4	Parallax .....	104
4.2.5	X and Y parallax .....	105
4.3	Stereomodel production process .....	106
<b>4.3.1</b>	<b>Interior orientation .....</b>	<b>106</b>
4.3.1	Relative orientation .....	108
4.3.2	Absolute orientation.....	110
4.3.3	Analytical aerotriangulation.....	110
4.3.4	Image matching.....	111
4.3.5	Extraction techniques.....	111
4.3.6	Visualisations .....	113
4.3.7	Summary of DEM production .....	114
4.4	Methods and site selection .....	115
4.4.1	Aerial photograph acquisition.....	115
4.4.2	Differential GPS survey .....	116
4.4.3	Ground control points .....	117
4.4.4	Post-processing .....	119
4.4.5	DEM construction .....	121
4.4.6	Interior orientation .....	121
4.4.7	Absolute orientation.....	122
4.4.8	DEM extraction.....	122
4.4.9	Mosaic and orthophotograph production .....	123
4.4.10	Results.....	123
4.4.11	Volumetric Change Detection: Processing .....	124
4.4.12	Error measurement.....	124
4.5	Summary .....	128

<b>Chapter 5</b>	<b>Glacier margin fluctuations .....</b>	<b>129</b>
5.1	Introduction: Recession and lowering of Skeiðarárjökull 1945-2007 .....	129
5.2	Eastern region .....	133
5.2.1	Eastern region 1945 .....	133
5.2.2	Eastern region 1965 .....	134
5.2.3	Eastern region 1968-1996 .....	136
5.2.4	Eastern region 1997 .....	136
5.2.5	Eastern region 2003 .....	138
5.2.6	Eastern region 2003 – 2009 .....	140
5.2.7	Channel profiles 1965-2007 .....	143
5.3	Central region.....	147
5.3.1	Central region 1904.....	147
5.3.2	Central region 1945.....	148
5.3.3	Central region 1965-1968 .....	149
5.3.4	Central region 1986.....	153
5.3.5	Central region 1992.....	156
5.3.6	Central region 1997.....	162
5.3.7	Central region 2003.....	163
5.3.8	Central region 2007-2009 .....	166
5.4	Western region .....	168
5.4.1	Western region 1904 .....	168
5.4.2	Western region 1945 .....	169
5.4.3	Western region 1965 .....	171
5.4.4	Western region 1968 .....	172
5.4.5	Western region 1979 .....	174
5.4.6	Western region 1986 .....	175
5.4.7	Western region 1997 .....	177
5.4.8	Western region 2003-2009.....	180
5.5	Summary .....	185
<b>Chapter 6</b>	<b>Jökulhlaup legacy .....</b>	<b>186</b>
6.1	Introduction.....	186
6.2	Site 1: Double Embayment (DE)/ice-walled canyon complex .....	187
6.2.1	Site 1: Description.....	187
6.2.2	Site 1: Interpretation .....	190
6.3	Site 2: Depression .....	191
6.3.1	Site 2: Description.....	191
6.3.2	Site 2: Interpretation .....	195

6.4	Site 3: Loop Complex .....	196
6.4.1	Site 3: Description.....	196
6.4.2	Site 3: Interpretation (Loop Complex).....	200
6.5	Site 4: Western ridges .....	202
6.5.1	Site 4: Description.....	202
6.5.2	Site 4: Interpretation (western ridges).....	203
6.6	Site 5: Remnant outwash fan apex.....	204
6.6.1	Site 5: Description.....	204
6.6.2	Site 5: Interpretation .....	206
6.7	Site 6: Central Gígjukvísl 1965.....	206
6.7.1	Site 6: Description.....	206
6.7.2	Site 6: Interpretation .....	208
6.8	Summary .....	209
<b>Chapter 7</b>	<b>Post-depositional modification of proglacial outwash .....</b>	<b>210</b>
7.1	Introduction.....	210
7.2	Hardaskríða depressions .....	211
7.2.1	Depressions .....	214
7.3	Volumetric change detection .....	216
7.4	Interpretation.....	220
7.5	Emplacement mechanisms.....	221
7.6	Discussion .....	223
<b>Chapter 8</b>	<b>Discussion.....</b>	<b>226</b>
8.1	Introduction.....	226
8.2	Margin fluctuations: margin advance, surges and retreat .....	228
8.2.1	Margin advance and surges: diagnostic landform assemblages, impact and persistence.....	228
8.2.2	Glacier margin retreat and ice surface lowering over the 20 <sup>th</sup> century .....	229
8.2.3	Glacier margin retreat: impact of fluctuations on incision/aggradation .....	230
8.2.4	Glacier margin retreat: channel incision and braiding.....	232
8.2.5	Glacier margin retreat: temporal variability .....	234
8.3	Jökulhlaups: diagnostic signatures, persistence and impact .....	235
8.3.1	Jökulhlaups: diagnostic signatures.....	235
8.3.2	Jökulhlaups and glacier margin fluctuations.....	237
8.3.3	Jökulhlaups: pre-existing topography and substrate .....	238

8.3.4	Jökulhlaups: persistence.....	238
8.4	Post-depositional modification .....	239
8.4.1	Post-depositional modification: diagnostic landform signatures of buried ice, controls on ablation and melting rates .....	239
8.4.2	Post-depositional modification: impact on sandur evolution and persistence .....	240
8.5	Holistic model of sandur evolution.....	242
8.5.1	Introduction.....	242
8.5.2	Relationship between glacier margin fluctuations and jökulhlaup behaviour .....	242
8.5.3	Large-scale processes: impact and persistence .....	243
8.5.4	Large-scale processes: interdependence .....	245
8.5.5	Holistic model of the sandur evolution .....	246
1.1.3	Holistic model.....	246
<b>Chapter 9</b>	<b>Conclusions .....</b>	<b>249</b>
9.1	Introduction.....	249
9.2	Holistic model of large-scale processes and long-term sandur evolution.....	250
9.3	Implications.....	254
9.4	Future work.....	255
9.5	Wider Implications.....	257
<b>Appendix A</b>	<b>Photomosaics .....</b>	<b>259</b>
<b>Appendix B</b>	<b>Data quality: check points vs DTMs .....</b>	<b>263</b>
<b>Appendix C</b>	<b>Location maps of figures.....</b>	<b>283</b>
<b>References</b>	<b>.....</b>	<b>287</b>



## List of Figures

Figure 1.1 An ice-cored drumlin at Brúarjökull, Iceland, and the resultant landform following meltout illustrates the difficulty in recognizing landforms diagnostic of emplacement mechanisms over long time-scales with what in this case is only a ‘transitional landform’: a) terrain prior to surge, b) surge event, c) glacier snout following surge, d) present-day ice-cored drumlin, e) future ice free landscape. (Schomacker et al., 2006). ....	7
Figure 1.2 Geological map of region surrounding Vatnajökull (Thorarinsson et al., 1951). ....	12
Figure 1.3 Location map of Skeiðarárjökull (top) showing the three major lobes, the retreat of the margin since 1945, the location of the 19 <sup>th</sup> century moraines (as defined by (Galon, 1973a)), the location of the proglacial depression (red hue) and the major drainage channels (imagery: 2010 Google Earth). Draping aerial photographs over DEMs (bottom) provides an oblique view of the proglacial depression (2007 imagery on 5 m DEM). ....	13
Figure 1.4 Overview map of field area divisions east, central and west depicted upon a 1997 photo-base map provided by Vegagerðin (Icelandic Roads Authority), including the five main drainage outlets of Skeiðarárjökull during the 20 <sup>th</sup> century: the Súla, the Gígjukvísl, Háöldukvísl, Sælhúsakvísl and the Eastern and Western Skeiðará. ....	14
Figure 1.5 Location of the Gjálp fissure, subglacial lake Grímsvötn and the path of the meltwater beneath Skeiðarárjökull during the November 1996 jökulhlaup (Flowers et al., 2004)...	15
Figure 1.6 Lowering of the glacier surface during glacier margin retreat since 1938 has decoupled the glacier from the sandur, leading to the formation of an ice-marginal depression and development of lateral drainage (Gomez et al., 2000). ....	18
Figure 1.7 Location map of outlet glaciers of the Vatnajökull ice cap known to surge and dates of documented surges; (Björnsson et al., 2003). ....	19
Figure 2.1 Schematic plan of the proximal, middle and distal portions of an Icelandic sandur from Boothroyd and Nummedal (1978), modified by Zielinski and van Loon (2002). .	24
Figure 2.2 Relationship between channel migration, aggradation and frequency of channel belt avulsion (Bristow and Best, 1993). ....	24
Figure 2.3 Comparison of braided streams and alluvial fan development in Iceland and Alaska (Boothroyd and Nummedal, 1978). ....	25
Figure 2.4 Classic model of sandur development, from Price (1969) page 33. ....	26

- Figure 2.5 Development of blowout structures and sediment wedges during a surge (from Benediktsson et al., 2008, page 232): 1) During the quiescent phase, features and sediments are deposited during ice lowering, 2) compressive flow during advance results in thrusts, debris entrainment and deposition of material on the glacier surface, 3) thinning following passage of surge waves results in expansion of crevasse network while at glacier front blow out structures, elevated drainage and reverse slope sediment wedge develops, 4) a drop in pore pressure results in coupling of ice/bed interface, deforming the substrate in a brittle manner and 5a) (enlargement) in fine-grained strata, high-pore pressure will deform the material in a ductile, fold dominated manner, while 5b) in coarse-grained strata, it deforms in a brittle manner, resulting in slabs with low-angle thrusts. .... 28
- Figure 2.6 Crevasse-cast ridge formational model from Bjarnadóttir (2007) based upon observations at Brúarjökull, Iceland. A) Crevasses open up as a result of the propagation of down-glacier compressional flow during surge, and sediment is dragged up into the crevasses as a result of the pressure differences, forming bed-anchored crevasse casts. B) Ablation of glacier surface during retreat reveals crevasse cast ridges and flutes. .... 30
- Figure 2.7 Model of landforms created during surging events (Evans and Rea, 1999): a) outer zone of proglacial thrust pre-surge sediment; b) zone of weakly developed hummocky moraine; c) zone of flutings, crevasse-squeeze ridges and concertina eskers; 1) proglacial outwash fans; 2) thrust block moraine; 3) hummocky moraine; 4) crevasse-squeeze ridge; 5) concertina esker; 6) fluting; 7) glacier. .... 30
- Figure 2.8 Proglacial landsystem model of a surging glacier based upon observations at Skeiðarárjökull (van Dijk, 2002): I) surge-related moraine-fan association with fine grained SFRs II) surge-related, coarse-grained, subglacially-fed ice-contact fans, III) surge-related deltas and fan deltas in proglacial depressions, IV) ice-proximal quiescent phase fans QPF's, V) ice-proximal basin and pond sediments, VI) quiescent phase fans on the distal side of the surge moraines. .... 31
- Figure 2.9 Diagram of morphosequences, or landsystem models, of various proglacial systems: A) fluvial ice-contact sequence, B) fluvial non-ice contact sequence, C) lacustrine ice-contact sequence, D) fluvial-lacustrine ice-contact sequence, E) fluvial-lacustrine non-ice

contact sequence, F) lacustrine-fluvial ice contact sequence (after Koteff and Pessl, 1981, page 7).....	32
Figure 2.10 1, 2 and 3) represent progressive abandonment of moraine gap drainage following ice margin recession (Klimek, 1973): 4) ice margin positions, 5) end moraines, 6) moraine ‘gates’, 7) inherited gates, 8) youngest gates.....	33
Figure 2.11 Relationship between margin position and drainage development, modified from Klimek (1973) .....	35
Figure 2.12 Jökulhlaup-related landforms within limno-glacial valley sandur landsystem (Maizels, 1997): 1) expansion bar, 2) pendant bar, 3) mega-ripples or dunes, 4) slack-water deposits, 5) large-scale dune cross-bedding with reactivation surfaces, 6) large-scale bar front cross-bedding, 7) imbricated boulder lag, 8) channel fill deposits, 9) small scale ripples, 10) chute channel and lobes, 11) kettle holes and kettle fills, 12) ice-block obstacle marks, and 13) wash limit on adjacent valley-side slopes.....	37
Figure 2.13 Jökulhlaup-related landforms within volcanogenic landsystem (Maizels, 1997): 1) massive bedded sediments, 2) terraced boulder deposits, 3) abandoned sandur terrace, 4) washed sandur, 5) lobate fan deposited by hyper-concentrated jökulhlaup flows, 6) incised jökulhlaup channel with streamlined residual hummocks, boulders and mega ripples, 7) hummocky distal jökulhlaup deposits, 8) streamlined, hummocky erosional bars mantled with rimmed and till-fill kettles, 9) incised jökulhlaup channel, 10) incised active meltwater channel, 11) streamlined erosional bars, wash limits and scattered boulders and dune forms downstream of bedrock obstacles. ....	37
Figure 2.14 Two common types of hydrograph shape: (a) an exponentially rising limb followed by a steep falling limb, typically associated with tunnel drainage through the progressive enlargement of an ice-tunnel; (b) a linearly rising limb often associated with the emptying of a subglacial reservoir, such as outburst floods frequently associated with a subglacial volcanic eruption. Modified from Walder and Costa (1996) and Duller (2007). ....	39
Figure 2.15 Model depicting the numerous factors that control flow and sediment characteristics of jökulhlaup floods (Maizels, 1997).....	40
Figure 2.16 Model for the formation of upward infilled hydrofractures beneath an ice sheet (Rijsdijk et al., 1999). ....	43

Figure 2.17 Coupled vs. decoupled scenarios for routing of jökulhlaup discharge. Inset demonstrates the effects of meltwater ponding in the proglacial zone on the flood hydrograph (Gomez et al., 2002). .....	44
Figure 2.18 Kettle hole obstacle/scour mark genesis. Type 1: partial or total burial and subsequent exhumation of block results in kettle scours with both proximal and lateral scour and tail. Type 2: partial exhumation of partially buried ice blocks on margins of main channels results in semi circular obstacle marks. Types 3 and 4: obstacle marks with proximal and lateral scour crescent, a ridge stoss-side of the scour crescent and a large, anti-clinal aggradational tail. Type 5: obstacle marks <5 m in diameter with fine-grained gravel in the immediate lee of the scour hollow and coarse gravel lag characterising the distal part of the tail. Formed by waning stage deposition, followed by late waning stage erosion. Type 6: erosional obstacle marks formed by total exhumation of buried ice blocks or by scour around ice blocks grounded by the late waning stage (Russell et al., 2006). .....	46
Figure 2.19 Collection of ablation studies conducted at different glaciers, where $a$ is the thickness of maximum ablation, $b$ is the thickness where ablation rates begins to decrease (Nicholson and Benn, 2006) based on Østrem's estimation of the effects of thin layer of debris on ablation rates (1959). .....	48
Figure 2.20. Simplified model depicting the evolution of stagnation topography following glacial retreat (Price, 1969). .....	49
Figure 2.21 Classification of jökulhlaup-related kettle holes, based on debris content of the original ice blocks. After Maizels (1992). .....	50
Figure 2.22 Stages of evolution of a rimmed-normal kettle following the emplacement, and gradual burial, of a block of ice. Modelled after observations at the Höfðabrekkujökull forefield, Mýrdalssandur, Iceland. A-G are individual facies observed around ice block (Olszewski and Weckwerth, 1998). .....	50
Figure 2.23 a) Back and downwasting processes in ice cored moraines, b) and measuring backwasting in the field (Schomacker, 2008). .....	53
Figure 2.24 Formation of low-relief hummocky topography due to melting of high angle debris bands (Boulton, 1967) illustrating before (a) and after (b) meltout. ....	53

Figure 3.1 Radio echo soundings of Skeiðarárjökull (Björnsson, 1999). a) profiles taken across the glacier's width reveal subglacial 'channels' while b) depicts profiles taken at the western (C-C'), central (D-D') and eastern (E-E') reveal the position of the underlying, over-deepened slopes beneath the glacier ice. ....	58
Figure 3.2 Depiction of the progress of the 1991 surge (solid black lines) and the resulting advance of the ice margin (dashed lines)(Björnsson et al., 2003). This map displays the suspect location of an ice tunnel that may drain jökulhlaups from the subglacial lake Grímsvötn to the river Skeiðará. ....	60
Figure 3.3 Section of the Gígjukvísl push moraine and fan complex that depicts the relationship between buried glacier ice, push moraine, overridden and pushed outwash sediments and push moraine related fans (Russell et al., 2001a). ....	62
Figure 3.4. Aerial photographs depicting surge related fans (SRFs) and quiescent phase fans (QPFs) emplaced on the elevated portions of the sandur (van Dijk, 2002). ....	62
Figure 3.5 Profiles of the sandur margin in the east (top), central (middle) and west regions (bottom) (Klimek, 1973). ....	63
Figure 3.6 Evolution of drainage from A) 1946, B) 1960 and C) 1965 depicting the abandonment of the central sandur and the development of the Skeiðará, Gígjukvísl and Súla channels (Galon, 1973a) ....	65
Figure 3.7 Advances and retreat of Skeiðarárjökull's western lobe (Molewski, 2000). The solid line represents systematic measurements carried out on profile since 1932, while broken line represents estimated position. A = advance, R = recession, S = Stagnation (Thorarinsson, 1943), while circles represent jökulhlaups and triangles represent surges. ....	67
Figure 3.8 A) Generalised map of the extent of the 1934 jökulhlaup upon the sandur: note the near total inundation of the eastern Skeiðará region (Nielson, 1937). B) Map of the extent of the 1954 jökulhlaup; the (main flood outlets numbered 1-10) (Rist, 1955). C) Location map depicting the extent of the 1996 jökulhlaup on the Skeiðarársandur as well as the supraglacial emergence of floodwaters north of the margin and D) a comparison of jökulhlaup hydrographs from 1934 to the recent 1996 event (Snorrason et al., 2002).....	70

Figure 3.9 Map showing the major outlets of the 1996 jökulhlaup, the development of supraglacial fractures and discharge, and the location of the Gígjukvísl Double Embayment (DE) (black box) (Russell et al., 2001b).....	72
Figure 3.10 Discharge and duration of the 1996 jökulhlaup in the Skeiðará, Gígjukvísl and Súla Rivers (Roberts et al., 2001). .....	73
Figure 3.11 Chronological development of outlets and fracturing across the margin of Skeiðarárjökull during the November 1996 jökulhlaup between 0720h - 1330h (A-E). From Roberts et al., 2000, page 1432. ....	74
Figure 3.12 Model of controls on englacial sediment deposition during the November 1996 jökulhlaup –from Roberts et al., 2001 page 949- depicting the main intra-glacial flood routes (Roberts et al., 2000). Panel A) depicts the formation of an infill within a near-surface englacial cavity and vertical bed deposition as a result of supercooling, while panels B) and C) depict main phases on the development, and preservation, of a rising supraglacial fracture outlet.....	75
Figure 3.13 Morphological and sedimentological characteristics of ice-contact jökulhlaup: a) Rising stage deposition topographically-controlled by presence of backwater lake resulting in radial, delta-like fan, b) topographically unrestricted fan allows for the aggradation of sheet-like layers, c) heavily dissected fan and exhumation of ice blocks as a result of sediment poor waters during waning stage fans (Russell and Knudsen, 2002). .....	76
Figure 3.14 During the 1996 jökulhlaup, while subaqueous efflux into the upper Sæluhúsavatn basin occurred at 110 m, substantial discharge ascended the flanks of the lower Sæluhúsavatn basin through a tunnel channel to exit at an elevation of 120 m. Temporarily raised lake levels acted as a hydraulic dam, deflecting subglacial jökulhlaup flow up from the western flank of the upper basin to exit the glacier margin at 120 m (Russell et al., 2007). ....	77
Figure 3.15 Double embayment, ice-walled canyon, proximal and distal fans. 1997 ice margin is depicted in red and shown in inset. Modified from Cassidy et al. (2003). ....	78
Figure 3.16 Location of airborne laser altimetry transects taken in 1996, 1997 and 2001 (for Track 1, additional tracks 1992, 2001 only) overlaid upon SAR DEM, from Smith et al. (2006). ....	80

Figure 3.17 a) Laser altimetry profiles along Track 1 for 1996, 1997 and 2001; b) net topographic changes after the 1996 jökulhlaup; c) net post modification 2001-1997; d) net topographic changes after 5 years (Smith, 2006).....	80
Figure 3.18 Exposure of the supraglacial double-embayment and ice-walled channel sediments following the lowering of the ice surface and retreat of the margin (Russell et al., 2001b). .....	81
Figure 3.19 Map showing routing of subglacial jökulhlaups from Grænalón. ....	85
Figure 3.20 Observations of melting at Skeiðarárjökull by Jewtuchowicz (1973); a) accumulation moraine ridge transverse to the glacier edge (1) glacier ice, (2) moraine ridge and b) bending of layers caused by dead-ice melting (1) dead ice, (2) sand layers.....	87
Figure 3.21 Molewski and Olsewski's (2000) interpretation of the development of ice-cored end moraines due to a series of glacier advances near the Gígjukvísl river Gap, Skeiðarársandur based on exposed stratigraphic sections. a) Following an advance of Skeiðarárjökull, a period of retreat, b) leaves behind ice at the terminal moraine, covered by a deposit of till; a further advance over the existing ice creates a sharp unconformable contact, c) the next episode of retreat deposits till that buries the ice again, d, e, f) and a lateral fluvial system develops behind the ice cored moraine. ....	89
Figure 4.1 Collinear relationship between an object on the ground, the object in the image and the position of the exposure station (modified from (Wolf and Dewitt 2000). ....	102
Figure 4.2 Focal length B captures a wider ground area than focal length A, responsible for the differing distance ratios between the two the film planes.....	103
Figure 4.3 Similar triangles demonstrating the relationship between elevation ( $H'$ ) and focal length ( $f$ ) with ground ( $A-B$ ) and photo ( $a'-b'$ ) distances on a flat terrain (Wolf & Dewitt, 2000). ....	103
Figure 4.4 Illustrates the effecting of uneven terrain (changing elevation ( $H$ )) on the scale of a vertical photograph, while focal length ( $f$ ) remains constant and $h(\text{avg})$ represents the average elevation height (Miller, 2007).....	104
Figure 4.5 Perceived depth of photographs when viewed with stereo-glasses (Miller, 2007). ..	105
Figure 4.6 Absolute parallax (Miller, 2007). ....	105
Figure 4.7 Differential parallax(Miller, 2007). ....	106

Figure 4.8 Fiducial marks on a typical aerial photograph found either in the corners or along the edge of a photograph.....	107
Figure 4.9 Diagram of relative orientation between two aerial photographs (Wolf & Dewitt, 2000). .....	108
Figure 4.10 Presents the relationship between a point in object space and the corresponding point within image space (Wolf and Dewitt, 2000). .....	109
Figure 4.11 Relative orientation between two aerial photographs (Miller, 2007).....	110
Figure 4.12 Epipolar geometry. Both ground point A and ground point A', with a different elevation, appear on the left epipolar plane at the same location; however, ground point A only matches one point in the right epipolar plane (Miller, 2007). .....	111
Figure 4.13 Geometric distortion caused by elevation changes seen from different observation points (Miller, 2007). .....	113
Figure 4.14 Point P shown in its position on the DEM model and the corresponding coordinates for point p on the orthophotographs (Miller, 2007).....	114
Figure 4.15 Base station initializing (left) and rover unit (right) collecting a point feature.....	116
Figure 4.16 An example of features documented in aerial photographs (a-d) at the mouth of the Haoldokvisl, such as kettle holes and ridges, collected with the dGPS equipment (e) and the corresponding features that have persisted over the past sixty years.....	118
Figure 4.17 Example of terrain-shaded relief DEM of the central and eastern margin of Skeiðarárjökull, depicted as a hillshade, extracted from 2007 aerial photographs using SocetSet 5.5 (after manual clean-up). .....	123
Figure 4.18 Error distribution curve, displaying confidence intervals (modified from (Miller, 2007a). .....	126
Figure 5.1 Georeferenced GeoEye images depicting the changing position the fluctuating position of the glacier margin from 1945 to 2009 (mosaic contains: left image from Aug 2009, right from Sept 2009). The three lobes of the glacier (west, central and east) are demarcated by red dashed lines. Note that all 2009 drainage of the eastern (E) and central (C) lobes drains into the Gígjukvísl channel.....	130
Figure 5.2 Profiles of the west (a), central (b) and eastern (c) regions of Skeiðarárjökull depicting changes in glacier surface topography from 1965-2007 (not all photo-years available for each profile). Prior to 1997, with the exception of the 1992 surge, there has been a	



progressive lowering of the glacier surface and recession of the ice-margin. Since 1997, there has been an increase in the lowering of the glacier surface, in some locations by over 100 m. ....	131
Figure 5.3 Glacier margin parallel profiles of the sandur (S-S'), glacier margin (I-I'), and proglacial depression (T-T'). Vertical lines denote no data/breaks in DEM coverage. .	132
Figure 5.4 1945 photomosaic of eastern region: 1) meltout features, 2) alluvial fan, 3) outwash fan apex and 4) recessional push moraines.....	133
Figure 5.5 1965 photomosaic of the eastern region. Inset A) 1) expansion of terrace has resulted in the removal of a significant portion of the sandur, 2) and 3) two channels of the western Skeiðará that have been widened/deepened since 1945, 4) smoothed alluvial fan, and 5) retreat of margin has exposed a esker 240 m long that leads to former alluvial fan. ....	135
Figure 5.6 Photomosaic of the eastern region in 1997: 1) low, drumlinised ridge, 2) 1996 outlets, 3) outwash fan.....	137
Figure 5.7 Aerial photograph of the eastern region in 2003 indicating 1) drumlinised terrain, 2) drumlinised esker and 3) proglacial lake. ....	139
Figure 5.8 2007 photomosaic of the Eastern region showing 1) drumlinised terrain, 2) drumlinised, ascending eskers 3) three lakes separated by two rounded ridges. ....	141
Figure 5.9 Profile depicting the development of the proglacial depression in the Eastern region from 1965 - 2007; the progressive retreat of the glacier margin has resulted in a series of ice-front parallel channels that have permitted meltwater to drain along the glacier margin into the western Skeiðará channel.....	142
Figure 5.10 Profiles of the eastern Skeiðará channel taken from 1965, 1997 and 2007. Profiles depict the removal of material and incision between 1965 and 1997 and subsequent influx and removal of material between 1997 and 2007. ....	144
Figure 5.11 Profile of western Skeiðará channel between 1965-2007. Between 1965 and 1975 the margin was relatively stable and exhibits comparatively little channel change. Note the lowering of the elevation in places between 1975 and 1997 interpreted to be related to the 1996 jökulhlaup. Lowering between 2003 and 2007 is interpreted as relating to erosion by the 2004 jökulhlaup.....	146

Figure 5.12 1904 topographic map of the central region (overlain upon 2003 photomosaic for reference). Features 1-3 represent active drainage channels draining the margin: 1) the Sandgigjukvisl, 2) the Sigurdarfitaralar, and 3) another unnamed channel.....	147
Figure 5.13 1945 Central region photomosaic: 1) proglacial lake Háöldulón, 2) kettled terrain, 3) Gígjukvísl, 4) unnamed channel, 5) region of elevated terrain blocking westward flow of drainage, 6) marginal outlets and 7) remnant of 19 <sup>th</sup> century moraine (Háalda mound).148	
Figure 5.14 1965 photomosaic with insets of the two largest kettled outwash fans.....	150
Figure 5.15 Photomosaic with insets of the two largest kettled outwash fans on 1968 imagery. .....	151
Figure 5.16 Comparison of ice surface profiles between 1965 and 1986, displayed on the 1965 photo basemap. ....	152
Figure 5.17 Central region 1986. Drainage channels that have developed adjacent to former 1965 flood outlets; retreat around these 1965 outlets exposed elongated, rounded ridges.....	154
Figure 5.18 Alluvial fans observed on 1965 images (A and B) and the adjacent thrust blocks and depressions exposed on the subsequent 1986 images (C and D).....	156
Figure 5.19 Central region 1992. Numbers 1-4 (and insets) are alluvial fans emplaced during the 1991 surge; 5) represents large-scale meltout features. ....	157
Figure 5.20 Comparison of the advance of the central margin between 1986 and 1992 between imagery (a) and contours (b). The contour maps illustrate the steep, near vertical front of the snout of the margin (contours in 5 m intervals). ....	158
Figure 5.21 The steepening of the ice front in response to the 1991 surge is depicted with profiles taken perpendicular to the ice front both pre-surge (1986) and during-surge (1992). In elevation alone, the ice thickness increased by over 100 m in the west and over 40 m in the east profiles. ....	159
Figure 5.22 Location map and profiles of 1991 surge fans (A, B, C and D). Note - B depicts glaciotectonically disturbed glaciolacustrine deposits formed during the surge. ....	161
Figure 5.23 Central region following 1996 jökulhlaup capturing infilling of the proglacial depression with sediment and the development of the: 1) double embayment, 2) Gígjukvísl gap, 3) Gígjukvísl channel and erosion of an overridden alluvial fan. ....	162
Figure 5.24 Development of drainage and retreat of the margin following the 1996 jökulhlaup. Numbered features are: former 1997 terrace, 2) Double Embayment and esker complex,	

3) elongated ridge, 4) fluted ground, 5) and 6) chaotic meltout terrain and 7) large meltout regions.....	164
Figure 5.25. Lowering of ice surface between 1997 and 2003 DEMs overlain on 2003 imagery. ....	164
Figure 5.26 Supra- and englacial features melting out of the margin in 1997 (top) and 2003 (middle, bottom DEM). DEM depicts only 5 m lowering of the largest landform in the area following the retreat of the margin (3 m contour interval). Note – profile transects highest profile of landform to measure secondary alteration.....	165
Figure 5.27 Oblique photograph depicting landforms developing following the retreat of the central margin (2008).....	166
Figure 5.28 2007 mosaic showing the development of proglacial lakes and further exposed subglacial terrain. Features include 1) esker, 2) meltout features, 3) lake, 4) chaotic terrain and western lake, 5) depressions. ....	167
Figure 5.29 1904 map of Western Skeiðarárjökull depicting the position of the glacier margin and generalised drainage networks including the Blautakvísl and Sandgígjukvísl channel. Numbered features are 1) Súla, 2) Blautakvísl, 3) 19 <sup>th</sup> century moraine, 4) Sandgígúr moraine complex, 5) unidentified moraine, 6) remnant fan apex.....	169
Figure 5.30 1945 photomosaic of western region. 1) Súla, 2) Blautakvísl, 3) proglacial trench region with small lakes, 4) 1890 moraine, 5) isolated 1890 moraine, 6) and 7) remnant fan apices. ....	170
Figure 5.31 Retreat of the Western margin in 1965 (> 2 km). Numbered features are 1) Súla, 2) and 3) are rectilinear ridges.....	171
Figure 5.32 Western region 1968. Numbered features are 1) Súla, 2) kettle holes.....	173
Figure 5.33 1979 images containing kettle holes and obstacle marks downstream of Súla outlet (Feature 1).....	174
Figure 5.34 Western region 1986 taken following the 1985-86 surge and jökulhlaup: 1) Súla and ice blocks and obstacle marks and 2) erosion along Blautakvísl.....	176
Figure 5.35 Western region 1997 photographs. Numbered features are 1) Súla, 2) kettled jökulhlaup fan and channel formed during 1996 jökulhlaup. ....	178
Figure 5.36 Profile of Súla channel, 1968 and 1997 photo sets. ....	179

Figure 5.37 Western Region 2003. 1) Súla, 2) erosional scarp east of Blautakvísl, 3) 1996 outlet. .....	180
Figure 5.38 Comparison of Súla and Blautakvísl outlets in 1997 (a) and 2003 (b). Note the development of the 42 m wide Blautakvísl channel and removal of material west of terrace (orange) on the 2003 image. ....	181
Figure 5.39 Channel straightening and incision of the Blautakvísl following Grænalón jökulhlaup in 2005 (photographs courtesy of Dr. A. J. Russell).....	181
Figure 5.40 2007 snapshot of Sula (obtained from Loftmyndir). Note the eastward migration of the channel as well as the incision of the single channel for ~2 km, before developing into braided channels.....	182
Figure 5.41 Changing ice levels along the western lateral margin of Skeiðarárjökull in 1945 (red dashed line), 1968 (blue dashed line) and 1997. Since 1945, the glacier has lowered 30+m and over 160 m laterally. Oblique aerial photograph shows the lake itself and the flow of water between the glacier and the massif. Upper right image shows lake Grænalón and lateral subaerial drainage to the ice dam in 2008 (photograph courtesy of Dr. A.J. Russell).....	183
Figure 5.42. Retreat of the Western lobe: red (1945), and blue (1968) on 1997 imagery. Elevation profiles of 1968 and 1997 are shown in upper left, depicting a lowering of over 30 m of the Western lobe. The ice has retreated laterally from the massif over 150 m since 1945, and lowered along the massif between 5-15 m.....	184
Figure 6.1 Double Embayment (DE) and ice-walled canyon complex generated during the 1996 jökulhlaup (A) and the same region following retreat of the glacier margin (B). Features in the 2007 image are: (DE) Double-Embayment complex (blue), esker (E), fracture fills (F).....	188
Figure 6.2 Profiles of the DE complex: for both profiles (A-A' and B-B') the 2007 surface is shown in blue, while the 1997 surface is shown in red. ....	189
Figure 6.3 Linear gravel ridge (foreground); fracture filled ice (background); ground photo taken approximately 500 m west of DE complex, 2006.....	190
Figure 6.4 Profile across elongate depression (outlined in black)on 2007 imagery/DEM. ....	192

Figure 6.5 Oblique photographs of elongate depressions (red arrows) and drainage channel (white arrow): A) looking north, b) looking south. Photographs courtesy of Dr. A. J. Russell 2008.....	193
Figure 6.6 Profiles along bottom of elongate depression (A - A') and drainage channel (B-B') (2007 imagery/DEM).....	195
Figure 6.7 Oblique aerial oblique view of the Loop Complex (2003 DEM).....	197
Figure 6.8 North-south transect of Loop Complex and margin (1992 in red, 1997 in blue), depicting removal of material following the 1996 jökulhlaup.....	197
Figure 6.9 Loop Complex in 1992: 1) fluted ground, 2) esker (dashed line indicates present on earlier photoseries prior to erosion) 3) proglacial drainage, 4) fracture fills, 5) disturbed ground, 6) outline of drumlinised landform.....	198
Figure 6.10 Oblique photograph of the region in 2007, depicting the fluted ground and the location of disrupted terrain (A), stratigraphic section of undisturbed terrain (B) and disturbed terrain (C). Photographs and stratigraphic sections courtesy of Dr. A. J. Russell. ....	199
Figure 6.11 'Loop Complex' region in 1945 prior to retreat. Purple hatched polygon depicts the approximate location of a major 1934 jökulhlaup outlet. ....	201
Figure 6.12 Western region in 1945 (left)c and 1997 (right). Retreat of the margin has exposed long, rectilinear ridges (red lines), an esker (orange) and a ridge interpreted to be the location of a former jökulhlaup outlet (blue) and the location of the former margin (purple).....	203
Figure 6.13 Profile of remnant outwash fan apex and position of western margin since 1965 (flat line indicates lack of data). ....	205
Figure 6.14 1965 photomosaic of the Gígjukvísl gap in the 19 <sup>th</sup> century moraine: 1) smoothed ground, 2) esker, 3) drainage channels, 4) fracture fills, 5) disturbed terrain, 6) moraines, 7) jökulhlaup outlets, 8) surge-advance related outwash fan (Russell et al., 2001a).....	207
Figure 7.1 1a) Location map of several large depressions on the central sandur (Hardaskriða), with approximated margin position in 1904 and 1934 taken from georeferenced maps - the largest depressions in this region are circled in red. 1b) Location of the depressions in 2003 and the same undisturbed terrain in 1945 (1c).....	211

Figure 7.2 Geomorphological map of depressions. 1) kettle holes, 2) concentric crevasses and horst and graben, 3) normal faulting, 4) gullies, 5) dirt road, 6) outwash. ....	212
Figure 7.3 Profiles of depressions 1 –4 in 2007 is shown in blue; 1968 surface, when available, is shown in red. ....	213
Figure 7.4 Profile of sandur and proglacial depression (1), and drumlinised ridges (profiles 2-4) exposed by the retreat of the glacier margin since 1945. The majority of these ridges had been removed in later photoseries. ....	215
Figure 7.5 Combined elevation profiles of the drumlinised ridges located within the proglacial depression. ....	216
Figure 7.6 Total elevation loss (m) between 1945 – 2007 and estimated volume loss estimated by using an artificial 1945 surface (top); profiles of depressions between 1945 (red), 1968 (brown) and 2007 (blue) (bottom). ....	217
Figure 7.7 Profile of depressions found on the central sandur; 1968 is shown in red, 2007 in blue. ....	218
Figure 7.8 Location map and long profile of the glacier and the sandur, demonstrating the retreat of the margin and the base level lowering of drainage within the proglacial depression, and assumed lowering of groundwater table. ....	219
Figure 7.9 Approximate locations of 19 <sup>th</sup> century moraines estimated from georeferenced 1904 topographic map (dashed red line). Dashed blue lines represent depressions that have developed since 1945 south of the 19 <sup>th</sup> century moraines. Solid blue line (top) represents position of margin in 1945. ....	222
Figure 7.10 Approximate extent of 1934 ice margin (dashed blue line) and location of jökulhlaup routing (blue hashed polygons) on top of 2003 photomosaic (1997 photomosaic underlain to fill gaps). Red polygons delineate location of depressions. (Thorarinsson, 1974). ....	223
Figure 8.1 Stylised timeline of major events documented in Chapters 5, 6 and 7, including jökulhlaups, surges and the gradual melt out of buried ice. Major drainage capture events or periods of channel abandonment are also shown. For a complete list of all jökulhlaups at Skeiðarárjökull see Table 3.1 and 3.2. ....	227
Figure 8.2 Comparison of landforms emplaced by a minor rapid advance, or possible surge, observed on 1965 (A) and 1986 (B) imagery and DEMs. Features include 1) steep, near	

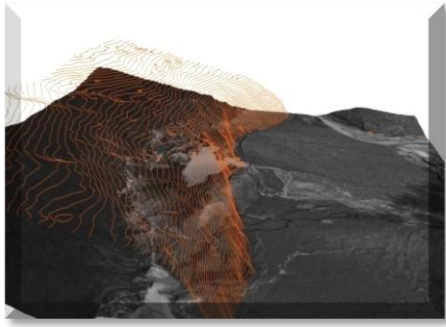
vertical margin, 2) thrust block moraine, 3) alluvial fan, 4) proglacial lake and braided stream network.....	229
Figure 8.3 Stylised diagram of the abandonment of drainage systems within an overdeepened basin at a retreating margin based on Skeiðarárjökull: 1) abandoned drainage channels along central sandur, the first channels to be abandoned during margin retreat, 2) detached snout comprised of moraines, abandoned moraine gates, buried ice and outwash plains, 3) lowest area (maximum) of overdeepening of the proglacial depression infilled with sediment and proglacial drainage and lakes, 4) lateral drainage channel that remain actively coupled to the sandur until glacier retreats past the maximum overdeepening, 5) lateral drainage channel that has remained active and coupled to sandur despite retreat of glacier margin due to incision resulting from glaciolimnic jökulhlaups, 6) main central drainage channel that drains drainage contained within the overdeepening out onto the sandur. ....	231
Figure 8.4 Approximate position of braided stream networks over time in relation to the decoupled glacier margin, demonstrating the long-term, downstream shifting of braided stream networks associated with margin retreat and the marked, yet brief, impact of a high-magnitude jökulhlaup. ....	233
Figure 8.5 Landforms created by jökulhlaups are dependent upon margin position. A) Glacier margin coupled: jökulhlaups emplace, then buries ice blocks on the sandur, B) Glacier margin retreats and ice blocks melt, creating negative landforms on the sandur, C) Glacier margin decoupled: within proglacial depression, jökulhlaup deposits sediment on ice (en- or supra glacial), D) Glacier margin retreats further: during and following melt out creates positive landform (dashed line = jökulhlaup routing). ....	244
Figure 8.6 Large-scale processes and resulting landforms and landform assemblages observed at Skeiðarárjökull. ....	247
Figure 8.7 Schematic diagram depicting the interdependence of large-scale processes and proglacial landsystem model. Numbered landforms are: 1) glacier; 2) proglacial lake; 3) jökulhlaup landform fracture fills, eskers and small proglacial lakes, 4) recent jökulhlaup landform assemblage comprised of fracture fills, sinuous esker, and outwash fan apex and associated fan with kettles and obstacle marks; 5) drumlinised eskers associated with former jökulhlaup; 6) apex of jökulhlaup outwash fan and former abandoned lateral	

drainage channel; 7) thickly-bedded jökulhlaup deposits; 8) drumlinised surge fan with jökulhlaup landform assemblage comprised of fracture fills, disturbed terrain, sinuous esker, and outwash fan apex and associated fan with kettles and obstacle marks; 9) surge-related outwash fan, thrust block and depression with minor proglacial lake; 10 (two instances) jökulhlaup-associated drumlinised eskers; 11) jökulhlaup tunnel channel and former proglacial lake basin; 12) proglacial trench; 13) moraine gap and jökulhlaup-related kettled outwash fan; 14) surge-related fan and hanging outlet; 15) jökulhlaup-modified incised channel that is the dominant channel on the sandur; 16) proglacial depressions associated with ice blocks buried by jökulhlaup; 17) abandoned moraine gap and braided stream channels. .... 248



## List of Tables

Table 1.1 Non-flood average discharges, sediment and chemical concentrations of three major rivers of Skeiðarárjökull (Snorrason et al., 1997).....	15
Table 2.1 Mechanisms involved in jökulhlaup generation and their possible triggers (Walder and Costa, 1996, Tweed and Russell, 1999, Roberts et al., 2005, Duller, 2007). ....	38
Table 2.2 Summary of jökulhlaup-related landforms. ....	42
Table 3.1 List of jökulhlaups at Skeiðarárjökull (Ives, 2007). ....	71
Table 3.2 of Grænalón jökulhlaups.....	84
Table 3.3 Signatures and persistence: the table above presents hypotheses in the literature concerning landform signatures associated with large-scale processes such as margin fluctuations and jökulhlaups, as well as their persistence on the sandur over time.....	93
Table 3.4 Reference table of landforms used to identify some of the common landforms on aerial photographs.....	98
Table 4.1 Features collected with dGPS in the field for use in georeferencing images .....	119
Table 4.2 Average height difference between DEM and control (check) points surveyed at the field site with error estimates given as root mean square (RMS) errors. Random errors are reported at the 95th percentile limit (all units are in m). Note ‘*’ designates 1997 and 2003 Roads Authority Vegagerðin DEMs compared against field data.....	125
Table 4.3 Standard deviation multipliers for percentage of probable errors of the normal distribution (Wolf and Ghilani, 1997, Miller, 2007a).....	126
Table 8.1 Landforms associated with jökulhlaups documented on aerial photographs (see Chapter 6).....	236



## Chapter 1 Introduction, aims and rationale

---

*This chapter introduces large-scale, temperate proglacial landsystems and the processes that are associated with their development. The rationale, aims and structure for this study are presented.*

---

### 1.1 Introduction

Landsystem models of temperate glacial systems relate processes to the resulting landform-sediment assemblages and have been employed worldwide to identify proglacial landforms (Clayton and Moran, 1974, Boulton and Eyles, 1979, Eyles, 1983, Gustavason and Boothroyd, 1987, Benn and Evans, 1998, Evans et al., 1999, Evans and Rea, 1999). Any landsystem model, in its simplest terms, attempts to relate geomorphology and subsurface material to the processes responsible for their creation (Eyles, 1983). Developed to rapidly characterise large tracts of unmapped terrain, landsystems group together a recurring pattern of topography, soil and/or vegetation that is predictably different from adjacent regions (Christian and Steward, 1952, Evans, 2005). Studies of glaciated terrain have identified landform-sediment suites to create landsystem models that encompass fluctuation of glacier ice (advance and retreat) as well as the additional complexity of pre-advance, supra-, en-, and subglacial elements following glacier recession (Clayton and Moran, 1974, Eyles, 1983, Knudsen, 1995, Evans, 2005). To date, these models have primarily been derived from observations of individual, large-scale events which are defined in this study to include processes and landforms associated with rapid glacier margin advances (surges) (Kamb et al., 1985, Kamb, 1987, Knudsen, 1995, Andrzejewski and Molewski, 1999, Russell et al., 2001a, van Dijk, 2002, Evans and Rea, 2003, Waller et al., 2008), glacier margin recession (Price, 1969b, Galon, 1973a,

Klimek, 1973, Wojcik, 1973a, Wisniewski, 1997, Marren, 2002b) or sudden, high-magnitude outburst floods (jökulhlaups) (Maizels, 1991, Maizels, 1992, Russell, 1993, Russell and Knudsen, 1999, Tweed and Russell, 1999, Gomez et al., 2000, Roberts et al., 2000, Knudsen et al., 2001, Roberts et al., 2001, Russell et al., 2001b, Fay, 2002, Carrivick, 2004, Russell et al., 2006, Smith, 2006, Russell et al., 2007, Burke et al., 2010). Few studies however, account for further modification of the proglacial terrain or outwash plain (sandur) by repeated occurrences of these large-scale events, nor have they addressed the effects of post-depositional modification on this landscape following glacier advance or retreat.

Additionally, few studies have examined the evolution of landforms over a decadal time scale (Hjulström, 1952, Price, 1969, Price and Howarth, 1970, Evans and Twigg, 2002); instead, they have been restricted to very short time windows of observation (days to years) or inferred from stratigraphic sections and are therefore subject to misinterpretation and are restricted to single events and processes. More insight is needed to provide an understanding of the ice-marginal deposits generated by numerous advance and retreat cycles at contemporary glacier margins that have resulted in polygenetic landforms (Harvey, 2006). Understanding the processes responsible for the creation of complex landsystem suites that have been emplaced by repeated events is important in deciphering the palimpsests, or overprinted landsystems, that constitute much of the Pleistocene landforms that persist today across North America, Europe and Asia (Evans, 2011). This study will examine three large-scale processes that affect the long-term ( $10^2 - 10^3$  decades) development of the temperate glacier sandur landsystem – namely glacier margin fluctuations, jökulhlaups and post-depositional modification due to ice melt in order to produce a holistic model of the long-term, large-scale evolution of a sandur.

As a result of the 20<sup>th</sup> century's warming trends, Icelandic glaciers have retreated more than one kilometre since the end of the Little Ice Age (Björnsson, 1979, Sigurðsson et al., 2007) providing an opportunity to understand the internal dynamics of these glaciers by examining the proglacial terrain and the sub-, supra- and englacial landforms revealed by the retreating margins. The retreat of Skeiðarárjökull, a glacier in southeast Iceland, provides a unique opportunity to correlate processes to landforms and to examine how these landforms evolve over a decadal timeframe. This chapter presents the aims and objectives of this research and provides an overview of the major large-scale processes thought to affect the long-term glacio-fluvial development of proglacial terrain and the sandur.

## 1.2 Rationale

Justification of this research is presented below and briefly described. These themes are expanded upon in greater detail in the literature review.

- A) Although several researchers have examined the link between large-scale fluctuations of glacier margins, ice surface elevation and the development of glacio-fluvial systems, few have been able to model the impact of large-scale glacier margin advance/retreat upon the proglacial ice-marginal landsystem over long periods of time.

Fluctuations in glacier margin position and the elevation of the glacier snout have been recognised as being major controls on the development of proglacial landscape and meltwater drainage pattern (Björnsson, 1998, Evans et al., 1999, Evans and Twigg, 2002, Marren, 2002b). Glacier margin advance increases aggradation and steepening of the sandur, encouraging the development of braided streams (Maizels, 1979). Glacier surges have been associated with rapid glacier margin advances and a re-organisation of the subglacial drainage systems of temperate glaciers, a cycle that may repeat in periods of  $10^1$  to  $10^2$  years (Kamb et al., 1985, Björnsson, 1998). Surges are independent of climate forcing and are the result of internal instabilities of a glacier, and are capable of transferring large volumes of ice to the margin from a reservoir area with velocities of up to one thousand times the normal flow rate (Clark et al., 1984, Kamb et al., 1985, Evans and Rea, 1999). During surges, drainage undergoes a transition from being routed through a few established, lateral subglacial tunnel channels (conduit system) (Shreve, 1974, Björnsson, 1998) to a distributed drainage system dominated by a series of linked cavities (Kamb et al., 1985, Kamb, 1987). This distributed drainage system may result in numerous, regularly spaced en- and supraglacial outlets across the glacier margin (van Dijk, 2002). Observations of recent surges have documented the emplacement of large volumes of material and landforms that have altered the erosional/depositional characteristics of the glacio-fluvial system, often within a span of a few days - months (Fleisher et al., 1998, Russell et al., 2001a, van Dijk, 2002).

While several authors have suggested that these landforms, or landform assemblages, emplaced during recent surge events comprise diagnostic signatures that could be used to identify past surges (Croot, 1988, Sharp, 1988, Knudsen, 1995, Evans and Rea, 1999, Waller et al., 2008), it has been proposed that many of these features may also develop in response to rapid ice advance in response to changing climatic conditions (Sharp, 1988,

Evans and Rea, 1999, Waller et al., 2008), and no single landform, assemblage or deposit can be uniquely tied to identifying surges.

Glacier margin retreat may lead to the development of proglacial lakes (Jonsson, 1955, Howarth and Price, 1969) and alterations to channel and terrace geometry (Maizels, 1979, Marren, 2002b) and meltwater distribution (Klimek, 1973). Both glacier margin advance and retreat may affect the geomorphology of the proglacial area without any alteration in sediment or water supply, as channel incision may result simply from the lowering of the upstream meltwater outlet (Marren, 2002b). While there have been several studies that attempt to chart the development of proglacial drainage systems (Hjulström, 1952, Price, 1969, Price and Howarth, 1970, Evans and Twigg, 2002), there has been little work documenting the impact of fluctuations of the glacier margin on the evolution of the proglacial environment over decadal periods of time or that also encompasses the effects of other large-scale processes (Gomez et al., 2002, Marren, 2002b).

B) Little is known about the role that jökulhlaups of varying magnitude play in determining sandur volume, area of deposition, style and morphology of erosion and deposition or the resulting overall impact on the evolution of the sandur on a decadal scale. Until an understanding can be gained of the current processes affecting glacier landsystems, the accuracy of any interpretations derived from stratigraphic sequences or relic landforms remains in question.

The term ‘jökulhlaup’ is employed across the world to describe a glacial outburst flood caused by a rapid release of meltwater that has become impounded within sub-, en- or supraglacial or ice-marginal reservoirs (Thorarinsson, 1939, Björnsson, 1975, Russell, 1993, Walder and Costa, 1996, Roberts et al., 2003) as a result of topography or hydraulic pressure gradients (Björnsson, 1974, Nye, 1976). The release of water may be the result of several possible mechanisms including drainage of an ice-marginal/ice-dammed lake, drainage of a supra- sub or –en glacial lake, the drainage of an intra glacial cavity, as a result of meltwater release during a surge termination or as a result of a volcanically-induced melting (Walder and Costa, 1996, Tweed and Russell, 1999, Roberts et al., 2005, Duller, 2007). Water may accumulate over time (‘storage release’ type) or build up rapidly in response to a volcanic eruption or rainfall and become impounded within, below, upon or adjacent to a glacier for periods ranging from as brief as a few minutes or hours (Fountain et al., 1999) to several hundred years (Teller, 1995). When these reservoirs drain, they may produce floods of varying magnitude and duration occurring on a yearly

or decadal scale, resulting in significant sedimentological and geomorphological change on the proglacial landsystems (Maizels, 1997). Reservoirs, however, are not necessarily required for jökulhlaups, as rainfall or volcanogenically induced floods may occur without any residence time ('direct release' type) (Thorarinsson, 1939, Björnsson, 1992, Warburton and Fenn, 1994). Such cataclysmic flooding events were important processes during global periods of glaciation and may result in dramatic erosional and depositional landsystem changes as seen at Lake Missoula, USA (Bretz et al., 1956, Baker, 1973), Bonneville (O'Conner, 1993) and at the Altai Mountains, Siberia (Rudoy and Baker, 1993, Carling, 1996). While these models of jökulhlaup-related processes and landforms in the literature dwell upon the immediate impact of single floods, nearly all neglect to quantify the effects of such events on the long-term ( $10^1 - 10^2 \text{ year}^{-1}$ ) development of the sandur, thereby further highlighting the need for a comprehensive model of the impact of jökulhlaups on sandur evolution.

It has been observed that low-magnitude, high-frequency events (annual meltwater and nival discharge) in proglacial systems are responsible for large volumes of material emplaced by coalescing alluvial fans and braided streams (Krigström, 1962, Churski, 1973, Boothroyd and Ashley, 1975, Church and Gilbert, 1975, Miall, 1977, Miall, 1985, Bridge, 1993), while other authors have proposed that high-magnitude, low-frequency events have been a dominant factor (Maizels, 1992, Gudmundsson et al., 1995, Maizels, 1997). Following recent high-magnitude glacier outburst floods or jökulhlaups, another model that is characterised by alternating high-frequency, high-magnitude flooding events with high-frequency, low-magnitude regimes has been proposed (Marren, 2002a, Marren, 2005, Russell et al., 2006), while other researchers (Gomez et al., 2000, Magilligan et al., 2002) purport that the surficial expressions of high-magnitude jökulhlaups are ephemeral and their impact are removed within years or decades.

It has also been proposed that it is the sequence and recurrence intervals between such large-scale events that may be the dominant control, rather than their magnitude alone (Wolman and Miller, 1960, Anderson and Calver, 1975). Therefore it is the period between such events (relaxation time) that determines their eventual impact (Anderson and Calver, 1975, Baker and Kochel, 1988, Carling, 1989); i.e., the greater the period between floods, the greater the impact of the flood upon the sandur, as there is greater availability of sediment both delivered and reworked.

C) It has been proposed that glacier margin retreat, surges and floods produce unique landforms that are diagnostic of the processes that emplaced them (Kamb et al., 1985, Maizels, 1992, Knudsen, 1995, Marren, 2002b, van Dijk, 2002, Russell et al., 2006, Burke et al., 2010). Few studies, however, have examined the long-term, post-depositional modification these landforms due to ice melt that may limit the viability of using such landforms as diagnostic signatures outside of a narrow window of time ( $10^1$ - $10^3$  yr).

Although some proglacial landforms and stratigraphic sections have been proposed to be diagnostic signatures of events such as surges (Knudsen, 1995, Evans and Rea, 1999, van Dijk, 2002, van Dijk and Sigurðsson, 2002, Waller et al., 2008) or jökulhlaups (Munro-Stasiuk et al., 2008, Hooke and Jennings, 2006, Burke et al., 2010, Burke et al., 2008, Roberts et al., 2000, Russell et al., 2006, Burke et al., 2009, Maizels, 1992, Maizels, 1977, Fay, 2002, Russell et al., 2001b, Price, 1969, Carrivick, 2004, Cassidy et al., 2003, Clayton et al., 1999, Colman, 2002, Carling, 1989), few studies have measured the long-term effect of post-depositional modification as a result of meltout on such diagnostic signatures to determine the final landform stage (Østrem, 1959, Clayton and Moran, 1974, Johnson, 1992b, Krüger and Kjær, 2000, Russell and Knudsen, 2002, Nicholson and Benn, 2006, Schomacker et al., 2006).

Paraglacial reworking describes the adjustment of glacial landsystems to non-glacial conditions through such processes as debris flows, slope failure and fluvial re-sedimentation (Church and Ryder, 1972, Woodward et al., 2008). Such secondary modification is recognised as a significant mechanism in sculpting deglaciaded landscapes (Ballentyne, 2002), and ice-cored topography may contain a variety of landforms that may be subject to frequent secondary modification. The correlation between climatic parameters and melting rates of buried ice bodies is weak, suggesting that processes and topography play a key role (Nicholson and Benn, 2006). Additionally, different components of a de-glaciaded landsystem reach equilibrium over greatly different timescales (Ballentyne, 2002). As a result of these processes, it may be difficult, if not impossible, to determine the initial emplacement conditions of some resultant secondary landforms (Johnson, 1992a), as seen in the example of an ice-cored drumlin in Figure 1.1.

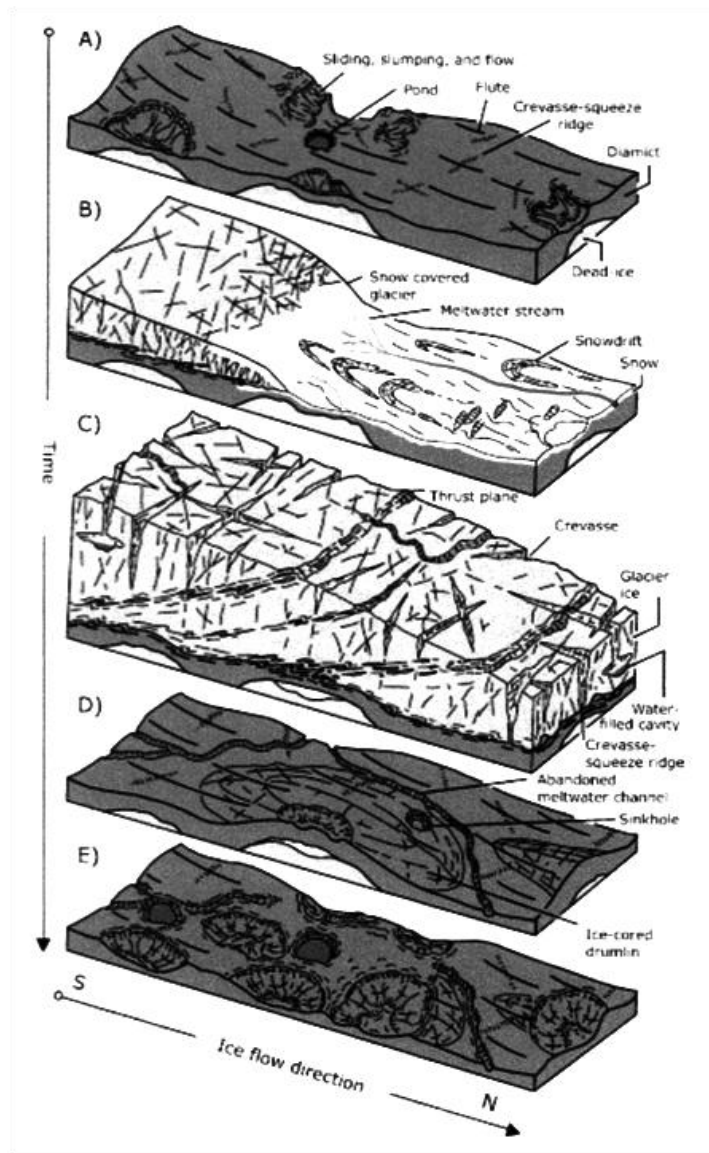


**Figure 1.1** An ice-cored drumlin at Brúarjökull, Iceland, and the resultant landform following meltout illustrates the difficulty in recognizing landforms diagnostic of emplacement mechanisms over long time-scales with what in this case is only a ‘transitional landform’: a) terrain prior to surge, b) surge event, c) glacier snout following surge, d) present-day ice-cored drumlin, e) future ice free landscape. (Schomacker et al., 2006).

Little research exists that examines the persistence of features generated by flood or surge events, nor the sub- or englacial emplacement of material during and following these events (Evans and Rea, 2003, Waller et al., 2008, Woodward et al., 2008). While such individual events may repeatedly produce distinct, recognizable landforms and drainage patterns, over time these landforms may become modified or removed by repeated events, erosion or the melting out of buried ice, rendering the final landform unrecognizable. Further work is needed to document the rate of secondary modification of such features due to the gradual melting of ice buried by sediment. Examining melt processes and rates within buried ice masses in the forelands of temperate glaciers will also provide an



analogue for the evolution of proglacial terrain following the retreat of glaciers at the end of the Pleistocene.

### **1.3 Summary**

It is evident from the above rationale that the existing models of the geomorphic evolution of proglacial landsystems have focused primarily on observations made during short windows of time and have often focused on individual floods and glacier surges. Little work has been done to examine the rates of change over decadal time-spans to provide a control on processes and their role in the evolution of the sandur and ice-marginal proglacial terrain. Developing a model that addresses these factors will help us understand not only how proglacial systems will respond to future advances, retreats or flooding events, but will also aid in interpreting landforms and stratigraphic signatures generated during the Pleistocene. This research is significant as it is the first to observe, document and quantify the rate of formation and development of proglacial landforms and processes on a decadal scale.

### **1.4 Overall research aims**

The overall aim of this project is

- To evaluate models of proglacial landscape development derived from relatively short-duration field campaigns and observation windows, as well as those models derived from interpretations of sediment and landform records of formerly glaciated areas.

This aim will be achieved by fulfilling the following objectives:

- 1) To present a literature-based model of the evolution of ice-marginal proglacial terrain and sandur morphology including the large scale processes of glacier margin fluctuations, jökulhlaups and secondary modification due to ice melt.
- 2) To test models of processes that affect sandur morphology and evolution in order to characterise the emplacement, exposure and subsequent evolution and persistence of proglacial landforms of Skeiðarárjökull over decadal time frames.
- 3) To evaluate models of landscape-forming processes using evidence obtained from (2).

- 4) To develop a landform/landsystems model of a temperate glacier which may be applied/tested elsewhere in the world, both in modern glacial environments as well as during the Pleistocene.

## 1.5 Research approach

*'It's not what people don't know that gets them into trouble,' an American humorist once said, 'it's what people know that ain't so.'* (Glasner, 2009)

The impact of glacier surges and jökulhlaups on proglacial landscapes have been documented using aerial photographs taken before and after such events; manual surveying techniques and ground photographs; and, more recently, by using Synthetic Aperture Radar (SAR) and Light Detection and Ranging (LiDAR) to document the erosion and deposition of sediment. Larger-scale, and lower-resolution, change detection may also be obtained using satellite imagery. While these techniques capture the short-term, two-dimensional impacts of such recent events (or three-dimensional impacts in the case of LiDAR), the development of cost-effective automated terrain extraction from aerial photographs, both digital and historic, presents an opportunity to quickly model large ( $>30 \text{ km}^2$ ) terrains, often with sub-metre accuracy (Baily et al., 2003). Greater availability of historic imagery of a region presents an advantage over modelling with LiDAR; while LiDAR provides a higher resolution, the development of the technology remains relatively recent enough that a substantial archive of landscapes over periods of more than one or two decades does not yet exist to compare change over time. Comparing surfaces constructed from imagery before and after an event is often utilised as a cost-effective method to quickly quantify large-scale volumetric changes due to melt out, subsidence, flooding, human interference or other causes (Gilbert and Scheifer, 2007).

Due to the relatively inexpensive cost and often large number of historical aerial photographs available in many regions, this study will test models of landscape change using sequential aerial photographs taken over the past six decades. The explanations of these landforms and interpretations about the processes that formed them are developed by identifying the landform(s) that formed after a given event and developing hypotheses to explain their formation. These hypotheses may either be refuted or supported by examining other events in the field, in the literature or preserved within the sedimentary record. The principle of induction purports that research may develop a scientific law through repeated observations; however, as pointed out by Hume in the 18<sup>th</sup> century, it only takes one contrary test result or observation to invalidate a law (Glasner, 2009). For

example, while a jökulhlaup or a surge may repeatedly emplace a ‘unique’ set of geomorphic features, one could use this ‘unique’ landform as a diagnostic signature of such an event *until* another process is discovered that might emplace the same landforms.

For the purpose of this research, landsystem models and related hypotheses are presented and critically tested. Landsystem models and related hypotheses found in the literature will be evaluated by attempting to identify large-scale landforms or processes on historical imagery. Once identified, an attempt will be made to correlate processes or landforms to events or processes (such as jökulhlaups or surges) documented in the historical literature, maps or even folklore. If events occurred that support the model, then it is probable that the landforms are associated with it; if there is no known event or process documented in the literature to correlate a landform or process observed on the imagery, it is possible that the landforms are associated with the process suggested by the landsystem models and hypotheses – it is also possible that not all events have been recorded, particularly minor one. It is acknowledged that not all landforms and processes in the literature will be found; these are not testable in this study. However, where landforms and/or processes are identified on imagery, they will be examined and their evolution over time documented in order to expand existing models and processes in the literature. These observations will be used to test the validity of hypotheses found in the literature and, where applicable, derive new hypotheses. It is important to recognise that landforms developed at one period of time may influence the development of later landforms over a series of time frames (Williams, 1987) and that many polygenetic landforms will have been emplaced or modified as a result of numerous, repeated processes.

## **1.6 Site Selection: Skeiðarárjökull, Iceland**

### **1.6.1 *Skeiðarárjökull: introduction***

The temperate glaciers of Iceland have been identified as contemporary analogues for landscape and paleogeographic reconstructions for the southern margins of Pleistocene mid-latitude ice sheets (Clayton and Moran, 1974, Koteff and Pessl, 1981, Waite, 1985, Boulton, 1986, Gustavson and Boothroyd, 1987, Croot, 1988, Dredge and Cowan, 1989, Mooers, 1990, Blewett and Winters, 1995, Evans et al., 1999, Evans and Twigg, 2002, Magilligan et al., 2002). Over the 20<sup>th</sup> century, large-scale alterations of glacier drainage patterns have significantly impacted Iceland’s transportation and communication networks and have been responsible for damage to property and loss of livestock and human life (Thorarinsson, 1974, Snorrason et al., 1997, Snorrason et al., 2002, Björnsson,

2003, Sigurðsson, 2005, Ives, 2007) demonstrating the need for developing a greater understanding of the active processes in the region and their future behaviour.

The following sections provide an overview of the field site Skeiðarárjökull and the large-scale processes active at this location. This brief introduction is provided to supply the reader with context to understand the scope of the study, the structure of the literature reviews, and the application of photogrammetry and GIS to such a large-scale and diverse field site. A comprehensive examination of large-scale glacial processes is provided in Chapter 2, and those specifically observed at Skeiðarárjökull is presented in Chapter 3.

#### 1.6.2 *Skeiðarárjökull: location*

Skeiðarárjökull is an outlet glacier of Vatnajökull (Figure 1.2), the largest ice cap in Europe (8,100 km<sup>2</sup>). Vatnajökull is located in the southeastern region of Iceland and straddles the active western volcanic zone (Thorarinsson et al., 1951). In this zone, magma fluctuations may affect the overlying ice, causing changes in heat and mass distribution that are capable of generating instabilities and large reservoirs of meltwater. Skeiðarárjökull is a temperate glacier, with a climate characterised by low summer temperatures and heavy winter precipitation, a result of its position within the confluence of the warm Gulf Stream and the polar East Greenland Current (Björnsson, 1979). Skeiðarárjökull consists of three confluent ice lobes that together cover an area of 1,370 km<sup>2</sup> and flow onto Skeiðarársandur, the outwash plain, creating a glacier snout that spans ~23 km (Björnsson, 1999). Skeiðarárjökull lies within an over-deepened basin located at approximately 200 m below mean sea level (msl). Skeiðarárjökull and Skeiðarársandur, are bordered on the east by mountainous Örafajökull and to the west by the cliffs of the basalt spur of Lómangupúr and the Eystrafrjall massifs (Figure 1.2). These massifs are composed of palagonites, tuffs, breccias and basalts of the Quaternary Moberg formation (Thorarinsson et al., 1959). The proximal zone of Skeiðarársandur is comprised of proglacial lakes, elongated depressions and arcuate terminal moraine ridges (Figure 1.3), while its distal zone extends more than 20 km to the sea.

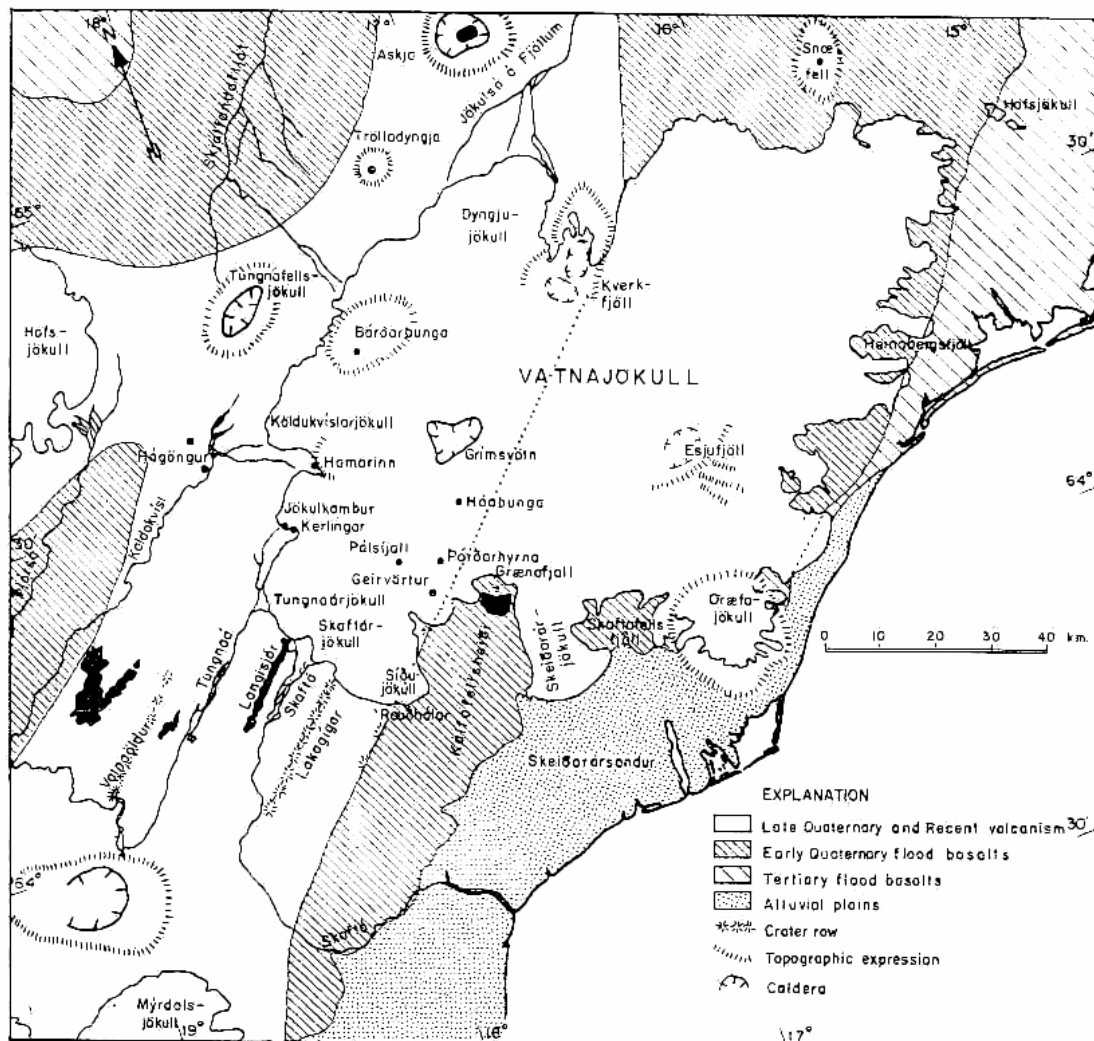
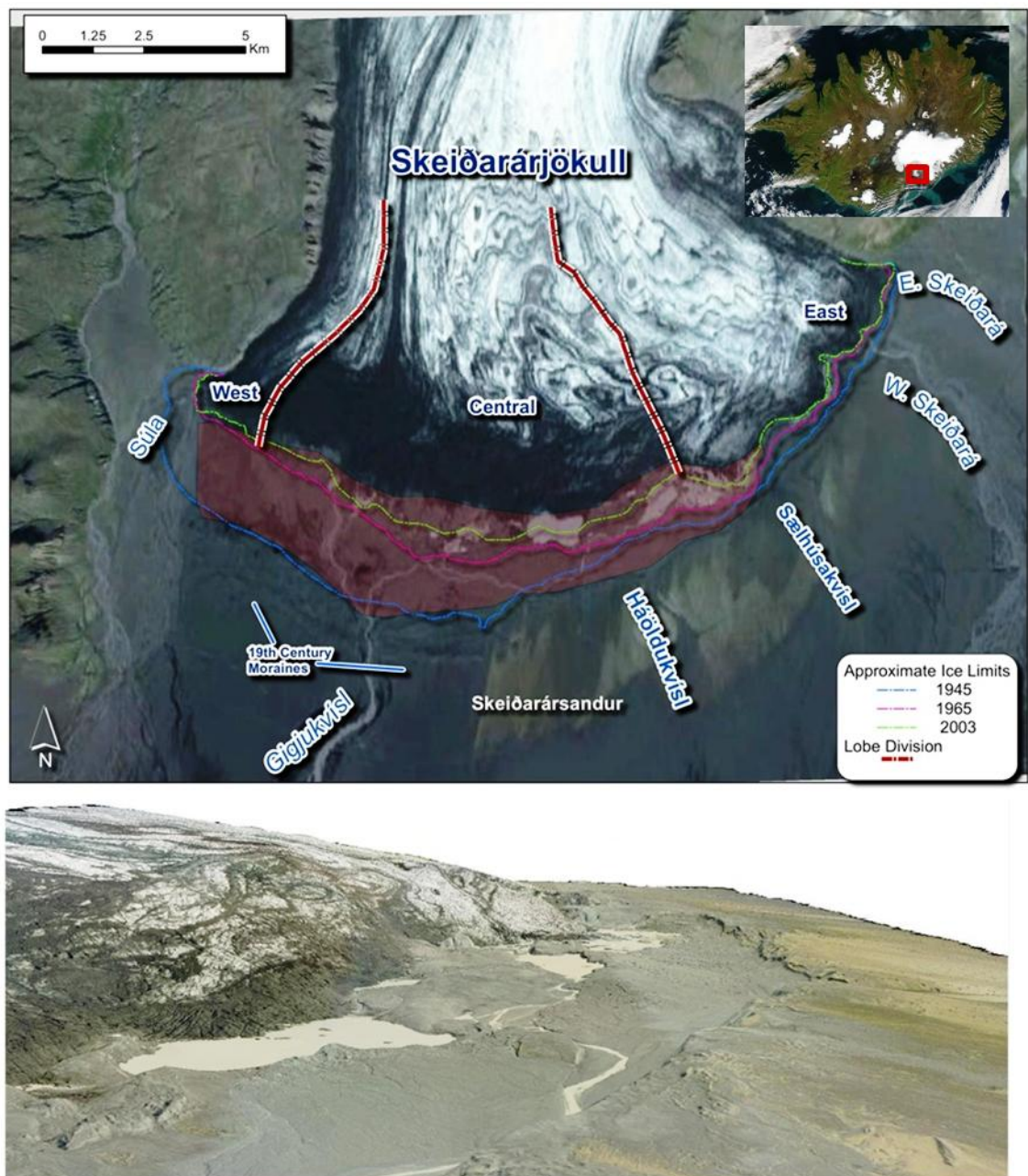


Figure 1.2 Geological map of region surrounding Vatnajökull (Thorarinsson et al., 1951).



**Figure 1.3** Location map of Skeiðarárjökull in Iceland (top inset) and it's margin showing the three major lobes, the retreat of the margin since 1945, the location of the 19<sup>th</sup> century moraines (as defined by (Galon, 1973a), the location of the proglacial depression (red hue) and the major drainage channels (imagery: 2010 Google Earth). Draping aerial photographs over DEMs (bottom) provides an oblique view of the proglacial depression (2007 imagery on 5 m DEM).

Documented by historical aerial photographs repeatedly over the past sixty years, Skeiðarárjökull and Skeiðarársandur have been subject to repeated surges and jökulhlaups and the proglacial terrain has been subject to extensive modification as a result of post-depositional modification due to the melting of buried ice. The ice-marginal zone of Skeiðarárjökull has been extensively documented in the literature over the last few decades, due in part to the frequency of jökulhlaups and surges as well as its proximity to



Iceland's Route 1 highway. For the purposes of this study, Skeiðarársandur is divided into three regions: east, central and west (Figure 1.4).

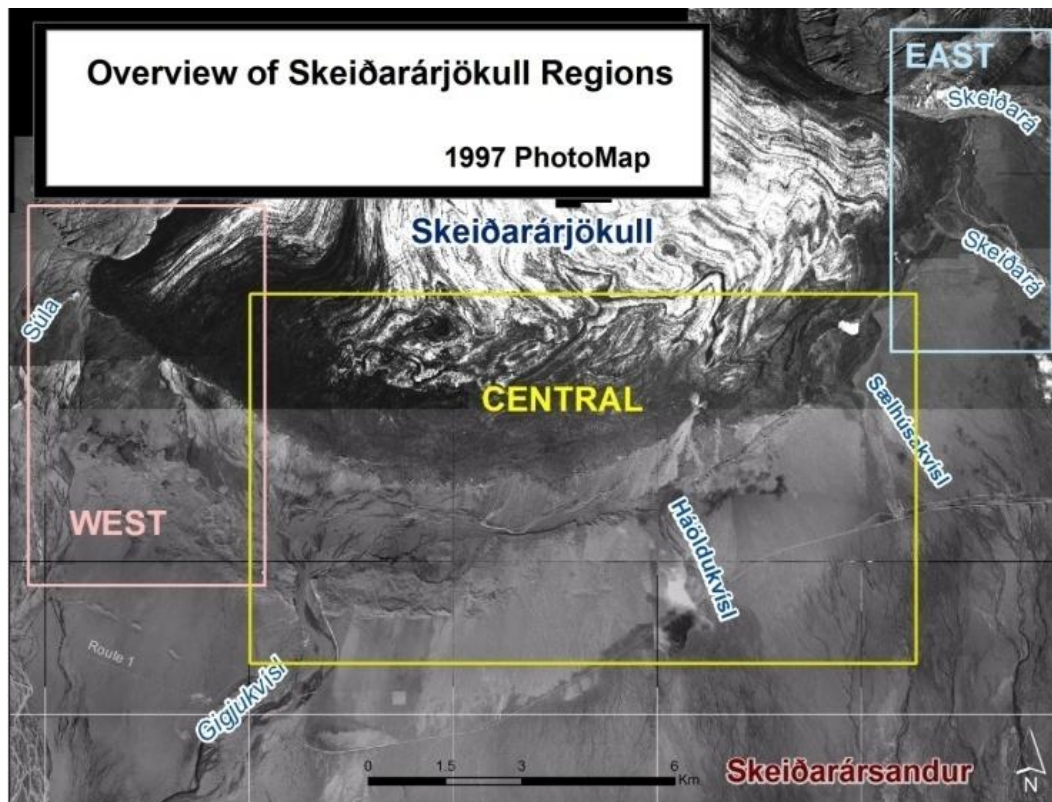


**Figure 1.4** Overview map of field area divisions east, central and west depicted upon a 1997 photo-base map provided by Vegagerðin (Icelandic Roads Authority), including the five main drainage outlets of Skeiðarárjökull during the 20<sup>th</sup> century: the Sula, the Gígjukvísl, Háöldukvísl, Sælhúsakvísl and the Eastern and Western Skeiðará.

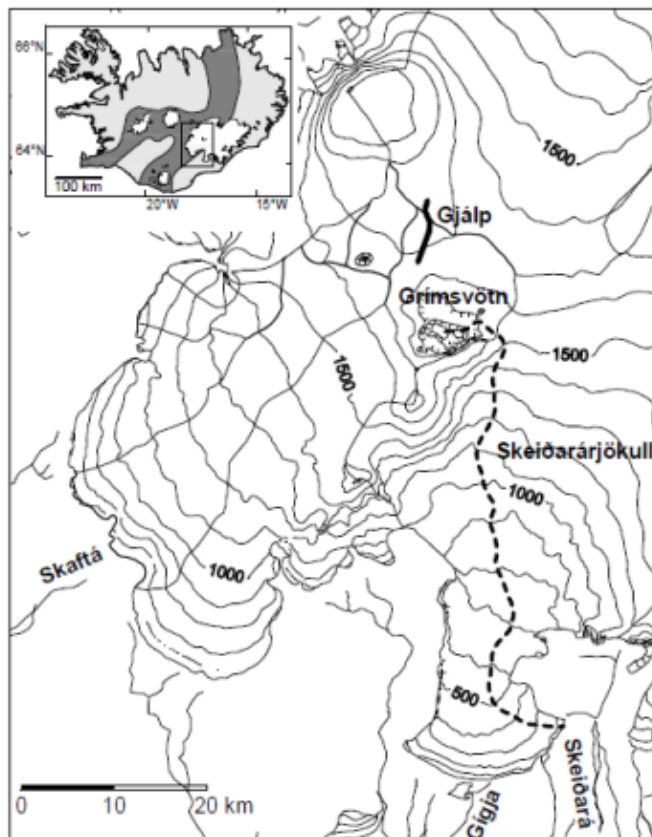
The eastern region is dominated by two features: the eastern lobe of Skeiðarárjökull and the Skeiðará rivers. Historically, the Skeiðará has been fed by meltwater routed subglacially to the base of the Skeiðarárjökull overdeepening (Björnsson, 1998) that flows onto the sandur via two artesian springs: one feeding the eastern Skeiðará and the Kaldakvísl and a second supplying the channel to the western Skeiðará (

Table 1.1); at present these channels are no longer active. The Skeiðará river also receives jökulhlaups from the drainage of ice-marginal lakes on the eastern margin of Skeiðarárjökull (Galon, 1973a, Björnsson, 1992). The eastern Skeiðará channel is bordered to the east by the steep incline of the basalt massif Skaftafellsfjöll and is separated from the western Skeiðará by an elevated region of heavily-kettled terraces. Near the margin of the glacier, the channels of both rivers commonly ranged from 30-50 m in width and 1-3 m in depth during normal meltwater conditions, while during flooding, the river may grow to widths of 8 km and depths of 30 m. Numerous jökulhlaups have inundated the Skeiðará channels over the past two hundred years, as a

result of jökulhlaups generated in association with eruptions from the Grímsvötn caldera (Figure 1.5) (Klimek, 1973, Björnsson, 1992, 1997, 1998, and 1998). During the November 1996 jökulhlaup, for example, 1.2 km<sup>3</sup> of water flooded through the Skeiðará, with discharge in the channel exceeding 15,000 m<sup>3</sup>s<sup>-1</sup> (Snorrason et al., 2002).

River	Discharge (m <sup>3</sup> ·s <sup>-1</sup> )	Sed Concentration (mg·L <sup>-1</sup> )
<b>Skeiðará</b>		
Summer	200 - 400	1500 - 4000
Winter	15 - 80	100 - 1000
<b>Gígjukvísl</b>		
Summer	20 - 70	1000 - 4000
Winter	2 - 20	50 - 2000
<b>Súla</b>		
Summer	10 - 60	1000 - 3000
Winter	1 - 10	200 - 2000

**Table 1.1 Non-flood average discharges, sediment and chemical concentrations of three major rivers of Skeiðarárjökull (Snorrason et al., 1997).**



**Figure 1.5 Location of the Gjalp fissure, subglacial lake Grímsvötn and the path of the meltwater beneath Skeiðarárjökull during the November 1996 jökulhlaup (Flowers et al., 2004).**



Drainage in the central region is dominated by the Gígjukvísl, a channel that has incised directly through the moraines estimated to date back to the 19<sup>th</sup> century (Galon, 1973a). These moraines form an arcuate belt of multiple ridges that spans over 3 km and separates the inner zone of marginal deposits emplaced since the 1930s from the end moraines and outwash deposits. Across the moraine belt, transverse depressions, moraine gates or ‘gaps’ exist that once provided access to the forefield for drainage across the glacier margin (Bogacki, 1973). Recent glacier surface lowering and margin retreat has led to the development of a proglacial depression 2 km across, with a depth of over 30 m. This retreat, and the development of the trench, has led to the abandonment of former channels, the formation of large lakes and meltwater drainage parallel to the ice margin. Retreat has also exposed a wide tract of sub-, en- and supraglacial features including drumlins, eskers, fracture fills, large kettle holes, ice-walled canyons and fracture-fill ridges that may provide insight into the dynamics of large-scale, temperate ice flow (Roberts et al., 2000, Fay, 2002, Russell et al., 2007, Woodward et al., 2008).

For the purposes of this study, the western region is defined as the portion of the sandur that lies west of the drainage flowing into the Gígjukvísl and east of the massif Lómangupúr as shown on Figure 1.4. This region encompasses both the Súla and the Blautkavísl, two channels that drained the western lobe of Skeiðarárjökull during the 20<sup>th</sup> century. The Súla emerged from artesian vents near the base of the Eystrafljall massif before flowing across a wide (>1.5 km), braided floodplain. Along the base of Lómangupúr, flows the Núpsvötn which drains the adjoining valley and frequently inter-braided with the Súla. Approximately 7 km south of the glacier margin lie partially preserved moraine ridges that may date back to at least the mid-18<sup>th</sup> century (Thorarinsson, 1943, Molewski, 2000).

Over the past sixty years, the western lobe of Skeiðarárjökull, with the exception of minor glacier margin advances, has retreated markedly. As early as 1756, Skeiðarárjökull extended so far south that it lay against the walls of Lómangupúr (Klimek, 1973) cites (Thorarinsson, 1939), an obstruction that formed the ice-dammed lake Núpsalón, which at its greatest extent possessed a surface area of 5 km<sup>2</sup> and potentially contained 100 million m<sup>3</sup> of water, further demonstrating the vast amount of change that this region has experienced in the relatively recent past.

In addition to floods from Grímsvötn, the western region has also been subject to outburst floods from Grænalón, Europe’s largest ice-dammed lake that possesses an area up to 18

km<sup>2</sup> (Björnsson, 2009). It is estimated that from at least 1785 to 1945, high-magnitude jökulhlaups from this lake were routed beneath the base of the ~250 m deep ice-dam flanking Grænalón (Björnsson, 1998, Thorarinsson, 1939, Thorarinsson, 1974). Grænalón jökulhlaups have reached peak discharges of 5000 m<sup>3</sup> s<sup>-1</sup> (Roberts, et al., 2005). Over the three decades following the retreat and lowering of the margin, the behaviour of the floods has altered, increasing in frequency (as often as 23 days apart) and appearing to be routed through the glacier (Roberts et al., 2005). While recent flooding events are lower in magnitude than their historical, less-frequent counterparts, peak flows into the Blautakvísl of 200-800 m<sup>3</sup> s<sup>-1</sup> have been documented and have significantly altered the nature of this channel.

#### 1.6.3 *Large-scale processes at Skeiðarárjökull: glacier margin fluctuations*

Like many other glaciers in Iceland, Skeiðarárjökull has retreated significantly since 1933 in response to the increase in temperature (Thorarinsson, 1943). Skeiðarárjökull's retreat has not been uniform: while the eastern and western lobes maintain active single point outlets, the central portion of the glacier has effectively decoupled from its terminal moraine, acting to 'behead' former drainage pathways (Figure 1.6) (Church and Ryder, 1972, Jewtuchowicz, 1973, Klimek, 1973, Wojcik, 1973a, Russell and Knudsen, 2002). During glacier recession, proglacial drainage typically collects in lakes within this depression before exiting onto the sandur via the eastern and western braided river systems.

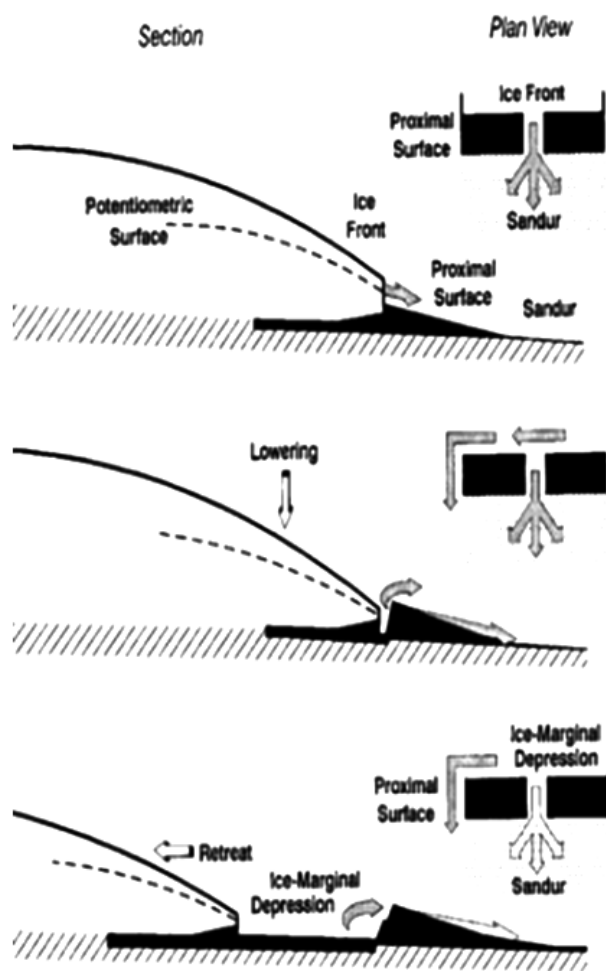


**Figure 1.6 Lowering of the glacier surface during glacier margin retreat since 1938 has decoupled the glacier from the sandur, leading to the formation of an ice-marginal depression and development of lateral drainage (Gomez et al., 2000).**

Over the past 300 years, Skeiðarárjökull has surged numerous times: 1787, 1812, 1857, 1873, 1929, 1985, and 1991 (Björnsson et al., 2003). Skeiðarárjökull shares characteristics with other surging glaciers in Iceland (Figure 1.7) including: flat ablation zones, low annual velocities and gentle slopes ( $1.6 - 4^\circ$ ) and it occupies an over-deepened basin that widens at the glacier mouth (Björnsson et al., 2003). Different regions of the sandur, however, are affected differently by surges that provide a wide range of landforms and processes: the central and western margins advanced significantly, while the eastern branch does not as it is sheltered behind the massif Skaftafellsfjöll that deflects most of the ice flow westwards. The subsequent retreat of Skeiðarárjökull following the 1991 surge exposed several suites of subglacial landforms that have provided insight into the internal mechanics of the surge itself (Pálsson et al., 1992), as well as examples of landforms and landsystems that may be used to identify other surge events on the sandur, at other locales and within the geological and geomorphic record (Russell et al., 2001a, van Dijk, 2002, Waller et al., 2008).

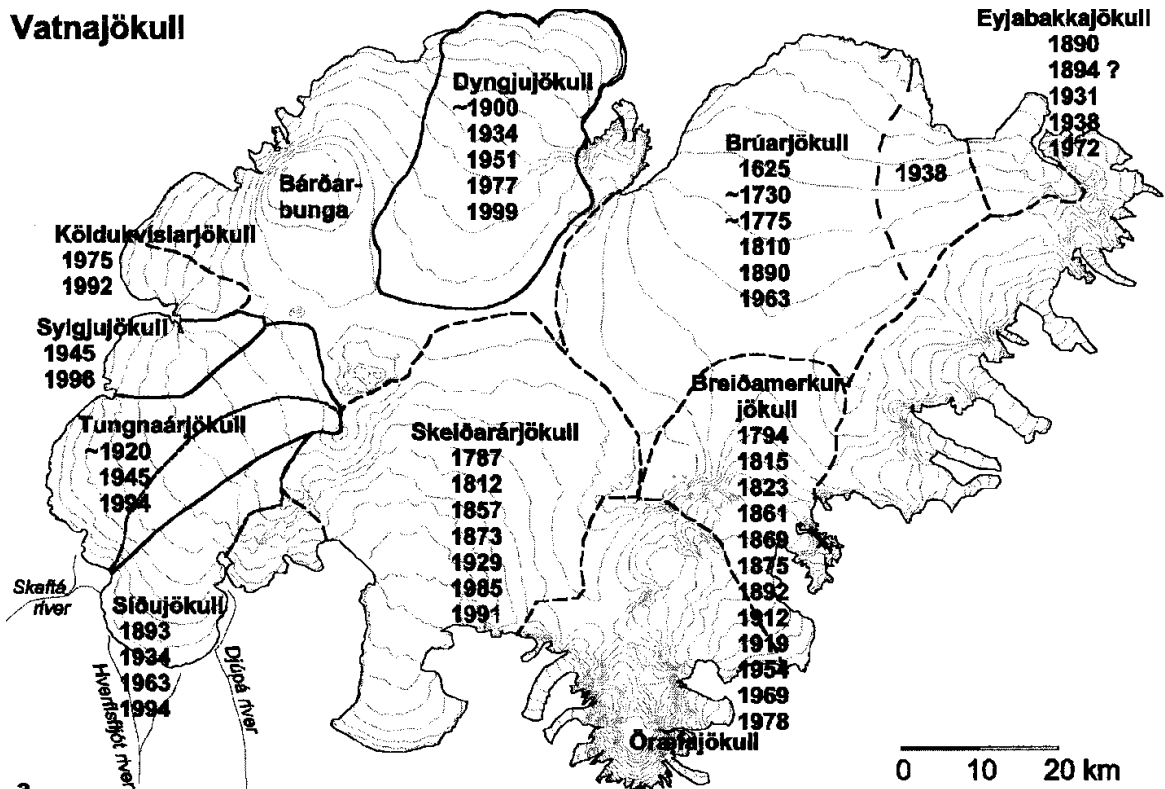


Figure 1.7 Location map of outlet glaciers of the Vatnajökull ice cap known to surge and dates of documented surges; (Björnsson et al., 2003).

#### 1.1.1 *Large-scale processes at Skeiðarárjökull: jökulhlaups*

High-magnitude, high-frequency jökulhlaups at Skeiðarárjökull have been recorded in folklore for eight centuries and documented as early as 1681 (Wadell, 1935). Indeed, Skeiðarársandur, the largest outwash plain in the world, has been termed a jökulhlaup ‘type-site’ (Maizels, 1991, Maizels and Russell, 1992, Russell et al., 1999b). Jökulhlaups here have been severe enough to cause the glacier ice to billow like ‘rollers of the sea’, devastating the ice margin and transporting large blocks of ice great distances (Wadell, 1935). ‘Skeiðarárhlaups’ have been identified as being the primary emplacement mechanism for the estimated 100 km<sup>3</sup> of sediment found between the glacier snout and the sea, occurring approximately five times per century over the last 10,000 years (Guðmundsson et al., 2002). The largest of these jökulhlaups are closely associated with volcanic eruptions at Vatnajökull and may occur roughly every decade (Thorarinsson, 1974, Guðmundsson et al., 2002), varying in scale and duration depending on their origin and frequency. Due to their sheer scale and legacy of devastation, comparisons of the effects of Skeiðarárjökull’s jökulhlaups to those released by the retreating Quaternary ice sheets have been postulated as early as 1934 (Wadell, 1935). Examinations of the 1996 high-magnitude jökulhlaup have revealed that a single flooding event may contain

distinct stages that emplace unique landforms or sedimentary structures (Russell and Knudsen, 2002, Roberts et al., 2001, 2003). In addition to being subject to volcanically-generated flooding from subglacial lake Grímsvötn, Skeiðarárjökull is also subject to frequent (months to annual) flooding from the ice-marginal lake Grænalón (Thorarinsson, 1939, Thorarinsson, 1974, Roberts et al., 2005).

#### 1.1.2 *Large-scale processes at Skeiðarárjökull: post-depositional modification*

Large bodies of buried glacier ice exist beneath the surface of Skeiðarársandur, often more than 1 km distant from the active ice margin and buried beneath layers of debris that may exceed 3 m in thickness (Russell et al., 1999b, Fay, 2002, Everest and Bradwell, 2003). An ice-cored terminal moraine complex, for example, found ~4 km south of the margin was documented as far back as 1815 (Henderson, 1819). Typically, ice-cored terrain documented in the western and central regions of the sandur are characterised by supersaturated muds, ice-cored moraines, subaerial thermokarst drainage networks, ponds and collapsing surfaces (Klimek, 1972, Bogacki, 1973, Jewtuchowicz, 1973, Jewtuchowicz, 1971, Andrzejewski and Molewski, 1999, Klimek, 1973). In addition to large bodies of buried ice, secondary modification on a smaller scale has been observed within the ice-marginal areas following the emplacement of landforms following recent jökulhlaups and glacier surges (Fay, 2002, Waller et al., 2008, Woodward et al., 2008). These landforms may include en- or supraglacial features such as kettle holes, fracture-filled ridges or eskers (Björnsson, 1997, Fay, 2002, van Dijk, 2002, van Dijk and Sigurðsson, 2002, Russell et al., 2001a, Russell et al., 2006). However, a comprehensive examination of the impact of secondary modification of macro- and meso-scale landforms and assemblages on the sandur, from emplacement to final meltout, has not yet been undertaken.

#### 1.6.4 *Summary*

Skeiðarárjökull has experienced several well-documented glacier surges and high-magnitude jökulhlaups. The glacier itself consists of three lobes that exhibit distinct behaviour as a result of climate and position. The recession of the glacier margin since the 1940s, and the subsequent evolution of its glacio-fluvial drainage patterns, provides an ideal site to examine the impact of ice lowering, and frontal retreat, on sandur development. The retreat of the glacier margin has also resulted in the exposure of an array of supra-, en- and subglacial landforms that may provide further insight into major sub-, en- and supraglacial processes. Finally, the recession of the glacier margin has been documented over the last six decades using historical aerial photographs, providing an

opportunity to examine how proglacial landforms, and the glacial landsystem as a whole, have been subsequently affected by post-depositional modification processes over a decadal time-frame.

## **1.7 Thesis structure**

In order to determine the impact of large-scale processes such as jökulhlaups, surges and post-depositional modification on the evolution of the sandur, it is necessary to identify landforms diagnostic of these processes to locate similar events on historical imagery. This requires the testing of existing landsystem models and an examination of their persistence over time in order to evaluate their usefulness as diagnostic signatures and the overall impact of the events on sandur evolution. These models will be tested by comparing them against historical events of similar magnitude on imagery (and used to identify previously unrecorded events), and observing their subsequent evolution over time; new hypotheses and models will be generated based upon these observations. The overall structure of the dissertation is presented below:

Chapter 1 presents the approach, goals, structures and objectives of this research. The literature review, due to the large volume of material and topics that are covered in this thesis, is broken up into two chapters, Chapters 2 and 3: Chapter 2 examines the salient literature on jökulhlaups, surges and post-depositional modification due to the melting of buried ice, while Chapter 3 focuses on literature pertaining to these three suites of processes at Skeiðarárjökull. Chapter 3 describes the field area and determines key criteria of landforms and structures that are diagnostic of large-scale proglacial processes and presents competing hypotheses for research questions specific to Skeiðarárjökull. Chapter 4 presents the basic principles and applications of analytical photogrammetry, and the details the process of extracting and analysing 3-D models with SocetSet and ArcGIS software including constraints, error estimates and other data collection issues.

Chapters 5, 6 and 7 examine each of the three large-scale processes with respect to the large scale landforms and documented historical accounts, where available. Chapter 5 describes historic fluctuations of the glacier margin at Skeiðarárjökull observed on imagery since 1945 for each of the three lobes (east, central and west); local interpretations are made regarding margin fluctuations and jökulhlaups and their impact on the evolution of the adjacent sandar. Chapter 6 examines the legacy of jökulhlaups on the sandur order to ascertain the impact, persistence and overall geomorphic signature of jökulhlaups on the proglacial landsystem of Skeiðarárjökull.

Chapter 8 discusses the controls, impact and persistence of features on the proglacial landscape and the interaction between processes and compares models and hypotheses presented in Chapter 2 and 3 with results of Chapters 5, 6 and 7. Chapter 9 provides a summary of the research and conclusions as well as a comprehensive model of sandur evolution. In this final chapter, the wider implications of the research are discussed and the possibilities for future research are presented.



## Chapter 2 Literature review: context of the research

---

*This section presents theories in the literature that address large-scale processes and landforms associated with glacier margin advance and retreat (including rapid advances such as surges), jökulhlaups (volcanogenic and limno-glacial) and post-depositional modification as a result of the melting out of buried ice. This review focuses on models of meso- and macro-scale processes and landforms present at large, temperate glaciers and their adjacent proglacial areas worldwide, with a particular emphasis on decadal-century timescales. Specific studies of landforms and processes found at Skeiðarárjökull are explored in detail in Chapter 3.*

---

### **2.1 Dynamics of glacier margins: controls on drainage and sedimentation regimes in response to margin fluctuations, floods and secondary modification**

#### **2.1.1 Introduction**

This chapter examines the processes and landforms associated with glacier margin fluctuations, jökulhlaups and post-depositional modification found in the literature. Hypotheses, landsystem models and their deficiencies are presented. Chapter 3 examines observations in the literature that deal specifically with the field site.

### **2.2 Glacier margin fluctuations**

#### **2.2.1 Introduction**

It has long been recognised that glacier margin position affects large-scale proglacial topography (Maizels, 1979). At advancing and stable glacier margins, for example,



meltwater flows directly onto the sandur, distributing sediments eroded from beneath the glacier and eventually raising the level of the sandur (Arnborg, 1955). In regions where meltwater is not confined by topography, alluvial fans may coalesce, forming a broad sandur (Figure 2.1) (Boothroyd and Nummedal, 1978). Sandar are characterised by braided rivers that divide and rejoin around bars in a regular pattern, the characteristics of which are controlled by a variety of factors, including channel migration rate, avulsion, frequency and aggradation rate (Figure 2.2) (Bristow and Best, 1993, Marren, 2005).

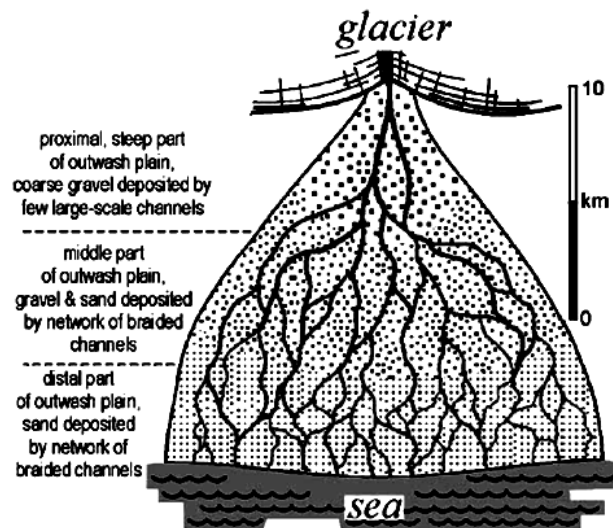


Figure 2.1 Schematic plan of the proximal, middle and distal portions of an Icelandic sandur from Boothroyd and Nummedal (1978), modified by Zielinski and van Loon (2002).

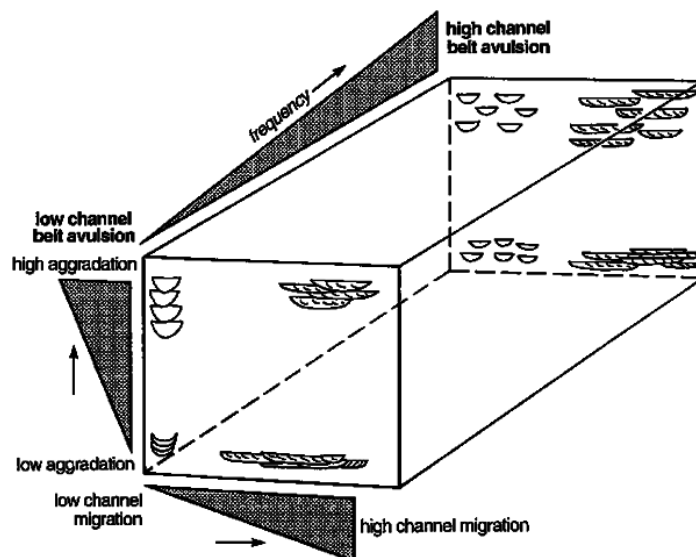
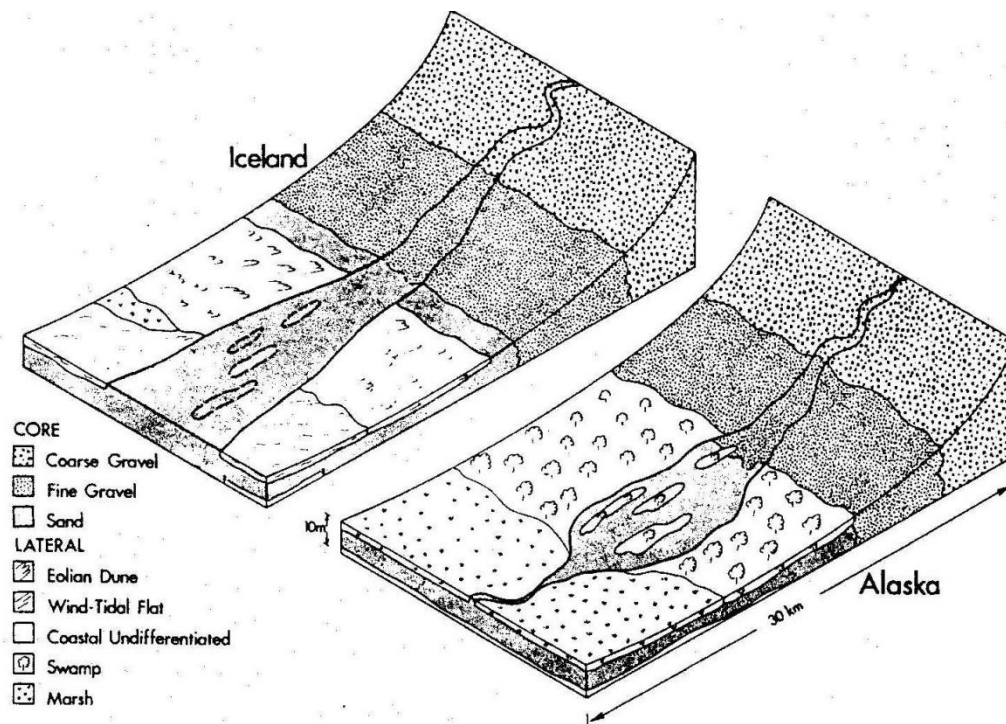


Figure 2.2 Relationship between channel migration, aggradation and frequency of channel belt avulsion (Bristow and Best, 1993).

Glacier advance increases aggradation and steepening of the sandur, encouraging the development of braided streams (Maizels, 1979). Boothroyd and Nummedal (1978) examined the development of alluvial fans in humid, proglacial settings and identified three distinct channel patterns: 1) single, or few, channels incised into coarse gravel deposits that extend from the glacier margin 2-5 km, 2) channels that bifurcate into a larger number of channels (termed ‘coarse braided’) and are bisected by individual and multiple longitudinal bars and 3) a distal region characterised by fine braiding channels (Figure 2.3).



**Figure 2.3 Comparison of braided streams and alluvial fan development in Iceland and Alaska (Boothroyd and Nummedal, 1978).**

Retreat is commonly characterised by entrenched channels, large regions of hummocky terrain, dead ice and proglacial lakes (Boulton, 1967, Thompson, 1988, Marren, 2002b), The associated lowering of the ice surface and resulting frontal retreat plays an important role on the development of the glacio-fluvial system (Price, 1969, Churski, 1973, Björnsson, 1999), as glacier retreat may lead to the development of proglacial lakes (Jonsson, 1955, Howarth and Price, 1969), channel and terrace geometry (Maizels, 1979, Marren, 2002b) and meltwater distribution (Klimek, 1973). Glacier advance and retreat may affect the geomorphology of the proglacial area without any alteration in sediment or water supply, as channel incision may result simply from the lowering of the upstream meltwater outlet (Marren, 2002b).

Price (1969) noted at Breiðamerkurjökull, Iceland that the descent of terrain away from moraines in a series of steps encourages the development of drainage parallel to the margin (Figure 2.4). While Price's model depicts many of the landforms commonly found on proglacial terrain where glaciers are subject to glacier margin recession and floods, often glaciers in similar regions and climatic conditions exhibit different patterns of retreat. For example, in southeast Iceland, Skaftafellsjökull has experienced rapid retreat that has exposed an extensive region of ground moraine, while the adjacent glacier, Svínafellsjökull, was subject to successive recession and re-advances, resulting in the formation of a series of push moraine complexes (Thompson, 1988). The ability of two adjoining glaciers to respond differently to climate and internal fluctuations demonstrates the complexity of predicting and modelling glacier fluctuations and the resulting proglacial landforms generated in response to these fluctuations. The following section examines processes and landforms associated with surges and glacier margin recession.

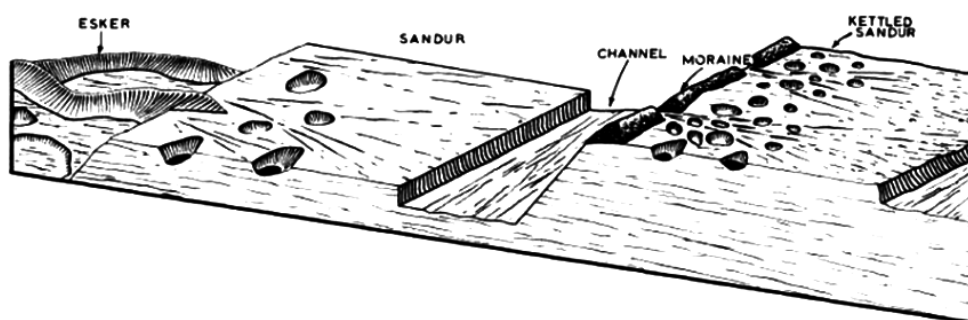


Figure 2.4 Classic model of sandur development, from Price (1969) page 33.

### 2.2.2 *Glacier advance and surges*

Glacier advance, and normal glacier flow, is often characterised by meltwater draining through a few established, lateral subglacial tunnel channels (conduit system) (Shreve, 1974, Björnsson, 1998). The advance of the glacier margin may result in the formation of moraines, drumlins and thrust blocks; these landforms may also be generated during the active phase of the 'surge cycle'. Glacier surging is a result of cyclic flow instabilities triggered from within the glacier and may produce flow velocities up to one thousand times that of ice flow during non-surge phases (Clarke et al., 1984, Raymond, 1987, Evans, 2003). The 'surge cycle' differs from a continued advance of the ice margin as the cyclic flow instabilities that the glacier experiences result in changes in internal drainage

that emplace suites of landforms beneath the glacier and proximal to the glacier margin (Evans and Rea, 2002).

Surges occur in both temperate glaciers (glaciers that are at melting point all year with the exception of the top few metres of ice) and poly thermal glaciers (glaciers that contain both ‘cold ice’ (below 0°C) at their margins and ‘warm’ ice (at 0°C) at their interior where ice is warmed to the pressure melting point). The initiation of a surge is commonly characterised by a rapid increase in velocity in the upper part of the accumulation area, an event that may last for several months (Björnsson et al., 2003). The excess ice travels down-glacier in a kinematic wave, often visually recognizable as a heavily-crevassed bulge, although it may take several months for this influx of ice to reach the glacier margin (Kamb et al., 1985, Björnsson et al., 2003). During a surge event, the glacier profile may develop a steep, near-vertical front, while the surface may develop looped medial moraines and extensive crevassing (Meier and Post, 1969, Clarke et al., 1984, Kamb et al., 1985, Raymond, 1987, van Dijk, 2002).

Several mechanisms for glacier surges have been proposed, including the critical mass hypothesis, the deformable bed hypothesis, the thermal switch model and the hydrological switch model. The critical mass hypothesis proposes that upon glacier ice accumulating to a critical mass, basal melting occurs that acts to reduce friction, and lifts the glacier from the bed permitting the rapid flow of ice (Meier and Post, 1969). The underlying geology of the glacier may also dictate the location and frequency of a surge in areas that contain substrate that fail under stress, termed the deformable bed hypothesis, although this phenomenon may be quite rare (Evans and Rea, 1999). The thermal switch model has been derived from observations at polythermal glaciers where surges occur as a result of the ‘warmer’ ice (at pressure melting point in the interior of the glacier) forcing the cold ice at the margin that is frozen to the bed forward (Murray et al., 2000, Fowler et al., 2001, Benn and Evans, 2010). As the field site Skeiðarárjökull is a temperate glacier, so the thermal switch model is not examined in this study.

The hydrological switch model ascribes surging events due to alterations in subglacial hydrological conditions. During a surge drainage changes from a conduit system to one that is dominated by a series of linked cavities, or a distributed system (Kamb et al., 1985, Kamb, 1987). As a consequence of the ice travelling faster over the irregular ground surface, small cavities (< few metres) develop links via narrow connections perpendicular to ice flow (Lliboutry, 1981, Walder, 1986). This conduit system restricts the flow of

water and exists beneath the entire glacier, persisting for some time (Björnsson, 1979). The resulting increased water pressure, combined with the reduced friction caused by the presence of the basal cavity system, increases basal sliding. In turn, the velocity increase via basal sliding provides the stability for the cavities that maintain the increased water pressure (Kamb et al., 1985). The increased water pressure may result in blowout structures (Figure 2.5) (Benediktsson et al., 2008) and the formation of deltas/deposits on elevated portions of sandur, such as the emplacement of fans across moraines where there are no gaps (van Dijk, 2002). Both systems may co-exist throughout the glacier, changing in response to seasonal and diurnal meltwater inputs (Björnsson, 1998).

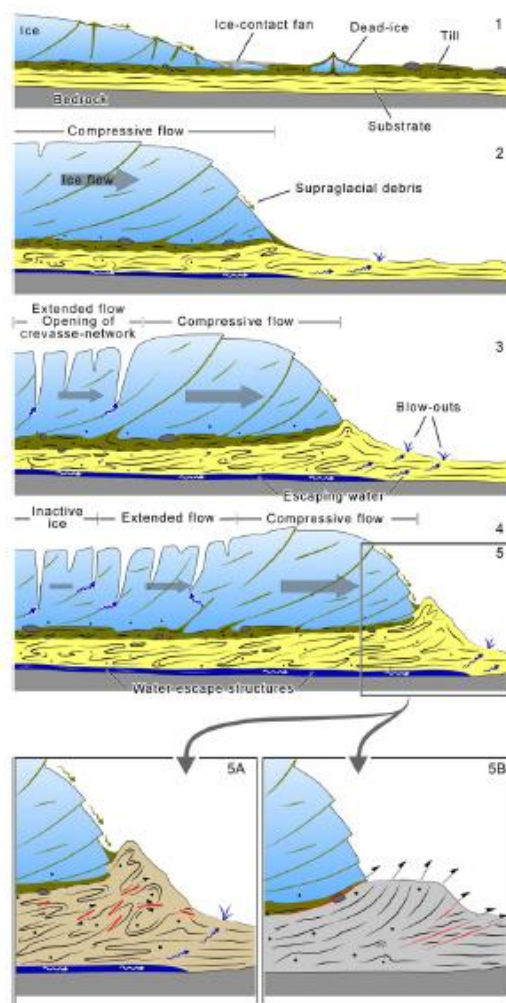


**Figure 2.5 Development of blowout structures and sediment wedges during a surge (from Benediktsson et al., 2008, page 232):** 1) During the quiescent phase, features and sediments are deposited during ice lowering, 2) compressive flow during advance results in thrusts, debris entrainment and deposition of material on the glacier surface, 3) thinning following passage of surge waves results in expansion of crevasse network while at glacier front blow out structures, elevated drainage and reverse slope sediment wedge develops, 4) a drop in pore pressure results in coupling of ice/bed interface, deforming the substrate in a brittle manner and 5a) (enlargement) in fine-grained strata, high-pore pressure will deform the material in a ductile, fold dominated manner, while 5b) in coarse-grained strata, it deforms in a brittle manner, resulting in slabs with low-angle thrusts.

During a cavitation-dominated system, it has been noted that the sediment concentration of meltwater greatly increases, and new marginal englacial outlets and alluvial fans may develop (Kamb et al., 1985, Fleisher et al., 1998, Björnsson et al., 2003). The cavitation-dominated system serves to laterally distribute subglacial drainage (Björnsson et al., 2003), determine the spatial distribution of surge related landforms, and restrict the size of the fans (van Dijk, 2002). While this marked increase in sedimentation may infill channels or proglacial lakes, erosion due to increased meltwater may also alter existing proglacial drainage channels (Russell et al., 1999b, Russell et al., 2001a). As the surge reaches the glacier front, however, the recursive system is broken and the cavities collapse, returning the drainage system to a tunnel/conduit system.

At this terminal stage of the ‘surge cycle’, large volumes of water may be released during an outburst flood (jökulhlaup), observed to excavate ice canyons and transport large ice blocks (Kamb et al., 1985, Fleisher et al., 1998). The drop in pore pressure leads to a strengthening of the ice/bed interface, and this may cause the sediment to deform, creating a sediment wedge end moraine characterised by ice blocks and thrust blocks (Figure 2.5) (Benediktsson et al., 2008). Following retreat, en- and subglacial features may be exposed including hummocky terrain, concertina eskers, flutes, drumlins, and crevasse casts (Knudsen, 1995, Evans and Rea, 1999, Bjarnadóttir, 2007, Waller et al., 2008). Margin retreat may also leave hanging outlets, alluvial fans and overridden moraines on proglacial distal regions (Russell et al., 2001a, van Dijk, 2002, van Dijk and Sigurðsson, 2002), as well as terrain steps (Andrzejewski and Molewski, 1999).

### 2.2.3 *Surges: diagnostic landforms and landsystem models*

Hummocky moraines (Clayton et al., 1985), fields of flutes terminating at major moraines (Sharp, 1988, Dredge and Cowan, 1989), large stacks of contorted and faulted blocks or wide belts of arcuate thrust ridges (Evans, 2003), concertina eskers (Knudsen, 1995), meandering ridges/conduit fills (Christoffersen et al., 2005) and crevasse-cast ridges (Figure 2.6) (Sharp, 1985a, Evans and Rea, 2003, Bjarnadóttir, 2007) are all examples of landforms, taken singly or en suite, that have been described as diagnostic landforms for surge events. However, they are not present at all surging glaciers and may also develop as a result of rapid ice advance (e.g. non-surge events) (Evans, 2003, Benediktsson et al., 2008). Recognizing the importance of recognizing surge events within the geomorphic record, and the landforms associated with distinct phases in the ‘surge cycle’, some models have been constructed that use a regional approach.

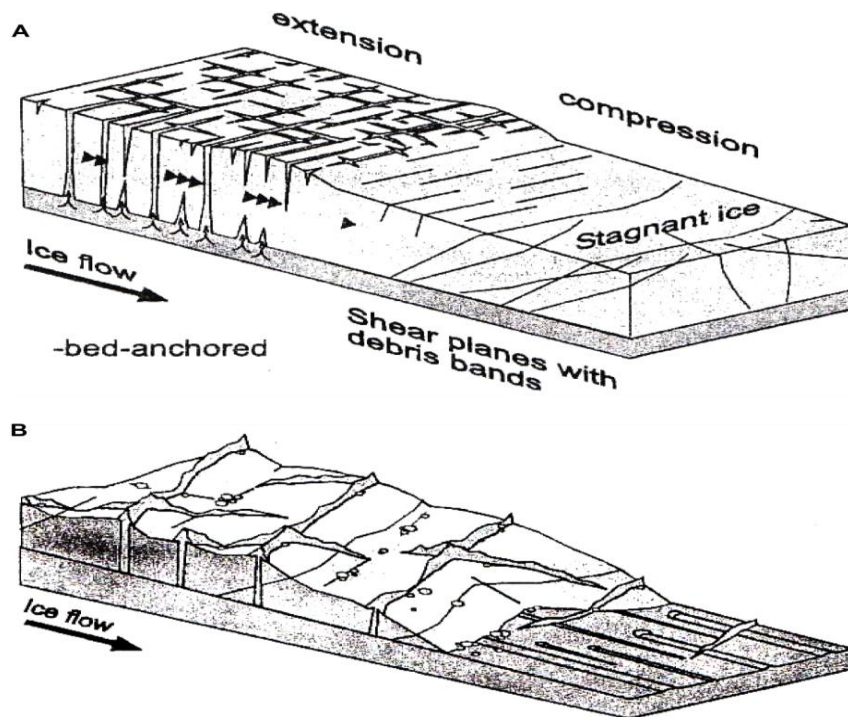


Figure 2.6 Crevasse-cast ridge formational model from Bjarnadóttir (2007) based upon observations at Brúarjökull, Iceland. A) Crevasses open up as a result of the propagation of down-glacier compressional flow during surge, and sediment is dragged up into the crevasses as a result of the pressure differences, forming bed-anchored crevasse casts. B) Ablation of glacier surface during retreat reveals crevasse cast ridges and flutes.

Evans and Rea (2003) presented a landsystem model (Figure 2.7) based upon the entire surge landform-sediment assemblage that consisted of three zones: an outer zone of thrust block moraine (Zone A) that grades into hummocky terrain (Zone B), then an inner zone of fluting/crevasses squeeze ridges and concertina eskers (C zone). This model captures some features common to surging glaciers, yet it lacks resolution with respect to features directly linked to the internal drainage fluctuations and terminal flood events.

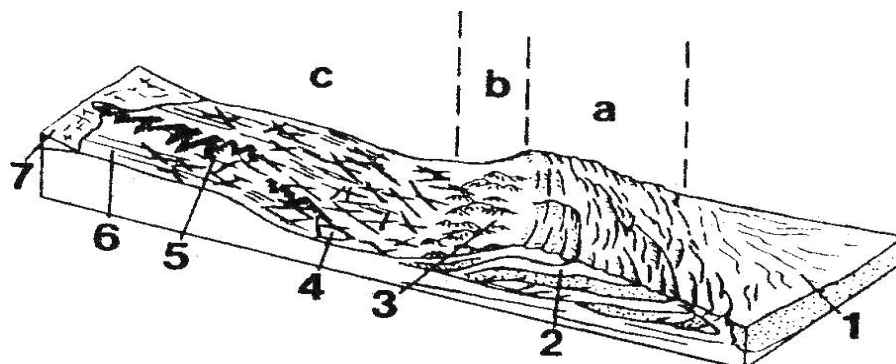
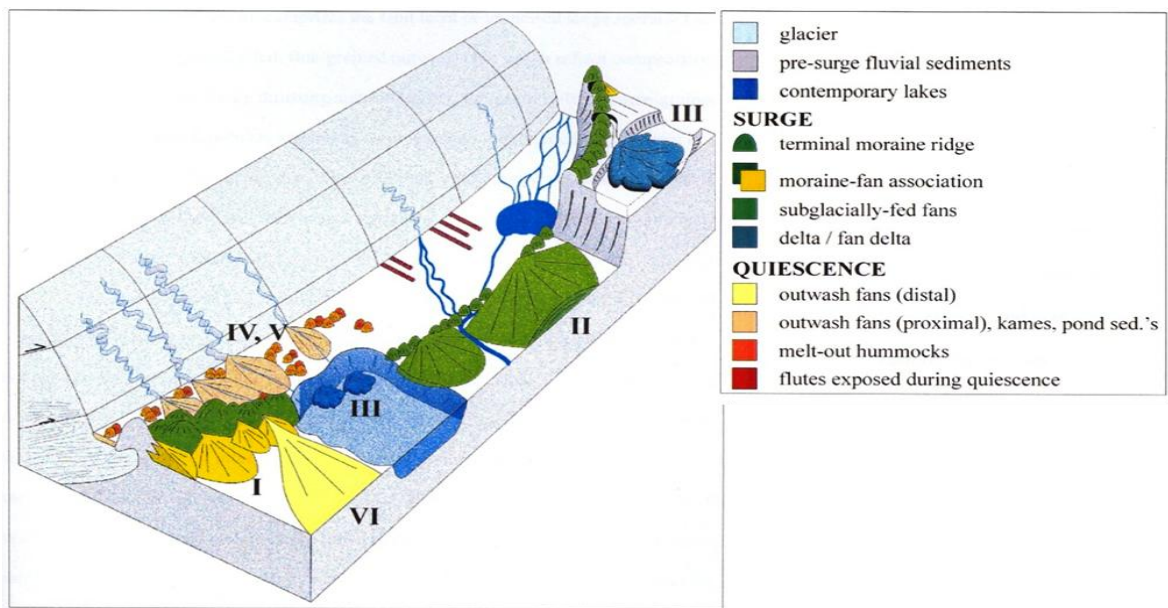


Figure 2.7 Model of landforms created during surging events (Evans and Rea, 1999): a) outer zone of proglacial thrust pre-surge sediment; b) zone of weakly developed hummocky moraine; c) zone of flutings, crevasse-squeeze ridges and concertina eskers; 1) proglacial outwash fans; 2) thrust block moraine; 3) hummocky moraine; 4) crevasse-squeeze ridge; 5) concertina esker; 6) fluting; 7) glacier.



Van Dijk's (2002) model (Figure 2.8) captures both the quiescent and surge phases of an event. In the surge phase, there exists: I, a terminal arc characterised by un-incised surge moraines and englacially-fed outwash fans, II, coarse-grained, subglacially fed ice contact fans; III, deltas and fan deltas emplaced on topographic highs (hanging outlets). The quiescent phase is marked by landforms IV and V consist of quiescent phase fans and pond/kame sediments with inter-bedded delta deposits; VI, fine-grained outwash fans lying within moraine gaps. van Dijk (2002) identified the internal drainage re-organisation from conduit-dominated to cavity-dominated as a main control on these surge related landforms and deposits.



**Figure 2.8 Proglacial landsystem model of a surging glacier based upon observations at Skeiðarárjökull (van Dijk, 2002): I) surge-related moraine-fan association with fine grained SFRs II) surge-related, coarse-grained, subglacially-fed ice-contact fans, III) surge-related deltas and fan deltas in proglacial depressions, IV) ice-proximal quiescent phase fans QPF's, V) ice-proximal basin and pond sediments, VI) quiescent phase fans on the distal side of the surge moraines.**

#### 2.2.4 *Retreat*

Koteff and Pessl's (1981) morphosequence was the first landsystem model to address retreat at glacier margins (Figure 2.9). Their 'dirt machine' model demonstrated that even during retreat debris is carried upwards along the live-ice/stagnant-ice interface, acting as a conveyor belt to bring material to the stagnation zone. The resulting landforms and deposits, however, are controlled by the regional topography, including the presence of proglacial lakes, moraines, dead ice, slope direction and angle (Koteff and Pessl, 1981). Slope is particularly important when examining retreating glacial landsystems that occupy over-deepened basins that commonly not only possess proglacial lakes and topographic constrictions, but whose rate of retreat may be accelerated when receding across a reverse slope (Price, 1969). The following section presents the overall effects of a retreating



margin on the proglacial glacio-fluvial system; specific landforms generated from stagnating ice margins are dealt with later in this chapter under the heading 'Post-depositional modification of proglacial outwash'.

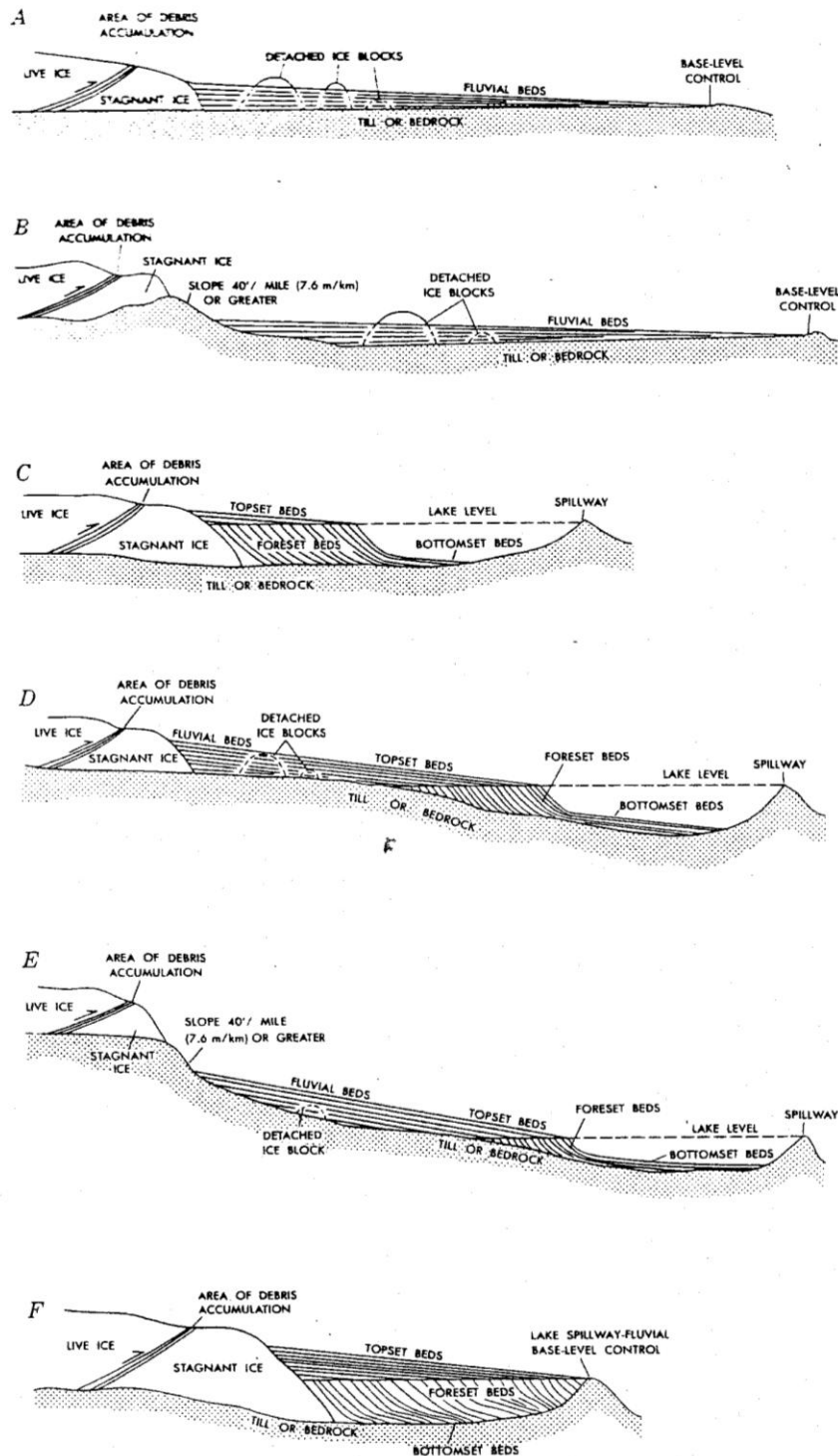
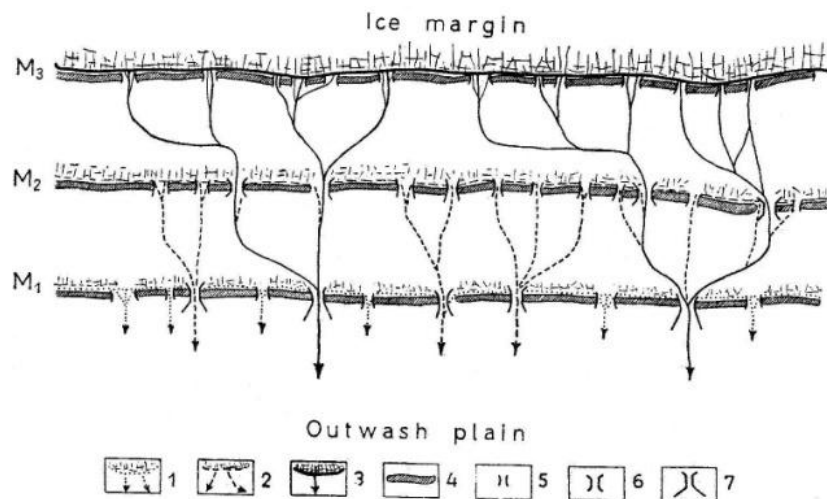


Figure 2.9 Diagram of morphosequences, or landsystem models, of various proglacial systems: A) fluvial ice-contact sequence, B) fluvial non-ice contact sequence, C) lacustrine ice-contact sequence, D) fluvial-lacustrine ice-contact sequence, E) fluvial-lacustrine non-ice contact sequence, F) lacustrine-fluvial ice contact sequence (after Koteff and Pessl, 1981, page 7).

During glacier frontal retreat, the number of active channels across the margin decreases (Price and Howarth, 1970), although the volume within a single channel increases, resulting in the enlargement and deepening of a few moraine gaps (Figure 2.10) (Klimek, 1972). Drainage proximal to the margin may be subject to continuous change as each successive standstill may be marked by a different altitude of the glacier base (Churski, 1973) and during retreat, channel incision and re-organisation may occur quite rapidly (Marren, 2002b). Incision has been observed to proceed in two stages on sandur in front of retreating margins (Roussel et al., 2008): during the first stage, incision is prohibited as a result of the release of sediment from the paraglacial and stagnating portions of the margin. The second stage is characterised by proximal sandur incision as this sediment supply dwindles. Continual alteration of drainage across the margin may be responsible for significant geomorphic changes within the marginal zone as lateral erosion may obliterate any existing landforms (Kozarski and Szupryczynski, 1973).



**Figure 2.10** 1, 2 and 3) represent progressive abandonment of moraine gap drainage following ice margin recession (Klimek, 1973): 4) ice margin positions, 5) end moraines, 6) moraine ‘gates’, 7) inherited gates, 8) youngest gates.

Landforms such as moraines, kame and kettle regions, flutes, eskers and crevasse-casts may, while they persist, act to control, direct and impound drainage (Howarth and Price, 1969, Galon, 1973a). Proglacial lakes may develop along topographic lows behind moraines (Boulton, 1967), often forming in regions where large drainage outlets were once present (Jonsson, 1955) and may also be collocated above or within depressions formed by large masses of buried ice (Thorarinsson, 1939, Arnborg, 1955, Jonsson, 1955, Howarth and Price, 1969). Proglacial lakes serve as sediment traps, capturing coarse-grained sediment and increasing the erosive potential of the meltwater as they flow across the sandur and during even during high-magnitude events such as jökulhlaups they may

act to impound flood waters until channel constrictions are eroded/expanded and the water is released (Russell et al., 2006).

At locations where lacustrine termini retreat into overdeepened basins, fracturing of the glacier margin and the development of calving ice blocks has been observed in many locations in the world, including Glacier Nef in Patagonia (Warren and Aniya, 1999), the Unteraargletscher glacier in Switzerland (Funk and Rothlisberger, 1989), the Tasman Glacier in New Zealand (Kirkbride and Warren, 1999) and the Mendenhall Glacier in Alaska (Boyce et al., 2007). Calving results from buoyant, upwardly directed forces that result in basal fractures in the glacier margin (van der Veen, 1996, Warren et al., 2001). Calving has been noted to play a major role in accelerating the rate of margin retreat, as it may result in the loss of large volumes of ice greater than possible through surface ablation alone (van der Veen, 2002).

Following glacier margin recession, proglacial topography may be subject to long periods of gradual modification as ice-cored moraines and dead ice fields are gradually occupied by lakes or develop into thermokarst topography/hummocky moraine (Boulton, 1967, Price, 1969, Krüger and Kjær, 2000). Steep moraine ridges subject to melting may be lowered into rounded hills, while sliding may produce wide, kettled, plains (Price, 1969, Jewtuchowicz, 1973). While it has been observed that actively advancing and eroding glaciers may generate larger volumes of debris than stagnating ice; this cannot necessarily be used as a stratigraphic signature, as during recession large volumes of glacial sediment may also be released into the system (Maizels, 1997). As recession continues, braided stream patterns may become established closer to the glacier margin confined within an incising channel (Figure 2.11); during re-advance, braiding will become re-established on the recently abandoned outwash surface (Marren, 2002b).

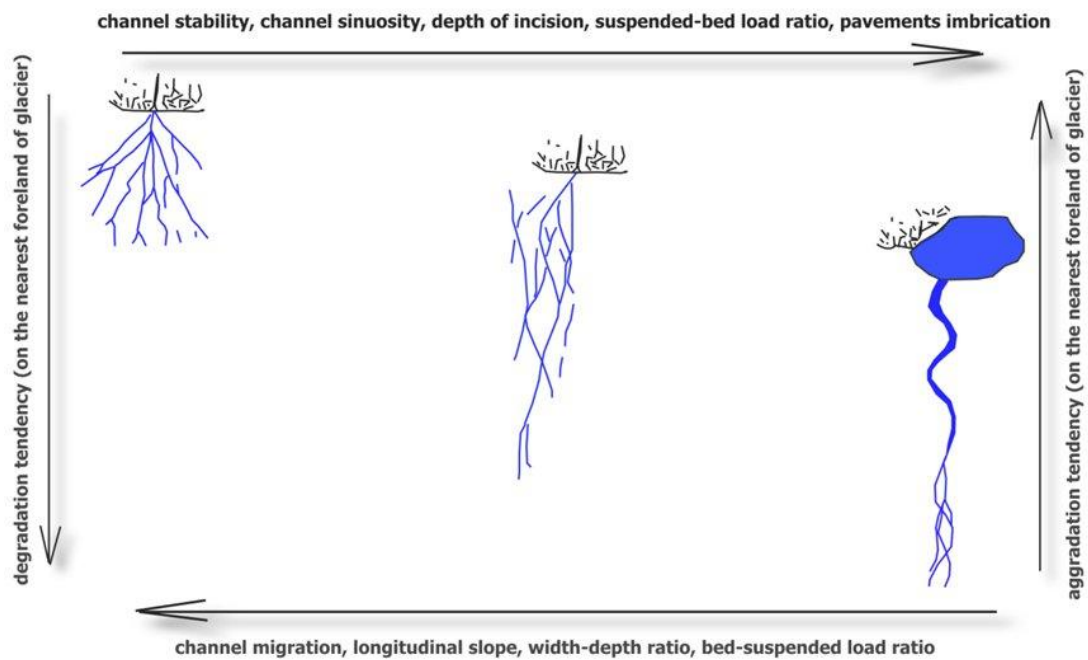


**Figure 2.11 Relationship between margin position and drainage development, modified from Klimek (1973) .**

If sufficient meltwater ascends out of an over-deepened basin, and the hydraulic potential increases more rapidly than the resulting mechanical energy can be transformed into heat, the water may become subject to supercooling (Shreve, 1985, Alley et al., 1998), a mechanism that may act to constrict meltwater conduits and result in the entrainment of large amounts of debris within the ice (Alley et al., 1998, Lawson et al., 1998, Evenson et al., 1999, Tweed et al., 2005). Supercooling may occur during large- and small-scale jökulhlaups (Roberts et al., 2002) and during ice-melt-dominated conditions as observed at artesian meltwater vents emerging at Skeiðarárjökull (Tweed et al., 2005) Matanuska Glacier (Lawson et al., 1998, Evenson et al., 1999) and at frazil ice rafts at the Bering Glacier (Natel and Fleisher, 1994, Fleisher et al., 1997). The reverse slope near the termini of these glaciers was sufficient during ice-melt-dominated conditions and during these jökulhlaups to generate supercooling. As a result, debris-rich ice accumulations were present in both sub- and englacial localities, further demonstrating the potential impact of ice margin position on the development of proglacial landsystems.

#### 2.2.5 *Summary*

Fluctuations of the glacier margin play an important role in the evolution of proglacial landsystems. Stable and advancing margins are characterised by a dispersed drainage system capable of delivering material across the front of the glacier, while recession is characterised by the development of proglacial lakes and drainage parallel to the glacier

margin and channel incision. Advance and retreat, therefore, directly affect the pattern and extent of both drainage and sedimentation processes and influence both the creation and persistence of landforms.

Recent research on glacier surges has focused on determining diagnostic landform(s) that may be used to recognize previous events. While glacier surges produce push moraines, alluvial fans, an increased number of drainage outlets and an increased sediment concentration in meltwater streams, these features may be found at both surging and non-surging glaciers. Concertina eskers, thrust block moraines and crevasse-cast ridges have also been proposed to be diagnostic signatures, although none of these may be considered exclusive to surges. Surges, however, are characterised by a switch in internal drainage configuration (from conduit to distributed drainage) that may result in the emplacement of different landforms during different phases of the surge cycle, including englacial outlets, wide alluvial fans, terminal stage jökulhlaups that may emplace ice blocks, and following the retreat of the glacier margin, the englacial drainage may result in the emplacement of 'hanging outlets' on the elevated sandur. Most studies of surges, however, have only examined features at surging glaciers during or immediately following a surge event. It is important to consider the longer-term impact (>10 years) that a surge event may have on the proglacial terrain when the glacier margin is coupled, or decoupled, from the sandur. Subsequent deflation, erosion, meltout, floods and margin fluctuations may further alter these diagnostic signatures.

## **2.3 Jökulhlaups: mechanics and related landforms**

### **2.3.1 *Introduction to jökulhlaups***

Maizels (1997) presented comprehensive landsystem models to identify jökulhlaup-related features in proglacial environments based on examinations of sedimentary sequences and landforms observed on sandar in southeast Iceland. These models depict possible large-scale landforms and sedimentary sequences that may be emplaced as a result of limno-glacial (Figure 2.12) and volcanogenic (Figure 2.13) jökulhlaups.

However, these landsystem models do not incorporate landforms or deposits emplaced supra-, en- or subglacially during a jökulhlaup, nor do they relate landforms to flood phases. In order to understand the depositional and erosional impact of jökulhlaups on the proglacial landsystem and develop a comprehensive spatio-temporal model, it is necessary to explore the mechanisms and processes affecting jökulhlaups and their deposits.

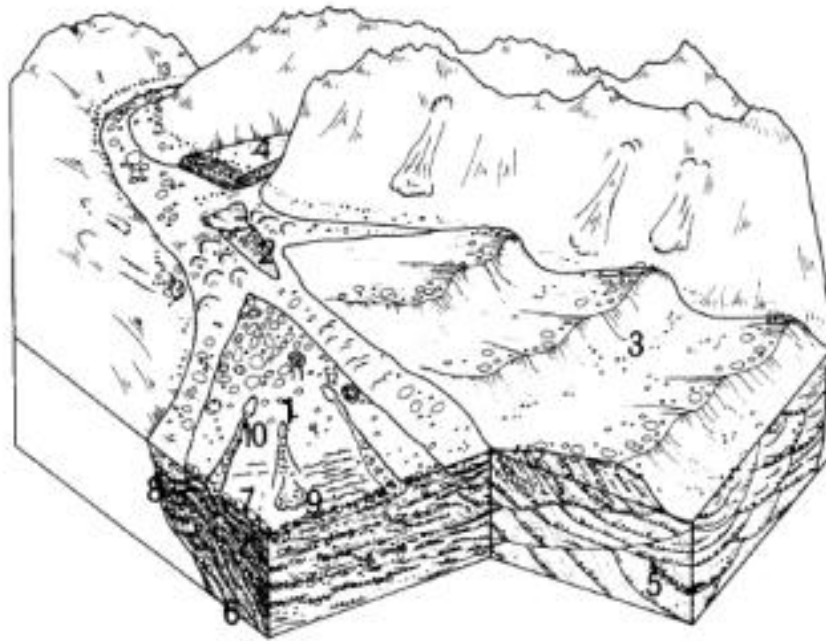


**Figure 2.12 Jökulhlaup-related landforms within limno-glacial valley sandur landsystem (Maizels, 1997): 1) expansion bar, 2) pendant bar, 3) mega-ripples or dunes, 4) slack-water deposits, 5) large-scale dune cross-bedding with reactivation surfaces, 6) large-scale bar front cross-bedding, 7) imbricated boulder lag, 8) channel fill deposits, 9) small scale ripples, 10) chute channel and lobes, 11) kettle holes and kettle fills, 12) ice-block obstacle marks, and 13) wash limit on adjacent valley-side slopes.**

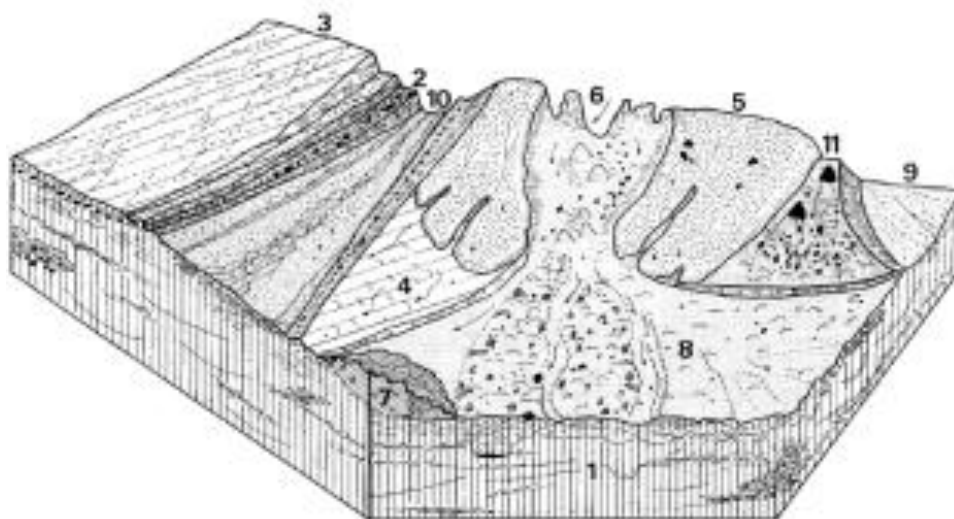


**Figure 2.13 Jökulhlaup-related landforms within volcanogenic landsystem (Maizels, 1997): 1) massive bedded sediments, 2) terraced boulder deposits, 3) abandoned sandur terrace, 4) washed sandur, 5) lobate fan deposited by hyper-concentrated jökulhlaup flows, 6) incised jökulhlaup channel with streamlined residual hummocks, boulders and mega ripples, 7) hummocky distal jökulhlaup deposits, 8) streamlined, hummocky erosional bars mantled with rimmed and till-fill kettles, 9) incised jökulhlaup channel, 10) incised active meltwater channel, 11) streamlined erosional bars, wash limits and scattered boulders and dune forms downstream of bedrock obstacles.**

### **2.3.2 Jökulhlaups: initiation and internal controls**

The mechanism of initiation, combined with drainage and reservoir characteristics, will determine a flood's frequency, timing and magnitude (Maizels, 1997). Jökulhlaups are

most commonly generated by the failure of an ice dam that had served to impound an ice-marginal lake (Maizels, 1997), although there are numerous other possible mechanisms (Table 2.1). Given the wide variety of mechanisms and possible environments, this study is restricted to jökulhlaups that are volcanically induced or generated by drainage from an ice-marginal or ice-dammed lake (limno-glacial). In addition to varying in residence time within the reservoir and in scale in regards to volume, these types of jökulhlaups may also experience different routing behaviours through the glacier that may be distinguished with a flood hydrograph.

<b>Jökulhlaup generation</b>	<b>Postulated Trigger Mechanisms</b>
Drainage of an ice-marginal, ice-dammed lake	<ul style="list-style-type: none"> <li>➤ Ice dam flotation due to hydrostatic stress</li> <li>➤ Glen mechanism: viscoplastic deformation of the ice dam when hydrostatic stress exceeds glaciostatic stress and the confining strength of ice</li> <li>➤ Supraglacial overspill (common at cold-based glaciers), resulting in thermodynamic erosion of an ice-lined spillway</li> <li>➤ Hydraulic tapping of a meltwater reservoir by intraglacial drainage</li> <li>➤ Darcian flow at the base of the ice dam</li> <li>➤ Enhanced glacier sliding close to the ice dam, leading to mechanical rupture of the dam base</li> <li>➤ Hydrodynamic enlargement of a breach formed between substrate and glacier ice</li> </ul>
Drainage of a supraglacial lake	<ul style="list-style-type: none"> <li>➤ Hydraulic tapping of a meltwater reservoir by intraglacial drainage</li> <li>➤ Nonlinear rate of spillway lowering due to viscous dissipation and conduction of heat from flowing meltwater</li> <li>➤ Release of meltwater into intraglacial drainage due to descent of a hydrofracture from the base of a supraglacial lake</li> </ul>
Volcanically induced jökulhlaup	<ul style="list-style-type: none"> <li>➤ Profuse ice melt due to subglacial volcanism, causing either subglacial or immediate drainage of floodwater with no significant storage</li> </ul>
Drainage of a subglacial lake	<ul style="list-style-type: none"> <li>➤ Ice dam flotation due to hydrostatic stress</li> <li>➤ Glen mechanism</li> <li>➤ Darcian flow at the base of the ice dam</li> </ul>
Drainage of an intraglacial cavity	<ul style="list-style-type: none"> <li>➤ Englacial rupture of a water-filled vault</li> <li>➤ Hydraulic tapping of a meltwater reservoir by intraglacial drainage</li> <li>➤ Enhanced glacier sliding close to the ice dam, leading to mechanical rupture of the dam base</li> <li>➤ Sudden input of meltwater to the glacier bed via crevasses and moulins</li> </ul>
Meltwater release during surge termination	<ul style="list-style-type: none"> <li>➤ Disruption of distributed subglacial drainage by the re-establishment of channelized subglacial drainage, resulting in the sudden evacuation of stored meltwater</li> </ul>

**Table 2.1 Mechanisms involved in jökulhlaup generation and their possible triggers (Walder and Costa, 1996, Tweed and Russell, 1999, Roberts et al., 2005, Duller, 2007).**

Flood discharge hydrographs characterise the release of the impounded water over time, which may range from hours to months based on whether the water is drained rapidly or slowly, respectively. In effect, the shape of a flood hydrograph conveys the morphology

and gradient of the flood route way (Maizels, 1997). A typical jökulhlaup hydrograph is characterised by a gradual rising limb followed by a rapid recession limb indicating a gradual expansion of the sub- or englacial conduit until the reservoir has been drained (Figure 2.14a), while irregularities in the hydrograph may reflect conduit constrictions, ice jams or complex routing paths (Maizels, 1997, Björnsson, 1998, Roberts et al., 2005). In contrast, Figure 2.14b presents a linearly rising hydrograph similar to that of the 1996 Skeiðarárhlaup, formed as a result of conduit enlargement due to frictional heat that increased the carrying capacity (Roberts et al., 2000, Carrivick, 2004). Numerous factors may affect a hydrograph, and they may not be immediately obvious. The increased hydrostatic pressure generated during a jökulhlaup, for example, may result in the retro-filling of ice-marginal basins by temporary lakes that may also affect the flood hydrograph (Roberts et al., 2003).

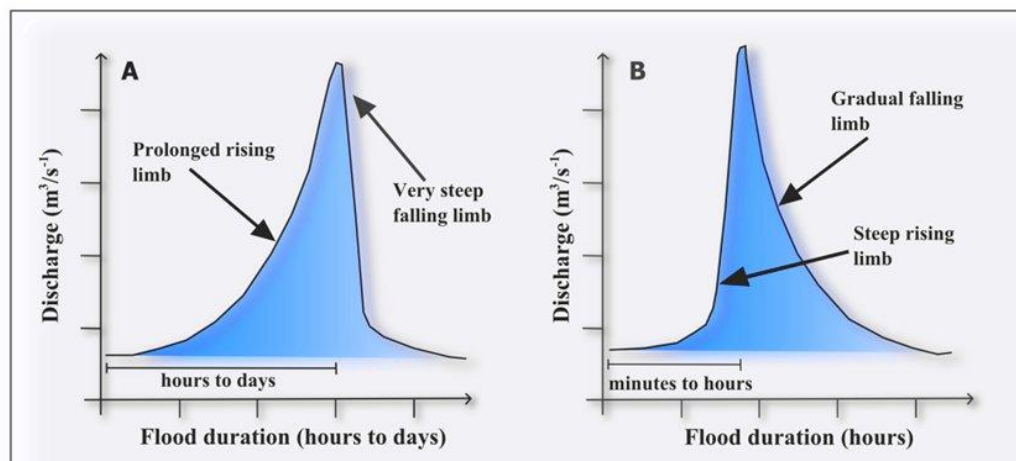


**Figure 2.14** Two common types of hydrograph shape: (a) an exponentially rising limb followed by a steep falling limb, typically associated with tunnel drainage through the progressive enlargement of an ice-tunnel; (b) a linearly rising limb often associated with the emptying of a subglacial reservoir, such as outburst floods frequently associated with a subglacial volcanic eruption. Modified from Walder and Costa (1996) and Duller (2007).

### 2.3.3 *Jökulhlaups: routing*

While early theories suggested that jökulhlaups discharged from pre-existing outlets across the glacier margin that remained stationary during flooding events, recent observations have demonstrated that internal routing may be far more complex. Under a steady-state regime, water is typically routed to the glacier bed via crevasses and moulins (Hooke, 1989, Fountain and Walder, 1998) to form an upwards-branching arborescent network (Shreve, 1972), or ‘R-channels’ (Fountain and Walder, 1998). During flooding events, drainage may occur either slowly and at low pressure as conduits slowly expand over days or weeks due to the release of frictional heating by flowing water or rapidly as a result of ice dam failure as observed at Vatnajökull, Iceland (Björnsson, 2009). During



large, linearly-rising flooding episodes, the capacity of pre-existing conduits may be overwhelmed by the influx of floodwaters, resulting in the development of a linked cavity system (Roberts et al., 2000) and in the formation of new outlets (supra-, en- and subglacial) that may vary both spatially and temporally across the margin as observed during the 1996 jökulhlaup event at Skeiðarárjökull (Roberts et al., 2001).

A single flooding event may display a wide range of flow conditions, possessing both a 'surge' phase characterised by a turbulent, hyperconcentrated flow, and more fluid pre-, inter-, and post-surge flows. As the rheology of the flow is dependent upon both sediment availability and concentration, this may also serve to control the hydraulics and flow regime of the jökulhlaup, directly affecting the sedimentology of the resulting deposits (Maizels, 1997). Numerous other factors that may affect jökulhlaups and their deposits are presented in Figure 2.15 and explored in depth by Maizels (1991, 1997).

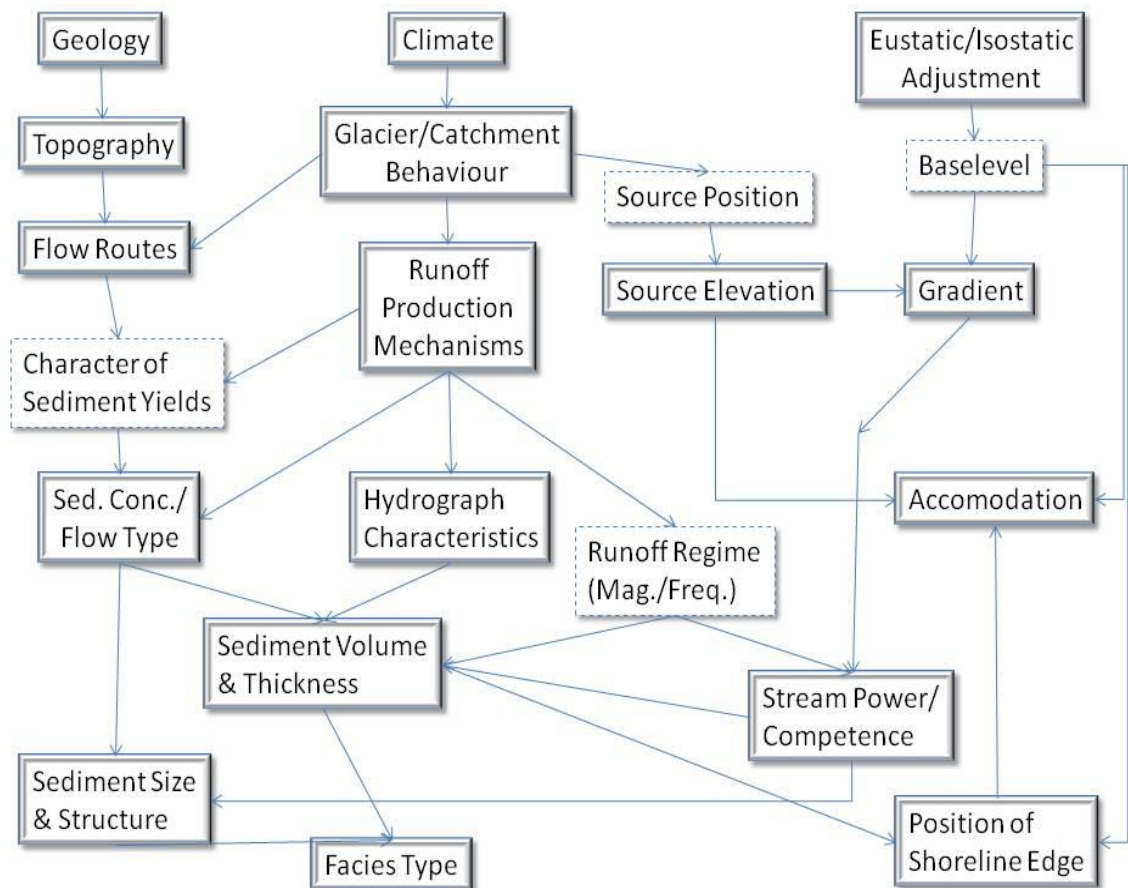


**Figure 2.15 Model depicting the numerous factors that control flow and sediment characteristics of jökulhlaup floods (Maizels, 1997).**

#### 2.3.4 *Jökulhlaups: landforms and controls*

While it is beyond the scope of this project to present all of the landforms produced by jökulhlaups that may occur in a variety of different settings, the following section describes meso- and macro-scale jökulhlaup-related landforms associated with unconfined, sandur landsystems generated by volcanogenic and glaciolimnic jökulhlaups. In the proglacial landsystem models described by Maizels (1997), sandur deposits were divided into three regimes: normal, ‘classic sandur’ outwash (Type I: non-jökulhlaup), characterised by braided streams and gravel bars (Churski, 1973); limno-glacial (Type II: ice-dammed jökulhlaups), characterised by boulder fields, pavements, chute channels, kettles and obstacle marks; and volcanogenic jökulhlaups (Type III) containing rimmed kettle holes, debris lobes/fans, boulder fields, incised channels and large ripples and gravel dunes.

Recent observations of material deposited supra- and englacially during jökulhlaups must be incorporated in order to compile a comprehensive landsystem model. The following section briefly presents features that may be indicative of past jökulhlaups by dividing the sandur into two generalised zones (Table 2.2): Zone 1 includes features formed sub-, en- and supraglacially during a jökulhlaup and later exposed by retreat; Zone 2 includes features deposited in the proximal sandur and distal sandur. Further details of many of these features are discussed in Chapter 3.

<i>Zone 1: Supra-, en- and subglacial landforms</i>	Fracture fills and crevasse-cast ridges (Roberts et al., 2000, Munro-Stasiuk et al., 2008)
	Subglacial canals (Russell, 2003) and tunnel channels (Clayton et al., 1999, Hooke and Jennings, 2006, Russell et al., 2007) (may also be associated with sinuous, rounded hills/drumlins (Clayton et al., 1999, Johnson, 1999))
	Conduit fills (eskers) (Brennand, 2000, Burke et al., 2008, Burke et al., 2009)
	Embayments/ice-walled canyons (Roberts et al., 2000, Russell et al., 2001b)
	Drumlins (Shaw, 1983, Shaw and Kvill, 1989, Johnson, 1999, Waller et al., 2008)

<i>Zone 2: Proglacial landforms</i>	Sandur, braided streams and bars (Krigström, 1962, Maizels, 1991, Maizels, 1997)
	Alluvial fans (Russell and Knudsen, 2002)
	Kettle holes and obstacle marks and ice blocks (Russell, 1993, Maizels, 1997, Russell et al., 2001b)
	Gravel dunes/anti-dunes (Rudoy and Baker, 1993, Carling, 1996, Carling, 1999)
	Terraces, incised active and inactive channels (Marren, 2002b)
	Expansion and pendant bars (Baker, 1984, Maizels, 1997)
	Chutes and lobes (Baker, 1973)
	Streamlined erosion bars, hills (Maizels, 1997)
	Scours, plunge pools and potholes (Baker, 1973)

**Table 2.2 Summary of jökulhlaup-related landforms.**

### **Zone 1**

Landforms emplaced within Zone 1 may vary across the glacier short periods of time and distance as a result of an increase in effective pressure (Roberts et al., 2000, Russell et al., 2007). Jökulhlaups with a rapid rate of discharge increase may impose temporary drainage circuits through the glacier, resulting in a variety of locations and morphologies of the outlets. These rapid increases in discharge may generate basal hydraulic pressures in excess of ice overburden, forcing floodwaters through to the surface of the glacier (Roberts et al., 2000). Hydraulic jacking may result in the formation of fractures and hydrofracturing. High porewater pressure within a confined gravel aquifer during a jökulhlaup, for instance, may result in the fracturing of the overlying till (Figure 2.16) (Rijsdijk et al., 1999). Water flowing into this fracture may fluidise the gravel and eject them into the overlying diamict and/or overlying ice, resulting in the formation of fracture fills (Boulton and Caban, 1995, van der Meer, 1998, Rijsdijk et al., 1999, Le Heron and Etienne, 2005, Kjaer et al., 2006). The resulting erosion of the diamicton unit and the glacier bed reduces pressure, and the jökulhlaup flow may then evolve from a complex fracture-fill network to conduit flow, ceasing as large, ice-roofed channels develop (Piotrowski, 1997, Sjogren et al., 2002, Russell et al., 2007). It has been suggested that

these landforms may be a diagnostic signature of high-magnitude jökulhlaups (Roberts et al., 2001, Russell, 2003, Munro-Stasiuk et al., 2008).

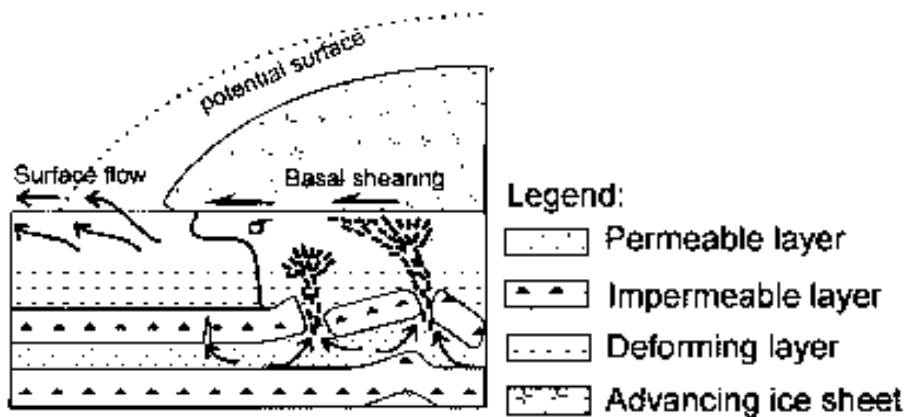


**Figure 2.16** Model for the formation of upward infilled hydrofractures beneath an ice sheet (Rijsdijk et al., 1999).

A large, single-event, englacial esker connected to a supraglacial, ice-walled canyon fill (Russell et al., 2006, Burke et al., 2008) has also been suggested to be emplaced by a single large flooding event. Furthermore, tunnel channels and drumlins have also been linked to jökulhlaups (Clayton et al., 1999, Hooke and Jennings, 2006, Russell et al., 2007); however, further research needs to be conducted to determine if these landforms, whether taken singly or as a collective suite, are diagnostic of jökulhlaups or if they may be generated by other mechanisms. Additionally, features in Zone 1 may be subject to alteration during glacial retreat, both in the short term ( $10^1$  years) and in the long term ( $10^2 - 10^3$  years), further affecting the usefulness of landforms as signatures (see 'Post-depositional modification' section). These sub-, en- and supraglacial landforms are discussed in greater detail in Chapter 3.

## Zone 2

The largest feature emplaced within Zone 2 is the sandur itself; the topography of the jökulhlaup route-ways may have a major impact on the resulting sandur deposits (Maizels, 1997). Confined sandur plains, for example, may result in increased flow depth, shear stress, flood power and erosive capacities, while unconfined outwash plains are characterised by flow depths and erosional capacities that rapidly decrease downstream (Maizels, 1997). High-energy zones of flood landforms may include erosional gorges, scoured bedrock, spillways and cataracts, while low-energy zones may include depositional landforms that include valley fills, bars and slackwater deposits (Maizels, 1997). When confined to narrow valleys, 'super rivers' may develop, capable of emplacing giant ripples over 10 m high and bars more than 200 m+ high and between 2-5

km in length (Rudoy and Baker, 1993). It is recognised, however, that even lower-magnitude floods are capable of producing landforms similar to those created during mega-floods if topographic constrictions and high relief due to bedrock topography are present (Carrivick, 2004, Carrivick, 2006, Carrivick, 2007) or as a result of confining outlets of glacier ice at over-deepenings (Cassidy et al., 2003). Russell et al. (2001b) determined that the geometry of a supraglacial, ice-walled channel system acted as a major control on the resulting sedimentology and morphology of the resulting jökulhlaup deposits as a result of the spatial variability of the flow conditions, similar to a bedrock-confined fluvial system (Baker, 1984, Baker and Kochel, 1988).

The position of the glacier margin may also play a key role in determining the impact of a jökulhlaup, as the presence or absence of an ice-marginal depression may act as a major control on depositional and erosional processes during high-magnitude jökulhlaups (Figure 2.17) (Gomez et al., 2002). When decoupled from the sandur, floodwaters may collect within the depression before exiting through point-sources, in contrast to the coupled model characterised by a diffuse, multipoint system where sediment and water are able to shift freely across the proximal sandur over time. Retreat of the glacier margin, as discussed in the previous section, may also result in rapid incision and terrace formation (Marren, 2002b).

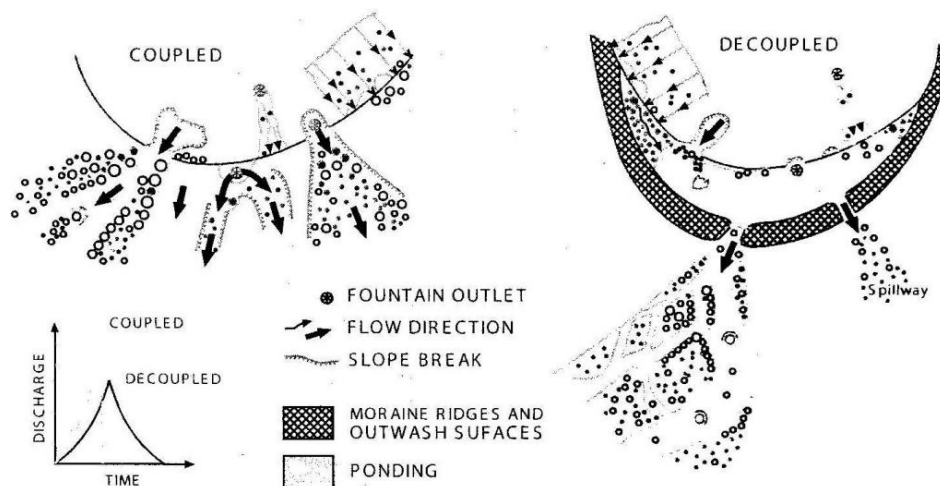


**Figure 2.17 Coupled vs. decoupled scenarios for routing of jökulhlaup discharge. Inset demonstrates the effects of meltwater ponding in the proglacial zone on the flood hydrograph (Gomez et al., 2002).**

The morphological impact of a jökulhlaup may be highly varied as different outlets may display unique activity during different phases of a single flooding event (Russell and Knudsen, 2002). For example, the rising phase of a flood is often contemporaneous with

the development of conduits and fan deposition, while the waning stage is commonly characterised by fan dissection and the exhumation of ice blocks.

Ice blocks themselves have been used as indicators of flood magnitude, as the depth of kettle holes may be used to indicate the minimum thickness of flood deposits (Russell, 1993, Fay, 2002). The presence of ice blocks, while long associated with outburst floods (Klimek, 1972, Klimek, 1973, Galon, 1973a, Galon, 1973b, Churski, 1973, Boothroyd and Nummedal, 1978, Maizels, 1992, Maizels, 1997), may also provide insight into flood behaviour and magnitude (Fay, 2002, Russell et al., 2006). Circular kettles are formed during the rising stage when ice blocks are completely buried, while obstacle marks may develop around partially-buried blocks during both rising and waning stages (Figure 2.18) (Russell and Knudsen, 2002). Both of these features are easily spotted on aerial photographs; however, as discussed in the previous section, ice blocks may be emplaced during floods associated with surge termination, and floods generated by varied mechanisms may occur at the same site. It is, therefore, important to consider all landforms when linking them to individual past events, or even portions of events as presented in the following section.

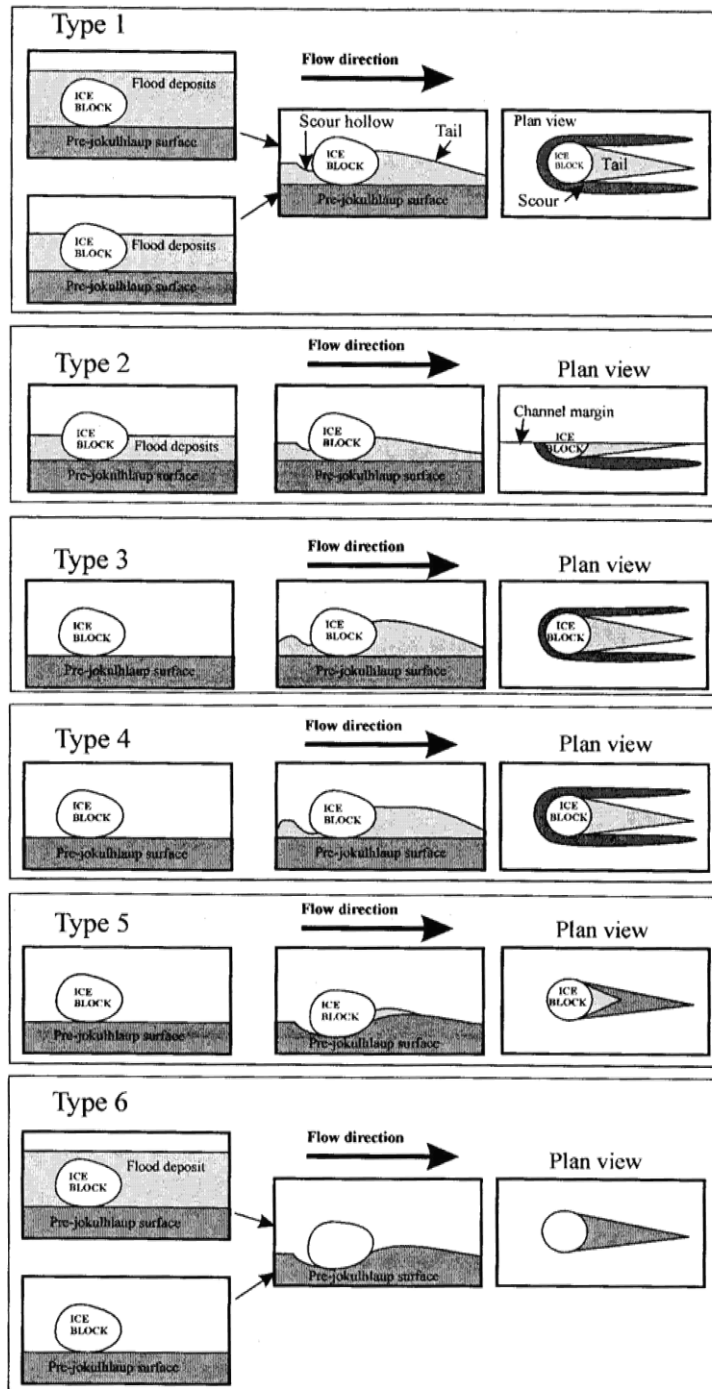


**Figure 2.18 Kettle hole obstacle/scour mark genesis.** Type 1: partial or total burial and subsequent exhumation of block results in kettle scours with both proximal and lateral scour and tail. Type 2: partial exhumation of partially buried ice blocks on margins of main channels results in semi circular obstacle marks. Types 3 and 4: obstacle marks with proximal and lateral scour crescent, a ridge stoss-side of the scour crescent and a large, anti-clinal aggradational tail. Type 5: obstacle marks <5 m in diameter with fine-grained gravel in the immediate lee of the scour hollow and coarse gravel lag characterising the distal part of the tail. Formed by waning stage deposition, followed by late waning stage erosion. Type 6: erosional obstacle marks formed by total exhumation of buried ice blocks or by scour around ice blocks grounded by the late waning stage (Russell et al., 2006).

### 2.3.5 Jökulhlaups: summary

In summary, several diagnostic landforms and sedimentary sequences are emplaced during jökulhlaups, although researchers caution that it may be difficult to correlate all

landforms to every initiation mechanism. The type, size and character of jökulhlaup deposits depend on a wide variety of factors, including routing, frequency, sediment availability and flow rheology, sub- and englacial topography and proglacial conditions. Individual landforms may be emplaced during distinct phases of a flood and provide lower limits of the amount of material deposited and the flood magnitude. Recent research has demonstrated that the spatial and temporal emplacement of landforms and deposits may vary considerably during a single event. Landforms may be emplaced sub-, en- and supraglacially during a flood, and these may be exposed later by glacier retreat. When taken in conjunction with landforms emplaced in the proglacial region, these features may be indicative of large-scale, low-frequency events.

## **2.4 Post-depositional modification: buried ice, collapse areas and en/subglacial meltout features**

### **2.4.1 *Introduction***

Relatively few long-term, qualitative studies of dead ice melt and their resulting landforms have been performed (Østrem, 1959, Clayton and Moran, 1974, Johnson, 1992b, Krüger and Kjær, 2000, Russell and Knudsen, 2002, Nicholson and Benn, 2006, Schomacker et al., 2006, Schomacker and Kjær, 2008). While hummocky fields of dead ice moraines (Boulton, 1972, Eyles, 1979, Krüger, 1997, Glasser and Hambrey, 2002, Spedding and Evans, 2002, Kjaer et al., 2006, Schomacker et al., 2006), as well as large depressions/collapse structures (Fleisher, 1986), are commonly interpreted to be the end result of buried masses of dead ice, few models encompass the full evolution of ice-cored landforms from emplacement to final meltout (Boulton, 1967, Schomacker et al., 2006, Waller et al., 2008). As a wide variety of emplacement mechanisms and localised factors may affect the final appearance of an ice-cored landform, this section presents a brief overview of a few of the large-scale processes that may emplace sub-, en- or supraglacial material upon, within or beneath ice and how these processes may impact both the rate of melt and appearance of the final landform. Specific parameters and hypotheses affecting macro-scale landforms (hummock fields, moraines and large buried bodies), as well as meso-scale features (kettle holes, ice-cored drumlins) specific to the field area, are described in detail in Chapters 3 and 7. The roles of other meltout features, such as the deformation of conduits and fracture fills, are addressed in the context of surges and jökulhlaup events within their respective chapters (Chapters 5 and 6).

Numerous studies have noted that even a thin layer ( $> 0.01$  m) of debris covering glacier ice can provide sufficient insulation to retard the ablation process (Figure 2.19) (Lister,



1953, Østrem, 1959, Nakawo and Young, 1981, Nicholson and Benn, 2006, Reid and Brock, 2010). Depending on the thickness of this debris layer, climatic conditions and the proximity of lakes or geothermal heat, buried ice may persist for extended periods exceeding decades or even centuries; studies of large bodies of buried ice around the globe under a variety of different conditions and climates have demonstrated that such masses may persist under a few metres of debris for periods ranging from hundreds to thousands of years in temperate to sub-arctic conditions (Østrem, 1961, Clayton, 1964, Boulton, 1972, Eyles, 1979, Driscoll, 1980, Krüger and Kjær, 2000, Spedding and Evans, 2002, Schomacker and Kjær, 2008). In Arctic environments, such as Greenland and Siberia, ice has persisted for more than 40,000 years (Astakhov and Isayeva, 1988, Houmark-Nielsen et al., 1994).

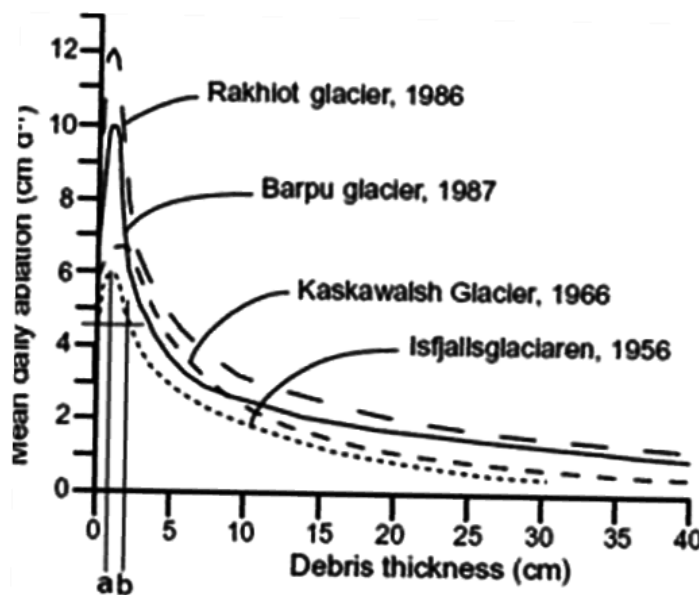


**Figure 2.19** Collection of ablation studies conducted at different glaciers, where *a* is the thickness of maximum ablation, *b* is the thickness where ablation rates begins to decrease (Nicholson and Benn, 2006) based on Østrem's estimation of the effects of thin layer of debris on ablation rates (1959).

Two generalised models of large buried ice bodies and their subsequent modification as a result of melt-out are shown in Figure 2.20. Price (1969) depicts the deposition of material on a retreating glacier margin, leading to the formation of kame and kettle topography. Others have examined the resulting morphology following the meltout of individual large bodies of ice (Fleisher, 1986), as well as the evolution of kettle holes formed by a wide range of ice blocks under different burial conditions as seen in Figure 2.21 and Figure 2.22 (Maizels, 1992, Olszewski and Weckwerth, 1998).

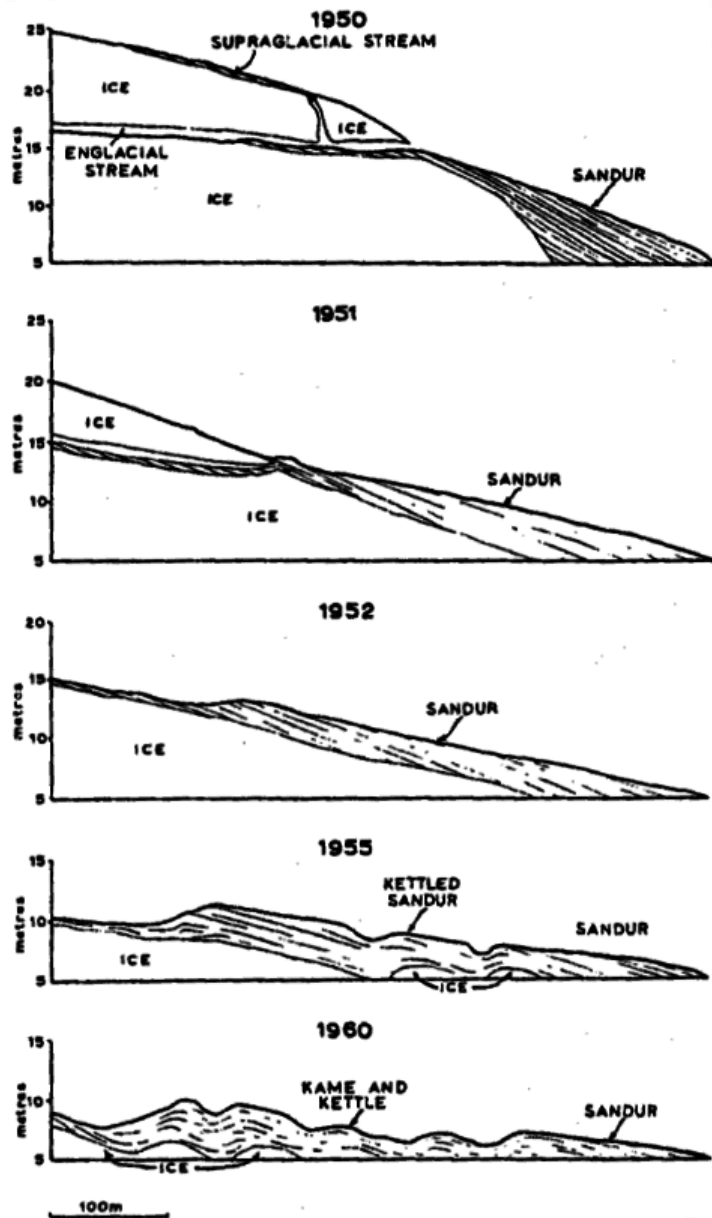


Figure 2.20. Simplified model depicting the evolution of stagnation topography following glacial retreat (Price, 1969).

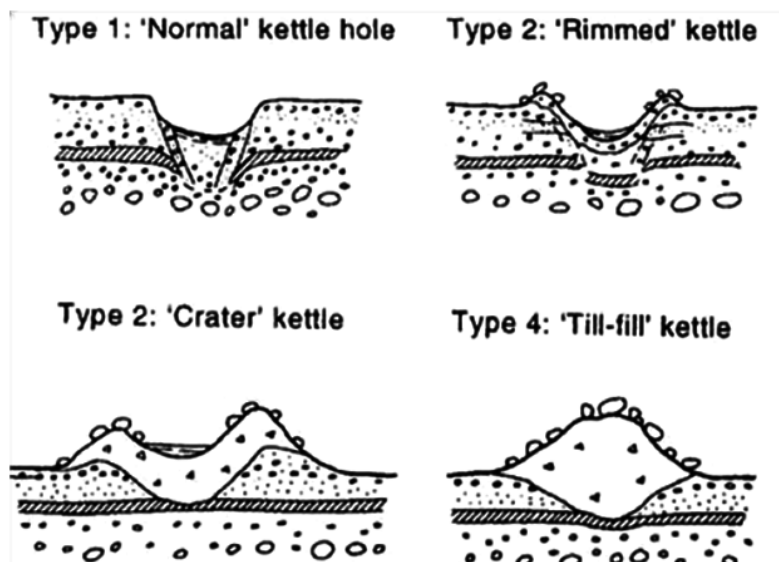


Figure 2.21 Classification of jökulhlaup-related kettle holes, based on debris content of the original ice blocks. After Maizels (1992).

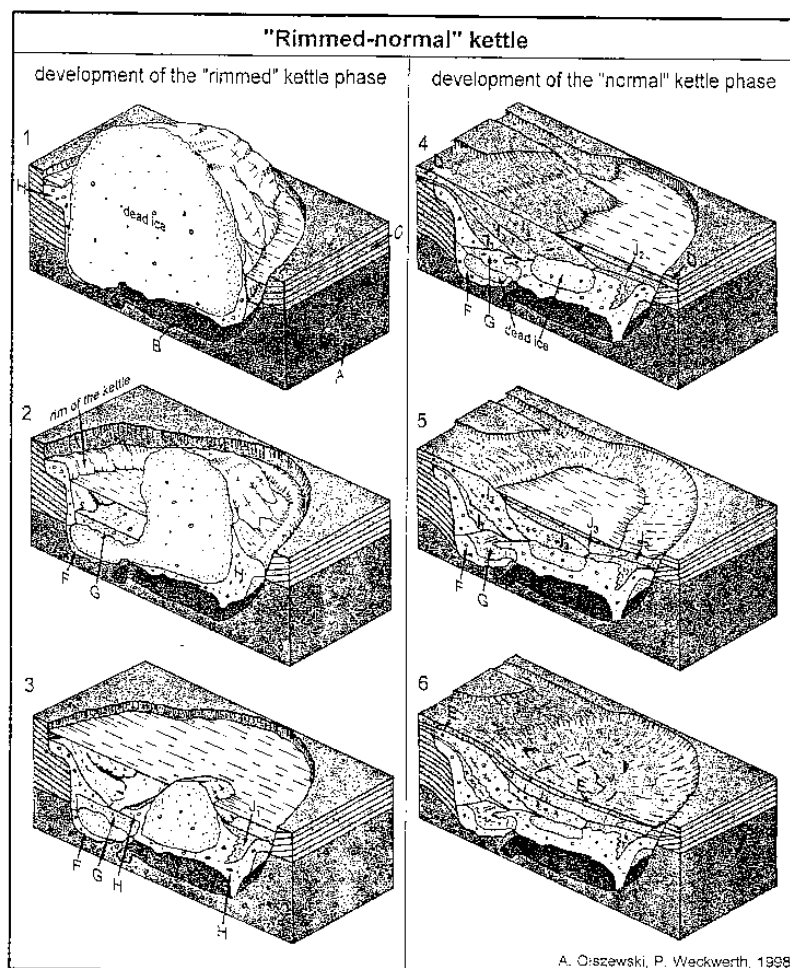


Figure 2.22 Stages of evolution of a rimmed-normal kettle following the emplacement, and gradual burial, of a block of ice. Modelled after observations at the Höfðabrekkujökull forefield, Mýrdalssandur, Iceland. A-G are individual facies observed around ice block (Olszewski and Weckwerth, 1998).

However, these diagrams simplify a process that is dependent upon numerous factors that may include local conditions, such as climate (precipitation, humidity, aeolian processes), the presence of groundwater or geothermal heat, topographic constrictions, mass movement and degree of solar exposure (Schomacker, 2008). The proximity of proglacial lakes may also increase melting rates due to active wasting processes such as calving, and also may act as heat reservoirs year-round; lakes may also act as settling basins, increasing the erosive capacity of meltwater streams that may incise the region, removing debris and exposing more ice (Driscoll, 1980, Stokes et al., 2007). The ice itself may contain debris that when melted further insulates the ice and may act to prevent additional thawing (French and Harry, 1990). While these authors have provided observations and assumptions of ice bodies in their localised regions, few have attempted to correlate the processes of the emplacement of these bodies with their subsequent pattern, and rate, of secondary modification.

#### 2.4.2 *Emplacement*

The formation and subsequent preservation of ice-cored terrain are determined by fluctuations in the terminus and velocity of a glacier, responses to changes in mass balance and ice flow, combined with the volume and mechanism of debris supplied to the surface of the glacier (Johnson, 1992a). The emplacement of this debris upon the ice surface itself may occur through a variety of mechanisms, including avalanching or rock falls from nunataks and mountain sides (Andre, 1990, Hambrey, 1999, Glasser and Hambrey, 2002, Schomacker, 2008), supraglacial crevasse-squeezing (Johnson, 1971, Sharp, 1985a, Sharp, 1985b), the deposition of material via aeolian processes (Krüger and Aber, 1999), bursts of meltwater through glacier conduits and crevasse systems (Näslund and Hassinen, 1996, Krüger and Aber, 1999, Russell and Knudsen, 2002, Roberts et al., 2000), channel and tunnel fill material (Fitzsimons, 1991, Kirkbride and Spedding, 1996), the melting out of debris bands (Sharp, 1949, Boulton, 1967, Kirkbride and Spedding, 1996, Hambrey, 1999) as well as through the thrusting of subglacial material (Huddart and Hambrey, 1996, Hambrey, 1999, Krüger and Aber, 1999, Glasser and Hambrey, 2002). Although typically limited to regions with permafrost conditions, segregation injection, or segregated ice, may also occur when groundwater or basal ice freezes within a zone of porous gravels or sands under pressure at the glacier snout (French and Harry, 1990).

Other factors may play a role in isolating and burying large bodies of ice. Following retreat, large blocks of ice may become detached and partially or totally buried by

outwash (Ahlmann, 1938). Topographic conditions may result in the detachment of ice lobes where glacier flow is restricted across headward divides or along deeply incised valley meanders (Fleisher, 1986). The melting of these large, detached ice blocks may provide accommodation space for continued sediment accumulation as shown in Figure 2.20 and may create sediment sinks that are recognizable in the stratigraphic record and large-scale depressions that may be observed in air photographs. Similarly, climatic forcing may decouple the debris-laden glacier snout from the main body of the glacier (Stokes et al., 2007). This increase in debris cover may also be accompanied by a gradual migration of existing debris cover up-glacier, the resulting thinning and shrinkage of glacier ice increasing the likelihood of slope failure adjacent to the glacier, leading to the accumulation of more debris (Stokes et al., 2007). While shearing experienced during surges may emplace large volumes of debris and moraines, the shearing process itself may expose the moraine's ice-core, which may hasten melt (Johnson, 1971, Clapperton, 1975), demonstrating the potential complexity involved in a process as 'simple' as melting ice.

#### 2.4.3 *Meltout: primary and secondary*

It has been observed that the meltout process consists of two stages (Lister, 1953) in which the main mass first disintegrates into smaller, isolated blocks (primary), creating a 'thermokarst terrain' (Astakhov and Isayeva, 1988, Everest and Bradwell, 2003); these isolated blocks ultimately melt completely, often at a much slower rate (secondary). Following internment, buried ice masses under humid, sub-polar conditions are most commonly subject to down-wasting and back-wasting mechanisms (Figure 2.23) (Krüger and Kjær, 2000, Kjær et al., 2006). Down-wasting describes the process of ice mass thinning by melting along its top and bottom, while back-wasting describes the lateral retreat of slopes and ice core walls via slumping and sliding of debris, meltwater erosion (sapping), gully debris flows and stagnant ice bursts that occur when large volumes of water, trapped between ice and a fine sand or clay, are suddenly released (Johnson, 1971, McKenzie, 1969, Krüger and Kjær, 2000). Gravity is an important force that affects the re-sedimentation of material during melting (Sharp, 1949, Boulton, 1968), as well the presence of water which, through liquefaction, reduces the shear strength of debris covering the ice (Benn and Evans, 1998, Schomacker, 2008, Schomacker and Kjær, 2008, Woodward et al., 2008). Drainage through ice-cored terrain may develop via unstable subsurface conduits that develop through thermal erosion and percolation of meltwater. Whether water is delivered via these conduits, through groundwater or

precipitation, mudflows are common in this terrain, and the movement exposes more surface area and further melting (Johnson, 1992a).

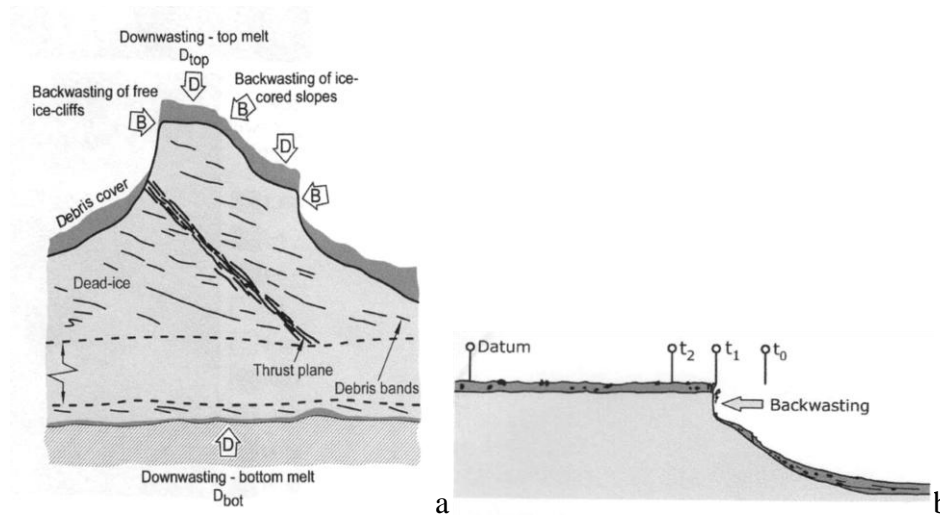


**Figure 2.23 a) Back and downwasting processes in ice cored moraines, b) and measuring backwasting in the field (Schomacker, 2008).**

As a result of these processes, the ice mass eventually disintegrates into discrete blocks that become buried by re-sedimentation, slowing the rate of melt and allowing only for down-wasting processes to occur. Regions with high levels of precipitation, however, may serve to rework the overburden via overland flow and avulsion. This reworking may expose the ice core and accelerate the rate of melt during the secondary alteration phase (Krüger and Kjær, 2000). Rainwater also has the ability to infiltrate the insulating layer of debris and transfer heat to the ice below (McKenzie, 1969). Some features that experience alteration following emplacement produce recognisable landforms, such as crevasse-cast ridges, at least in the short term, while other features may become completely unrecognisable from their original form (Figure 1.3). Figure 2.24 demonstrates another example, that of the transition of high angle debris bands within glacier ice into the final form of low-relief, hummocky topography.

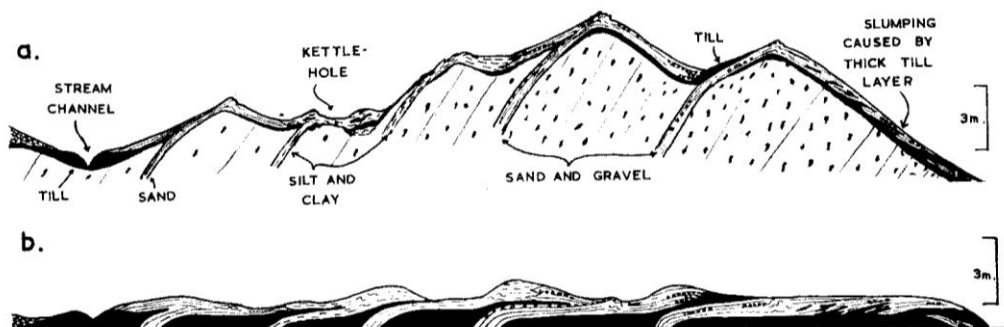


**Figure 2.24 Formation of low-relief hummocky topography due to melting of high angle debris bands (Boulton, 1967) illustrating before (a) and after (b) meltout.**

#### 2.4.4 *Quantification of melt rate*

The numerous factors involved in measuring the rate of melt in a buried ice body are shown in Figure 2.23 (Schomacker, 2008), in this case an ice-cored moraine, that is subject to both back-wasting and down-wasting. In permafrost regions, downwasting due to bottom melt is negligible, and the total amount of downwasting ( $D_{tot}$ ) can be measured by simply surveying the vertical lowering of the features to obtain the top melt ( $D_{top}$ ) (Krüger and Kjær, 2000). Similarly, back-wasting can be surveyed by marking the retreat of an ice face compared to a fixed point (Figure 2.23b). Benn and Evans (2008) proposed the following equation, assuming that other factors are constant, to capture down-wasting rates:

$$(h): D_{top} = k_d * T_0 / (h * L * \rho_{id})$$

##### **Equation 2.1**

Where top melt ( $D_{top}$ ) declines exponentially with the thickness of debris cover ( $h$ ),  $k_d$  is the thermal conductivity of the debris,  $T_0$  the surface temperature of the debris,  $L$  is the latent heat of fusion of the ice, and  $\rho_{id}$  is the density of the ice with debris (Benn and Evans, 1998, Schomacker, 2008). This equation attempts to encompass the effects of porosity, grain size distribution and water content on the ablation rate through  $k_d$ , where  $T_0$  accounts for the temperature (climate).

While DEMs are the most practical means of measuring melting rates in various locations, since climate is not the only factor involved, direct comparisons are difficult. Often, particularly in inaccessible regions, or in historical photographs, there is no method of determining porosity, debris content, debris cover, water table levels etc. For the purposes of this study, however, most of these parameters are unknown; the equations are presented to illustrate the complexities of attempting to average the rate of melt of buried bodies.

#### 2.4.5 *Summary of buried ice*

In summary, even in temperate, humid climates, relatively thin layers of debris may reduce the rate of ablation, preserving bodies of ice for years, decades or centuries. The mechanism responsible for their formation, whether the ice is transported in blocks during outburst floods, deposited during surging or rapid ice advance and left behind by glacier retreat, or buried by flood or gradual deposition, plays a vital role in the volume of ice deposited as well as the volume of material that covers, and protects the ice, resulting in varying rates of modification. Studies recognize that secondary modification may

proceed at two rates: the first, and most rapid, as primary melting following emplacement and the second, and longest, when the ice mass has been melted into smaller, discrete blocks. Other factors, such as margin position, climate, geothermal heat, the presence of lakes and groundwater levels as well as the type of sediment, debris content of the ice and erosional processes may also affect the rate of melt. Further work needs to generate a comprehensive model that captures how micro- and mesoscale landforms are modified during these two stages, and takes into account the additional secondary modification occurring at a regional scale at a retreating ice front, as the terrain upon which these landforms are emplaced may itself be experiencing these two stages of melt as well.

## **2.5 Summary of large-scale processes**

While numerous factors may contribute to the behaviour of a glacier and the resulting nature of the resulting landsystems, three major large-scale processes have been identified in the literature: glacier margin fluctuations, jökulhlaups and post-depositional modification as a result of ice melt. Fluctuations in glacier margin position play an important role in the development of drainage, depositional processes and persistence of landforms. Similarly both surges and large-scale outburst floods may deposit large volumes of material on the sandur, drastically altering the character of the landscape. Deposits from such events may display remarkable variability during an individual event, allowing spatio-temporal reconstruction from examining the resulting landforms. However, researchers caution that it may be difficult to absolutely ascribe a ‘diagnostic’ landform, as some may be the result of other processes. Surges, for example, may emplace push moraines, alluvial fans, and exhibit shearing, but these may also be found at non-surging glaciers.

Relatively thin layers of debris may also reduce the ablation rate, preserving bodies of ice for years, decades or centuries. This insulation may proceed at two different rates: the first, and most rapid, as primary melting following emplacement and the second, and longest, occurs when the ice mass has been isolated into smaller, discrete blocks. Most of these studies have only examined features at glaciers during or immediately following specific events. It is important to consider the long-term impact of erosion and meltout in order to model how diagnostic signatures are altered and what role these processes play in the overall evolution of the proglacial terrain, when the glacier margin is coupled to, or decoupled from, the sandur.



The literature presented in this chapter contains numerous landform models of these three large-scale processes in the literature that have been developed based on the observations of temperate glaciers both in Iceland and around the world. Several models have been repeatedly tested at numerous sites and are widely-accepted in relating process to form such as landforms associated with margin retreat (such as the development of proglacial lakes, exposure of subglacial landforms and development of ‘dead ice’ fields) or those associated with jökulhlaups (outwash fans and kettle holes, for example). Other processes, particularly those dealing with sub- and englacial drainage models (such as surges and jökulhlaup routing) have been developed within the last decade, however, and have been the subject of debate. Similarly, hypotheses regarding the role of these processes on the evolution of the sandur have also been contested. Chapter 3 examines landsystem models and hypotheses developed specifically at Skeiðarárjökull in greater detail.



## **Chapter 3 Literature review: large-scale processes and landforms at Skeiðarársandur**

---

*This chapter examines large-scale processes active at within, beneath, upon and proximal to Skeiðarárjökull and their subsequent impact on Skeiðarársandur. Large-scale processes documented in the literature at Skeiðarársandur including margin fluctuations, jökulhlaups, and meltout are presented and diagnostic landforms are identified.*

---

### **3.1 Introduction**

This chapter examines landforms and assemblages observed at Skeiðarársandur and expands upon the features and models presented in Chapter 2. Recent documented events and their processes are explored in detail, and hypotheses that test or refute these models are presented. Subsequent chapters will attempt to test/refute these hypotheses by a rigorous examination of landforms and models generated from historical reconstructions and present day observations at Skeiðarárjökull. The following sections explore the processes active during large-scale events at Skeiðarárjökull, including margin fluctuations, jökulhlaups, and large-scale ice meltout.

### **3.2 Margin fluctuations at Skeiðarárjökull: surges and retreat**

#### **3.2.1 Introduction**

The changing position of Skeiðarárjökull's margin over time (1904, 1945 and 1997-98) as well as its position relative to the subglacial topography as captured with radio echo soundings (Björnsson, 1999) is shown in Figure 3.1. The associated lowering of the ice surface during frontal retreat has been seen as playing a key role in the development of the glacio-fluvial system (Price, 1969, Churski, 1973, Björnsson, 1999). Overall, periods

of quiescence and retreat at Skeiðarárjökull over the 20<sup>th</sup> century has resulted in the development of entrenched channels, large regions of hummocks, dead ice and proglacial lakes (Boulton, 1967, Bogacki, 1973, Churski, 1973, Galon, 1973a, Jewtuchowicz, 1973, Klimek, 1973, Wojcik, 1973a, Thompson, 1988, Marren, 2002b). Active periods of advance, namely the two observed surges at Skeiðarárjökull have modified the proglacial terrain through the release of large volumes of meltwater and sediment and the emplacement of numerous evenly-spaced alluvial fans and braided streams and emplaced thrust blocks and ‘hanging’ outlets (Rist, 1955, Russell et al., 2001a, van Dijk, 2002). As the associated lowering of the ice surface during frontal retreat has been seen as playing a key role on the development of the glacio-fluvial system (Price, 1969, Churski, 1973, Björnsson, 1999), the following section examines recent fluctuations of Skeiðarárjökull, their impact on deposits and proposed diagnostic landforms.

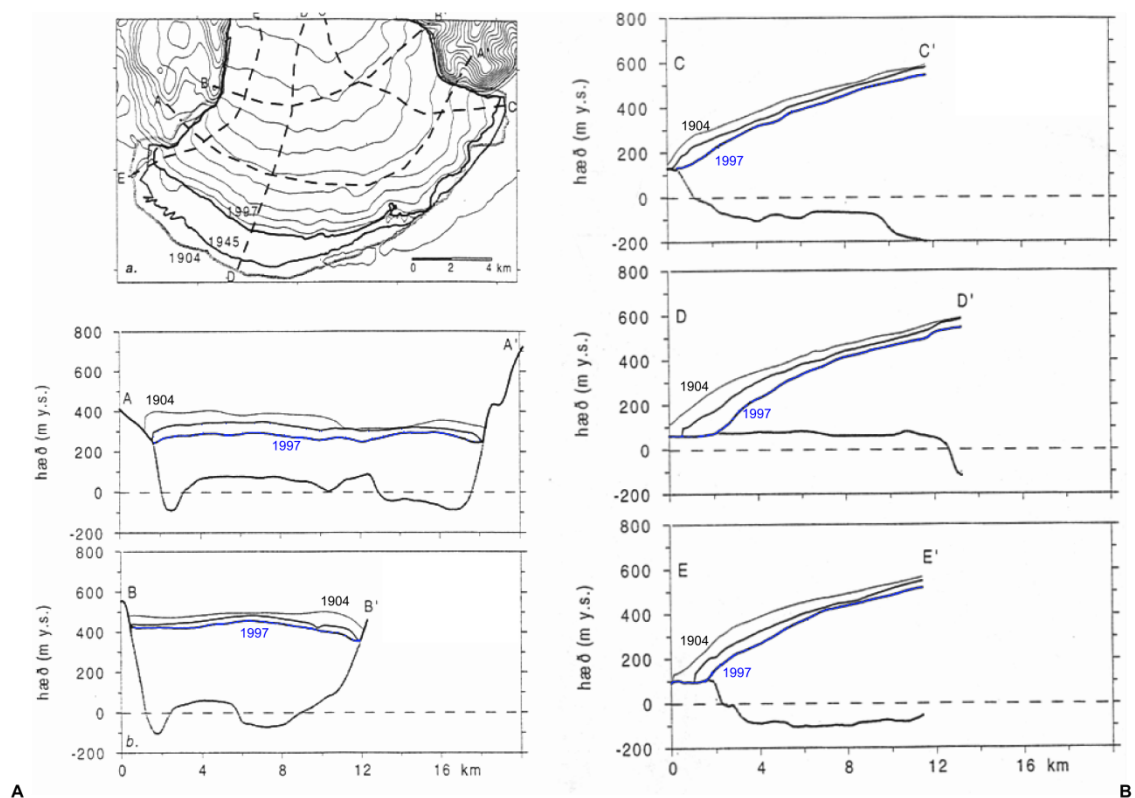


**Figure 3.1** Radio echo soundings of Skeiðarárjökull (Björnsson, 1999). a) profiles taken across the glacier’s width reveal subglacial ‘channels’ while b) depicts profiles taken at the western (C-C’), central (D-D’) and eastern (E-E’) reveal the position of the underlying, over-deepened slopes beneath the glacier ice.

### 3.2.2 Surges

Surges at Skeiðarárjökull have been documented for over two hundred years: the western lobe surged four times at increasing intervals of 25-118 years between 1787 and 1991, while the middle lobe surged four times between 1857 and 1991 at decreasing intervals of

72-6 years (Björnsson et al., 2003). While the ‘greatest advance’ of Skeiðarárjökull in historic time is thought to have occurred in 1929, when the margin extended approximately 400 m south of its recorded 1904 position (Sigurðsson, 2005), little scientific data of the event exists. In 1985-86, the western lobe advanced again approximately 450 m (Pálsson et al., 1992, Wisniewski, 1997, Sigurðsson, 1998). The most recent surge took place in 1991, the most documented of the known surge events, which resulted in advances of 450 m to 1 km (Pálsson et al., 1992, Björnsson, 1999, Russell et al., 2001a). The following sections describe observations of landforms and drainage networks affected by the 1991 surge and their subsequent modification by the November 1996 jökulhlaup and meltout over the following decades.

The 1991 surge began in March and continued through November (Sigurðsson, 1998), resulting in a total increase in surface area of  $10 \text{ km}^2$  (Pálsson et al., 1992, Waller et al., 2008). A region of crevassed ice was initially observed 10 km up glacier (Figure 3.2) and reached the central glacier front in May as a 50 m high surge front (Waller et al., 2008), although a steep margin profile developed even in regions where the surge was less noticeable (Wisniewski, 1997). Crevasses expanded upglacier ~45 km, extending over an area of  $\sim 1,000 \text{ km}^2$ , while the margin itself advanced in two distinct phases: the central lobe advanced ~ 450 m in May - July, and the western lobe advanced ~ 1 km between September and November (Pálsson et al., 1992, Björnsson, 1999, Russell et al., 2001a).

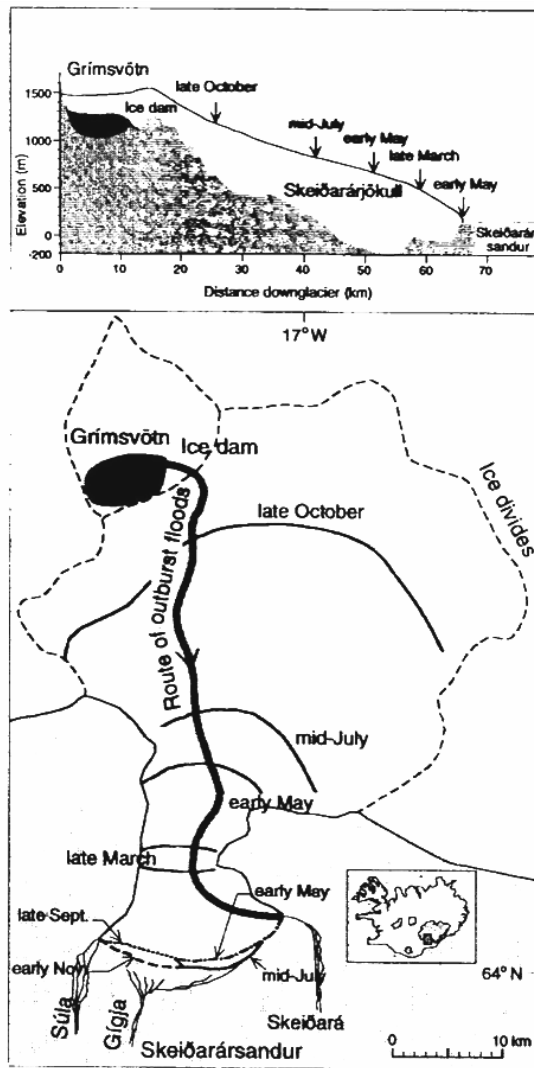


**Figure 3.2** Depiction of the progress of the 1991 surge (solid black lines) and the resulting advance of the ice margin (dashed lines) (Björnsson et al., 2003). This map displays the suspect location of an ice tunnel that may drain jökulhlaups from the subglacial lake Grímsvötn to the river Skeiðará.

The advance was accompanied by an increase in surface discharge, similar to that observed during the 1929 surge (Pálsson et al., 1992), as well as marked alterations in sub and englacial drainage patterns. By early May, meltwater containing high concentrations of sediment issued from small streams and crevasses along the east-central lobe instead of the normal large outlet channels; by July, drainage returned to the main Skeiðará and Gígjukvísl channels (Björnsson, 1998). During this same period, the discharge into the Gígjukvísl increased three-fold compared to the Skeiðará, corresponding with the appearance of several new drainage outlets across the glacier margin (Russell et al., 2001a). These outlets were characterised by large en- and subglacially-fed alluvial fans approximately 400 m in diameter; some contained ice blocks, which are indicative of flooding (van Dijk and Sigurðsson, 2002). The appearance of these new outlets, along with the emplacement of smaller alluvial fans in the west located upon topographic highs,

was assumed to be an expression of the increased basal water pressure characteristic of a linked cavity network by van Dijk (2002).

While surges are known to produce flooding events (Kamb et al., 1985, Fleisher et al., 1998), the ability of this large-scale linked cavity network to store water resulted in both the truncation of a flooding event from Grímsvötn in September and for the low-velocity discharge into Skeiðará (Pálsson et al., 1992, Björnsson, 1998). A second Grímsvötn flood took place between late October and November, near the end of the surge event, that drained into the Skeiðará with a hydrograph typical of Grímsvötn floods during non-surge periods. Björnsson (1998) suggests that during a surge even an outburst flood is not capable of destroying the distributed drainage system, directly affecting the impact of glacio-fluvial flooding events during surges.

The surge limit itself was marked by a push-moraine complex 5 m high and 10 m in breadth (Russell et al., 2001a) and the advance of the margin into a proglacial lake resulted in a unique displacement of glaciolimnic deposits over 12 m high (Wisniewski, 1997). A series of regularly-spaced proglacial fans (~30) that range in size from 4-10 m were emplaced during the 1991 surge that have persisted following the ongoing retreat of the margin (Russell et al., 2001a). This association of glacier ice thrust over older outwash sediments with outwash fans originating from a push moraine complex is similarly reflected in exposures through the Gígjukvísl section (Figure 3.3) (Galon, 1973a, Russell et al., 2001a). Similarities between the numerous proglacial outwash fans emplaced during the 1991 surge and relic fans on the distal sandur (Figure 3.4) suggest that surge-related processes may control the development of much of Skeiðarársandur (Russell et al., 2001a).

Although several of the alluvial fans emplaced by the 1991 surge were obliterated as a result of the 1996 jökulhlaup, alluvial fans emplaced on topographic highs and large, coarse-grained fans that develop during surge related flooding events were proposed by van Dijk (2002) to have a high preservation potential. Indeed, pre-surge coarse-grained, highly permeable ice contact fans were overridden during the surge, resulting in the formation of kettled, drumlinised landforms, a possible diagnostic signature of surge or rapid ice advance (Waller et al., 2008). Additionally, the continuing retreat of Skeiðarárjökull has exposed several surge-associated landforms, including flutes and crevasse-cast ridges (Waller et al., 2008).

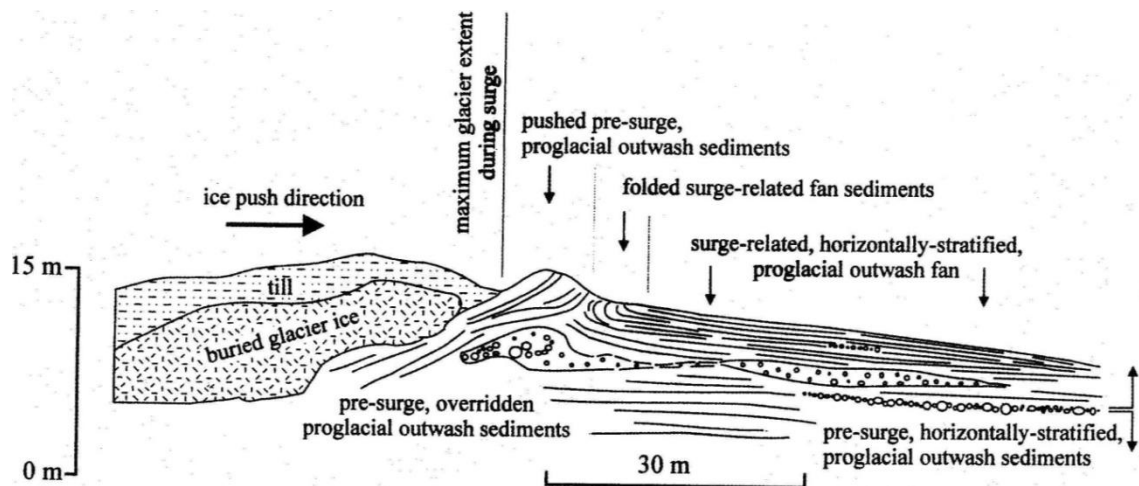


Figure 3.3 Section of the Gígjukvísl push moraine and fan complex that depicts the relationship between buried glacier ice, push moraine, overridden and pushed outwash sediments and push moraine related fans (Russell et al., 2001a).

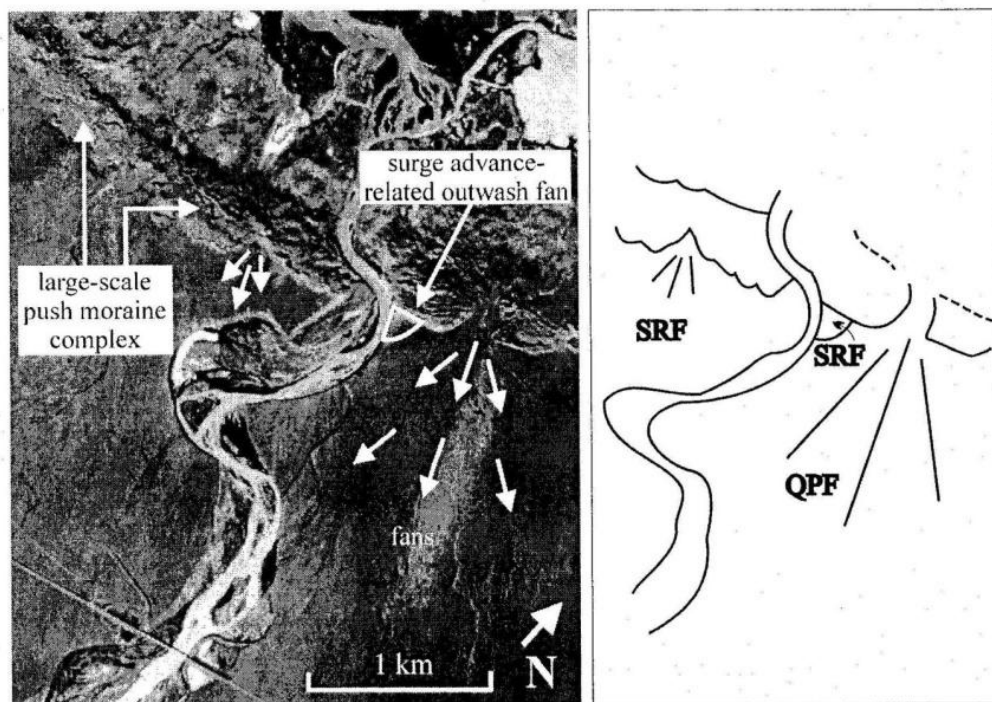


Figure 3.4. Aerial photographs depicting surge related fans (SRFs) and quiescent phase fans (QPFs) emplaced on the elevated portions of the sandur (van Dijk, 2002).

### 3.2.3 *Glacier Margin Retreat: 20<sup>th</sup> century to present*

In an attempt to account for the formation of the proglacial trench, Arnborg (1955) noted that when Skeiðarárjökull was at its maximum (up until 1890), the increased thickness of ice, and related pressure, would have steepened the basin inside the end moraine. Additionally, Arnborg reasoned that the increased erosive action in this region (shearing) would have emplaced large volumes of material towards the moraine; the height difference would increase the longer the stationary stage persisted, resulting in the development of the proglacial trench which now spans most of the central depression.

The development of the depression, however, as seen in Figure 3.1 and Figure 3.5, has not been uniform, but rather a reflection of the behaviour of the three glacier lobes and the processes that affect them, as these lobes have each experienced different rates and patterns of retreat. The following sections describe landforms and processes that have been documented in these three regions in the literature.

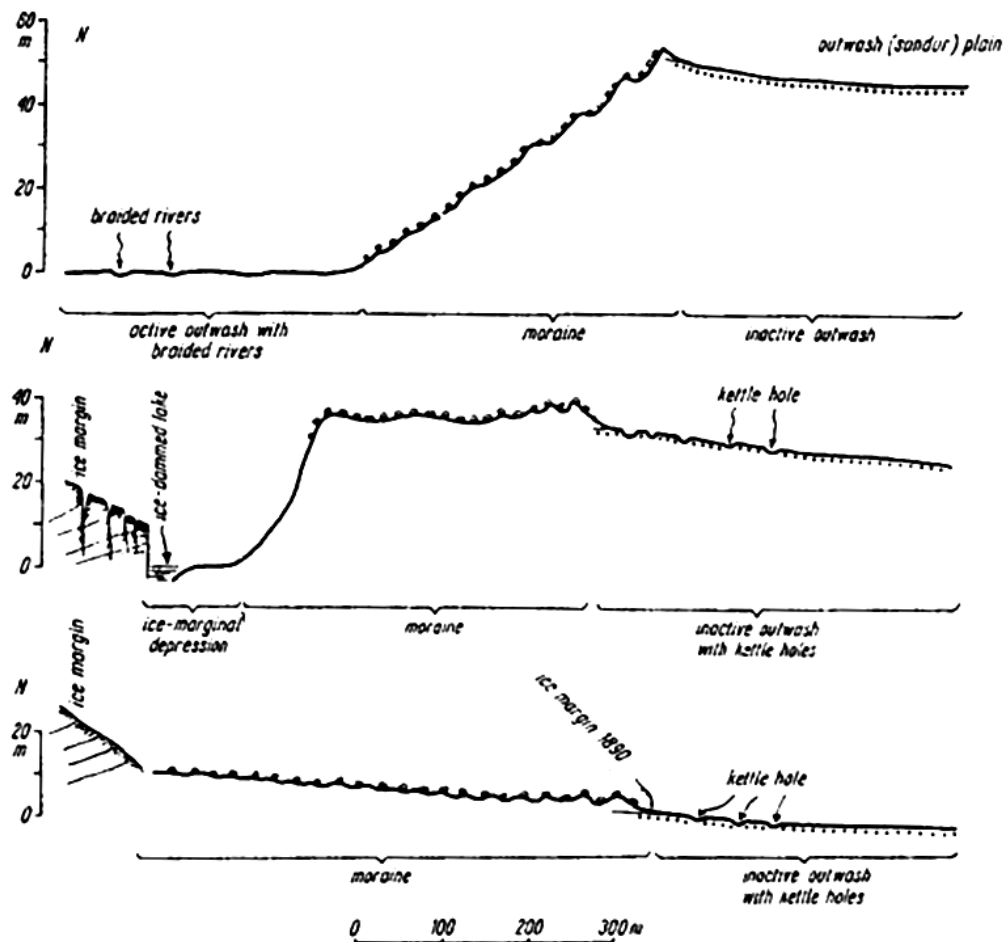


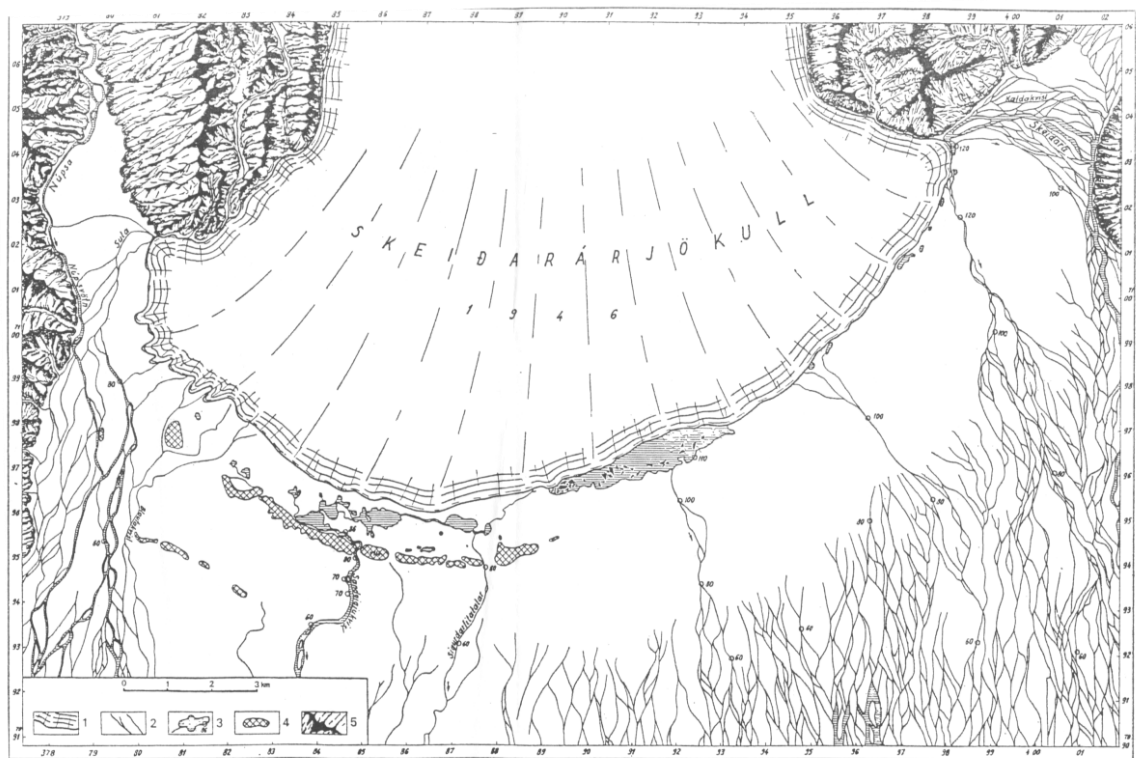
Figure 3.5 Profiles of the sandur margin in the east (top), central (middle) and west regions (bottom) (Klimek, 1973).

#### 3.2.4 *Eastern Skeiðarárjökull*

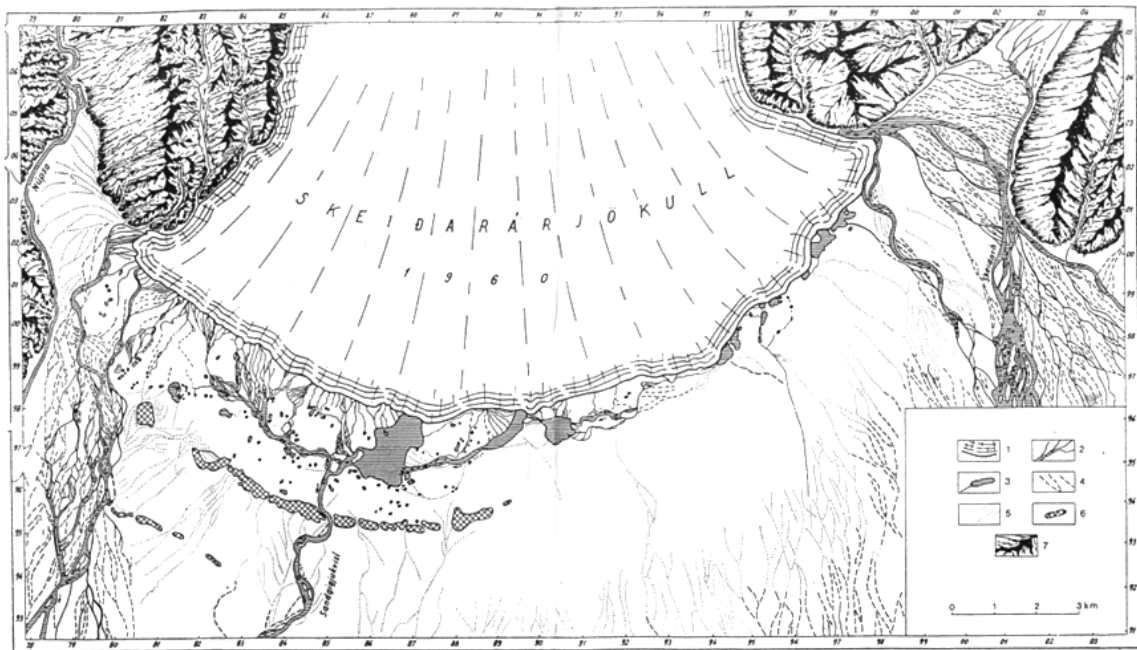
While the eastern region has been subject to several periods of fluctuation over the past two hundred years, the rate of this fluctuation, and retreat in particular, has been tempered by the colder climatic conditions (Wojcik, 1973b). The proglacial trench is nearly absent here and instead restricted to a narrow depression with a few small lakes that abut the steepened glacier snout. This region is characterised by a successive series of end moraines that mark the repeated retreat of the margin as described by Klimek (1973). Following the 1890 maximum, from 1904-1920 the eastern portion of Skeiðarárjökull



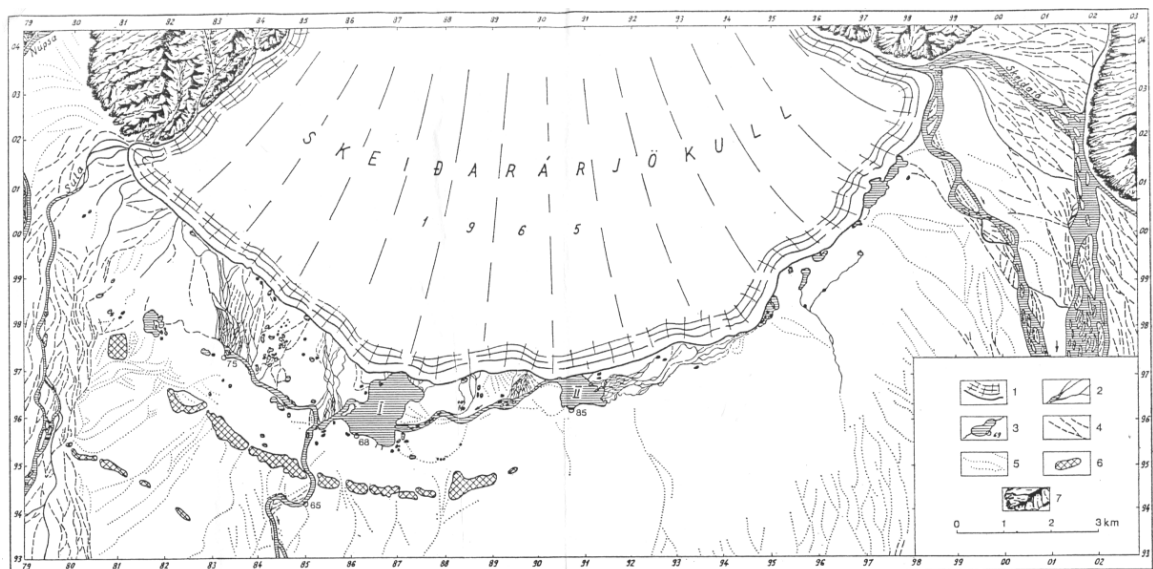
was stagnant, and recession was noted from 1932 - 1947, retreating at a rate of 24 m/year (Klimek, 1973). During subsequent retreats, moraine gaps grew fewer and wider (Figure 3.6). Retreat was accompanied by an increase in meltwater discharge which was restricted to, and continued to incise, a few channels. This was a result of the stagnation of the glacier that prohibited direct drainage onto the sandur and encouraged the development of large, marginal rivers that were frequently inundated by jökulhlaups from the Skeiðará outlets. Overall, the recession in the region is characterised by a series of abandoned, heavily kettled terraces. During retreat, the glacier ice was insulated by layers of debris which detached as dead ice fields and ice ridges. Following the November 1996 jökulhlaup, the glacier has rapidly retreated, resulting in the capture of the eastern Skeiðará by the western Skeiðará in 2004 and, as of August 2009 (personal communication by Dr. A. J. Russell), nearly all the drainage of this lobe flows parallel to the ice margin westward into the Gígjukvísl.



A) 1946- 1- glacier, 2- rivers, 3- lakes, 4- end moraines, 5- basalt massifs.



**B) 1960: 1-glacier, 2-rivers in the area of acting sandy tracks, 3-lakes, 4-traces of larger river humid beds, 5-traces of larger river dry beds, 6-end moraines, 7-basalt massifs.**



**C) 1965: 1-glacier, 2-rivers in the area of active sandy tracks, 3-lakes, 4-traces of larger river humid beds, 5-traces of larger river dry beds, 6-end moraines, 7-basalt massifs.**

**Figure 3.6 Evolution of drainage from A) 1946, B) 1960 and C) 1965 depicting the abandonment of the central sandur and the development of the Skeiðará, Gígjukvísl and Súla channels (Galon, 1973a)**

### 3.2.5 *Central Skeiðarárjökull*

Recession in the central region was differentiated by Galon (1973a) into five main zones: eroded end moraines and abandoned channels, the band of the main 1890 moraine, zones of elongated depressions, an inner zone of marginal deposits that pass into an undulating plain of ice-dammed basins and a zone comprising ice dammed lakes, ice moraine ridges and outwash deposits. The moraine ridges may exceed 30 m in height and comprise older

morainic plateaus and hummocks, and younger moraine ridges (Galon, 1973a). The landscape between this belt and the glacier margin is characterised by elongate depressions, boulders, and fluted smoothed ground moraine (Galon, 1973a). As the glacier retreated, the older moraines were partially removed by meltwater issuing from the margin, resulting in the formation of moraine gaps or ‘gates’ (Bogacki, 1973, Galon, 1973a). The number of ‘gates’ decreased during recession in the pattern described by Klimek (1972), (Figure 2.9). A wide break in the moraine belt exists across the middle of the sandur, a span occupied by extensive sheets of outwash.

North of the end moraines, an extensive plain of ‘degradation and aggradation’ was observed by Galon (1973a), formed as a result of recession and standstill followed by brief periods of advance. Behind this region is the zone of ‘elongated depressions’, a result of the glacio-fluvial stage of recession, in which meltwaters emerged from the ‘gates’ to flow across the forefield; following glacier retreat and lowering, the glaciolimnical stage developed, as water could no longer escape through the gaps and ponded to form proglacial lakes. Moraine deposits in the distal portions are noticeably absent here, possibly as a result of the 1904 and 1922 jökulhlaups (Galon, 1973b). Consideration is given later in this chapter to the impact on ice bodies emplaced beneath sediments as a result of floods and surges, and the resulting pattern of retreat. Further examples of this, as well as an examination of landforms exposed by retreat in the central region and the development of the now dominant Gígjukvísl channel, are explored later in this chapter.

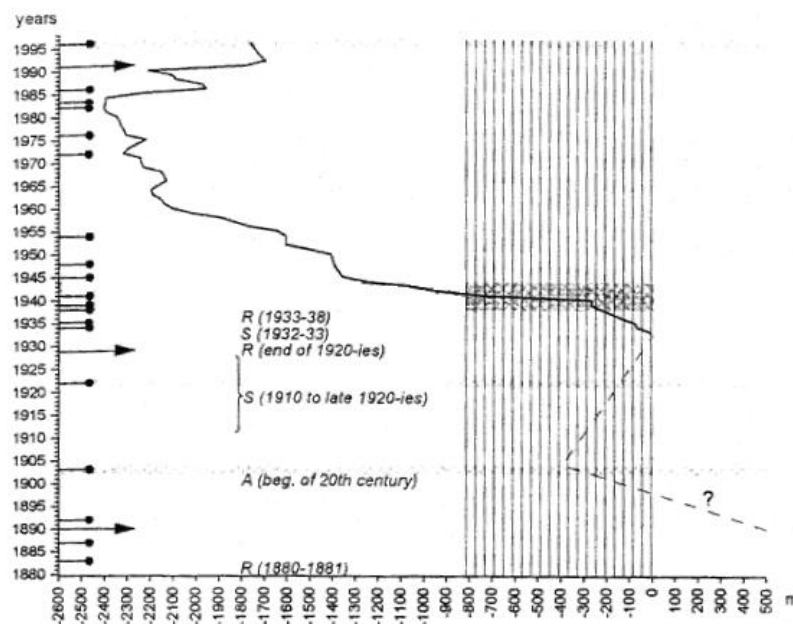
### 3.2.6 *Western Skeiðarárjökull*

Figure 3.7 presents a detailed examination of retreat in the western region and demarcates surges and jökulhlaups (Molewski, 2000). The ice is heavily mantled with debris, and an extensive surficial drainage network has developed upon its surface, terrain which makes ground observations and estimations of the ice margin position very difficult. The surface of the ice has lowered gradually and is heavily crevassed, unfavourable for the formation of larger end moraines (Jewtuchowicz, 1973). This region has retreated more than 5 km over the past two hundred years. A detailed examination of the resulting extensive low, undulating plains and morainic plateaus are described by Klimek (1973).

From 1904 to 1965, the western margin retreated 2600 m, while the eastern section retreated only 500 m, illustrating the asymmetrical response of the glacier during recession (Wojcik, 1973a). The western edge of this region possesses a greater humidity

and precipitation than the rest of the sandur (Wojcik, 1973b). This microclimate may be a contributing factor for the increased ablation and the few shallow lakes that have developed over 1.5 km distant from the ice margin (Wojcik, 1973b). It has been proposed that in the east, cold winds descending from the Oræfajökull ice cap may act as a barrier, lowering ablation rates, while in the west, warm winds from the ocean bring precipitation and higher rates of ablation (Wojcik, 1973a)

During the western lobe's initial recession, Galon (1973a) postulates that a series of fissures formed in which the glacio-fluvial material was melted out, insulating the debris beneath and resulting in a successive process of marginal stagnation which resulted in the formation of five distinct morphogenic zones: 1) the forefield of the main end moraine zone and remnants of older moraines; 2) the main end moraine zone, 3) the zone of elongated depressions, 4) an inner zone of marginal deposits and landforms passing into an undulating plain of ablation and ice-dammed basins, drained by a peripheral rivers; and 5) ice moraine ridges, morainic plains, outwash deposits and ice-dammed lakes. Galon mentions that the internal structure (crevasses and fractures) played a role in the formation of these regions but does not tackle the topic of how this internal structure originated. Overall, recession in the region is described by Klimek (1973) as being the result of gradual stagnation, as opposed to repeated detachment of dead ice fields and ridges as seen in the eastern region of Skeiðarársandur.



**Figure 3.7** Advances and retreat of Skeiðarárjökull's western lobe (Molewski, 2000). The solid line represents systematic measurements carried out on profile since 1932, while broken line represents estimated position. A = advance, R = recession, S = Stagnation (Thorarinsson, 1943), while circles represent jökulhlaups and triangles represent surges.

### 3.2.7 *Summary of fluctuations at Skeiðarárjökull*

In summary, the three lobes that comprise Skeiðarárjökull responded differently during periods of transgression and regression, resulting in different suites of landforms within a single field area. These fluctuations have played an important role in the organization of glacio-fluvial systems and, as a result, have played a major role in the development of the landforms. Lying within an over-deepened basin, the underlying topography has also played a critical role in the determining the location of outlets during such fluctuations. The 1991 surge that dramatically affected the central and western lobes provided researchers with an opportunity to observe the development of large alluvial fans and contemporaneous flooding events and to examine the persistence of surge-related landforms following the margin's retreat; these observations have provided new insight into the internal glacier hydraulics during surge events. Recession since 1945 has been asymmetrical across the margin, and the difference in the behaviour of the lobes and differences in their internal structure have resulted in three distinct proglacial topographic regions.

## 3.3 **Jökulhlaups at Skeiðarárjökull**

*“Where the seas used to be 60 m deep, a sandur grew up almost over night...The activity of the volcano must then have been so great that not only one of the glaciers which covered it slid down, but the majority of them hurled themselves with immeasurable masses of gravel, sand and water over the surrounding country.” 1362 Oræfa eruption (Ahlmann, 1938)*

### 3.3.1 *Introduction*

Ahlmann's quotation above captures the impact that historic jökulhlaups have had on the sandur. High-magnitude jökulhlaups have occurred at Skeiðarárjökull in 1903, 1923, 1934, 1938, 1954 and 1996 (Wadell, 1935, Björnsson, 1997), while Grænalón-related floods have occurred in even more frequent intervals at a lower magnitude, presently occurring only months apart (Roberts et al., 2005). The behaviour of these floods, and their resulting impact on the sandur, has altered in response to Skeiðarárjökull's retreat since the 1940s (Galon, 1973a, Björnsson, 1974, Björnsson, 1992, Gudmundsson et al., 1997, Roberts et al., 2001, Russell et al., 2006). The floodwaters of the 1996 Grímsvötn jökulhlaup, for instance, behaved quite differently than previous floods of the same source: while occupying the two main channels (the Súla and Eastern Skeiðará) and re-

activating old channels, a large volume of the flood was routed through the Gígjukvísl channel. This section presents an overview of these changing flood patterns over the course of the twentieth century and provides specific details and observations of the November 1996 jökulhlaup, including studies conducted in the area as recently as 2009. Further specifics regarding individual models, landforms and their persistence may be found in Chapter 6.

### 3.3.2 *Glacier recession and jökulhlaups at Skeiðarárjökull: 1934-2009*

An overview of the development of the proglacial depression since 1934 and its subsequent impact on jökulhlaup routing is shown in Figure 3.8. In contrast to the drainage across the sandur evident during the 1934 jökulhlaup (Figure 3.8a), the 1954 floodwaters were routed parallel to the margin and into the Sandgígjukvísl (Figure 3.8b), bypassing most of the sandur completely (Rist, 1955). Observations of the 1996 event (Figure 3.8c), a flood several orders of magnitude larger than previous events (Figure 3.8d), indicated that the greatest amount of geomorphic change took place within the depression, not upon the sandur (Gomez et al., 2002). During this event, floodwaters ponded within the depression, resulting in meltwater bypassing Skeiðarársandur's proximal zone, less than 25% of which was inundated (Gomez et al., 2000). A complete list of jökulhlaups at Skeiðarárjökull is shown in Table 3.1. The following section explores not only the impact of the proglacial depression on the landsystem but also the impact of vertical lowering of the glacier's surface on glacio-fluvial processes.

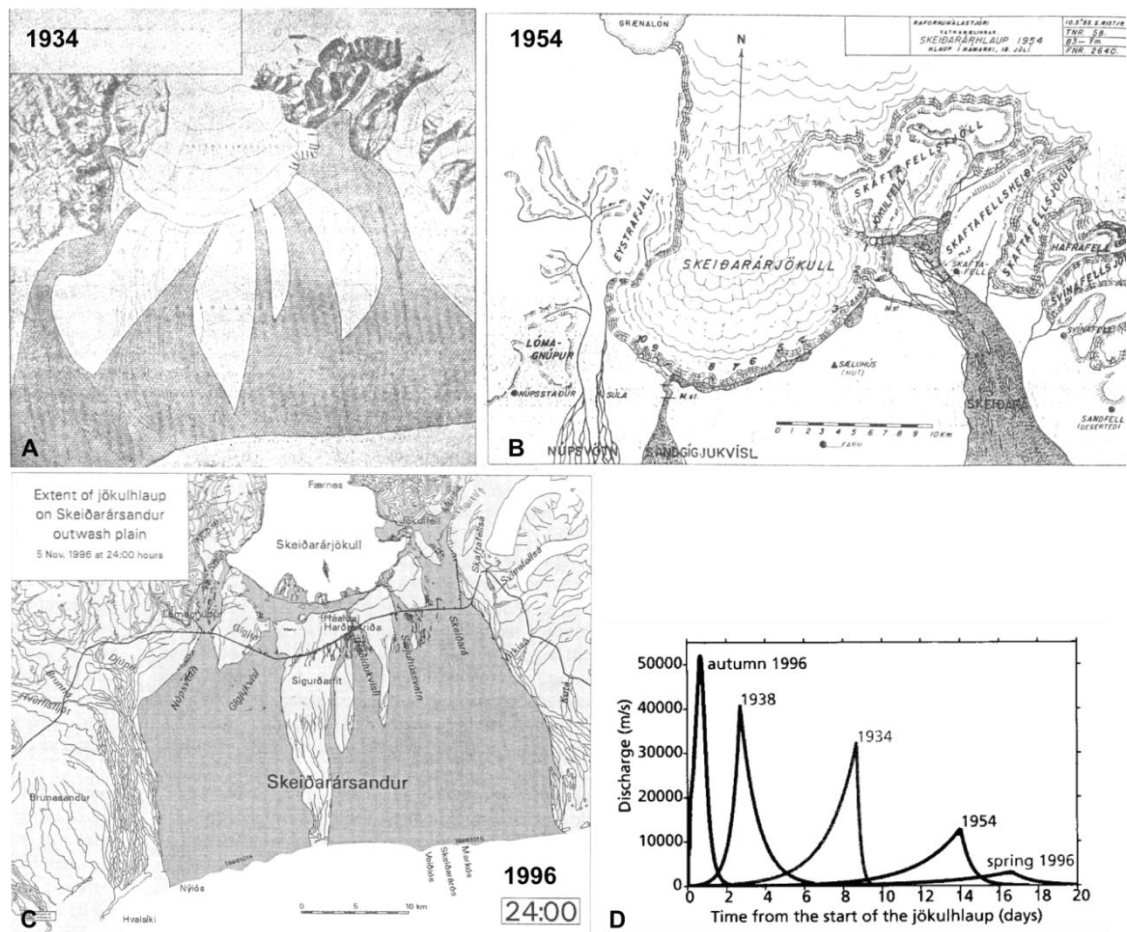


**Figure 3.8** A) Generalised map of the extent of the 1934 jökulhlaup upon the sandur: note the near total inundation of the eastern Skeiðará region (Nielson, 1937). B) Map of the extent of the 1954 jökulhlaup; the (main flood outlets numbered 1-10) (Rist, 1955). C) Location map depicting the extent of the 1996 jökulhlaup on the Skeiðarársandur as well as the supraglacial emergence of floodwaters north of the margin and D) a comparison of jökulhlaup hydrographs from 1934 to the recent 1996 event (Snorrason et al., 2002).

<b>Jökulhlaup</b>	<b>Grímsvötn Eruption</b>
1816 (June)	?
1838 (June)	?
1851 (May)	1851
1861 (May) (Stórahlaup)	1861
1873 (Jan)	1873
1883 (March)	1883
1892 (March)	1892
1897 (medium hlaup in Jan)	no eruption
1903 (major hlaup in June)	1903
1913 (major hlaup in March)	1913
1922 (major hlaup in September)	1922
1934 (major hlaup in March)	1934
1938 (major hlaup in May-June)	1938
1939 (minor hlaup in May-June)	no eruption
1941 (minor hlaup in April)	no eruption
1945 (minor hlaup in September)	no eruption
1948 (minor hlaup in February)	no eruption
1954 (medium hlaup in July)	no eruption
1960 (medium hlaup in Jan)	no eruption
1965 (small hlaup in Sept)	no eruption
1972 (medium hlaup in March)	no eruption
1976 (medium hlaup)	no eruption
1982 (medium hlaup)	no eruption
1983 (very small hlaup)	no eruption
1986 (small hlaup)	no eruption
1991 (small hlaup)	no eruption
1996a (small hlaup)	no eruption
1996b (massive hlaup)	massive eruption <sup>1</sup>
1998a (small hlaup)	no eruption
1998b (very small hlaup)	small eruption followed
1999 (small hlaup)	no eruption
2002 (very small hlaup)	no eruption
2003 (very small hlaup)	no eruption
2004 (small hlaup in November)	small eruption

<sup>1</sup> Following an eruption within the water Gjálp catchment of Grímsvötn.

**Table 3.1 List of jökulhlaups at Skeiðarárjökull (Ives, 2007).**

### 3.3.3 *November 1996 jökulhlaup*

Unmatched in both discharge and time to peak (Figure 3.8d), the November 1996 jökulhlaup at Skeiðarárjökull has been studied numerous times in recent years, with much debate focusing on the impact of jökulhlaups on a sandur's development (Björnsson, 1997, Roberts et al., 2000, 2001, Gomez et al., 2002, Snorrason et al., 2002, Russell et al., 2006, Smith et al., 2000, 2006). This jökulhlaup was a result of a 6 km long subglacial fissure eruption at Gjálp (Figure 1.5) which lasted from September 30<sup>th</sup> - October 13<sup>th</sup> and melted large quantities of the overlying Vatnajökull ice cap (~3 km<sup>3</sup>). Meltwater flowed away from the fissure over a 200 m high subglacial ridge and began to fill the subglacial



lake that occupied the Grímsvötn caldera (Snorrason et al., 2002). Further details of the fissure eruption and the filling of lake Grímsvötn are described by Gudmundsson et al. (1997, 2004) and Björnsson (2009). The following sections provide an overview of how the event progressed in order to understand how the floodwaters were routed during the event and how the behaviour of the floodwaters affected the resulting deposits.

By November 4<sup>th</sup> 1996, the ice barrier containing lake Grímsvötn failed; ten hours later, and 50 km down glacier, the floodwaters breached the front of Skeiðarárjökull, emerging approximately 2-3 km up from the glacier margin and at the eastern Skeiðará outlet (Figure 3.9), a total volume of 3.6 km<sup>3</sup> (Björnsson, 1997). The floodwaters continued to breach the ice, moving progressively westward along the terminus, effectively filling the proglacial trench and inundating the major contemporary channels (Núpsvötn, Súla, Gígjukvísl, and Skeiðará) and reactivating two abandoned channels (Sælhúsakvísl and the Háöldukvísl) (Figure 3.10). It is estimated that the jökulhlaup achieved a peak discharge of 50,000 m<sup>3</sup> s<sup>-1</sup> in just 15 hours, covering approximately 750 km<sup>2</sup> of area and transporting an estimated 180 million tons of suspended sediment (Björnsson, 1997, Snorrason et al., 2002). It is estimated that this single event added approximately 7 km<sup>2</sup> of sediment to the coastline (Snorrason et al., 2002). Observations of the spatio-temporal variability of the 1996 jökulhlaup have provided vital insight into the interaction of the floodwaters within a glacier during a single event and how different landforms may be emplaced during different phases of a flood.

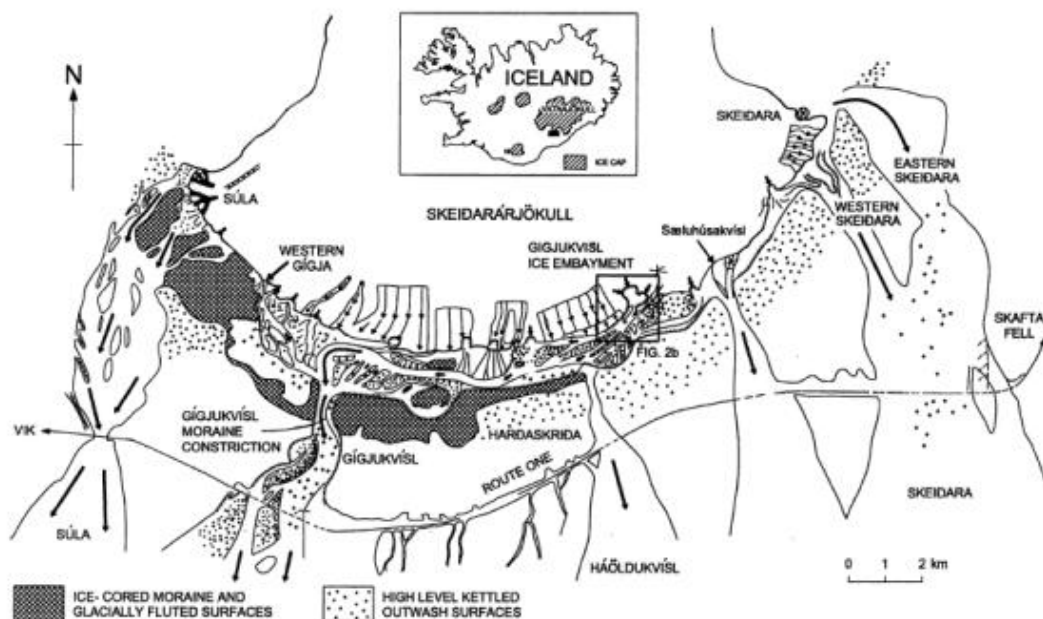


**Figure 3.9** Map showing the major outlets of the 1996 jökulhlaup, the development of supraglacial fractures and discharge, and the location of the Gígjukvísl Double Embayment (DE) (black box) (Russell et al., 2001b).

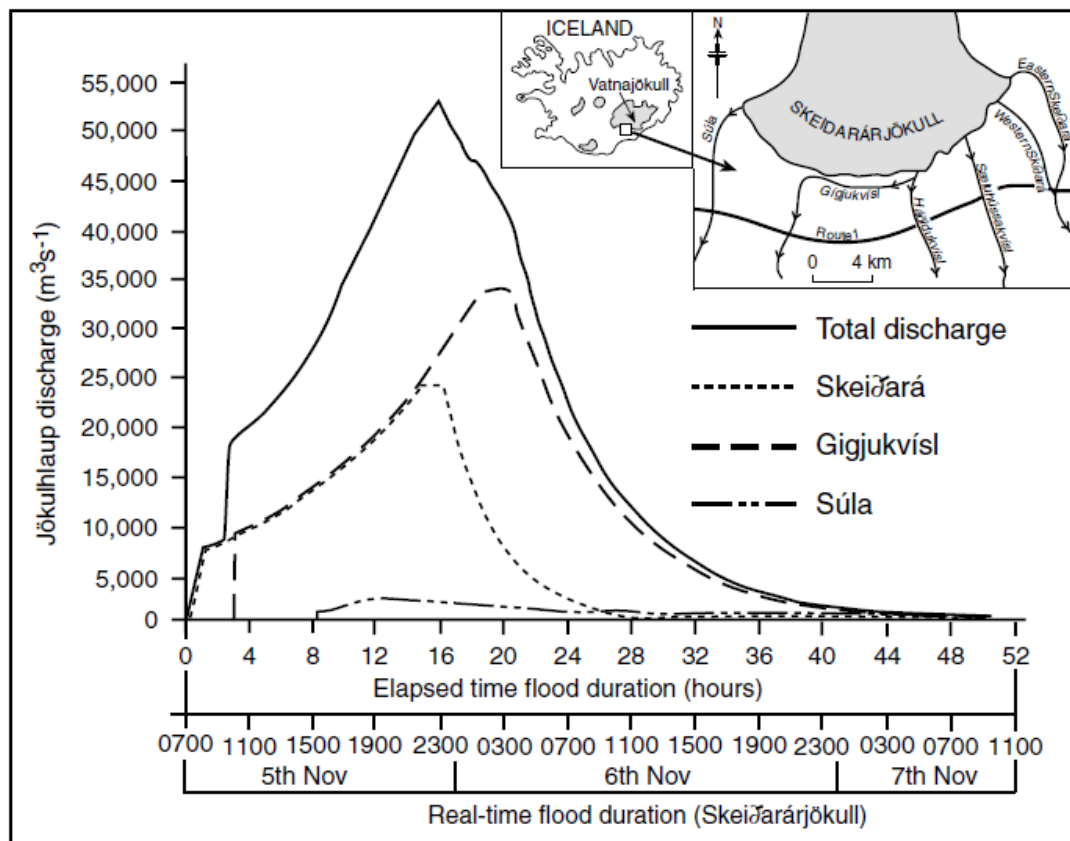
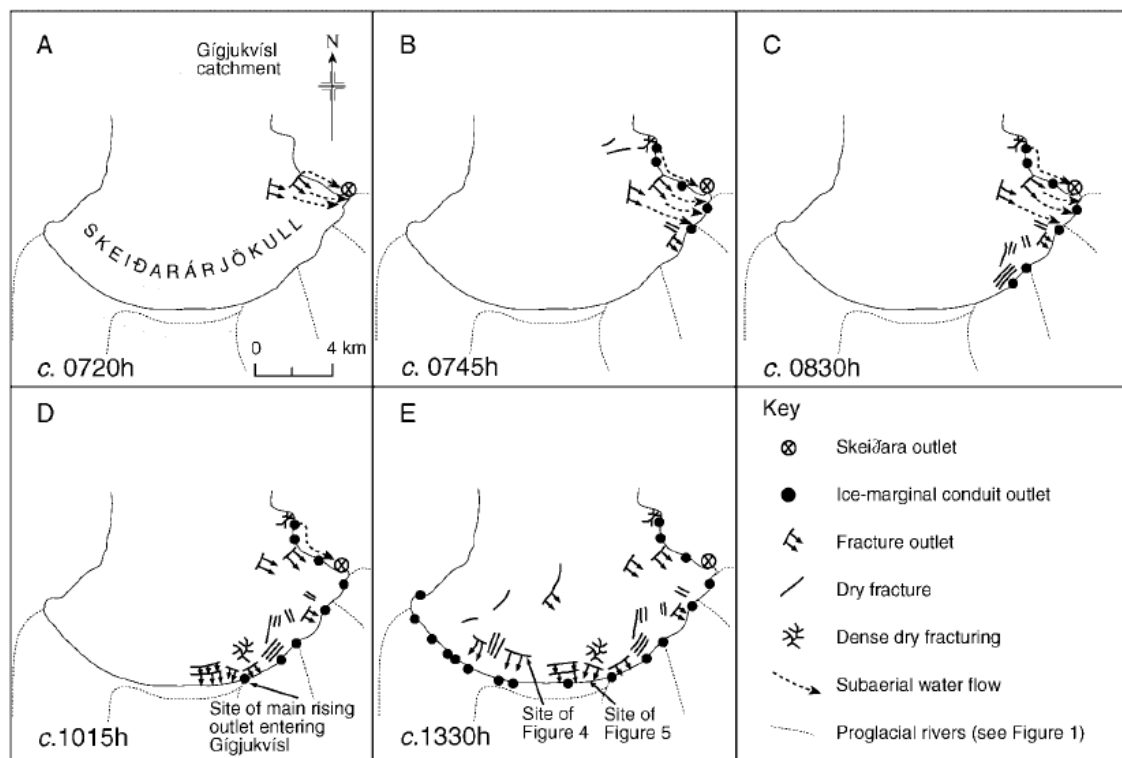


Figure 3.10 Discharge and duration of the 1996 jökulhlaup in the Skeiðará, Gígjukvísl and Súla Rivers (Roberts et al., 2001).

### 3.3.4 November 1996 jökulhlaup: controls on floodwater routing

The emergence of sediment-rich floodwaters through supraglacial fractures more than 3 km upglacier from the Skeiðará outlet, as well as jetting via moulins and crevasses that progressed westward during the event, indicated a shift of internal hydraulics (Figure 3.11), an observation that has led to several key insights into jökulhlaup routing. During the rising stage of the flood, pre-existing conduits were incapable of accommodating floodwaters, resulting in the formation of new outlets (Roberts et al., 2001) and forcing meltwater upwards through approximately 350 m of ice (Björnsson, 1999). Burke et al. (2009) suggest that the waters were routed englacially along pre-existing, porous tephra bands and that the resulting rapid increase in discharge caused hydrofracturing of the surrounding ice. Fractures developed across the entire glacier margin and were superimposed onto pre-existing structures such as crevasses. These were rapidly in-filled via deposition from sediment-laden, super-cooled waters, resulting in vertical bedding structures (Figure 3.12) (Roberts et al., 2001). Continual accretion within these fractures led to blockage, causing pressurized floodwater to fracture the frozen sediment, producing secondary infill (Roberts et al., 2001).

The presence of rip-up clasts and subglacial diamict deposited within numerous fracture fills further suggests a direct link between sub-, en-, and supraglacial drainage networks. During the late-rising and waning stages of the flood, such englacial conduits were in-filled by glacio-fluvial sediments (Burke et al., 2009). Following glacier retreat, these sub-, en- and supraglacially emplaced landforms may be preserved in the form of fracture fills (Roberts et al., 2000, Roberts et al., 2001, Munro-Stasiuk et al., 2008) and conduits (eskers) (Burke et al., 2008, Burke et al., 2009) although these features may be modified, eroded or buried following subsequent large-scale events, secondary alteration and the actions of aeolian and fluvial activity.



**Figure 3.11** Chronological development of outlets and fracturing across the margin of Skeiðarárjökull during the November 1996 jökulhlaup between 0720h - 1330h (A-E). From Roberts et al., 2000, page 1432.

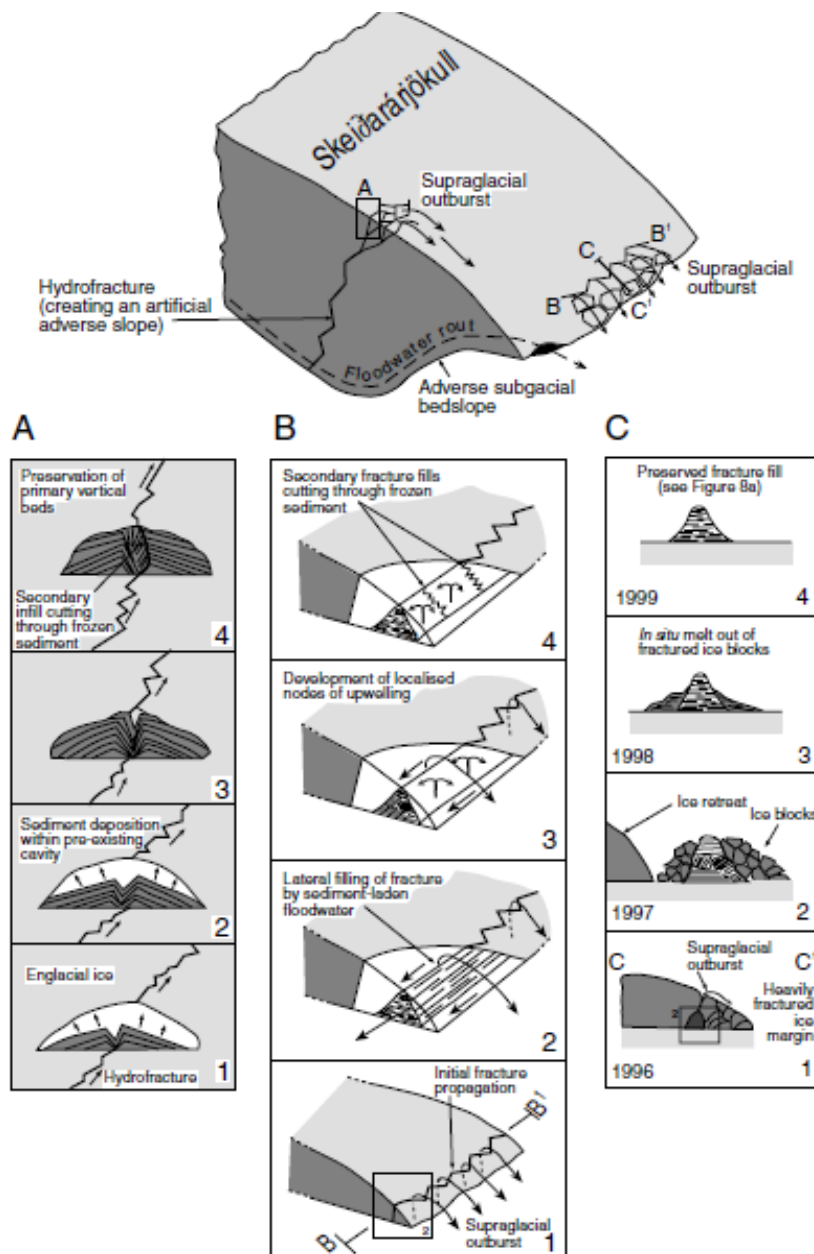


**Figure 3.12 Model of controls on englacial sediment deposition during the November 1996 jökulhlaup –from Roberts et al., 2001 page 949- depicting the main intra-glacial flood routes (Roberts et al., 2000). Panel A) depicts the formation of an infill within a near-surface englacial cavity and vertical bed deposition as a result of supercooling, while panels B) and C) depict main phases on the development, and preservation, of a rising supraglacial fracture outlet.**

### 3.3.5 1996 jökulhlaup: proglacial controls

The ponding of water within the reverse slope of Skeiðarárjökull's proglacial depression was identified as a major control on the November 1996 jökulhlaup (Russell and Knudsen, 1999). In addition to possessing only a few outlet channels, the configuration also acted as a sediment trap, allowing coarse particles to settle out, thereby increasing the erosive capacity of the meltwater (Smith et al., 2000) and serving to attenuate the hydrograph and delay the flood peak (Russell et al., 1999a). Rising-stage deposition of material into topographically restricted backwater lakes during the 1996 jökulhlaup

resulted in the formation of distinctive, relatively flat-topped, delta-like radial outwash fans (Figure 3.13) (Russell and Knudsen, 2002).

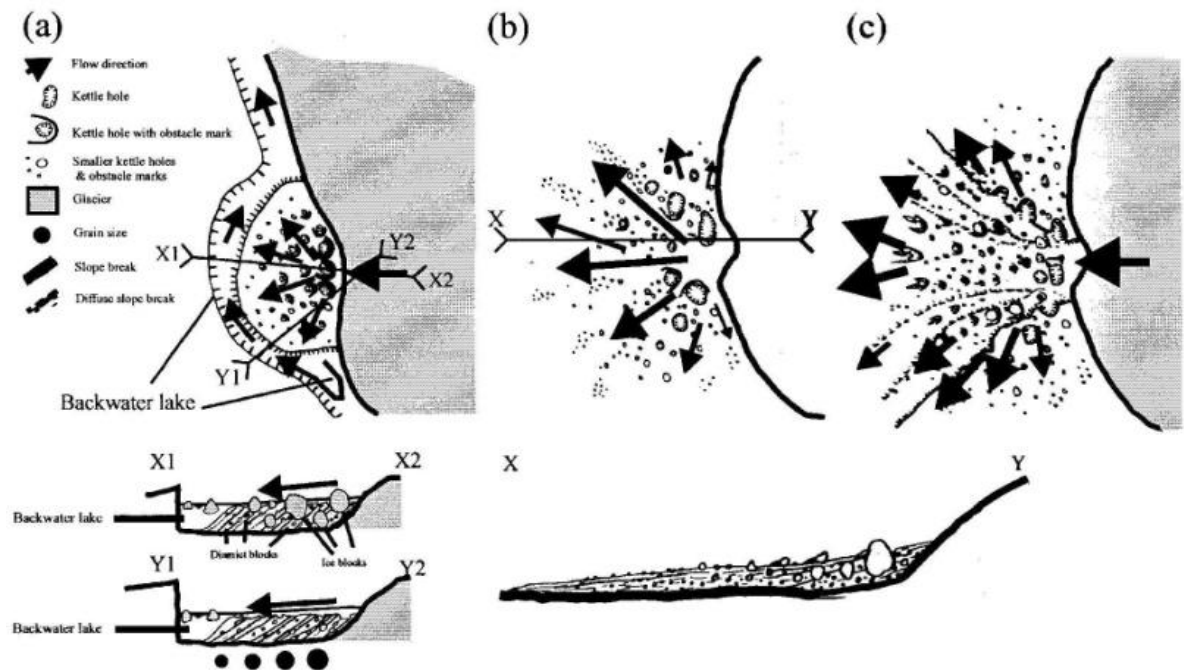


**Figure 3.13 Morphological and sedimentological characteristics of ice-contact jökulhlaup: a) Rising stage deposition topographically-controlled by presence of backwater lake resulting in radial, delta-like fan, b) topographically unrestricted fan allows for the aggradation of sheet-like layers, c) heavily dissected fan and exhumation of ice blocks as a result of sediment poor waters during waning stage fans (Russell and Knudsen, 2002).**

It has also been suggested that an over-deepened basin may also retain meltwater within subglacial lakes, providing a source of water for release during tunnel channel-forming bursts, as evidenced at the Sæluhúsavatn basin tunnel channel outlet (Russell et al., 2007). These authors propose that over-deepening may encourage the formation of tunnel channels, as the ascending subglacial water will find the most effective route through the glacier substrate (Figure 3.14). Additionally, the excavation of the ice-walled canyon and double embayment corresponded to a location of maximum over-deepening (Björnsson, 1999), highlighting the role of ice thickness on internal glacier hydraulics and the ability of topographic constrictions to generate supercritical conditions and associated large-scale macro landforms (Roberts et al., 2000). Russell et al. (2007) also noted that a comparatively ‘modest number of ice blocks when compared to other outlets’ as flood flow within sediment-walled tunnel channels will result in less ice removal as en- or supraglacial conduits that are subject to extensive erosional processes during large-scale jökulhlaups (Roberts et al., 2001, Roberts, 2005)

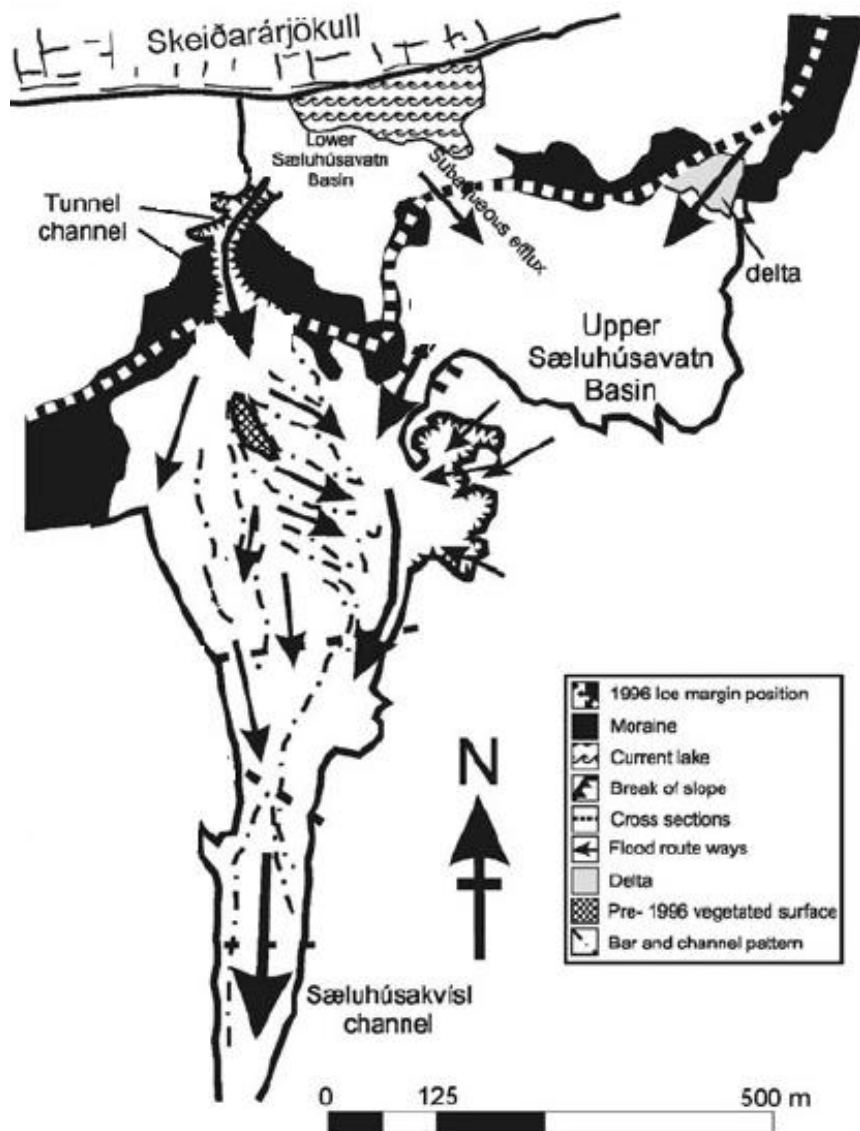


**Figure 3.14** During the 1996 jökulhlaup, while subaqueous efflux into the upper Sæluhúsavátn basin occurred at 110 m, substantial discharge ascended the flanks of the lower Sæluhúsavátn basin through a tunnel channel to exit at an elevation of 120 m. Temporarily raised lake levels acted as a hydraulic dam, deflecting subglacial jökulhlaup flow up from the western flank of the upper basin to exit the glacier margin at 120 m (Russell et al., 2007).

The Gígjukvísl experienced the most notable change of the pre-existing river channels: while the Súla and Skeiðará outlets had waned considerably by November 6th, floodwaters in the persisted in the Gígjukvísl River until November 7<sup>th</sup>, achieving a maximum discharge of 34,000 m<sup>3</sup>/s (Russell and Knudsen, 1999, Snorrason et al., 2002) and doubling the width of the Gígjukvísl moraine gap (Russell et al., 1999b, Smith et al., 2000). The floodwaters reached the Gígjukvísl by 1015h on November 5th, emerging via crevasses up to 2 km in length and single conduit outlets (Roberts et al., 2000, Roberts et al., 2001, Snorrason et al., 2002). The main flow into the Gígjukvísl channel emerged from a fracture complex outlet that, during the mid to late rising, peak and early waning stages migrated retrogressively, resulting in the excavation of a double-headed

embayment and ice-walled canyon that extended more than 500 m into the glacier margin (Russell and Knudsen, 1999, Roberts et al., 2000, Roberts et al., 2001).

Based upon these observations, and by examining the sediments and landforms deposited during the flood, Cassidy, et al. (2003), were able to subdivide the outlet into three distinct regions (Figure 3.15): 1) the ice-walled canyon and double embayment region were characterised by restricted, high-energy, deep flows that occurred during the late rising phase capable of transporting of large boulders, ice blocks and high concentrations of sediment, resulting in the removal of over 5 million m<sup>3</sup> of ice, 2) the proximal fan region was characterised by rapid flow expansion, deposition of ice blocks in distinct, flow-parallel linear zones and prolonged waning stage deposits and channelling, and 3) the distal outwash fan region characterised by widening of the fan, deposition of finer grained sediments and ponding of outwash waters. Further details of the stratigraphic sections and flow hydraulics may be found in Cassidy, et al. (2003); however, this study provides an example of interpreting three stages of a single, high magnitude event from a single outwash channel and landforms.

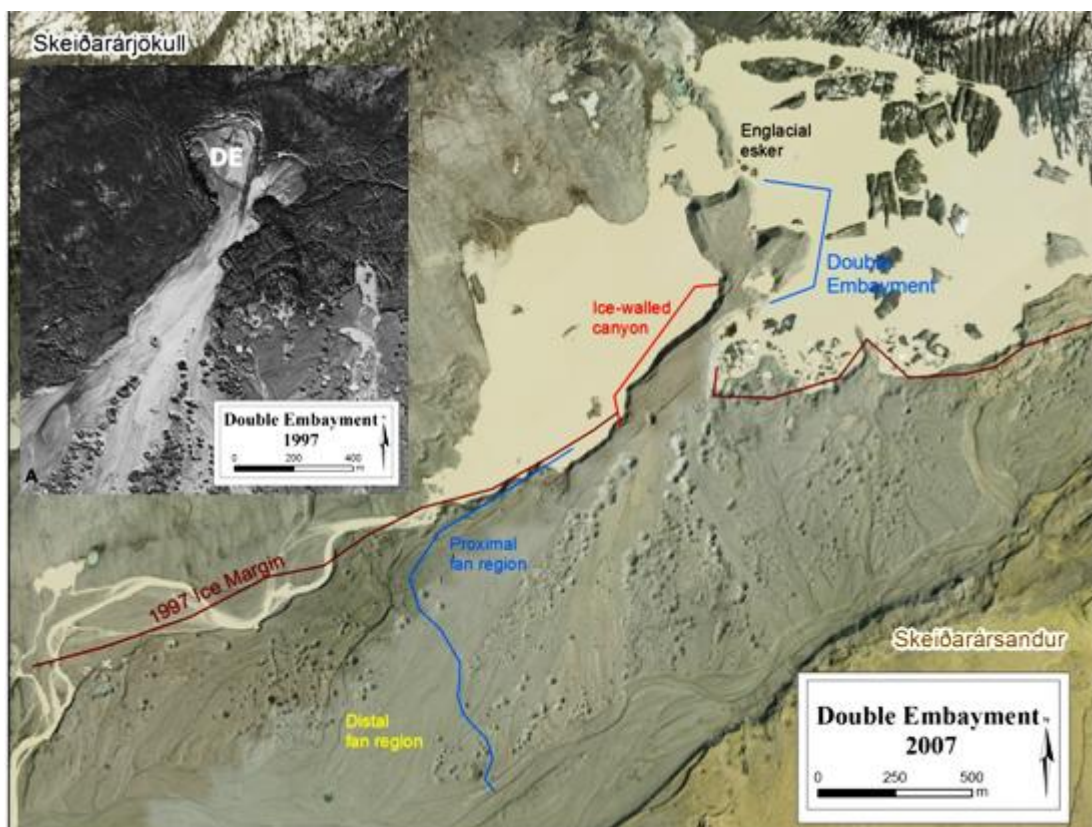


**Figure 3.15 Double embayment, ice-walled canyon, proximal and distal fans. 1997 ice margin is depicted in red and shown in inset. Modified from Cassidy et al. (2003).**



### 3.3.6 *November 1996 jökulhlaups: landforms and persistence*

Since 1996, the persistence of deposits emplaced during the floods have been examined through numerous projects including examining the impact on the sandur as a whole (Gomez et al., 2000, Smith et al., 2000, Gomez et al., 2002, Magilligan et al., 2002, Smith, 2006); documenting the emplacement and subsequent modification of ice blocks, kettle holes and obstacle marks (Fay, 2002, Russell et al., 2006); and monitoring the meltout of an englacial esker (Burke et al., 2008, Burke et al., 2009) and the paraglacial alteration of the adjoining double embayment (Russell et al., 2001b, Woodward et al., 2008). The overarching goal of all of this research was to determine what diagnostic landforms are generated during jökulhlaups, including how they are preserved/altered over time, and what, if any, are the lasting impacts of such events on the sandur as a whole.

As presented in Chapter 1, Smith et al. (2006) suggest that despite a net gain of +20 cm and +24 cm of sediment deposited in the Gígjukvísl and Skeiðará, respectively, half of the material emplaced during the 1996 jökulhlaup was removed within four years, implying that the impact of jökulhlaups on the fluvial system are ephemeral. The 12 m of sediment deposited within the trench is attributed to the ‘atypical’ position of the margin relative to the sandur. The Airborne Topographic Mapper elevation data presented in this study (Figure 3.16 and Figure 3.17), collected before the flood in 1996, immediately following in 1997 and again in 2001 contained an average height error of 8.5 cm, yet the authors attempt to quantify net losses of 9-10 cm. This data in their study cannot be correlated with this thesis; digital elevation models (DEMs) cannot measure at such an ‘accurate’ level, and all but one of the transects (transect 2a) are not captured by the available imagery, so it is unlikely that these results can be disputed directly. However, the DEMs in this thesis may be employed to mensurate the proximal sandur, and individual channels, over a much longer period (1965-2007) to ascertain if the impact of a jökulhlaup on a sandur is indeed ephemeral as these authors suggest.



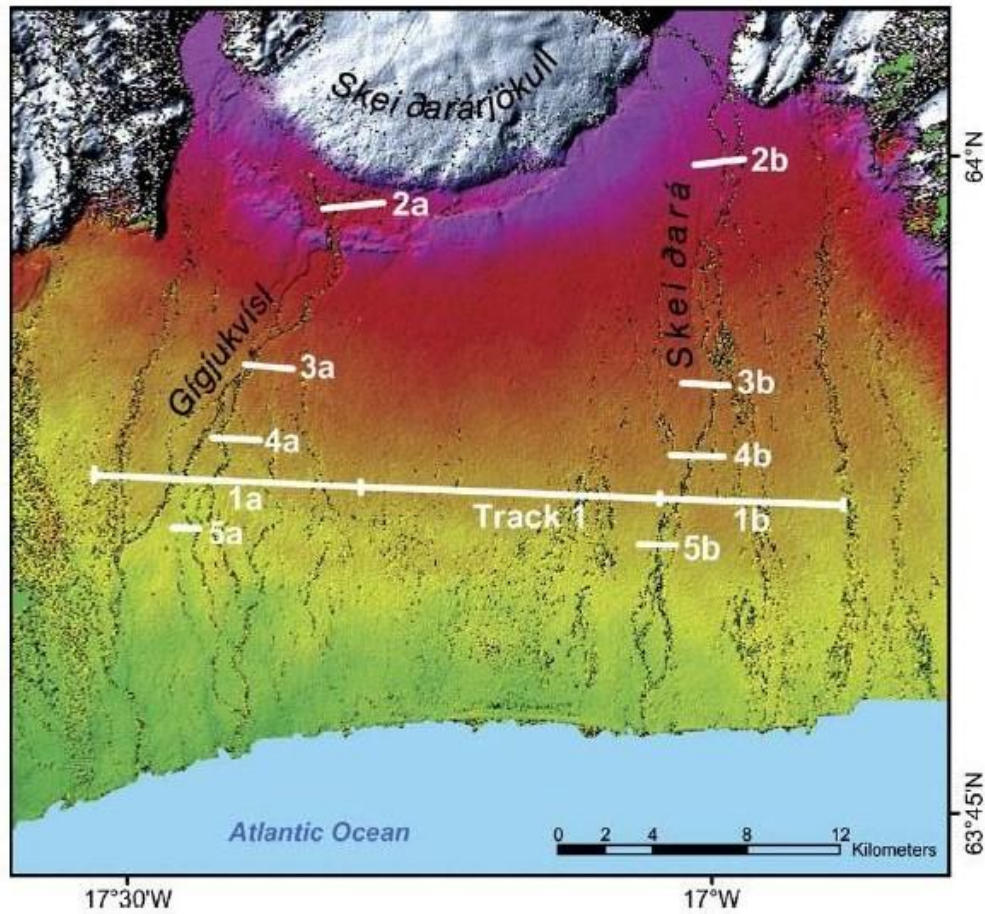


Figure 3.16 Location of airborne laser altimetry transects taken in 1996, 1997 and 2001 (for Track 1, additional tracks 1992, 2001 only) overlaid upon SAR DEM, from Smith et al. (2006).

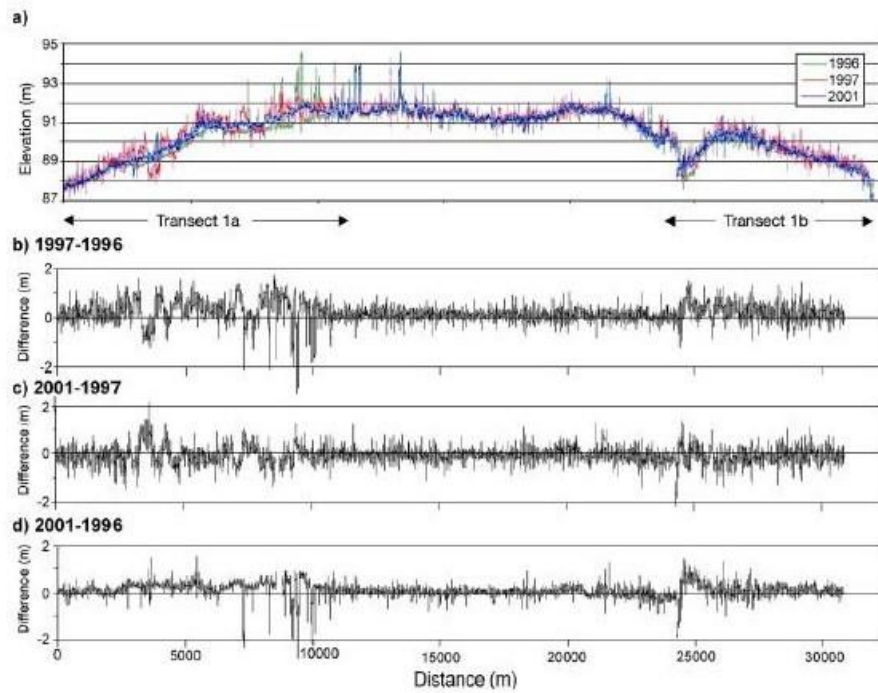
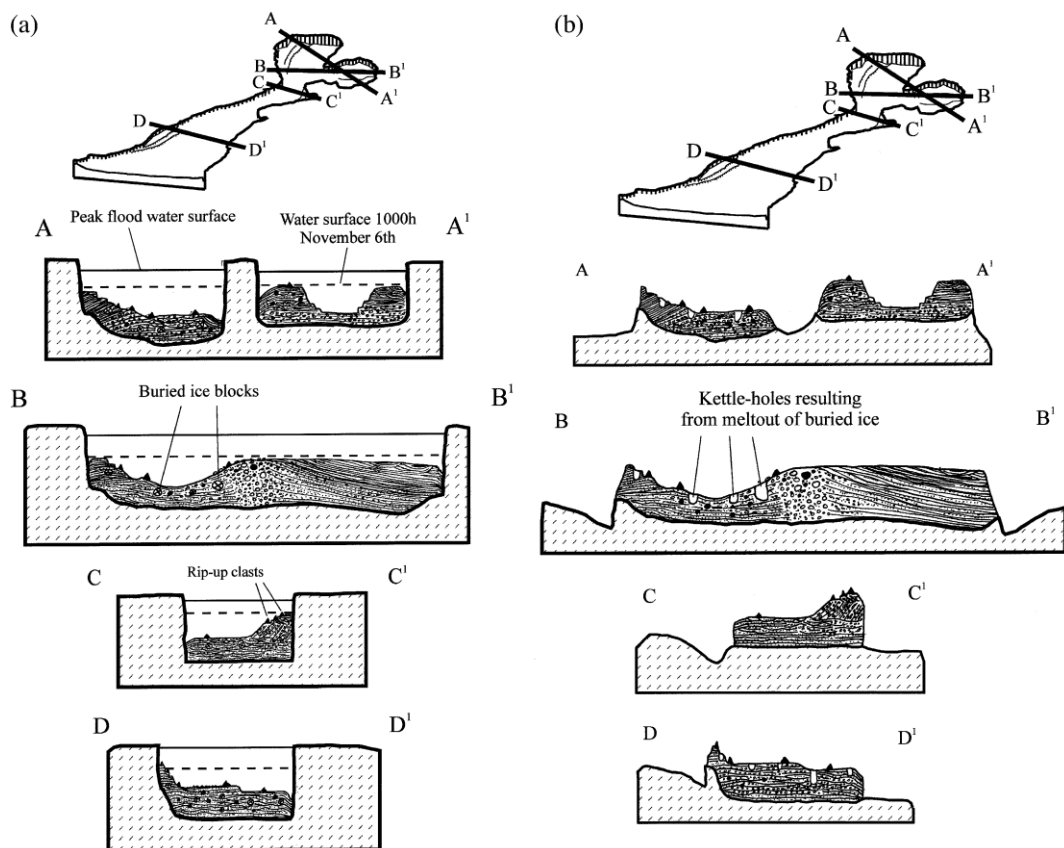


Figure 3.17 a) Laser altimetry profiles along Track 1 for 1996, 1997 and 2001; b) net topographic changes after the 1996 jökulhlaup; c) net post modification 2001-1997; d) net topographic changes after 5 years (Smith, 2006).

Perhaps one of the most striking landforms emplaced during the November 1996 flood was the supraglacial emplacement of the double embayment and ice-walled channel; the retreat and lowering of the glacier ice resulted in the exposure of the sediments as seen in Figure 3.18 (Russell et al., 2001b). This, combined with proximal crevasse-clast ridges, fracture fills and the large, single-event englacial esker connected to the double embayment, suggests that this may be a diagnostic composite landform of central outlets during large-scale jökulhlaups (Russell et al., 2006, Burke et al., 2008). Further ground-penetrating radar (GPR) investigations conducted in 2006 and 2007 of the sediments that were deposited in the ice-walled canyon during the 1996 jökulhlaup (Woodward et al., 2008), revealed that 12 m of sediments overlaid buried ice. These sediments exhibited normal and reverse faulting due to the melting and movement of frozen sediment and buried ice at or beneath the water table, calling into question the preservation potential of such a diagnostic, supra/englacial landform, as this feature in this englacial location at least may only be considered transitional at present.



**Figure 3.18 Exposure of the supraglacial double-embayment and ice-walled channel sediments following the lowering of the ice surface and retreat of the margin (Russell et al., 2001b).**

While greater in spatial distribution, if smaller in vertical extent, rectilinear fracture fills distributed within the proglacial depression have been presented as landforms diagnostic of past events characterised by high water pressure such as jökulhlaups or possibly during

the release of en- or supraglacial water during the terminal phase of a surge (Bennett et al. 2000). These fracture fills are ridges between 20-200 m in length, 2-10 m in width and 0.5-5 m high covered by pebbles, cobbles and boulders. A GPR survey conducted by these researchers taken across several ridges revealed that these features are a network of clastic dykes, proposed to be the relics of hydro-fracture fills that formed during jökulhlaups (Munro-Stasiuk et al., 2008). These authors suggest that the increased water pressure during these flooding events forced water out of over-pressurized subglacial channels up through the overlying ice. The ridges are the surficial expression of where water escaped from the ice surface; as the floodwaters waned, sediment was deposited in the fractures.

Observations of fracture and channel fills at stratigraphic sections at the Blautakvísl (Russell, 2003) suggested that these features developed as a result of a multiple flood phases including a) an onset of jökulhlaup flow marked by high water pressures capable of fluidizing sediment, permitting gravel from the lower unit to be injected into the overlying diamicton – as water pressure and discharge increase rapidly, hydrofractures are driven through the overlying diamicton and overlying ice (Rijsdijk et al., 1999, Russell, 2003, Le Heron and Etienne, 2005, Kjaer et al., 2006); b) hydrofractures widen, and a broad, anastomosing channel system is formed by erosion at the glacier bed; c) flow through vertical hydrofractures is reduced as pressure is relieved by channel erosion beneath the diamict unit and large sections of the fractured diamicton unit drop into the channel and jökulhlaup flow evolves from a complex fracture-fill network to conduit flow; flow ceases as large ice-roofed channels develop (Piotrowski, 1997, Sjogren et al., 2002, Russell et al., 2007). They suggest that as a result, event-related Quaternary eskers may be associated with undulating terrain, partially or wholly inset into undisturbed subglacial surfaces, terrain that may otherwise be mistaken for kettled terrain and associated with the meltout of *in situ* glacier ice.

### 3.3.7 ***Grænalón jökulhlaups***

While large-scale, volcanogenic jökulhlaups are infrequent, other glaciolimnic jökulhlaups at Skeiðarárjökull may occur more regularly, although the behaviour of these floods has also altered in recent years (Table 3.2). As the glacier surface has lowered over time in response to climate, so have the levels of ice-proximal lakes; the drainage mechanisms of these lakes, specifically those of lake Grænalón, have also changed. At its maximum extent during the Little Ice Age, Grænalón spanned from the western edge of Skeiðarárjökull across to a small outlet glacier 5 km to the west, and the water drained out

over a ridge into the Núpsá (Roberts, et al., 2005). Between 1890-1951, the thinning of the glacier allowed the meltwater to lift the ice dam (~250 m deep) and drain the lake, resulting in jökulhlaups being routed through Skeiðarárjökull; the largest of these floods occurred in 1935 and 1939 (Roberts et al., 2005). As Skeiðarárjökull's surface lowered, the reduction of hydrostatic stress has instead caused the glacier to drain beneath a shallow 'ice buttress' via the southeast corner of the lake (Figure 3.19) (communication Dr. Matthew Roberts). Between 1981 and 1992 annual drainage of Grænalón passed from the ice buttress along an 18 km sub-aerial route between the glacier and Eystrafljall (Roberts et al., 2005). Recent seismic measurements made since 2002, however, have tracked frequent (sometimes monthly) jökulhlaups indicating that jökulhlaups now flow through Skeiðarárjökull (Roberts et al., 2005). As a result of changes in climate and associated ice level lowering, outburst floods from Grænalón are now typically small, frequent events that release only ~1% of the lakes volume in contrast to the jökulhlaups of fifty years ago that released all of the lake volume at infrequent intervals (Roberts et al., 2005).

YEAR	DATE	RIVER	DISCHARGE	COMMENTS
(1785)		Núpsvötn		fertile land was destroyed
1898	End of November	Súla, (Núpsvötn)	took 5-6 days to reach peak	one man drowned
(1913)		Núpsvötn		
1935	5 Sept - 12 Sept	Súla, (Núpsvötn)	peak discharge: 12 Sept	lake volume ca. 1.5 km <sup>3</sup> , the lake emptied
<a href="#">1939</a>	23 July - 31 July	Súla, (Núpsvötn), Blautakvísl	4,000 - 5,000 m <sup>3</sup> /s	large icebergs were carried downstream, fertile land was destroyed
1943				Glacier much thinner, waterlevel lower, no more discharge to Núpsá (ever). Jökulhlaups not as large.
1946				
1949				
1951	15 Oct - 22 Oct	Súla		First time that water breaks through beneath the very eastern end of glacier tongue, lake level change: 22m
:	typical total Vol. 0.3 km <sup>3</sup> , often one jökulhlaup per year			
1973	6 Aug - 9 Aug		peak discharge 7 Aug 2,000 m <sup>3</sup> /s	total volume: 0.2 km <sup>3</sup>
:				
1977				
1981	10 July	Súla	750 m <sup>3</sup> /s	jökulhlaup flow irregular, nonsteady as in 1977
<a href="#">1983</a>	16 Aug - 18 Aug	Súla	2200 m <sup>3</sup> /s	seemed to be steady outflow after the jökulhlaup for 2 months
1984	15 Aug - 16 Aug			
1986	29 Aug - 31 Sept	Súla and Gígukvísl	2,000 m <sup>3</sup> /s and 800 m <sup>3</sup> /s	dikes were damaged
1987	10 Aug - 11 Aug			
1988	20 Aug - 21 Aug			
1989	1 Aug - 2 Aug			
1990	11 July - 12 July		peak discharge 12 July	
1991	16 Aug, 15 Sept, 30 Sept			
1992	3 Oct - 6. Oct			
1995	15 Jan - 22 Jan			
2001	23 Sept - 31 Sept			

Table 3.2 of Grænalón jökulhlaups obtained from the Geophysics Division of the Science Institute of Iceland website (<http://www.raunvis.hi.is/~alexandr/glaciorisk/jokulhlaup/GLOF/vatna/graen.htm>)



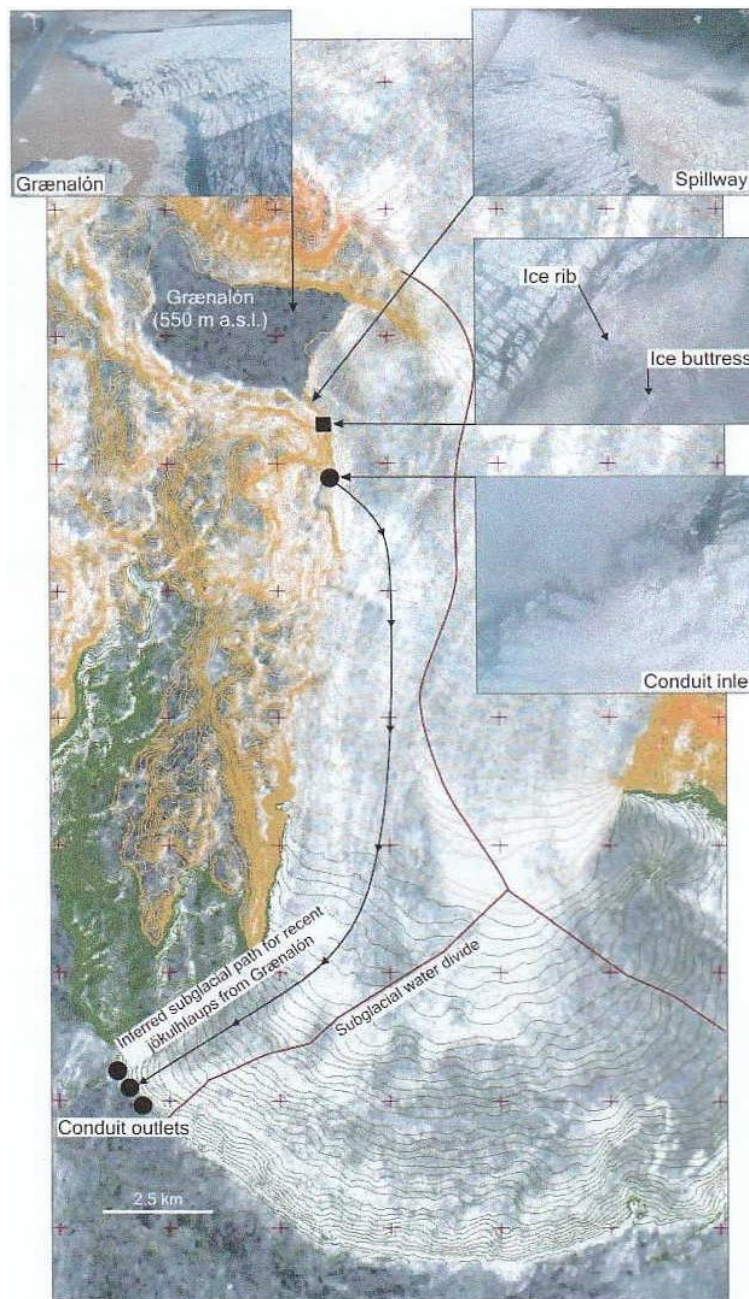


**Figure 3.19** Map showing routing of subglacial jökulhlaups from Grænalón.

### 3.3.8 *Summary of jökulhlaups at Skeiðarárjökull*

Observations of volcanogenic and limnoglacial jökulhlaups at Skeiðarárjökull have provided valuable insight into englacial routing and controls during glacial recession. As the ice surface lowered and the glacier margin receded within its overdeepened basin, proglacial drainage has altered accordingly, collecting within the depression as lakes and flowing parallel to the glacier margin. These factors served to alter the impact of jökulhlaups, restricting floodwaters to a few outlets that bypassed the proximal sandur, as well as increasing the erosive capacity of the water by acting as a sediment trap. Observations of the emplacement of supra- and englacial material during the catastrophic

November 1996 flood revealed that the existing conduits were not capable of channeling the influx of meltwaters, resulting in the generation of new channels, hydrofracturing the ice, and depositing sub- and englacial sediments via supercooled waters. Numerous macro- and meso-scale landforms were emplaced including eskers, an ice-walled canyon, a tunnel valley channel, fracture fills, large ice blocks and kettle holes, obstacle marks and alluvial fans. Perhaps most importantly, however, was the recognition of temporal and spatial variations during the single event that resulted in a variety of landforms that could be tied to different phases of the flood. Recognizing these landforms, and how they have altered over the last ten years, may enable this study to locate older signatures of jokulhlaups on the sandur, as well as attempt to quantify the persistence of a single event on the long-term evolution of the sandur.

### **3.4 Post-depositional modification of proglacial outwash at Skeiðarárjökull**

#### **3.4.1 *Introduction***

Initial studies of buried ice at Skeiðarárjökull focused primarily on documenting the extensive landforms and melting processes while only briefly exploring the emplacement mechanisms (Jewtuchowicz, 1971, Klimek, 1972, Bogacki, 1973, Churski, 1973, Jewtuchowicz, 1973, Klimek, 1973). These studies attributed most of the large bodies of buried ice adjacent to Skeiðarárjökull to be the result of retreat of the margin and emplacement of sediment upon the stagnant ice front via ice marginal fans. The expansive 1890 moraine that characterises much of the central sandur was recognised as a portion of the glacier broken off during retreat or separation by the erosive action of ablation waters (Galon, 1973a). Numerous dead ice fields across the front of the glacier formed by ‘meltwater and debris cover’ were also documented as well as dead ice ridges and series of ridges parallel to the glacier (Jewtuchowicz, 1973). Observations of the development of smaller forms created by differential melting were documented such as dirt cones and dirt bands (Wojcik, 1973a).

The observations of these expeditions appear limited to the processes active at the time, although Galon (1973a) recognised that these dead ice regions developed as a function of the internal structure of the glacier itself (crevasse systems, medial moraines, shear planes), yet limited work focused on the emplacement mechanisms. Numerous eskers were observed, although their origin was attributed to the melting out of englacial conduits that later infilled with debris as the ice roof collapsed or was let down by the melting medial moraines (Figure 3.20a) (Jewtuchowicz, 1973). These investigations did,

however, detail meteorological conditions, as well as the various melting and erosive processes present along the margin.

In a similar manner to previous researchers, the expedition observed that secondary alteration proceeded at more than one rate. Jewtuchowicz's (1973) three-stage model identified three stages: 1) intensive ablation that results in thick debris layers over the ice, 2) following burial melting leads to deformation (lower, rounded features) resulting in the appearance of chaotic kettles and basins (Figure 3.20b) and 3) thermokarst melting leads to the formation of proglacial lakes as the depression collects water (Jewtuchowicz, 1971, Jewtuchowicz, 1973). This cycle of development of dead ice fields was proposed to result in the 'rapid and irregular' retreat of the glacier edge, which in turn intensifies the acceleration. However, the volume of material emplaced across the sandur (in some places in excess of 4 m) is unlikely to have been emplaced due to the simple process of 'intensive ablation'. While these authors recognised that large portions of the terminal moraines had been removed/buried by large volumes of sediment and meltwater, they did not examine these features in detail. Later studies at Skeiðarárjökull paid greater attention to the mechanisms responsible for deposition of material within and upon the ice generated by individual, recent surges and jökulhlaups.

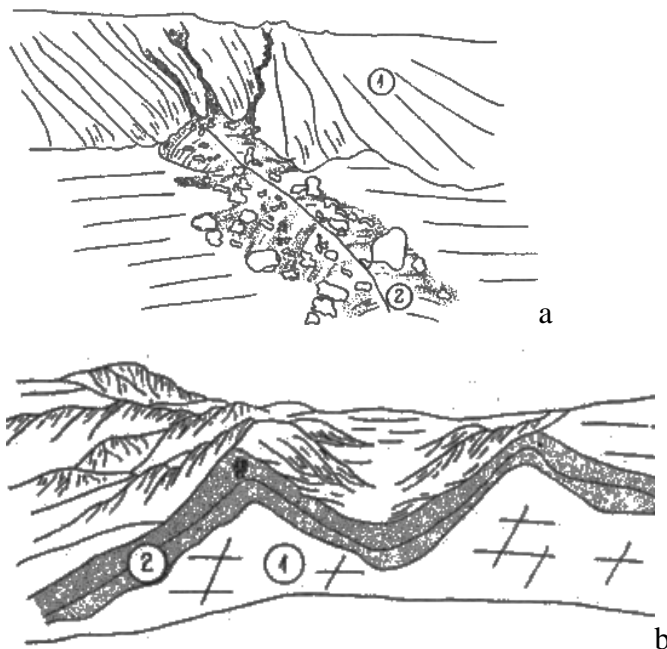


**Figure 3.20** Observations of melting at Skeiðarárjökull by Jewtuchowicz (1973); a) accumulation moraine ridge transverse to the glacier edge (1) glacier ice, (2) moraine ridge and b) bending of layers caused by dead-ice melting (1) dead ice, (2) sand layers.



### 3.4.2 *Emplacement mechanisms: surges and floods*

Recent investigations of secondary alteration at Skeiðarárjökull have focused on observations made following the 1991 surge and the 1996 jökulhlaup following the rapid retreat of the glacier margin as described in the previous sections. These have included observations of buried ice bodies emplaced via supra- and englacial processes: arterial fracture outlets formed via hydro-fracturing, alluvial fan emplacement, multiple and single channel outlet and esker/conduit systems, and the incorporation of ice blocks within/above sediment (Björnsson, 1997, Roberts et al., 2000, Roberts et al., 2001, Russell et al., 2006) during the November 1996 jökulhlaup. Similarly, the ability of surges to emplace large blocks/ridges of ice and debris via thrusting was investigated during the 1991 surge, as well as the emplacement of numerous large alluvial fans and the later transportation of large ice blocks during surge termination (van Dijk, 2002, van Dijk and Sigurðsson, 2002, Björnsson et al., 2003, Russell et al., 2006). GPR studies carried out in 2006 on the double embayment revealed 12 m of sediment overlying buried ice, the material being reworked by rotational slumping as well as normal and reverse faulting (Woodward et al., 2008).

The 1996 jökulhlaup also widened the Gígjukvísl gap by 200%, exposing a 30 m thick section of glacier ice buried within the 1890 moraine complex (Russell et al., 1999b). The horizontally foliated glacier ice was overlain by 2-5 m of poorly sorted, loosely consolidated gravel and sands; further bodies of ice were later identified beneath 3 - 4 m of debris on either side of the channel using geo-electrical resistivity surveys in 1999-2000 (Everest and Bradwell, 2003). Based on their estimates, they suggest that the moraine complex had persisted for over 200 years, highlighting the need for caution in utilizing radiocarbon dating, lichenometry and cosmogenic surface-exposure dating in deglaciated regions. Molewski and Olszewski (2000) also documented a similar deposit of buried ice over 18 m thick exposed at the fresh sections; their interpretation of this ice-cored moraine suggests that the buried ice was emplaced as a result of sequential re-advances, indicating the complexity of attempting to determine the history of such features (Figure 3.21).

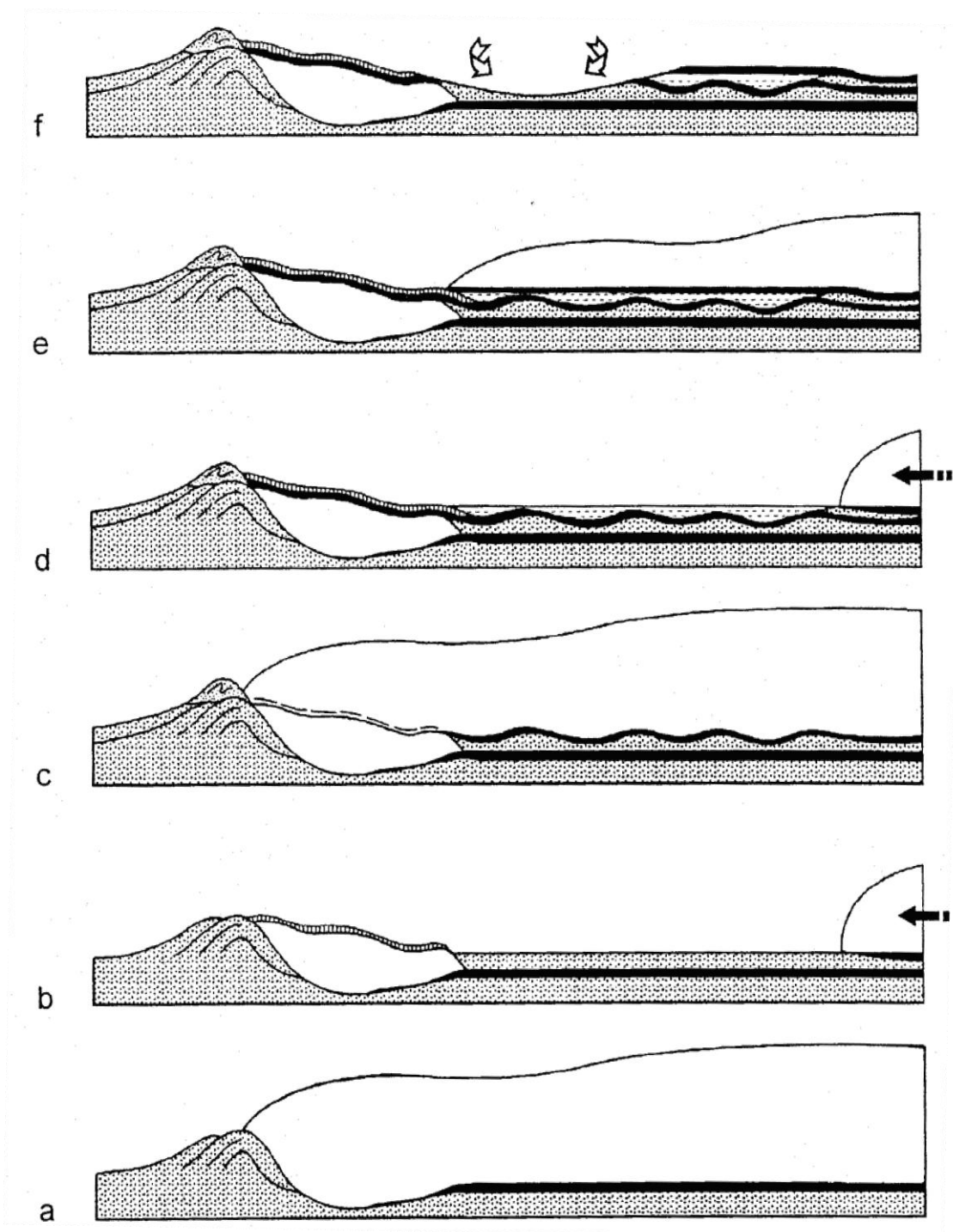


**Figure 3.21** Molewski and Olsewski's (2000) interpretation of the development of ice-cored end moraines due to a series of glacier advances near the Gígjukvísl river Gap, Skeiðarársandur based on exposed stratigraphic sections. a) Following an advance of Skeiðarárjökull, a period of retreat, b) leaves behind ice at the terminal moraine, covered by a deposit of till; a further advance over the existing ice creates a sharp unconformable contact, c) the next episode of retreat deposits till that buries the ice again, d, e, f) and a lateral fluvial system develops behind the ice cored moraine.

### 3.4.3 *Summary: post-depositional modification at Skeiðarárjökull*

Post-depositional modification through back- and down-wasting mechanisms has been observed along the margin of Skeiðarárjökull for many decades. Large bodies of ice buried beneath >1 m of sediment have been identified in cross sections, through geo-

electrical resistivity surveys, and observed being emplaced during events such as surges and jökulhlaups. Little research, however, has been done to quantify the rate of melt, to determine the mechanisms for emplacement or to understand the long-term impact of this modification on landforms proposed to be used as diagnostic landforms of other large-scale processes. It is evident from the literature that there has been little done to examine the relationship between emplacement mechanisms and the rate and development of subsequent post-depositional modification in order to understand their role in the evolution of the sandur as a whole, including their effects on drainage development and glacier margin retreat. The observation that most of the sandur contains large regions of buried ice needs to also be taken into account when proposing models of diagnostic signatures and the long-term evolution of the sandur.

### 3.5 Summary of large-scale landsystem models and hypotheses

Landsystem models, processes and related hypotheses collected from the literature in Chapter 2 and 3 are presented in Table 3.3. These are presented in order of decreasing confidence as some landform models associated with jökulhlaups are quite common and have been observed for decades during actual flood events. For example, the landsystem model that *Proglacial landform signatures associated with jökulhlaups include kettled outwash fans, obstacle marks, channel modification and moraine dissection* (Maizels, 1992, Fay, 2002, Evans, 2003, Russell et al., 2006) has a much higher confidence (probable) than the more recent model that proposes *Landform assemblages consisting of fracture fills, single-event conduits and proglacial kettled outwash fans have been suggested by Russell et al. (2006) and Burke et al. (2008) are diagnostic of major outlets emplaced during single event, high-magnitude jökulhlaups*. This second model has only recently been proposed and may be subject to further modification through future observations or at other locales and therefore possesses of a lower degree of confidence (possible). Limitations to testing may include resolution of historical aerial photographs and resultant DEMs, lack of data regarding percentage of debris within ice or detailed climate information for various portions of the glacier.

As presented in Chapter 1, Chapters 5, 6 and 7 will evaluate the landsystem models and hypotheses relating to large-scale processes found in the literature by first attempting to identify them on historical imagery. Once identified, an attempt will be made to correlate processes or landforms to events or processes (such as jökulhlaups or surges) documented in the historical literature, maps or even folklore. If events occurred that support the

model, then it is probable that the landforms are associated with it; if there is no known event or process documented in the literature to correlate a landform or process observed on the imagery, it is possible that the landforms are associated with the process suggested by the landsystem models and hypotheses – it is also possible that not all events have been recorded, particularly minor one. It is, however, acknowledged that not all landforms and processes in the literature will be found; these are not testable in this study. However, where landforms and/or processes are identified on imagery, they will be examined and their evolution over time documented in order to expand existing models and processes in the literature. These observations will be used to test the validity of hypotheses found in the literature and, where applicable, derive new hypotheses.

<b>Landform models, processes and hypotheses related to diagnostic signatures and processes of large-scale glacier margin fluctuations, jökulhlaups and meltout</b>	
<b>A. Margin fluctuation models and hypotheses</b>	
<b>Margin fluctuations – landsystem models and processes</b>	
A.1	Numerous landform assemblages have been proposed to be diagnostic signatures to differentiate glacier surges including: thrust block moraines, ice locks and evenly-spaced, ice-contact alluvial fans (Boulton, 1967, Sharp, 1985a, Croot, 1988, Knudsen, 1995, Evans and Rea, 1999, Russell et al., 2001a, Benediktsson et al., 2008, Waller et al., 2008).
A.2	Following retreat, en- and sub-glacial features may be exposed including hummocky terrain, concertina eskers, flutes, drumlins, and crevasse-casts (Knudsen, 1995, Evans and Rea, 1999, Bjarnadóttir, 2007, Waller et al., 2008).
A.3	Glacier margin retreat may also leave hanging outlets, alluvial fans and overridden moraines on proglacial distal regions (Russell et al., 2001a, van Dijk, 2002, van Dijk and Sigurðsson, 2002).
A.4	Glacier retreat provides accommodation space, permitting the development of proglacial lakes and drainage parallel to the margin (Jonsson, 1955, Howarth and Price, 1969, Klimek, 1973, Gustavason and Boothroyd, 1987, Bristow and Best, 1993).
<b>Margin fluctuations - hypotheses</b>	
A.5	Fluctuations of glacier margins exert a direct control on the spatial distribution and rate of proglacial aggradation or incision (Maizels, 1979, Marren, 2002b).
A.6	Glacier margin advance/retreat may affect the geomorphology of the proglacial area without any alteration in sediment or water supply, as channel incision may result simply from the lowering of the upstream meltwater outlet (Marren, 2002b).
A.7	Glacier margin position affects proglacial drainage networks: during retreat, as channel incision may result simply from the lowering of the upstream meltwater outlet (Marren, 2002b) and result in braided stream patterns near to the glacier margin confined within an incising channel. During advance, braiding will become re-established on the recently abandoned outwash surface (Marren, 2002b) and braiding will develop further away from the

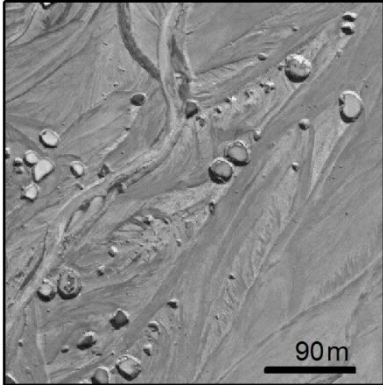
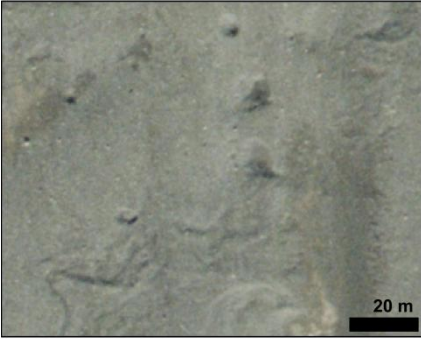
	margin (Maizels, 1979, Churski, 1973).
A.8	During retreat, channel incision and reorganization occur quite rapidly (Marren, 2002b).
<b>B. Jökulhlaups</b>	
<b>Jökulhlaups – landsystem models and processes</b>	
B.1	Proglacial landform signatures associated with jökulhlaups include kettled outwash fans, obstacle marks, channel modification and moraine dissection (Maizels, 1992, Fay, 2002, Evans, 2003, Russell et al., 2006).
B.2	Landform assemblages consisting of fracture fills, single-event conduits and proglacial kettled outwash fans have been suggested by Russell et al. (2006) and Burke et al. (2008) are diagnostic of major outlets emplaced during single event, high-magnitude jökulhlaups.
<b>Jökulhlaups - hypotheses</b>	
B.3	During a jökulhlaup, as pressure decreases flow may evolve from a complex fracture-fill network to conduit flow, demonstrating that it is possible to determine different phases of a jökulhlaup from the resulting landforms and sedimentary sequences (Piotrowski, 1997, Sjogren et al., 2002, Roberts et al., 2000, 2002, Russell et al., 2007).
B.4	The scale, type and position of jökulhlaup-related proglacial landforms may vary depending on the position of the glacier margin (Maizels, 1997).)
B.5	The position of the glacier margin plays a key role in the impact of flood (Maizels, 1997, Gomez et al., 2002).
B.6	Pre-existing topography may affect the routing of jökulhlaups and the location and type of resulting deposits (Magilligan et al., 2002, Russell et al., 2006).
<b>C. Post-depositional modification</b>	
<b>Post-depositional modification – landsystem models and processes</b>	
C.1	Post-depositional modification of landforms by large bodies of buried ice are characterised by normal faulting, hummocky topography and large depression / collapse structures (Boulton, 1972, Eyles, 1979, Fleisher, 1986, Krüger, 1997, Glasser and Hambrey, 2002, Spedding and Evans, 2002, Kjaer et al., 2006, Schomacker et al., 2006).
C.2	Even a thin layer (> 0.01 m) of debris covering glacier ice can provide sufficient insulation to retard the ablation process (Lister, 1953, Østrem, 1959, Nakawo and Young, 1981, Nicholson and Benn, 2006).
C.3	Melting takes place at two rates (Lister, 1953): primary, in which the main mass first disintegrates into smaller, isolated blocks (primary) creating a ‘thermokarst’ and secondary, when these isolated blocks ultimately melt completely, often at a much slower rate (Astakhov and Isayeva, 1988, Everest and Bradwell, 2003).
C.4	Emplacement of debris affects melting rate and controls development of glacio-fluvial systems; process and topography play a key role (Nicholson and Benn, 2006).
C.5	Ice blocks and obstacle marks are indicators of flood and flood magnitude; their position and morphology are diagnostic signatures of different flood phases providing: flow depth, margin position and ice thickness, and the location of major outlets during a single jökulhlaup (Klimek, 1972, Churski, 1973, Galon, 1973a, Galon, 1973b, Klimek, 1973, Boothroyd and Nummedal, 1978, Maizels, 1997, Maizels, 1992, Fay, 2002, Russell, 1993).

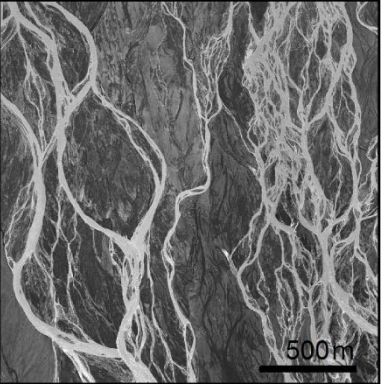
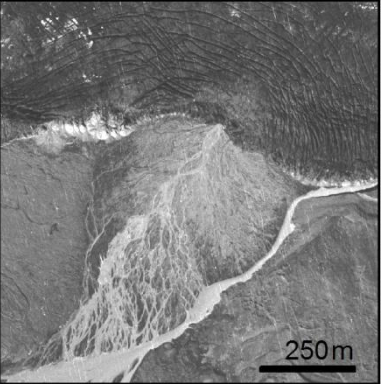
<b>Post-depositional modification – hypotheses</b>	
C.6	It is often difficult, if not impossible, to determine the initial emplacement processes and conditions of landforms following secondary modification (Johnson, 1992a, Schomacker et al., 2006).
C.7	High magnitude jökulhlaups may have buried much of the central snout of Skeiðarárjökull insulating the glacier ice, retarding ablation (Galon, 1973a, Thorarinsson, 1974).
C.8	Large volume of material on the central snout of Skeiðarárjökull resulted in differential ablation rates that led to the detachment of the snout and the subsequent development of the proglacial trench (Stokes et al., 2007).
<b>D. Hypotheses that address the overall evolution of the sandur</b>	
D.1	During high-magnitude jökulhlaups the presence or absence of an proglacial trench may act as a major control on depositional and erosional processes (Gomez et al., 2002) and on sandur sedimentology (Russell and Knudsen, 1999).
D.2	The present decoupled state of the glacier margin is atypical; majority of sediment were laid down by a coupled, diffuse distributed drainage system (Gomez et al., 2000).
D.3	The development of the landscape of Skeiðarársandur is characterised by a combination of sudden, high-magnitude, low-frequency events and diffuse gradual processes (Marren, 2002a, Russell et al., 2006).
D.4	Impact of flooding on sandur is ephemeral, and is quickly removed within a few years (Smith, 2006).

**Table 3.3 Signatures and persistence: the table above presents hypotheses in the literature concerning landform signatures associated with large-scale processes such as margin fluctuations and jökulhlaups, as well as their persistence on the sandur over time.**

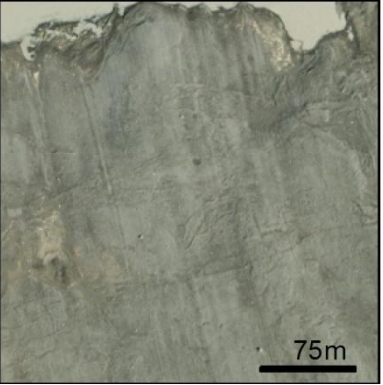
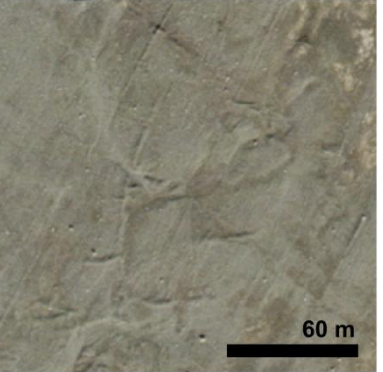
### **3.6 Guide to large-scale processes and landforms commonly found at Skeiðarárjökull**

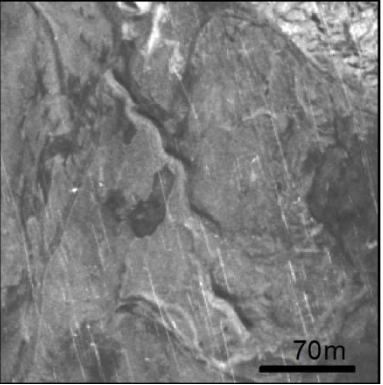
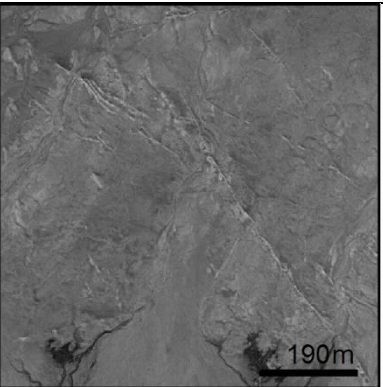
Landforms commonly found on proglacial terrains, as well as examples of these landforms on aerial photographs, are presented in Table 3.3. This table is presented to aid the reader in identifying landforms that are commonly found on proglacial terrains associated with temperate glaciers worldwide and have repeatedly been observed at Skeiðarárjökull. The table is presented in order to facilitate the identification of common landforms and associated events and therefore permit a more detailed discussion of more complex, controversial or newly discovered landforms or landform assemblages that may be documented in this study. When such less common, and more complex, landforms are encountered, the features are first described in detail and an emplacement mechanism proposed.

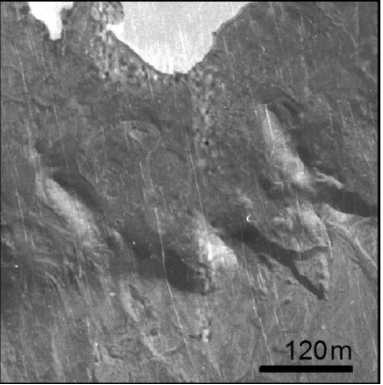
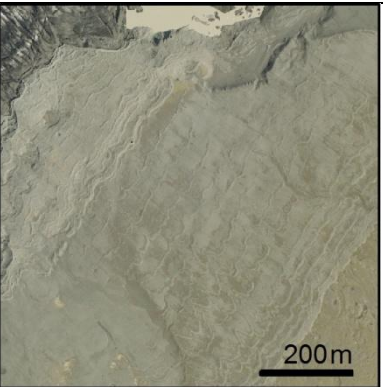
<i>Example of landform on aerial photograph</i>	<i>Landform</i>	<i>Feature/process</i>	<i>Source</i>
	Shadows around kettle holes pointing in direction of flow.	Obstacle marks	(Maizels, 1977, Fay, 2002)
	Circular depressions ranging from 1-50m+ in diameter. May contain water or ice blocks.	Kettle holes	(Maizels, 1977, Branney, 1995, Branney and Gilbert, 1995, Fay, 2002)

	<p>Shallow, interlacing streams or rivers containing pendant and or expansion bars.</p>	<p>Braided streams/rivers</p>	<p>(Krigström, 1962, Baker, 1973, Boothroyd and Nummedal, 1978, Maizels, 1997)</p>
	<p>Fan-shaped ramps emanating from outlet or apex. Fan may contain pitted surface, boulders and drainage.</p>	<p>Ice-marginal fan</p>	<p>(Boothroyd and Nummedal, 1978, Maizels, 1979)</p>



	<p>Low, linear ridge parallel to direction of glacier flow, often with boulder at head</p>	<p>Flutes and streamlined topography</p>	<p>(Boulton, 1976, Sharp, 1988)</p>
	<p>Low, irregular ridges of gravel and boulders orientated parallel and transverse to the direction of glacier flow</p>	<p>Crevasse cast ridges</p>	<p>(Sharp, 1985a, van der Meer, 1998, Bjarnadóttir, 2007)</p>

	<p>Sinuuous, steep-sided, sharp-crested ridges, single or anabranching in form</p>	<p>Esker</p>	<p>(Price, 1969, Shreve, 1985, Knudsen, 1995, Burke et al., 2009)</p>
	<p>Low, rectilinear ridges, often intersecting at right angles</p>	<p>Rectilinear fracture fills</p>	<p>(Rijsdijk et al., 1999, Roberts et al., 2000, Russell et al., 2006, Munro-Stasiuk et al., 2008)</p>

	<p>Elongated, rounded hills, often mantled with streamlined features (grooves) and boulders and flutes</p>	<p>Drumlin or drumlinoid</p>	<p>(Mooers, 1990)</p>
	<p>Low ridge laying perpendicular to glacier flow</p>	<p>Push moraine</p>	<p>(Sharp, 1985b, Sharp, 1988)</p>

**Table 3.4 Reference table of landforms used to identify some of the common landforms on aerial photographs.**



## Chapter 4 Principles of photogrammetry and field methods

---

*In this chapter, the basic principles of photogrammetry and the automated process of extracting elevation models from historical aerial photographs are presented. Issues, such as working with imagery of varying data quality, as well as common processing errors will be discussed, including the suitability of using historical aerial photographs to quantify landscape change over time. Field methods used to collect ground control points in the field are described and problems and challenges encountered at the site are also documented.*

---

### 4.1 Introduction to Photogrammetry

Photogrammetry, and indeed to an extent photography, has been employed by geomorphologists since its inception to document and analyse changes in landscapes over time, often in locations where physical monitoring or surveying of the region would otherwise be impossible (Wolf and Dewitt, 2000). Previous data extraction from photographs through analytical photogrammetry was both time-consuming and laborious. Topographic maps, for a time, were the only cost-effective means of creating three dimensional models, but the resolution was dependent upon the contour interval and suffered from the associated poor resolution (Smith et al., 1997). Advances in technology have provided researchers from a variety of backgrounds with the ability to derive digital terrains from these images, often at sub-metre resolutions, quickly and cheaply, enabling both volumetric quantification of change (Lane et al., 1993, Chandler, 1999, Lane et al., 2000, Baily et al., 2003).

Over the last twenty years, geomorphological studies of these digital terrains have grown rapidly, spanning topics as numerous as they are varied: monitoring of gully development and associated sediment production in New Zealand (Derose et al., 1998, Betts et al., 2003), glacier monitoring in the Swiss Alps (Baltsavaia et al., 2001b), estimating rock-glacier creep rates (Wangenstein et al., 2006) and quantifying volcanic avalanches in Nicaragua (Kerle, 2002). The majority of these studies involved creating surfaces before and after a depositional or erosional event and subtracting the elevation values of these surfaces to quantify the net change.

A review of these studies shows that such an approach, which may seem simplistic on the ‘surface’, may in fact hold several challenges, not least amongst them being the quality of the archival photographs available. In many regions, the canopy height of vegetation may need to be estimated and removed, the presence of steep cliffs and shadows may result in a high degree of interpolation and even smooth surfaces, such as water or clean ice, may similarly flummox the software (Gilbert and Scheifer, 2007). For example, in this study the barren nature of the sandur removes the necessity for stripping vegetation, attempts to model this landscape were complicated by braided streams, featureless plains, lakes studded with the subtle snouts of icebergs and the continued gradual settling of large regions due to the presence of buried ice.

A variety of techniques to generate digital terrain models are available for geomorphic analysis. Elevation data may be acquired via airborne and/or terrestrial laser scanning, global positioning systems and passive remote sensing techniques, including aerial photogrammetry (Wolf and Dewitt, 2000). Due to the sheer volume of archival aerial photographic data available, as well as due to time and fiscal constraints, creating digital terrain models from aerial photography, combined with a detailed differential Global Positioning Survey (dGPS), was deemed the most effective method to achieve the goals and objectives set for this project.

It has been recognised that when a high-quality digital scanner and the appropriate digital processing techniques are used, highly accurate models can be generated from historical images (Walker, 1996). However, as software and hardware becomes less expensive and digital terrain models are increasingly being applied to solve geomorphic problems, this influx of new users may lack a photogrammetric background and may subsequently be unaware of the limitations and error inherent in the models that they are presenting (Miller, 2007). In order to understand the benefits and limitations of spatial data derived

from aerial photographs, both recent and historical, it is important to understand the underlying principles of photogrammetry.

## **4.2 Principles of photogrammetry: How does it work?**

### **4.2.1 *Background***

While photogrammetry is the science of obtaining information from photographic images, analytical photogrammetry involves utilizing photographs to determine the location, size, shape and volume of surfaces on such images based on the relationship between the internal camera parameters and the corresponding points on the ground, otherwise known as the object space (Miller, 2007). This concept was employed by Laussedat in 1898 who first published a mathematical technique for obtaining measurements from aerial photographs taken aboard a hot air balloon. Since that time, advances in film and camera technology, coupled with the widespread use of aeroplanes both in war and peacetime, enabled aerial photographs to be employed as a common surveying technique during the 20<sup>th</sup> century (Wolf and Dewitt, 2000). Initially, photogrammetric measurements were obtained by using the analogue photogrammetric approach, where the user made measurements manually with a plotter. Over the last sixty years, however, advances in camera and computing technologies, coupled with the ability to monitor flights with GPS allows the automatic generation of maps from digital aerial photographs with greater precision and at a lower cost than was possible using manual processing methods (Lane et al., 1993). While these advances have reduced error and dramatically increased production time, the process of analytical photogrammetry continues to rely on the same techniques employed by Laussedat in the 19<sup>th</sup> century.

### **4.2.2 *Analytical photogrammetry***

Analytical photogrammetry is based on the condition of collinearity, the principle that states that an object in space, the projection centre, and the exposure station all lie along a straight line, demonstrated in Figure 4.1 (Miller, 2007). Ground, or Cartesian, coordinates may then be equated to the photographic coordinates, enabling measurements, such as distance and area, to be obtained from a photograph. Using two overlapping images taken from two different positions allows the measurement of height, and therefore volume, to be accurately measured. In order to understand this process of extracting volumetric data, it is first necessary to review the basic principles of vertical aerial photography, the concepts of stereoscopic viewing/stereo models and how measurements are extracted from these models. While the theoretical and mathematical principles may be found in

any photogrammetric textbook (Wolf and Dewitt, 2000, McGlone et al., 2004, Miller, 2007), the basic concepts are presented in the following sections.

#### 4.2.3 *Aerial photography basics*

A vertical, or near vertical ( $< 5^\circ$  tilt), aerial photograph is one taken from a platform, usually an aircraft, with the optical axis of the camera vertical to the ground as shown in Figure 4.1 (Miller, 2007). The camera's focal length ( $f$ ) is defined as the distance between the film plane and the centre of the lens when the lens is focused on infinity (Miller, 2007). As demonstrated in Figure 4.2, increasing the focal length (A and B) increases the field of view, and determines the ratio of distances between ground points on the film plane.

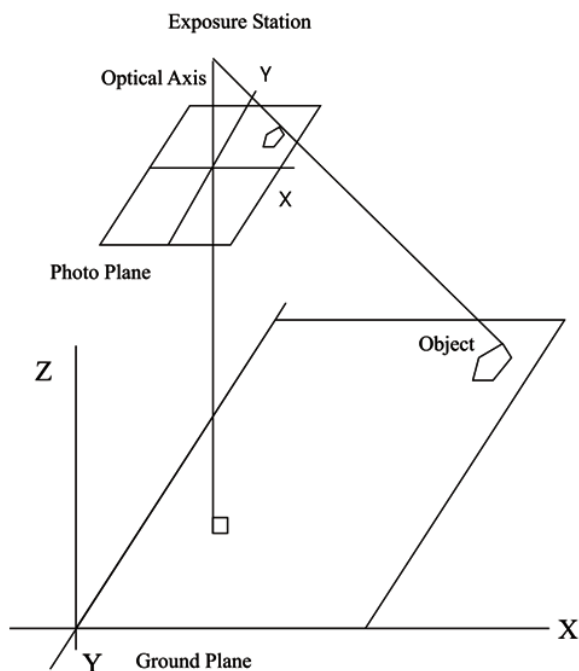


**Figure 4.1 Collinear relationship between an object on the ground, the object in the image and the position of the exposure station (modified from (Wolf and Dewitt 2000)).**

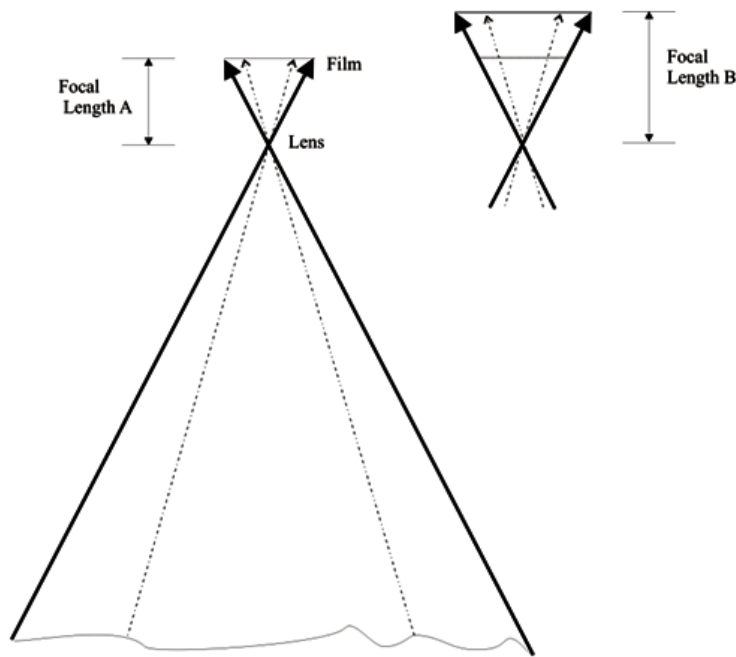


**Figure 4.2** Focal length B captures a wider ground area than focal length A, responsible for the differing distance ratios between the two the film planes.

To compare distances on the ground with those on a photograph, and to therefore obtain the scale of a photograph, it is first necessary to know both the focal length ( $f$ ) and the elevation of the camera ( $H'$ ) when photograph was taken (Figure 4.3).

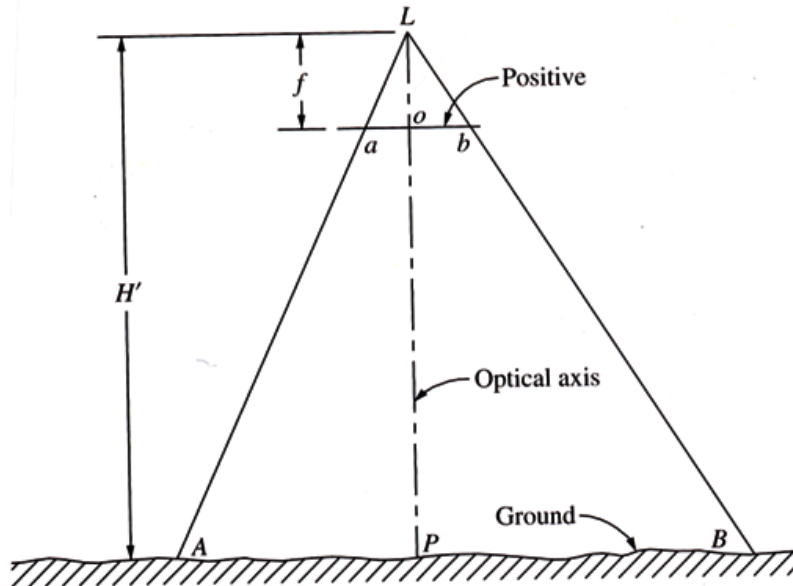


**Figure 4.3** Similar triangles demonstrating the relationship between elevation ( $H'$ ) and focal length ( $f$ ) with ground (A-B) and photo (a'-b') distances on a flat terrain (Wolf & Dewitt, 2000).

If the distance between two points, A and B, on the ground are known and the distance between the two corresponding points,  $a$  and  $b$ , on the photograph taken at elevation  $H'$  from the law of similar triangles, scale ( $S$ ) can be found by:



$$S = \frac{ab}{AB} = \frac{f}{H'}$$

**Equation 4.1 Determining scale (S) (Wolf and Dewitt, 2000).**

It is important to remember that while the focal length of a camera and flying altitude of the plane may remain constant, the topography of the ground below does not (Figure 4.4). This is particularly true of the glaciated regions examined in this study. Since elevation (H) will vary across the photograph while the focal length will remain constant, so will the scale vary throughout the photograph. However, calculating the average elevation from the highest and lowest points in the field of view, the average scale of the photograph (H) can be determined (Miller, 2007).

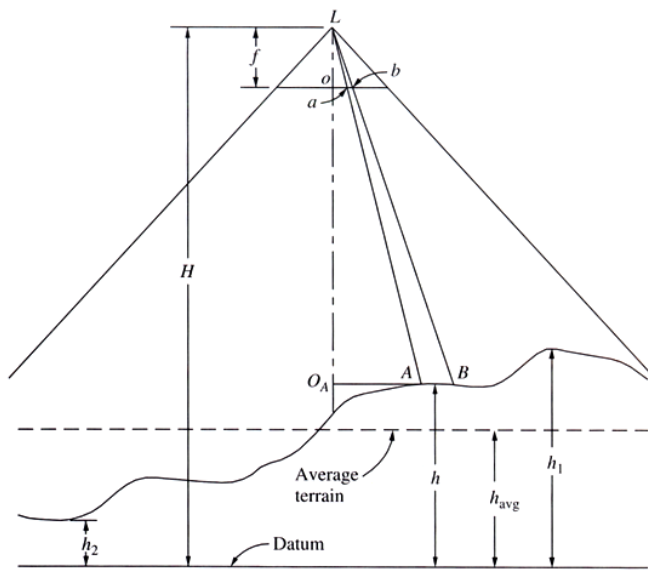


**Figure 4.4 Illustrates the effecting of uneven terrain (changing elevation (H)) on the scale of a vertical photograph, while focal length (f) remains constant and h(av) represents the average elevation height (Miller, 2007).**

#### 4.2.4 Parallax

When sightlines converge upon an object, the angle of this convergence depends upon the distance of the object from the observer (Miller, 2007). The closer the object is, the greater the angle of parallax. This perceived depth is utilised in stereoscopy: a pair of stereo-glasses, for example, allows the left eye to only see the left photo and the right eye to only see the right photo (Figure 4.5). The observer discerns the height of the building on the photos by associating heights A and B with the *faux* parallactic angles  $\Phi_a$  and  $\Phi_b$  (Miller, 2007).

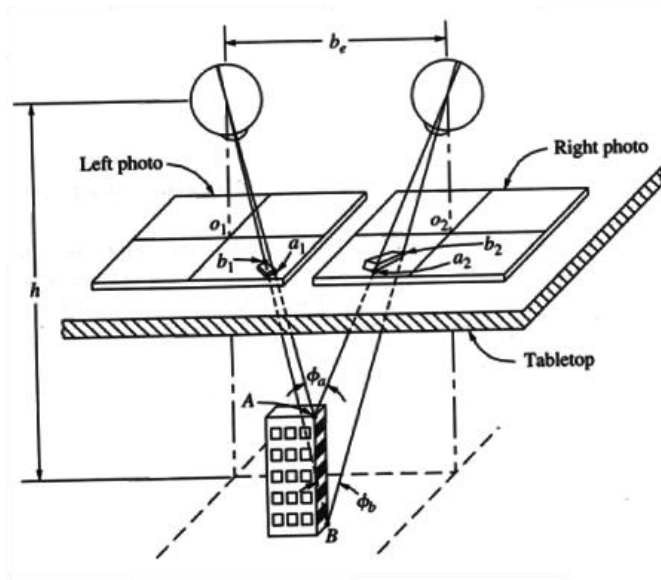


Figure 4.5 Perceived depth of photographs when viewed with stereo-glasses (Miller, 2007).

#### 4.2.5 *X and Y parallax*

In order to calculate the elevation and position of an object from aerial photographs, it is necessary to define the point on both photographs in terms of x and y coordinates. The offset of points along the x-axis, parallel to the direction of flight, can be used to determine the height of an object using the following method. Firstly, the x coordinate of the object must be measured on both photographs. Subtracting these two values provides the absolute parallax (Figure 4.6). For example, if the point was located at +12 mm and is -5 mm on the right, this would be an absolute parallax of 17 mm, or  $(12 - (-5))$ . Finally, the differential parallax must be measured, which is obtained by calculating the difference between the absolute parallax of the top of an object from the absolute parallax at the base of an object, shown in Figure 4.7 with a differential parallax of 0.7 mm (Miller, 2007).

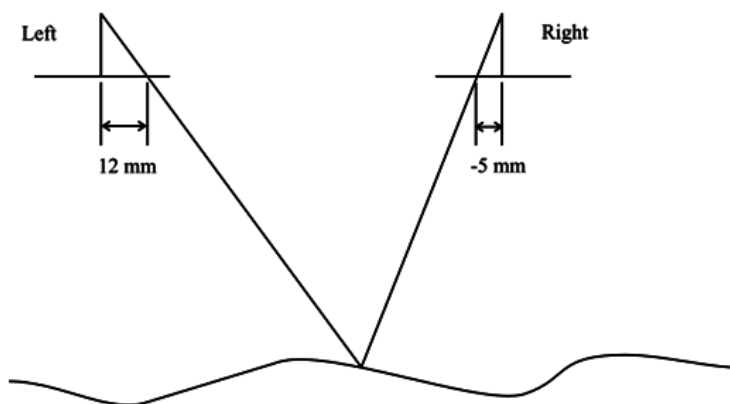
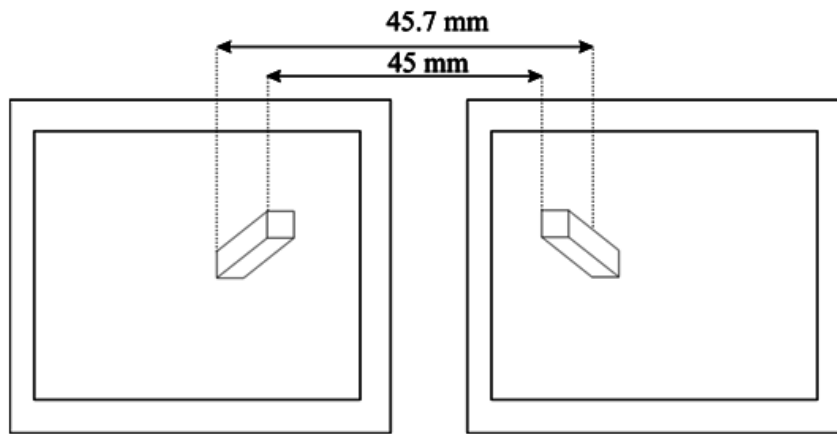


Figure 4.6 Absolute parallax (Miller, 2007).



**Figure 4.7 Differential parallax**(Miller, 2007).

The height of the object may then be calculated using:

$$\text{Object height} = \frac{dP}{P+dP} \times H$$

**Equation 4.2 Height of object using differential parallax** (Warner et al., 1996).

Where P is the absolute parallax measured at the base of the object, dP is the differential parallax, and H is the flying height. Displacement along the y-axis can be determined by measuring the y parallax, which may be caused by tilt or extreme elevation differences (common in glaciated landscapes) and must be removed during the automation process.

### 4.3 Stereomodel production process

The common method for creating an analytical stereomodel requires orientating the image in three steps: interior, relative and absolute orientation (Warner et al., 1996).

When these steps have been completed, the features in the image will be successfully mapped spatially to real-world coordinates. The resulting stereo model can then be used to produce elevation models for quantitative analysis, animated visualizations, or spatially accurate photographs (orthophotographs), or even photomosaics.

#### 4.3.1 Interior orientation

In order to accurately measure real-world terrain with a photograph, it is necessary to be able to reconstruct the parameters of the camera at the instant the picture was taken.

Cameras used in aerial photography are carefully calibrated in order to later replicate its interior orientation, and these attributes, or constants, are documented in the camera calibration certificates (Warner et al., 1996). These constants include camera focal length, fiducial marks, the principal point of autocollimation and the symmetrical and radial

distortion of the lens. The fiducial marks (Figure 4.8) are usually found in either the corners or along the edge of a photograph (sometimes both) and are used to provide a two-dimensional reference system for the photograph (Warner et al., 1996). The principal point, where the principal axis intersects the film plane, is determined by the intersection of lines drawn between opposing fiducial marks, and coincides with the point on the image plane perpendicular to the centre of the lens (Miller, 2007). Radial and symmetrical distortion is a by-product of manufacturing lenses, and like the rest of the values for these constants, their corrections can be found with the camera calibration certificates that may be provided with the imagery (Wolf and Dewitt, 2000).

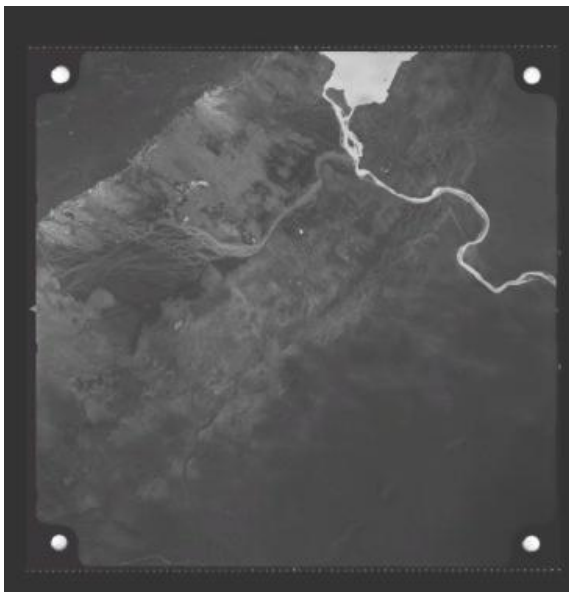


**Figure 4.8 Fiducial marks on a typical aerial photograph found either in the corners or along the edge of a photograph.**

In order to relate points in a photograph to those on the ground, however, it is necessary to establish a coordinate system for both. While terrestrial maps commonly employ latitude/longitude or northing/easting coordinates, aerial photographs have their own conventions. The x-axis on a photograph is parallel to the direction of flight, while the z-axis is the flying height and the y-axis is perpendicular to both: an aeroplane, not being a stable platform, may rotate around each of these axes, defined by  $\Phi$  (phi),  $\Omega$  (omega), and  $\kappa$  (kappa) (Warner et al., 1996). If the plane dips its nose, it is termed a phi rotation, rotating about y-axis. If the plane tips its wings, it is rotating on the x- axis (the direction of flight) and is termed an omega rotation. The kappa, rotation about the z-axis, is also the flight direction, and often the only angle obtainable from historic flight planning maps (Warner et al., 1996). For all of the photos in this study, the phi and omega rotations were assumed to be negligible.

#### 4.3.1 *Relative orientation*

Once the internal orientation and coordinate system of a photograph has been determined, it is then necessary to establish the angular and positional orientation of two photographs with respect to each other, otherwise known as the relative orientation (Wolf and Dewitt, 2000). Figure 4.9 demonstrates how this relative orientation is determined by setting values for the left hand photograph to zero, as well as fixing  $Z_{L1}$  to  $f$  and assigning the distance  $X_{L2}$  of the right photograph equal to the photo base  $B$ . Using collinearity equations, it is possible to solve for the variables  $Y_{L2}$  and  $Z_{L2}$ . These equations are described at length in photogrammetry text books (Wolf and Dewitt, 2000, Miller, 2007), but are presented briefly below.

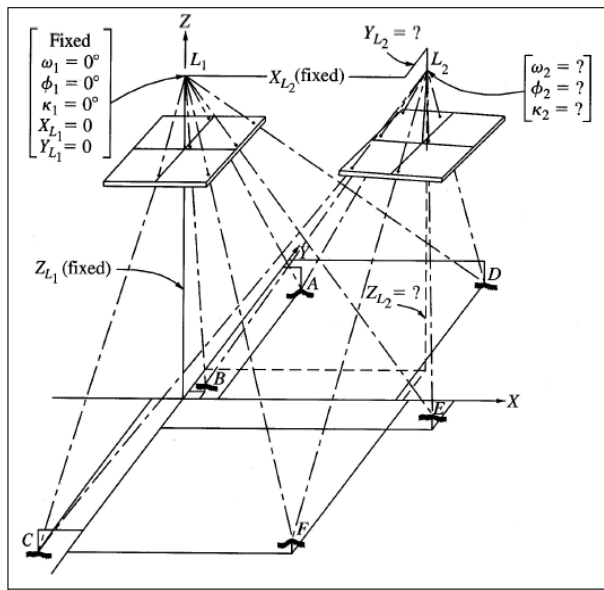


**Figure 4.9** Diagram of relative orientation between two aerial photographs (Wolf & Dewitt, 2000).

Given that light reflected from a point on the ground travels in a straight line through the lens and onto the exposure station,

$$\begin{pmatrix} x \\ y \\ z \end{pmatrix} = kM \begin{pmatrix} X-X_0 \\ Y-Y_0 \\ Z-Z_0 \end{pmatrix} \quad \text{Equation 4.3}$$

Where  $x, y$  and  $z$  are the coordinates of a point in the image space (such as the photographic negative), while  $X, Y$  and  $Z$  are the coordinates of the point in the object space (on the ground), and  $X_0, Y_0$  and  $Z_0$  are the coordinates of the perspective centre of the lens and  $k$  is a scale factor (Lane et al., 1993).

$$M \text{ is the rotation matrix} = \begin{bmatrix} m_{11} & m_{12} & m_{13} \\ m_{21} & m_{22} & m_{23} \\ m_{31} & m_{32} & m_{33} \end{bmatrix} \quad \text{Equation 4.4}$$

The rotation matrix elements ( $m_{11}$ ,  $m_{12}$ ...) are a function of  $\omega$ ,  $\phi$ , and  $\kappa$  on Figure 4.10, and are required to determine the position of the object space coordinates relative to the ground coordinates. Expanding upon this relationship for a point upon the ground, a corresponding point on the photograph exists:

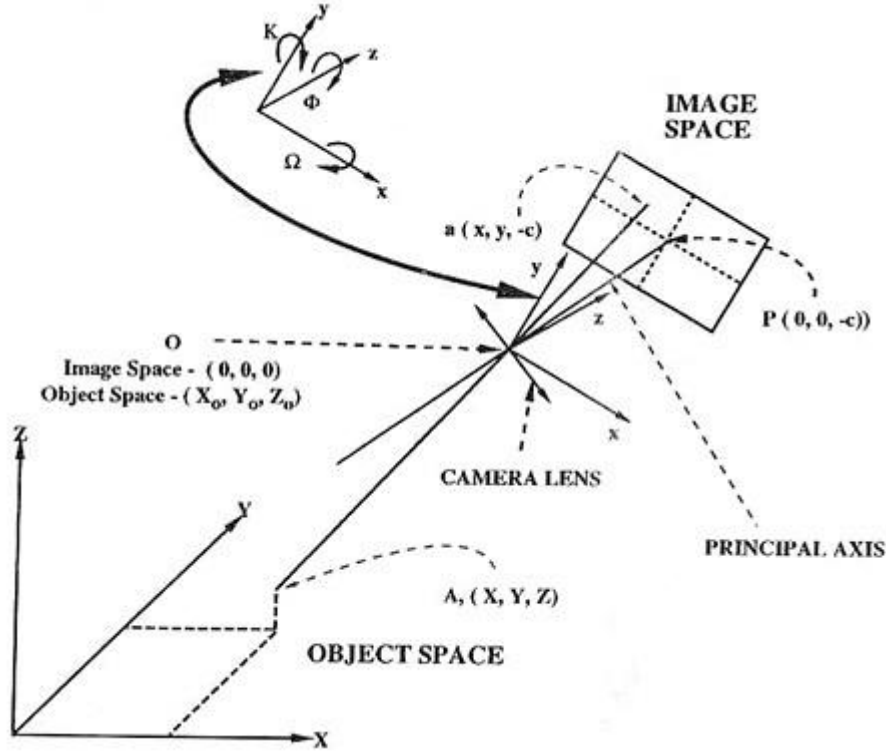


Figure 4.10 Presents the relationship between a point in object space and the corresponding point within image space (Wolf and Dewitt, 2000).

$$x = \frac{-c[m_{11}(X - X_0) + m_{12}(Y - Y_0) + m_{13}(Z - Z_0)]}{[m_{31}(X - X_0) + m_{32}(Y - Y_0) + m_{33}(Z - Z_0)]}$$

Equation 4.5

$$y = \frac{-c[m_{21}(X - X_0) + m_{22}(Y - Y_0) + m_{23}(Z - Z_0)]}{[m_{31}(X - X_0) + m_{32}(Y - Y_0) + m_{33}(Z - Z_0)]}$$

$c$  is the focal length of the camera.

Equation 4.6

From (Lane et al., 1993)

The advantage of these equations lies in the fact that if the points on the image and the ground are known, then other unknown variables, such as focal length, may be solved for, or distortions within the camera lens corrected for, allowing for such advantages of using nonstandard cameras or even photographs taken from angles greater than  $10^\circ$  (Lane et al.,

1993). A minimum of three known height (z) points and two plan ground control points are required for a successful application of these equations, although further points should be used to increase precision (Lane et al., 1993).

#### 4.3.2 *Absolute orientation*

Absolute orientation relates the stereomodel to ground coordinates using a three-dimensional conformal coordinate transformation (Wolf and Dewitt, 2000). An x, y and z coordinate in the stereo model must be matched to a ground point that also possesses a different x, y and z coordinate. In addition, the two systems may possess different scales and origins. In order to solve for the unknowns and accomplish the transformation of scale and rotation around all three axes, at least two horizontal and three vertical control points are required (Miller, 2007).

#### 4.3.3 *Analytical aerotriangulation*

The concepts and processes used to create a stereomodel from a pair of photographs can be used to link series of several adjoining photographs together in a strip. These strips may be sewn together using tie points, discussed below, to create blocks (Figure 4.11) that may be produced simultaneously using a process known as aerotriangulation (Miller, 2007). Creating these blocks in a single process is known as a ‘bundle adjustment’, where all of the light rays, or ‘bundles’, from the photographs that pass through the lens are all adjusted simultaneously. The ability to interpolate points based on only a few known ground control points provides the ability to model large areas with minimal fieldwork quickly and cheaply with modern digital photogrammetric workstations, or DPWs (Wolf and Dewitt, 2000).

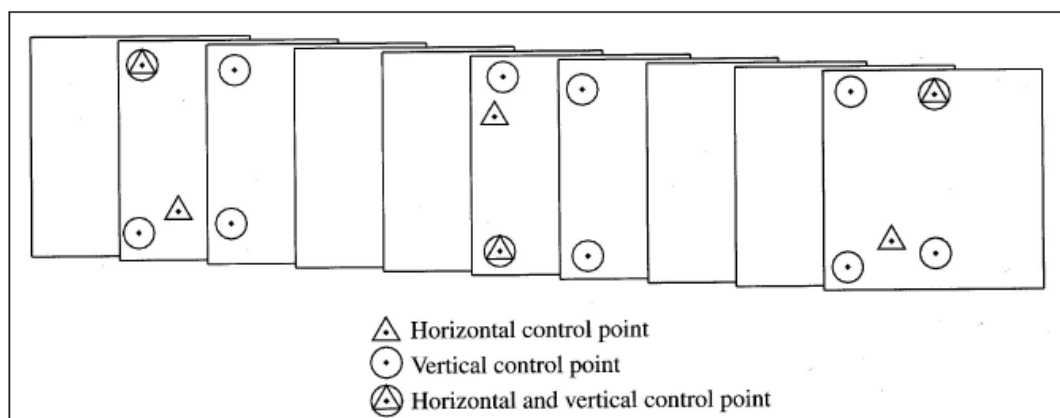


**Figure 4.11** Relative orientation between two aerial photographs (Miller, 2007).

#### 4.3.4 *Image matching*

Tie points are automatically generated using image matching, a procedure that identifies identical points found within the overlapping images. Instead of comparing two entire images at once, image matching utilizes a roving window that examines pixel values of small portions of the images at a time (Wolf and Dewitt, 2000). The pixels are compared for matching areas of gray-scale values (area-based) and edges (feature-based), or both. To further reduce the search area and increase computational efficiency, single lines can be searched by using the principle of epipolar geometry. This utilizes the previously described condition of collinearity and its associated condition, coplanarity, which states that an object, a camera and the images all lie on a common plane as shown in Figure 4.12 (Wolf and Dewitt, 2000). As shown, both ground point A and ground point A' of a different elevation, both appear on the left epipolar plane at the same point; however, ground point A only matches one point in the right epipolar plane. The roving window searches along a line for this geometric match and calculates the coordinate of this point, quickly obtaining matches across both images. DPWs produce DEMs by automatically matching these points and these points, may be extracted as coordinates, generally in predefined, regularly-spaced grids at intervals defined by the user (Miller, 2007).

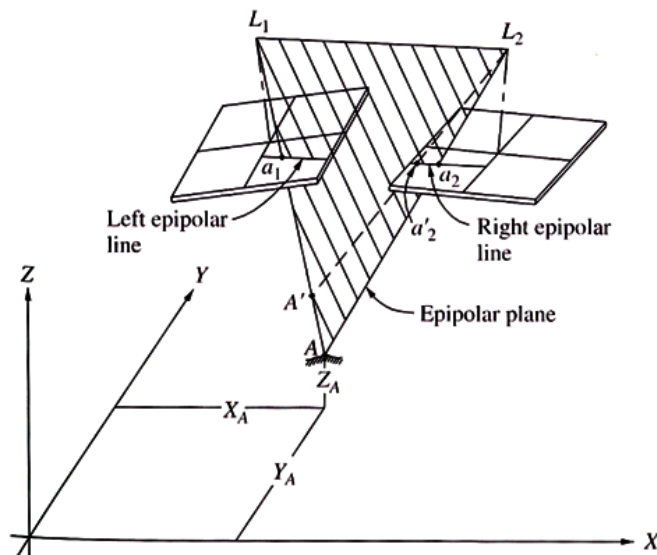


**Figure 4.12 Epipolar geometry.** Both ground point A and ground point A', with a different elevation, appear on the left epipolar plane at the same location; however, ground point A only matches one point in the right epipolar plane (Miller, 2007).

#### 4.3.5 *Extraction techniques*

*SocetSet* is a digital stereo feature extraction and light table software package created by BAE Systems that provides two methods for DEM extraction: adaptive and nonadaptive automatic terrain extraction (ATE) (Baily et al., 2003). The nonadaptive ATE technique



relies on the application of specific algorithms with associated parameters and filters tailored to specific characteristics of the image. The adaptive ATE alters its strategy as it encounters variations in the terrain as it crosses the image. As flat plains transition from hills to cliffs, for example, ATE adopts the best extraction strategy to match these variations. When creating models, it is important to tailor the extraction strategy to the characteristics of the landscape and the resolution of the image (Gooch and Chandler, 1999). In this study, the automated ATE option was utilised, due to the variable nature of the proglacial terrain. This strategy is often recommended for most terrains, as the ATE is capable of rapidly producing large numbers of points with relatively low residuals, although it is less reliable in areas of steep cliffs, extensive shadows or poor texture (Gooch and Chandler, 1999, Baltsavaia et al., 2001a, Baily et al., 2003). Error involved in this collection strategy, and error measurement associated with the collection of ground control and utilizing historical photographs, is discussed later in this chapter.

Regions with uniform texture, lighting or gradient often lack contrasting gray scale values, hindering the ability of the search window to find corresponding points, causing interpolation and decreasing the accuracy for these regions (Gooch and Chandler, 1999). Another factor that may affect data quality is sudden relief changes, which create geometric distortion shown in Figure 4.13. This occurs since two different areas of a terrain are seen from two different points of observation and do not appear to ‘match’. While commonly a problem during grid extraction, where points are produced at every stated interval regardless of the quality of the matching, triangular irregular network (Woodward et al.) models reduce this geometric error by ignoring points with poor suitability.

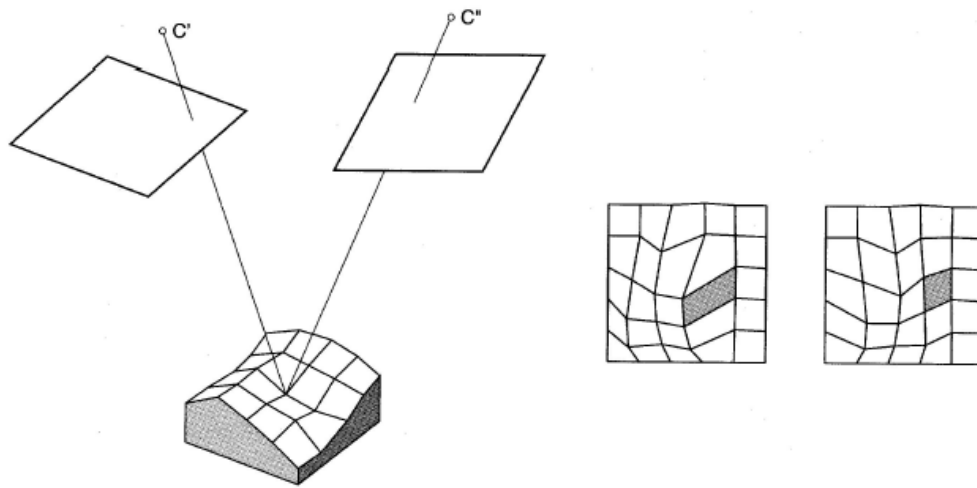


**Figure 4.13 Geometric distortion caused by elevation changes seen from different observation points (Miller, 2007).**

For the purposes of this study, DEMs were extracted at two resolutions: large (i.e. 10 x 10 m, or 20 x 20 m) to compare against the DEMs provided by Landmælingar Íslands and create large mosaics. Smaller, 5 x 5 m, grids were produced for more detailed studies. The DEMs were extracted using SocetSet's ATE area matching method using low smoothing, high precision and medium breaklines and exported as an ASCII text file.

#### 4.3.6 *Visualisations*

In addition to producing digital elevation data, SocetSet is also capable of producing several other products useful in analyzing and viewing terrain. These products include the ability to create virtual 'fly throughs' of the scene and other two-dimensional products that may be viewed in printable (and more portable) formats, including anaglyphs, that render the 3D terrain in two-colour layers slightly offset from each other to simulate depth perception and orthophotographs. Orthophotographs are images possessing the planimetric precision of a map. Just as aerial photographs can be used to create DEMs, DEMs can be used to spatially correct imagery. Collinearity equations can be used to match the  $x$ ,  $y$  and  $z$  coordinates of a point  $P$  in a DEM array with the  $x_p$  and  $y_p$  coordinates on the photograph (Figure 4.14) (Wolf and Dewitt, 2000). This process, known as differential rectification, removes from the photograph the effects of camera tilt and terrain displacement. This can then be transformed to match the row and column coordinates of the digital image. This process is repeated across the entire array to produce a final orthophotographs (Miller, 2007), although manual quality checks are frequently necessary.

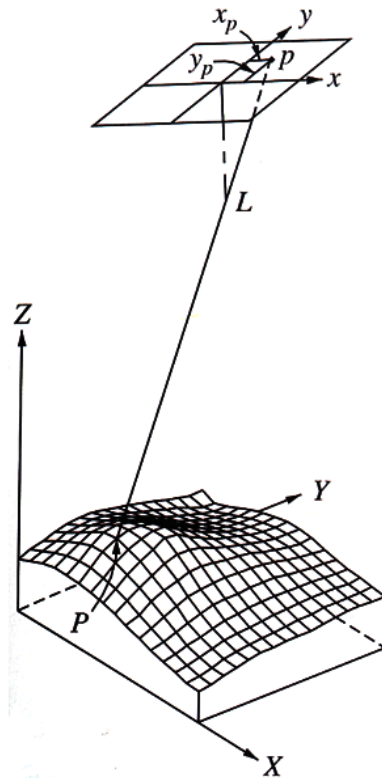


**Figure 4.14** Point P shown in its position on the DEM model and the corresponding coordinates for point p on the orthophotographs (Miller, 2007).

#### 4.3.7 *Summary of DEM production*

In summary, DEMs produced through the automated production process are dependent upon numerous factors including the terrain, the quality of the photographic image (film preservation, contrast, textures), camera and flight parameters, the scanning resolution of the image, the algorithms used during image matching and the final post spacing selected by the user (Smith et al., 1997). While the error introduced by these factors may be minimized, no DEM will be completely free of artefacts (Smith and Clark, 2005). Nonetheless, automated digital extraction has proven to be a cost-effective technique capable of rendering terrain models that may encompass large areas, both rapidly and with quantifiable error margins.

For future studies, it is recommended that surface matching algorithms be tested against future, repeated LiDAR surveys (and associated aerial photographs) to compare change over time. Surface matching orientates a photogrammetric DEM against an existing DEM (Buckley et al., 2004) without the need for acquiring ground control points and may be particularly useful for measuring change in regions that may be inaccessible by foot, or are newly exposed/formed and, as such, lack ground control points. This technique was not applied due to the poor quality of many of the historical photographs and the fact that the area is subject to region-wide melt out and ice surface fluctuations. However, as the

technique is improved, it may be a valuable venue for further study for parts of the field areas that demonstrate relative stability.

#### **4.4 Methods and site selection**

When selecting regions of the proglacial area to study, it was important to locate sites that had experienced change but also contained stable zones with large-scale, persistent features that could be collected to use as control points. It was also important to select sites that were present in as many photographs as possible, as many of the historic aerial photographs/flight paths did not possess the same footprint.

##### **4.4.1 *Aerial photograph acquisition***

All vertical aerial photographs of the field site collected for DEM creation were obtained from the National Land Survey of Iceland, Landmælingar Íslands, who maintain an archive of aerial photographs for most of Iceland dating back to the 1940s. The images were scanned by Landmælingar Íslands with an Eversmart Jazz+ Scitex scanner, at a resolution of 2000 dpi and delivered as tagged image format (tif) files. Camera calibration documentation and flight lines drawn on 1:100,000 topographic maps were provided with the purchased images for all photographs taken after 1954. The black and white scanned negatives were purchased for the years 1965, 1968, 1972, 1975, 1979, 1986, 1992, 1997 and 2007. Photographs from 1945, taken by the U.S. Air Force, were also purchased from Landmælingar Íslands, who provided known flight elevations and camera focal lengths, but unfortunately the images lack standard fiducial markings, known flight lines or other camera information. All of the files obtained from Landmælingar Íslands vary in quality, scale, elevation and resolution. Many of the older negatives were poorly stored and are scratched and torn, have poor contrast or were actually scanned prints instead of negatives. The 1972 and 1979 photosets, due to coverage issues and cloud cover, were not processed as DEMs and only used as a visual aid. A recent survey, completed thanks to a NERC grant, was flown in 2007, and the colour, digital images were made available for this study.

Oblique colour photographs of the field site were also collected from previous years, courtesy of Dr. Andrew Russell and Andrew Gregory, and were also taken from a twin propeller plane at low altitude during the 2006 and 2008 field seasons. Low-resolution colour orthophotographs were provided by the Icelandic Roads Authority, Vegagerðin, for flights taken in 1997 and 2003 as jpgs, along with 10 m ASCII DEMs in ISN93.

#### 4.4.2 *Differential GPS survey*

A differential GPS (dGPS) survey was conducted between the glacier margin and Highway 1 using Thales-brand ProMark III units. Known sites surveyed by the Icelandic Roads Authority were used to establish control points. The daily collection routine involved establishing a static base station on a tripod on a known landmark, while one or two rover units collected point features (Figure 4.15). An initialization period of fifteen minutes was required between each rover and the base station and is essential for the GPS unit to be able to synchronize its internally-generated code with the signal actively being received from the satellite. Once these two signals are synchronised, the dGPS unit is able to determine its geographic location based on the travel time between the satellite and the position on the ground (Leick, 2004). After initialization, a stop and go survey was conducted, with a rover remaining on a point for twenty seconds, with one second sampling intervals. However, should a rover or base unit lose satellite lock, either due to poor satellite configurations or user error, the units had to be re-initialised on a known point. Improper initialisation settings may also result in collecting useless data. All elevation data is presented as metres above mean sea level (m asl).



**Figure 4.15** Base station initializing (left) and rover unit (right) collecting a point feature.

In accordance with the requirements provided by the *Thales* vendor, only points with Position Dilution of Precision (PDOP) values of less than 3.0 were collected during this survey. The GNSS Solutions Mission Planning software was employed to determine periods during the day when the constellation of satellites would lack sufficient geometry, providing unacceptable PDOP. Due to the extreme latitude of the field site and the obstruction of the horizon to the north, east and west by the large basalt massifs and ice caps, there were often two one-hour gaps during the day that had poor, or negligible, satellite coverage; samples were not collected during these periods.

Contributing factors to data collection errors included atmospheric conditions and user error. Maintaining stability of the rover pole proved difficult during the duration of sampling due to strong winds and other adverse weather conditions, as well as the physical prowess of the volunteer manning the unit. It must also be noted that without the help of the EarthWatch volunteers, it would have been impossible to collect the volume of points required for this project in the given time span.

#### 4.4.3 *Ground control points*

Large-scale, persistent features such as terraces, kettle holes, boulders and ridges visible in all of the aerial photographs were collected with the dGPS units, although points along the crests of ridges and kettle holes were the most common feature collected during the survey (Figure 4.16). Point collection favoured unique, distinct formations. Several regions were unreachable due to melt-water or other topographic obstacles. Although features were selected based upon their visibility on the aerial photographs, an effort was made to ensure that features were as evenly spaced as possible across the region to ensure that widespread coverage is available for image rectification. Their number and type are listed in Table 4.1.

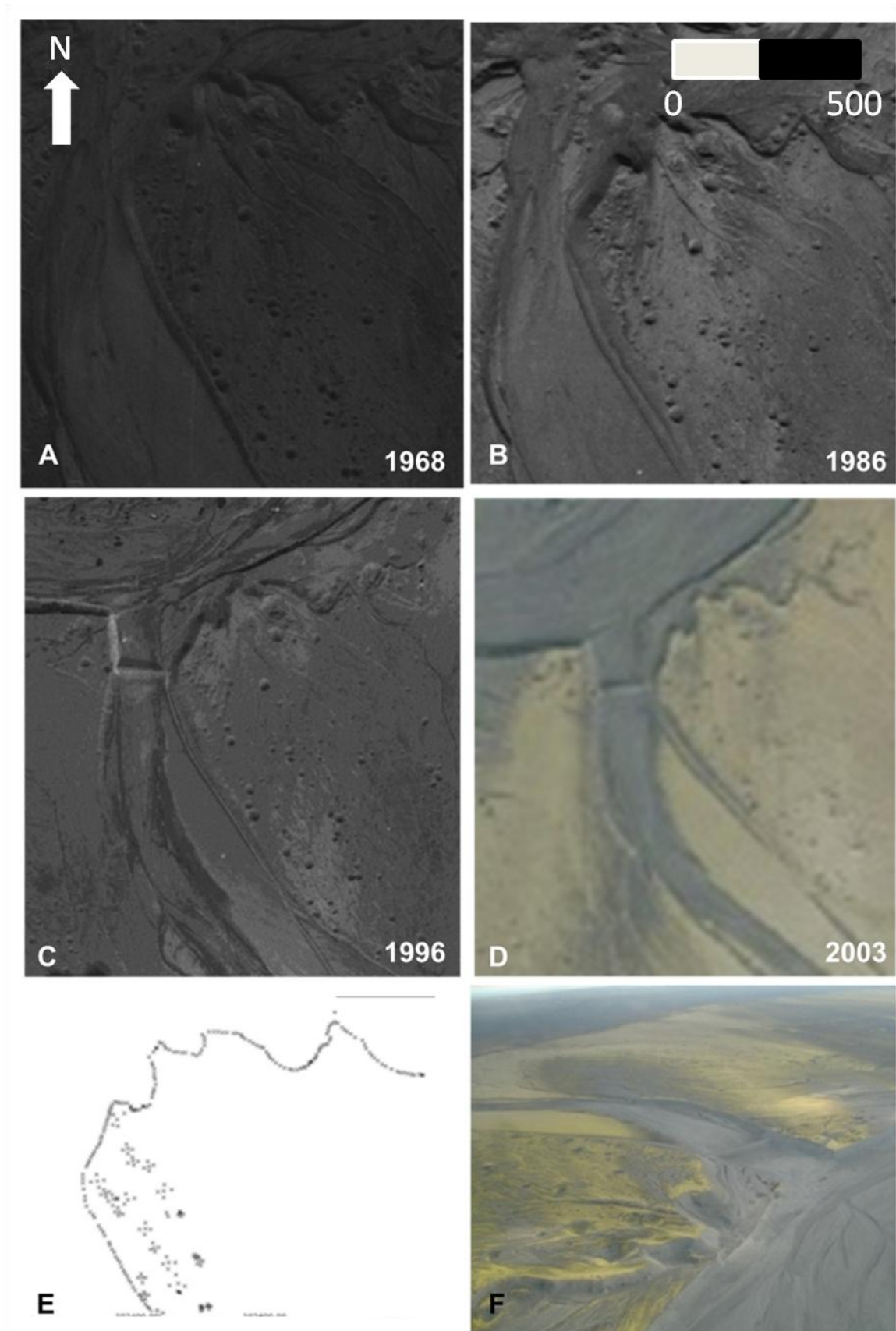


**Figure 4.16** An example of features documented in aerial photographs (a-d) at the mouth of the Haoldokvisl, such as kettle holes and ridges, collected with the dGPS equipment (e) and the corresponding features that have persisted over the past sixty years.

<i>Feature Type</i>	<i>Feature Count</i>
Kettle Holes (rim and centre points)	692
Moraine (ridge and base)	455
Boulders	127
Terraces	1850
Ridges	1478
Misc	499

**Table 4.1 Features collected with dGPS in the field for use in georeferencing images**

Terraces and large boulders proved to be the most accurate features for georeferencing the images. Kettle holes were also very useful; although easily spotted on the aerial photographs, mapping them in the field was challenging as it was difficult in undulating topography to ascertain which depression was being mapped. For this reason, only distinctive groupings of kettle holes were mapped to aid in later identification. Four points were taken around the rim of each kettle hole, at roughly equidistant positions at the north, south, east and west quadrant points measured with a Brunton compass, with a final point taken in the centre. Determining the exact break in slope of the rim of the kettle, or even the centre point, was often difficult. Kettles, as well as moraine ridges/terraces, may be delineated clearly by vegetation changes or steep slopes, but the transitional areas are not always so clearly defined. It is important to note that most of these features are subject to erosion by wind, rain, fluvial processes and settling/subsidence from melt out. Due to their persistence and distribution, boulders were the best target for dGPS collection; however, many regions simply lacked boulders of sufficient diameter that could be discerned in the photographs.

#### 4.4.4 *Post-processing*

On a daily basis, data was downloaded from the handheld units and processed using the GNSS Solutions software. Points were collected in NAD WGS84 Zone 28 North, both in Lat/Long and Northing/Easting format. When possible, erroneous satellite data was corrected by masking the individual signals of poor or erratic satellites. If this correction was not possible, the points were discarded, and a decision made as to whether it was worth recollecting the points in question or to carry on with the survey as planned. Points that fell within the acceptable error limit ( $< 3$  cm) were exported as a text file. Points were



corrected relative to a static station set up over a Vegagerðin-surveyed site at Svínafell, located 12 km to the east. The manufacturer (Thales) provided a precision of less than 3 cm on the x, y and z for surveys corrected to known Icelandic Roads Authority Survey station. This was deemed acceptable, as the goal was to measure large-scale change and matching the average mapped feature (kettle hole, slope edge, and even boulder) to a photo with a scale of 1:35,000 inherently possessed an error of 1- 3 m. While this is still acceptable within the scope of the project, cross-sectional profiles of the Súla and eastern Skeiðará depicted in this project are presented to highlight horizontal change (aggradation/erosion) as opposed to vertical change.

It was recognised early on in the project planning stages of fieldwork that much of the proglacial terrain may subject to subsidence due to ice melt or deflation by wind erosion over long periods (decades to centuries). In order to limit the scope of the project and generate landscapes suitable for comparison landscapes derived from the aerial photographs were to be compared to each other, maintaining an internal consistency. Further, by mensurating only the emplacement, erosion and modification of large-scale features and processes, it was considered the subsidence/deflation of the landscape would be within the vertical limit of error.

These x,y,z text files were brought into the mapping software provided by the vendor, MobileMapper, in an effort to overlie the collected points and the 1997 imagery to facilitate future data collection planning efforts. However, this software package proved cumbersome as it was necessary to manually research and enter the three-dimensional coordinates of individual points. Another limitation of the software was that it was unable to render full-scale versions of the imagery, to uniquely symbolise the points based on attributes), to label the points by id or to control how the imagery beneath was displayed, making it difficult to interpret. A copy of Leica Imagine software was provided by the University of Newcastle Geomatics department, thanks to Dr. Williams, that was capable of resolving these issues and was used for the remainder of the field seasons to create maps for planning purposes.

Upon returning from the field, the collected points were re-processed and exported into ESRI's ArcGIS for display and initial georeferencing of the images. The WGS84 coordinates were then transformed into local Icelandic coordinates (ISN93 datum) using the online transformation website Cocodat-i provided by Landmælingar Íslands. Conversion was necessary to compare ground control points and final DEMs against

those provided by Vegagerðin (in ISN93). Ground control points were selected after all of the available imagery was purchased and spaced as evenly as possible to ensure the best geometry in creating photogrammetric models. Due to the presence of the glacier to the north, the rivers and mountains on the western and eastern sides, and the lack of identifiable features south of the highway, this disproportionate concentration of points across the centre of the photographs will skew the RMS errors outside of these regions.

#### 4.4.5 *DEM construction*

DEMs were generated using Leica's SocetSet 5.3/5.5 (Ngate) software. Information such as flight direction, elevation and camera specifications (see previous sections) were entered when available. Triangulation (interior and exterior orientation) was accomplished for all photosets, although difficulties and solutions to various challenges are described below.

#### 4.4.6 *Interior orientation*

Images were imported into SocetSet and prepared for interior orientation. While the flying heights were provided by Landmælingar Íslands and the flight lines could be approximated from historical flight maps, camera type and position/axes not only varied from flight to flight, but so did their coordinate system and axes. It often took several attempts correct for left- vs. right-hand coordinate systems and varying camera orientations.

After the files were successfully imported, if they were discernable, the fiducial marks were measured in order to establish a reference x, y coordinate system for features within the image frame and to correct for any distortion such as expansion or shrinkage in the film (Wolf and Dewitt, 2000). The coordinates of the fiducials were measured using SocetSet's manual orientation; residual line and sample errors of less than 1m were accepted. As previously documented, the earliest photo set from 1945, did not possess any information other than flight elevation and camera focal length. While the flight direction was approximated based on the footprints of the photographs, the process of restitution was undertaken manually following the approach used by Smith and Clark (2005) (Smith and Clark, 2005). Four fiducial marks, although often only three were discernable due to the poor quality of the photograph, were measured in Adobe Photoshop, with the central 0, 0 of the axes defined by the intersection of these four, or three, points for all of the photographs. The mean values of these fiducials were calculated and used to locate the fiducials in Socet Set as described by Miller (2007a) and

Walstra (2006). However, due to the poor quality of the photographs, these images and resultant DEMs are only used for visual reference in this study.

#### 4.4.7 *Absolute orientation*

Once an internal coordinate system was established within the photographs, the control points measured in the field could be used to relate the image to the ground (absolute orientation). The ISN93 coordinates of the ground control points (GCPs) were imported as a text file and were used to identify points on the images. Once the x, y and z values of GCPs have been identified on both (or more) images, SocetSet can then perform point measurement automatically, using digital image matching (Baily et al., 2003). Check points (dGPS points measured in the field) were compared against the resultant photogrammetric models to measure consistency of the z that frequently produced errors of less than 3 m, often less than 1 m prior to manual cleanup ('post pushing'). Following all DEM cleanup, GCPs fell under 1 m. It should be noted that while the software was able to perform these calculations successfully to under one pixel, due to the high concentration of control points in the centre of the image (along the glacier margin) and the lack of points at the edges of the photographs, the images rarely 'passed' the blunder detection tool. However, as only DEMs of the glacier margin were extracted, this region should be internally consistent, as demonstrated by the accuracy of the check points.

#### 4.4.8 *DEM extraction*

DEMs were extracted from the photogrammetric models using SocetSet's internal Automatic Extraction image matching utility (Figure 4.17). Primarily, two DEMs were produced: large-scale, 10 x 10 m grids with medium smoothing, precision, breaklines and mass points were created across the entire glacier margin in order to create orthophotographs and assess the DEMs against those provided by Landmælingar Íslands, and smaller, 5 x 5 m grids with low smoothing, high precision and few breaklines were produced for areas undergoing detailed change studies.

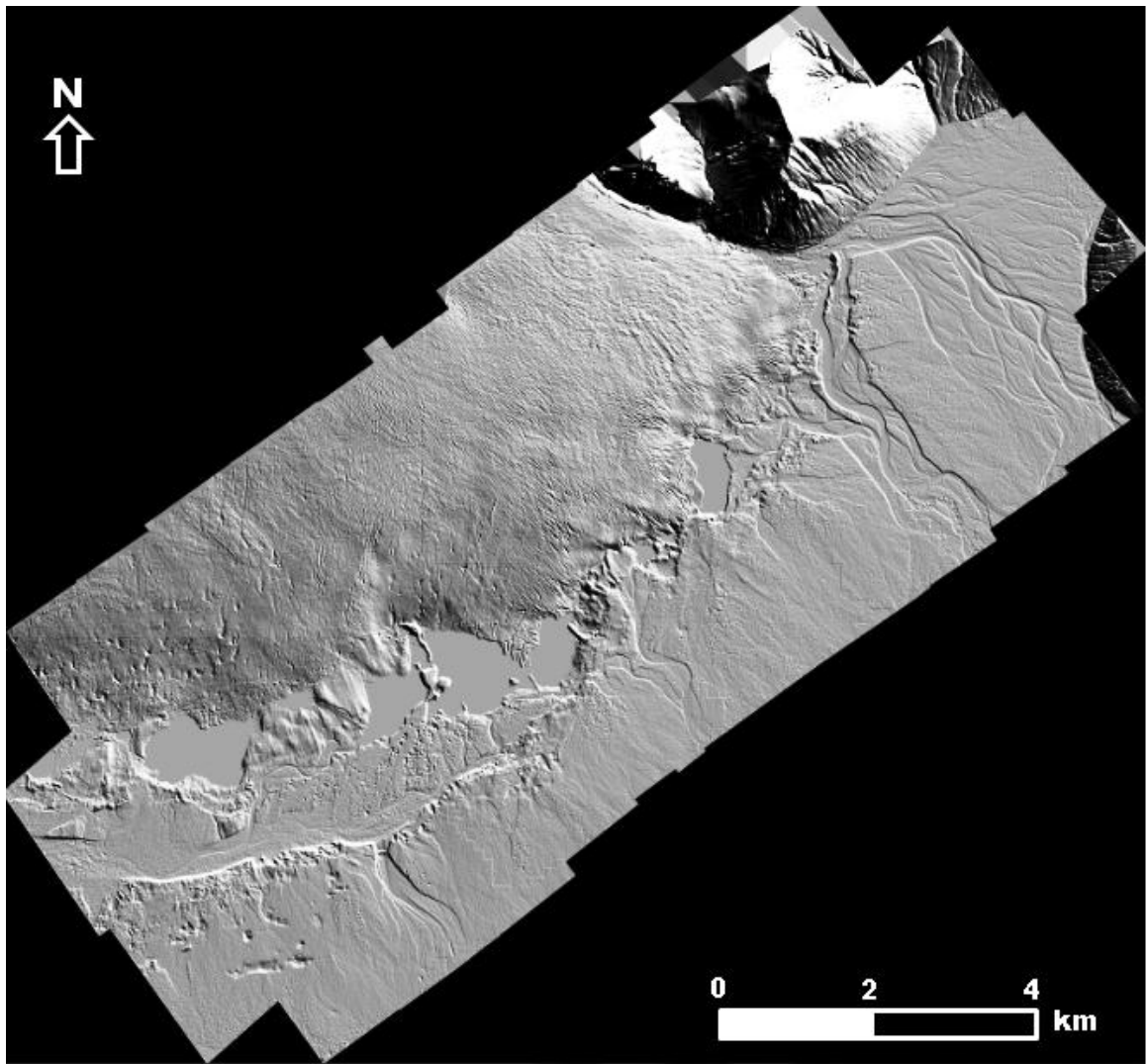


**Figure 4.17** Example of terrain-shaded relief DEM of the central and eastern margin of Skeiðarárjökull, depicted as a hillshade, extracted from 2007 aerial photographs using SocetSet 5.5 (after manual clean-up).

#### 4.4.9 *Mosaic and orthophotograph production*

In addition to generating DEMs, mosaics and orthophotographs were produced within SocetSet. The resulting mosaics (Appendix A) were produced in order to aid in visual inspection of the field area, while the orthophotographs were created to not only drape over the finished DEMs, but to aid in assessing the accuracy of the DEMs themselves.

#### 4.4.10 *Results*

The quality of the resultant DEMs was assessed in several ways, the most obvious being a visual inspection of the end product against the imagery and the DEMs provided by Landmælingar Íslands. The second method, previously described, entailed measuring the virtual DEM surface against the check points measured by dGPS in the field. While errant ground control points, those with high residuals, were occasionally removed and replaced with nearby points with lower error values and the photographs reprocessed, many were

left unless their values were a result of shadowing or texture rendered them unsuitable for use. However, often accurately measured points lying near the edge of the photograph that possessed larger than average residuals were not removed. Socet Set provides an additional internal measure of accuracy, ascribing each point in the image with a value, or figure of merit, that details how the point was generated. By assigning these points a symbol in ArcMap, or simply summarizing their values in a table, the user is able to ascertain the reliability of the points. On average, DEMs derived from all photosets displayed residuals of less than 1 metre in the centre of the photographs, and approaching 2 metres in regions with little ground control points or poor image quality.

#### 4.4.11 *Volumetric Change Detection: Processing*

Comparing surfaces constructed from two subsequent time periods (before and after) is often utilised as a cost-effective method to quickly quantify large-scale volumetric changes due to meltout, subsidence, flooding, human interference or other causes (Schiefer and Gilbert, 2007). In this study, volumetric comparisons between the various DEM sets possessing differing resolutions, however, present several difficulties. The datasets provided by Vegagerðin for the 2003 were delivered with only 20 m post spacings, and no ground control points were provided for either the 1997 or the 2003 series. When compared with the datasets and ground control points generated in this study, the z values for the Vegagerðin data sets change can differ up to 3 m, with no apparent correctable standard offset (Appendix B, Figures B8 and B9). Small-scale, subtle changes in the proglacial terrain over short time spans, between 1997 and 1992 for example, may be less than the margin of error, and the resultant DEM may display little or no change.

Comparing DEMs of the same resolution, created with the same ground control points, is the most reliable method to quantify change between stages. While the DEMs created from historical photographs in this study possess a resolution of 3 x 3 m and are internally consistent with z values averaging 1 m or less for GCPs and under 3 m for check points (see Appendix B), the field areas may often lie on the edge of the images, often the least accurate area of an optical exposure and the most susceptible to the later physical effects of deterioration and aging.

#### 4.4.12 *Error measurement*

Error, the difference between the recorded value and the actual value, is a theoretical quantity that can never truly be determined, and is often categorized into three types:

blunder (or gross), systematic or random (Cooper and Cross, 1988). Blunder, or gross, errors occur due to measuring or recording mistakes (such as a volunteer tilting the dGPS surveying pole or writing down incorrect values); systematic errors occur due to applying the incorrect functional model (such as one DEM having a consistent offset); and random errors are inherent in any measuring process and cannot ever be truly removed (Lane et al., 2000, Derose et al., 1998). Systematic errors and random errors were evaluated by comparing apparent elevation differences between the DEMs over check (or ‘control’) points measured with the dGPS. The location of the check points, and ground control points, are shown in Appendix B, and summarised in Table 4.2. Systematic errors are given as root-mean-square error (RMS) measures, and the 95<sup>th</sup> percentile limit is given for random errors (all units are in metres), a technique commonly used in DEM quality analysis (Schiefer and Gilbert, 2007). RMS was calculated by measuring DEM heights against dGPS check points, providing a measure of deviation of observed values from what can be considered their ‘true’ values (Miller, 2007a). The differences in height (dH) permit RMS to be calculated (Equation 7).

<b>Photo Year</b>	<b>Ave Z dif</b>	<b>RMS</b>	<b>SD</b>	<b>95% confidence (2xSD)</b>
<i>1945</i>	<i>-41.5643</i>	<i>84.0704</i>	<i>76.0609</i>	-
1965	0.0773	3.4536	3.6062	7.2124
1968	1.8190	2.5760	1.8769	3.7538
1975	-0.3217	2.7856	2.8900	5.7800
1986	1.0386	2.0768	1.8665	3.7330
1992	-1.2334	2.0994	1.7512	3.5024
1997	1.1436	2.7784	2.6015	5.2030
1997*	1.5002	2.7248	2.3369	4.6738
2003*	-0.9224	2.7059	2.6221	5.2442
2007	0.1575	1.6187	1.6442	3.2884

**Table 4.2 Average height difference between DEM and control (check) points surveyed at the field site with error estimates given as root mean square (RMS) errors. Random errors are reported at the 95th percentile limit (all units are in m). Note ‘\*’ designates 1997 and 2003 Roads Authority Vegagerðin DEMs compared against field data.**

$$\text{RMS} = \sqrt{\sum_1^n dh^2/n}$$

**Equation 7 Root Mean Square error formula (n = number of observations (check points)) (Li, 1988).**

Random error is usually assessed by employing probability statistics where it is assumed that the data is distributed about the mean, as shown by a normal distribution curve (Figure 4.18) (Wolf and Ghilani, 1997). Approximately 68.3% of all measurements are expected to fall within the range of  $\pm 1$  standard deviation ( $\sigma$ ), while approximately 99.7% will fall within  $\pm 3 \sigma$  (Table 4.3). Random errors for check points in this study are reported at the 95<sup>th</sup> percentile, as is common when reporting summary statistics of DEM quality (Gilbert and Scheifer, 2007).

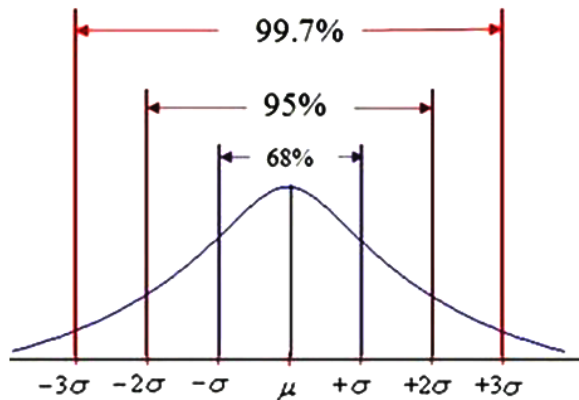


Figure 4.18 Error distribution curve, displaying confidence intervals (modified from (Miller, 2007a)).

Multiplier	Percentage Probable Error (%)
0.6745 $\sigma$	50.0
1.0000 $\sigma$	68.3 ( $\pm 1 \sigma$ )
1.6449 $\sigma$	90
1.9600 $\sigma$	95.0 ( $\sim \pm 2 \sigma$ )
2.5760 $\sigma$	99.0
2.9650 $\sigma$	97.9 ( $\sim \pm 3 \sigma$ )
3.2900 $\sigma$	99.9

Table 4.3 Standard deviation multipliers for percentage of probable errors of the normal distribution (Wolf and Ghilani, 1997, Miller, 2007a).

It should be noted that visual inspection of the DEMs showed the highest accuracy in the centre of the photographs and on sandy or ice-covered terrain, and had to be manually corrected in areas containing lakes, shadows or braided streams. The 1945 photographs, for example, while containing a high degree of error, demonstrated remarkable validity in the centre of the photographs that maintained a high quality of image; given the poor condition of these aerial photographs as a whole, however, this photo year is not mensurated in this study.

Throughout this study, the regions (posts) of the DEM that were used to extract profiles or volumetric data were manually corrected in SocetSet to improve accuracy of less than 2 m; lakes and rivers were smoothed to base level where possible. Given the large study area (in some cases 25 x 5 km), manually cleaning each post for ten photo sets (over 80 images) was not feasible; portions of the DEM that were not examined in this study may therefore require further manual correction ('post-pushing'). Elevation profiles extracted for high-resolution areas such as channel cross-sections were cleaned manually, however due to the error on the z axis, these profiles are constructed to illustrate channel erosion and deposition (x,y) changes greater than 1 m, rather than water level or surface lowering (z).

Due to the position of the ice margin, the changing terrain within the proglacial depression and the location of the imagery footprints, the check points in the 1965 imagery display a disproportionate degree of error, most likely as a result as their position on the far edges of the available imagery. It should also be noted that the 1997 photosets contained more than 30% cloud cover, resulting in poor correlation and were not used for elevation profiles in this study. The 1997 and 2003 DEMs obtained from the Icelandic Roads Authority were measured against dGPS points measured in the field (Table 4.2); however, no other metadata was provided with the DEM files (error, ground control points, or calibration information) of these substantially lower resolution data sets. The DEMs do not contain consistent offsets, although the general trends are consistent with the higher quality 2007 dataset, and to a lesser degree the 1997 datasets. For future analysis, further attempts should be made to obtain the metadata and GCPs for these two Icelandic Roads Authority datasets, or even higher resolution DEMs should be extracted. All previous attempts to obtain this data from the vendor through the Icelandic Roads Authority have so far proven unsuccessful.

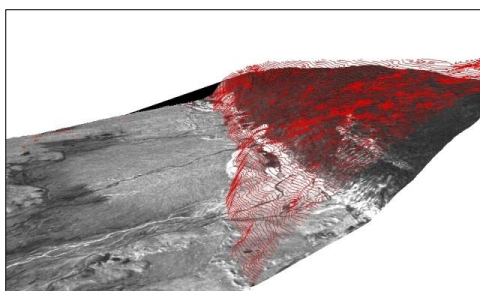
In subsequent chapters, mensurations were conducted in ArcMap and exported as portable network graphics (png) files at 300 dots per inch (dpi). All horizontal measurements (x,y) were considered to be accurate to 1 metre and, unless otherwise stated, contain a standard deviation of  $\pm 1.41$  m, while all vertical measurements (z) are presented in the text with the appropriate error depending on the relevant image years described in Table 4.2. It should be noted that graphics exported out of ArcMap cannot compare in resolution to viewing aerial photographs with electronic light tables (ELT's) such as SocetSet, Socet GXP or RemoteView. If the reader wishes to view the imagery, it is recommended that the image files be viewed with one of these applications if possible.



The aerial photographs themselves are interesting in the years that were captured; the reason for their existence is sometimes obvious (such as following a large flood or surge) while in other cases it is not known why the flight was flown. It should be noted that the action of taking a photograph due to an event applies a non-random prejudice to a historical study which may provide a weighting towards observing one process/event more heavily than another. When possible, caution is used to present the reader with a reason why an image may have been taken, and that other processes may have been active during time-steps that may equally be as important.

#### **4.5 Summary**

This chapter detailed the methodology employed for generating the terrain models that will be used to fulfil the aims and objectives of this study. This involved obtaining archived and recent images for the region and collecting ground control points in the field. Utilizing analytical photogrammetry, the image and field data were combined to produce digital terrain models. Throughout these stages of collecting and processing data, several issues became apparent. Complications encountered in the field, such as equipment failure and the difficulty involved in mapping complex landforms in a constant state of flux, were experienced on a daily basis and must be taken into account when using the DEM for areas outside of the regions that were cleaned and corrected for this study. Additionally, complications encountered during photogrammetric processing including poor image resolution and preservation, surface texture and variable lighting conditions, location relative to control points, highlight the importance of paying careful consideration when selecting regions for further study, both in modelling as well as in the field.



## Chapter 5 Glacier margin fluctuations

---

*This chapter describes and quantifies fluctuations of Skeiðarárjökull and the associated morphological changes of the proximal sandur between 1945 and 2009. The evolution of the glacio-fluvial systems and landforms adjacent to Skeiðarárjökull's three lobes (east, central and west) over the past six decades are examined following margin retreat, advance and following numerous jökulhlaups. These observations are used to test existing landsystem models and hypotheses. Further discussion of the relationship between margin fluctuations, jökulhlaups and surges on the evolution of Skeiðarárjökull's glacio-fluvial system and the proximal sandur is presented in Chapter 8.*

---

### 5.1 Introduction: Recession and lowering of Skeiðarárjökull 1945-2007

The retreat of Skeiðarárjökull's margin between 1904 and 2009 is shown in Figure 5.1. Elevation profiles of the glacier reveal that the surface of gradually lowered  $20 \pm 4.06$  m between 1965 and 1986; excluding the 1991 surge, the surface lowered drastically between 1997 and 2003 (up to  $70 \pm 3.45$  m) and up to  $170 \pm 2.78$  m by 2007 (Figure 5.2). In order to understand the relationship between glacier margin, ice surface fluctuations and the development of the proglacial terrain, area-wide, accurate transects of the margin, proglacial depression and proximal sandur were extracted (Figure 5.3). Large-scale observations are combined with detailed examinations of aerial photographs of Skeiðarárjökull's three lobes (east, central and west) and the corresponding proximal proglacial terrain. Due to the large number of photosets available, not all are presented in detail in this chapter, and the reader is directed to Plates I, II and III in Appendix A. Regions are presented chronologically, and observations are interpreted using literature specific to processes and landforms documented in the field area. Landforms specific to jökulhlaups and large-scale meltout are presented only briefly and explored in greater depth in their respective chapters. A holistic assessment of the literature-based hypotheses and models is further examined in Chapter 8. For locations of figures cited throughout this chapter, see Appendix C (Figures C.1 and C.2).

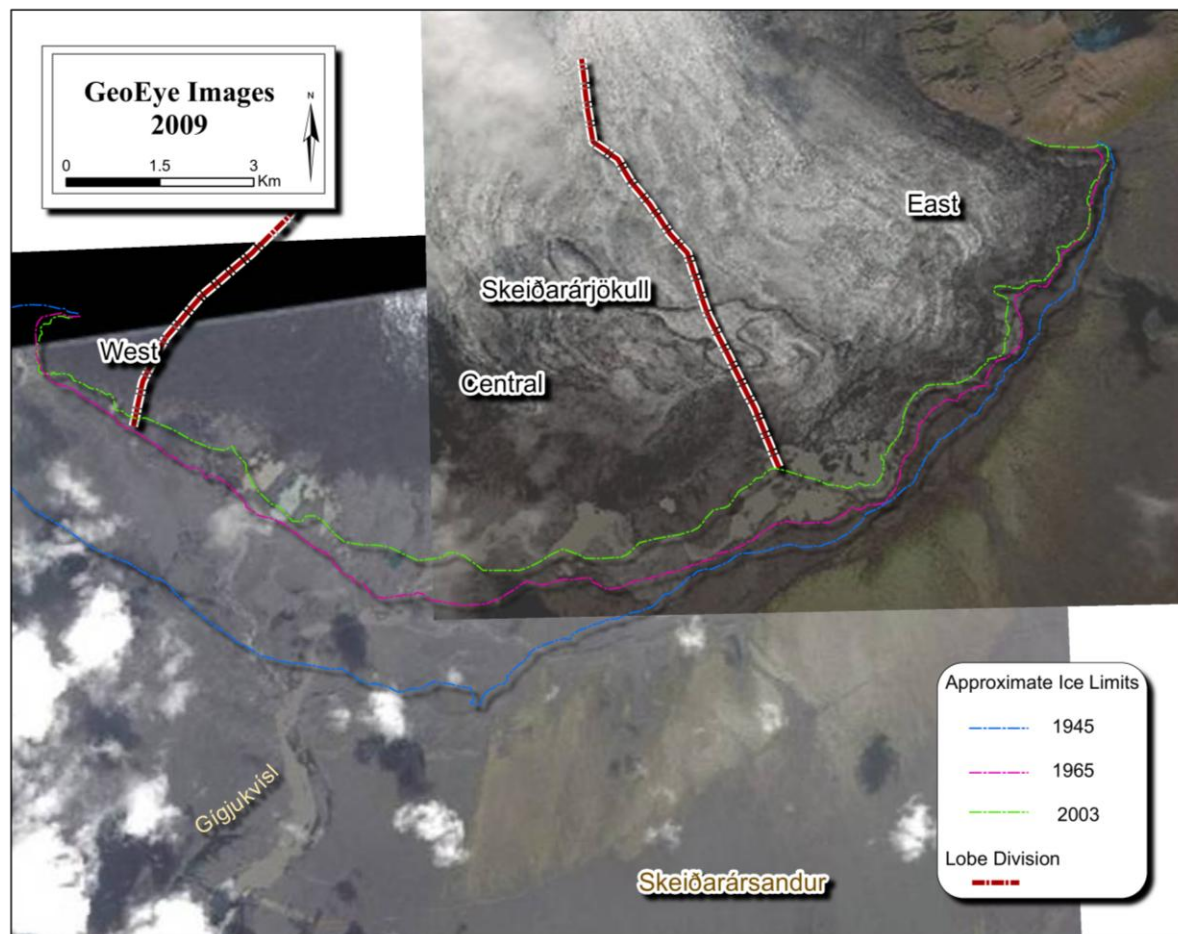


**Figure 5.1** Georeferenced GeoEye images depicting the changing position the fluctuating position of the glacier margin from 1945 to 2009 (mosaic contains: left image from Aug 2009, right from Sept 2009). The three lobes of the glacier (west, central and east) are demarcated by red dashed lines. Note that all 2009 drainage of the eastern (E) and central (C) lobes drains into the Gígjukvísl channel.

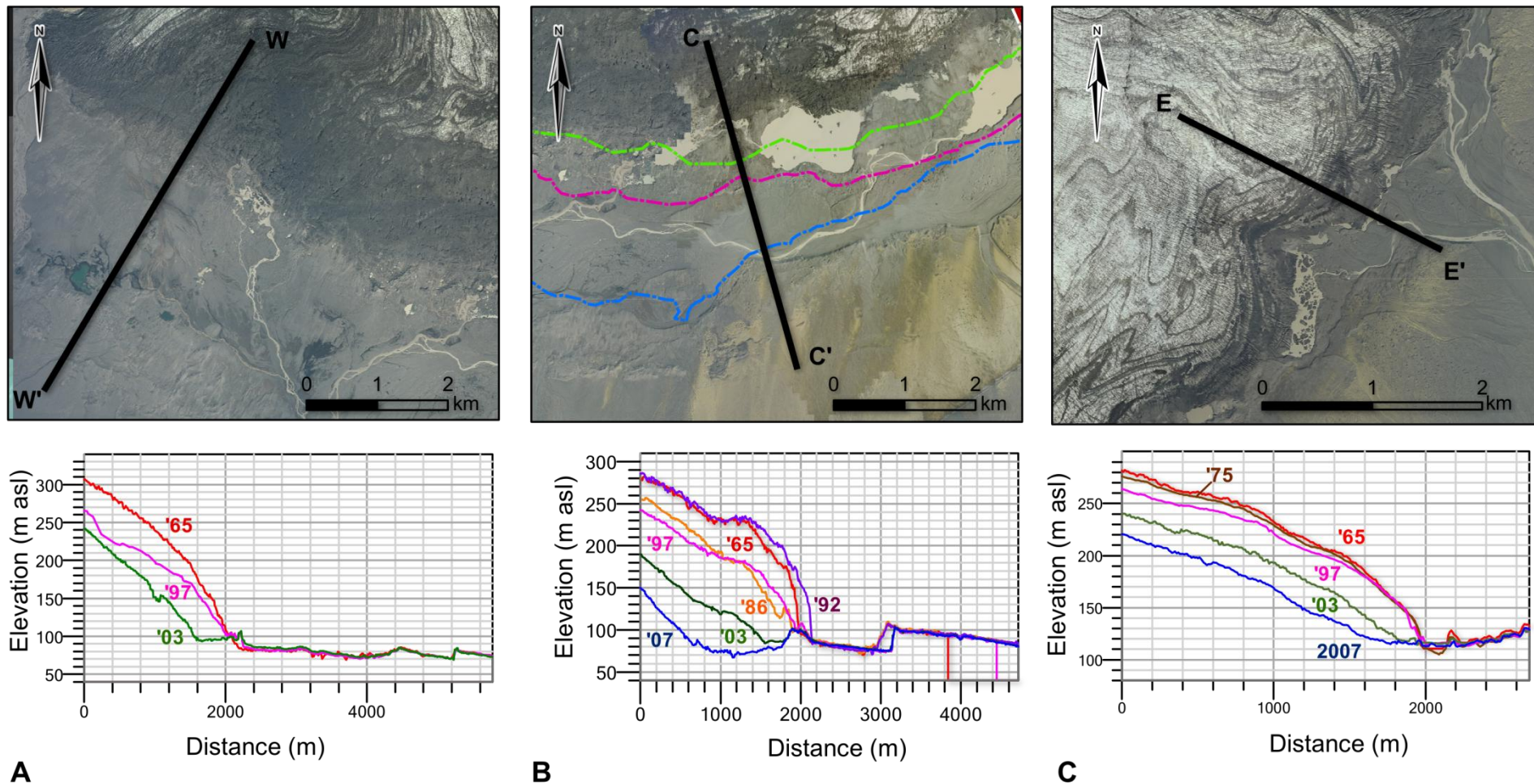


**Figure 5.2** Profiles of the west (a), central (b) and eastern (c) regions of Skeiðarárjökull depicting changes in glacier surface topography from 1965-2007 (not all photo-years available for each profile). Prior to 1997, with the exception of the 1992 surge, there has been a progressive lowering of the glacier surface and recession of the ice-margin. Since 1997, there has been an increase in the lowering of the glacier surface, in some locations by over 100 m.



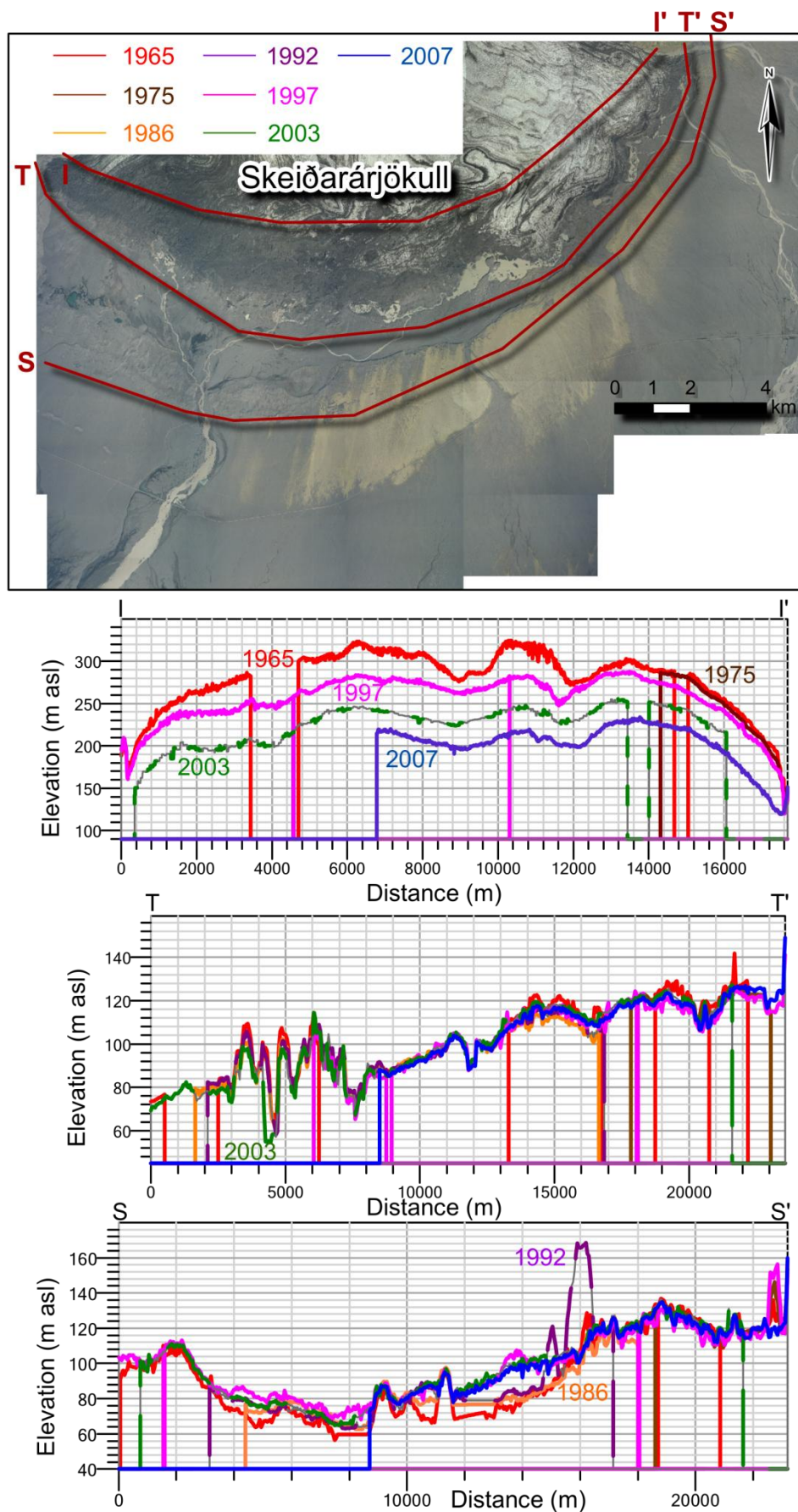


**Figure 5.3** Glacier margin parallel profiles of the sandur (S-S'), glacier margin (I-I'), and proglacial depression (T-T'). Vertical lines denote no data/breaks in DEM coverage.

## 5.2 Eastern region

### 5.2.1 Eastern region 1945

The eastern region in 1945 is characterised by three main channels (the eastern and western Skeiðará and the Sælhúsakvísl), minor proglacial lakes and moraines (Figure 5.4). While the poor quality of images prevented accurate reconstruction to extract elevation profiles, an examination the ice surface against the Jökulfell massif reveals that the ice is at its highest vertical extent of any of the photo series ( $> 230$  m). The snout of the glacier possesses numerous crevasses that exceed 300 m in length and are orientated perpendicular to the direction of ice flow. The margin itself appears to be heavily fractured and numerous supraglacial drainage channels drain the margin and flow out onto the kettled sandur.

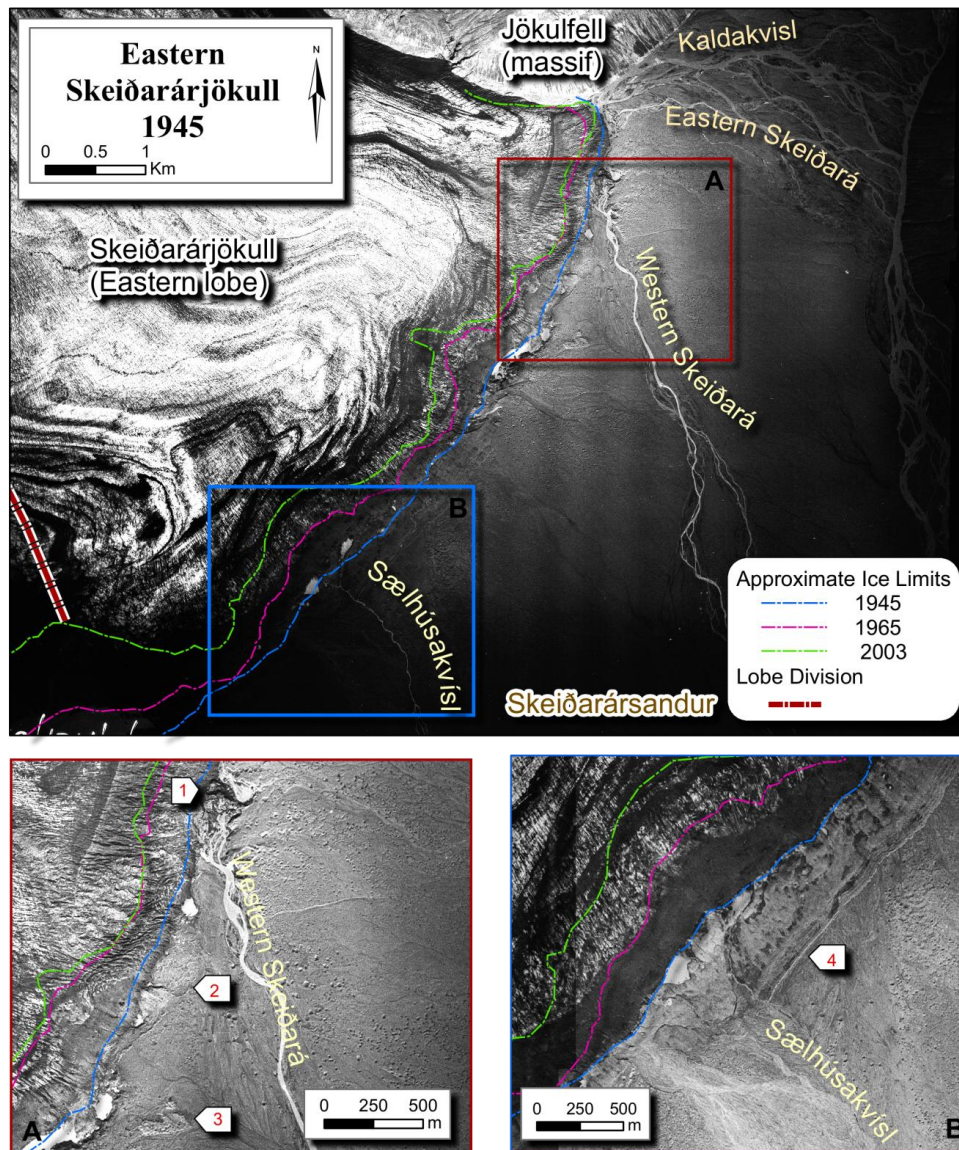


Figure 5.4 1945 photomosaic of eastern region: 1) meltout features, 2) alluvial fan, 3) outwash fan apex and 4) recessional push moraines.

The eastern Skeiðará and a minor channel, the Kaldakvísl, emerge from the base of Jökulfell before flowing together to form an extensive braided channel complex that is more than 500 m in width. The western Skeiðará emerges from the glacier as a single, well-defined channel that flows past outwash fans continue south for over 3 km before dispersing into a network of braided streams. The Sælhúsakvísl, although not active at this time, possesses a channel that spans over 750 m at its greatest width. The head of the Sælhúsakvísl channel is characterised by numerous recessional moraines, flutes, boulders and water-filled, elongate depressions that exceed over 150 m in width.

Both the Skeiðará and Sælhúsakvísl channels contain circular depressions that range from 10 - 30 m in diameter. These depressions are similar in geometry and position to the kettle holes described by Klimek (1973) and Galon (1973a) on other older, elevated terraces in the eastern region. The kettle holes and obstacle marks on the 1945 photographs are discernable more the 2 km away from the glacier margin.

The large size of ice marginal depressions, kettle holes and obstacle marks along the Skeiðará and Sælhúsakvísl channels, combined with the wide, steep terraces, suggest that large volumes of meltwater have inundated these channels and broke apart, or buried, the marginal ice in this area. This assemblage of jökulhlaup landforms was probably created by the 1934 and 1938 Grímsvötn jökulhlaups that are known to have inundated this area (see Table 3.2) (Thorarinsson, 1974). Kettle holes and channels, and possible outwash fan apex found on the elevated terraces were emplaced by other, older floods (Klimek, 1973); the size, depth and distribution of the kettle holes and obstacle marks are indicative that these were high-magnitude flooding events.

#### 5.2.2 *Eastern region 1965*

Taken eleven years after the 1954 jökulhlaup (Figure 3.8), the 1965 images reveal that the margin has retreated approximately 300 m (Figure 5.5). Proglacial lakes and proglacial meltwater outlets observed on the 1945 images at 120 m asl have been re-established at 108 m asl, a lowering of  $12 \pm 3.61$  m. The eastern Skeiðará is now confined to a single channel and contains numerous kettle holes and obstacle marks. As seen in Figure 5.3, significant portions of the elevated sandur abutting the south-western portion channel have been eroded. The western Skeiðará channel has also altered significantly: there are two new 100 m wide dry channels that expand to cover an area of over 1 km wide on the southern boundary of the study area.



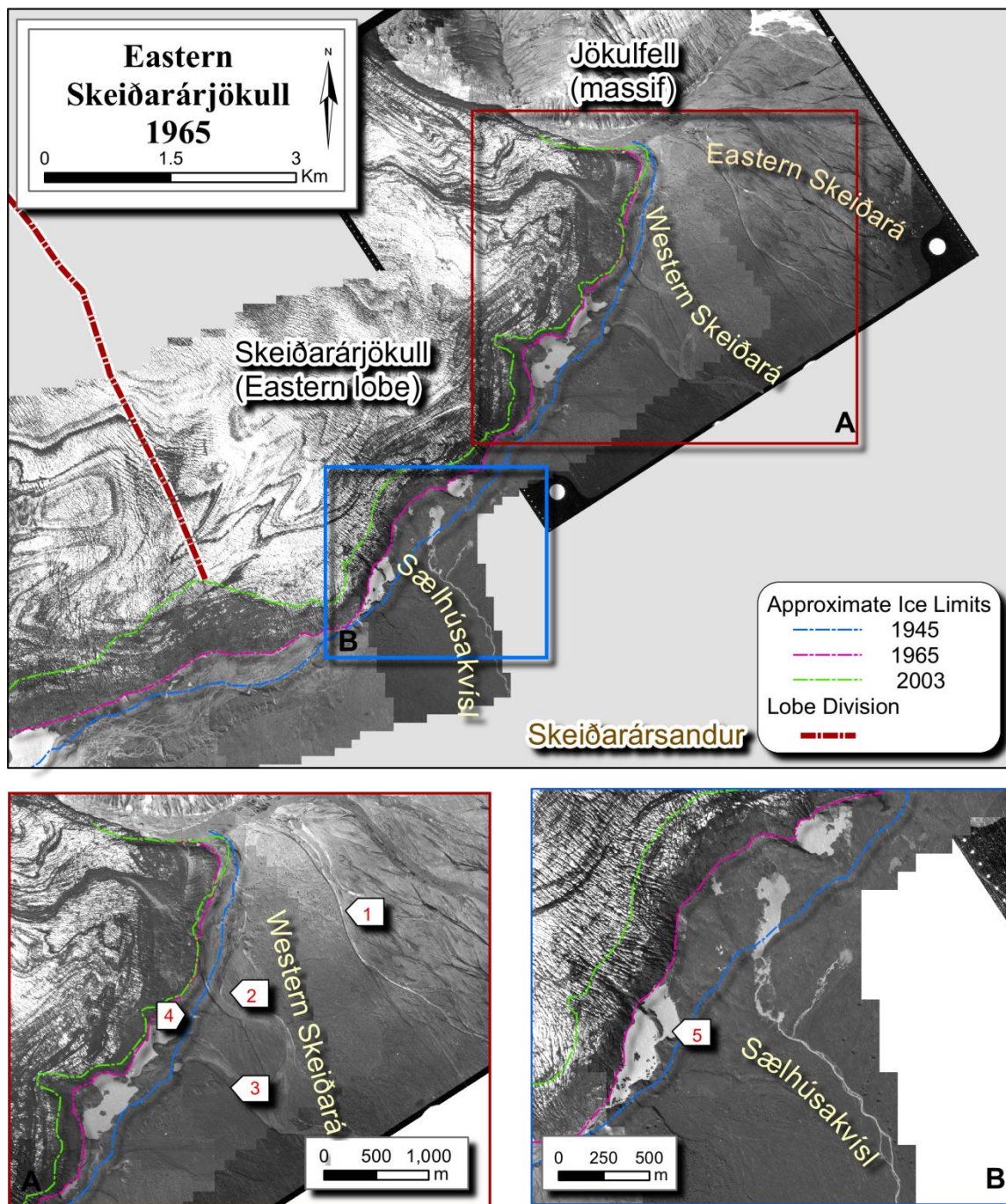


**Figure 5.5** 1965 photomosaic of the eastern region. Inset A) 1) expansion of terrace has resulted in the removal of a significant portion of the sandur, 2) and 3) two channels of the western Skeiðará that have been widened/deepened since 1945, 4) smoothed alluvial fan, and 5) retreat of margin has exposed a esker 240 m long that leads to former alluvial fan.

The morphology of the Sælhúsakvísl region has not been significantly altered, although the margin has retreated over 450 m, exposing large, water-filled depressions. The western most of these lakes is bifurcated by a drumlinised esker 240 m in length that joins the apex of an outwash fan on the sandur.

The proglacial lakes and drainage along the glacier margin has shifted northwards, with water levels in the lakes 12 m lower than in 1945, consistent with models of frontal



margin retreat (Arnborg, 1955, Jonsson, 1955, Kirkbride, 1993, Kirkbride and Warren, 1999, Benn et al., 2004, Dykes et al., 2010). The presences of kettle holes (Maizels, 1992, Maizels, 1997), obstacle marks (Russell, 1993, Fay, 2002), channel incision and expansion (Krigström, 1962) and the infilling of depressions proximal to the sandur are most likely the result of the 1954 jökulhlaup (Churski, 1973). The geometry of a drumlinised esker that leads to a kettled outwash fan on at the head of the Sælhúsakvísl is consistent with that of a sub- or englacial conduit that may have been generated during a jökulhlaup (Price, 1969, Burke et al., 2008, Burke et al., 2009), consistent with observations by Rist (1955) who documents that three out of the ten main outlets of the 1954 jökulhlaup emerged from in this area (Figure 3.8). Unfortunately, the lack of imagery over the two decades since 1945, prevents observations of any impact of proglacial drainage shifts, which have been noted in other locations to affect proglacial drainage evolution (Krigstrom, 1962, Marren, 2002).

#### 5.2.3 *Eastern region 1968-1996*

Only limited coverage of the eastern region was available post 1965 and pre 1992 (see Plate I for photographs from 1968, 1975, and portions of 1986 and 1992). The 1975 photographs are the only complete photoset of this area during this 28-year period. The 1975 images indicate that the position of the glacier margin is approximately the same position as it was 1968, although there was an ice surface lowering of  $12 \pm 3.45$  m (Figure 5.2). By 1975, the eastern Skeiðará is confined to a single channel over 80 m wide that emerges from the base of Jökulfell. This incision of this channel prevented meltwater from flowing parallel to the glacier margin, resulting in the abandonment of the many braided stream channels visible on the 1945 and 1965 aerial photographs. Little, if any, meltwater flows into the western Skeiðará on the 1975 images. The lowering of water in the proglacial lake at the head of this channel exposed two drumlinised eskers that are coincident with the location of the 1954 jökulhlaup outlet, suggesting that these may be the product of deposition within a large sub- or englacial jökulhlaup conduits (Price, 1969, Burke et al., 2008, Burke et al., 2009).

#### 5.2.4 *Eastern region 1997*

The 1997 images, taken less than a year after the 1996 jökulhlaup, reveal that Skeiðarárjökull's margin, while in approximately the same position as in 1965, now has a completely different character (Figure 5.6). The margin contains numerous crevasses, both orientated perpendicular to flow and arcuate in geometry. Numerous kettled outwash fans are visible along the margin. Large areas of topographic lows, including a lake

situated at the head of the western Skeiðará that has been present since 1965, have been completely infilled with sediment. The eastern Skeiðará now emerges from the glacier margin as a wide, braided channel that ranges from 100-160 m in width. Approximately 2.7 km east of the margin, the braids become smaller and more numerous, spanning an area more than 1 km wide. In 1975, however, the eastern Skeiðará was dominated by a primary channel over 150 m wide, with braids not appearing until more than 7 km downstream.

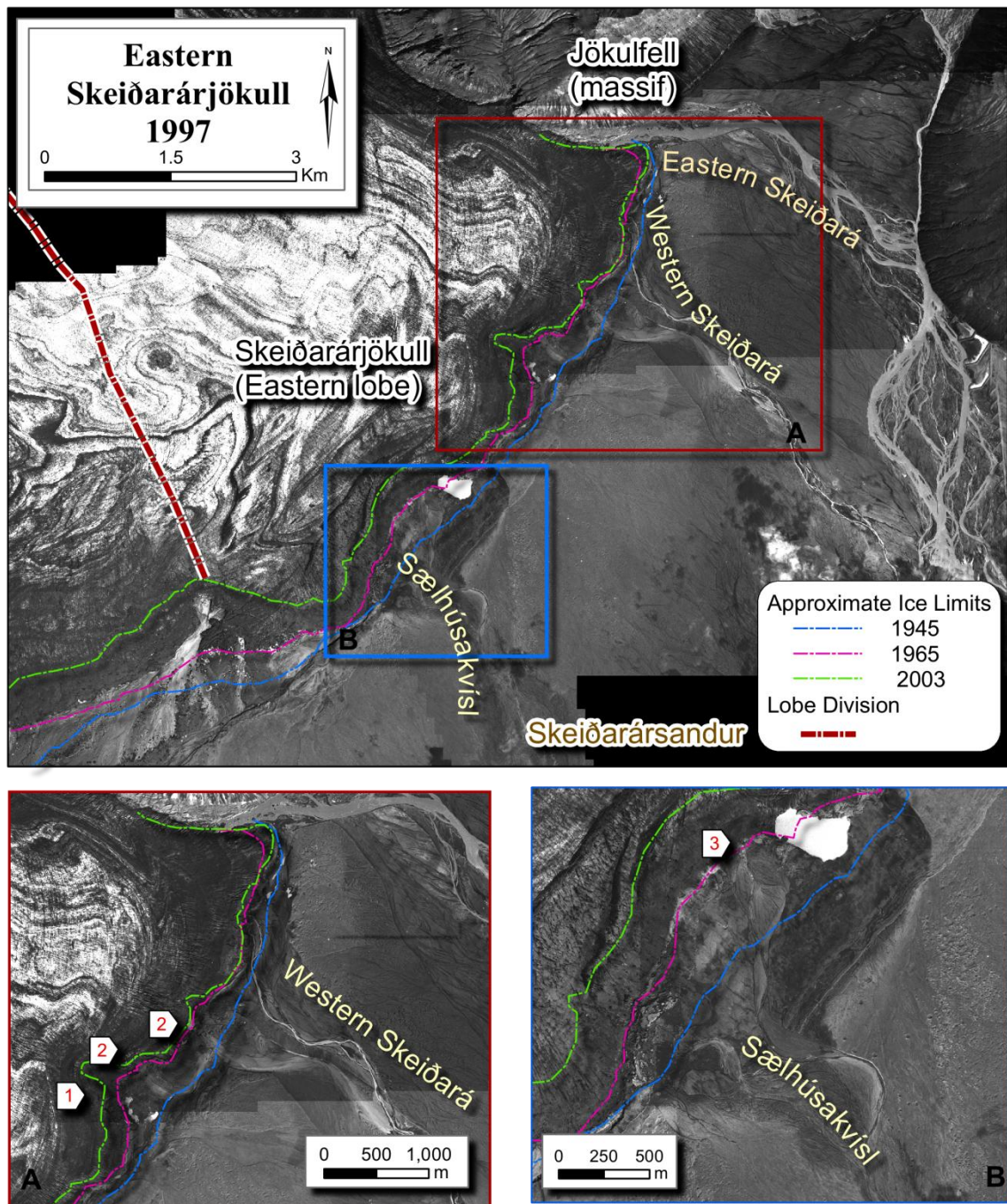


Figure 5.6 Photomosaic of the eastern region in 1997: 1) low, drumlinised ridge, 2) 1996 outlets, 3) outwash fan.

In the Sælhúsakvísl region, two new channels have been incised into the mouth of the Sælhúsakvísl, ranging from 100-150 m in width. The southernmost lakes, topographic lows and subglacial features present in earlier photographs appear to have been inundated with sediment. The surviving lake has had material eroded from its western shores, while further south, the easternmost channel has incised a steep cut bank into the sandur. A large outwash fan has developed along the margin to the west that contains numerous obstacle marks and kettles.

The influx of large volumes of sediment, channel incision, the presence of numerous outlets across the margin and the emplacement of fans containing obstacle marks and kettle holes is consistent with observations of high-magnitude jökulhlaups in the literature and documented during this event (Boothroyd and Nummedal, 1978, Maizels, 1977, Maizels, 1979, Russell, 1993, Snorrason et al., 1997, Roberts et al., 2000, Russell et al., 2001b, Fay, 2002, Snorrason et al., 2002, Russell et al., 2006). The lack of significant alteration in the Skeiðará channel following the 1996 jökulhlaup is consistent with observations by Klimek (1973) who proposed that the channels had become ‘hardened’ following previous floods in 1934, 1938 and 1954 (see the following section for a detailed description of channel modifications from 1965-2007). The close proximity of the extensive network of braided trains of the eastern Skeiðará to the glacier margin are consistent with increased aggradation as a result of the November 1996 jökulhlaup (Maizels, 1979, Bristow and Best, 1993, Marren, 2005). The rapid development of these trains following a single event demonstrates that the position of braided channels in relation to the glacier margin is not entirely dependent upon margin position suggesting the expansion of other models (Boothroyd and Nummedal, 1978).

#### 5.2.5 *Eastern region 2003*

The 2003 DEMs document the first substantial vertical lowering and horizontal retreat of the eastern lobe of Skeiðarárjökull since 1945 (Figure 5.2). After approximately thirty-two years of relative stability, the glacier surface lowered approximately  $30 \pm 3.45$  m, and the glacier margin retreated approximately 350 m within a span of only five years. The proglacial drainage system has also changed dramatically, with proglacial lakes present once more along the margin (Figure 5.7). On the 2003 images, the eastern Skeiðará lacks the numerous braids present on the 1997 images. Instead, the eastern Skeiðará has incised into the sandur as a single 100-150 m wide channel that flows eastward until reaching the flood levees adjacent to Skaftafellsheiði. Here, the braided stream pattern returns and these merge with the western Skeiðará (off-map).



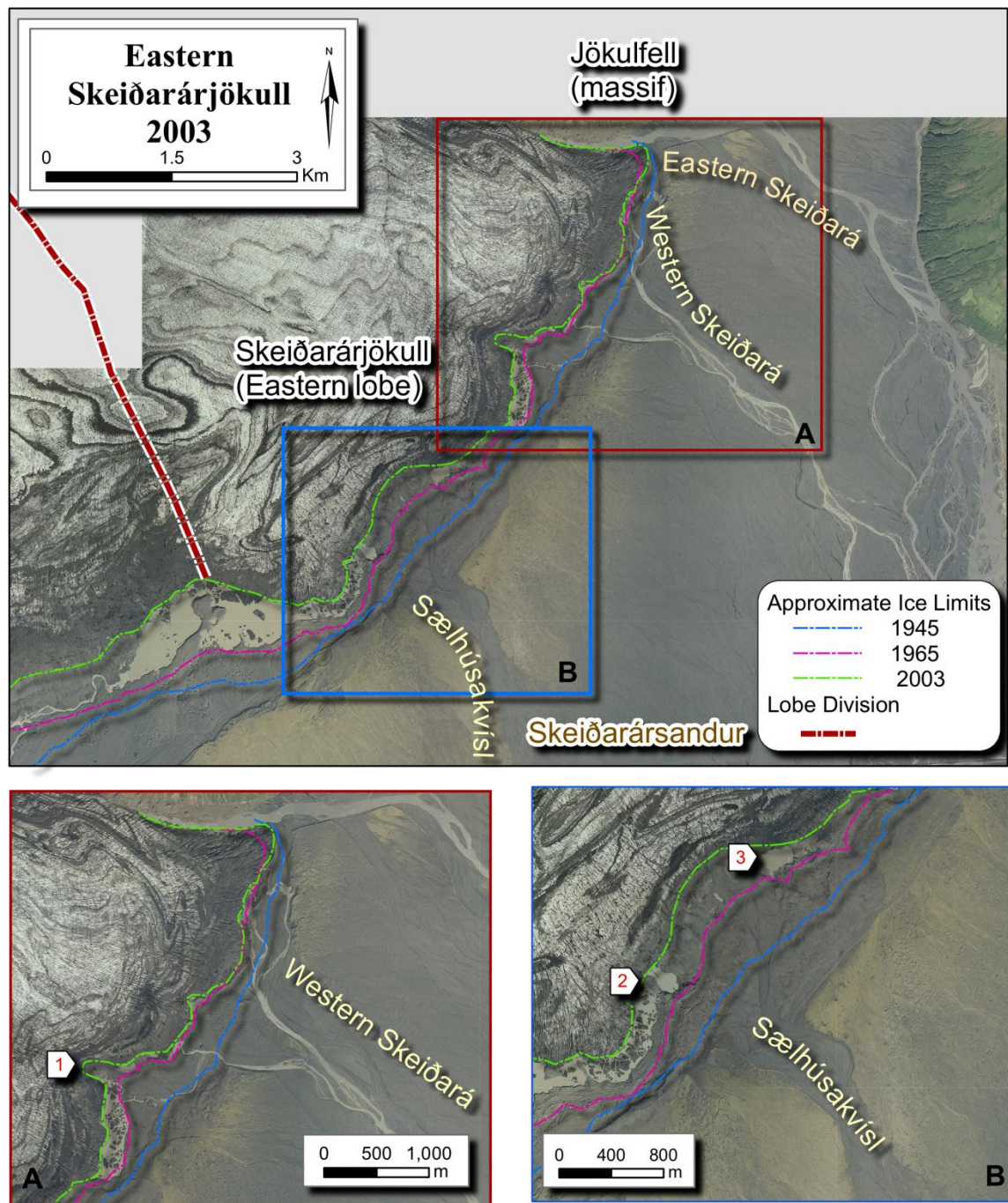


**Figure 5.7** Aerial photograph of the eastern region in 2003 indicating 1) drumlinised terrain, 2) drumlinised esker and 3) proglacial lake.

The western Skeiðará comprises two 30-40 m wide channels that flow within the extent of the 1954 flood channel, incising into the 1996 jökulhlaup deposits. The western Skeiðará possesses several broad, braided reaches and drains the large iceberg-filled lake at the head of the channel. The retreat of the glacier margin around the head of the western Skeiðará channel has exposed large depressions and drumlinised eskers orientated parallel to glacier flow.

The retreat of the glacier in the Sælhúsakvísl area has exposed fluted ground as well as numerous lakes and basins located immediately behind the lakes observed on the 1997 images, but at a lower elevation. The easternmost lake, previously at 114 m asl, has now been re-established at 98 m asl. Two lakes that have developed directly to the north of the lakes that were in-filled during the 1996 flood are bifurcated by a drumlinised esker over 260 m in length that trends north-west/south east. This esker is similar in orientation to an esker located on the 1965-1975 photographs that was eroded or buried by the 1992 surge fan and the 1996 flood deposits. If this is indeed a single continuous feature, its total length is in excess of 580 m. The retreat of the margin has permitted drainage from the southernmost lake to flow west into the Gígjukvísl catchment. The margin adjacent to these lakes has been subject to flotation and calving that has generated large ice blocks, some over 100 m in length.

The incision of the eastern Skeiðará channel is consistent with models of outlet lowering (Marren, 2002b). The corresponding dramatic lowering of the ice surface immediately following the November 1996 jökulhlaup suggests a correlation between high-magnitude jökulhlaups and excavation of material beneath the glacier and the subsequent rapid lowering and retreat of the glacier. This relationship is discussed in further detail in Chapter 8.

The presence of large ice blocks calving from the thinning glacier margin is consistent with descriptions of retreating lacustrine margins within overdeepened basins (Funk and Rothlisberger, 1989, van der Veen, 1996, Kirkbride and Warren, 1999, Warren and Aniya, 1999, Warren et al., 2001, Van der Veen, 2002, Boyce et al., 2007) and reinforces the importance of the influence of topography on the pattern and rate of margin retreat.

#### 5.2.6 *Eastern region 2003 – 2009*

Between 2003-2007, the ice surface of the eastern lobe lowered  $20 \pm 3.1$  m, a net vertical loss of  $60 \pm 2.78$  m since 1997 (Figure 5.2). This trend continues up-glacier with thinning ranging from 40 to 60 m. The character of the ice elevation profiles since 1997 are also noticeably different: instead of possessing a steep front, the lobe now possesses a gently sloping, thinning margin that gradually begins to increase in thickness away from the sandur. Compared to the 2003 images, by 2007 the proglacial drainage of the eastern lobe has altered drastically (Figure 5.8). The retreat of the glacier margin away from the sandur and the Jökulfell massif has permitted the flow of all proglacial drainage to drain 2.5 km westward along the glacier margin and into the western Skeiðará, effectively



abandoning the eastern Skeiðará. The drainage along the glacier margin is now confined within a channel approximately 130 m wide that resides at a base level  $5 \text{ m} \pm 3.45 \text{ m}$  lower than the smaller ( $\sim 20 - 60 \text{ m}$  wide) channels that were present in 2003 (Figure 5.9).

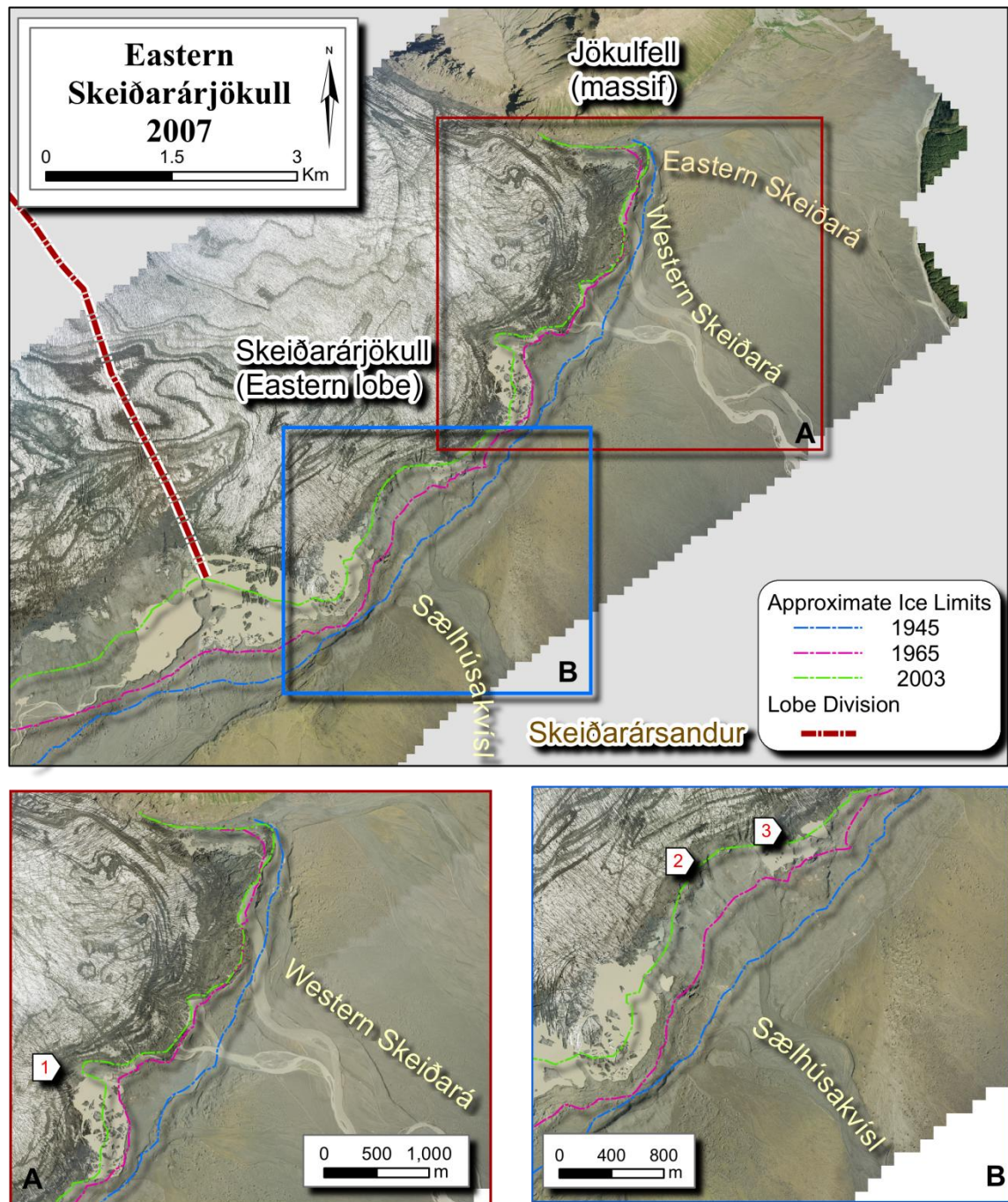


Figure 5.8 2007 photomosaic of the Eastern region showing 1) drumlinised terrain, 2) drumlinised, ascending eskers 3) three lakes separated by two rounded ridges.



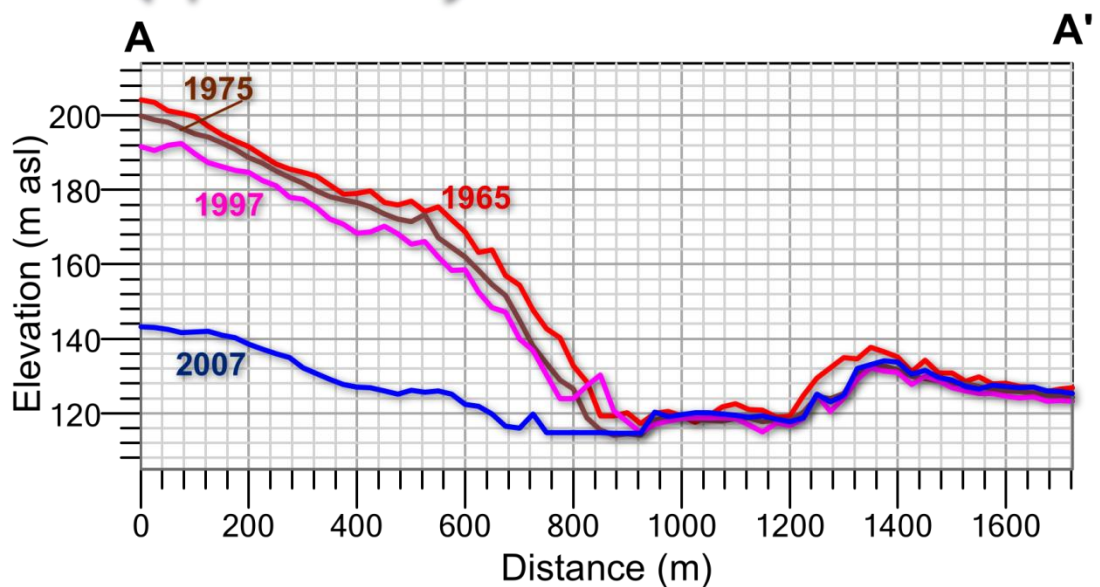
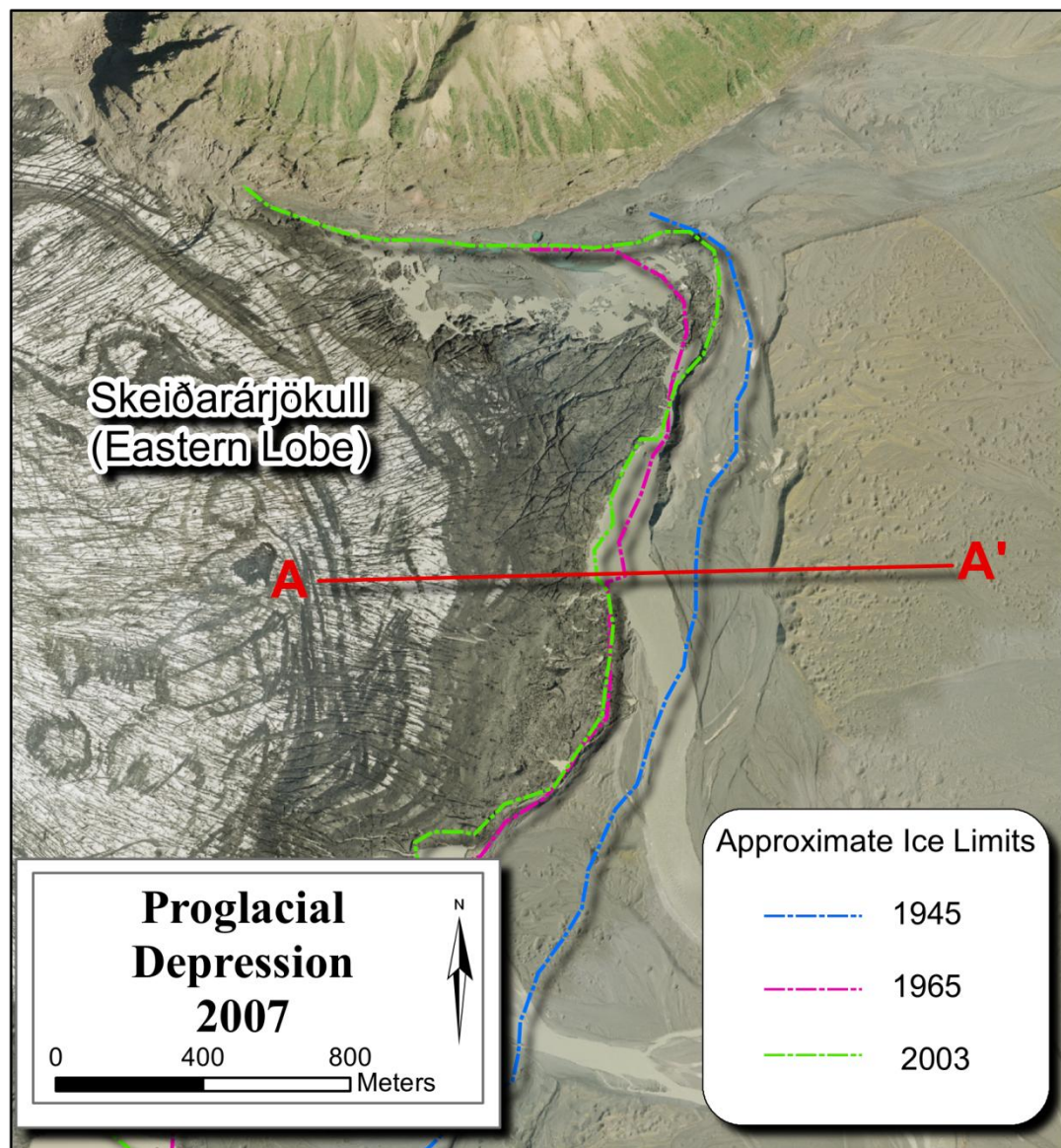


Figure 5.9 Profile depicting the development of the proglacial depression in the Eastern region from 1965 - 2007; the progressive retreat of the glacier margin has resulted in a series of ice-front parallel channels that have permitted meltwater to drain along the glacier margin into the western Skeiðará channel.

The glacier margin at the head of the eastern Skeiðará has retreated over 400 m. The head of the abandoned eastern Skeiðará in 2007 is characterised by numerous kettle holes (1-15 m in diameter) that have developed since 2003. The western Skeiðará has straightened and widened from 65 m to 125 m. It is joined by a secondary channel ( $75 \pm 1.41$  m wide) that collects drainage from the glacier margin proximal to the former 1996 jökulhlaup outlets. Further downstream, large portions of the 1996 kettled deposits that lay within the 1954 channel visible on the 2003 images have been removed.

In the Sælhúsakvísl region, retreat of the margin has revealed that two elongate eskers have ‘trifurcated’ the eastern lake into three lakes that are 1) ~80 m, 2) ~90 m and 3) 260 m wide. In contrast, the western lakes have merged, spanning westwards over 3.3 km in width (off-map). Numerous elongate eskers, some upwards of 380 m in length, appear to be ascending the slope up to the elevated sandur. The surfaces of the drumlinised eskers are relatively smooth, characterised by lineations, recessional moraines and occasional boulders. These ridges also contain newly formed kettles and collapse features that have developed since 2003.

A detailed review of the development of the 1996 outlets in this region are described in Chapter 3, as is the development of a tunnel channel complex at the Sælhúsakvísl. The eskers that ascend upslope to the sandur in the Sælhúsakvísl region are indicative of floodwaters and sediment emplaced as a result of supercooling generated during the flood within the overdeepened basin (Roberts et al., 2002, Tweed et al., 2005). The widening and straightening of the western Skeiðará is most likely the result of the October 2004 jökulhlaup, generated by the eruption of Grímsvötn (Roberts, 2005, Vogfjord et al., 2005), that reached a peak discharge of  $3.3 \times 10^3 \text{ m}^3 \text{ s}^{-1}$  in the Skeiðará in November, primarily affecting the western Skeiðará. The resulting channel incision allowed proglacial river channels to keep pace with the rate of glacier surface lowering and remain coupled to the sandur (*personal communication Dr. A.J. Russell*). While the poor resolution of the 2009 GeoEye images prevented accurate mensuration or description of features in this region, they clearly depict that a second capture has already taken place: the glacier has retreated sufficiently for all subaerial proglacial drainage adjacent to the eastern lobe to flow westward into the Gígjukvísl (Figure 5.2).

#### 5.2.7 *Channel profiles 1965-2007*

The removal of material and subsequent lowering of the eastern Skeiðará channel between 1965 and 2007 is shown in Figure 5.10. The changes depicted over these four



decades are relatively minor within this wide channel, with a net erosion of  $< 5$  m. As presented in Chapter 3, the lack of significant change in this channel is most likely the result of the numerous past floods that have excavated the wide flood plain, while the presence of the massif to the north and the elevated sandur to the south have acted to laterally confine the channel. The following sections compare the eastern and western Skeiðará channels and their response to glacier margin fluctuations, as well as the effects of hardening following flooding events.

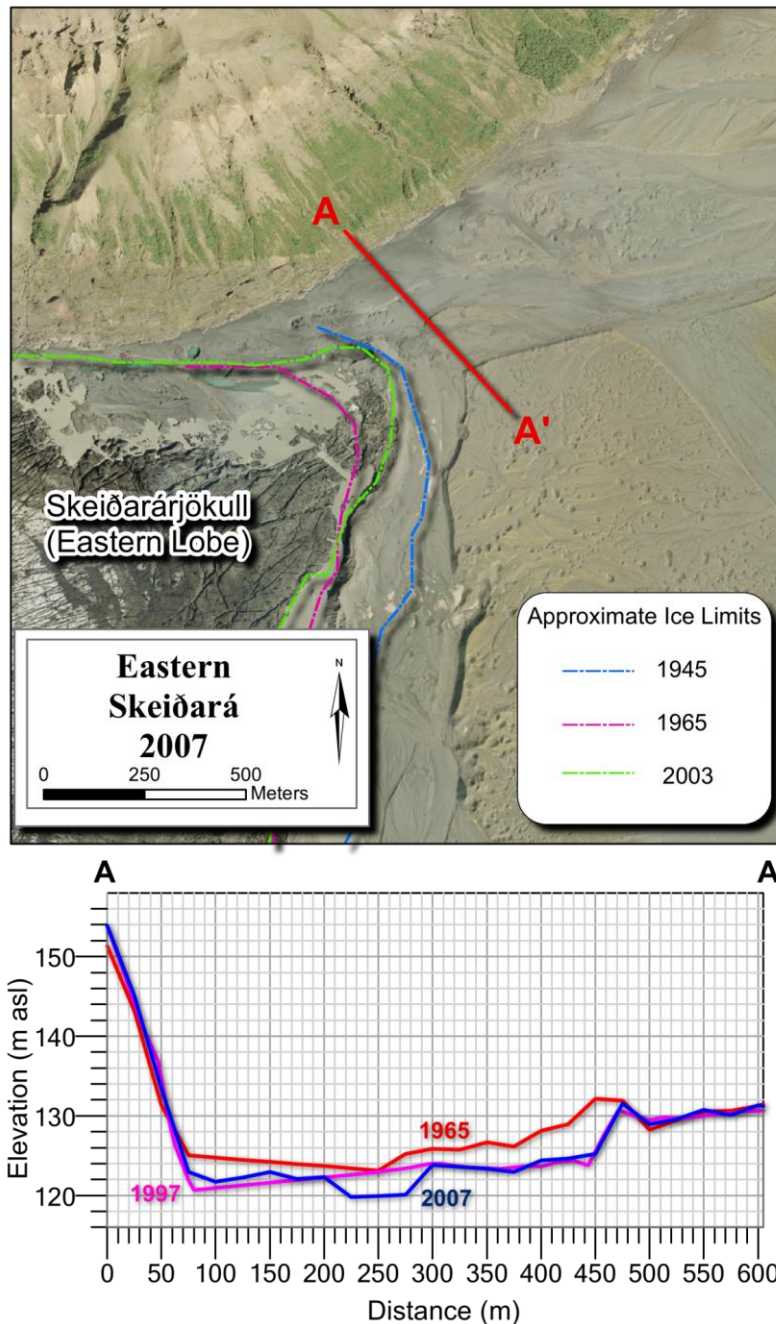


**Figure 5.10** Profiles of the eastern Skeiðará channel taken from 1965, 1997 and 2007. Profiles depict the removal of material and incision between 1965 and 1997 and subsequent influx and removal of material between 1997 and 2007.

In the western Skeiðará, the channel was subject to lateral erosion between 1965 and 1975 (approximately 160 m) and further lateral modification is apparent on the 1997 profile (approximately 200 m), presumably the result of the 1996 jökulhlaup (Figure 5.11) [Note: this transect also requires further GCPs for accurate control on the z axis, additionally 2003 GCPs were not provided by vendor]. The 2007 profile shows further incision and lateral erosion of material (approximately 60 m), presumably as a result of the increased discharge during the 2004 jökulhlaup and the capture of the eastern Skeiðará increasing non-flood discharge into the Skeiðará. While as late as 2003, the eastern Skeiðará has been the primary drainage channel in the region since at least 1945, the elevation data reveals that the base eastern Skeiðará is 5 – 10 m higher than the base of the western Skeiðará channel. The observation that the proglacial drainage has been routed under hydraulic pressure upslope is consistent with hydraulic models of glaciers lying within overdeepened basins (Alley et al., 1998, Lawson et al., 1998, Evenson et al., 1999, Tweed et al., 2005). This is also consistent with upwellings noted at the glacier margin near the head of the eastern Skeiðará in 2006 (*personal observation*).

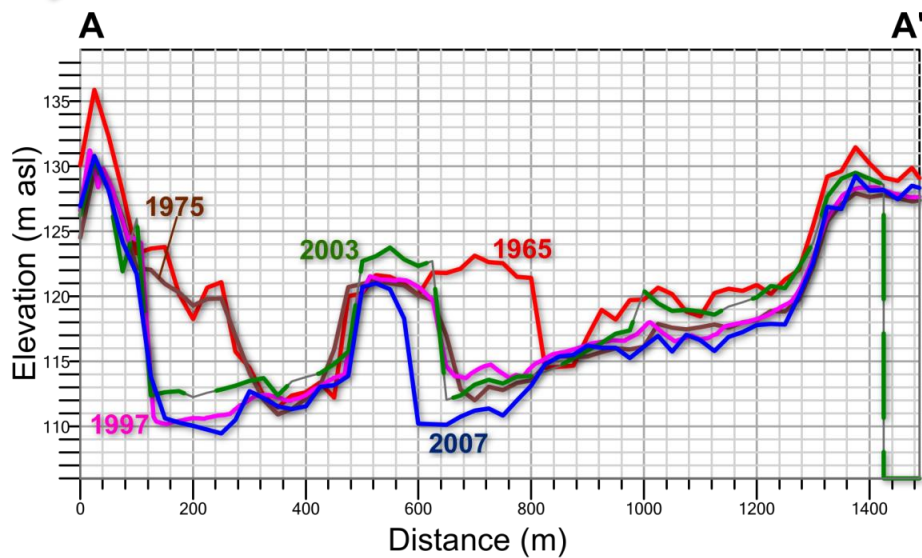
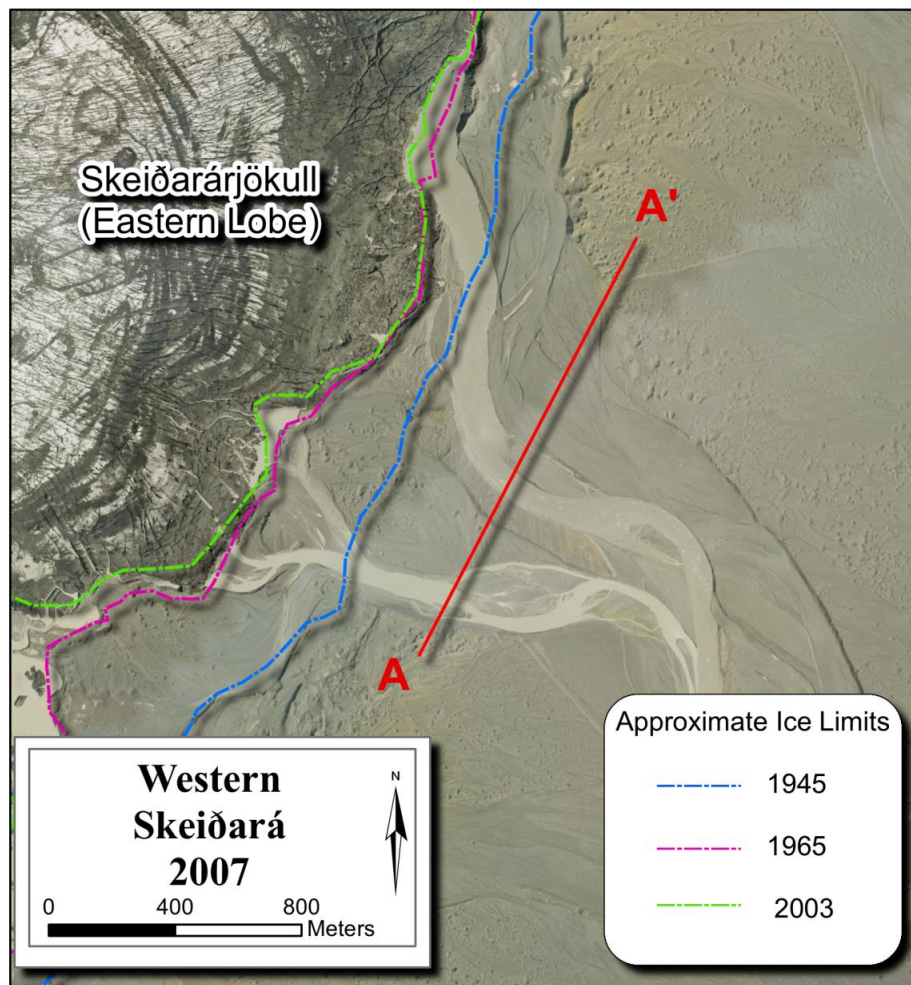


Figure 5.11 Profile of western Skeiðará channel between 1965-2007 constructed to highlight lateral erosion and aggradation. Between 1965 and 1975 the margin was relatively stable and exhibits comparatively little channel change. Note the lowering of erosion in profiles between 1975 and 1997 interpreted to be related to the 1996 jökulhlaup. Erosion between 2003 and 2007 is interpreted as relating to erosion by the 2004 jökulhlaup.



## 5.3 Central region

### 5.3.1 *Central region 1904*

The 1904 topographic map (Figure 5.12), although lacking the resolution of aerial photographs, depicts the position of the glacier margin, the location of active drainage channels and numerous abandoned channels. These channels pass through gaps in the central moraine belt that dates back to at least the 19<sup>th</sup> century (Galon, 1973a). The active channels include the Sandgígjukvísl (Figure 5.12, Feature 1), the Sigurdarfítaralar (Figure 5.12, Feature 2), an unnamed channel (Figure 5.12, Feature 3) and a portion of the Háöldukvísl (on map). These channels drain directly from the ice margin through the moraine gaps and out onto the sandur. All of these channels appear to display little or no braiding, however it should be noted that the cartographers may have only depicted active channels and that the map lacks any fine detail. Proglacial lakes, so ubiquitous today, are not present.

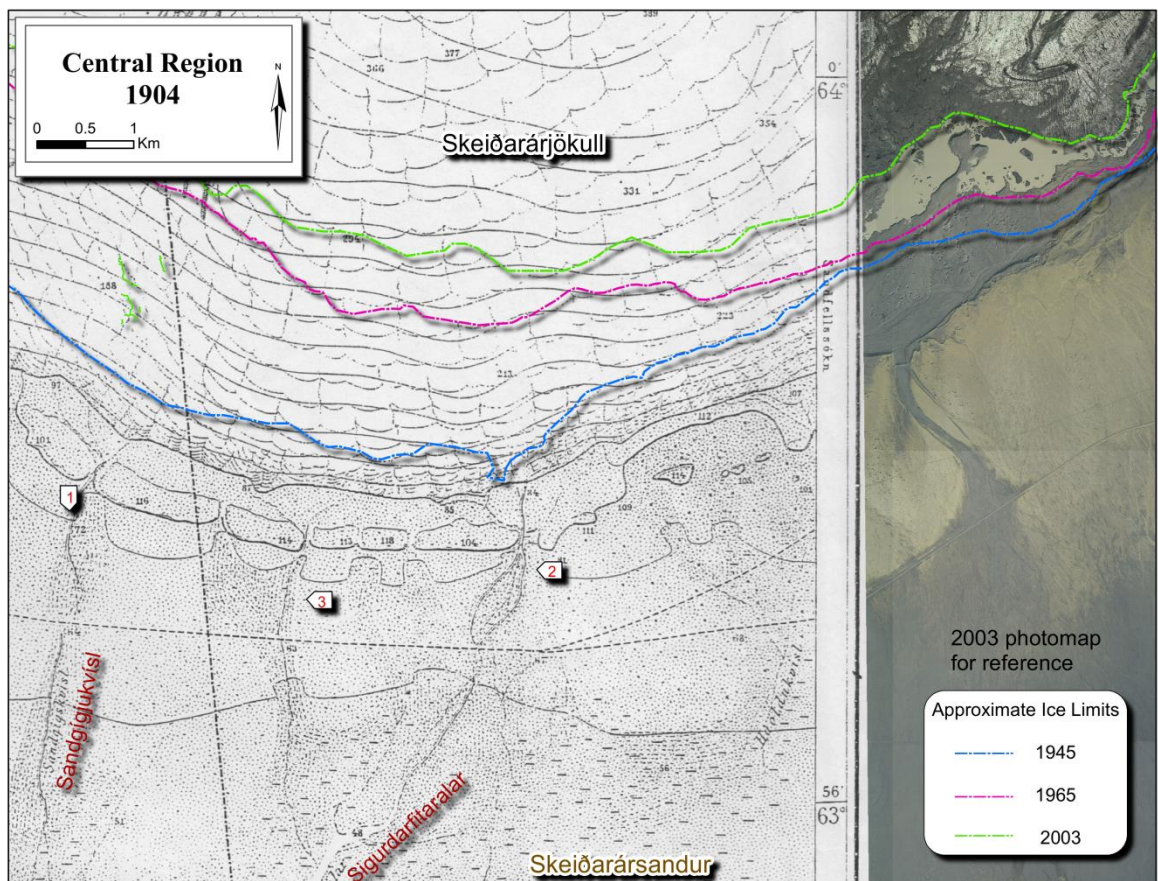


**Figure 5.12** 1904 topographic map of the central region (overlain upon 2003 photomosaic for reference). Features 1-3 represent active drainage channels draining the margin: 1) the Sandgígjukvísl, 2) the Sigurdarfítaralar, and 3) another unnamed channel.

Inferences obtained from the 1904 map corroborate existing models of drainage networks at stable or advancing glacier margins whereby evenly-spaced drainage channels flow out on to the sandur through gaps in the moraines (Arnborg, 1955, Bogacki, 1973, Galon,

1973a, Boothroyd and Nummedal, 1978). The lack of proglacial lakes, often associated with retreating margins (Arnborg, 1955, Jonsson, 1955, Kirkbride, 1993, Kirkbride and Warren, 1999, Benn et al., 2004, Dykes et al., 2010), further suggests that the 1904 margin was stable or advancing.

### 5.3.2 *Central region 1945*

By 1945 the glacier margin has retreated more than 300 m. The proximal proglacial topography consists of smoothed ground, chaotic terrain and wide depressions (Figure 5.13). The number of active drainage channels in this area has reduced to three: the Gigjukvísl, the Sigurdarfítaralar and the Háöldukvísl; the unnamed channel on the 1904 map is no longer active. Proglacial lake Háöldulón is 4.4 km in length, ranges from 300-700 m in width and has surface elevation of 90 m asl. Háöldulón drains into the Háöldukvísl, prevented from draining the westward regions by a ~1 km wide drumlinised convex terrain consisting of flutes, numerous boulders and kettle holes. The Haoldokvisl channel itself possesses a maximum width of only 22 m, a misfit that resides within a much wider channel (~115 m) that is incised within the heavily kettled sandur.

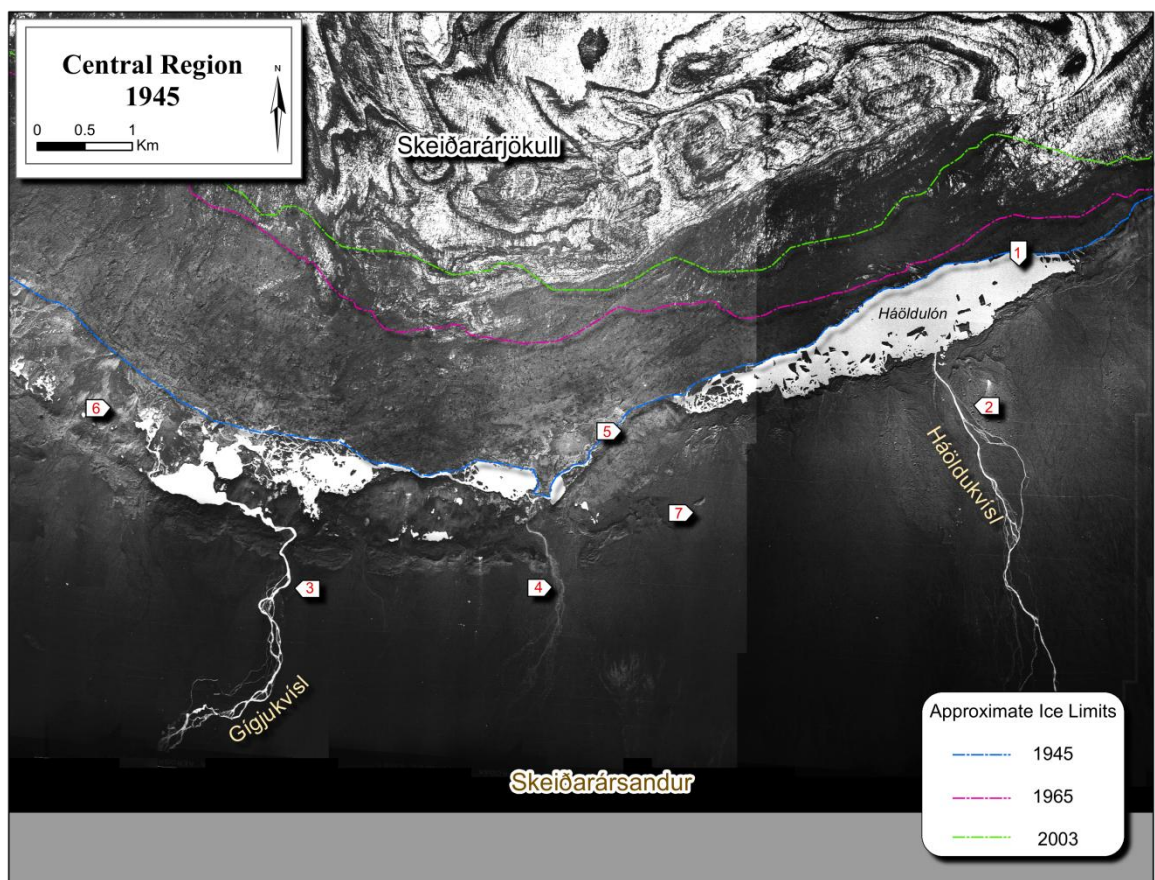


Figure 5.13 1945 Central region photomosaic: 1) proglacial lake Háöldulón, 2) kettled terrain, 3) Gigjukvísl, 4) unnamed channel, 5) region of elevated terrain blocking westward flow of drainage, 6) marginal outlets and 7) remnant of 19<sup>th</sup> century moraine (Háalda mound).

The elevated sandur near this channel contains numerous kettle holes and kettle-scours that are up to 50 m in diameter. The proximal and lateral scour and tails, more clearly visible on later photo years, is consistent with descriptions of the kettle scours by Fay (2002) that suggests that total or partial burial and subsequent exhumation of the ice blocks during a large-scale jokulhlaup event. Many of the 19<sup>th</sup> century moraines between the Gígjukvísl and the Háöldukvísl present on the 1904 map are no longer visible. This portion of the sandur, and historical accounts of geomorphic processes in this region between 1904 and 1945, are presented in greater detail in Chapter 7.

The Gígjukvísl captures the majority of the drainage along the western margin before passing through a 23 m wide gap in the 19<sup>th</sup> century moraines. The development of this channel, and the overall shift in drainage in this region, is thought to have occurred within a relatively short period of time (1938-1944) (Galon, 1973a). The lakes that drain into the Gígjukvísl appear to be constrained by higher, fluted ground and the elevated sandur to the south. Boulders, depressions, drumlinised topography and shallow lakes dominate this terrain. The proglacial depression between the glacier margin and the sandur extends west of the Gígjukvísl and is characterised by numerous lakes, shallow streams and ice blocks residing within a 5 km swath of exposed subglacial features; this region is described in higher resolution photosets later sections.

### 5.3.3 *Central region 1965-1968*

By 1965, all of the drainage in the central region flows into the Gígjukvísl (Figure 5.14). Several heavily kettled ice-marginal outwash fans that contain active drainage channels are present along the retreating glacier margin, the largest of these are shown in Figure 5.14. These fans, as well as the presence of recessional moraines, direct and control proglacial drainage in this region. Háöldulón has lowered by  $20 \pm 4.07$  m and the Háöldukvísl channel is no longer active. The lowering of Háöldulón has exposed a 2.5 km by 600 m wide plain that is covered by finely braided shallow streams.



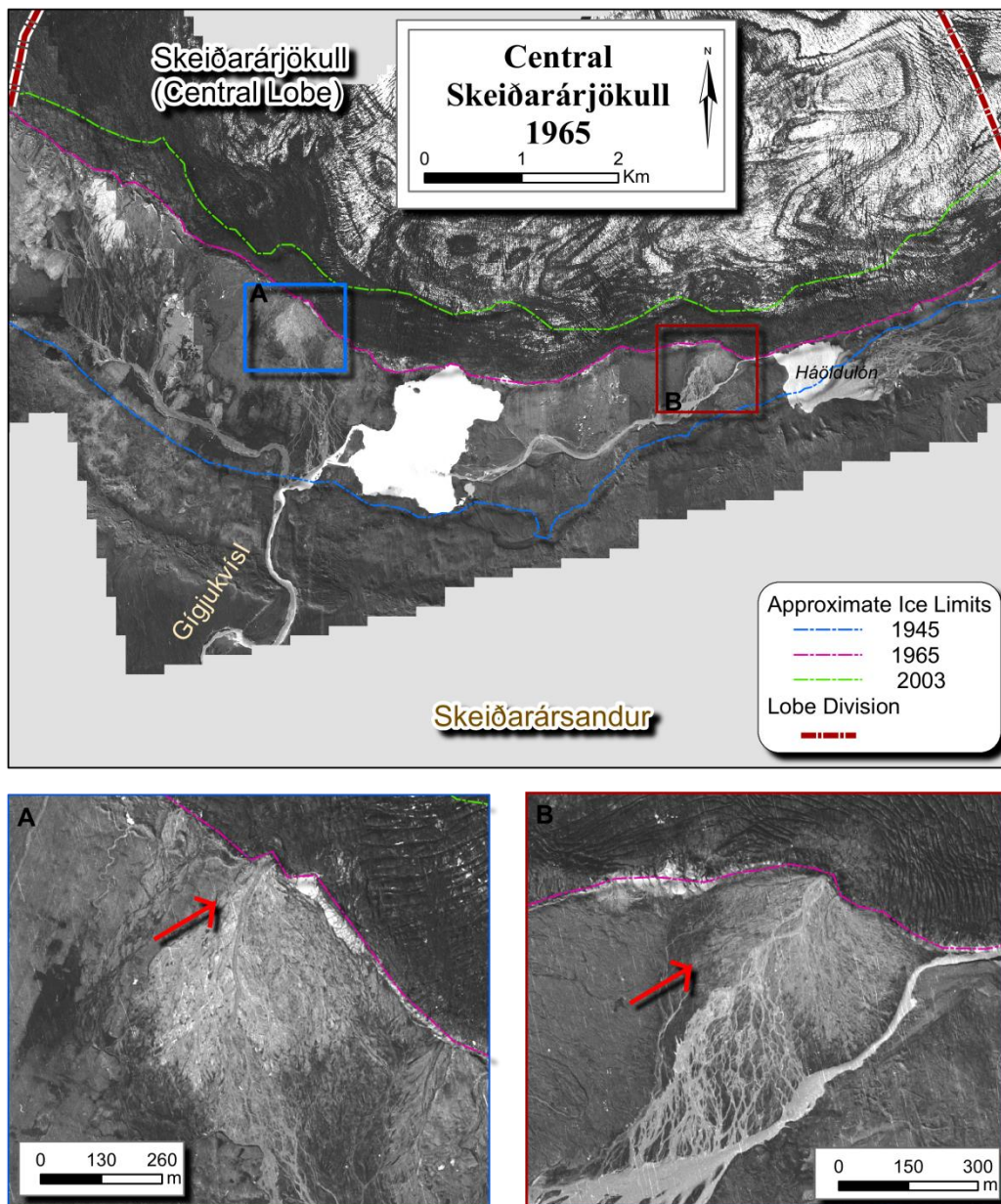


**Figure 5.14** 1965 photomosaic with insets of the two largest kettled outwash fans.

Between 1965 and 1968, the kettled ice-marginal outwash fans have widened, channels within these fans have become incised (Figure 5.15), and discharge across the central margin has increased, raising the level of Háöldulón. Between 1965 and 1968, the glacier margin retreated up to 20-50 m in some areas. Profiles of the ice surface in 1965 and 1968 are shown in Figure 5.16. In 1965, the glacier snout possessed a steeply sloping front, the ice surface 42 m higher compared to 1968 profile. The observed increase in ice thickness, steep slope, the emplacement of large outwash fans and increased number of drainage outlets observed on the 1965 images is possibly indicative of a minor advance of the glacier margin or possibly even a previously undocumented minor surge event. It is documented that western lobe also experienced a similar advance at this time (Figure 3.7) (Molewski, 2000). Advances in southeastern Iceland are generally ascribed to be a

response to a cold period experienced in Iceland in the mid to late 1960s (Sigurðsson, 1998); however, the 1965 advance may pre-date these conditions, and surges are not climate-dependent (Evans and Rea, 2003). The position of the glacier margin in 1965 is similar to that depicted on the hydrographic map from 1960 (Figure 3.6) (Galon, 1973a), indicating that the advance was comparatively minor. Further sedimentological investigations of the ice marginal fans may be needed to determine if this was a minor surge or simply a rapid advance.

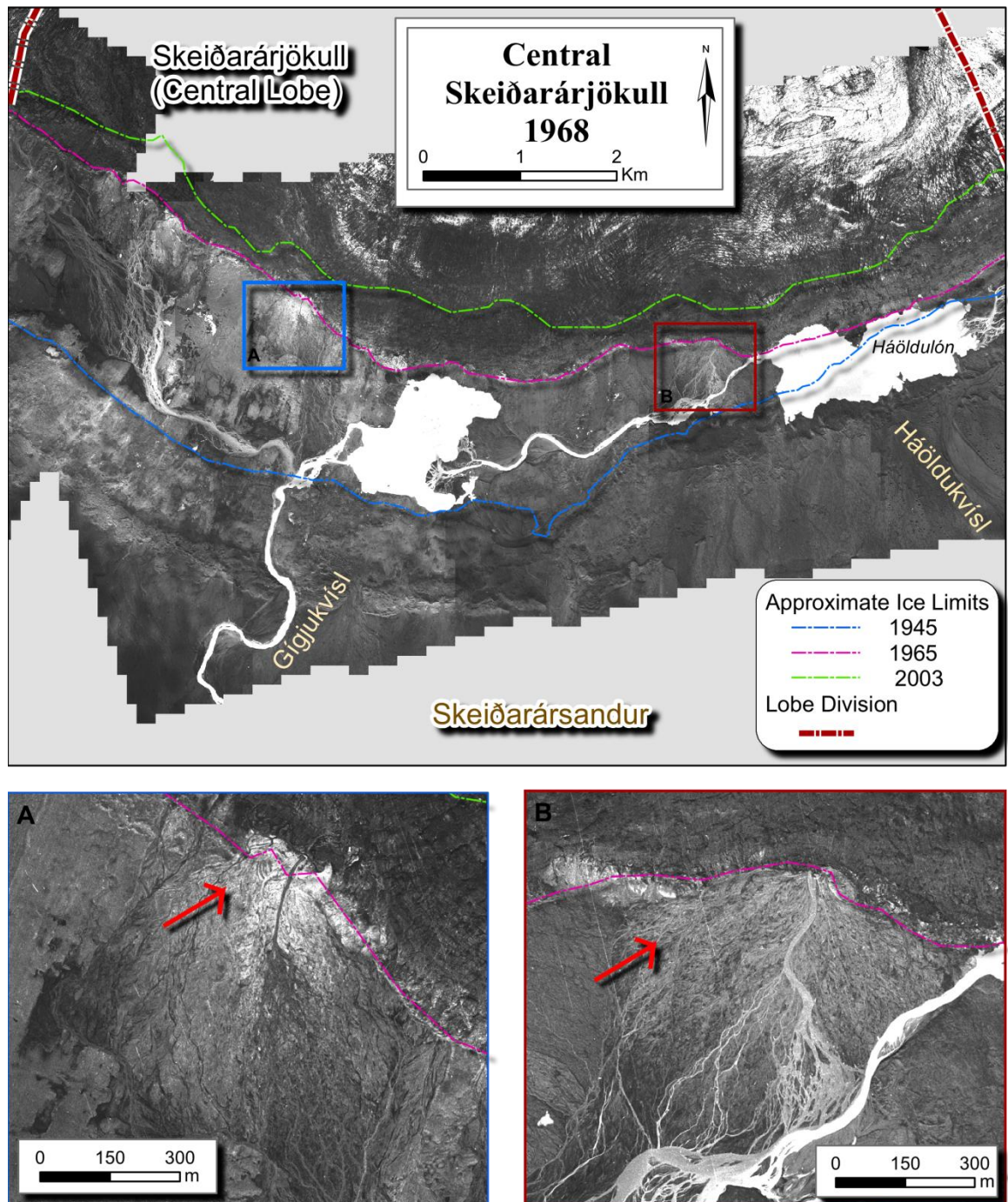
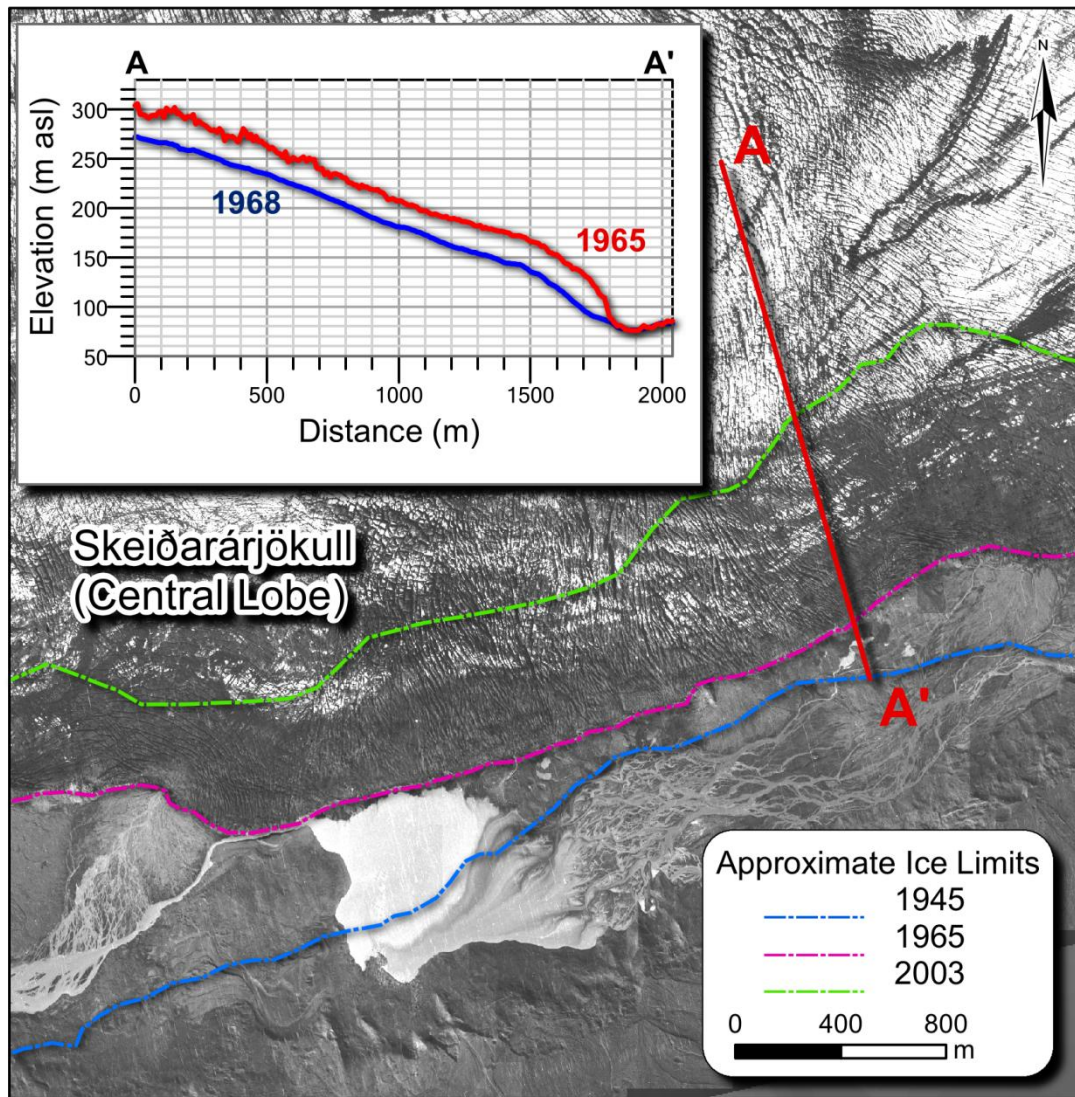


Figure 5.15 Photomosaic with insets of the two largest kettled outwash fans on 1968 imagery.





**Figure 5.16** Comparison of ice surface profiles between 1965 and 1986, displayed on the 1965 photo basemap.

Between 1945 and 1965, the drainage of Háöldulón (Figure 5.14) has exposed two drumlised eskers along the southern wall of the proglacial depression that range from 14 to 55 m in width and are oriented towards the apex of a large, heavily kettled ice-marginal outwash fan situated on the elevated sandur. Although separated by a distance of 560 m, these eskers extend more than 850 m. The kettle holes on the fan range from 2 to 43 m in diameter. By 1968, these fans have continued to expand, and have been incised by new channels (Figure 5.15).

Further west (1.5 km) of the Háöldukvísl, three more drumlinised ridges extend from the kettled Harðaskriða outwash plain into the proglacial depression. These ridges are orientated north-south and measure, from west to east, 161 m, 105 m, and 165 m in length and approximately 38 m, 50 m and 41 m in width. The Gígjukvísl drains a lake approximately 1.4 km in diameter and approximately 15 m in depth (Churski, 1973) with

a surface elevation of 50 m asl. The Gígjukvísl gap is approximately 240 m wide, and the Gígjukvísl channel itself is approximately 90 m wide as it passes through the 19<sup>th</sup> century moraines. Downstream of the moraines, the Gígjukvísl has incised within a older terrace over 380 m wide that has been eroded since 1945.

The retreat of the glacier margin, the corresponding reduction in the number of active drainage channels across the elevated sandur and the lowering of lake levels, observed between 1945 and 1965/68, are consistent with models of glacier recession (Arnborg, 1955, Jonsson, 1955, Howarth and Price, 1969). The drumlised eskers exposed by the retreat of the glacier margin and the draining of Háöldulón that are associated with the heavily kettled outwash fans located on the elevated sandur are consistent with models of sub- and englacial conduits (Burke et al., 2008, Russell et al., 2006) that may have been emplaced during jökulhlaups prior to 1945.

While the the capture of the Háöldukvísl river after 1945 and the influx of drainage during the minor advance observed on the 1965 images will have contributed to the expansion and incision of the Gígjukvísl channel, it should be noted that a major jökulhlaup also affected this area in 1954 (Rist, 1955) (see Table 3.1). These factors may responsible for the observed large-scale modification of the channel and the erosion of the wide terraces south of the 19<sup>th</sup> century moraines.

The 1954 margin was positioned south of two large ice marignal fans shown in Figure 5.14 and Figure 5.15, suggesting that the heavily kettled fans, and the channels incised within them, may be a result of the the 1960 or 1965 jökulhlaups. Over the following eleven years (1968-1979), the central portion of Skeidararjökull only experienced minor margin recession and small-scale changes in its proglacial drainage patterns (Plate I) until the 1985-86 surge.

#### 5.3.4 *Central region 1986*

The 1986 photographs reveal that since 1965, the glacier margin has retreated over 650 m and has lowered by at least  $60 \pm 4.06$  m (Figure 5.2; Figure 5.17). The 1986 images depict two ice-marginal outwash fans that contain kettle holes up to 5 m in diameter, boulders up to 3 m in diameter and incised channels that are up to 10 m wide. West of Háöldulón, the drumlinised terrain exposed by retreat is extensively covered with extensive, shallow, braided streams that drain into the Gígjukvísl. The Gígjukvísl itself continues to flow through the same gap in the 19<sup>th</sup> century moraines, however south of this gap, the Gígjukvísl is incised within a terrace that is now over 540 m wide. The elevated sandur



east of the Gígjukvísl contains numerous large elongate depressions over 1 km long and over 160 m wide and circular depressions that are over 160 m in diameter. These depressions were not present on the 1945 images. The dirt road that traverses this area in 1945 is visible on the 1986 images, although in 1986 it is distorted, possessing improbable slopes. The gradual distortion of the road and surrounding terrain as well as the geometry and position of the depressions suggests that this area has been subject to subsidence due to the melting of buried ice bodies. The origin and emplacement mechanisms of these large bodies are presented in greater detail in Chapter 7.

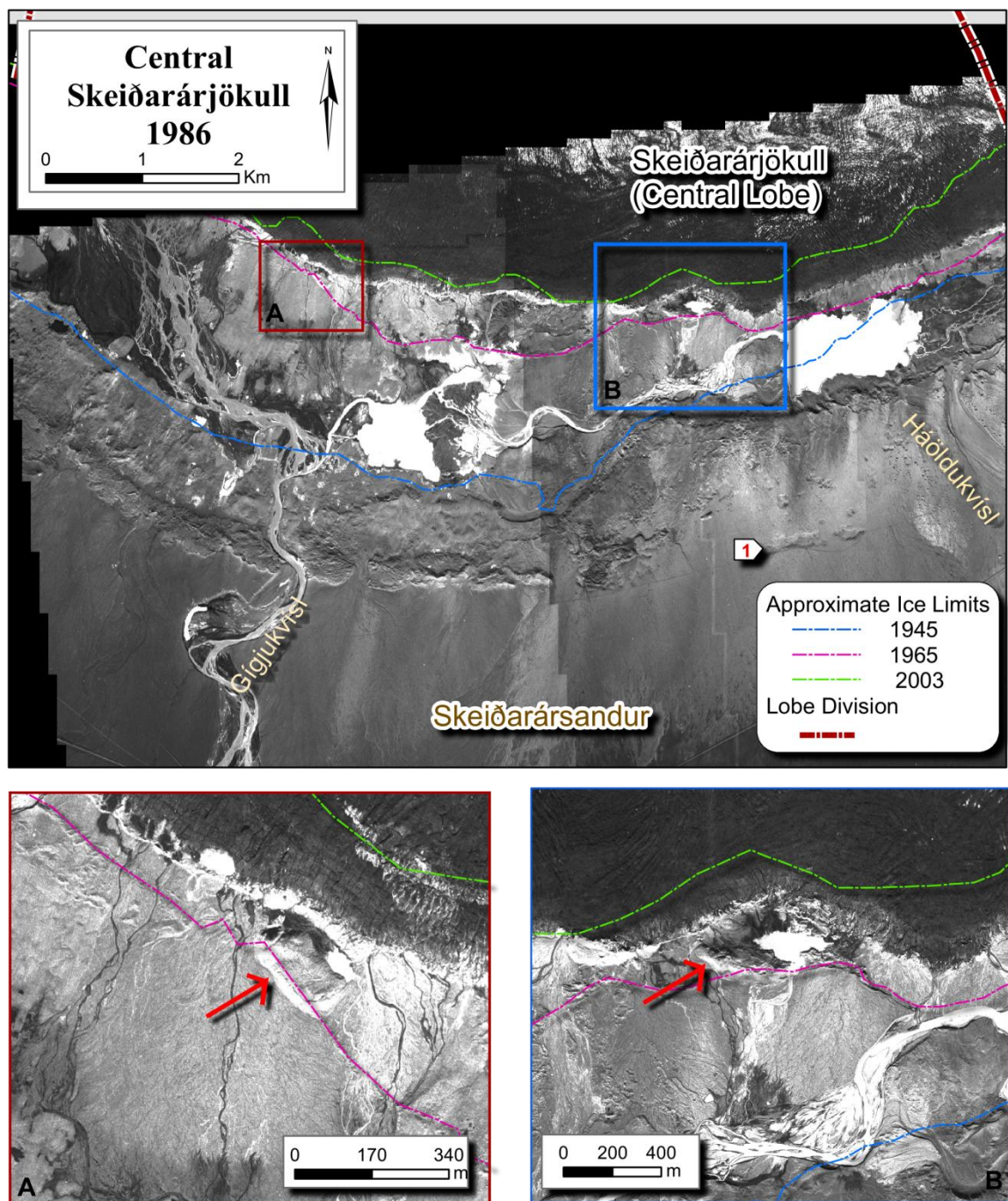


**Figure 5.17** Central region 1986. Drainage channels that have developed adjacent to former 1965 flood outlets; retreat around these 1965 outlets exposed elongated, rounded ridges.

The increased number of drainage outlets across the margin, increase in discharge and the development of ice-marginal fans at regular intervals along the glacier margin are indicative of a distributed drainage system associated with a glacier surge (Kamb et al., 1985, Kamb, 1987, Fleisher et al., 1998, van Dijk, 2002, Björnsson et al., 2003). The increased number and density of braided stream networks within the proglacial depression suggests a coincident increase in sedimentation, consistent with established surge models presented for these images (see Chapter 3) (Russell et al., 1999b, Russell et al., 2001a).

The retreat of the margin north of the two fans shown in Figure 5.14 and Figure 5.15 has exposed two elongate blocks of terrain and adjacent depressions that are orientated perpendicular to glacier flow Figure 5.18. The ridges are both situated northwest of the each fan, contain smoothed surface, and were both partially visible along the ice margin on both the 1965 and 1968 images. The eastern block is 400 m long, 80 m wide and 17 m high, while the western block is 232 m long, 108 m wide and 15 m high. The position of the fans and associated channels suggest that these blocks have served to direct subglacial drainage. The orientation, geometry and smoothed surface of the blocks, and the corresponding depressions are consistent with overridden thrust-blocks (Evans and Twigg, 2002) produced by glacier advance or surges, possibly during the minor surge event observed on the 1965 images.

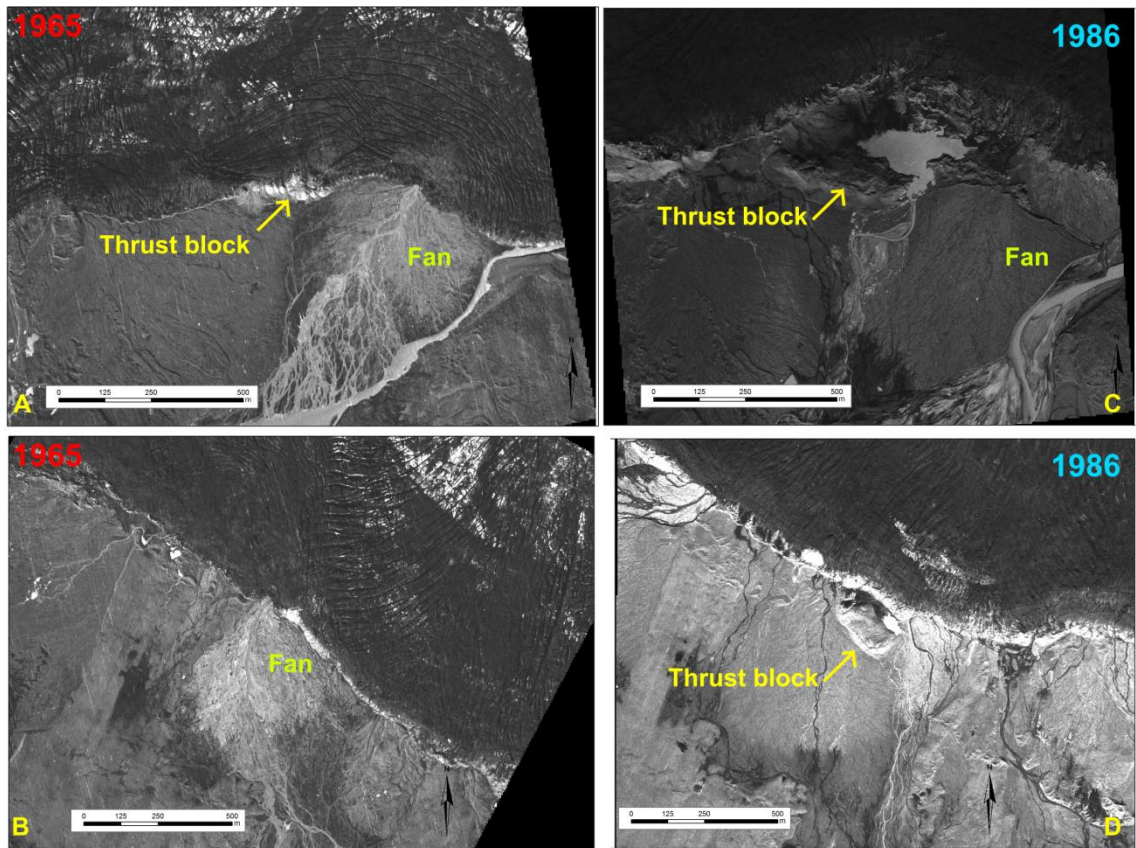


**Figure 5.18** Alluvial fans observed on 1965 images (A and B) and the adjacent thrust blocks and depressions exposed on the subsequent 1986 images (C and D).

#### 5.3.5 *Central region 1992*

The 1992 photographs reveal that the glacier margin has advanced beyond its 1965 limit by approximately 300 m (Figure 5.19). The glacier snout has developed a steep, near vertical face (Figure 5.2) with a surface elevation increase of  $80 \pm 2.56$  m since 1986 (Figure 5.20). A comparison of elevation profiles of between 1986 and 1992 (Figure 5.21) at two locations along the glacier margin reveals an increase in ice thickness of up to 100 m (west profile) and 40 m (east profile).



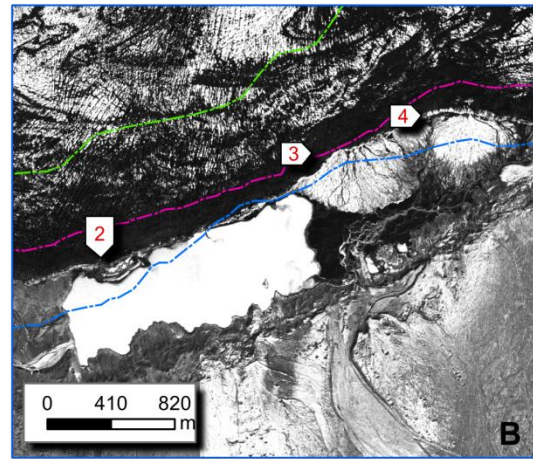
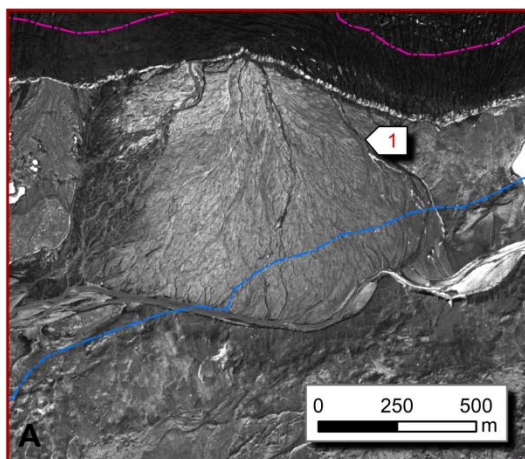
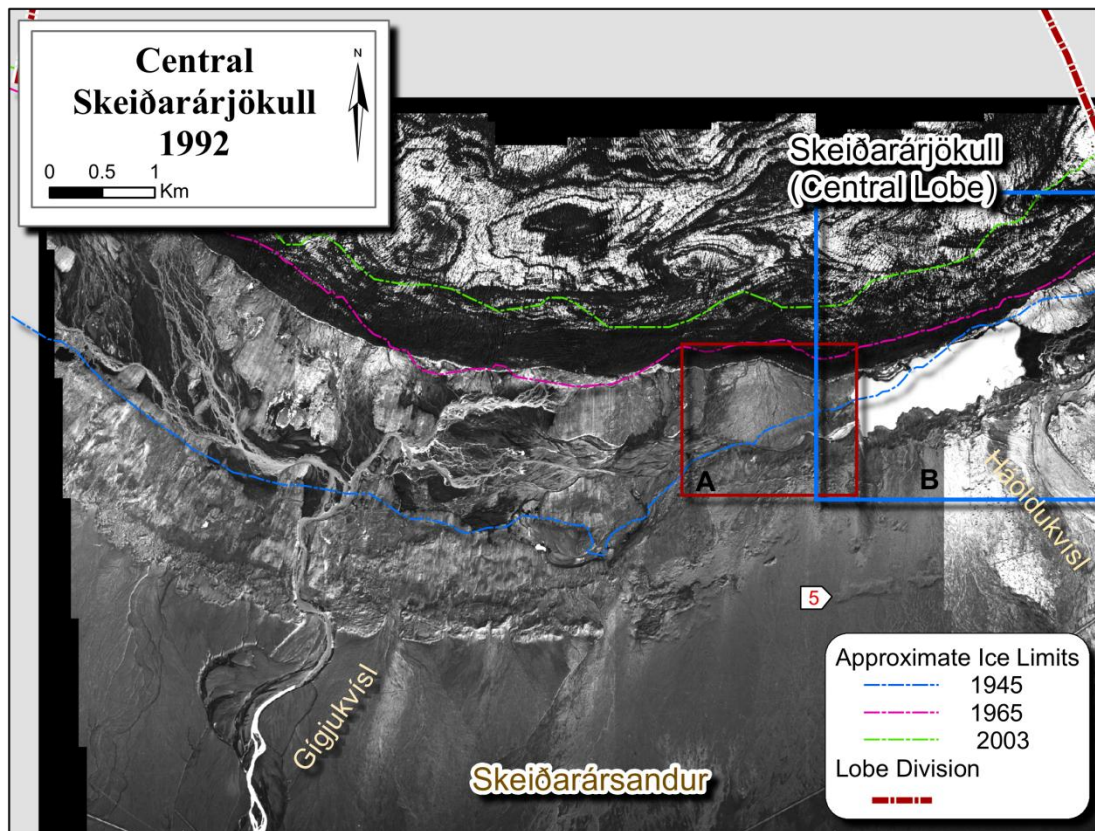
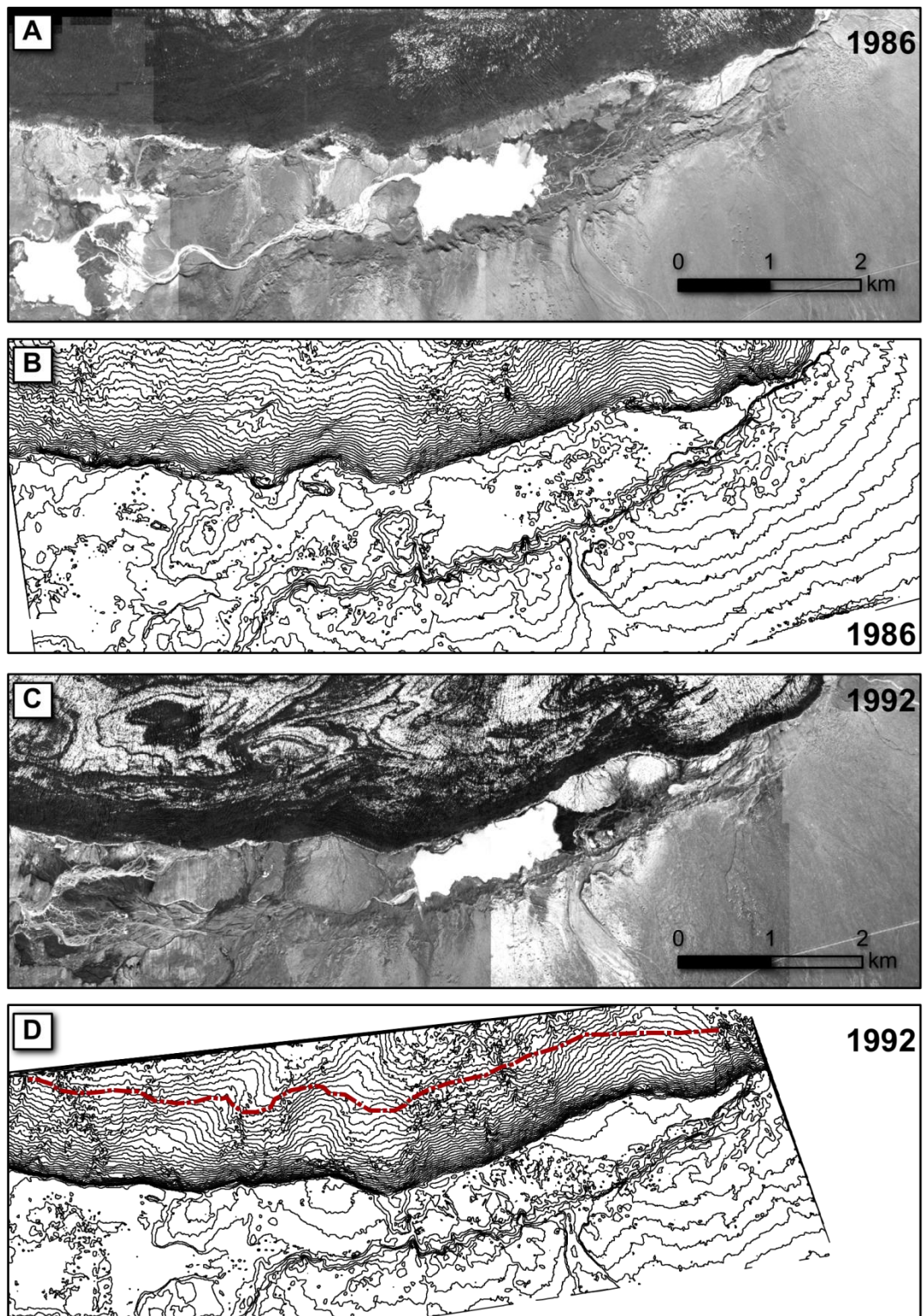
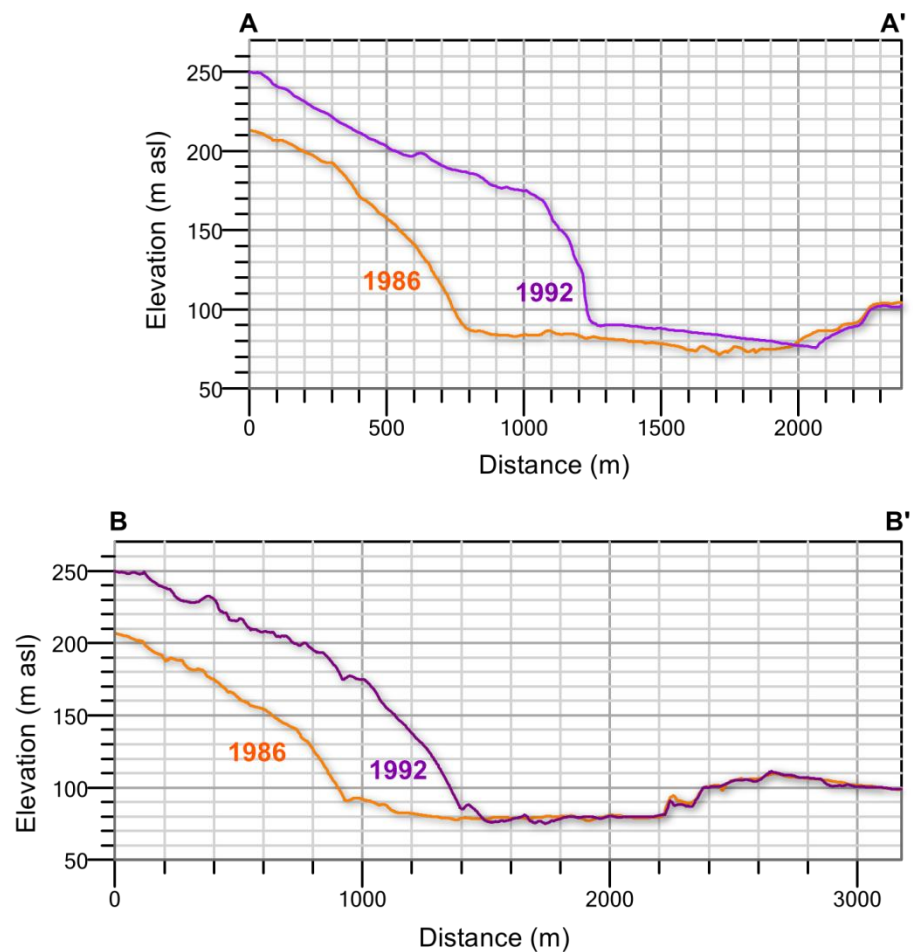
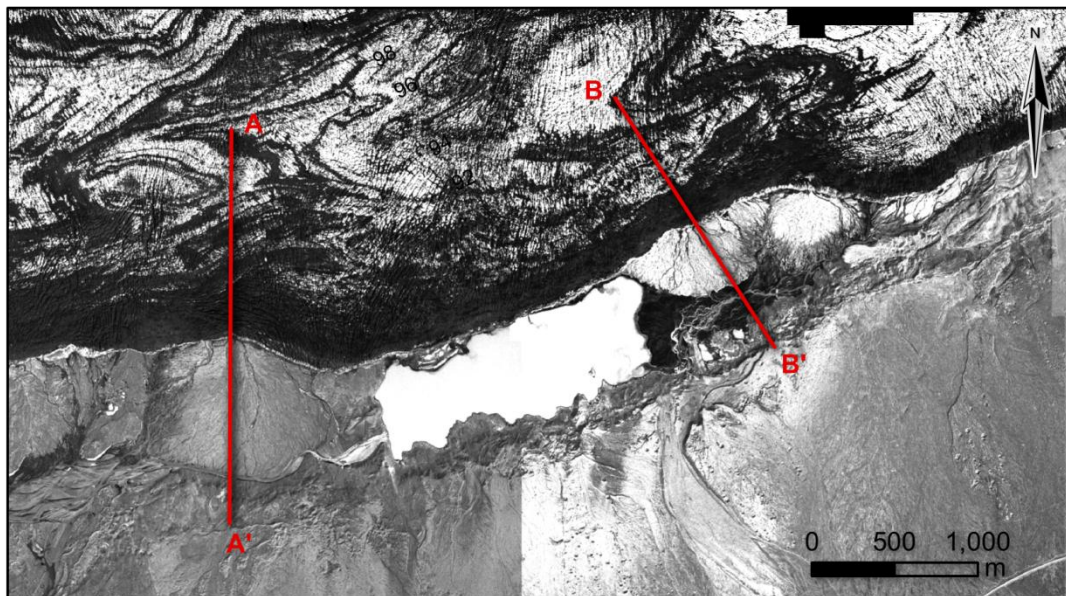


Figure 5.19 Central region 1992. Numbers 1-4 (and insets) are alluvial fans emplaced during the 1991 surge; 5) represents large-scale meltout features.





**Figure 5.20** Comparison of the advance of the central margin between 1986 and 1992 between imagery (a) and contours (b). The contour maps illustrate the steep, near vertical front of the snout of the margin (contours in 5 m intervals).



**Figure 5.21** The steepening of the ice front in response to the 1991 surge is depicted with profiles taken perpendicular to the ice front both pre-surge (1986) and during-surge (1992). In elevation alone, the ice thickness increased by over 100 m in the west and over 40 m in the east profiles.

The proglacial lake at the head of the Gígjukvísl in 1986 has been completely infilled with sediment. The drainage in this area is now comprised of shallow, intricately braided streams. Large fans ranging from 500-900 m in width have been deposited along the



glacier margin and into Háöldulón itself (Figure 5.22). Westward drainage into the Gígjukvísl from Háöldulón has been completely blocked by the largest of these fans. With the exception of the fan emplaced into Háöldulón, the fans possess an average angle of 9 degrees and range in thickness from 8 to 10 m.

The increase in ice thickness, and the steep, near vertical front of the margin, development of lateral drainage across the margin and the establishment of ice-marginal fans is consistent with observations of vertical ice fronts that develop during surge events (Meier and Post, 1969, Kamb et al., 1985, Wisniewski, 1997, Björnsson et al., 2003). The elevation data also corroborate observations made by previous authors (Andrzejewski and Molewski, 1999, Russell et al., 2001a, van Dijk, 2002, van Dijk and Sigurðsson, 2002) regarding the extent and thickness of the outwash fans emplaced during the 1991 surge and their impact on local drainage patterns and is described in detail in Chapter 3.

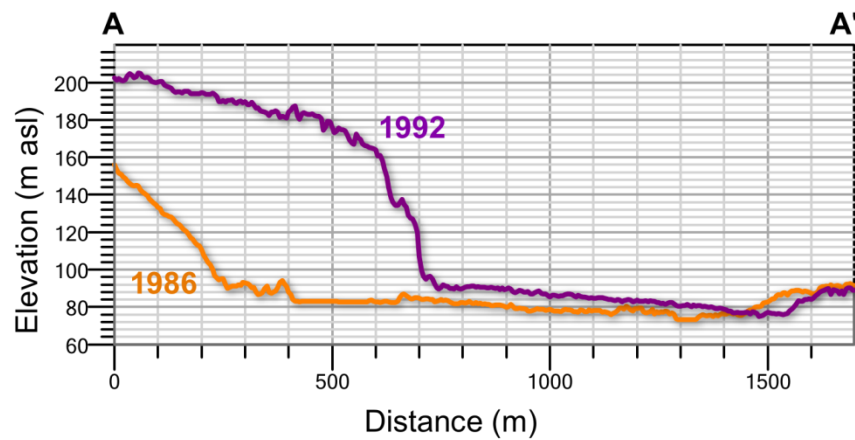
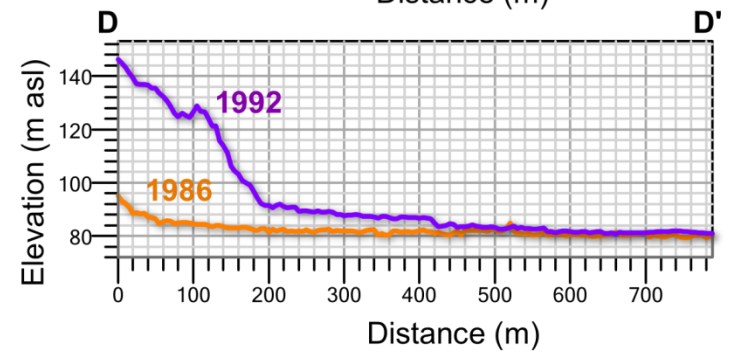
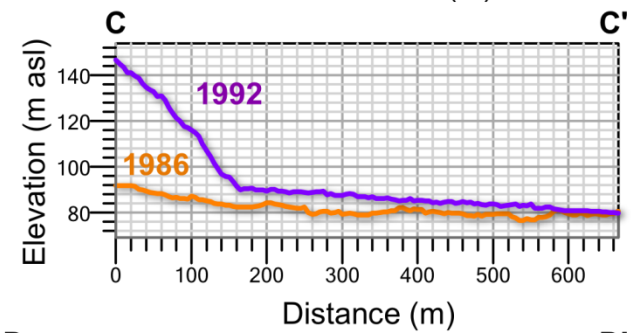
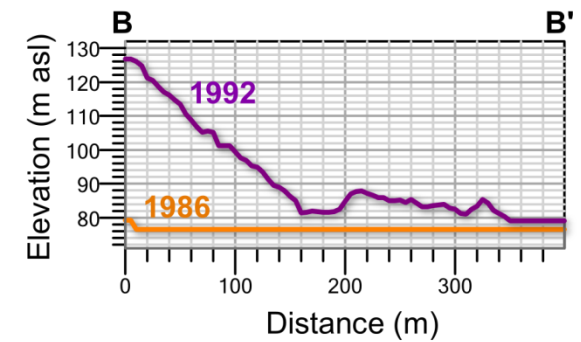
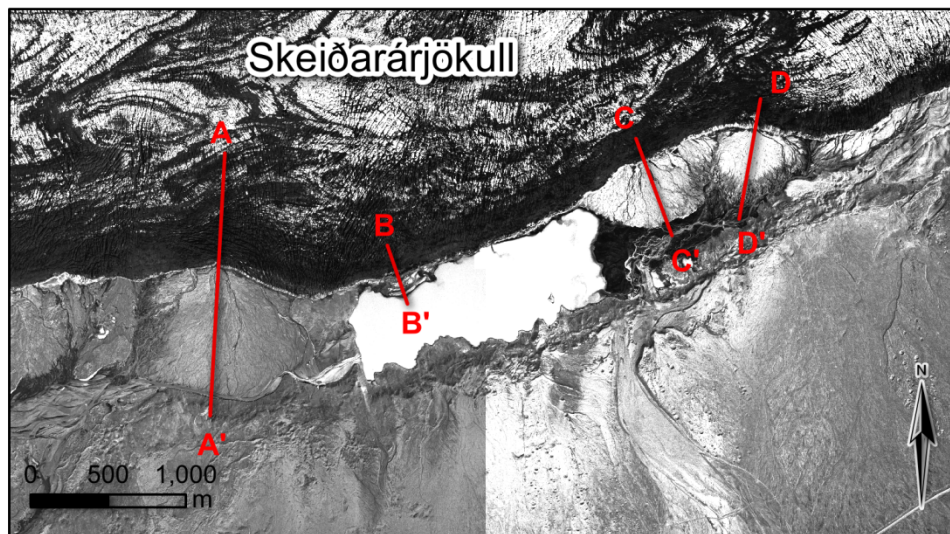
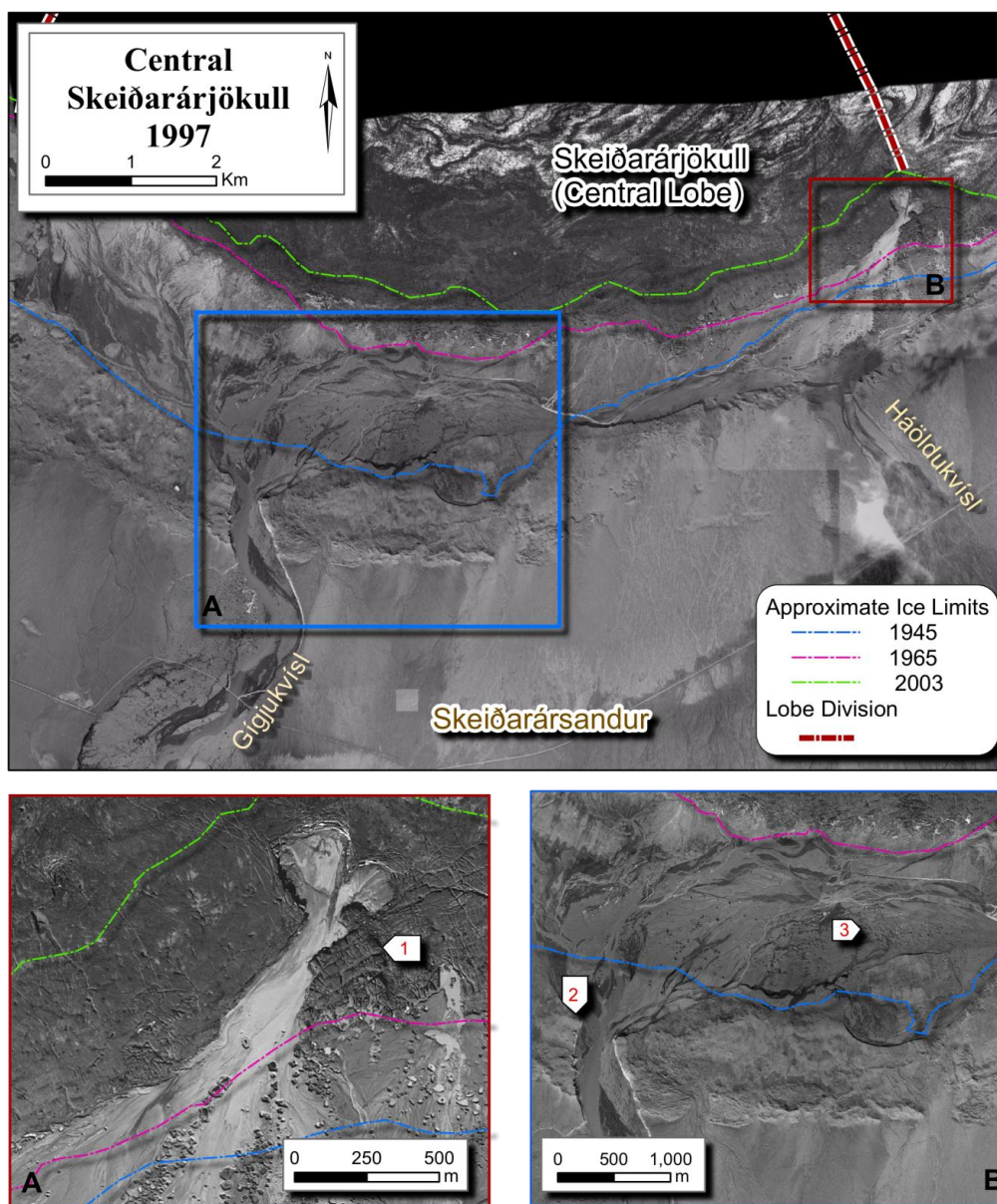


Figure 5.22 Location map and profiles of 1991 surge fans (A, B, C and D). Note - B depicts glaciotectonically disturbed glaciolacustrine deposits formed during the surge.

### 5.3.6 Central region 1997

Between 1992 and 1997, the central region of the glacier margin retreated by 100 m (Figure 5.2) and lowered by  $68 \pm 2.32$  m, returning to similar positions observed in 1986 (Figure 5.23). All proglacial lakes present on the 1992 images have been infilled with sediment. Large portions of the 1991 surge fans are no longer visible, and over 300 m of the southern wall of the proglacial depression has been removed. The Gígjukvísl moraine gap has widened from 50-100 to 500 m (Russell et al., 1999a), and downstream the Gígjukvísl channel has widened over 1.5 km. For detailed descriptions of kettle holes, outlets and other depositional and erosional features associated with the 1996 jökulhlaup, including the effects of overdeepening and margin position, see Chapters 3 and 6.



**Figure 5.23** Central region following 1996 jökulhlaup capturing infilling of the proglacial depression with sediment and the development of the: 1) double embayment, 2) Gígjukvísl gap, 3) Gígjukvísl channel and erosion of an overridden alluvial fan.

The impacts of the retreat of the glacier margin in the central region since 1945 on the high-magnitude 1996 jökulhlaup were noted by several researchers. The formation of large-volume backwater lakes ( $60\text{-}100 \times 10^6 \text{ m}^3$  of water) upstream of the Gígjukvísl moraine gap (Russell and Knudsen, 1999), and the associated settling of coarse-grained particles resulted in increased the erosive capacity of the floodwaters (Russell and Knudsen, 1999, Russell and Knudsen, 2002, Gomez et al., 2002) and permitted the reworking of rising stage sediments as local backwater controls were removed. Unlike earlier large floods, the greatest amount of geomorphic change took place within the depression, not upon the sandur, less than 25% of which was inundated (Gomez et al., 2000). Observations from the 2003 and 2007 photo-series are presented in the following section and chapters to examine the evolution of the central depression, the persistence of the 1996 jökulhlaup-related landforms and the Gígjukvísl itself.

#### 5.3.7 *Central region 2003*

Between 1997 and 2003, the glacier margin retreated 1 km (Figure 5.24) and its surface lowered extensively across the central region, up to  $84 \pm 3.45$  m (Figure 5.2; Figure 5.25). Drainage across the front of the margin has re-established at a base level 13 m lower than prior to the 1996 jökulhlaup, and numerous proglacial lakes up to 2 km in width have developed. Drainage within the proglacial depression flows east-west, as flow to the south is blocked by the sediment emplaced during the 1996 jökulhlaup. West of the Double Embayment, retreat of the margin has exposed a 1.5 km wide area of drumlinised terrain that deflects drainage southward. The retreat and lowering of the glacier margin has resulted in and supraglacial features, such as the ice-walled canyon and Double Embayment landforms that have become topographic highs that serve to restrict and direct surficial drainage.



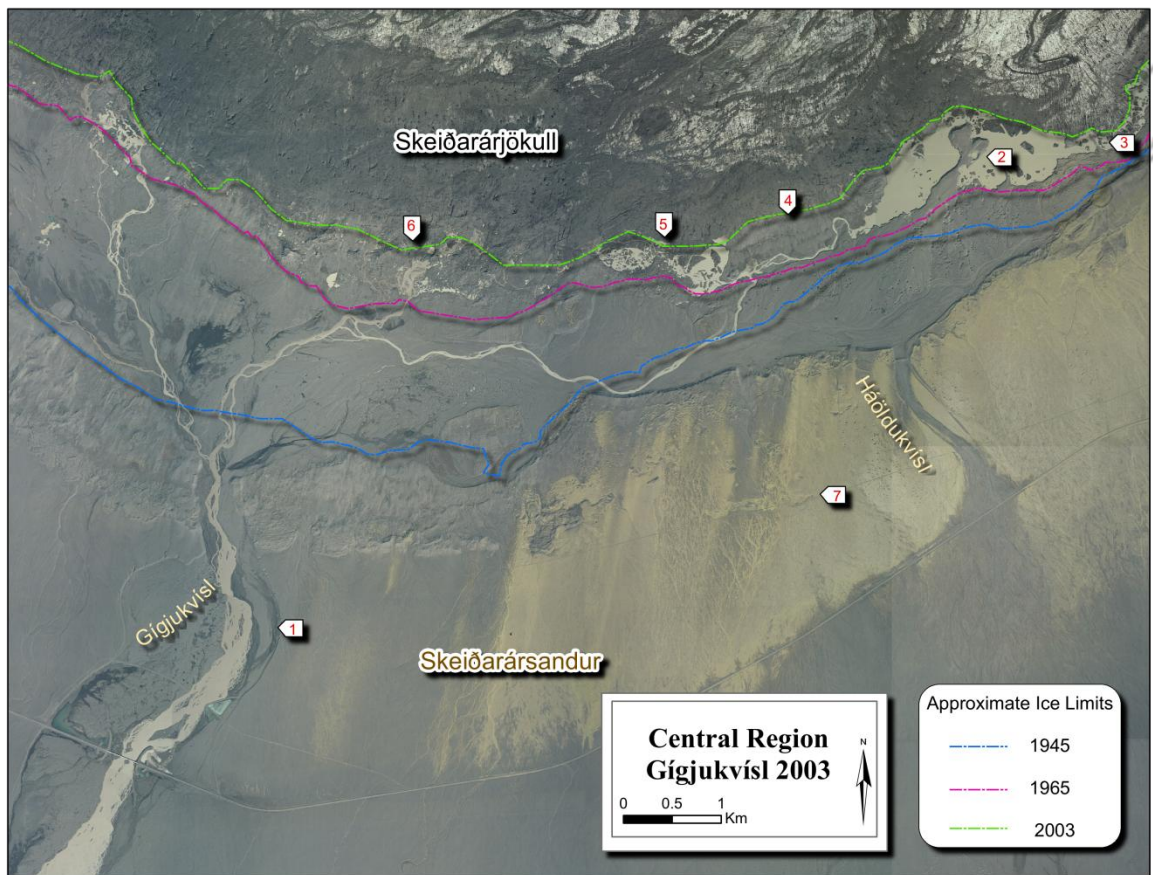


**Figure 5.24** Development of drainage and retreat of the margin following the 1996 jökulhlaup. Numbered features are: former 1997 terrace, 2) Double Embayment and esker complex, 3) elongated ridge, 4) fluted ground, 5) and 6) chaotic meltout terrain and 7) large meltout regions.

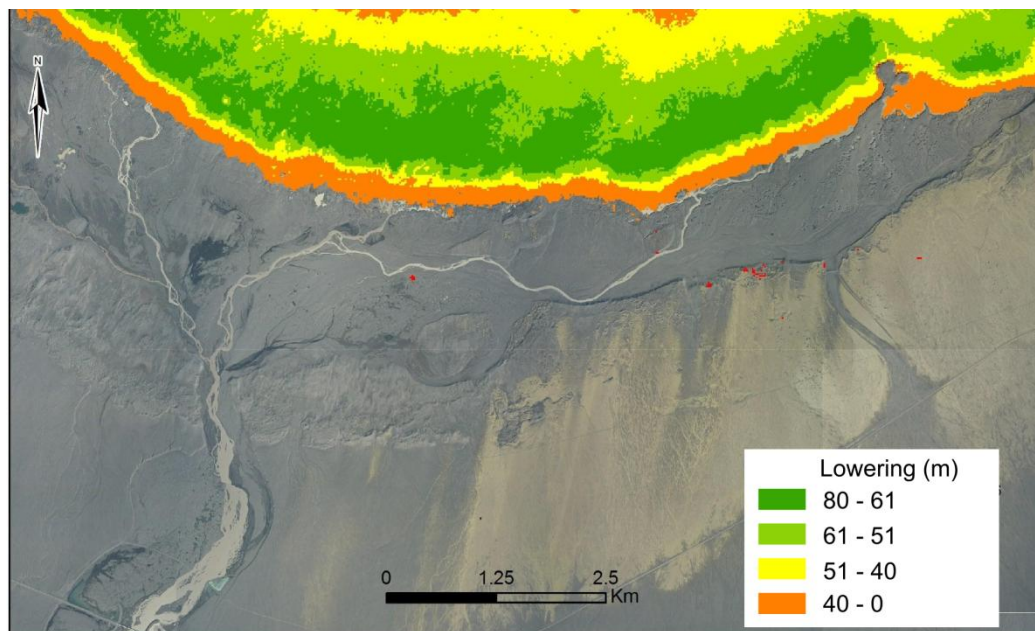


**Figure 5.25.** Lowering of ice surface between 1997 and 2003 DEMs overlain on 2003 imagery.

Retreat west of the Gígjukvísl has exposed a band of chaotic terrain (Figure 5.26) characterised by numerous irregular depressions and topographic highs. A profile of the tallest landform ( $40 \pm 2.62$  m high and 300 m wide) reveals that there has been minimal

(<5 m) lowering since 1997. Supraglacial landforms can be seen on both photo years, extending 2 km across the margin and on the 2003 images correspond to similar irregular terrain. As seen in Figure 5.27, by 2008, the supraglacial deposits in this region have developed gentle slopes and still contain ice cores that are draining onto the surrounding hummocky topography.

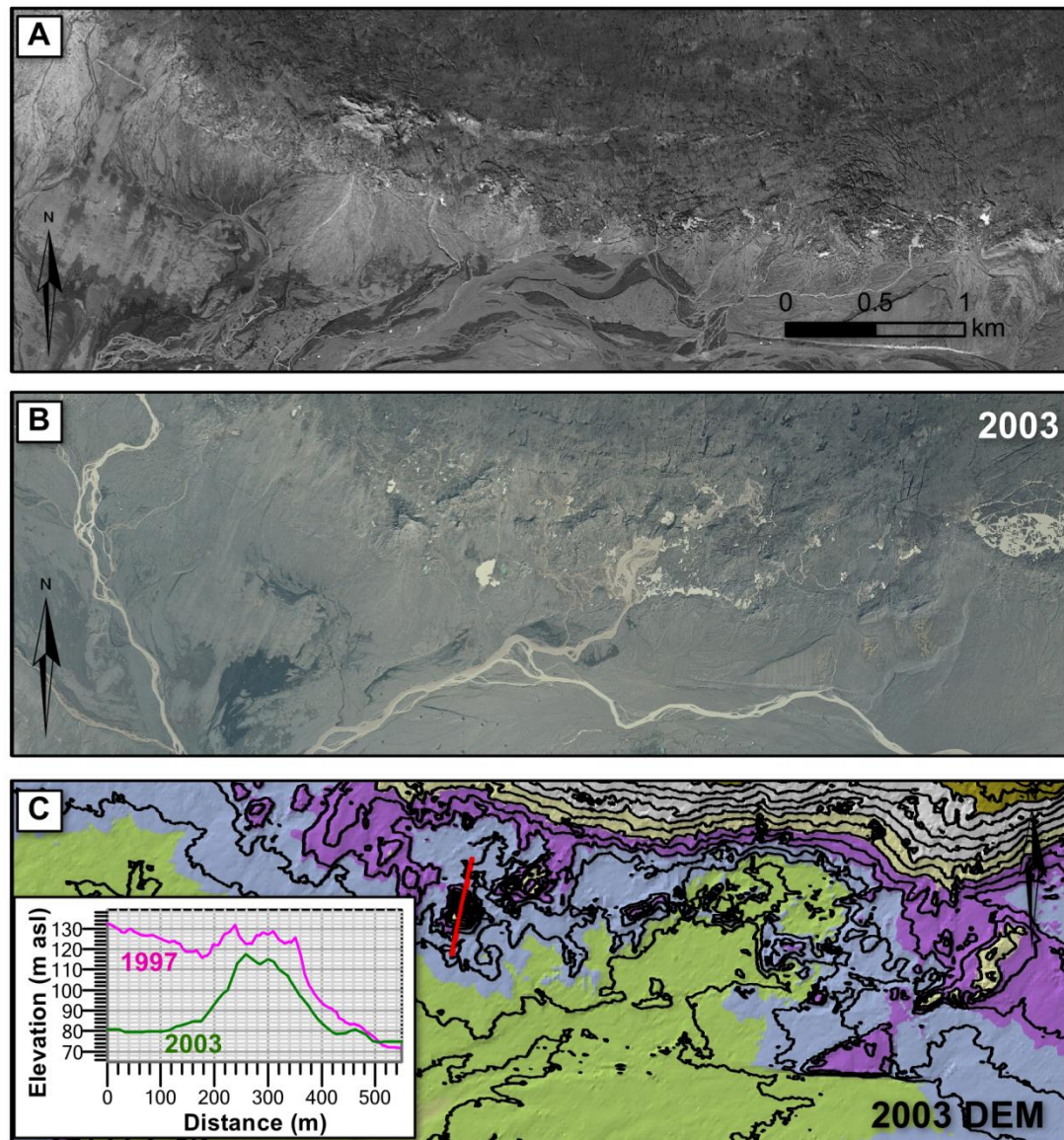


**Figure 5.26** Supra- and englacial features melting out of the margin in 1997 (top) and 2003 (middle, bottom DEM). DEM depicts only 5 m lowering of the largest landform in the area following the retreat of the margin (3 m contour interval). Note – profile transects highest profile of landform to measure secondary alteration.





**Figure 5.27** Oblique photograph depicting landforms developing following the retreat of the central margin (2008).

Given that the ice surface of Skeiðarárjökull experienced a dramatic lowering immediately following the 1996 high-magnitude jökulhlaup, this suggests that there may be a correlation. As observations of the 1996 jökulhlaup indicated that large volumes of material were transferred from beneath the ice onto the sandur (Snorrason et al., 1997) and that large volumes of material were entrained within the ice as a result of the overdeepening and associated supercooling conditions (Alley et al., 1998, Lawson et al., 1998, Evenson et al., 1999, Tweed et al., 2005), it is reasonable to assume that these conditions may have excavated the new ‘step’ now being exposed within the proglacial depression. The relationship between margin position and large-scale flooding events and the impact on the proglacial sandur are further explored in Chapter 8.

The chaotic terrain that corresponds to supraglacial debris on the 1992 and 1997 photographs suggest that the debris emplaced upon, and within, the ice has acted to retard ablation (Lister, 1953, Østrem, 1959, Nakawo and Young, 1981, Nicholson and Benn, 2006, Reid and Brock, 2010). While these are transitional landforms, as their ice cores may melt out and develop into hummocky topography in a matter of decades (or less), these features have an impact on local drainage patterns and provide insight to the processes occurring during a jökulhlaup.

#### 5.3.8 *Central region 2007-2009*

While the 2007 images (Figure 5.28) provide only partial coverage of the central region, they reveal that the glacier margin retreated another 500 m. The lake surrounding the Double Embayment complex has expanded 2.7 km and now contains icebergs that exceed 250 m in length. Two other lakes have developed since 1997: the larger lake extends over



1.3 km in length with a water level at  $85 \pm 1.64$  m asl, while the second, westernmost lake that extends off photo resides at  $75 \pm 1.64$  m asl. These lakes are separated by drumlinised terrain characterised by flutes and fracture fills. Westward, the retreat of the margin has exposed chaotic terrain that is described in detail in Chapter 6.

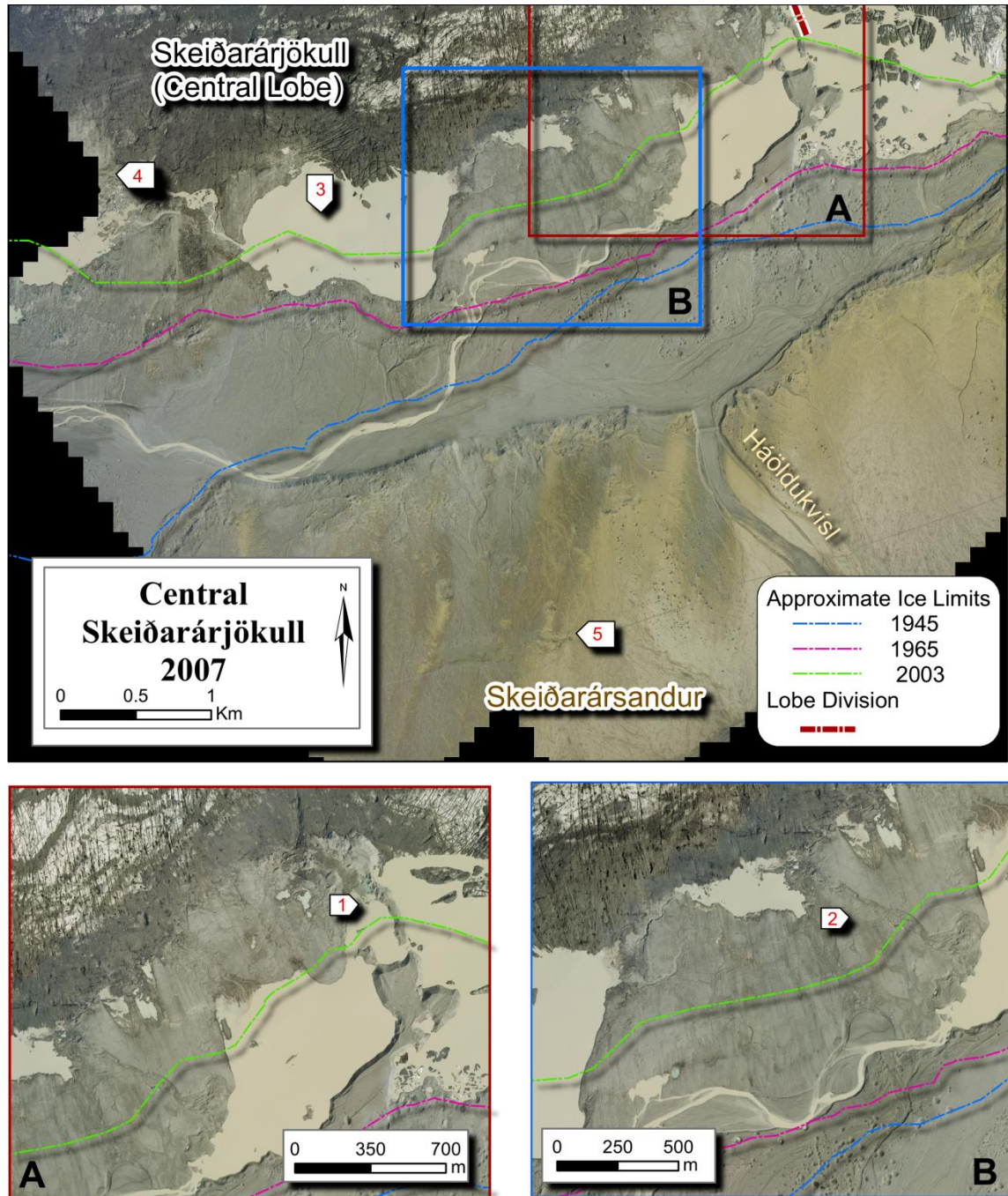


**Figure 5.28** 2007 mosaic showing the development of proglacial lakes and further exposed subglacial terrain. Features include 1) esker, 2) meltout features, 3) lake, 4) chaotic terrain and western lake, 5) depressions.

By 2009, while the glacier margin does not appear to have retreated significantly (Figure 5.1), it is apparent that the majority of the proglacial lakes are now connected via a channel that flows to the Gígjukvísl. The westernmost lake appears to have been greatly

reduced in size, with much of the former lake now replaced by shallow braided streams and extensive incision and erosion appears to have occurred north of the Háöldukvísl channel. The Gígjukvísl, now the sole channel in the eastern and central regions, also captures some of the drainage from the western portion of the central lobe.

Since 1997, the retreat of the glacier margin (approximately 1 km) within the overdeepened basin has provided accommodation space that has permitted development of proglacial lakes and drainage parallel to the glacier margin. The presence of extensive proglacial lakes along the margin and numerous large icebergs within the lakes on the 2003 and 2007 images suggests that the ice-margin may be floating and undercutting the thinning glacier margin (Funk and Rothlisberger, 1989, van der Veen, 1996, Kirkbride and Warren, 1999, Warren and Aniya, 1999, Warren et al., 2001, van der Veen, 2002, Boyce et al., 2007). Most notably, the capture of first the Eastern, then the western Skeiðará by the Gígjukvísl occurred within just six years (between 2003 and 2009). As demonstrated in the eastern region, this capture does not appear to have been the result of extensive retreat of the glacier margin, but rather by the lowering of the glacier surface, and development the flow of drainage along, and beneath the glacier margin into the Gígjukvísl catchment.

## **5.4 Western region**

### **5.4.1 *Western region 1904***

On the 1904 map (Figure 5.29), the proglacial drainage across the western glacier margin is characterised by narrow, evenly spaced channels that emerge through gaps in the moraines before draining directly south onto the sandur. The Súla drains directly west-northwest from between Skeiðarárjökull and Eystrafljall massif before joining the Núpsa. These braided channels flow southward along the base of Lómangupúr into the Núpsvötn channel and lake (off-map). The Blautakvísl, a narrow channel, flows over 3 km south before joining the Súla and the Núpsvötn (off map). Approximately 2 km south of the glacier margin are a series of low ridges orientated parallel to the glacier margin: the Sandgígúr moraine complex. The terrain between the Sandgígúr moraine and the 1890 moraines to the north (80-100 m asl) appear to have experienced little change from 1904 to the present day. Narrow, elongate ridges orientated parallel to flow may be the remains of outwash fan apices, similar to the Double Embayment; these are described later in the context of photoyears that contain higher resolution.



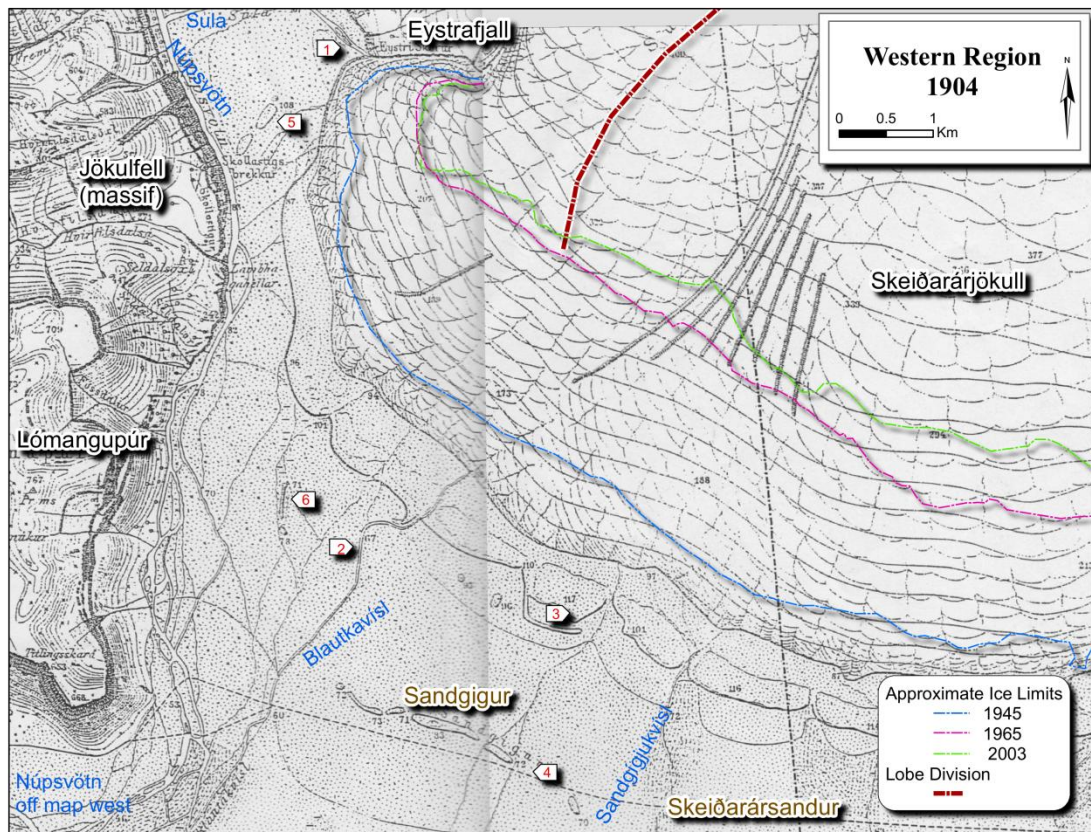


**Figure 5.29** 1904 map of Western Skeiðarárjökull depicting the position of the glacier margin and generalised drainage networks including the Blautakvísl and Sandgígjukvísl channel. Numbered features are 1) Súlá, 2) Blautakvísl, 3) 19<sup>th</sup> century moraine, 4) Sandgígur moraine complex, 5) unidentified moraine, 6) remnant fan apex.

The depiction of evenly spaced drainage channels that pass through gaps in the moraines and out on to the sandur is consistent with models of a stable, or advancing, glacier margin (Arnborg, 1955, Boothroyd and Nummedal, 1978). While Klimek (1973) suggests that the Sandgígur moraine complex was emplaced during the glacier's maximum extent in 1740, this was not confirmed during the course of this study

#### 5.4.2 *Western region 1945*

By 1945, the glacier margin has retreated 850 m, and most of the drainage channels across the sandur have been abandoned (Figure 5.30). Only two channels remain: the Súlá and the Blautakvísl. These channels join together and inter-braid upon a 2 km wide sandur. The Súlá emerges from the between the margin of Skeiðarárjökull and the base of Eystrafrjall as a series of braided streams that cover an area > 500 m across before combining to form a single channel that incises several older, larger channels. In contrast to the 1904 map, the Súlá flows directly south instead of cutting immediately west. As it passes across the floodplain, the Súlá channel narrows (20-50 m in width) before its channels merge with those of the Núpsa. The Súlá channels, and the plains to the south and west, are littered with obstacle marks and kettle holes up to 15 m in diameter.

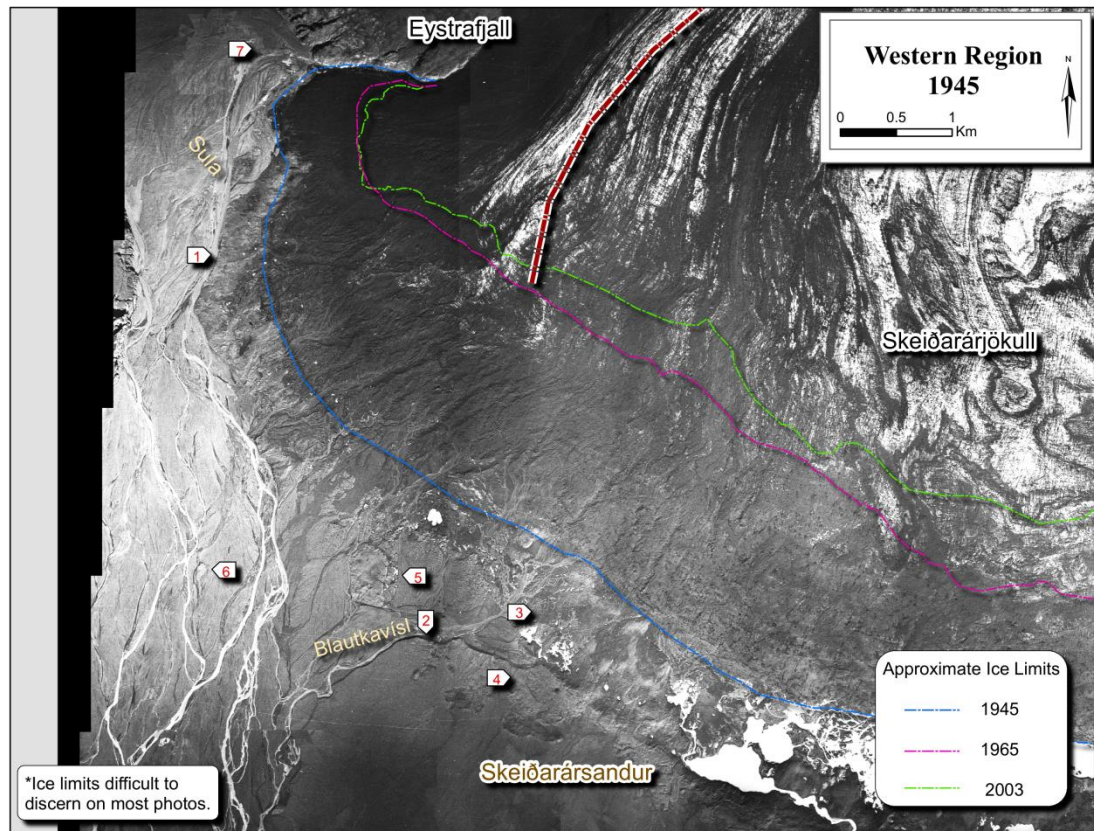


**Figure 5.30** 1945 photomosaic of western region. 1) Sula, 2) Blautakvísl, 3) proglacial trench region with small lakes, 4) 1890 moraine, 5) isolated 1890 moraine, 6) and 7) remnant fan apices.

The Blautakvísl is 30 m wide and drains the eastern portion of this glacier lobe, undercutting a larger, older terrace before inter-braiding with the other channels. The ~2 km long erosional scarp that has developed adjacent to the Blautakvísl restricts flow from reaching the elevated sandur to the east. The proglacial trench between the glacier margin and these braided channels is characterised by a low, wide, undulating plain of hummocky topography and isolated plateaus. The terrain exposed by the retreat of the glacier margin contains a few very small lakes, often no more than 30 m wide. The only drainage visible on this terrain flows around a series of low, rounded ridges before incising into a heavily kettled, older terrace and into the Blautakvísl. Two elongated ridges are orientated parallel to the glacier flow and contain kettles, obstacle marks and boulders.

The reduction in the number of channels in response to ice margin retreat corroborates observations made by Price and Howarth (1970). The hummocky topography exposed by retreat is consistent with descriptions of kame and kettle topography at a retreating margin (Boulton, 1967, Price, 1969, Krüger and Kjær, 2000). The numerous kettle holes and obstacle marks, as well as the straightening of the Sula, are interpreted in this study to



be the result of the high-magnitude jökulhlaup(s) that affected this region in 1922, 1934, or 1938 as noted by other authors (Wadell, 1935, Thorarinsson, 1974, Björnsson, 1997). The elongated ridges are interpreted to be the apex out of outwash fans emplaced during a high-magnitude jökulhlaup event and are described in detail in Chapter 6.

#### 5.4.3 *Western region 1965*

By 1965 the glacier margin retreated over 2 km and has exposed an array of subglacial features (Figure 5.31). In addition to the frontal retreat of the margin, a comparison between the ice against the massif Eystrafljall between 1945 and 1965 illustrates the vertical lowering of the ice surface over the two decades (~30 m). The Súla remains the dominant drainage channel along the western margin and it continues to flow southward, if from a greatly eastward-shifted position along the ice front. The Súla is established within a channel 25 m wide, possessing much the same character as it did in 1945. The Blautakvísl consists of a series of braided streams, the largest channel not exceeding more than 5 m in width.

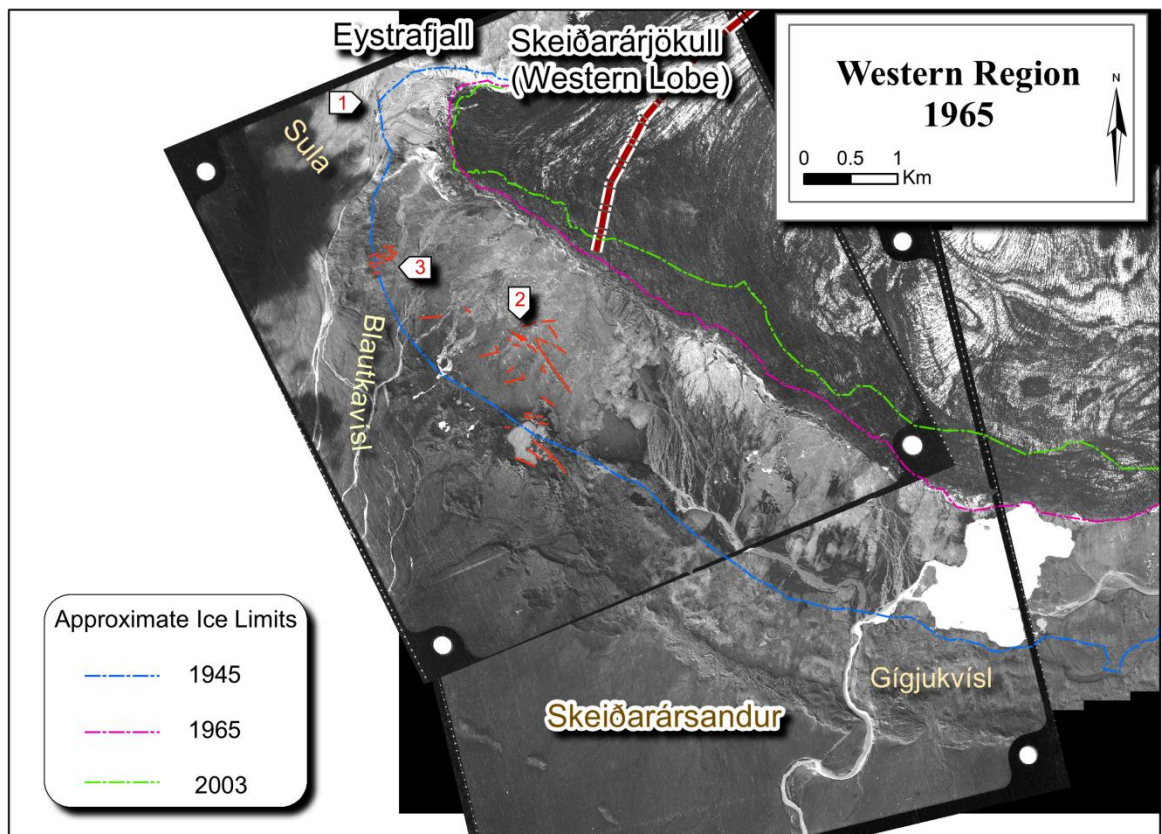


**Figure 5.31** Retreat of the Western margin in 1965 (> 2 km). Numbered features are 1) Súla, 2) and 3) are rectilinear ridges.

Between the glacier margin and 1890 moraines lies a region of low relief, broken by a series of elongated ridges. These ridges are less than 2 m in height and extend over distances of > 600 m. These ridges, while often perpendicular to the direction of glacier

flow, intersect each other at right angles. The ridges and sinuous esker that leads to the limit of the former 1945 margin serve to impound local drainage, resulting in numerous shallow lakes and pools.

The wide expanse of low relief was described by Klimek (1973) as being ‘flattened’ due to the deposition of alluvial fans by the retreating ice front, effectively levelling the topography. It is worth noting that if the region was indeed ‘flattened’ by the deposition of successive alluvial fans during margin retreat as posited by Klimek, it is unlikely that ridges with such low relief ( $< 2$  m) would persist, suggesting that the topography, and the features deposited upon it, are primarily the result of lowering and melting the glacier ice with minimal deposition. The rectilinear ridges are consistent with descriptions in the literature of fracture fills (Rijsdijk et al., 1999, Roberts et al., 2000, Russell et al., 2006, Munro-Stasiuk et al., 2008); the evolution of these ridges from 1965-2003, and their association with the sinuous esker are explored in more detail in Chapters 6 and 8.

#### 5.4.4 *Western region 1968*

Between 1965 and 1968, the Súla has dramatically altered in character: it now possesses a large central channel (60 m in width) and displays no braids (Figure 5.32). The kettle holes present along this channel in 1965 are absent. East of the elongate ridge that abuts the Súla is a heavily kettled alluvial fan, 420 m in width. The kettle holes on this fan range from 3 to 13 m in diameter. The Blautakvísl has also dramatically altered its planform character, now comprised of four braided channels; these channels have removed a portion of the old 1890 moraine. Most of the small moraines present in 1965 are also no longer visible.

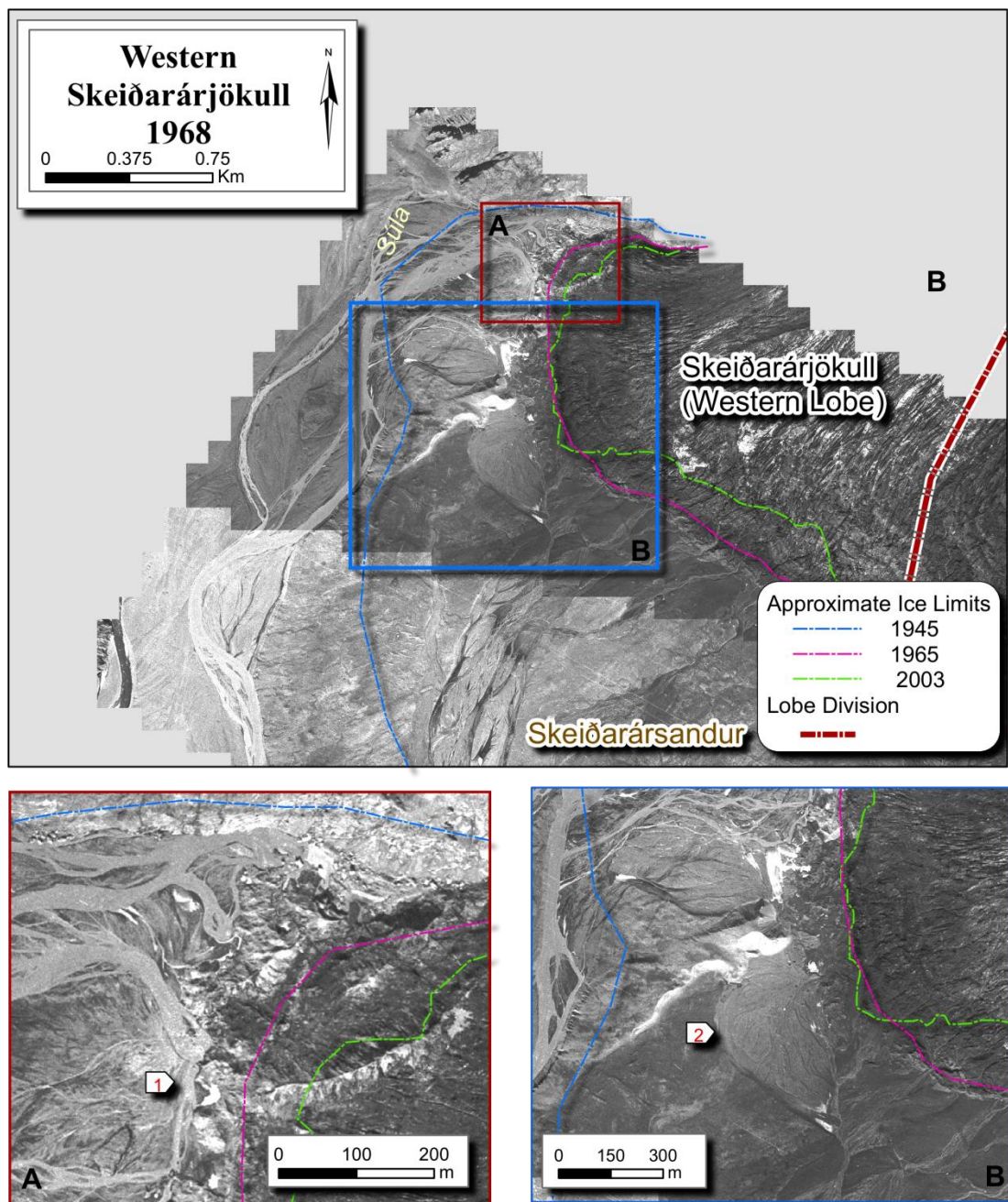


Figure 5.32 Western region 1968. Numbered features are 1) Súla, 2) kettle holes.



The presence of a kettled alluvial fan, the removal or burial of other landforms (moraines, kettle holes and obstacle marks) and the widening and deepening of the channels is consistent with observations of proglacial terrain following jökulhlaups (Russell, 1993, Maizels, 1997, Fay, 2002). This may be the result of a low-magnitude Grænalónhlaup as would be suggested by the lowering of the ice surface (Roberts et al., 2005). While the position of the glacier margin has not fluctuated in three years, there has been a marked increase in incision and reduction of channel braiding in the Súla; these observations demonstrate that glaciolimno-jökulhlaups that affect a relatively restricted area may result in a dramatic alteration in large-scale drainage patterns within a small time step (days to weeks).

#### 5.4.5 *Western region 1979*

While the margin position appears unchanged, by 1979 the central Súla channel has again changed character and its single channel has been replaced by extensive braided channels. At the head of the Súla are a dense concentration of kettle holes (> 10 m in diameter) and similar kettle holes may be found as far as 2.5 km downstream (Figure 5.33). The character of the Blautakvísl drainage outlets near the ice margin has also changed: instead of possessing multiple outlets spaced across the margin, a single incised channel emerges near the elongated ridge that separates it from the Súla.

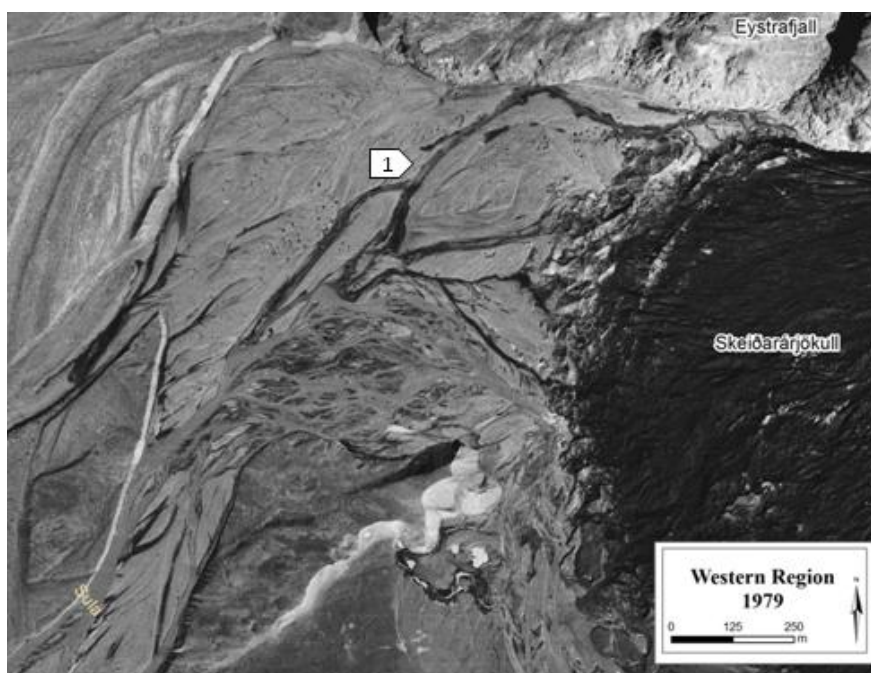


**Figure 5.33** 1979 images containing kettle holes and obstacle marks downstream of Súla outlet (Feature 1).

The presence of kettle holes, obstacle and scour marks as well as the alteration of the channel geometry suggests another Grænalónhlaup. The most likely process responsible for the emplacement of these features is a Grænalón flood documented in 1979 (Table 3.2). It should be noted that while the position of the glacier margin remained unchanged the two channels were affected differently: the braided channels of the Súla increased in density and proximity to the margin, while the Blautakvísl incised within a single channel.

#### 5.4.6 *Western region 1986*

Taken during the 1986 surge, the photographs reveal that the glacier margin has advanced up to 100 m since 1979 (Figure 5.34). An alluvial fan, over 500 m wide, is present in the eastern portion of this region, incised by a channel over 200 m long and up to 25 m wide. In 1979 the Súla contained few channels wider than 50 m in width, while in 1986, the Súla is comprised of numerous channels that range from 150 to 195 m in width. The Súla and the Blautakvísl channels merge together between the base of Lómangupúr and the elevated sandur to the east, spanning an area more than 2 km across. Ice blocks are present along the length of the Súla, but the highest concentration are located at the head of the Súla, south of Eystrafjall. Here ice blocks greater than 15 m in diameter lie within the Súla channel.

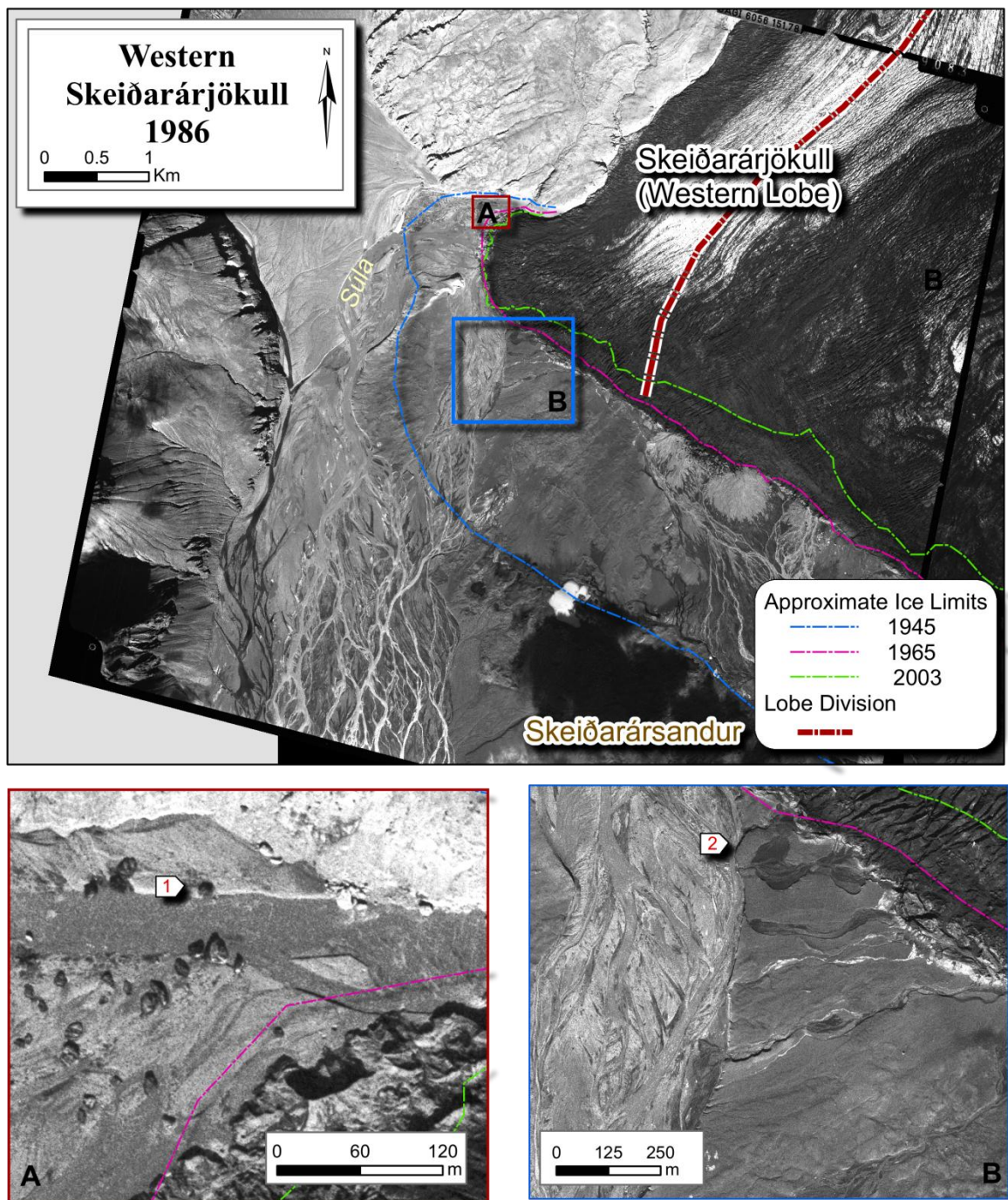


**Figure 5.34** Western region 1986 taken following the 1985-86 surge and jökulhlaup: 1) Sula and ice blocks and obstacle marks and 2) erosion along Blautakvísl.

The advance of the glacier margin, the increase in proglacial drainage outlets across the margin, and the presence of the large alluvial fan are indicative the internal reorganisation of drainage into a distributed system associated with a glacier surge (Kamb et al., 1985, Kamb, 1987, Fleisher et al., 1998, van Dijk, 2002, Björnsson et al., 2003). The intense braiding observed in these channels is interpreted to be a response to the increase in discharge and sediment load (Krigström, 1962). While the surge may have contributed to the discharge into the Sula, the presence of large ice blocks is consistent with the

documented the documented 1986 Grænalón jökulhlaup that obtained recorded discharges of  $2,000 \text{ m}^3 \text{ s}^{-1}$  in the Súla (van Dijk, 2002).

#### 5.4.7 *Western region 1997*

Taken a year after the 1996 jökulhlaup, the images of the Súla and the Blautakvísl channels contain kettle holes, obstacle marks, and boulders that may be found over 3 km south of the outlets (Figure 5.35). These kettle holes and obstacle marks are not confined to the two main channels but are also found near the eastern edge of the Western region. A new outlet is present along the glacier margin, 300 m west of the 1986 outlet, and contains kettle holes and ice blocks over 11 m in diameter. A channel flowing from this outlet has been incised into the hummocky terrain, displaying numerous obstacle marks and kettle holes before flowing >1.5 km south east into the Gígjukvísl. Similar to the eastern Skeiðará following this same event, profiles the Súla between 1968 and 1997 (Figure 5.36) display minimal modification. DEMs of the intervening years were not available, so it cannot be ascertained from this data if the aggradation (~5 m) observed on the profiles occurred solely as a result of the November 1996 jökulhlaup.



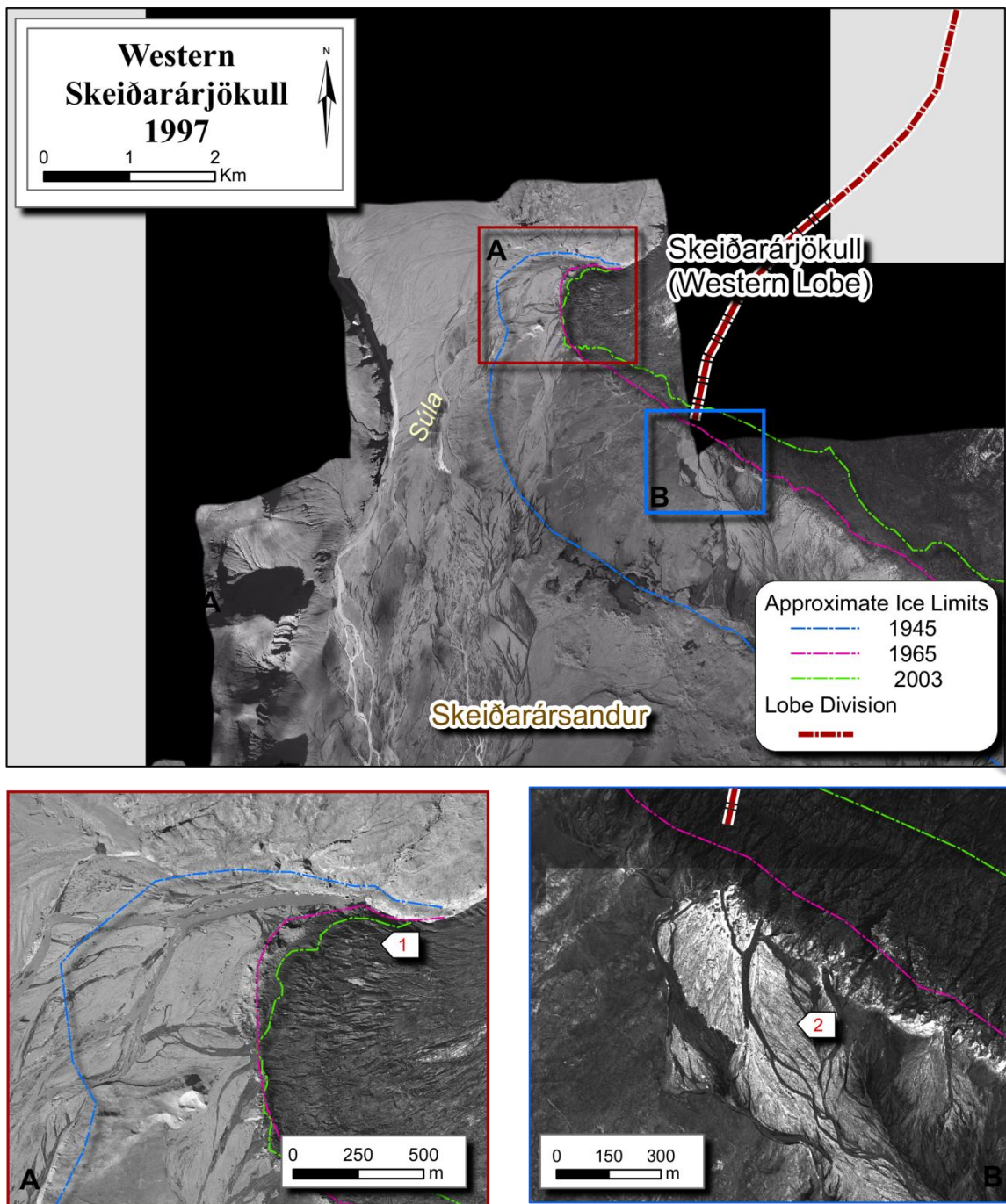


Figure 5.35 Western region 1997 photographs. Numbered features are 1) Súla, 2) kettled jökulhlaup fan and channel formed during 1996 jökulhlaup.

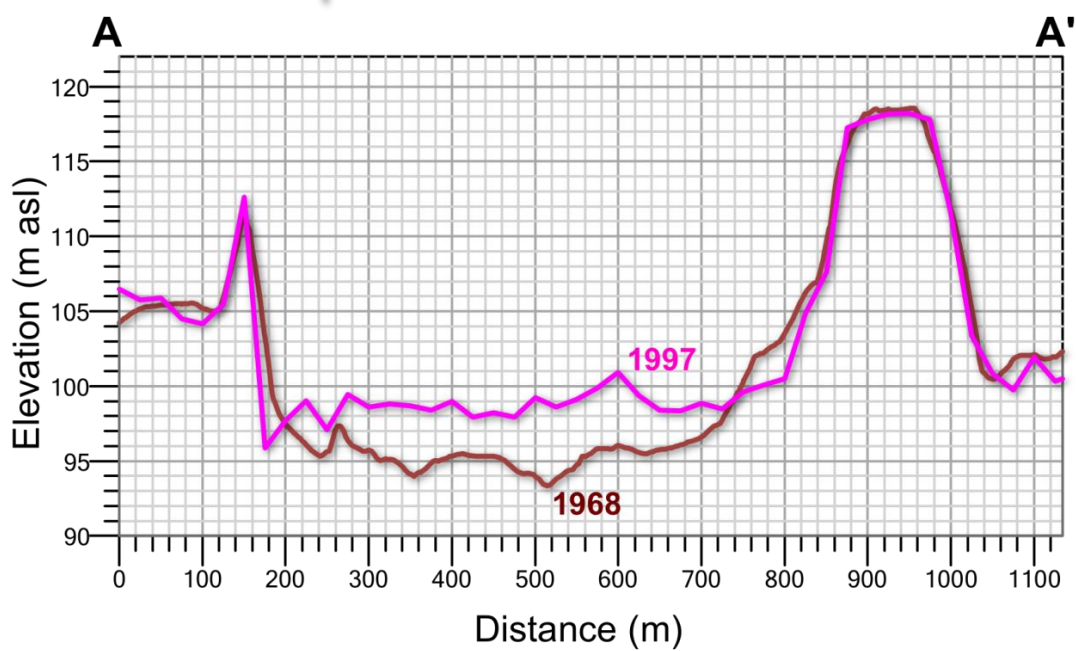
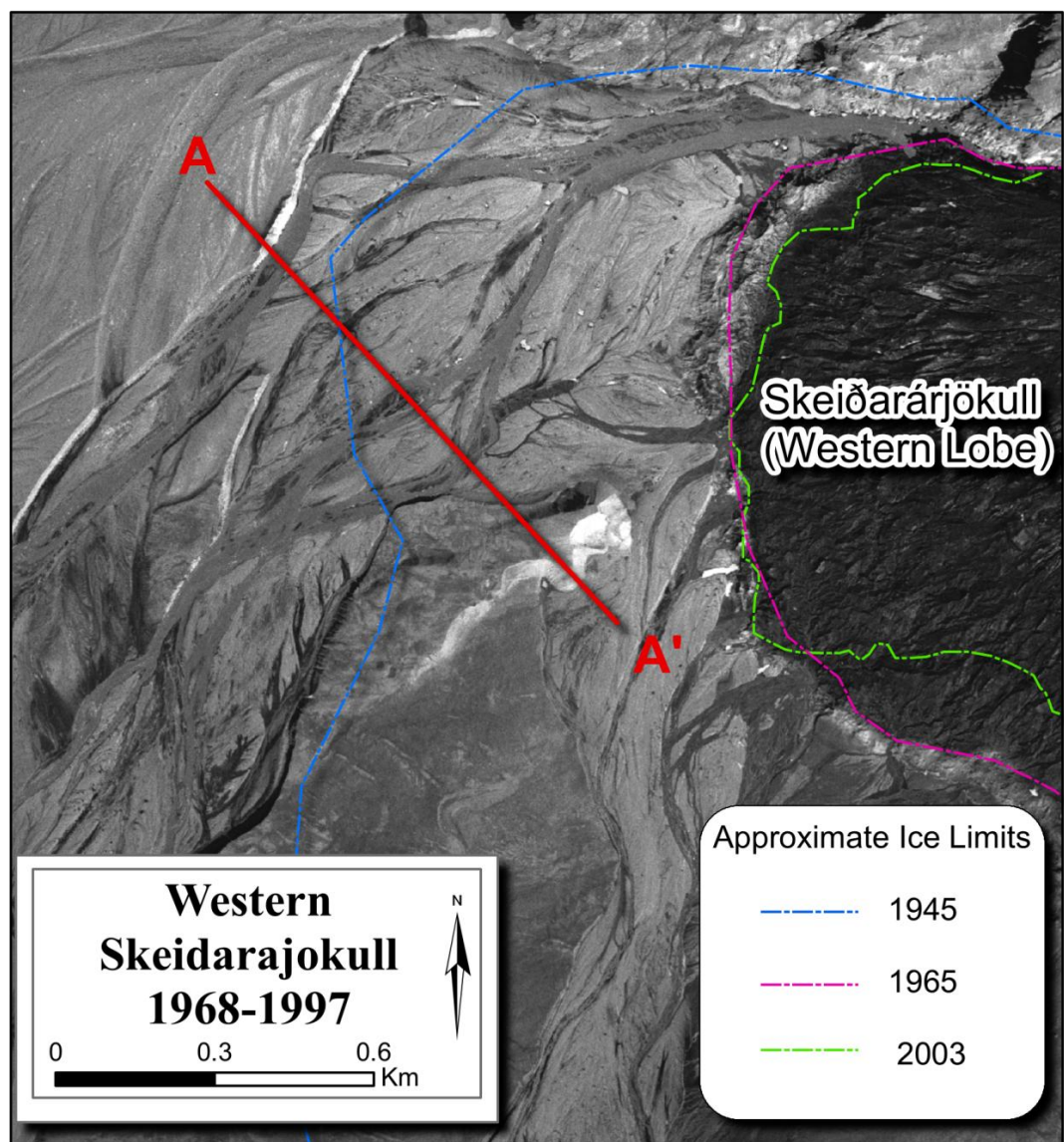


Figure 5.36 Profile of Súlá channel, 1968 and 1997 DEMs constructed to highlight lateral erosion and aggradation.



#### 5.4.8 Western region 2003-2009

By 2003, the glacier has retreated over 3 km from its 19<sup>th</sup> century moraines, over 2 km since 1945 alone (Figure 5.37). The glacier surface is heavily crevassed, and contains extensive supraglacial drainage channels and numerous supraglacial lakes. While full 2003 coverage of the western area was not acquired, it is apparent on the existing imagery that the Blautakvísl channel has altered drastically since 1997. Drainage now emerges along the glacier margin from two main outlets, feeding channels that range from 20-60 m in width that flow into the Blautakvísl, now a single channel 42 m across at its widest point. Figure 5.38 depicts the incision of the Blautakvísl channel and eastward lateral erosion.

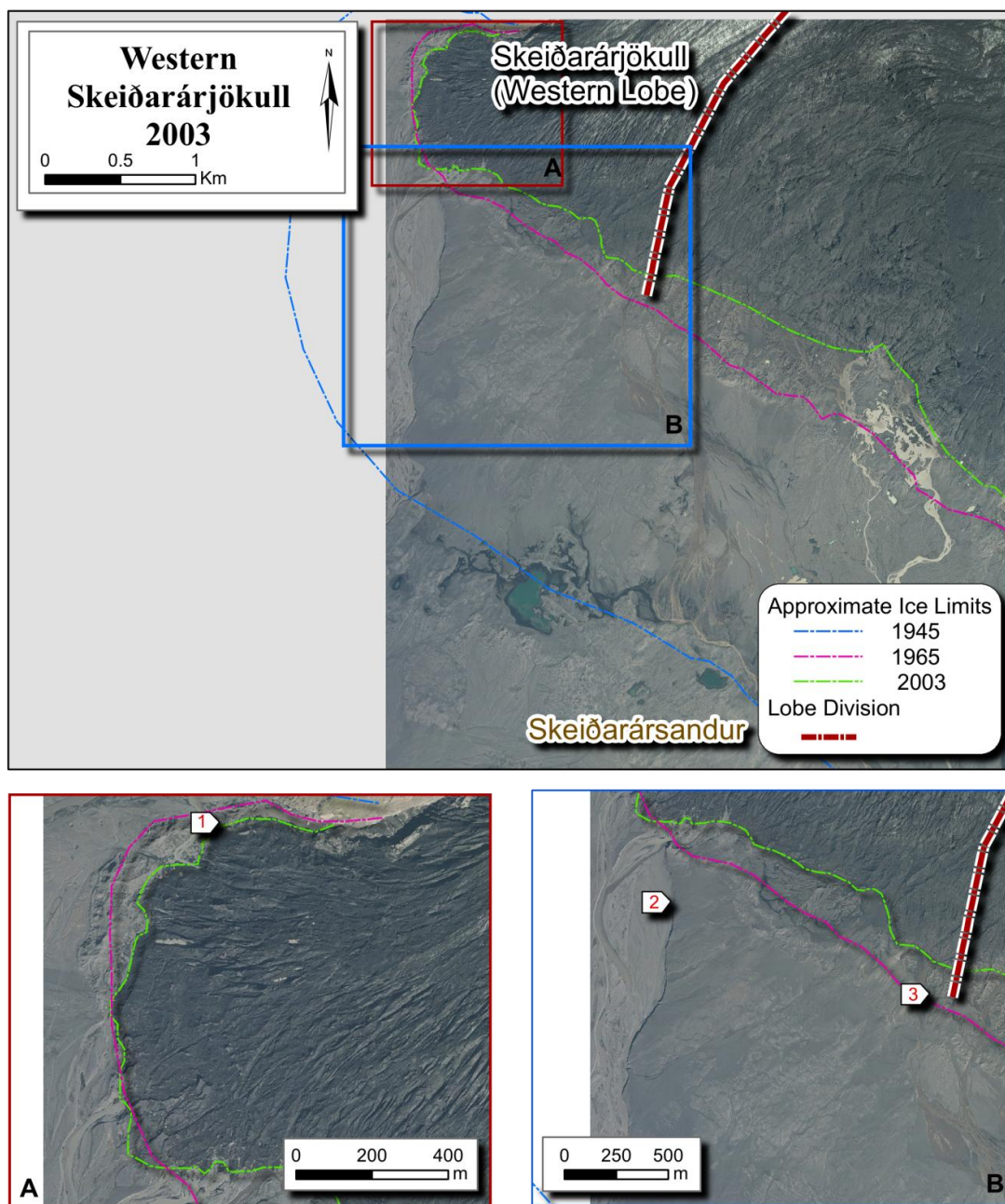
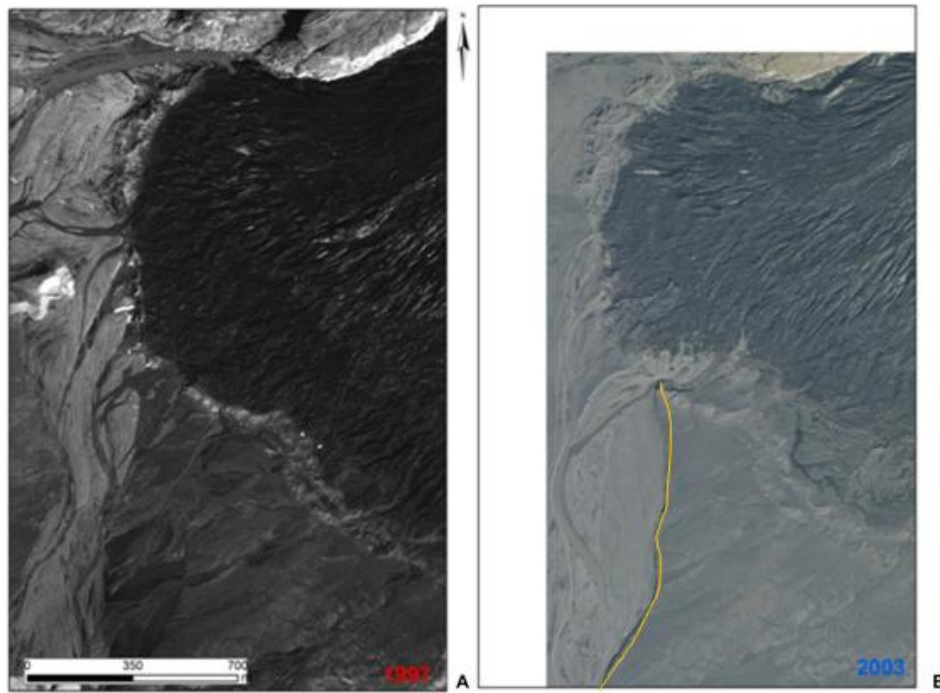


Figure 5.37 Western Region 2003. 1) Súla, 2) erosional scarp east of Blautakvísl, 3) 1996 outlet.





**Figure 5.38** Comparison of Súlá and Blautakvísl outlets in 1997 (a) and 2003 (b). Note the development of the 42 m wide Blautakvísl channel and removal of material west of terrace (orange) on the 2003 image.

Oblique aerial photographs of the Blautakvísl were taken in July and August 2005, before and after a Grænalón jökulhlaup (Figure 5.39). Prior to the jökulhlaup, there are numerous, shallow channels present that drain the glacier margin. Taken a week after the jökulhlaup, drainage on the photograph appears confined into a few, wide channels that appear to have incised into the sandur and flow into the main Blautakvísl channel. The low-resolution 2009 GeoEye thumbnails reveal that the Súlá is no longer active and all supraglacial drainage has shifted eastward into the Blautakvísl (Figure 5.40). While the resolution of these images is poor, it also appears that the western edge of ice margin is broken apart. Drainage into the Blautakvísl in 2009 is confined to 1 – 2 channels as it flows south for 1 km, before transitioning to braided channels as it passes onto the broad expanse between Lómangupúr and the elevated sandur.



**Figure 5.39** Channel straightening and incision of the Blautakvísl following Grænalón jökulhlaup in 2005 (photographs courtesy of Dr. A. J. Russell).

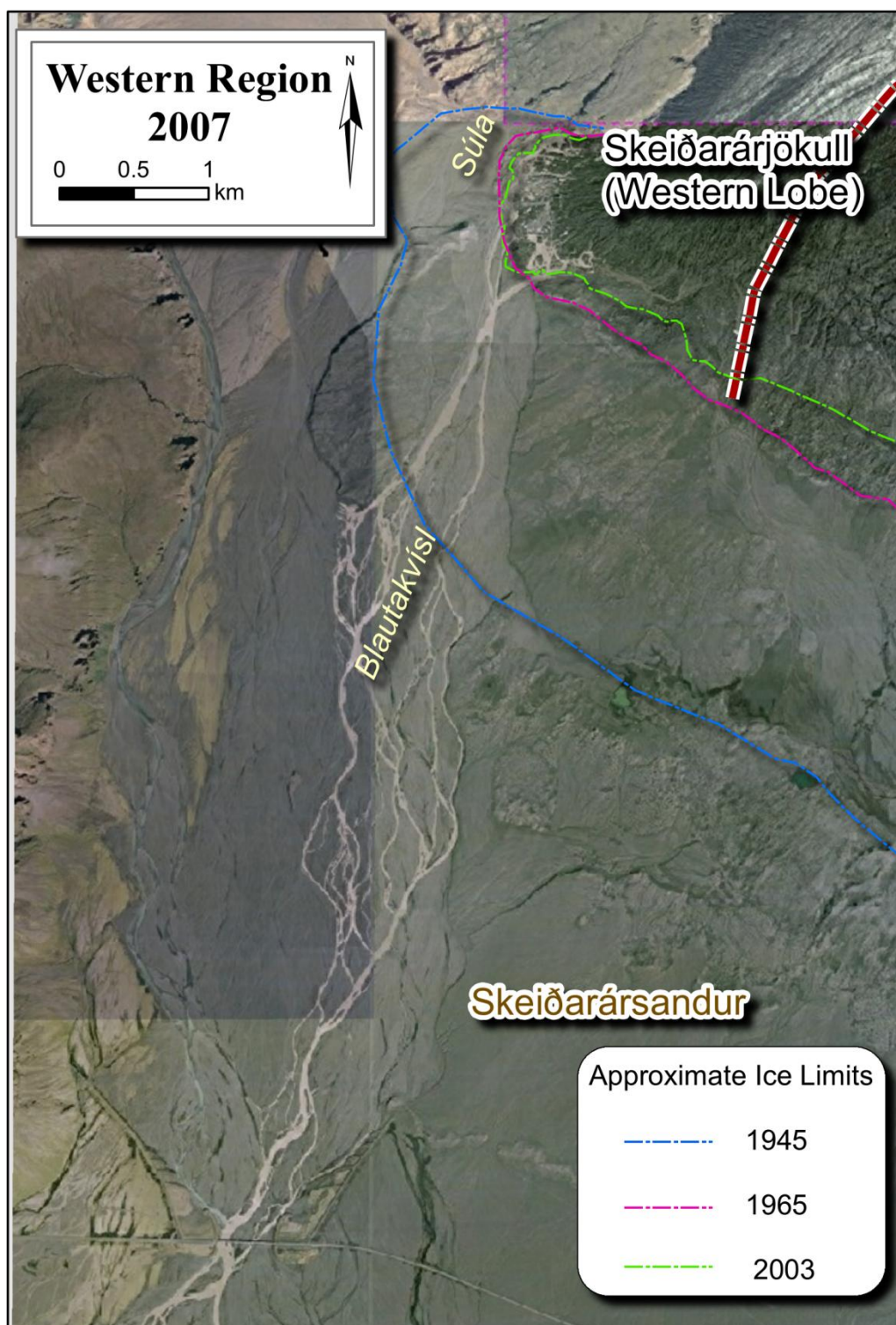


**Figure 5.40** 2007 snapshot of Sula (obtained from Loftmyndir). Note the eastward migration of the channel as well as the incision of the single channel for ~2 km, before developing into braided channels.

Limited elevation data of the lateral margin of the western lobe was available for this study. While 1997 data was available, only the 1968 images provided substantial coverage of the same region. No photographs extended to lake Grænalón or the ice dam described in Chapter 3, nor were images of the region available between the 1981-1992,



the period reported by Roberts et al. (2005) that described a sub-aerial 18 km long drainage route along the glacier's flank. Figure 5.41 presents a comparison of photosets of the Western region from 1945, 68 and 1997. Comparison of 1945 photographs illustrate retreat of over 150 m away from the wall of the massif, and elevation profiles between 1968 and 1997 reveal a lowering of 30-40 m of the Western lobe itself (Figure 5.42). Vertical retreat along the massif itself is less pronounced (ranging between 5-15 m).

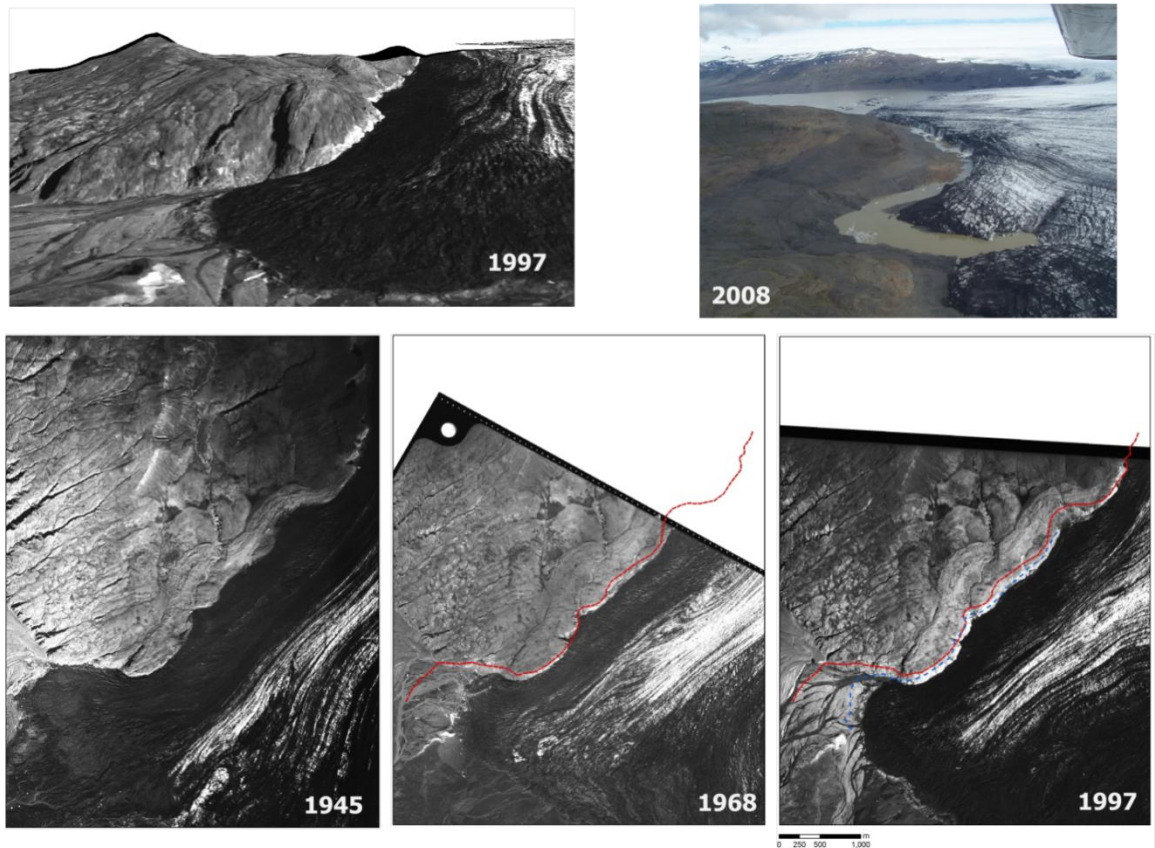


**Figure 5.41** Changing ice levels along the western lateral margin of Skeiðarárjökull in 1945 (red dashed line), 1968 (blue dashed line) and 1997. Since 1945, the glacier has lowered 30+m and over 160 m laterally. Oblique aerial photograph shows the lake itself and the flow of water between the glacier and the massif. Upper right image shows lake Grænalón and lateral subaerial drainage to the ice dam in 2008 (photograph courtesy of Dr. A.J. Russell).

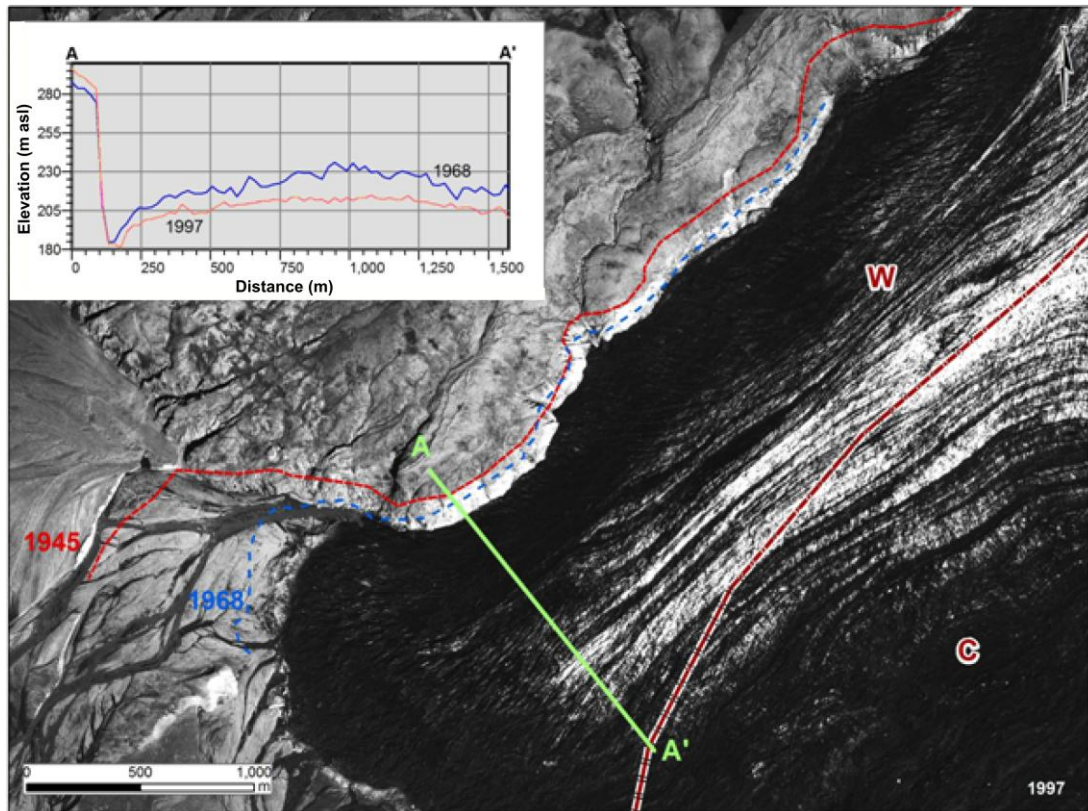
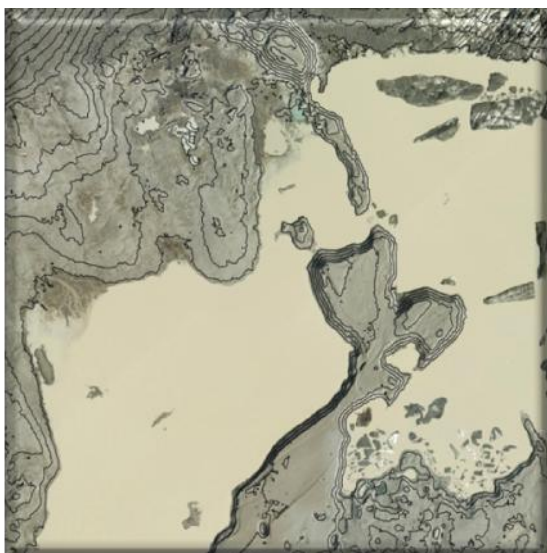


**Figure 5.42.** Retreat of the Western lobe: red (1945), and blue (1968) on 1997 imagery. Elevation profiles of 1968 and 1997 are shown in upper left, depicting a lowering of over 30 m of the Western lobe. The ice has retreated laterally from the massif over 150 m since 1945, and lowered along the massif between 5-15 m.

Roberts et al. (2005) proposed that as a result of ice surface lowering since 1992, Grænalón jökulhlaups began to drain eastwards into the Blautakvísl channel instead of the Súla, down-cutting and incising into the pre-existing terraces. The oblique 2005 photographs taken before and after a jökulhlaup (Figure 5.39) clearly demonstrate the ability of a jökulhlaup to straighten and incise drainage. The 2009 images that depict both the retreat of the margin and the abandonment of the Súla confirm the eastward migration of drainage in this region. While further eastern migration of the Blautakvísl drainage on the sandur is confined by the terrace depicted on Figure 5.38, as observed by Roberts et al. (2005) and corroborated by personal observations by Dr. A. R. Russell, the continued lowering of the glacier is permitting the flow of water subglacially into the Gígjukvísl catchment. This underscores the potential impact of ice level on sub and englacial routing behaviour. If additional photosets may be acquired, future research should be conducted to fully analyse the retreat and lowering of the glacier and the corresponding impact on the drainage in this system.

## 5.5 Summary

Observations of the Skeiðarárjökull on historical imagery and maps examined in this chapter have provided the opportunity to observe the response of the landscape to the large-scale advance and retreat of the glacier margin as well as observing the impact of high-magnitude jökulhlaups (1934, 1938, 1954 and 1996) and areas affected by decadal post-depositional modification due to ice melt. The evolution of drainage channels, proglacial lakes, alluvial fans, terraces, meltout features and moraines, as well as subglacial landforms exposed by glacier retreat were documented and the mechanisms responsible for their formation were interpreted. Landsystem models presented in Chapter 2 and 3 were used to identify landforms on the images and when possible correlated with historical events described in the literature. At least two probable events were identified using these models: the 1965 minor advance or surge and the Grænalón jökulhlaup (circa 1977). While this chapter focused primarily on the development proglacial drainage systems and terrain in response to the advance and retreat of the glacier margin, Chapter 6 examines specific landforms and processes that relate to high- magnitude jökulhlaups in greater detail. Chapter 7 then focuses on modifications of the proglacial terrain that have developed in response to the melting of buried ice bodies emplaced by jökulhlaups and margin fluctuations.



## Chapter 6 Jökulhlaup legacy

---

*The evolution of landform assemblages at Skeiðarárjökull associated with jökulhlaups, including those exposed by margin retreat, is described and models for their emplacement presented. These models are employed to test hypotheses in the literature in order to understand the role of jökulhlaups in the evolution of the sandur including style and morphology of deposition and erosion, the impact on the volume of material deposited on the sandur and where it is deposited. The persistence of these features is examined as well as the development of these features in relationship to the pre-existing topography and glacier margin position.*

---

### 6.1 Introduction

The retreat of Skeiðarárjökull's margin since 1997 has exposed several landform assemblages associated with the large-scale processes observed during the November 1996 jökulhlaup (Björnsson, 1997, Russell et al., 1999a, 1999b, Russell and Knudsen, 1999, Russell et al., 1999a, Gomez et al., 2000, Smith et al., 2000, Roberts et al., 2000, Roberts et al., 2001, Russell et al., 2001b, Waller et al., 2001, Gomez et al., 2002, Magilligan et al., 2002, Roberts et al., 2002, Russell and Knudsen, 2002, Snorrason et al., 2002, Cassidy et al., 2003, Carrivick, 2004, Smith and Clark, 2005, Russell et al., 2006, Smith, 2006). In addition to presenting observations of how these landforms have evolved since 1996, this chapter tests the emplacement mechanisms and models presented in the literature against other landforms and landform assemblages located on both on other



areas of the present-day sandur as well as on aerial images in order to 1) identify landform assemblages diagnostic of jökulhlaups, 2) identify the processes and controls on these landforms during emplacement and 3) attempt to determine the impact of high-magnitude jökulhlaups on the sandur. For locations referenced throughout this chapter, see Appendix C (Figure C.3).

## **6.2 Site 1: Double Embayment (DE)/ice-walled canyon complex**

### **6.2.1 *Site 1: Description***

As observed on the 1997 imagery, the Double Embayment was approximately 300 m across at its widest point, while the ice-walled canyon was >100 m wide and  $50 \pm 2.6$  m deep. On these images, the floor of these features contain large volumes of sediment and large trains of ice blocks and obstacle marks that extend from the Double Embayment out onto the proglacial outwash fans, a distance over 800 m (Figure 6.1 and Figure 6.2). Some kettle holes exceeded 45 m in diameter (Russell et al., 1999b, Russell and Knudsen, 1999, Russell et al., 2001b) and some still contain ice, although these are absent on the 2003 images. By 2007, the retreat of the glacier margin (> 1,100 m) served to ‘elevate’ the sediments deposited within the ice-walled canyon and embayment (Figure 6.1). The 2007 profiles shown in Figure 6.2 reveal minimal surficial lowering of the sediments deposited within the Double Embayment or the ice-walled canyon over the last decade, although some normal faulting and lateral slumping of the sediments has occurred (Woodward et al., 2008). The retreat of the ice margin has also exposed a 700 m long esker that leads from the glacier margin into the former Double Embayment and ice-walled canyon complex. In the north-west, the esker is approximately 150 m wide and is intersected by numerous rectilinear ridges of various lengths (between 5 - 270 m). These ridges are orientated perpendicular and parallel to glacier flow (Figure 6.1 and Figure 6.3). As the esker trends southeast, it narrows along its length to 30 m in width before joining the Double Embayment landform. The Double Embayment complex, the esker and outwash fans have diverted and impounded local drainage, resulting in development of proglacial lakes.

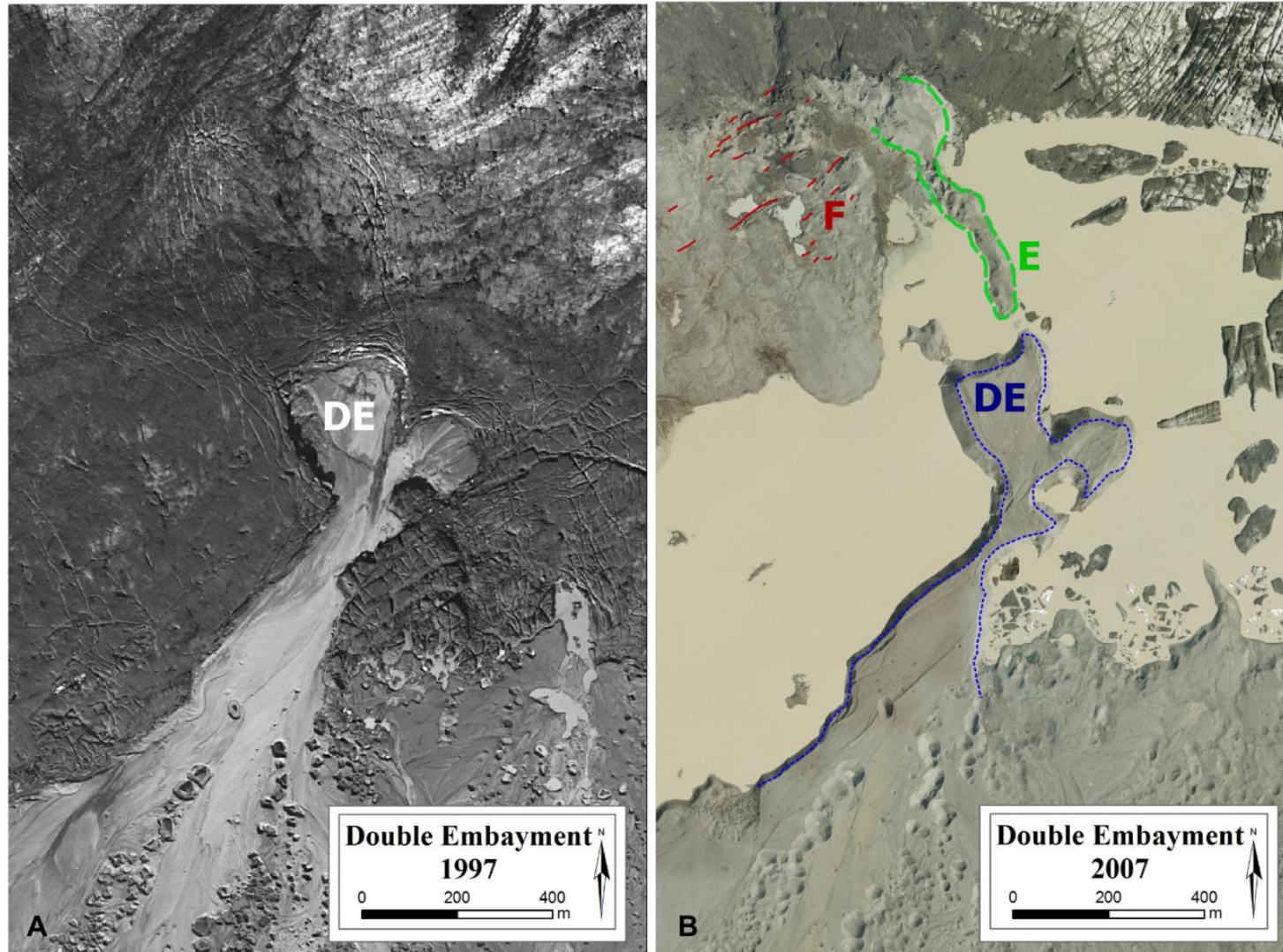


Figure 6.1 Double Embayment (DE) and ice-walled canyon complex generated during the 1996 jökulhlaup (A) and the same region following retreat of the glacier margin (B). Features in the 2007 image are: (DE) Double-Embayment complex (blue), esker (E), fracture fills (F).

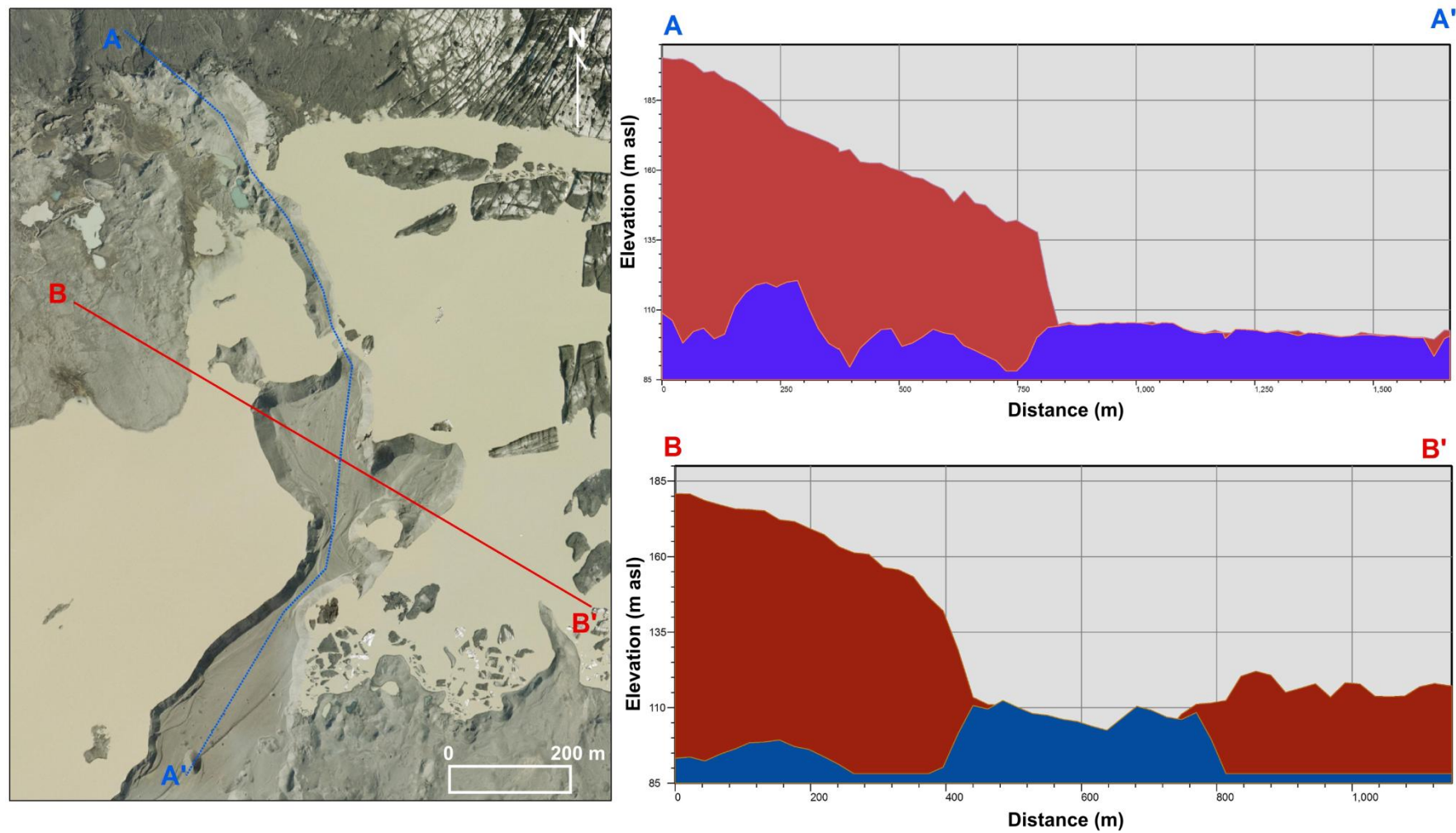
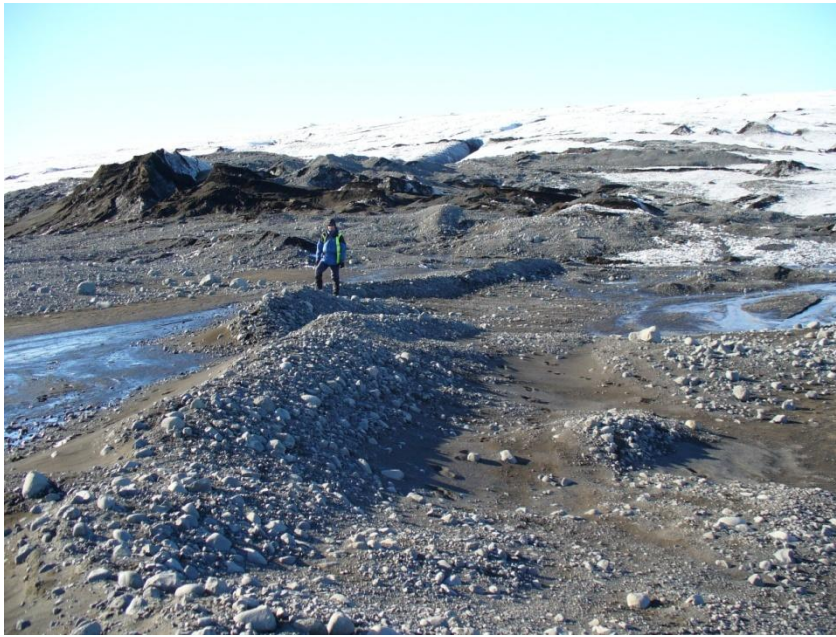


Figure 6.2 Profiles of the DE complex: for both profiles (A-A' and B-B') the 2007 surface is shown in blue, while the 1997 surface is shown in red.





**Figure 6.3** Linear gravel ridge (foreground); fracture filled ice (background); ground photo taken approximately 500 m west of DE complex, 2006.

#### 6.2.2 *Site 1: Interpretation*

Observations made during the 1996 jökulhlaup and examinations of landforms following margin retreat indicate that the Double Embayment and ice-walled canyon were eroded from the ice rapidly (less than 17 hours), ice that was already heavily fractured by high water pressure (Roberts et al., 2001, Roberts et al., 2000, Russell et al., 2006), resulting in the removal of  $5 \times 10^6 \text{ m}^3 \text{ s}^{-1}$  of glacier ice (Russell et al., 2001b). The rectilinear ridges exposed by the retreat of the margin around the north-west portion of the esker correspond to the extensive hydro-fracturing and debris covered regions observed in the 1997 photographs. These ridges were interpreted by Roberts et al (2000, 2001) to be fracture fills, formed as a result of englacial deposition of sediment within pre-existing and jökulhlaup-generated ice fractures (Waller et al., 2001, Roberts et al., 2000, Roberts et al., 2001, Roberts et al., 2002) (see Chapter 3).

As observed during the 1996 event, within the first 9 hours of the jökulhlaup, outlets spread rapidly westward across the snout of Skeiðarárjökull, through which floodwaters emerged on the glacier surface, persisting for minutes to an hour before flow was established through conduits (Roberts et al., 2000). The deposition of material within these conduits was attributed to sediment accretion via super-cooled discharge that was generated by floodwaters ascending up through the glacier in an overdeepened basin (Lawson et al., 1998, Evenson et al., 1999, Roberts et al., 2001). The 700 m esker was interpreted by Burke et al. (2008, 2009, 2010) to be an englacial esker emplaced during the first twenty-four hours of the jökulhlaup. Their analysis of ground-penetrating radar

(GPR) data related these deposits and bedforms to a multistage model: following the initial development of supraglacial fracture outlets, cavities and ice blocks fractured during the initial floodwave were excavated leading to conduit growth (Roberts et al., 2000). Further excavation and downstream unroofing resulted in the development of the ice-walled canyon.

The association of landform assemblages of fracture fills, the large, single-event englacial esker and the DE/ice-walled canyon outlet was suggested by Russell et al. (2006) and Burke et al. (2008) to be a landform signature diagnostic of central outlets during high-magnitude, volcanogenic jökulhlaups (Russell et al., 2006, Burke et al., 2008). The 1997 - 2007 images provide the opportunity to observe the preservation potential of these landform assemblages in response to margin retreat, and paraglacial modification. It is inferred from the profiles in Figure 6.2 that the large volume of sediment deposited within the Double Embayment and ice-walled canyon served to insulate the ice beneath, reducing ablation. This confirms GPR investigations conducted in 2006 and 2007 by Woodward et al. (2008) that revealed 12 m of sediments overlain on buried ice. This ridge of sediment exposed by the retreat and lowering of the surrounding ice is posited by Russell et al., (2005) to be analogous to Quaternary eskers.

It is evident, however, that post-depositional modification of these features that were deposited on, and within, the glacier continues to this day (Woodward et al., 2008, Burke et al., 2010), indicating that this landform assemblage will continue be subject to post-depositional modification.

## **6.3 Site 2: Depression**

### **6.3.1 Site 2: Description**

Approximately 1 km west of the Double Embayment (DE) complex, the retreat of the glacier margin since 1997 has exposed an convex area of fluted ground approximately 800 m wide that contains linear ridges and an elongate depression (Figure 6.4). This area of drumlinised ground is convex in profile and contains numerous erratics up to 3 m in diameter. Linear ridges are aligned parallel to glacier flow and range from 10 to 270 m in length and 1 - 3 m in width. The elongate depression that ranges in width from 5 to 250 m, over 7 m deep, and up to 1 km in length. The elongate depression and a drainage channel trends northwest/southeast (Figure 6.5), and both extend from a 500 m wide water-filled proglacial depression and terminate near the approximate location of the 1996 margin. While the 1996 floodwaters emerged through supraglacial fractures along

this portion of the margin, these features do not appear to correspond with any of the observed 1996 marginal en- or subglacial outlets (Roberts et al., 2000).

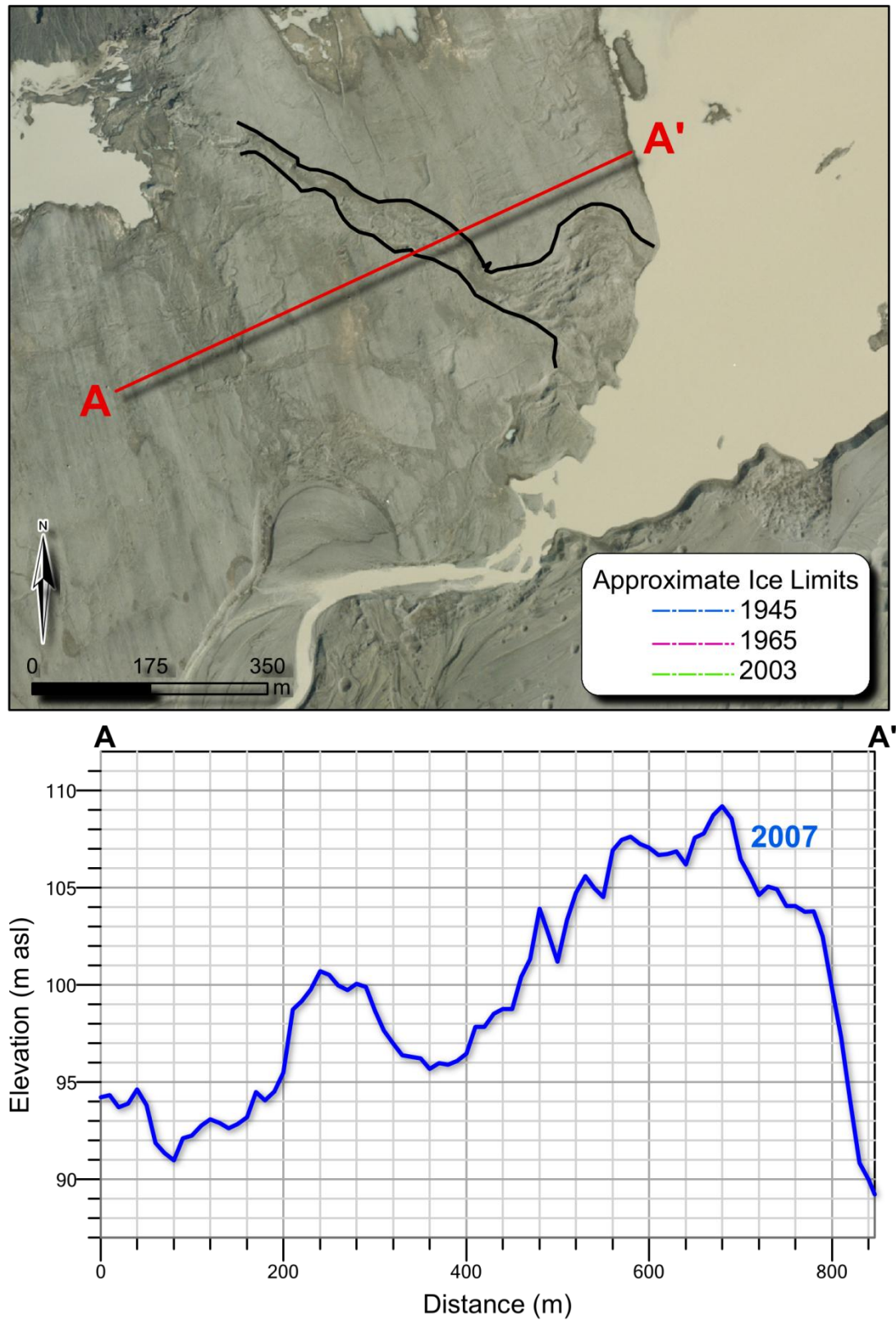
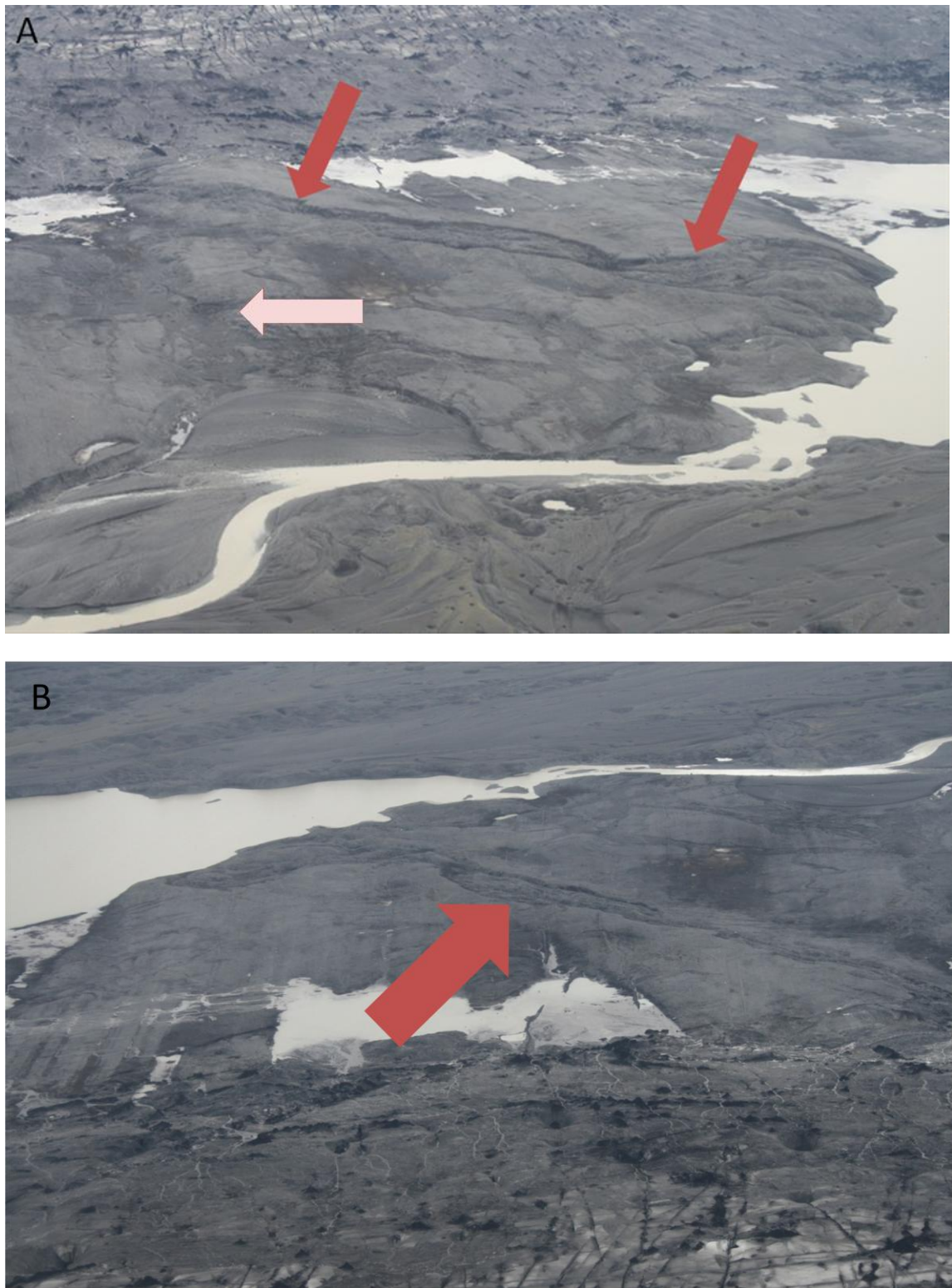


Figure 6.4 Profile across elongate depression (outlined in black)on 2007 imagery/DEM.





**Figure 6.5** Oblique photographs of elongate depressions (red arrows) and drainage channel (white arrow): A) looking north, b) looking south. Photographs courtesy of Dr. A. J. Russell 2008.

The base of the depression (Figure 5.6, Profile A – A') resides at 91 m in the northwest, rises 14 m over the first 200 m then lowers to 88 m before terminating in a proglacial lake in the southeast, a drop of over  $17 \pm 1.64$  m (Figure 6.6). The floor of the depression is uneven and chaotic. The walls of the depression appear to be subject to normal faulting and appear larger in the 2007 images than the 2003 images. Directly across the lake from

this feature is a semi-circular region of highly disturbed terrain that, on the 1992 imagery, lies at the same location of the apex of the 1991 surge fan. The base of the drainage channel to the west (Figure 5.6 Profile B – B') resides on average 5 m lower than the eastern depression. The base level of the western channel resides at 91 m in the northwest, rises 5.5 m over the first 80 m, then the profile lowers 11.5 m to terminate, possibly below water, at 85 m, a total drop in elevation of 11.5 m. The western channel appears to have been subject to negligible subsidence in comparing the 2003 and 2007 images and on both images appears to contain active or recent proglacial drainage.

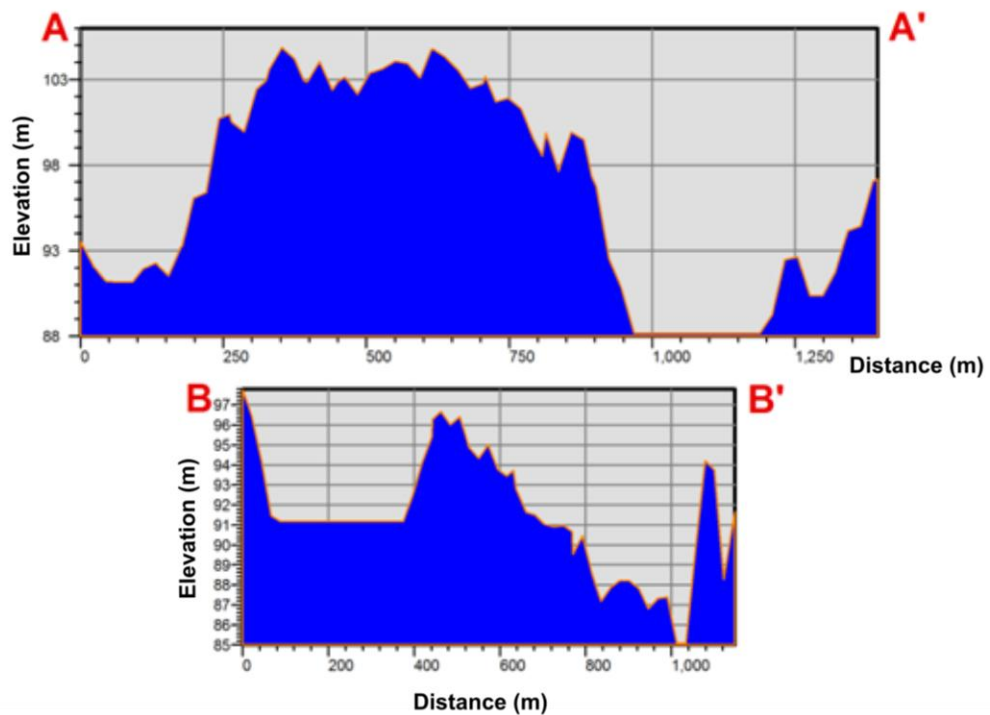
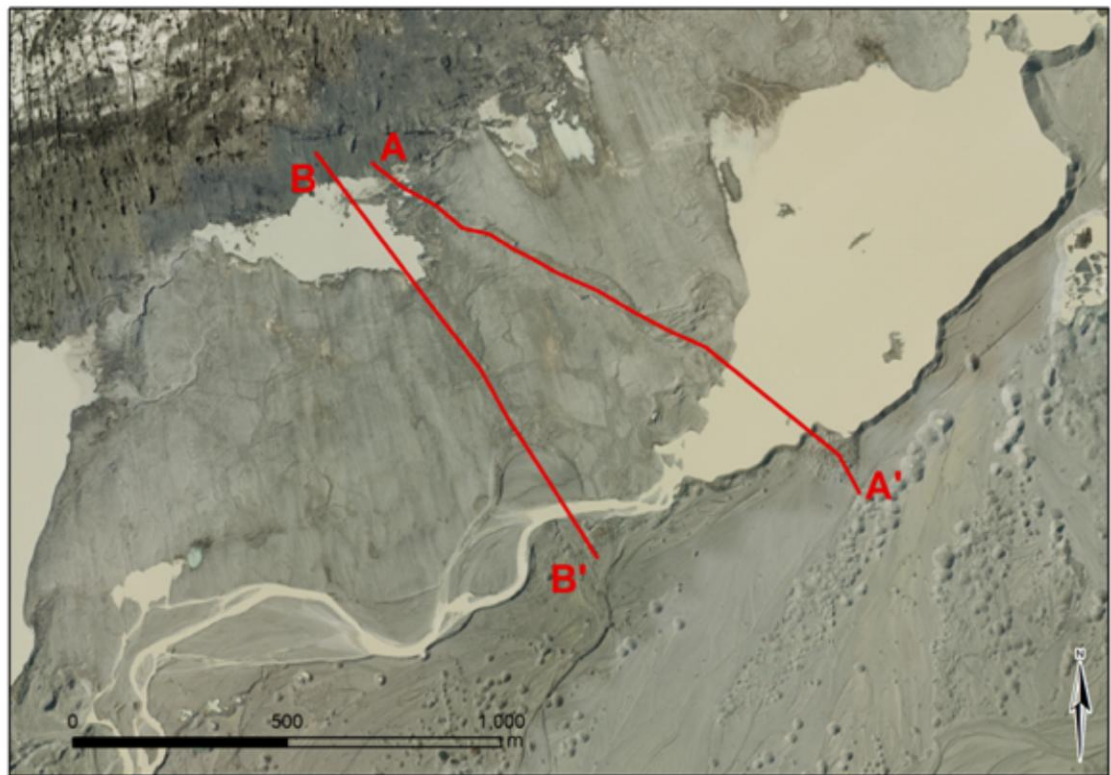


**Figure 6.6** Profiles along bottom of elongate depression (A - A') and drainage channel (B-B') (2007 imagery/DEM).

#### 6.3.2 *Site 2: Interpretation*

The smoothed ground, the presence of flutes and large boulders are consistent with a landform that that has been overridden or 'drumlinised' (Boulton, 1987, Evans and Twigg, 2002). As the margin retreated between 2003-2007, the depression (Figure 5.6, Profile A – A') appears to have become progressively more defined and has experienced

normal faulting along its margins, suggesting post-depositional modification due to the melting of buried ice (Branney, 1995, Olszewski and Weckwerth, 1998), unlike the channel to the west (B-B') which has experienced no subsidence. The vertical loss of 7 m within depression (A-A') suggests that at least this thickness of ice bodies has melted out, and indicates that the ice body was insulated by a thick (> 1 m) of debris that served to insulate the ice and reduce ablation (Østrem, 1959), indicating that this material was originally emplaced en or supraglacially.

Interpreting the origin of the ice bodies from imagery alone is difficult. Field work conducted in this area revealed the presence of numerous blocks of buried ice incorporated within non-stratified sediment (personal communication, Dr. A.J. Russell, 2012). The chaotic assemblage of sediment and blocks fractured from the overlying ice may have been caused during the onset of jökulhlaups during the formation of subglacial canal and tunnel channels (Rijsdijk et al., 1999, Russell, 2003, Le Heron and Etienne, 2005, Kjaer et al., 2006). During a jökulhlaup, ground water within the gravel aquifer may have become highly pressurized, ascending through hydrofractures into the overlying ice. The resulting erosion of the sediment and ice blocks then reduce pressure, and the jökulhlaup flow may have then evolved from a complex fracture-fill network to conduit flow (Piotrowski, 1997, Sjogren et al., 2002, Russell et al., 2007). Dr. Russell also indicated that field work suggested that the strata, and drumlinised landform, are englacial, and may have been emplaced during the 1991 surge event, suggesting a direct link between surge-related landforms and their subsequent impact on jökulhlaup routing. Further sedimentological investigation of this site is needed, however, to support this interpretation.

## **6.4 Site 3: Loop Complex**

### **6.4.1 Site 3: Description**

Since 1945, the retreat of the central glacier margin has exposed a wide, elongated drumlinised area of fluted terrain located 5 km west of the DE complex. This smoothed ground is bordered to the south by a 100 m wide, 1 km long channel-arc (Figure 6.7), an area referred to as the Loop Complex. The fluted ground is bisected by an east/west flowing channel on the 1965 photographs that was further widened 700 m following the 1996 jökulhlaup (Figure 6.8 and Figure 6.9). The fluted ground is interrupted by a wide region of undulating terrain that contains numerous low, rectilinear ridges (Figure 6.9). These ridges extend over 200 m in length and are orientated both transverse and parallel to present glacier flow. This undulating terrain also contains a low, sinuous 500 m long



esker that covers a region 300 m in length from north to south. This esker possesses a relatively constant width (~15 m) as it passes in tight loops across the undulating terrain and leads to a 300 m wide gap in the moraines. An outwash fan extends from this gap out onto the sandur that is characterised by a dense distribution of kettle holes and obstacle marks. Approximately 300 m east of the Loop Complex there are numerous arcuate ridges that are 100-300 m in length and trend southwest-northeast (Figure 6.9).

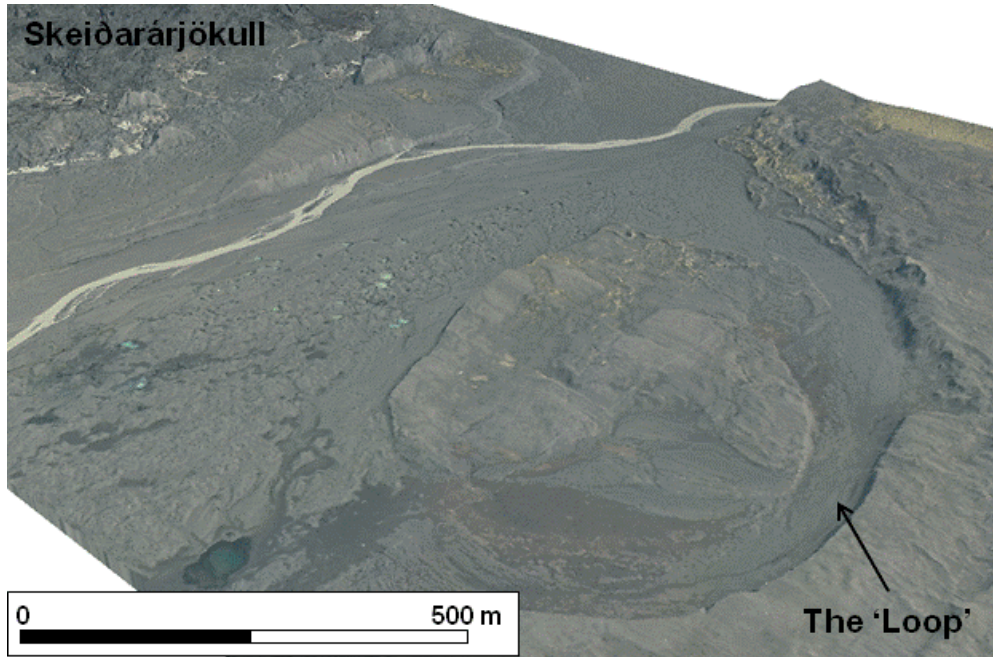


Figure 6.7 Oblique aerial oblique view of the Loop Complex (2003 DEM).

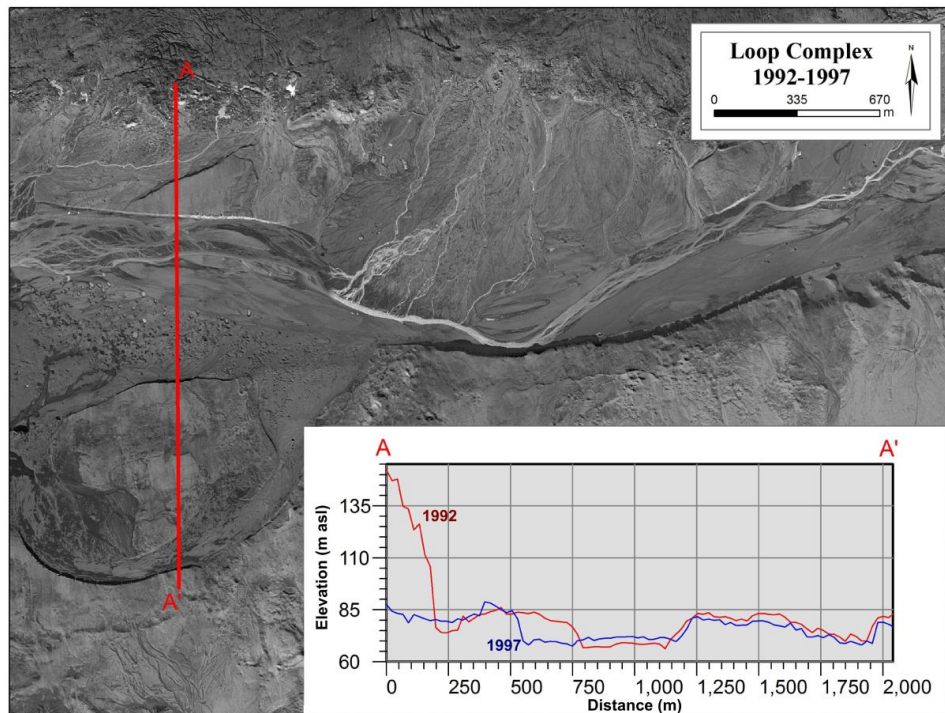
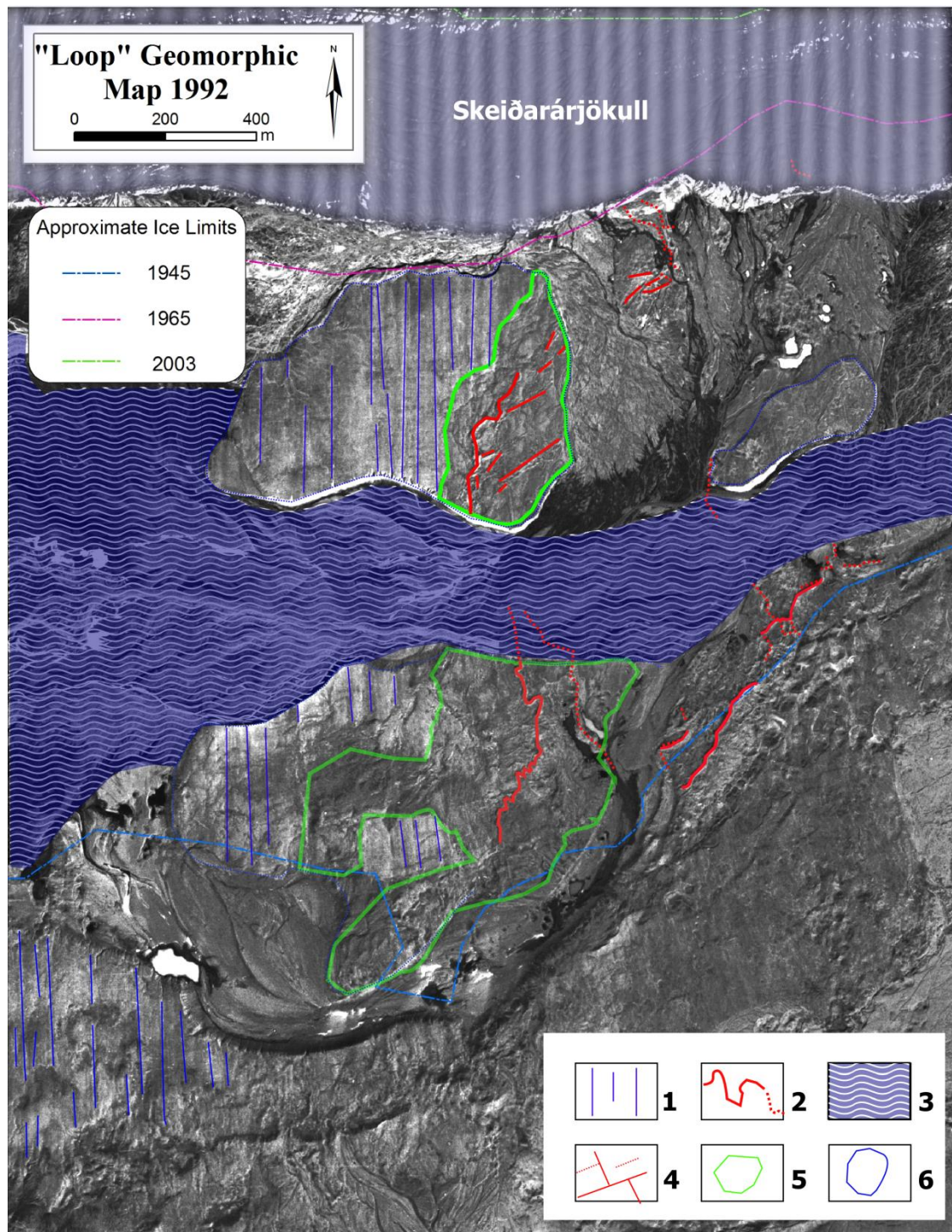


Figure 6.8 North-south transect of Loop Complex and margin (1992 in red, 1997 in blue), depicting removal of material following the 1996 jökulhlaup.





**Figure 6.9 Loop Complex in 1992: 1) fluted ground, 2) esker (dashed line indicates present on earlier photoseries prior to erosion) 3) proglacial drainage, 4) fracture fills, 5) disturbed ground, 6) outline of drumlinised landform.**

Ground photographs that compare stratigraphic sections of both disturbed and undisturbed terrain shown in Figure 6.10. While the zone of undulating terrain is characterised by irregular elongate depressions and ridges with isolated blocks of undisturbed ground (Figure 6.10 A), exposures of the undisturbed terrain (Figure 6.10, B) appear to consist of two distinct beds, each 1-3 m thick. The lower bed contains bedded gravels and sands, while the upper unit appears to be comprised of a massive layer of till



(silt, sands and gravels). At exposures of the disturbed terrain, large (0.5 – 3 m) blocks of the upper till unit appear randomly distributed within the lower gravel unit (Figure 6.10, C).

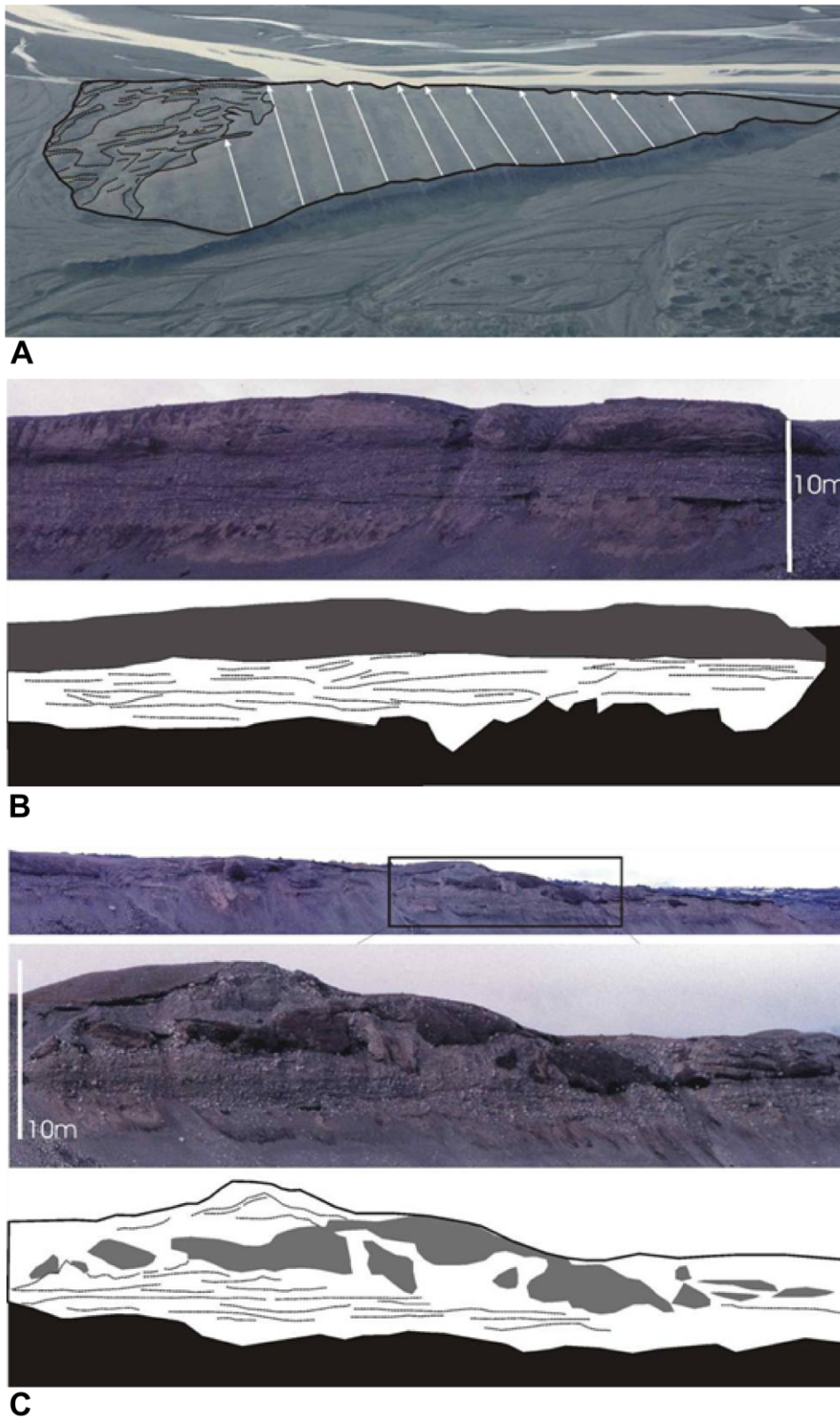


**Figure 6.10** Oblique photograph of the region in 2007, depicting the fluted ground and the location of disrupted terrain (A), stratigraphic section of undisturbed terrain (B) and disturbed terrain (C). Photographs and stratigraphic sections courtesy of Dr. A. J. Russell.

#### 6.4.2 *Site 3: Interpretation (Loop Complex)*

The drumlinised, fluted landform that is comprised of sands and gravels beds that are topped by till are consistent with that of a overridden alluvial fan (Krüger and Thomsen, 1984, Boulton, 1987, Shaw and Kvill, 1989, Evans and Twigg, 2002). The outwash fan containing a dense distribution of kettle holes and obstacle marks that stretch from the sinuous esker out onto the sandur is consistent with descriptions of jökulhlaup fans (Maizels, 1992); this interpretation is supported by the 1934 map that depicts a major jökulhlaup outlet at this location (Figure 6.10).

However, the chaotic displacement of large blocks of the overlying till incorporated within the gravel beds seen in the stratigraphic sections of the alluvial fan suggests that the ‘disrupted terrain’ was subject to severe mechanical modification. The injection of gravel beds into an overlying, less permeable substrate has been observed during the onset of jökulhlaups during the formation of subglacial canal and tunnel channels (Rijsdijk et al., 1999, Russell, 2003, Le Heron and Etienne, 2005, Kjaer et al., 2006). During a jökulhlaup, ground water within the gravel aquifer may have become highly pressurized, ascending through hydrofractures into the overlying impermeable diamicton unit. The resulting erosion of the diamicton unit and glacier bed may serve to reduce pressure, and the jökulhlaup flow may have then evolved from a complex fracture-fill network to conduit flow, ceasing as large ice-roofed channels developed (Piotrowski, 1997, Sjogren et al., 2002, Russell et al., 2007).

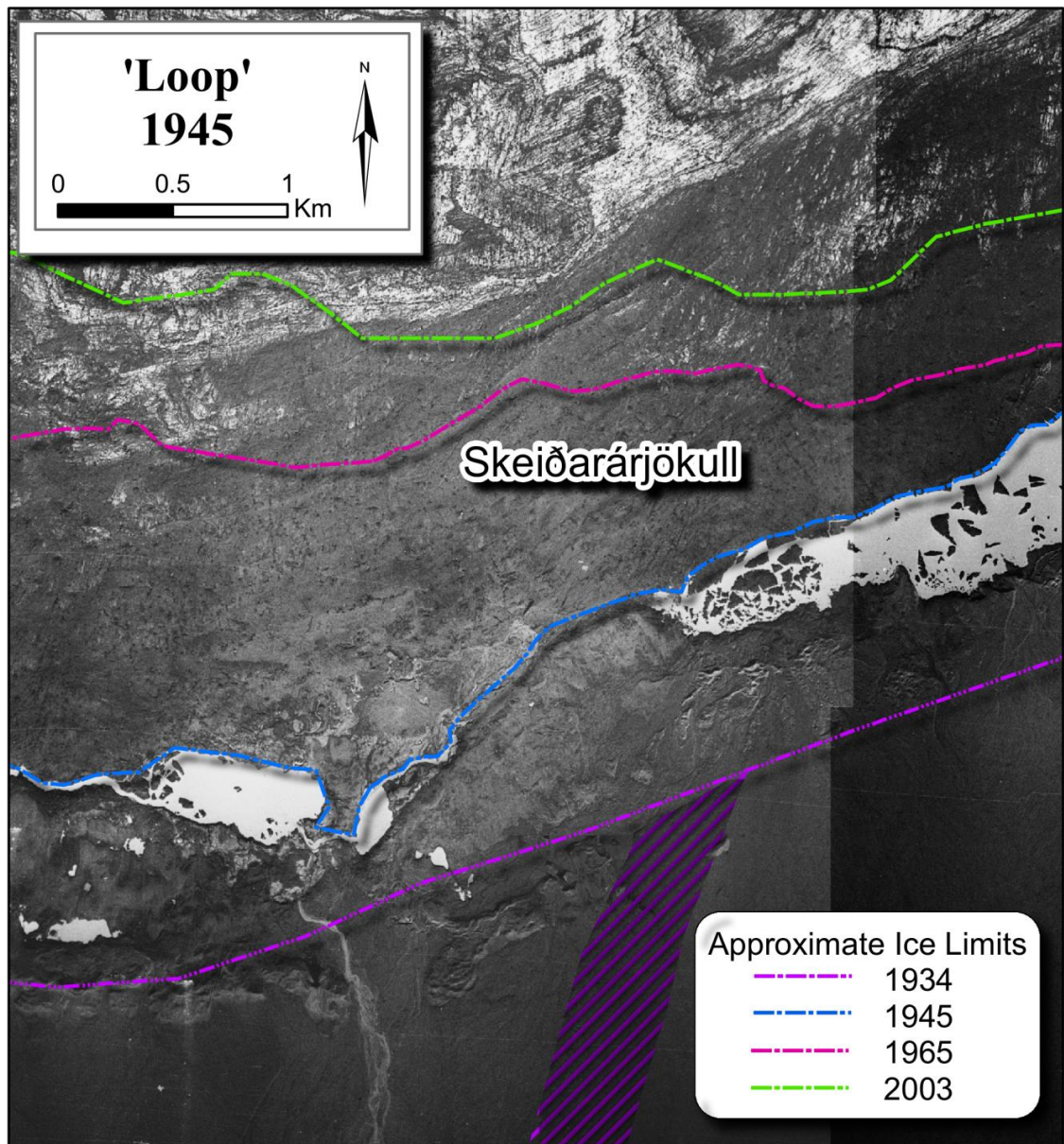


**Figure 6.11** ‘Loop Complex’ region in 1945 prior to retreat. Purple hatched polygon depicts the approximate location of a major 1934 jökulhlaup outlet.

The deposition of gravel above the fragmented diamicton layer may have resulted in the development of the observed mounds and ridges, resulting from the full incorporation of subterranean flow with the sub- and englacial drainage system. In regions where the diamicton was completely removed, the material was injected into hydrofractures within the ice, resulting in the formation of fracture fills developing into conduit flow, finally resulting in the deposition of eskers (Russell et al., 2006, Burke et al., 2008, Burke et al., 2009, Burke et al., 2010). This interpretation is supported by the corresponding size, location and geometry of the low rectilinear ridges, consistent with the fracture fills described by Roberts et al. (2000, 2001), and Russell et al. (2006) located proximal to the Double Embayment that were generated as a result of hydro-fracture fills formed during high-magnitude jökulhlaups.

## 6.5 Site 4: Western ridges

### 6.5.1 Site 4: Description

The retreat of the western margin has exposed a 4 km wide region of low, undulating terrain (Figure 6.12). This terrain is interrupted by rectilinear ridges that range between 0.5 - 10 m in width, 0.5 - 3 m in height, and may exceed 1 km in length. These ridges are orientated both perpendicular to and parallel to the glacier margin and were described by Monro-Stasiuk et al. (2008) as being composed of pebbles, cobbles and boulders. A comparison of the ridges on the 1965 and 1997 imagery reveals that they do not appear to have been subject to post-depositional modification during this period. However, ridges of a similar geometry and position are visible on the surface of the ice on the 1945 photographs. A 500 m long, sinuous esker of variable width (7- 30 m) and undulating profile extends from this area of rectilinear ridges southwest towards the moraine gap and kettled outwash fan. At the approximate location of the former 1945 glacier margin position, the ridge is no longer discernible; instead, this ridge grades into an outwash fan that contains a dense distribution of kettle holes and obstacle marks. The kettle holes on this fan range in width from 2 – 30 m and boulders range up to 3 m in diameter. Both the sinuous esker and the rectilinear ridges have served to impound and deflect local surface drainage on all images since 1965.



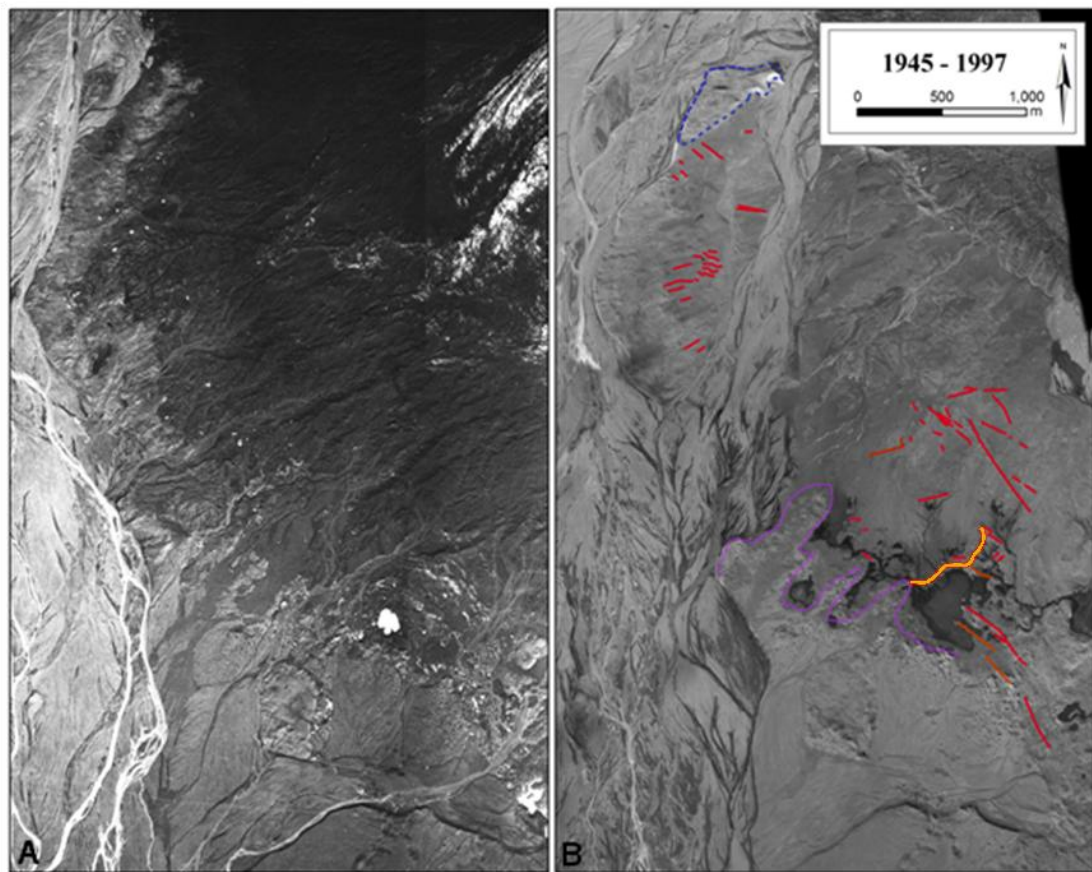


**Figure 6.12** Western region in 1945 (left) and 1997 (right). Retreat of the margin has exposed long, rectilinear ridges (red lines), an esker (orange) and a ridge interpreted to be the location of a former jökulhlaup outlet (blue) and the location of the former margin (purple).

#### 6.5.2 *Site 4: Interpretation (western ridges)*

The outwash fan containing kettle holes, obstacle marks and boulders is interpreted to be a jökulhlaup fan, consistent with those described at other locales along the margin (Russell, 1993, Maizels, 1997, Fay, 2002). The undulating profile and variable width of the sinuous esker suggests that it has been subject to post-depositional modification and is therefore likely en- or supraglacial in origin. The GPR investigations by Monro-Stasiuk et al. (2008) of the low gravel rectilinear ridges revealed these were a network of clastic dykes interpreted to be relics of hydro-fracture fills formed during high-magnitude volcanogenic jökulhlaups. They suggest that the increased water pressure during these flooding events forced water out of over-pressurized subglacial channels up through the overlying ice and that the rectilinear ridges are therefore the surficial expression as water escaped from the ice surface; as the floodwaters waned, sediment was deposited in the fractures. While this region this region has been subject to numerous jökulhlaups over the past 100 years (1887, 1897, 1903, 1934 (Thorarinsson, 1974)), these authors did not, however, relate the fracture fills to the other landforms in the area. While different in scale and extent, the association of the fracture fills, esker and jökulhlaup outwash fan is

again consistent with the high-magnitude jökulhlaup assemblage described by Russell et al. (2006) and Burke et al. (2008) and suggests that the position of the glacier margin, underlying topography and substrate and thickness of the ice surface may play a role in determining the size and extent of these landforms. The landforms observed at this site also demonstrate the decadal persistence of such assemblages, particularly the relatively low <3 m ridges, precluding glacier advance or inundation by later jökulhlaups.

## **6.6 Site 5: Remnant outwash fan apex**

### **6.6.1 Site 5: Description**

A 750 m long ridge of sediment that trends northeast to southwest is visible on all photoyears, including the 1945 photographs where the ridge can be seen above the ice surface (Figure 6.12). The ridge contains boulders up to 2 m in diameter and kettle holes that range in size from 2 – 27 m in diameter. Seen in profile (Figure 6.13), this ridge is highest near the glacier margin and decreases in elevation as it grades southwest into the proglacial terrain. Although the 1945 historical photographs were too degraded to extract a full DEM, it is apparent from sampled data that this ridge was approximately level with the ice surface at this time. Elevation profiles of this ridge in 1968, 1997 and 2003 (Figure 6.13) demonstrate that this landform has not been significantly modified. While the retreat of the glacier margin north of the feature has been heavily affected by proglacial drainage and jökulhlaups, this ridge has remained relatively intact.



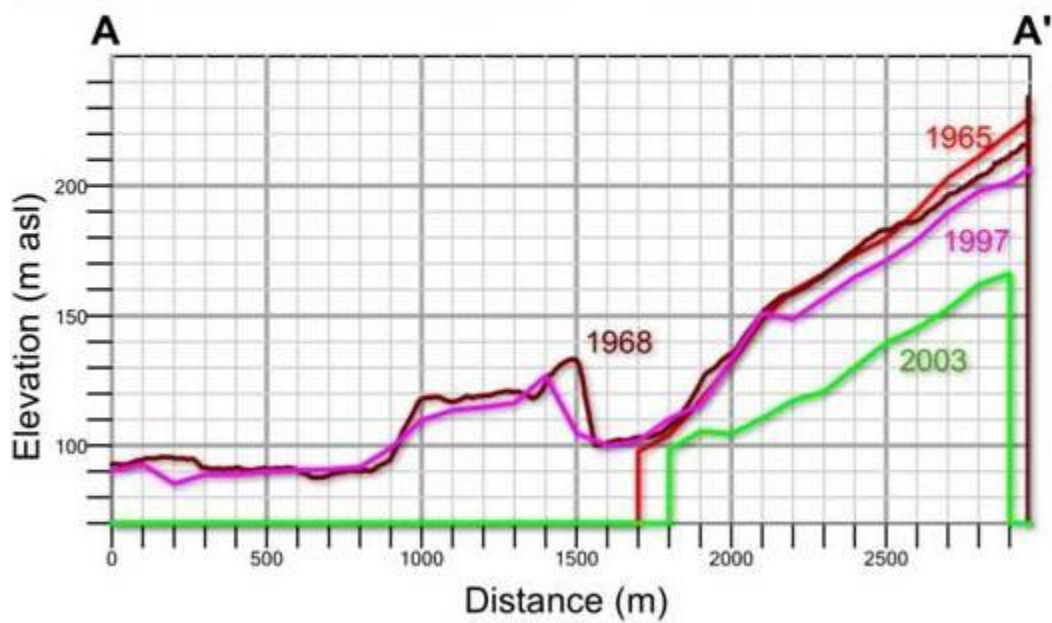
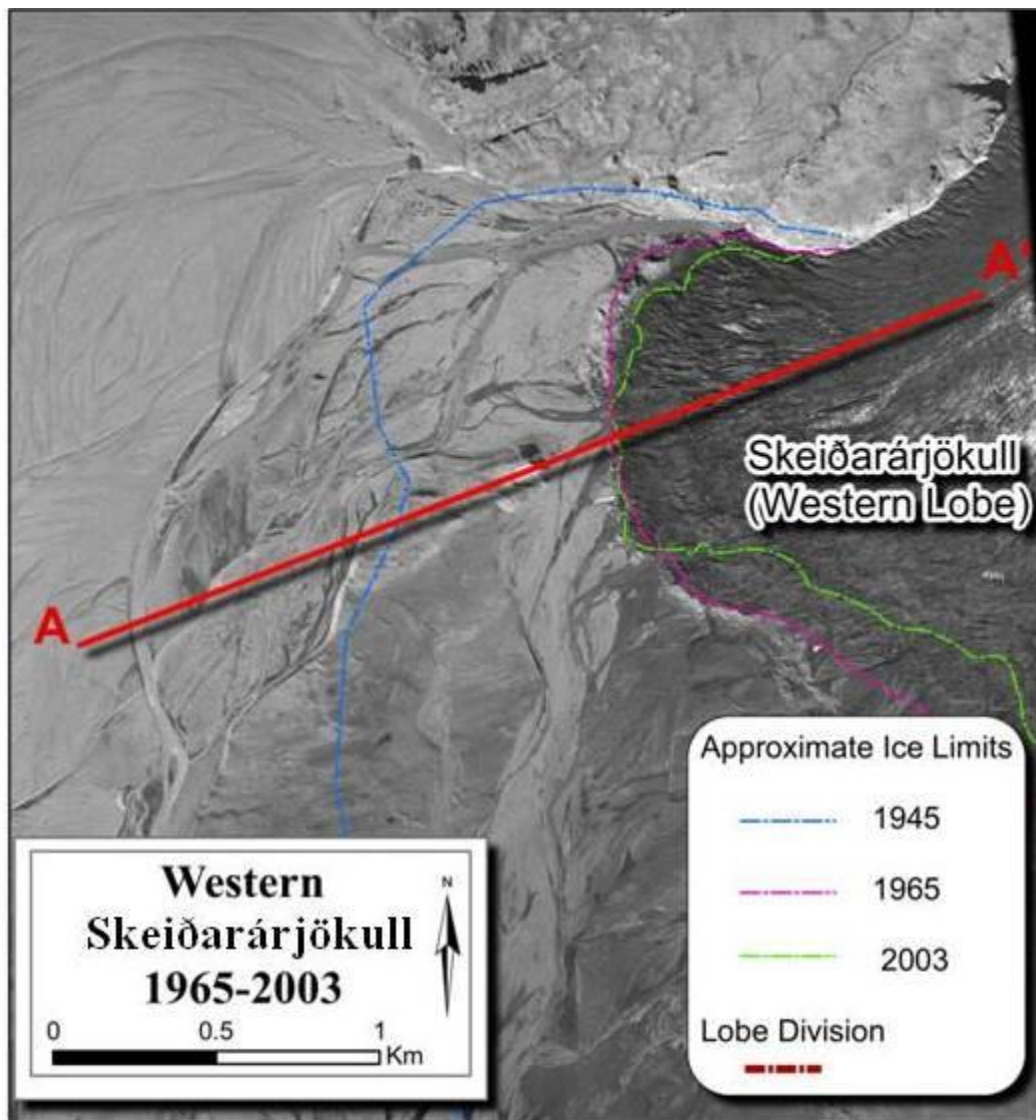


Figure 6.13 Profile of remnant outwash fan apex and position of western margin since 1965 (flat line indicates lack of data).

#### 6.6.2 *Site 5: Interpretation*

The feature displays no significant post-depositional modification following the retreat of the glacier margin since 1945, suggesting that it was not emplaced en- or supraglacially, but deposited along the ice-bed interface. The orientation of the large, elongate ridge to glacier flow, combined with the presence of large boulders and kettle holes, is consistent with descriptions of the ice-walled canyon, or outwash fan apex, generated during the November 1996 jökulhlaup (Russell et al., 2001b, Russell et al., 2006, Cassidy et al., 2003, Russell and Knudsen, 1999). In this case, a single supraglacial, ice-walled canyon was excavated during a jökulhlaup along the ice-bed interface, and flowed out onto the sandur. Similar to the routing of the jökulhlaup flow observed through the ice-walled canyon in 1996, routing flow through a confined conduit may permit jökulhlaup flows to maintain high sediment efflux and aggradation rates (Russell and Knudsen, 2002), and may have emplaced this large ridge of sediment, boulders and ice blocks. Following emplacement, the retreat and lowering of the ice margin ‘elevated’ the ridge of sediment to be the topographic high that persists today.

### 6.7 **Site 6: Central Gígjukvísl 1965**

#### 6.7.1 *Site 6: Description*

On the 1965 imagery, the Gígjukvísl gap in the 19<sup>th</sup> century moraines is 300 m across, while the Gígjukvísl itself resides in a channel that is only 72 m wide (Figure 6.14). Another gap in the moraines lies 500 m east of Gígjukvísl gap that is 150 m wide and contains boulders up to 4 m in width upon a heavily kettled outwash plain. This outwash fan is characterised by a dense distribution of kettle holes (up to 10 m in diameter) and obstacle marks. The terrain north and east of this gap is characterised by smoothed ground that is interrupted by kettle holes up to 15 m in diameter and boulders up to 3 m in width. In contrast, the adjacent terrain to the north and west is uneven, containing depressions and ridges.

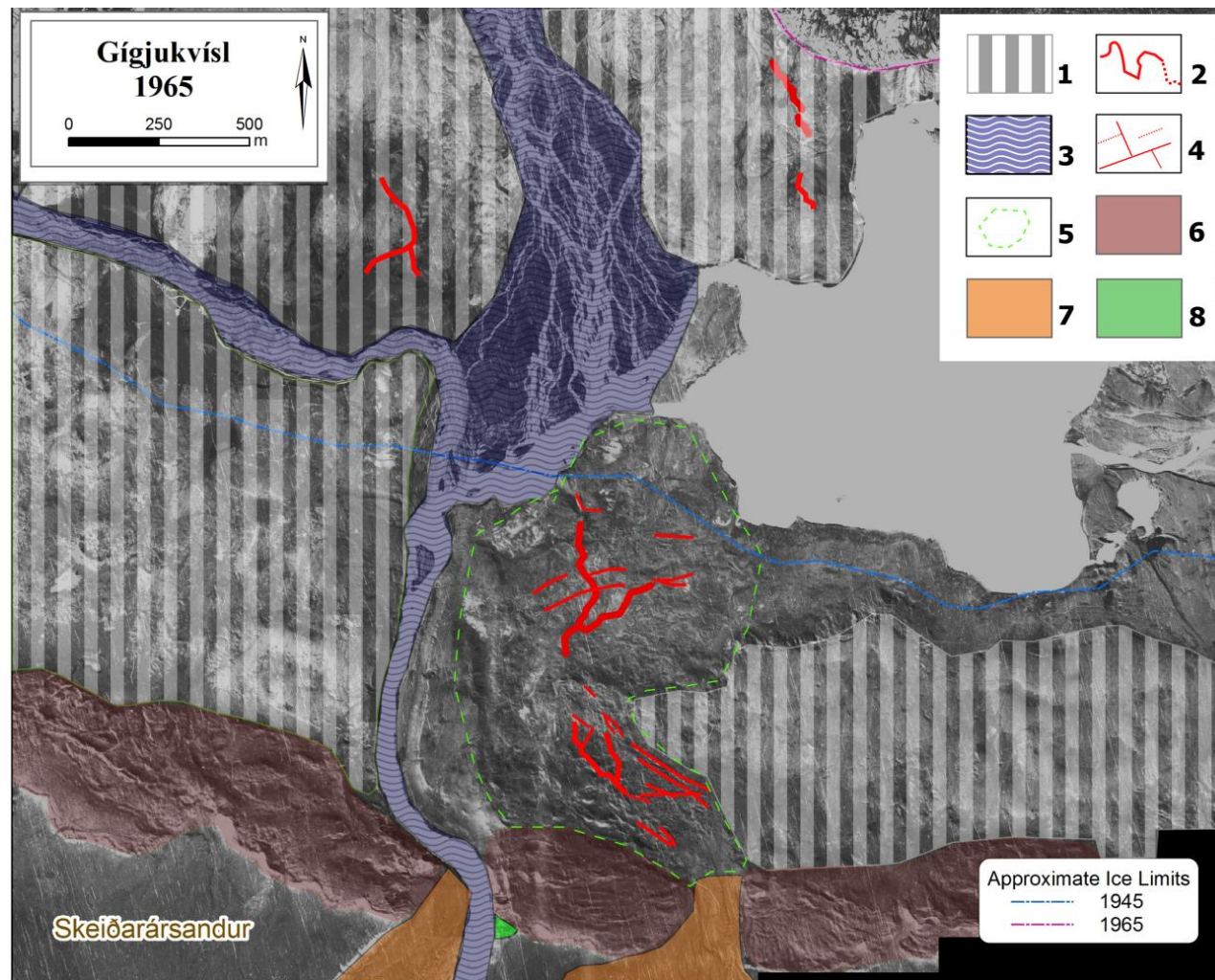


Figure 6.14 1965 photomosaic of the Gígjukvísl gap in the 19<sup>th</sup> century moraine: 1) smoothed ground, 2) esker, 3) drainage channels, 4) fracture fills, 5) disturbed terrain, 6) moraines, 7) jökulhlaup outlets, 8) surge-advance related outwash fan (Russell et al., 2001a).

This area of ridges was previously covered by a proglacial lake on the 1945 images. By 1960, the lake was gone and Klimek (1973) simply describes this terrain as ‘lake bottom deposits’, and the odd patterns were proposed to be the result of ice blocks drifting along the lake floor. However, on subsequent imagery (1986, 1992, 2003) these ridges have become progressively more defined. There are two types of ridges in this area, linear ridges intersecting at right angles and sinuous eskers. The linear ridges range from 5-260 m in length while the sinuous ridge, steep-sided eskers may exceed 400 m in length and cover a transect of 740 m, and trend northwest-southeast, leading to the eastern gap in the moraines and rising upslope an elevation of 20 m. While proglacial drainage networks and a lake obscure much of the terrain to the north, a second series of sinuous eskers 420 m in length that possess the same orientation extend 1 km to the north.

#### 6.7.2 *Site 6: Interpretation*

The description of the outwash fan that leads south from the gap in the 19<sup>th</sup> century moraines that contains kettle holes, obstacle marks and boulders is consistent with descriptions of a jökulhlaup-related outwash fan (Maizels, 1997, Russell, 1993, Fay, 2002). The increasing definition of ridges observed within the depression over the past forty years suggests that these have been subject to post depositional modification as a result of the melting of ice. The esker that ascends (20 m) up the reverse slope from the fracture-filled depression to the 19<sup>th</sup> century moraines suggests that it was generated under conditions of high pressure. The intersecting rectilinear ridges within the depression are consistent with descriptions of fracture fills (Rijsdijk et al., 1999, Roberts et al., 2000, Le Heron and Etienne, 2005, Russell et al., 2006, Munro-Stasiuk et al., 2008) and not the result of icebergs scours within the lake as proposed by Klimek (1973).

The association of these sub-, en- and proglacial features is consistent with the development of fracture fills, and their subsequent evolution into conduits/eskers during a high-magnitude jökulhlaup as described by Russell et al. (2006) and Burke et al. (2008, 2009, 2010). A comparison of the 1945 and 1965 photographs reveal that while the Gígjukvísl gap was heavily modified by the 1954 jökulhlaup (see Chapter 5), this region of smoothed ground and irregular topography lies at a higher elevation and was not affected by this event. Neither were these outlets of the 1934 event (Nielson, 1937), suggesting an earlier flood is responsible for their emplacement.

## 6.8 Summary

This chapter examined several jökulhlaup-related landsystem models that have been developed at Skeiðarárjökull and documented their modification over the past decade. Using these landsystem models, and the hypotheses of their genesis, photographs and DEMs were examined to locate other occurrences of similar landforms or landform assemblages, past and present, to support or expand these landsystem models. Several landforms and landform assemblages were identified across the glacier margin that may also corroborate with historical accounts in the literature. The following chapter examines large-scale post depositional modification of the landscape due to ice melt and the relationship to both jökulhlaups and fluctuations of the glacier margin in order to understand the temporal and spatial impact of these processes on the evolution of the sandur.





## Chapter 7 Post-depositional modification of proglacial outwash

---

*This chapter examines the effects of post-depositional modification on large-scale proglacial landforms, resulting specifically from the meltout of buried glacier ice. The development of several depressions in the central portion of the sandur between 1945 and 2007 is described. In order to determine a mechanism for the emplacement of these buried ice bodies, the dimensions, orientations and locations of the depressions were combined with descriptions of events found in historical records. Observations were used to test hypotheses of emplacement models of buried ice bodies that were presented in Chapter 1. Further discussion of the relationship between margin fluctuations, jökulhlaups and subsequent post-depositional modification is presented in Chapter 8.*

---

### 7.1 Introduction

In order to determine the impact of post-depositional modification on large-scale landforms on Skeiðarársandur over decadal timescales, historical imagery and DEMs from 1945 to 2007 were used to quantify changes in sandur surface morphology and elevation in order to identify large areas that appear to have been subject to extensive meltout. Numerous maps and journal articles have extensively mapped individual ice ridges, ice blocks and dead ice fields across the margin of Skeiðarársandur and closely detailed the melting out of individual ice blocks following jökulhlaups (Galon, 1973a, Jewtuchowicz, 1973, Wojcik, 1973a, Wisniewski, 1997, Fay, 2002, Russell et al., 2006). However, the origin of an area of larger depressions that have developed progressively since 1945 on central Skeiðarársandur, in an area known as Hardaskriða, remains to be investigated. This area was specifically selected due to its size, distinct pattern and



references in the literature that made passing judgements to their emplacement via jökulhlaups (Thorarinsson, 1974, Galon, 1973a, Knudsen et al., 2001). This chapter examines the development of these depressions over six decades and examines a possible mechanism for their emplacement that may be more complex than the literature suggests. The relationship between the process, or combination of processes, responsible for the development of these landforms is explored, while further discussion of the implications of long-term, large-scale impact of post-depositional modification and other large-scale processes is presented in Chapter 8 (Theme C). For the locations of figures in this chapter, see Appendix C (Figure C.4).

## 7.2 Hardaskriða depressions

The area of Hardaskriða is located between the Háöldukvísl and Gígjukvísl channels (Figure 7.1) and, unlike eastern and western regions of Skeiðarársandur, the 19<sup>th</sup> century moraines are not present here, reportedly buried or removed by jökulhlaups (Galon, 1973a, Jewtuchowicz, 1973, Wojcik, 1973a, Wisniewski, 1997, Thorarinsson, 1974, Knudsen et al., 2001). Hardaskriða comprises an outwash plain that contains numerous kettle holes, obstacle marks, outwash terraces and large depressions. The largest of these depressions are up to 600 m wide, and possess steep walls and uneven floors. A geomorphological map of these depressions is shown in Figure 7.2 and dGPS profiles of these depressions are presented in Figure 7.3.

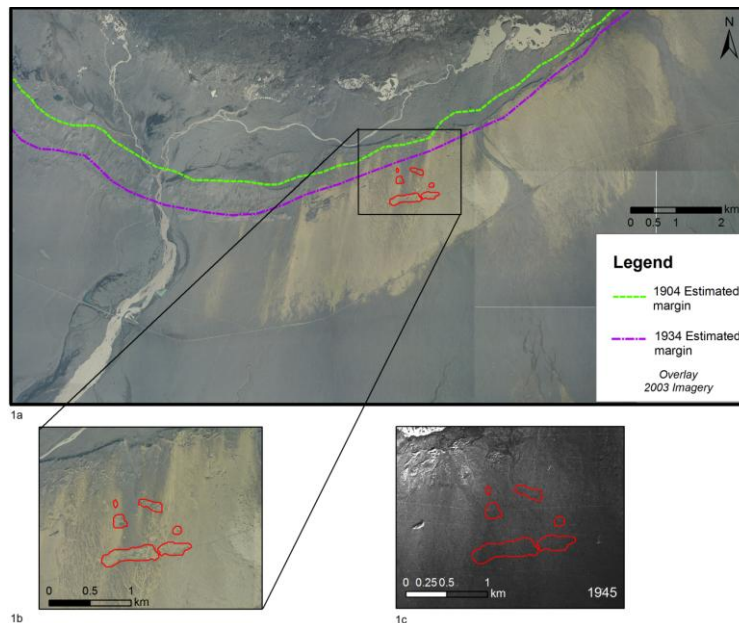


**Figure 7.1** 1a) Location map of several large depressions on the central sandur (Hardaskriða), with approximated margin position in 1904 and 1934 taken from georeferenced maps - the largest depressions in this region are circled in red. 1b) Location of the depressions in 2003 and the same undisturbed terrain in 1945 (1c).

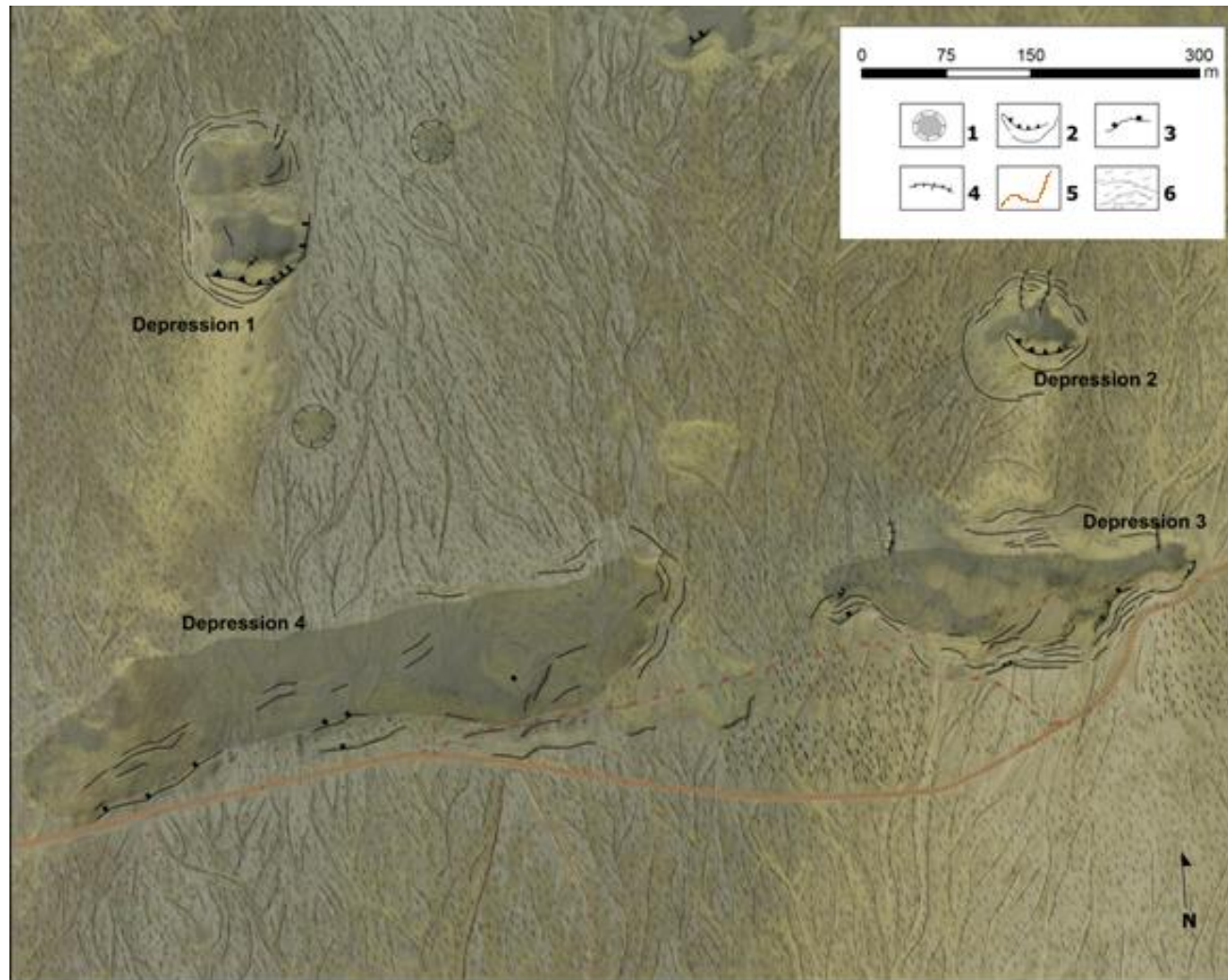


Figure 7.2 Geomorphological map of depressions. 1) kettle holes, 2) concentric crevasses and horst and graben, 3) normal faulting, 4) gullies, 5) dirt road, 6) outwash.

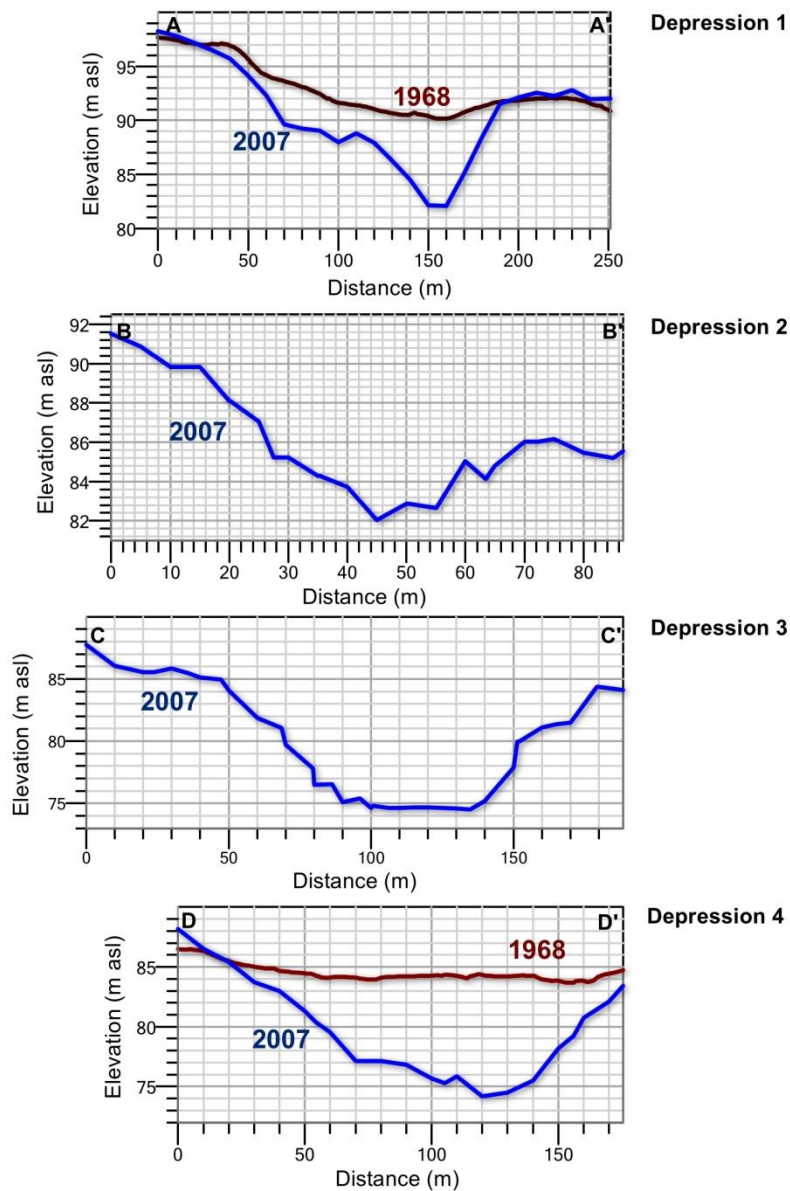
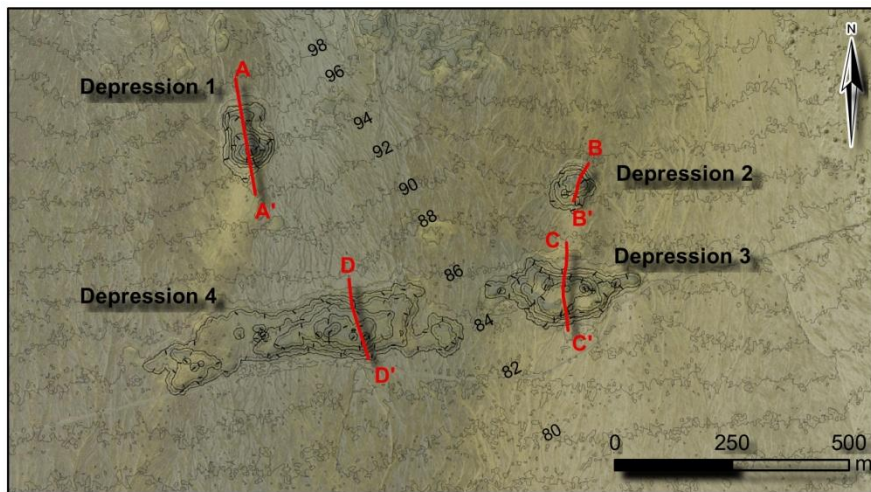


Figure 7.3 Profiles of depressions 1 –4 in 2007 is shown in blue; 1968 surface, when available, is shown in red.

### 7.2.1 *Depressions*

Depression 1 is approximately oval in shape and ranges in width from 164 m (north-south) to 108 m (east-west). The northern and southern rims are characterised by outwardly dipping arcuate and concentric normal faults. Along the southern rim, normal faulting has resulted in the rotation of two large blocks (up to 60 m in length and 15 m wide) have developed. The base of this depression is characterised by sagging, uneven terrain, and is divided into two portions of unequal depth. The northernmost part of the depression ranges in depth from 8-10 m, while the southern part of the depression is  $12 \pm 1.64$  m in depth.

Depression 2 is approximately circular in shape and ranges in width from 89 m (north-south) to 104 m (east-west) and  $13 \pm 1.64$  m deep. The northern portion contains of concentric normal faults and two extensional faults that trend north-south (40 m and 50 m in length). Along the southernmost rim of this depression, normal faulting has resulted in the rotation of two blocks, the largest 60 m long and 13 m wide.

Depression 3 possesses an irregular, elongate morphology that trends east-west. The depression ranges in width from 342 m (east-west) and 116 m (north-south) and is  $12 \pm 1.64$  m deep. The margin, while not circular in shape, contains numerous normal faults and embayments that surround the depression. The southern margin is marked by several rotated blocks and steep walls. The margin appears to slump in rotational blocks towards the centre, resulting in 'steps' that dip outwards from the depression. A dirt road observed on the 1945 photographs (Figure 7.1) is visible on the 2007 photographs and its original surface, although now undulating, remains discernable as it traverses the depression, suggesting that the subsidence has been gradual in nature.

Depression 4, the widest of the depressions, is similar in shape to depression 3, and possesses an irregular shape and trending east-west. The depression ranges in width from 604 m (east-west) to 148 m (north-south). Similar to the other depressions, the walls are steepest along the southern margin, and the margin is characterised by horst and graben blocks and concentric extensional fractures. Numerous embayments have developed along the northern, eastern and western margin. These portions of the depression margin possess a relatively gentle, stepped slope, compared to the steeper southern margin.

The proglacial depression directly north of this site contains three drumlinised, elongate ridges that join the elevated sandur as seen on 1965 imagery (Figure 7.4). These ridges



trend north-south and, from east to west, are 176 m, 79 m and 151 m in length and 30, 37, and  $34 \pm 1.64$  m in height respectively. Figure 7.5 displays elevation profiles of the area immediately adjacent to these ridges (Profile 1) and the ridges themselves (Profiles 2-4) that lie within the rectangular region that has been removed from sandur. While varying in height, the ridges all span an average of 33 m from the base of the depression to the sandur. Later photoseries indicate that these ridges have been largely removed by the fluvial erosion by shifting proglacial drainage channels and by the November 1996 jökulhlaup.

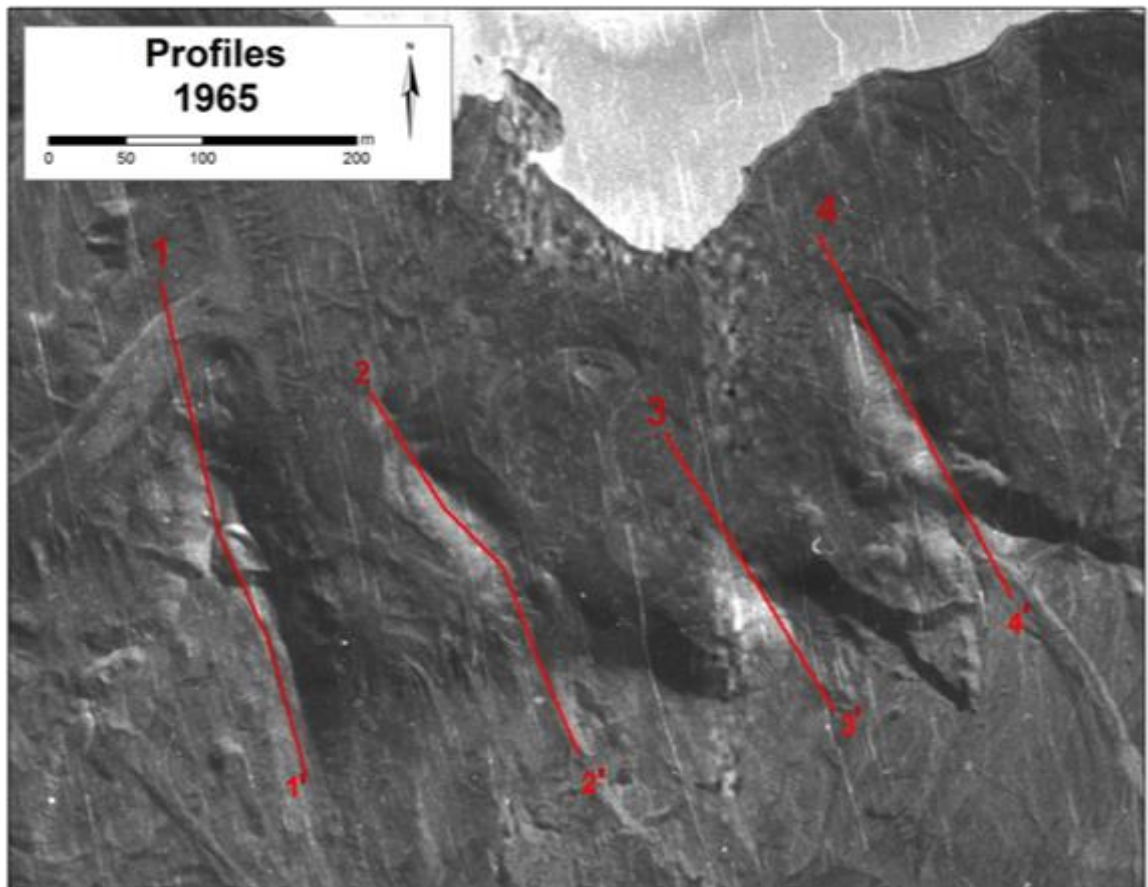


**Figure 7.4** Profile of sandur and proglacial depression (1), and drumlinised ridges (profiles 2-4) exposed by the retreat of the glacier margin since 1945. The majority of these ridges had been removed in later photoseries.

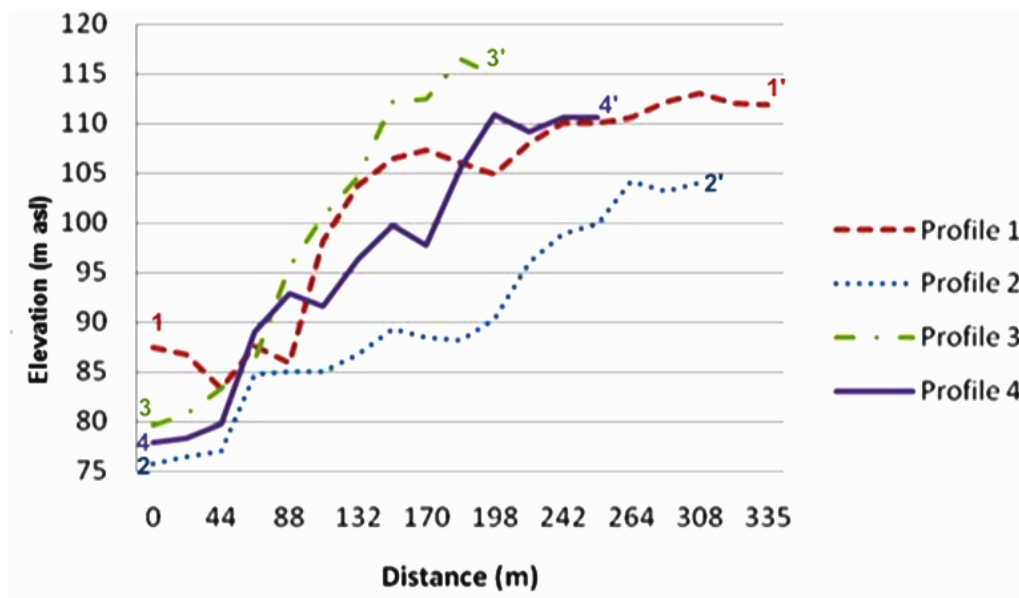


Figure 7.5 Combined elevation profiles of the drumlinised ridges located within the proglacial depression.

### 7.3 Volumetric change detection

While the poor quality of the 1945 images precluded the production of a 1945 DEM surface to quantify subsidence over the last sixty-two years, an attempt was made to provide an approximation. By removing elevation points that lay within the depressions on the 2007 imagery and generating a triangular irregular network, or TIN, across the missing data points, a 1945 surface was simulated. Elevation values from the two datasets were subtracted using ArcMap's Spatial Analyst tool to provide an approximate estimate of the volumetric loss for four of the major collapse areas in this region. A vertical lowering of  $12 \text{ m} \pm 1.64$  over 62 years was calculated from the height difference between the *faux* 1945 and 2007 sandur surfaces (Figure 7.6), representing an average rate of 19 cm per year. Figure 7.7 depicts the depth of the depressions (in 1968 and in 2007) compared with the depth of the proglacial depression directly to the north. Figure 7.8 depicts the location of the southernmost depressions compared with proglacial depression as well as the overall surface elevation of the ice surface since 1997.



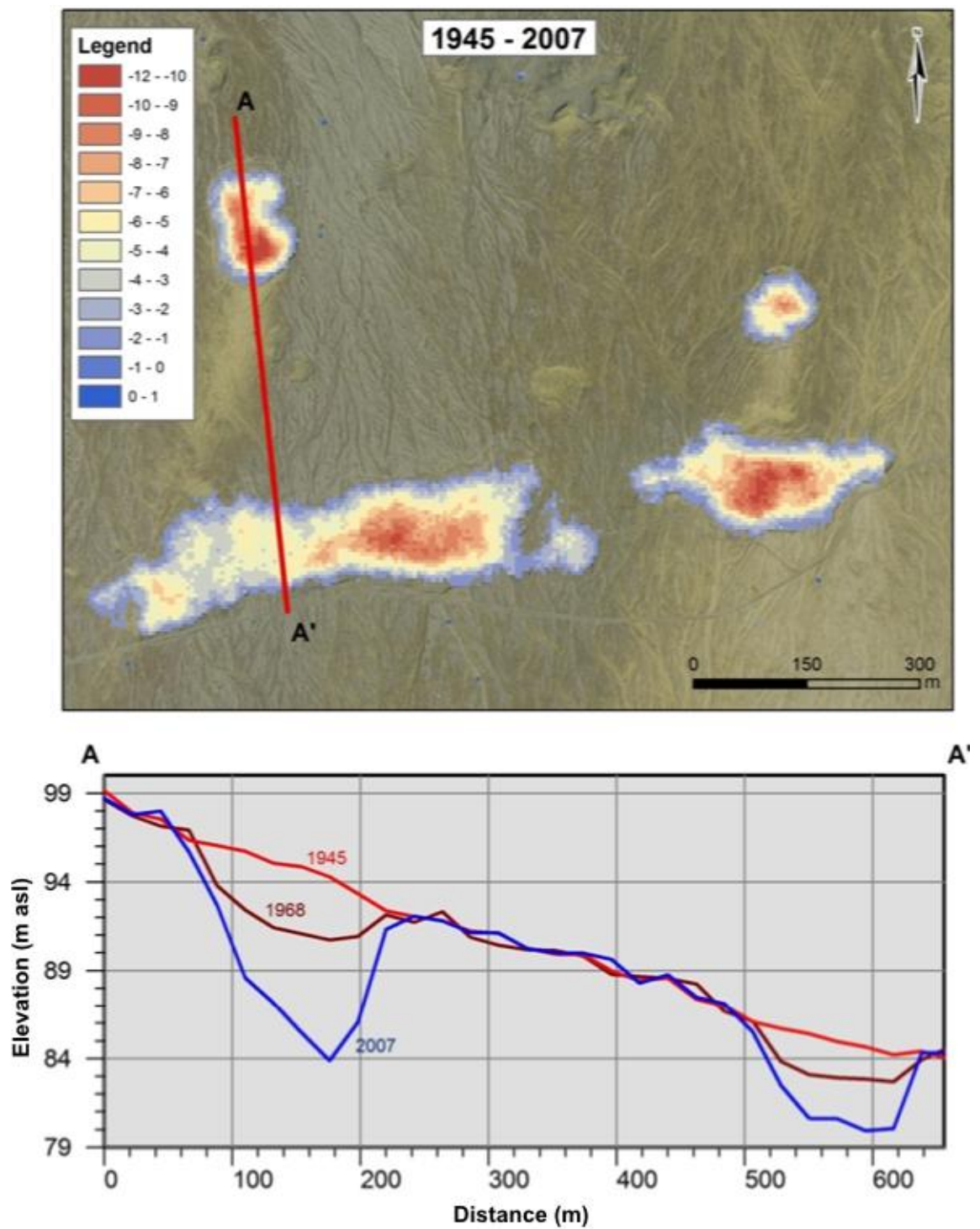


Figure 7.6 Total elevation loss (m) between 1945 – 2007 and estimated volume loss estimated by using an artificial 1945 surface (top); profiles of depressions between 1945 (red), 1968 (brown) and 2007 (blue) (bottom).

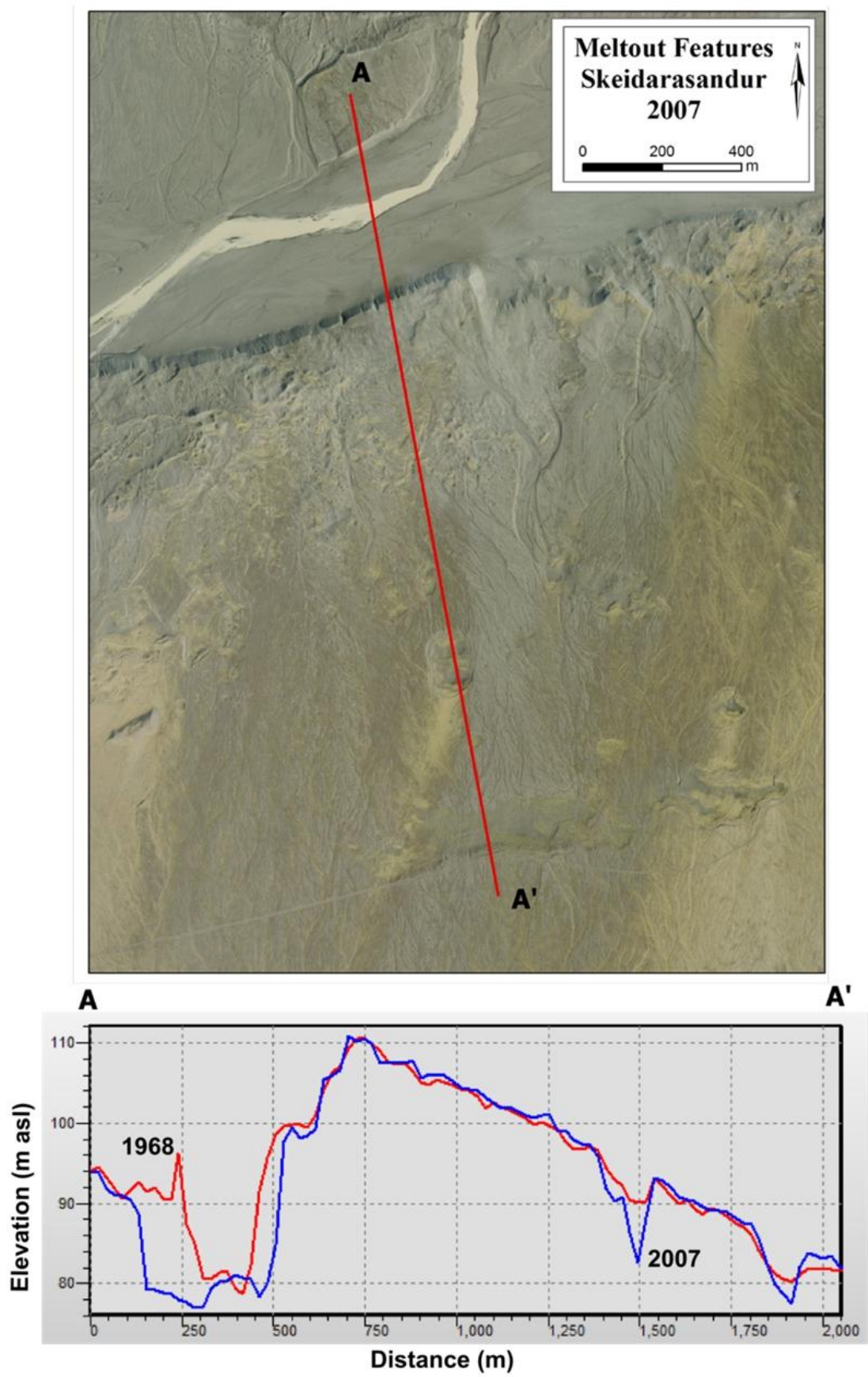
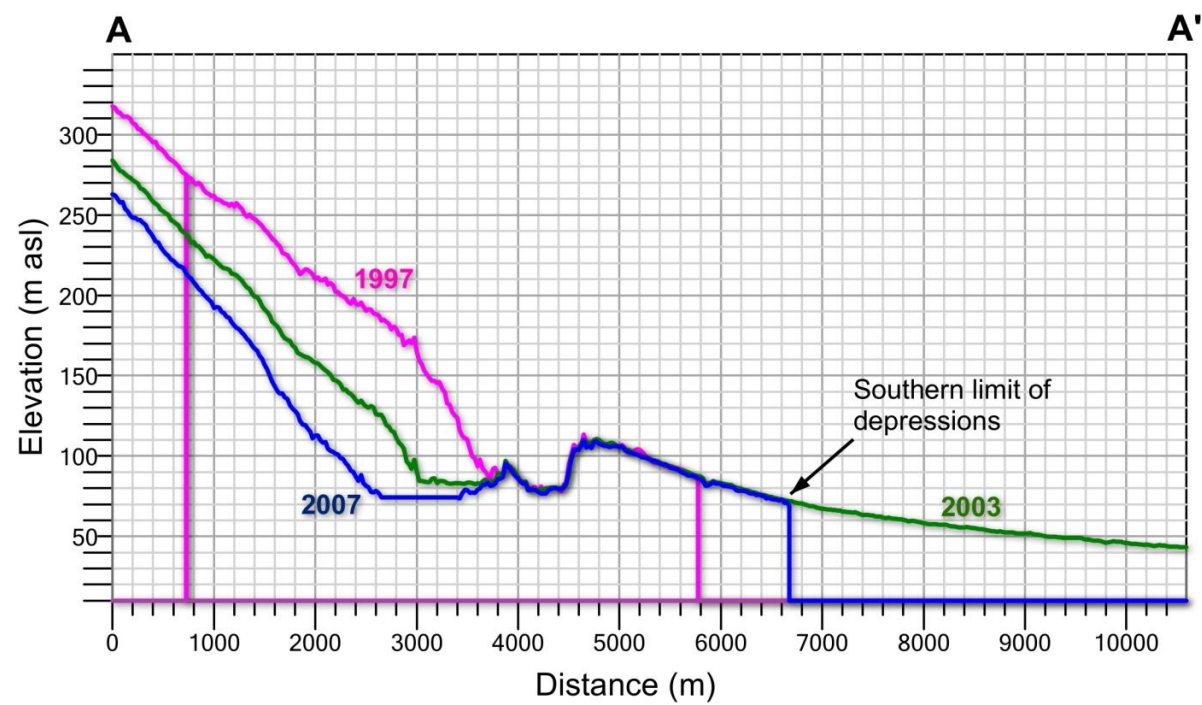


Figure 7.7 Profile of depressions found on the central sandur; 1968 is shown in red, 2007 in blue.



**Figure 7.8** Location map and long profile of the glacier and the sandur, demonstrating the retreat of the margin and the base level lowering of drainage within the proglacial depression, and assumed lowering of groundwater table.

#### 7.4 Interpretation

DEMs and dGPS measurements reveal that the Hardaskriða depressions experienced the greatest vertical loss within their centres. The terrain appears to slump in rotational blocks towards the centre, characteristic of horst and graben structures, resulting in ‘steps’ that have developed along the side of the feature into the centre. The concentric rings of normal faulting, horst and graben, normal and extensional faults described at the Hardaskriða depressions 1-4 are consistent with observations made at other field sites involving smaller bodies of ice that have been transported by lahars and jökulhlaups (Maizels, 1992, Branney, 1995, Branney and Gilbert, 1995, Olszewski and Weckwerth, 1998). Such features have been employed to provide indirect evidence of buried bodies of ice at other locales (Boulton, 1972, Hambrey, 1984, Dickson and Head, 2006).

As these buried ice bodies began to melt, the loss of volume and drainage of subsurface water results in the subsidence of the overlying sediment (McDonnald and Shilts, 1975, Maizels, 1992). This subsidence may result in the formation of an outward-dipping arcuate hairline fracture that elongates into a ring, causing the subsidence of a coherent block of sediment as seen in depressions 1 and 2 (Branney, 1995, Branney and Gilbert, 1995). These overhanging scarps become unstable and collapse along new arcuate faults, resulting in the development of extensional crevasses (Sanford, 1959, McDonnald and Shilts, 1975). Crevasses may continue to expand along small vertical and normal faults causing some walls to collapse, resulting in keystone graben. Continued collapse leads to intersection of arcuate fractures into blocks that tilt and subside into the pit. Mass movements and slumping produce even more rapid melt (Johnson, 1992a). At larger collapse pits, such as depressions 3 and 4, scalloped topographic margins with embayments may also develop (Branney, 1995, Branney and Gilbert, 1995). These features, combined with the steep walls of the depressions and undisturbed nature of the surrounding outwash plain are consistent with bodies of ice that have been completely surrounded by sediment (Maizels, 1991). The gentle slopes of the northern walls and the steeper slopes of the southern walls are consistent with the development of a ‘normal’ kettle hole (Maizels, 1992, Olszewski and Weckwerth, 1998) (see Chapter 3), as proglacial outwash resulted in the development of gravitational flow on the northern side, while block displacement and subsidence developed on the southern side following meltout.

Observations of other large bodies of buried ice greater than 30 m in thickness elsewhere on Skeiðarársandur have been documented via resistivity studies (Everest and Bradwell, 2003) and confirmed at exposures (Klimek, 1972, Bogacki, 1973, Churski, 1973, Jewtuchowicz, 1973, Russell et al., 1999a, Molewski, 2000). Ridges and detached plains of dead ice have also been described in the eastern and western portions of Skeiðarársandur deposited by the retreating ice margin (Galon, 1973a, Jewtuchowicz, 1973, Wojcik, 1973a). Unlike these ridges, plains or moraines elsewhere on the sandur, the descriptions of the Hardaskriða depressions are consistent with isolated blocks of ice emplaced by jökulhlaup-type floods (Maizels, 1992, Maizels and Russell, 1992, Branney, 1995, Branney and Gilbert, 1995).

### **7.5 Emplacement mechanisms**

In order to develop a sequence of when jökulhlaups emplaced these ice blocks and an estimate of their subsequent rate of melt, the 1904 topographic map and historical accounts of events on Hardaskriða were examined. The 1904 maps depict several elongated ridges on the central portion of Skeiðarársandur that appear to be continuations of the 19<sup>th</sup> century moraines seen in the western region (Figure 7.9). On the 1945 photographs these landforms are no longer visible and, as mentioned previously, the 19<sup>th</sup> century moraines on the central sandur were reportedly buried or removed by jökulhlaups (Galon, 1973a, Jewtuchowicz, 1973, Wojcik, 1973a, Wisniewski, 1997, Knudsen et al., 2001). While some of the depressions and landforms on Figure 7.9 correspond to the approximate positions of the 19<sup>th</sup> century moraines, several of the largest depressions developed 412 m south of this limit, suggesting that these depressions are not related to the pre-existing 19<sup>th</sup> century moraines.



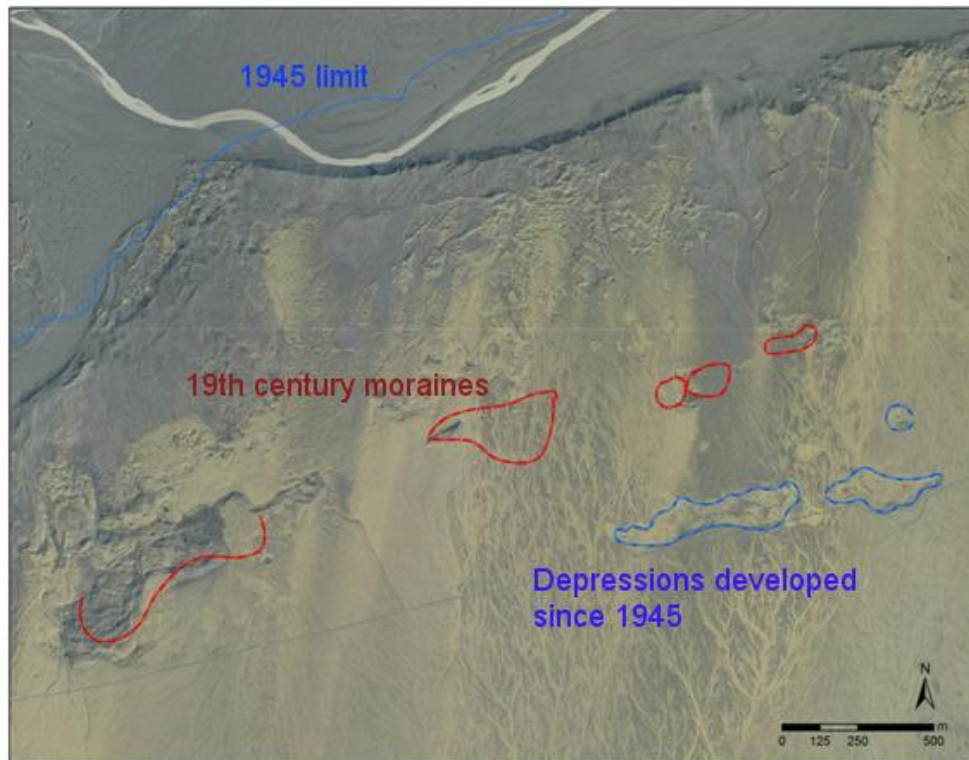


**Figure 7.9** Approximate locations of 19<sup>th</sup> century moraines estimated from georeferenced 1904 topographic map (dashed red line). Dashed blue lines represent depressions that have developed since 1945 south of the 19<sup>th</sup> century moraines. Solid blue line (top) represents position of margin in 1945.

According to Thorarinsson (1974), during the 1903 jökulhlaup a large piece of the glacier margin detached that was approximately 1 km in length and up to 150 m in height; it was also documented that a fracture of similar size and length developed upglacier located where the floodwaters burst from the glacier margin. This event also deposited ice blocks ‘the size of houses’ onto the sandur. These accounts also state that the 1903, 1913 and 1922 jökulhlaups inundated the central sandur with floodwaters and sediment (Thorarinsson, 1974) (see Table 3.1) and, during periods of glacier standstill, meltwater runoff was concentrated in the central part of the glacier forefield, responsible for the formation of the wide outwash channels (Galon, 1973b). The subsequent jökulhlaups in 1934 (Figure 7.10) and 1938 did not affect the Hardaskriða outwash plain (Thorarinsson, 1974), as the floodwaters were routed through the Háöldukvísl and other channels of lower elevation (Thorarinsson, 1974).



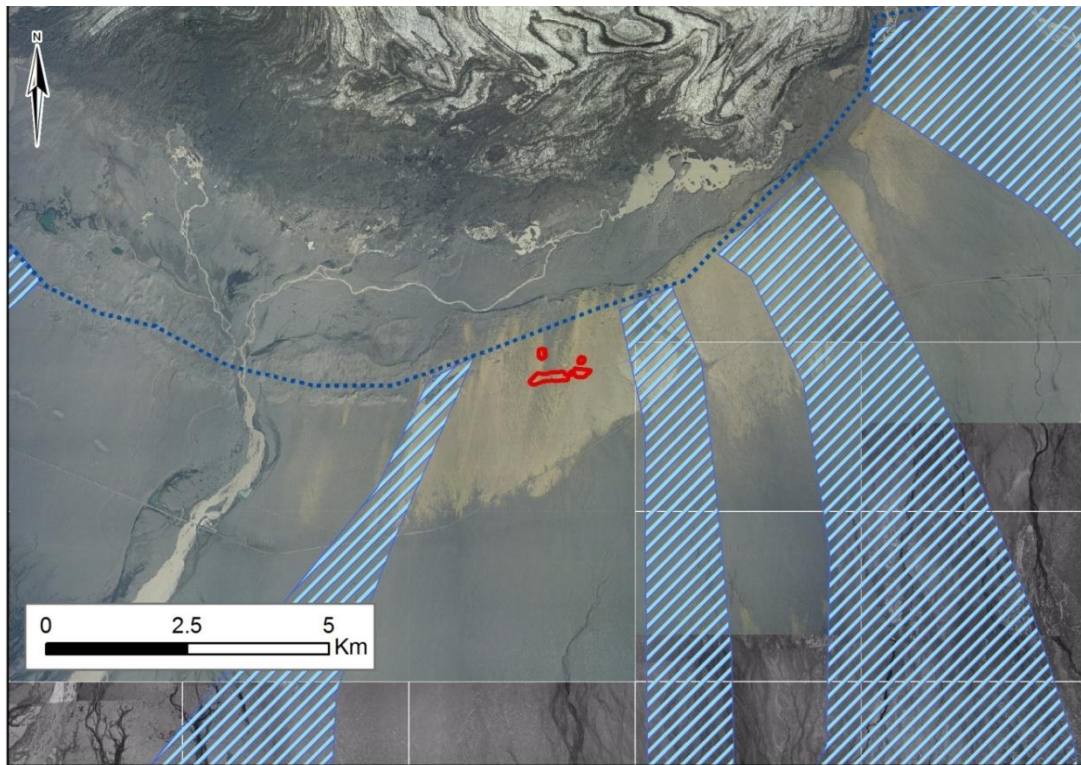


**Figure 7.10** Approximate extent of 1934 ice margin (dashed blue line) and location of jökulhlaup routing (blue hashed polygons) on top of 2003 photomosaic (1997 photomosaic underlain to fill gaps). Red polygons delineate location of depressions. (Thorarinsson, 1974).

In 1929, Skeiðarárjökull experienced a surge, with the western lobe advancing 390 m south of its 1904 position, while the eastern lobe only advanced 260 m south (Thorarinsson, 1943, Wojcik, 1973a, Wisniewski, 1997, Sigurðsson, 2005). While no measurement of the advance of the central lobe during this surge was documented, even if it advanced as far south of the 1904 position reported for the western lobe that experienced the greatest advance, the margin still would not have reached the location of the Hardaskriða depressions. Since 1933, Skeiðarárjökull has been receding (Thorarinsson, 1943) as a result of a warming trend that Iceland experienced that caused some glacier termini to retreat as much as 3-4 km (Sigurðsson, 2005).

## 7.6 Discussion

The largest, elongated Depressions 3 and 4 may be the result of the 1 km wide portion of the margin that detached during the 1903 jökulhlaup described by Thorarinsson (1974). During this same flood, house-size ice blocks were emplaced on the sandur and the flood waters ‘*dug down in deep sand channel...bank that...were...many human stories*’ (Thorarinsson, 1974). Ice blocks, regardless of their original shapes, result in circular depressions, such as depression 2; nested or dumbbell-shaped pits formed where circular

collapse pits from two closely adjacent buried blocks of ice overlap, such as depression 1 (Branney and Gilbert, 1995).

Ice blocks of a similar size were observed to be fully or partially buried during the 1996 jökulhlaup during the rising stage flood waters, and it was noted that when routed through a single conduit, waning stage flows may continue to maintain high sediment efflux and aggradation rates (Russell and Knudsen, 2002), capable of burying large bodies of ice. During the 1996 jökulhlaup,  $8.3 \times 10^6 \text{ m}^3$  of ice was transported onto Skeiðarársandur, including ice blocks as large as 45 m in diameter (Fay, 2002, Russell et al., 2005). Some of these ice blocks were deposited in a line, resulting in a single coalesced kettle hole approximately 130 m wide and 40 m long (Fay, 2002, Russell and Knudsen, 2002). The largest accumulation of ice blocks was over 1 km in length and extended up to 300 m in width (Fay, 2002, Russell and Knudsen, 2002), comparable in size to the Harðaskriða depressions.

However, as the majority of the ice blocks that were partially or completely buried during the 1996 jökulhlaup melted away within a just a few years, it is likely that the 1903 blocks were completely buried and further insulated by material deposited during the 1913 and 1922 jökulhlaups (Thorarinsson, 1974). The rate of melt of a buried ice body may be affected by a variety of factors, including the amount of material within the ice, depth of cover and geothermal heat flux (Nakawo and Young, 1981, Nicholson and Benn, 2006), making an initial estimate of the size of the buried ice body difficult. While the ice bodies may have been emplaced as early as 1903 and as late as 1922, any melting that occurred during that time is not captured on available imagery. It is evident that subsidence on the photographs was only observed following 1945, suggesting that the retreat of the glacier in the 1930s (Thorarinsson, 1943), lowering of the groundwater table and subsequent warming trend are responsible for increasing the melting rate of the buried ice (Sigurðsson, 2005).

The retreat of the ice between 1945 and 1965 also exposed several elongate, drumlinised ridges (Figure 7.4). These landforms may represent conduits, emplaced as material was forced up out of the proglacial depression and out onto the sandur during these historic jökulhlaups. As shown in Björnsson's (1999) profiles of the ice surface (Figure 3.1), the ice in this region in 1904 was ~100 m thicker than in 1945, which would have resulted in an increased hydraulic gradient during high-magnitude jökulhlaups and an increased

capacity to excavate and transport sediment (Roberts et al., 2000, Roberts et al., 2001, Roberts et al., 2002), reinforcing the importance of margin position on jökulhlaup processes and deposits. These landforms and their implications are further discussed in Chapter 8.



## Chapter 8 Discussion

---

*This chapter examines and tests models and hypotheses presented in the literature against observations made in the field pertaining to processes active at large-scale landsystems over decadal time frames. Models of large-scale landform assemblages diagnostic of surges, jökulhlaups and post-depositional modification identified on historical images and their correlation with historical events are used to determine the strengths of each model and used to modify or expand them. Observation from the imagery and these models are employed to support or refute hypotheses pertaining to each of the large-scale processes. A holistic model is presented that incorporates the overall impact of oscillations of the glacier margin, jökulhlaups and post-depositional modification on sandur evolution.*

---

### 8.1 Introduction

This chapter tests existing models and hypotheses of processes active in the proglacial environment presented in Chapter 2 and 3 by comparing them against observations made over a sixty-year period in Chapters 5, 6 and 7 in relation to themes A, B and C presented in Chapter 1. This chapter first examines, and in some cases expands upon, landform assemblages proposed to be diagnostic of glacier margin fluctuations, jökulhlaups and post depositional modification and subsequently tests hypotheses in the literature for each of these three processes. Finally, this chapter examines how each of the three large-scale processes and landforms relate to each other over a decadal timeframe and presents a diagrammatic holistic model of sandur evolution.

An overview of the events and processes described in the preceding chapters is depicted in a stylised timeline in Figure 8.1. This diagram does not contain every event to have affected Skeiðarársandur; however it is intended to depict major large-scale processes and events discussed in Chapters 5-7. Figure 8.1 also provides a visual means to compare periods of rapid change (such as the capture of the Skeiðará channels by the Gígjukvísl since 2003) when compared against the 100 year extent of this study. The long-term role of jökulhlaups on the sandur with regards to gradual melting of buried ice bodies at on the central sandur, and the relationship to margin position, is also depicted.

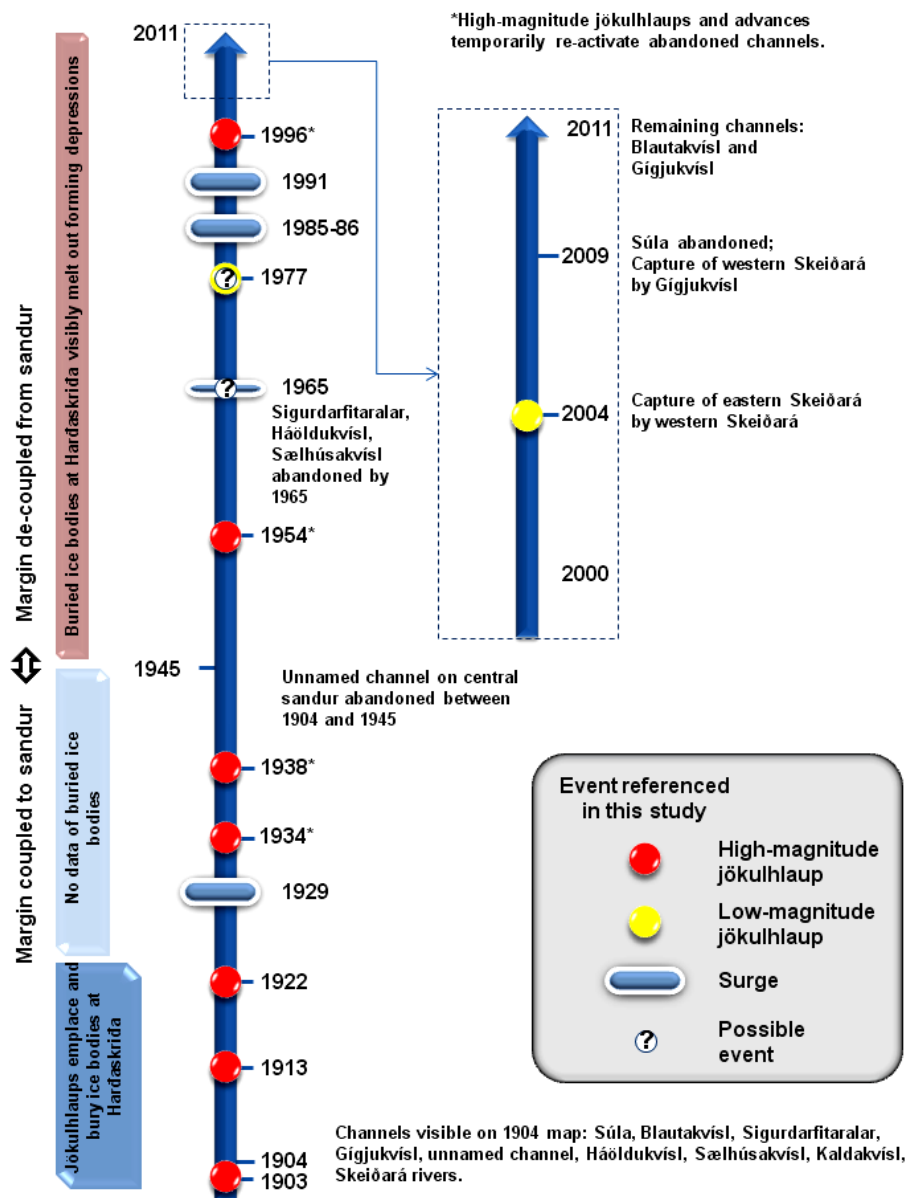


Figure 8.1 Stylised timeline of major events documented in Chapters 5, 6 and 7, including jökulhlaups, surges and the gradual melt out of buried ice. Major drainage capture events or periods of channel abandonment are also shown. For a complete list of all jökulhlaups at Skeiðarárjökull see Table 3.1 and 3.2.

## 8.2 Margin fluctuations: margin advance, surges and retreat

### 8.2.1 *Margin advance and surges: diagnostic landform assemblages, impact and persistence*

*(Landsystem model A.1 Numerous landform assemblages have been proposed to be diagnostic signatures to differentiate glacier surges including: thrust block moraines, ice blocks and evenly-spaced, ice-contact alluvial fans (Sharp, 1985a, Croot, 1988, Boulton, 1967, Evans and Rea, 1999, Knudsen, 1995, Russell et al., 2001a, Waller et al., 2008, Benediktsson et al., 2008); Landsystem model A.2 Following retreat, en- and sub-glacial features may be exposed including hummocky terrain, concertina eskers, flutes, drumlins, and crevasse-casts (Knudsen, 1995, Evans and Rea, 1999, Waller et al., 2008, Bjarnadóttir, 2007); Landsystem model A.3 Glacier margin retreat may also leave hanging outlets, alluvial fans and overridden moraines on proglacial distal regions (van Dijk and Sigurdsson, 2002, Russell et al., 2001a, van Dijk, 2002).)*

Several landform assemblages that have been presented in the literature as being diagnostic signatures of surges include hanging outlets, push moraines, thrust blocks, drumlised terrain, fluted ground, evenly-spaced ice-marginal outwash fans and an increase in proglacial drainage were based on observations of Skeiðarárjökull made following the 1985-86 and 1991 surge events (van Dijk and Sigurdsson, 2002, Russell et al., 2001a, van Dijk, 2002, Waller et al., 2008). While many of the surge-related alluvial fans generated by the 1985-86 and 1991 surges at Skeiðarárjökull were later eroded or buried by the influx of meltwater and sediment into the proglacial trench during the November 1996 jökulhlaup (Section 5.3.6), examination of earlier images (Section 5.3.3 and Section 5.3.4) revealed landforms consistent with the landsystem models A.1, A2, and A.3 (Figure 8.2).

The 1965 images (Section 5.3.3) revealed the presence of two ice-marginal, kettled alluvial fans, and an increase in drainage outlets spaced evenly along the glacier margin (Figure 5.18, Figure 5.19), and a steep, near vertical glacier snout along the central lobe (Figure 5.20, Figure 5.21). By 1986 (Section 5.3.4), the retreat of the margin revealed thrust blocks associated depressions where the two ice-marginal fans had been located on the 1965 and 1968 images (Figure 5.18). As seen in Figure 8.2, the alluvial fan, thrust blocks and associated depression have continued to affect proglacial drainage patterns and lakes two decades following their emplacement. While the observations of these



landforms appear to corroborate some of landform assemblages of the landsystem models of glacier surges A.1, A.2, and A.3, caution should be employed without further stratigraphic data or ground investigation; as described by other authors (Evans, 2003, Benediktsson et al., 2008) these features do not necessarily distinguish the 1965/68 possible surge from those that could be generated as a result of a minor rapid advance.

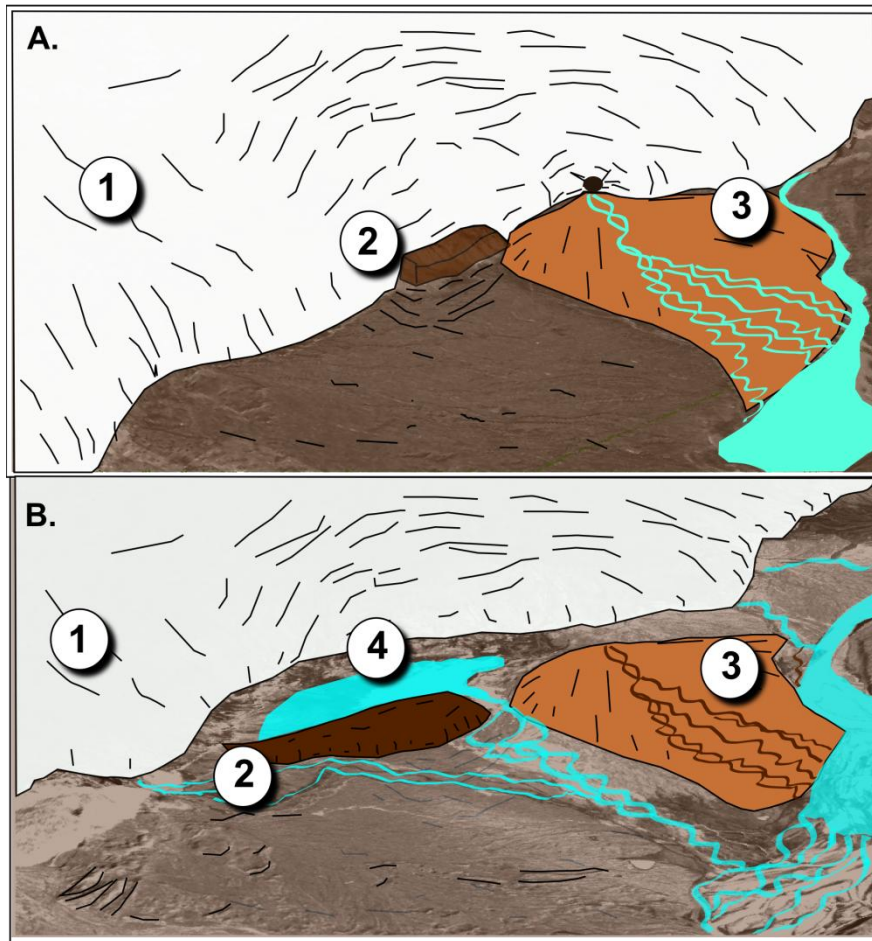


**Figure 8.2** Comparison of landforms emplaced by a minor rapid advance, or possible surge, observed on 1965 (A) and 1986 (B) imagery and DEMs. Features include 1) steep, near vertical margin, 2) thrust block moraine, 3) alluvial fan, 4) proglacial lake and braided stream network.

#### 8.2.2 *Glacier margin retreat and ice surface lowering over the 20<sup>th</sup> century*

*(Landsystem model A.4 Glacier retreat provides accommodation space, permitting the development of proglacial lakes and drainage parallel to the margin (Jonsson, 1955, Howarth and Price, 1969, Klimek, 1973, Bristow and Best, 1993, Gustavason and Boothroyd, 1987).)*

As shown in Section 5.3 and Appendix A-Plate III, the retreat of the glacier margin has permitted the establishment of proglacial drainage parallel to the central glacier margin, as well as the development of numerous large proglacial lakes, as proposed by landsystem model A.4. While the lowering of the ice surface has been observed to be a control on the

routing of the Grænalón jökulhlaups (Section 5.4.8, (Roberts et al., 2005), it was also observed that after decades of relative stability, the rapid lowering of the ice surface of the central glacier margin between 1997 and 2007 is pronounced (up to 80 m) (Figure 5.3; Figure 5.25). The dramatic thinning of the glacier margin since 1997 also suggests a relationship between the transfer of large volumes of sediment - approximately 180 million tons of suspended sediment (Björnsson, 1997, Snorrason et al., 2002) - through sub-, en- and supraglacial conduits observed during the November 1996 jökulhlaup from within and beneath the glacier and out onto the proglacial depression and sandur (Roberts et al., 2000, Snorrason et al., 2002). These observations suggest that high-magnitude jökulhlaups, by transferring such large volumes of material from beneath the glacier and onto the sandur, may also serve as a major control on the pattern of margin retreat, proglacial drainage patterns and the evolution of the sandur. As a result of the sediment emplaced by November 1996 jökulhlaup into the proglacial trench, post-1996 proglacial drainage and lakes have been restricted southward, and have developed along the glacier margin at a lower elevation (Figure 5.3). This interpretation may suggest the development of a new model that *The transfer of sub-, en- and supraglacial debris during jökulhlaups may exert a direct control on the pattern on glacier margin retreat by providing accommodation space for the development of proglacial drainage and lakes, and retarding the ablation rate of buried ice.*

### 8.2.3 ***Glacier margin retreat: impact of fluctuations on incision/aggradation***

*(Hypothesis A.5 Fluctuations of glacier margins exert a direct control on the spatial distribution and rate of proglacial aggradation or incision (Maizels, 1979, Marren, 2002b); Hypothesis A.6 Glacier margin advance/retreat may affect the geomorphology of the proglacial area without any alteration in sediment or water supply, as channel incision may result simply from the lowering of the upstream meltwater outlet (Marren, 2002b).)*

According to Klimek's (1973) model, continued retreat will result in the abandonment of all lateral drainage channels with only a single channel draining the central margin. However, in the case of the eastern Skeiðará, following the lowering of the glacier surface between 1997 and 2003 (Section 5.2.5), the retreat of the glacier margin resulted in the incision of a single, confined channel that temporarily, at least, served to restrict meltwater from flowing westward parallel to the glacier margin, resulting in abandonment of pre-existing drainage networks along the front of the margin in this area (Figure 5.7). This observation corroborates Hypotheses A.5 and A.6 and indicates that Klimek's model (Figure 2.10) may be oversimplified as minor margin fluctuations and both high and low

magnitude jökulhlaups may affect the rate, and pattern of channel development / abandonment. A simplified model based on the pattern of channel abandonment observed at Skeiðarárjökull is shown in Figure 8.3. This figure is presented to depict the relationship between glacier margin position, the proglacial depression and the selection and persistence of channels due to basin geometry and jökulhlaup-related incision.

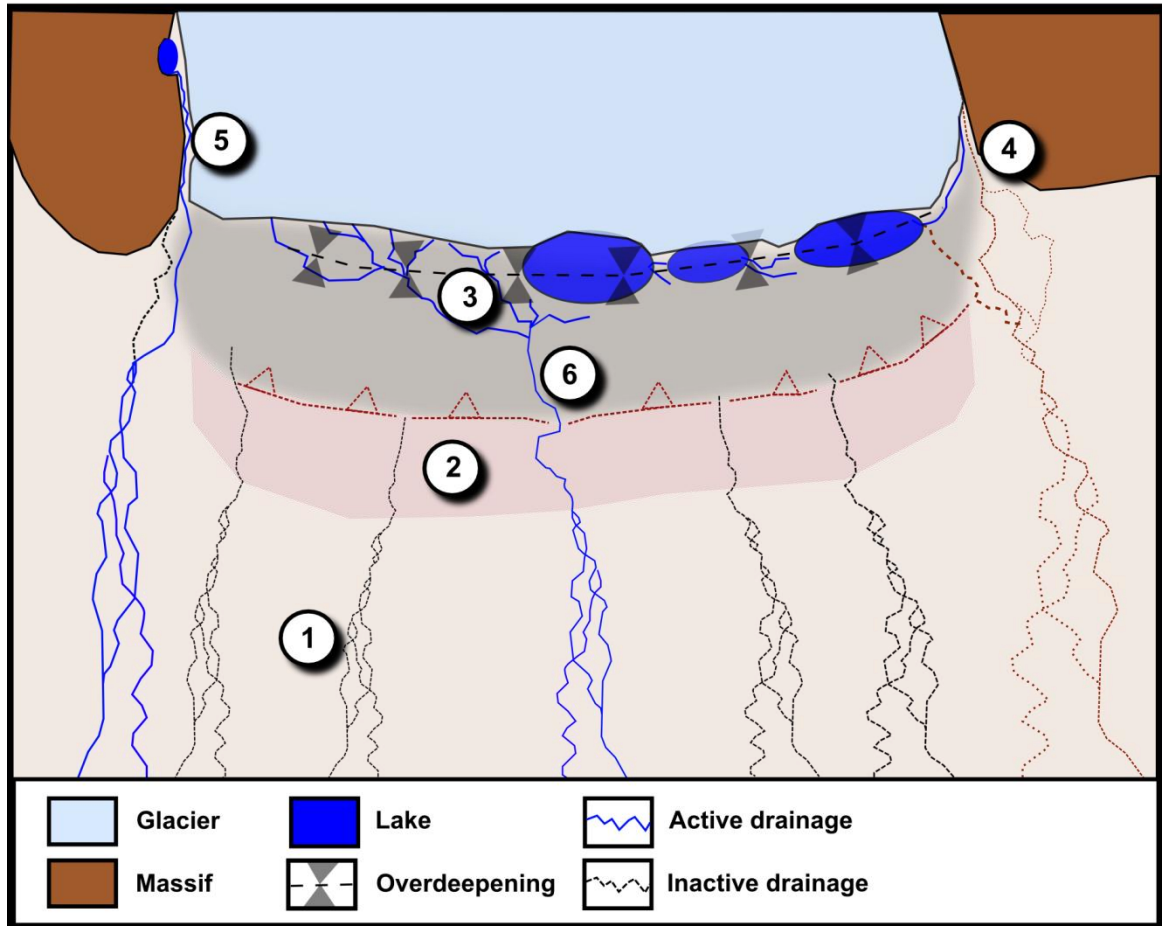


**Figure 8.3** Stylised diagram of the abandonment of drainage systems within an overdeepened basin at a retreating margin based on Skeiðarárjökull: 1) abandoned drainage channels along central sandur, the first channels to be abandoned during margin retreat, 2) detached snout comprised of moraines, abandoned moraine gates, buried ice and outwash plains, 3) lowest area (maximum) of overdeepening of the proglacial depression infilled with sediment and proglacial drainage and lakes, 4) lateral drainage channel that remain actively coupled to the sandur until glacier retreats past the maximum overdeepening, 5) lateral drainage channel that has remained active and coupled to sandur despite retreat of glacier margin due to incision resulting from glaciolimnic jökulhlaups, 6) main central drainage channel that drains drainage contained within the overdeepening out onto the sandur.

As noted at the field site, following the decoupling of the glacier margin from the sandur results in the abandonment of evenly-spaced proglacial streams (Figure 8.3, Feature 1). The retreat of the margin from the detached margin and moraines (Figure 8.3, Feature 2) results in the formation of a proglacial depression. During margin retreat, the glacier's lateral drainage remain may remain coupled due to the convex geometry of the sandur. Once the margin retreats beyond the point of maximum overdeepening (Figure 8.3,

Feature 3) however, these lateral drainage channels will no longer remain coupled to the sandur and will instead be captured by drainage within the proglacial depression (Figure 8.3, Feature 4).

A lateral drainage channel may remain coupled if repeated low magnitude jökulhlaups result in the continued incision of the channel that allows the channel to keep pace with margin retreat (Figure 8.3, Feature 5). This was observed that following a low-magnitude jökulhlaup at the Skeiðará in 2004 (Section 5.2.6), the resulting channel incision allowed the western Skeiðará channels to keep pace with the rate of glacier surface lowering, permitting it to remain coupled to the sandur. Similar channel incision was observed following two low-magnitude Grænalón jökulhlaup events at the Súla channel in 1968 and 1977 (Section 5.4.4) and at the Blautakvísl following repeated minor Grænalón jökulhlaups over the past decade that restricted the development of drainage parallel to the margin. These same events also served to widen and straighten several other ice-marginal channels that flowed into the Súla and the Blautakvísl, suggesting that jökulhlaups may also affect the rate and pattern of proglacial drainage systems during retreat. Drainage out of the proglacial depression and onto the central sandur occurs through a single, wide channel (Figure 8.3, Feature 6); in the case of Skeiðarárjökull, the evolution of the Gígjukvísl channel, both in terms of geometry and persistence, has been the result of the geometry of the overdeepening and as a result of volcanogenic jökulhlaups (1934, 1938, 1954 and 1997).

#### 8.2.4 ***Glacier margin retreat: channel incision and braiding***

*(Hypothesis: A.7 Glacier margin position affects proglacial drainage networks: during retreat, as channel incision may result simply from the lowering of the upstream meltwater outlet (Marren, 2002b) and result in braided stream patterns near to the glacier margin confined within an incising channel. During advance, braiding will become re-established on the recently abandoned outwash surface (Marren, 2002b) and braiding will develop further away from the margin (Maizels, 1979, Churski, 1973).)*

Observations of major channel outlets such as the Skeiðará and Súla (Sections 5.2 and 5.4) demonstrated that at a decoupled glacier margin the continued retreat of the glacier margin resulted in continued incision, shifting braided stream networks progressively further away from the glacier margin corroborating Hypothesis A.7. For example, at the eastern Skeiðará between 1945 and 2007 (Section 5.2.1), when the glacier margin was coupled to the sandur the braided stream channels were visible near the ice margin (< 50

m). Following the retreat of the glacier from 1965 – 1975 (Sections 5.2.2 and 5.2.3), the eastern Skeiðará was incised within a single broad channel (>150 m wide), with braided stream networks developing progressively further away from the glacier margin (over 5 km by 1975). Following the November 1996 jökulhlaup, however, while the eastern Skeiðará was subject to large-scale modification (widening and incision), ice-marginal braided channels appeared again close to the glacier margin on the 1997 images in response to the large influx of sediment, but were already further shifted downstream by 2003 (Section 5.2.5, Figure 8.4).

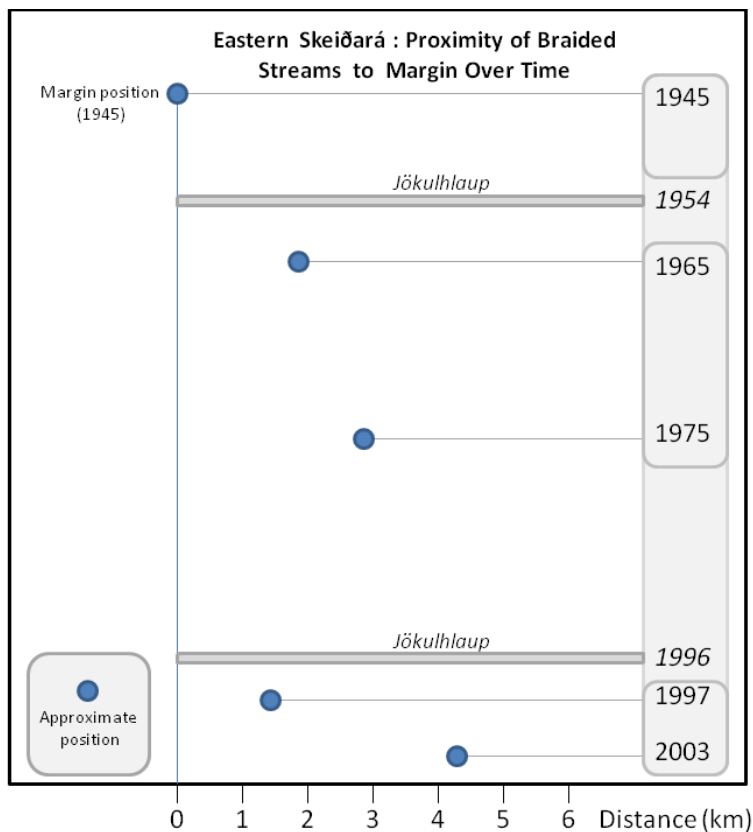


**Figure 8.4** Approximate position of braided stream networks over time in relation to the decoupled glacier margin, demonstrating the long-term, downstream shifting of braided stream networks associated with margin retreat and the marked, yet brief, impact of a high-magnitude jökulhlaup.

Additionally, the discharge of the 1979 jökulhlaup into the ‘non-hardened’ Blautakvísl resulted in a single, wide, incised channel (Section 5.4.5), where previously this channel had been dominated by a network of braided streams. In contrast, the sediment load deposited into the nearby ‘hardened’ Súla channel during this same event increased the proximity of braided streams to the glacier margin. This observation demonstrates that a jökulhlaup, not glacier margin fluctuations, may temporarily affect the position of braided streams differently within channels at different stages of evolution. While these observations do not refute Hypothesis A.7, they do suggest that these hypothesis be expanded. The shifting of the braided streams networks following jökulhlaups may only

persist for a short duration (months or years) as the channels re-distribute the sediments, however it has been observed at the field site that channel incision resulting from even minor jökulhlaups may have a decadal impact on the evolution of drainage at this retreating margin.

While observations from this study have demonstrated that the short-term impact (months to years) of jökulhlaups on channel development, Russell and Knudsen (1999) suggested a much longer term impact when they proposed that the 1954 high-magnitude jökulhlaup served to incise and widen the Gígjukvísl channel. This channel modification allowed drainage to remain coupled to the sandur during glacier margin retreat and was ultimately responsible for the selection of the Gígjukvísl as Skeiðarárjökull's dominant drainage channel (Figure 8.3). This, combined with the observations made in this study, suggests the development of a new hypothesis that *Jökulhlaups exert a direct control on the nature of proglacial aggradation or incision regardless of margin position.*

#### 8.2.5 ***Glacier margin retreat: temporal variability***

*(Hypotheses: A.8 During retreat, channel incision and reorganization may occur quite rapidly (Marren, 2002b).*

Glacier margin retreat at Skeiðarárjökull over the 20<sup>th</sup> century as observed on historical imagery (Sections 5.2, 5.3 and 5.4) was characterised by the gradual reduction of drainage channels through the 19<sup>th</sup> century moraines (Figure 8.1 and Figure 8.3), corroborating existing models of glacier retreat (Bogacki, 1973, Klimek, 1973, Price and Howarth, 1970). Within a relatively short span of time, between 1938 and 1944 (Galon, 1973a), the central lobe decoupled from the sandur, resulting in the abandonment of the Sælhúsakvísl and Háöldukvísl channels (Section 5.3.3); in a similarly rapid manner, since 2004 the number of channels reduced from five to one: drainage of the eastern Skeiðará channel was successively captured by first the western Skeiðará as recently as 2004 (Section 5.2.6), then both were captured by the Gígjukvísl channel as recently as August 2009, while drainage from the Súla and the Blautakvísl channels were captured by the Gígjukvísl between 2010-11 (Section 5.4.8 and Figure 8.1). Observations of these repeated and major shifts in drainage networks rapidly in response to the retreat of the glacier margin corroborate Hypothesis A.8.



### 8.3 Jökulhlaups: diagnostic signatures, persistence and impact

#### 8.3.1 *Jökulhlaups: diagnostic signatures*

*(Landsystem model B.1. Proglacial landform signatures associated with jökulhlaups include kettled outwash fans, obstacle marks, channel modification and moraine dissection (Maizels, 1992, Fay, 2002, Russell et al., 2006, Evans, 2003); Landsystem model B.2 Landform assemblages consisting of fracture fills, single-event conduits and proglacial kettled outwash fans have been suggested by Russell et al. (2006) and Burke et al. (2008) to be diagnostic of major outlets emplaced during single event, high-magnitude jökulhlaups; Hypothesis B.3. During a jökulhlaup, as pressure decreases flow may evolve from a complex fracture-fill network to conduit flow, demonstrating that it is possible to determine different phases of a jökulhlaup from the resulting landforms and sedimentary sequences (Piotrowski, 1997, Sjogren et al., 2002, Russell et al., 2007, Roberts et al., 2000, Roberts et al., 2002)).*

Landforms including kettled outwash fans, obstacle marks, channel modification and moraine dissection that have frequently been considered to be diagnostic landform signatures of jökulhlaups (Maizels, 1992, Fay, 2002, Russell et al., 2006, Evans, 2003) were observed throughout many of the images (Sections 5.2, 5.3 and 5.4) following numerous high and low-magnitude jökulhlaups, corroborating landsystem model B.1. For example, large-scale channel modification and moraine gap dissection of the Gígjukvísl was observed following both the 1954 (Section 5.3.3) and November 1996 jökulhlaups (Section 5.3.6). Similarly, channel modification and associated outwash fans containing kettle holes and obstacle marks were observed following the high-magnitude jökulhlaups of 1954 (Sections 5.2.2, 5.4.3) and 1996 (Section 5.2.4). Kettle holes, obstacle marks and channel modification were also observed following low-magnitude jökulhlaups (Sections 5.2.6, 5.4.5 and 5.4.8).

This study examined landform assemblages composed of fracture fills and sub-, en-, and supraglacial eskers that were associated with major ice-marginal, kettled outwash fans generated by the November 1996 high-magnitude jökulhlaup and later exposed by the retreat of the glacier margin (Table 8.1) (Site 1-Section 6.2). These landforms were used as the type site for an expanded model of jökulhlaup landform assemblages as presented in landsystem model B.2 (Burke et al., 2008, Russell et al., 2006). These landform assemblages, visible on the 2003 and 2007 images, are similar in scale and geometry to assemblages exposed by the retreating glacier margin at other locations at Skeiðarárjökull including Site 2 (Section 6.3), Site 3 (Section 6.4), Site 4 (Section 6.5), Site 5 (Section 6.6) and Site 6 (Section 6.7) that correspond to locations of documented high-magnitude

jökulhlaups. By examining these landforms over time, this study was able to further expand on these diagnostic landform assemblages of landsystem model B.2.

<b>Location</b>	<b>Landform assemblage</b>
<b>Site 1</b>	5 - 270 m long rectilinear fracture fills, <700 m long esker connected to ice-walled canyon and outwash fan containing large (>45 m diameter) ice blocks and obstacle marks.
<b>Site 2</b>	Linear, ascending channel (<1 km in length) of disturbed terrain and ice blocks.
<b>Site 3</b>	>200 m long rectilinear fracture fills, disturbed terrain and >500 m long sinuous esker leading to 300 m wide gap in moraines associated with an outwash fan characterised by kettle holes and obstacle marks.
<b>Site 4</b>	>500 m long sinuous esker, > 1 km long rectilinear fracture fills leading to outwash fan containing kettles (<30 m in diameter), obstacle marks and boulders (>3 m in diameter).
<b>Site 5</b>	750 m long ridge of sediment, outwash fan surface characterised by boulders up to 2 m in diameter and kettle holes up to 27 m in diameter.
<b>Site 6</b>	5- 260 m long rectilinear fracture fills, 740 m long sinuous esker leading to moraine gap 150 m wide and kettled outwash fan.

**Table 8.1 Landforms associated with jökulhlaups documented on aerial photographs (see Chapter 6).**

For example, at Site 3 (section 6.4) located in the central glacier margin, the retreat of the glacier margin exposed landforms consisting of several sinuous ridges over 1 km long that are interconnected with < 200 m long rectilinear ridges. The lack of post-depositional deformation or settling since their appearance in 1965, combined with the appearance of rip-up clasts and other signs of subsurface disruptions evident in stratigraphic exposures of the esker suggest that these landforms are subglacial in origin.

Another large-scale variation of this landform assemblage was identified along the western glacier margin at Site 4 (Section 6.5) comprising a series of low, sinuous ridges ~200 m long intersected by ~100 m – 1 km long rectilinear ridges may be observed on the images melting out of the ice from 1945 – present. As the ice retreated, the suite of en- and supraglacial ridges was lowered on to the glacier bed, subtly altering their geometry, acting to impound local runoff. A similar set of linear, rectilinear ridges > 200 m long that intersect a sinuous esker >400 m in length was identified in Site 6 (Section 6.7). All of these sub-, en- and supraglacial landforms were associated with moraine gaps, kettled outwash fans and known locations of prior jökulhlaup events, corroborating landform

models B.1 and B.2. These observations corroborate models of anastomosing esker ridges developing from a complex network of rectilinear fluvial hydro-fracture fills both within the glacier and glacier substrate during a high-magnitude jökulhlaup (Hypothesis B.3).

In other locations where fracture-fills and sinuous eskers were not visible on historical photographs, large-scale outwash apexes and fans emplaced by jökulhlaups on the proglacial terrain still persist. The Double Embayment and ice-walled canyon that were emplaced at Site 1 (Section 6.2) during the November 1996 jökulhlaup, features emplaced within a confined conduit that permitted jökulhlaup flows to maintain high sediment efflux and aggradation rates (Russell and Knudsen, 2002) during the event. The resulting large ridge of sediment, boulders and ice blocks were observed at Site 5 (Section 6.6) where similar outwash fan apexes were described that may have been generated during a jökulhlaup and emplaced during similar confined flow conditions.

### 8.3.2 *Jökulhlaups and glacier margin fluctuations*

*(Hypothesis B.4. The scale, type and position of jökulhlaup-related proglacial landforms may vary depending on the position of the glacier margin (Maizels, 1997).) Hypothesis B.5. The position of the glacier margin plays a key role in determining the impact of flood (Gomez et al., 2002, Maizels, 1997)).*

While several observers (Roberts et al., 2000, Russell et al., 2007) have noted the variability of landforms emplaced from multiple types of outlets across Skeiðarárjökull's margin during the November 1996 jökulhlaup, the historical aerial photographs used in this study have also revealed temporal variations of jökulhlaup-related landform assemblages relative to margin position and pre-existing topography. Jökulhlaup-related outlets and deposits at approximately the same geographic location generated different landform assemblages. For example, during the 1996 jökulhlaup, the position of the double embayment and ice-walled canyon 1996 outlets at Site 1 (Section 6.2) corresponded to a location of maximum overdeepening (Björnsson, 1999); the location and geometry of this outlet was interpreted to be the primary control on the size and these macro-scale landforms from this outlet and duration of flow. Analysis of historical imagery of an area only 500 m southwest of Site 1 revealed a different landform assemblage (Section 7.2): when the glacier margin was coupled to the sandur, jökulhlaups emplaced four, large sub- and englacial eskers (Figure 7.4) that routed material upslope 30 m over a distance of ~200 m (Figure 7.5) and inundating Hardaskriða (Section 7.4). These eskers are drumlinised and any smaller landforms that may have been associated with them do not persist on the 1965 images. However it demonstrates that margin

position may serve as a control on the type and scale of the jökulhlaup landform assemblage, corroborating Hypotheses B.4 and B.5.

#### 8.3.3 *Jökulhlaups: pre-existing topography and substrate*

*(Hypothesis B.6 Pre-existing topography may affect the routing of jökulhlaups and the location and type of resulting deposits (Magilligan et al., 2002, Russell et al., 2006).)*

While the hydrofracturing described by Roberts et al (2000) responsible for the fracture fills was evident at Sites 1, 3, 4 and 6, the extent and nature of the hydrofracturing and the resulting landforms varied. For example, at Sites 1, 4 and 6, hydrofracturing resulted in the emplacement of complex fracture fill networks located at the head of eskers, while at Site 3 hydrofracturing resulted in large ‘disrupted’ regions of terrain. This disturbed terrain is described in Section 6.4 to be the result of hydrofracturing of the overlying diamicton layer and ice blocks, and their incorporation within the underlying gravels due to conditions of substrate and hydraulic pressure experienced during jökulhlaups corroborated Hypothesis B.6 and observations by authors at other locales (Le Heron and Etienne, 2005, Kjaer et al., 2006, Rijdsdijk et al., 1999, Boulton and Caban, 1995, van der Meer, 1998, Russell, 2003). The region of disrupted terrain itself is within a landform identified as an overridden ice marginal surge fan, illustrating not only how pre-existing topography, but how landforms emplaced by large-scale processes impact the evolution of the sandur over time.

#### 8.3.4 *Jökulhlaups: persistence*

The diagnostic landform with the highest preservation potential appears to be the outwash fan apexes observed at Site 1 (Section 6.2) and Site 5 (Section 6.6). Over the last decade following its emplacement during the November 1996 jökulhlaup, Site 1 has also exhibited minimal vertical subsidence and only minor lateral slumping and normal faulting (Woodward et al., 2008). The fan apex at Site 5 has displayed negligible vertical lowering since 1945 and only minimal lateral erosion since 1965 (Figure 6.13), demonstrating the ability of major outwash fan apexes to persist for more than six decades.

Consisting of only pebbles, cobbles and boulders and often sub-metre in height, fracture fills have a surprisingly high preservation potential, and were easily identifiable even on the poorer quality 1945, 1965 and 1968 historical images. In addition to persisting for over six decades (Site 5, Section 6.6), this study also demonstrated the importance of considering the evolution of landform assemblages at a decadal scale: at Site 6 (Section

6.7) a chaotic terrain assemblage was initially identified by Klimek (1973) as being ice berg scours and lake-bottom deposits. It was only over several decades, as a result of secondary alteration due to melt out, the features became progressively more defined over later image-steps (1986, 1992 and 2003) and identifiable as an esker and fracture fills. The spatial association of these landforms with an associated wide moraine gap and kettled outwash fan is consistent with the jökulhlaup-related landform assemblages found at the other sites (1, 2, 3 and 4). Temporal control was provided by georeferencing maps of documented jökulhlaups in order to ascertain that this was the result of a flooding event prior to 1934.

## 8.4 Post-depositional modification

### 8.4.1 *Post-depositional modification: diagnostic landform signatures of buried ice, controls on ablation and melting rates*

*(Landsystem model C. 1. Post-depositional modification of landforms by large bodies of buried ice are characterised by normal faulting, hummocky topography and large depression / collapse structures (Boulton, 1972, Eyles, 1979, Fleisher, 1986, Krüger, 1997, Glasser and Hambrey, 2002, Spedding and Evans, 2002, Kjaer et al., 2006, Schomacker et al., 2006); Landsystem process C.2. Even a thin layer (> 0.01 m) of debris covering glacier ice can provide sufficient insulation to retard the ablation process (Lister, 1953, Østrem, 1959, Nakawo and Young, 1981, Nicholson and Benn, 2006); Landsystem process C.3. Melting takes place at two rates (Lister, 1953): primary, in which the main mass first disintegrates into smaller, isolated blocks (primary) creating a 'thermokarst' and secondary, when these isolated blocks ultimately melt completely, often at a much slower rate (Astakhov and Isayeva, 1988, Everest and Bradwell, 2003)).*

Landforms including hummocky topography, normal faulting, kettle holes, and large depressions and collapse structures that have been considered to be diagnostic landforms signatures of post-depositional modification (Boulton, 1972, Eyles, 1979, Krüger, 1997, Spedding and Evans, 2002, Glasser and Hambrey, 2002, Schomacker et al., 2006, Kjaer et al., 2006, Fleisher, 1986) were observed throughout many of the images (Sections 5.2, 5.3 and 5.4; Figure 5.26, Figure 5.27, Figure 6.1, Figure 6.2, Figure 6.4, Figure 6.14) , particularly at Hardaskriða (Section 7.2) , corroborating landsystem model C.1. The role of debris to insulate and retard the ablation process (landsystem process C.2) appeared to be corroborated by measurements of the ice bodies at Hardaskriða from 1945, 1968 and 2007 (Section 7.2, Figures 7.1 and 7.3). These observations are consistent with studies of buried ice observed (or inferred) elsewhere on the sandur (Klimek, 1972,

Bogacki, 1973, Churski, 1973, Jewtuchowicz, 1973, Russell et al., 1999a, Molewski, 2000, Everest and Bradwell, 2003). Utilising the Hardaskriða ice bodies to fully test process C.3., however, is difficult: data in this location was only available from 1968 – 2007 and any melting rates prior to 1945 were not available. Accepting the theory proposed in Section 7.4, that the bodies were emplaced during and subsequently buried by repeated jökulhlaups in 1913 and 1922, the initial rate of melt (primary) immediately following emplacement is not known from the available images or DEMs.

The DEMs that were available do provide information relating to the melting rate of these bodies from 1945-2007, presumably the ‘secondary’ rate. Melting certainly occurred at least two different rates: until 1945, there was no observable subsidence on the aerial photographs, suggesting a very low to negligible rate of melt. This appears to corroborate process C.3, however it is evident that this rate was controlled by more than just the thickness of overlying debris. Following the retreat of the glacier margin that occurred between 1945 and 2007, the subsidence of the terrain above the ice bodies ( $13 \pm 1.64$  m deep, Figure 7.3) suggests an average rate of melt of approximately 19 cm per year.

While the presence of an insulating layer of sediment above the ice bodies played a key role in reducing the rate of ablation as proposed by Østrem (1961) (landsystem model C1) and corroborates observations of other bodies of buried ice around the globe that may have persisted under a few metres of debris for periods ranging from hundreds to thousands of years in temperate to sub-arctic conditions (Østrem, 1961, Clayton, 1964, Boulton, 1972, Eyles, 1979, Driscoll, 1980, Krüger and Kjær, 2000, Spedding and Evans, 2002, Schomacker and Kjær, 2008), at Hardaskriða it is noticeable that on the images, the ice bodies do not exhibit melting until the 1965 photographs, following the retreat of the central lobe of the glacier margin and the subsequent formation of the proglacial trench since 1945. This observation and the sequence of events interpreted in this study to be responsible for the formation of these depressions suggests that the melting rate of the buried ice bodies may have been accelerated as a result of the retreat, and decoupling of the glacier margin and the associated increase in ambient temperatures. This suggests that glacier margin position may serve as a control on post-depositional modification processes C.2 and C.3, as buried ice bodies may be capable of persisting for much longer periods at a stable or advancing margin, rather than at a retreating or stagnating margin.

#### 8.4.2 ***Post-depositional modification: impact on sandur evolution and persistence***

*(Landsystem model C.4. Ice blocks and obstacle marks are indicators of flood and flood magnitude; their position and morphology are diagnostic signatures of different flood*



*phases providing: flow depth, margin position and ice thickness, and the location of major outlets during a single jökulhlaup (Klimek, 1972, Churski, 1973, Galon, 1973a, Galon, 1973b, Klimek, 1973, Boothroyd and Nummedal, 1978, Maizels, 1992, Russell, 1993, Maizels, 1997, Fay, 2002); Hypothesis C.5. Emplacement of debris affects melting rate and controls development of glacio-fluvial systems; process and topography play a key role (Nicholson and Benn, 2006); Hypothesis C.6. It is often difficult, if not impossible, to determine the initial emplacement processes and conditions of landforms following secondary modification (Johnson, 1992a, Schomacker et al., 2006); Hypothesis C.7. High magnitude jökulhlaups may have buried much of the central snout of Skeiðarárjökull insulating the glacier ice, retarding ablation (Galon, 1973a, Thórarinnsson, 1974); Hypothesis C.8. Large volume of material on the central snout of Skeiðarárjökull resulted in differential ablation rates that led to the detachment of the snout and the subsequent development of the proglacial trench (Stokes et al., 2007)).*

The interpretation that the Hardaskriða ice blocks may have been wholly buried during the 1903 jökulhlaup as a result of high rates of sedimentation that persisted through the waning stage of the flood corroborates landsystem model C.4. The interpretation that the continued melting of the Hardaskriða ice bodies nearly a century following their emplacement and burial by high-magnitude jökulhlaups may further demonstrates that jökulhlaups may continue to serve as important controls on sandur evolution on a decadal scale ( $10^1 - 10^2$  years), if not longer.

Observations of the estimated 180 million tons of suspended sediment transported by the November 1996 jökulhlaup and the interpretation that the Hardaskriða ice bodies were emplaced during and later buried by repeated jökulhlaups (Björnsson, 1997, Snorrason et al., 2002) corroborates Hypothesis C.5. The ability to interpret the emplacement mechanisms of the large-scale Hardaskriða ice bodies described in Section 7.4, after nearly a century following their burial may refute, in this instance, Hypothesis C.6 that *It is often difficult, if not impossible, to determine the initial emplacement processes and conditions of landforms following secondary modification*. Similarly, the interpretation of the formation of the Hardaskriða bodies corroborates Hypothesis C.7 that proposes when the glacier margin was coupled to the sandur *High magnitude jökulhlaups may have buried much of the central snout of Skeiðarárjökull insulating the glacier ice, retarding ablation (Galon, 1973a, Thórarinnsson, 1974)*. While it is probable that jökulhlaups emplaced *Large volume of material on the central snout of Skeiðarárjökull that resulted in differential ablation rates that led to the detachment of the snout and the subsequent development of the proglacial trench (Stokes et al., 2007)* (Hypothesis C.8), this may only be inferred from the data available in this study, and does not provide direct evidence of the mechanisms responsible for the detachment of the glacier snout.

## 8.5 Holistic model of sandur evolution

### 8.5.1 *Introduction*

Based upon the landsystem models and hypotheses tested and developed in the sections 8.2, 8.3 and 8.4, this study proposes the development of a holistic model for the evolution of a sandur in which the large-scale processes of glacier margin fluctuations, jökulhlaups and post-depositional modification due to ice melt are all interconnected. This holistic approach requires presenting these three large-scale landscape processes in context with the system as a whole in order to understand the evolution of the sandur over time. For the purposes of this discussion, the term holistic refers to the three large scale processes active at the glacier margin and the proximal proglacial terrain, rather than that of the entire glacier or ice cap. The following sections present an overview of the relationship between these three large-scale processes through observations made at the proglacial region of Skeiðarárjökull over the past 100 years in order to construct a schematic model that is may be employed against similar large-scale landsystems presently active worldwide, and in the past, that may be subject to so some, or all, of the three processes of margin fluctuations, jökulhlaups and post-depositional modification.

### 8.5.2 *Relationship between glacier margin fluctuations and jökulhlaup behaviour*

*(Hypothesis D.1. During high-magnitude jökulhlaups the presence or absence of an proglacial trench may act as a major control on depositional and erosional processes (Gomez et al., 2002) and on sandur sedimentology (Russell and Knudsen, 1999); Hypothesis D.2. The present decoupled state is atypical; majority of sediment were laid down by a coupled, diffuse distributed drainage system (Gomez et al., 2000); Hypothesis D.3. The development of the landscape of Skeiðarársandur is characterised by a combination of sudden, high-magnitude, low-frequency events and diffuse gradual processes (Marren, 2002a, Russell et al., 2006).)*

While the moraine-confined model proposed by Russell and Knudsen (2002) (Figure 2.17) was based upon observations of the November 1996 jökulhlaup (Section 5.2, 5.3, 5.4 and 6.2), the major fan apex emplaced at Section 6.5 and the large ice bodies observed at Section 7.4 corroborates their unconfined model of jökulhlaup deposition and the impact of a proglacial trench as a control on jökulhlaups (Hypotheses B.5 and D.1). Observations of the 1996 jökulhlaup, and the effect of the proglacial trench on jökulhlaup routing and deposits, also led Gomez et al. (2000) to state that a decoupled position of the glacier margin is atypical and that the sandur was instead built through diffuse deposition across the margin (Hypothesis D.2) rather than by a combination of sudden, high-

magnitude, low-frequency events and diffuse gradual processes (Marren, 2002a, Russell et al., 2006) as presented in Hypothesis D.3). However, Section 7.4 also demonstrated that when the glacier margin was coupled to the sandur, repeated jökulhlaups in 1904, 1913 and 1922 were capable of transferring sediment onto the central sandur of comparable volume to those emplaced during the November 1996 jökulhlaup (Site 1).

The ability of the high-magnitude jökulhlaups to transfer large volumes of material on the sandur are also supported by the presence of the large-scale outwash fan apex present at Site 6.5. These observations suggest that regardless of margin position (Hypothesis D.2) even when the glacier margin is coupled to the sandur, repeated high-magnitude jökulhlaups were capable of routing large volumes of sediment onto the sandur, as they have when the glacier was decoupled during the November 1996 jökulhlaup, corroborating Hypothesis D.3.

#### 8.5.3 ***Large-scale processes: impact and persistence***

*(Hypothesis D.4. Impact of flooding on sandur ephemeral, and is quickly removed within a few years (Smith, 2006).)*

A comparison of landform assemblages at Site 1 (Section 7.2) and Hardaskriða (Section 7.4) demonstrate that glacier margin position also plays a role in the evolution of the jökulhlaup landform signatures on a decadal scale. While the Hardaskriða ice bodies may have been emplaced and buried during a period when the glacier margin was coupled to the sandur, following the retreat of the glacier margin these buried bodies of ice melted out to become negative features (depressions) on the sandur (Figure 8.5a and b). However, when the glacier is decoupled from the glacier margin, jökulhlaups may generate landforms such as those observed along the central margin during and following the November 1996 jökulhlaup. The retreat and lowering of the glacier margin resulted in the exposure of eskers, outlets (Section 6.2) and a remnant outwash fan apex (Section 6.6) that became large-scale positive features on the terrain, acting to direct and impound drainage (Figure 8.5 c and d).

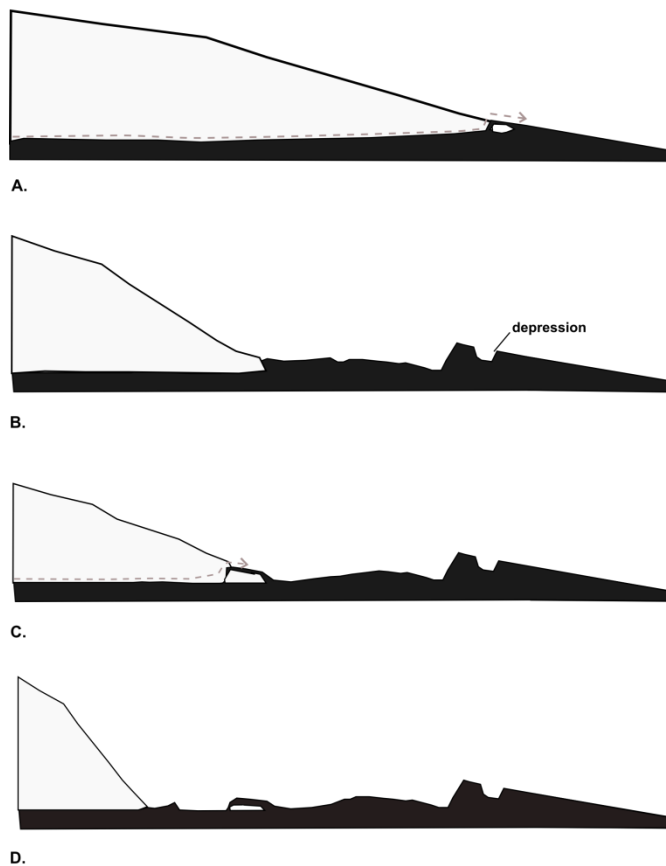


**Figure 8.5 Landforms created by jökulhlaups are dependent upon margin position. A) Glacier margin coupled: jökulhlaups emplace, then buries ice blocks on the sandur, B) Glacier margin retreats and ice blocks melt, creating negative landforms on the sandur, C) Glacier margin decoupled: within proglacial depression, jökulhlaup deposits sediment on ice (en- or supra glacial), D) Glacier margin retreats further: during and following melt out creates positive landform (dashed line = jökulhlaup routing).**

As seen at Site 1 (Section 6.2) and Site 5 (Section 6.6) secondary alteration of these landforms may then occur depending on the volume of material, and emplacement location (sub-, en- or supraglacially). While field observations concur with the observation of Woodward et al. (2008) that the ice-cored Double Embayment landform in Section 6.2 is only a transitional landform, it is evident from this study that even following subsequent secondary modification, jökulhlaup-related eskers and major outlet apexes continue to persist for many decades serving to act as a control on proglacial drainage networks (Section 6.3, 6.6 and Figure 7.4). Continued glacier retreat may result in an increase in ambient temperatures, lowering of the groundwater table and the subsequent gradual melting of bodies of buried ice, altering the proglacial topography and local drainage networks. The development of the Hardaskriða depressions decades following their emplacement (Figure 7.6), the macro-scale jökulhlaup-related landforms described in Chapter 6 at Sites 1-6, and indeed the long-term interrelationship between jökulhlaups and margin position and the sandur as a whole, refutes Hypothesis D.4., that

the impact of flooding on sandur is ephemeral, and quickly removed within a few years (Smith, 2006).

#### 8.5.4 *Large-scale processes: interdependence*

It was observed in this study that within less than six years the glacier margin retreated 1 km (Section 5.3.7, Figure 5.24). This rapid retreat occurred following the November 1996 jökulhlaup, which resulted in the excavation of approximately 180 million tons of suspended sediment from beneath the glacier and its subsequent deposition within proglacial lakes and drainage channels within the proglacial trench during the November 1996 jökulhlaup (Björnsson, 1997, Snorrason et al., 2002). Also within this same brief time period, the surface of the central lobe also lowered markedly across the central region, up to  $84 \pm 3.45$  m (Figure 5.3, Figure 5.25) for the first time in six decades. In response to this dramatic retreat and lowering of the central margin, proglacial drainage and large lakes (> 2 km) developed immediately behind the 1996 flood deposits, at a base level 13 m lower than those observed in 1996. These observations demonstrate that high-magnitude jökulhlaups that occur within short time-spans (hours, days, weeks) are capable of affecting the overall pattern and observed rate of glacier margin retreat within a short-time window (<6 years). Section 8.4.2 described the role that jökulhlaups may have played in the decoupling of the glacier margin, and the transfer of sediment from within and beneath the glacier onto the proglacial terrain via the November 1996 jökulhlaup that provided the accommodation space for development of proglacial lakes and drainage, further supports that Hypothesis A.4 be modified to include jökulhlaups as a large-scale process that may also affect the pattern of glacier margin retreat.

In turn, these proglacial lakes may affect later jökulhlaup behaviour, as the presence of proglacial lakes have demonstrated the ability to increase the variability of geomorphic response and sedimentary signature of later glacier outburst floods over distances as little as a few hundred metres (Russell et al., 2007) and increasing their erosive capacity (Russell et al., 1999b). Several of the proglacial lakes developed within depressions that appeared to be generated as a result of jökulhlaups, and surge related processes, requiring an expansion of existing models of proglacial lake development (Thorarinsson, 1939, Jonsson, 1955, Howarth and Price, 1969, Boulton, 1967). This suggests the formation of a new hypothesis that *In overdeepened basins, margin fluctuations and proglacial drainage may be affected as a result of the transfer large volumes of sediment from within the overdeepening to the proglacial terrain*. In addition to accelerating the rate of retreat of the glacier margin and encouraging the confining proglacial drainage along the glacier

margin, the large volume of sediment may serve to insulate large portions of the glacier snout, affecting the pattern of margin retreat and the long-term development ( $10^2$  - $10^3$  years) of the sandur.

#### 8.5.5 *Holistic model of the sandur evolution*

##### 1.1.3 *Holistic model*

Based on the models and hypotheses tested in this study that addressed themes A, B and C presented in Chapter 1, diagnostic landforms associated with the large-scale processes of glacier margin fluctuations, jökulhlaups and post-depositional modifications and their relationships were compiled (Figure 8.6). A holistic landsystem model was then developed in an attempt to encompass all of the landform assemblages associated with large-scale margin fluctuations, jökulhlaups and post-depositional modification and to schematically represent describe their relationship to each other over time (Figure 8.7). While this model does not describe every possible combination of landform assemblage or interaction, it does attempt to depict many of the more common landforms and interactions that were observed in this study.



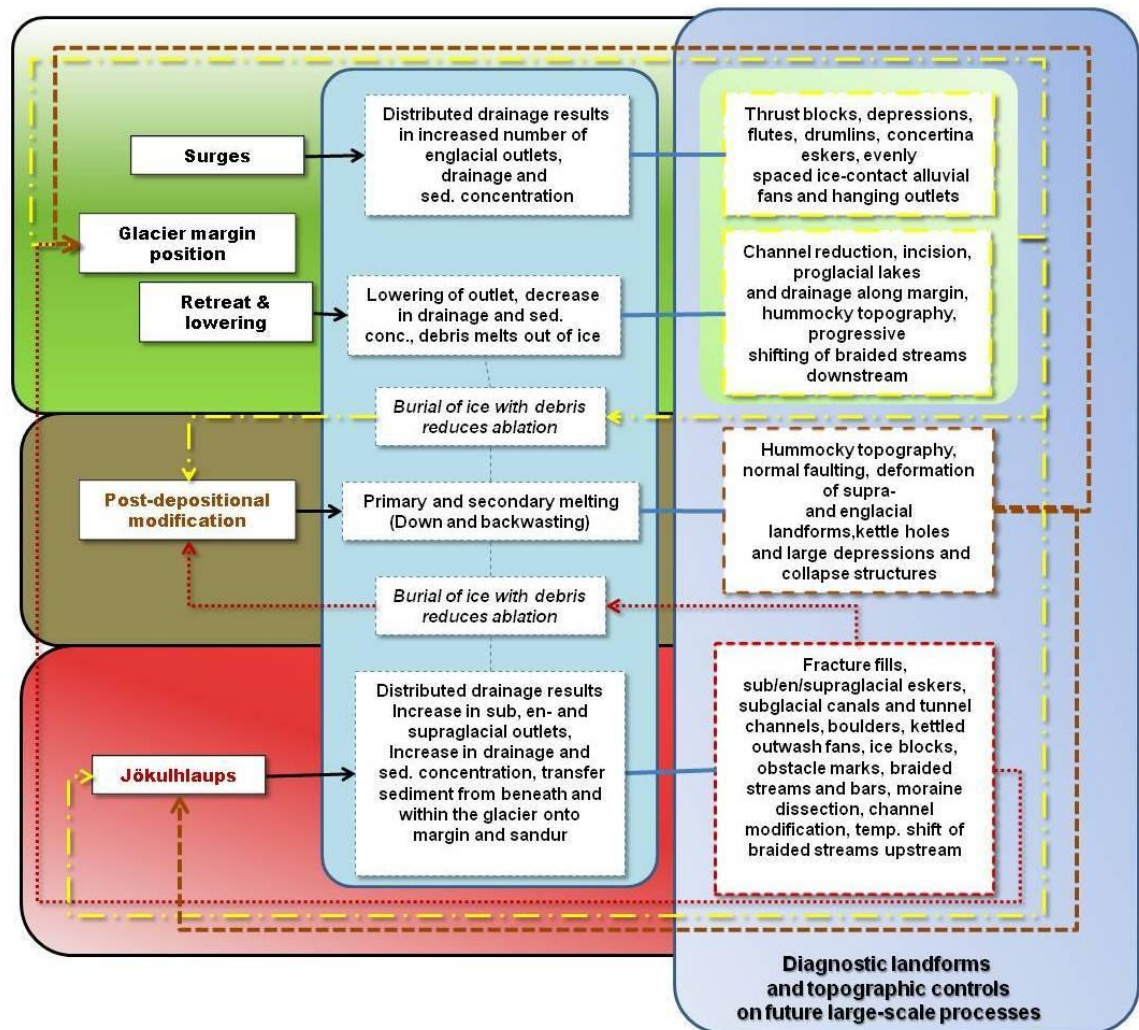


Figure 8.6 Large-scale processes and resulting landforms and landform assemblages observed at Skeiðarárjökull.

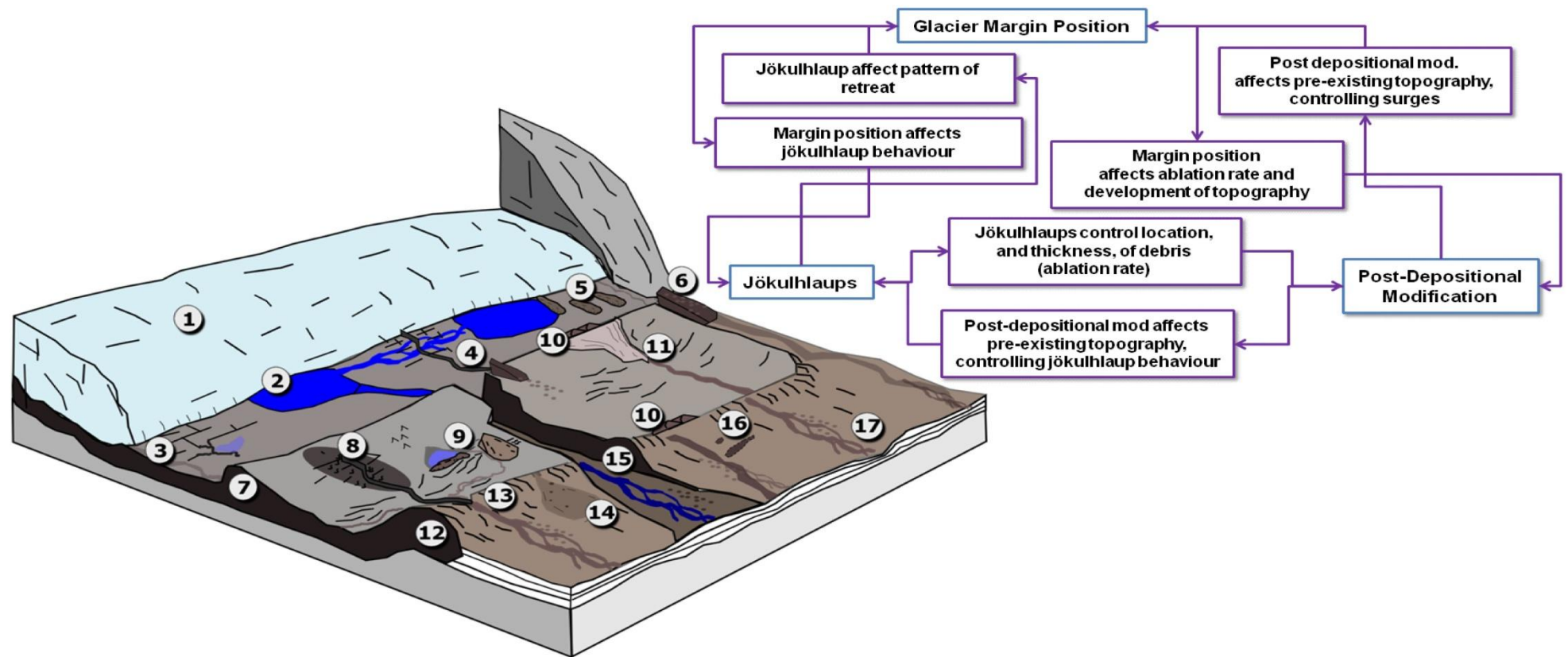


Figure 8.7 Schematic diagram depicting the interdependence of large-scale processes and proglacial landsystem model. Numbered landforms are: 1) glacier; 2) proglacial lake; 3) jökulhlaup landform fracture fills, eskers and small proglacial lakes; 4) recent jökulhlaup landform assemblage comprised of fracture fills, sinuous esker, and outwash fan apex and associated fan with kettles and obstacle marks; 5) drumlinised eskers associated with former jökulhlaup; 6) apex of jökulhlaup outwash fan and former abandoned lateral drainage channel; 7) thickly-bedded jökulhlaup deposits; 8) drumlinised surge fan with jökulhlaup landform assemblage comprised of fracture fills, disturbed terrain, sinuous esker, and outwash fan apex and associated fan with kettles and obstacle marks; 9) surge-related outwash fan, thrust block and depression with minor proglacial lake; 10 (two instances) jökulhlaup-associated drumlinised eskers; 11) jökulhlaup tunnel channel and former proglacial lake basin; 12) proglacial trench; 13) moraine gap and jökulhlaup-related kettled outwash fan; 14) surge-related fan and hanging outlet; 15) jökulhlaup-modified incised channel that is the dominant channel on the sandur; 16) proglacial depressions associated with ice blocks buried by jökulhlaup; 17) abandoned moraine gap and braided stream channels.



## Chapter 9 Conclusions

---

*This chapter presents the conclusions derived from the discussion of the results of this thesis. The controlling factors on the large-scale processes such as margin fluctuations, jökulhlaups and post-depositional modification on sandur evolution on a decadal scale are presented, as well as wider implications and potential areas for future research.*

---

### 9.1 Introduction

The overall aim of this project was to evaluate existing models of large-scale processes such as ice margin fluctuations, jökulhlaups and post depositional modification on proglacial landscape development that were previously only derived from relatively short-duration field campaigns and observation windows, as well as those derived from interpretations of sediment and landform records of formerly glaciated areas. By testing literature-based models of the major controls on sandur evolution and characterising the emplacement, and subsequent evolution, of proglacial landforms of temperate glaciers over decadal time frames, a holistic landsystem model was developed in an attempt to encompass all of the landform assemblages associated with large-scale margin fluctuations, jökulhlaups and post-depositional modification and to schematically represent describe their relationship to each other over time (Figure 8.6 and 8.7). While this model may be employed to interpret landforms and processes found at other locales, it cannot encompass all landform derivations. Instead it is intended to be used as a holistic model for the ways in which large-scale processes may interact with each other at similar sites, and provide examples of the resulting landforms assemblages.

## 9.2 Holistic model of large-scale processes and long-term sandur evolution

Prior to this study, little research had been conducted on the interactions and long-term impact of large-scale processes acting on proglacial landsystems. By combining observations taken from aerial photographs and derived DEMs with observations made in the field, models and hypotheses in the literature regarding large-scale processes and landform development could be tested. While numerous individual processes and landforms were examined in this study, a conclusion pivotal for the examination of proglacial landforms and the development of a holistic model based upon the understanding that long-term impact of large-scale processes associated with margin fluctuations, jökulhlaups and post-depositional modification on the evolution of the sandur are interconnected. Conclusions derived from this holistic approach are presented below.

Models of landforms diagnostic of large-scale processes including glacier margin fluctuations, jökulhlaups and post-depositional modification were tested by identifying key landform assemblages on historical photographs and DEMs that could be genetically linked to the processes responsible for their formation. The occurrence of surges was identified on historical imagery based on existing landform models that included near-vertical glacier margins, kettled alluvial fans, and drainage outlets spaced across the margin front, thrust blocks, depressions, drumlinised and fluted ground exposed following glacier margin retreat. A possible previously undocumented surge was identified based upon observations made on the 1965 images and 1986 images (Sections 5.3.3 and 5.3.4). The occurrence of jökulhlaups were identified on historical images based on landform assemblages of fracture fills, eskers, and kettled outwash fans (Sections 5.2, - 5.4; 6.3 – 6.7). Post depositional modification was identified on images based on landforms including normal faulting, hummocky terrain and collapse structures (Section 6.4 and 7.4). The observations of the emplacement and/or subsequent modification of these landforms, and of landform assemblages, in relation to margin position and post depositional modification were used to create the landform model in shown in Figure 8.7.

The ability to identify landforms and landform assemblages diagnostic of surges, jökulhlaups and meltout that have been described in this study was dependent upon the location of their emplacement on the sandur, as well as their alteration or deformation by subsequent glacier margin fluctuations, floods or post-depositional modification. For

example, following the November 1996 jökulhlaup, numerous pre-existing jökulhlaup and surge-related features, such as alluvial fans and eskers, were eroded or buried, demonstrating that their potential as identifiable diagnostic signatures on historical aerial photographs may be limited when emplaced within a confined, proglacial depression that is subject to such repeated, large-scale events. Similarly, ice-cored and ice-contact features, such as eskers or alluvial fans emplaced en- or supraglacially may be subject to post-depositional modification due to ice melt, making them difficult to identify.

Combining events documented in the literature with observations of gradual meltout captured on historical aerial photographs and derived DEMs provided an understanding of the holistic relationship between glacier margin fluctuations, jökulhlaups and post-depositional modification (Figure 8.7). In this holistic landsystem model, when coupled to the glacier margin the sandur is characterised by numerous, evenly-spaced braided streams that drain directly from the glacier and pass through gaps in the moraine onto the sandur (Figure 8.7: 17). Glacier surges may also emplace boulders, ice blocks and outwash fans through the moraine gaps (Figure 8.7: 14). Jökulhlaups may also be routed through moraine gaps across the margin, emplacing thickly-bedded outwash fans characterised by boulders, ice blocks, kettle holes and obstacle marks (Figure 8.7: 13). The location and thickness of deposits associated with jökulhlaups and surges may also affect the location and rate of later post-depositional modification due to large-scale meltout. In the event of repeated, high-magnitude volcanogenic jökulhlaups, the central margin of the glacier may become inundated with thick layers of debris, insulating portions of the snout as well as burying large ice blocks emplaced by previous floods (Figure 8.7: 16). In some instances, following the retreat of the glacier margin, debris emplaced en- or supraglacially by high-magnitude jökulhlaups may result in differential ablation rates, effectively decoupling the central glacier margin from the sandur and forming a proglacial trench.

As the glacier margin retreats, drainage outlets along the margin lower in elevation, and the drainage channels that flow through the moraine gaps decrease in number. While the retreat of the margin may be gradual, drainage capture by remaining channels occurs within relatively short time periods (days/weeks/months) (Figure 8.1). The remaining active channels become incised as the drainage outlets lower and braided streams progressively develop further away from the glacier margin. Depending on the trigger mechanism, source and magnitude, jökulhlaups that occur while the margin is retreating may be routed through lateral outlets and channels and through one, or a few, of the

remaining active channels that pass through the moraine and out onto the central sandur (Figure 8.7: 15). Jökulhlaups may alter channel geometry and the resulting widening and incising of the channels ‘harden’ them, permitting them to remain coupled to the glacier margin during subsequent margin retreat.

The retreat of the glacier margin from the central sandur, and the corresponding increase in ambient temperature, may permit the gradual melting out of ice bodies previously buried by jökulhlaup sediments on the sandur resulting in large depressions (Figure 8.7: 16). Within the proglacial trench, the retreat of the margin may provide accommodation space for the development of large proglacial lakes and drainage parallel to the glacier margin (Figure 8.7: 2) and expose features emplaced by large-scale processes when the glacier margin was coupled to the sandur. For instance, margin retreat within the trench may expose sub-, en-, and supraglacial features such as eskers (former conduits) of jökulhlaups that were routed onto the central sandur (Figure 8.7: 10).

Landforms exposed by retreat, both within the trench and along the glacier margin, may still be subject to large-scale erosional and depositional processes such as margin fluctuations and both high- and low-magnitude jökulhlaups. Surges, for instance, may result in the deposition of outwash fans, thrust blocks, boulders and ice blocks within the proglacial trench and lakes. Following the surge, the retreat of the glacier margin may expose eskers, crevasse casts, thrust blocks, drumlinised terrain and depressions that may serve to impound and direct proglacial drainage and lakes (Figure 8.7: 5, 8, 9). Surges, therefore, provide controls on the pattern of retreat and these landforms serve as controls for other subsequent surges and jökulhlaups.

Similarly, jökulhlaups that occur during the retreat of the glacier margin may emplace fracture fills, eskers, outwash fans, kettle holes and boulders and ice blocks that may meltout resulting in hummocky terrain (Figure 8.7: 3, 4, 6, 8, 13, 15). All of these features may serve to impound or direct proglacial drainage and control the development of proglacial lakes (Figure 8.7: 2,3). As seen in this study, the presence of proglacial lakes may serve to impound flood waters and increase the erosive capacity of floodwaters, and cause the incision and widening of major outlet channels. Pre-existing topography serves as a control that may result in a wide variety of landforms during a single event, producing numerous types of supra- and englacial outlets, tunnel channel complexes (Figure 8.7: 11) and large-scale eskers generated within ice-walled conduits (Figure 8.7: 4). Additionally, the transfer of large volumes of material during high-magnitude



jökulhlaups through supra-, en- and subglacial conduits from beneath the glacier up into the proglacial trench (Figure 8.7: 7, 10, 12). This transfer of subglacial sediment and debris to the proglacial terrain, lowers the surface of the glacier margin and provides the accommodation space for proglacial drainage along the margin and proglacial lakes to develop behind the deposits, but at a lower elevation (Figure 8.7: 7), and on a reverse slope may even appear to accelerate the rate of glacier retreat.

This study suggests that classic models of drainage development at retreating margins such as those proposed by Klimek (1973), Boothroyd and Nummendal (1978), Bristow and Best (1993) and Marren (2002b) may be overly simplistic. These models do not take into account the interdependence of margin fluctuations within overdeepened basins in context with repeated, high-magnitude jökulhlaups on channel modification and braided stream positions. For example, jökulhlaups may temporarily (months/years) shift braided streams closer to the glacier margin demonstrating that jökulhlaups may exert a direct control on the nature of proglacial aggradation or incision regardless of margin position (Figure 8.1; Figure 8.3).

Incision and channel modification as a result of high-magnitude jökulhlaups may also affect the rate of major drainage shifts and in selection of the ‘surviving’ channels, as demonstrated by the role that repeated jökulhlaups played on widening and incising the now dominant Gígjukvísl channel (Section 5.3.3; Figure 8.3). Additionally, the transfer of sub-, en- and supraglacial debris during jökulhlaups may exert a direct control on the pattern of glacier margin retreat by providing accommodation space for the development of proglacial drainage and lakes and retarding the ablation rate of large bodies of buried ice.

Over last 100 years, the evolution of Skeiðarárjökull has been marked by decades of relative stability followed by periods of rapid change (days, weeks, months, years) as observed by the channel capture of the eastern Skeiðará by the western Skeiðará, and the Gígjukvísl, as well as following the 1954 and 1996 jökulhlaups. While this study corroborates observations that alternating high-frequency, high-magnitude flooding events with high-frequency, low-magnitude regimes have played a dominant role in the evolution of the sandur (Marren, 2002a, Marren, 2005, Russell et al., 2006), it was also observed that in addition to magnitude, glacier margin position played a key role in the impact of jökulhlaups on topography.

High-magnitude jökulhlaups occurred six times over the 20<sup>th</sup> century, however their impact on the sandur varied with respect to the position of the glacier margin (Section 8.2). As fluctuations of the glacier margin may occur in relatively short time spans (months/years) and these may dramatically affect the routing behaviour of jökulhlaups, this suggests that examining the magnitude and frequency of jökulhlaups alone is not sufficient to understand the evolution of the sandur. At Skeiðarárjökull, by examining the magnitude and frequency of both large-scale processes of jökulhlaups and margin fluctuations, and combining those observations with the decadal impact of post-depositional modification, a holistic understanding of sandur evolution was derived (Figure 8.5).

The holistic model developed at Skeiðarárjökull may be applied to other warm-based, sediment-rich glaciers that may be subject to some or all of the large-scale processes observed at this site including margin fluctuations, jökulhlaup and secondary modification. The development of the jökulhlaup-related landform signatures identified at this site, and the ability to identify them at other locales, requires such sites to contain similar conditions, as the jökulhlaup-related landforms emplaced in this study area required the input of significant volumes of sediment and water. This, of course, does not preclude scenarios that lack the volcanogenic high-magnitude jökulhlaups at Skeiðarárjökull, as there are other mechanisms that can generate material and meltwater in similar magnitude. These models may provide a useful analogue for interpreting landforms and strata emplaced by margin fluctuations, jökulhlaups and meltout generated by the retreating continental Pleistocene ice sheets.

### 9.3 Implications

One of the most important implications of this study is the ability to provide controls on the spatial and temporal breadth with which past and future models of glacier processes should be evaluated. This study has provided the opportunity to:

- Test current diagnostic landform signatures of surges (and has potentially identified a previously undocumented minor surge).
- Test and expand current models of landform assemblages associated with jökulhlaups by identifying numerous combinations of landform types and assemblages observed on historical images across the sandur. In addition to identifying previously undocumented jökulhlaups, this also provided the

opportunity to monitor their evolution on a decadal scale, providing a more robust model for landform identification

- Relate landforms to processes over a period of  $10^2$  years as demonstrated by the ability to determine flow conditions of jökulhlaups during the early 20<sup>th</sup> century by examining large-scale post-depositional modification features on the sandur nearly 100 years later.
- Understand how large-scale jökulhlaups may affect the pattern of margin retreat, and understand the role that jökulhlaups may play in acting to decouple the glacier margin.
- Understand how margin retreat may affect the role of jökulhlaup magnitude and routing.
- Refute assumptions regarding the ephemeral (1-10 years) impact of high-magnitude jökulhlaups on sandur evolution.
- Understand the role of jökulhlaups on sandur topography and sedimentary architecture during both coupled and decoupled states.
- Document three periods of short time frames (days/weeks/months) that resulted in large-scale drainage shifts.
- Provide temporal controls on the persistence of large-scale, diagnostic landform signatures and demonstrate the importance of post-depositional modification, and margin position, over decadal time-frames to assess them.

Understanding the rate and pattern of large-scale drainage patterns shift in response to glacier margin retreat, surges and high-magnitude jökulhlaups may provide important implications for the infrastructure of Iceland. The ‘hardening’ of the Gígjukvísl following the 1996 event and subsequent channel modification following its capture of the other major drainage channels suggests that the Gígjukvísl bridge may require fundamental adjustments in order to handle the increased drainage influx and routing during future jökulhlaups of a magnitude similar to the November 1996 jökulhlaup. Other infrastructure, such as communication lines proximal to the Gígjukvísl channel should also be hardened, or relocated, in anticipation of such events.

#### **9.4 Future work**

While the three-dimensional models created from historical vertical aerial photographs have provided valuable insights to large-scale processes active at this field area, new

techniques may provide higher resolution detail on the evolution of landforms. LiDAR studies or terrestrial laser scanner have been employed recently at the site to monitor channel alterations following low-magnitude jökulhlaups and to model the melting of ice-cored landforms. Repeated surveys of these regions and other portions of the sandur over the next ten years could provide a high-resolution, three-dimensional baseline that could aid in quantifying the effects of future surges and jökulhlaups.

Obtaining more images that encompass a wider portion of the glacier could be combined with radio echo soundings obtained by Björnsson (1999) (Figure 3.1) and recent bathymetry studies of the proglacial lakes to accurately reconstruct fluctuations of the glacier within the over-deepened basin and the subsequent impact on the sandur. With this data, and the proper software, it would be possible to accurately model changes in the thickness of the glacier ice and margin position, changes in hydrostatic pressure, and the corresponding changes to the routing behaviour of jökulhlaups and their capacity to excavate and transport sediment as proposed by Roberts et al (2000, 2001, 2002).

Where possible, landforms identified on the historical aerial photographs that still persist should be mapped in detail through ground surveys and sedimentological examinations. In particular, the landform presented in Site 2 (Section 6.3), needs further ground investigations to determine if the disturbed strata were emplaced during the 1991 surge event, and the subsequent impact on jökulhlaup routing. Acquiring additional aerial photographs on the extreme south, east and west portions of the field area would provide more accurate and detailed models of the Gígjukvísl, Súla and Skeiðará channels and could be used to model hypothetical changes in discharge at the sub-decimetre level to aid in flood planning and mitigation. The evolution of existing landforms and drainage systems on Skeiðarársandur should continue to be monitored both in the field and through aerial photography (or LiDAR) in order to make a robust model for the evolution of ice-cored features, and to document the impact of future fluctuations and floods. Further retreat of Skeiðarárjökull's margin may expose further landforms that could provide a greater insight of the behaviour of the Grænalón drainage system in the western region, the development of sub- and englacial features in the central region, and the subglacial routing of flooding from Grímsvötn.

Additionally, little work has been done to monitor the fluctuations of the groundwater levels within the depression and on the elevated sandur. This research could be used to explore the relationship between the rate of melt of buried ice bodies and ground water

level fluctuations that may have been a factor in the development of the Hardaskrída depressions, as well as affecting the future development of other ice-cored terrain in the region. Similarly, the amount of debris within the buried ice bodies at Hardaskrída was unknown, making it difficult to accurately model the rate of melt. While it is known that the reverse slope of the overdeepened basin near the snout is sufficient during ice-melt dominated conditions and jökulhlaups to generate supercooling and entrain large amounts of debris within the ice (Hooke and Pohjola, 1994, Alley et al., 1998, Lawson et al., 1998, Evenson et al., 1999, Tweed et al., 2005), further research on the impact of this debris on meltout processes and rates could provide for more accurate reconstruction of the impact of post-depositional modification on the sandur.

The models and hypotheses presented in this study should also be tested against other temperate glaciers that are subject to similar large-scale processes. Glaciers across Iceland exhibit a wide variety of landforms and behaviour, while often emerging from the same ice cap; it would be beneficial to test the landform models and hypotheses derived from this study at these other locales in the region to determine their validity and to gain greater insight into this diversity of behaviour. This testing may involve returning to, and reinterpreting, other landforms across Iceland today, as well as delving into the Landmælingar historical photograph archive to find evidence of pertinent landform assemblages in the past.

The models and hypotheses tested in this study may also be employed to understand landform assemblages emplaced at temperate glaciers around the world and used as contemporary landscape analogues for the southern margins of Pleistocene mid-latitude ice sheets. The understanding of the interdependence of jökulhlaups and margin fluctuations could be used to revise existing glacial landsystem models such as those of Koteff and Pessel (1981), Clayton and Moran (1974), Boulton and Eyles, (1979), Eyles, (1983), and Gustavason and Boothroyd (1987). These models may not only be revised to include a greater variety of landform assemblages, but apply temporal constraints to the impact of processes and incorporate broader mechanisms for detachment mechanisms that may have played a role in the holistic evolution the processes responsible for the palimpsest of the resulting Pleistocene terrain.

## **9.5 Wider Implications**

The relationships between large-scale processes and their resulting landforms and their evolution over decadal time period that were presented in this study have provided an

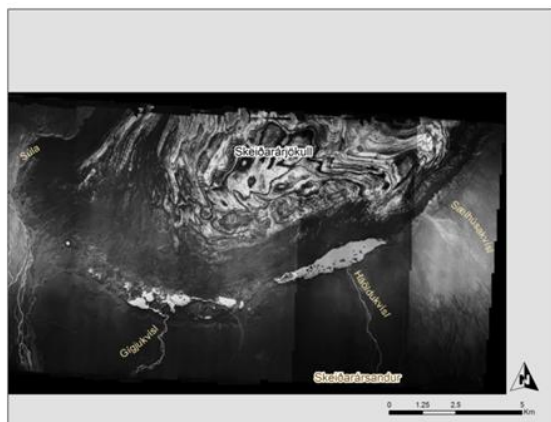
understanding of how to examine similar landforms in other locations. This includes other locales with similar climatic and structural regimes over the past century, as well as across Europe, Asia and North America during retreat of the Pleistocene ice sheets. This is particularly important when reconstructing glacier behaviour via Pleistocene landform assemblages. Such assemblages and sediment sequences have been created due to repeated occurrences of these three large-scale processes examined in this study, resulting in a palimpsests (overprinted) landsystems.

While understanding the behaviour of future flooding, margin fluctuations and meltout may affect drainage at Skeiðarárjökull is beneficial to the Icelandic Roads Authority for both engineering and safety reasons, these processes are not unique to Iceland. The present warming trend has lead to an increase in meltwater production worldwide, accelerating the retreat of many alpine glaciers that are also subject to outburst floods and meltout. Gaining insight into the relationships between fluctuations in ice thickness/extent, controls exerted by topography and substrate and climate, as well as identifying previous events in respective field areas, will facilitate mitigation efforts in all regions that are proximal to, or receive drainage from, temperate glacier systems.

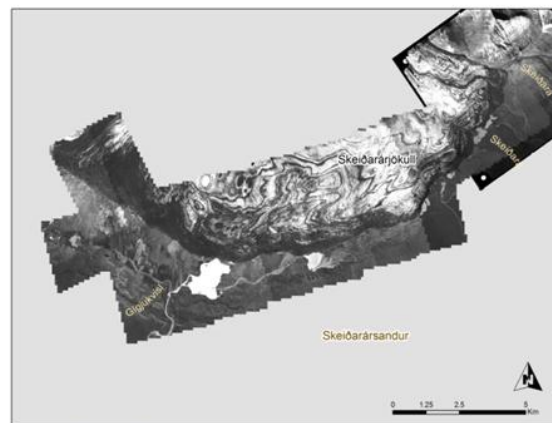
The ability to accurately model large-scale processes that may affect sandur evolution provides an insight into not only the evolution of the surficial topography but also may also provide valuable insight into the subsurface sedimentary architecture useful for exploiting mineral and oil deposits. Outburst floods generated during the retreat of these large ice sheets during the Pleistocene, for example, may have emplaced numerous sub-, en- and supraglacial features: the Geological Society of Canada has already expressed an interest in mapping thousands of eskers and possible fracture-filled features found across the Canadian shield, as understanding the routing of these sub- and englacial drainage networks may have value for mineralogical exploration.



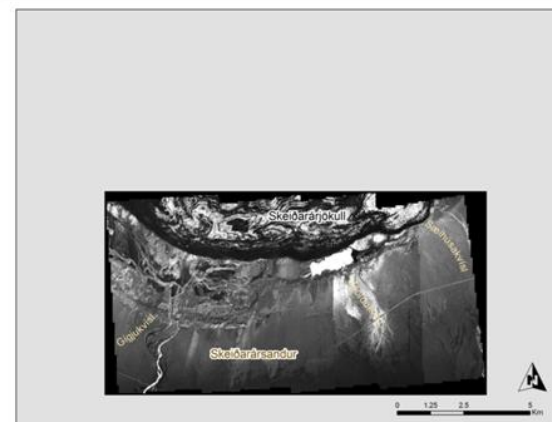
## Appendix A. Photomosaics



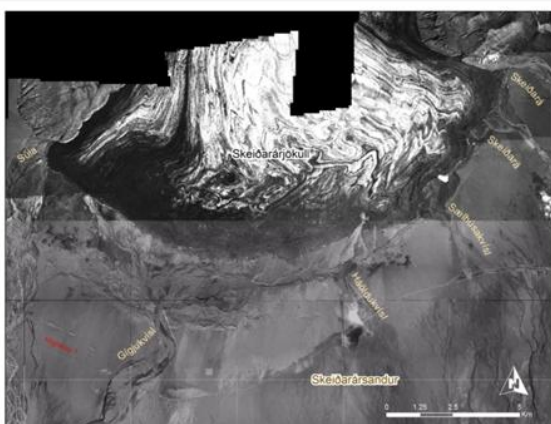
A. 1945



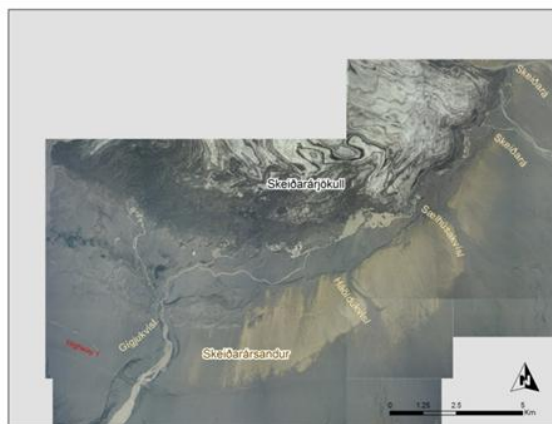
B. 1965



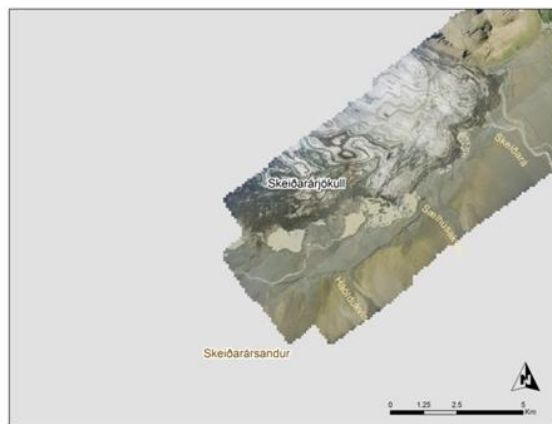
C. 1992



D. 1997

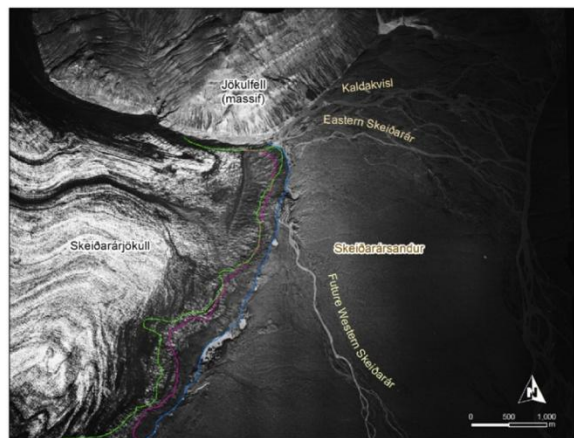


E. 2003

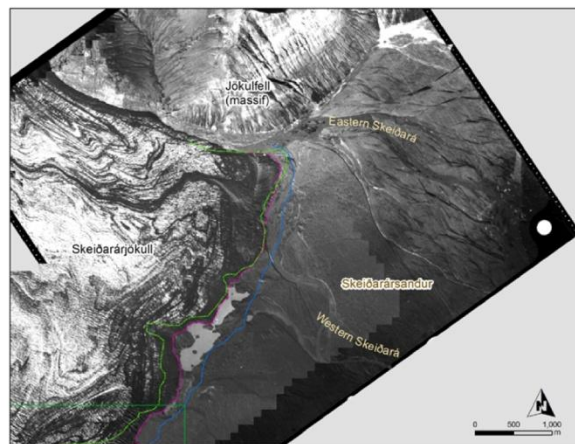


F. 2007

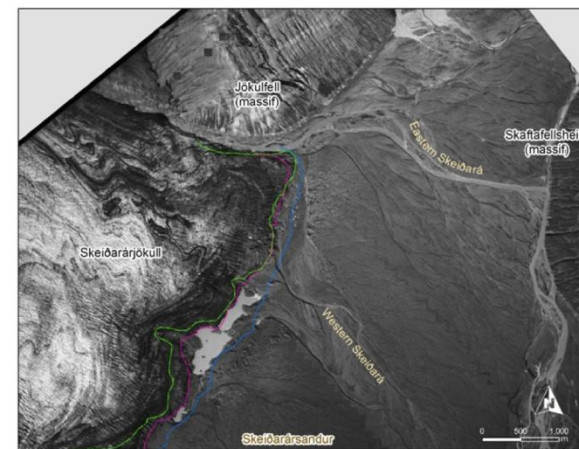
**Plate I.** Overview of available images that depict the retreat of Skeiðarárjökull's margin over the past sixty years. A-E are courtesy of Vegagerðin (Icelandic Roads Authority). Not represented are partial coverages from 1968, 1972, 1975, 1979 and 1986.



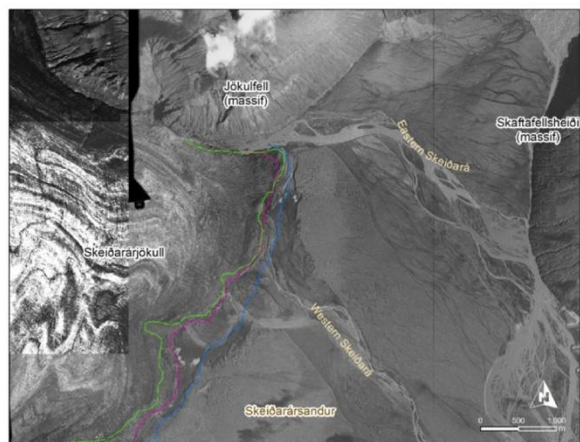
A. 1945



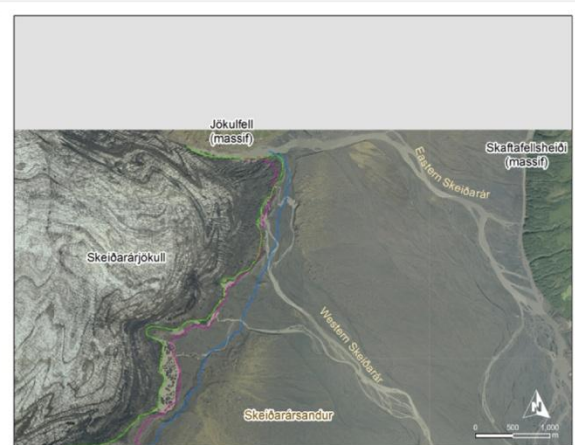
B. 1965



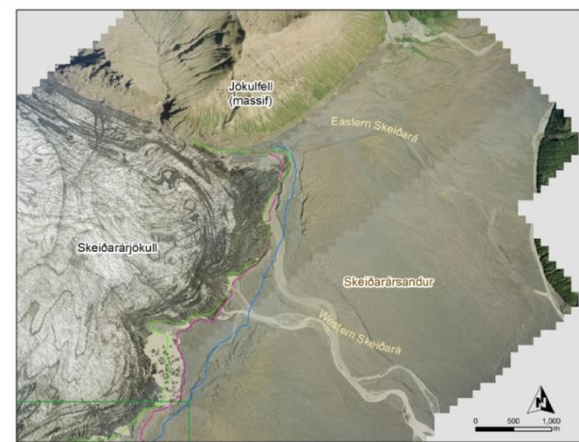
C. 1975



D. 1997



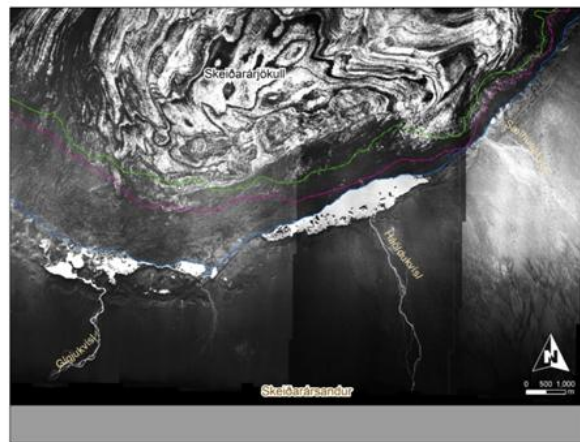
E. 2003



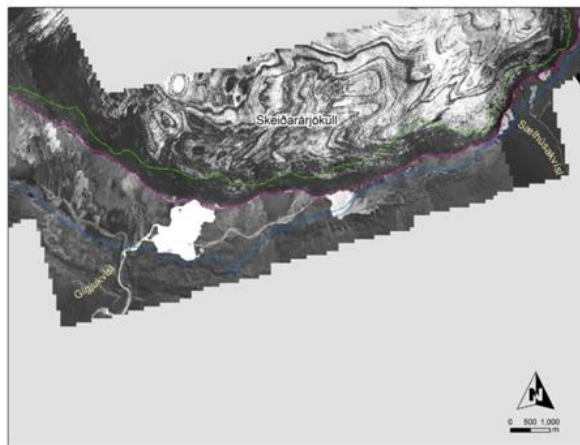
F. 2007

**Plate II. Overview of changes in the eastern margin of Skeiðarárjökull. A-E are courtesy of Vegagerðin (Icelandic Roads Authority). Not represented are partial coverages from 1968, 1972, 1979, 1986 and 1992.**

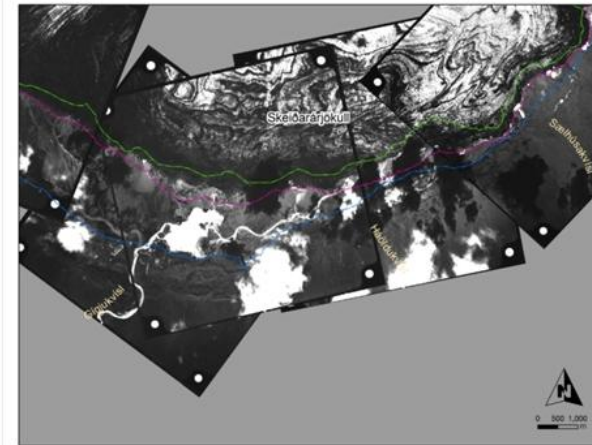




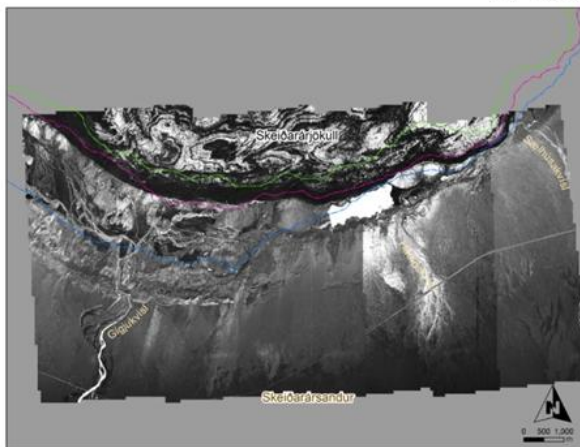
A. 1945



B. 1965



C. 1972



D. 1992

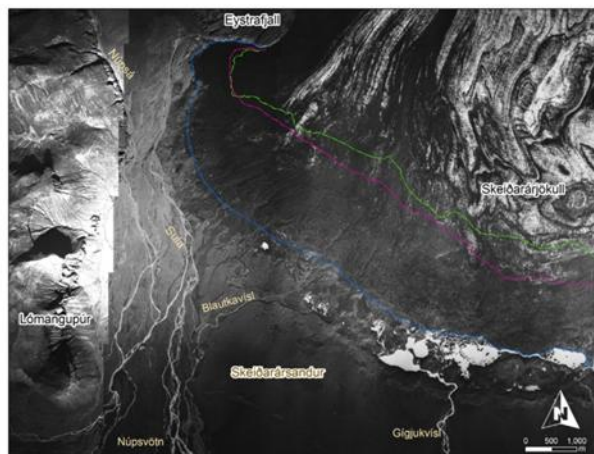


E. 2003

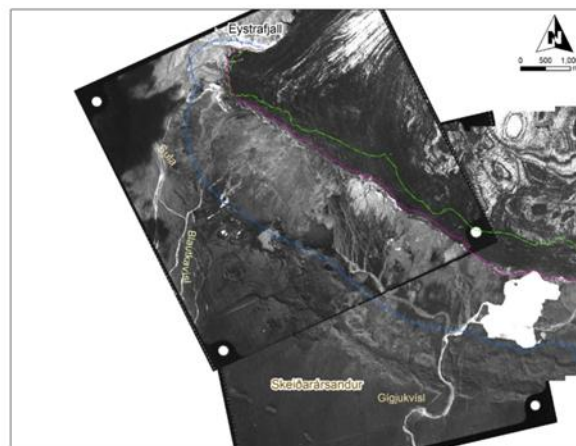


F. 2003

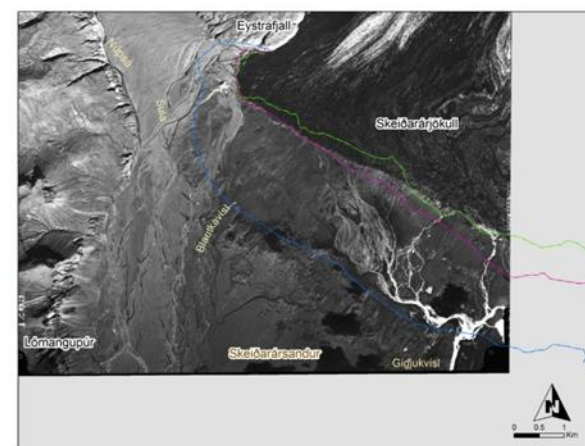
Plate III. Overview of changes in the central margin of Skeiðarárjökull. A-E are courtesy of Vegagerðin (Icelandic Roads Authority). Not represented are partial coverages from 1968, 1979, 1986 and 1997.



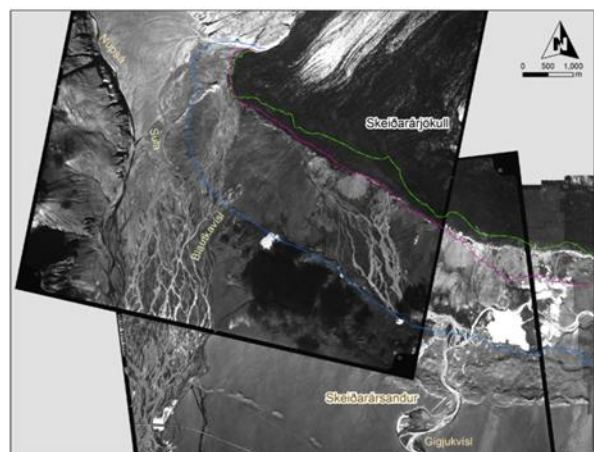
A. 1945



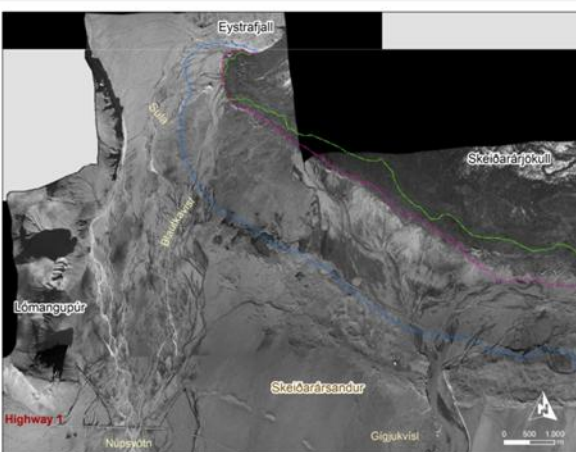
B. 1965



C. 1979



D. 1986



E. 1997



F. 2003

Plate IV. Overview of changes in the western margin of Skeiðarárjökull. A-E are courtesy of Vegagerðin (Icelandic Roads Authority). Not represented are partial coverages from 1968, 1972, 1975 and 1992.

## **Appendix B. Data quality: check points vs. DTM**

### **1945 COMPARISON OF CHECK POINT FILE TO DTM FILE**

Point# Point ID Z Diff

1	AUG2033	-136.1769
2	AUG2924	-128.6419
3	APR1909	2.9513
4	APR2126	-0.3065
5	APR2180	0.8730
6	APR3446	-177.0914
7	AUG5137	-157.3345
8	AUG5278	5.9248
9	APR1505	9.6633
10	AUG0219	4.4210
11	AUG0567	16.1779
12	AUG0350	15.5039
13	AUG5190	3.7000

Number of Points= 13

ave Z diff = -41.5643, rms = 84.0704, std = 76.0609 (Note : Z diff = ground points – dtm)



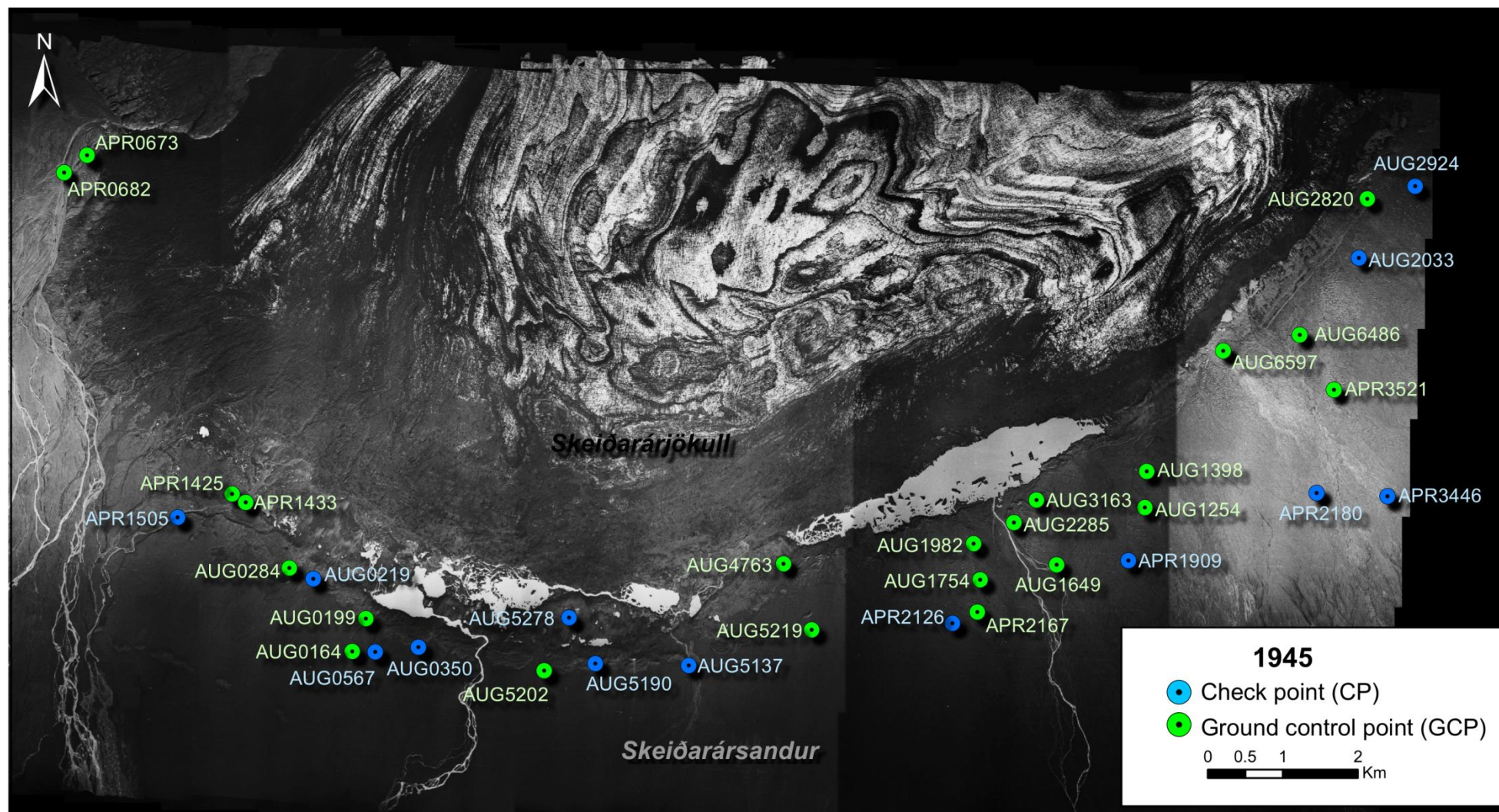


Figure B.1 1945 Ground control points and check points.



## 1965 COMPARISON OF CHECK POINT FILE TO DTM FILE

Point# Point ID Z Diff

2	AUG1982	1.2866
3	AUG3163	4.9820
4	AUG5936	-0.1646
5	AUG6486	-8.3907
6	AUG6597	-4.1935
7	AUG5269	2.1043
8	AUG5277	0.0208
9	AUG5148	0.0792
10	AUG4875	3.4289
11	AUG1989	-0.8482
12	AUG0526	-0.7233
13	APR1589	3.3464

Number of Points= 12

ave Z diff = 0.0773, rms = 3.4536, std = 3.6062

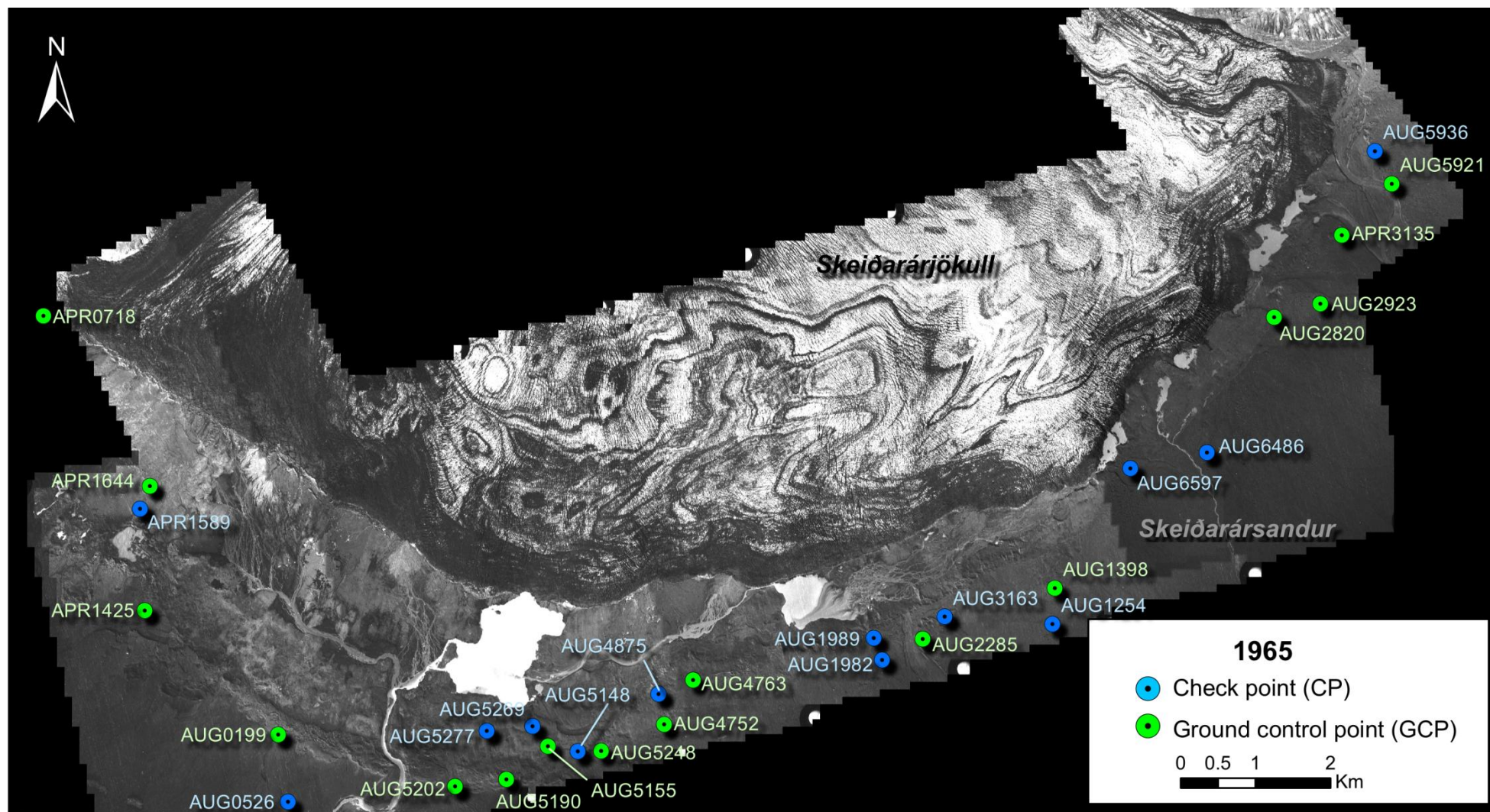


Figure B.2 1965 Ground control points and check points.

## 1968 COMPARISON OF CHECK POINT FILE TO DTM FILE

Point# Point ID Z Diff

2	AUG1982	1.3457
3	AUG2031	2.5741
4	AUG2818	2.7367
5	AUG3163	3.1816
6	AUG6002	4.2584
8	APR2167	-0.9971
9	APR2193	-0.1186
10	APR3137	1.7232
11	APR3185	6.8417
12	APR3228	0.8149
13	AUG5137	1.7518
14	AUG5155	0.6160
15	AUG0164	3.2526
17	AUG4757	-0.0808
18	AUG0348	2.5873
19	APR0746	1.2726
20	APR1505	1.1914
21	APR1458	-0.2101

Number of Points= 18

ave Z diff = 1.8190, rms = 2.5760, std = 1.8769

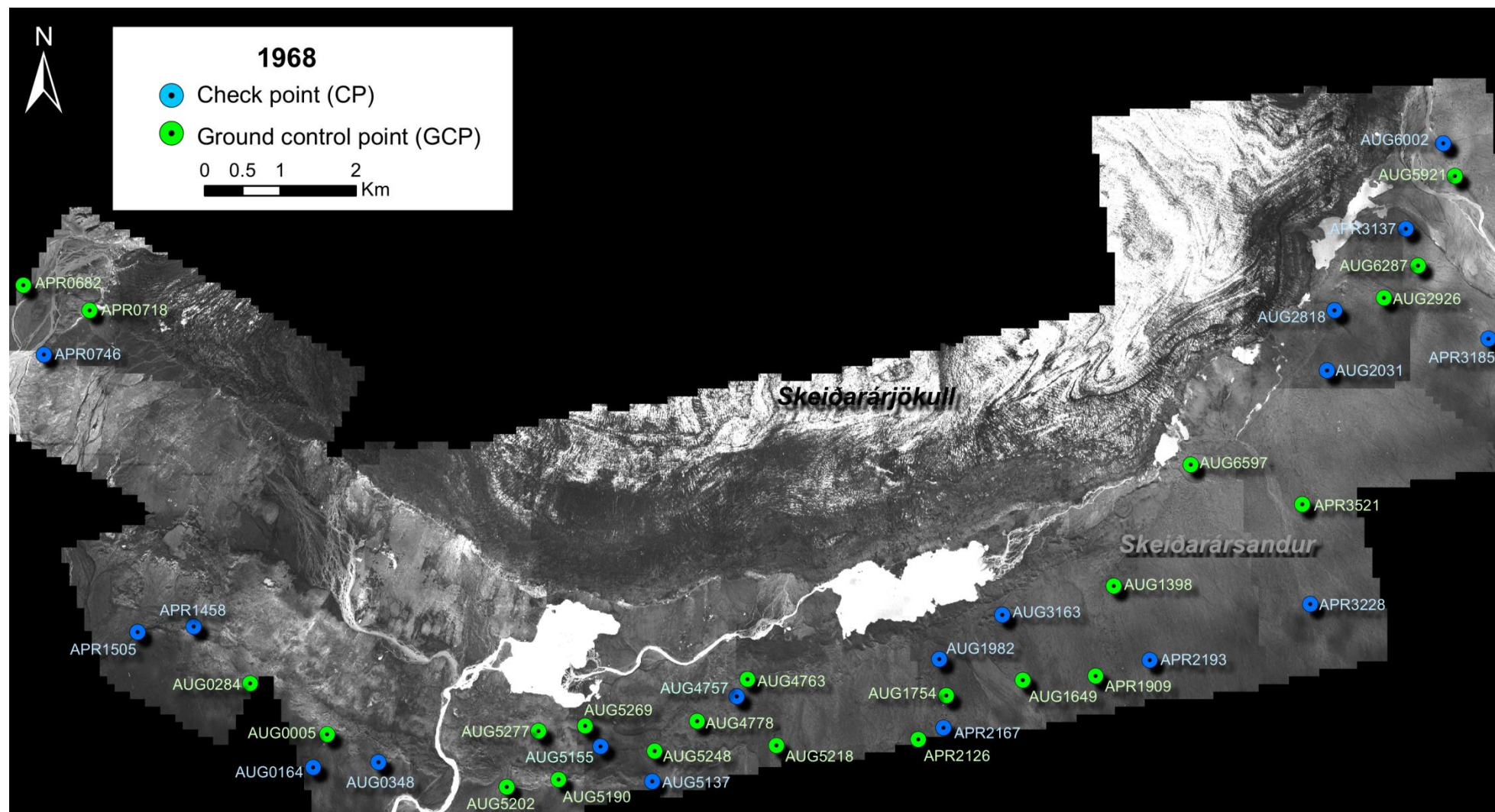


Figure B.3 1968 Ground control points and check points.

## 1975 COMPARISON OF CHECK POINT FILE TO DTM FILE

Point#	Point ID	Z Diff	X	Y	Z
1	AUG1398	2.2199	590041.8060	387564.3490	115.7650
2	AUG1649	-1.6309	588841.3900	386323.1650	84.9020
3	AUG1868	1.3403	588247.1250	386249.6790	92.7190
4	AUG1982	-0.0289	587737.2220	386600.5380	109.4180
5	AUG6597	-1.7657	591055.8520	389164.6160	120.0730
6	APR2167	-3.2555	587790.5800	385690.3060	84.8810
7	APR2193	-4.7922	590513.4840	386586.7650	84.7560
8	APR3462	2.1475	593968.8440	388195.1220	84.9440
10	AUG5822	2.1721	594220.2900	394616.9090	131.8180
11	AUG5936	0.5993	594323.7100	393411.6330	128.0960
12	AUG2673	3.8673	593883.7650	392289.9600	128.5620
13	APR3520	-4.7336	592545.6690	388639.8250	96.2750

Number of Points= 12

ave Z diff = -0.3217, rms = 2.7856, std = 2.8900



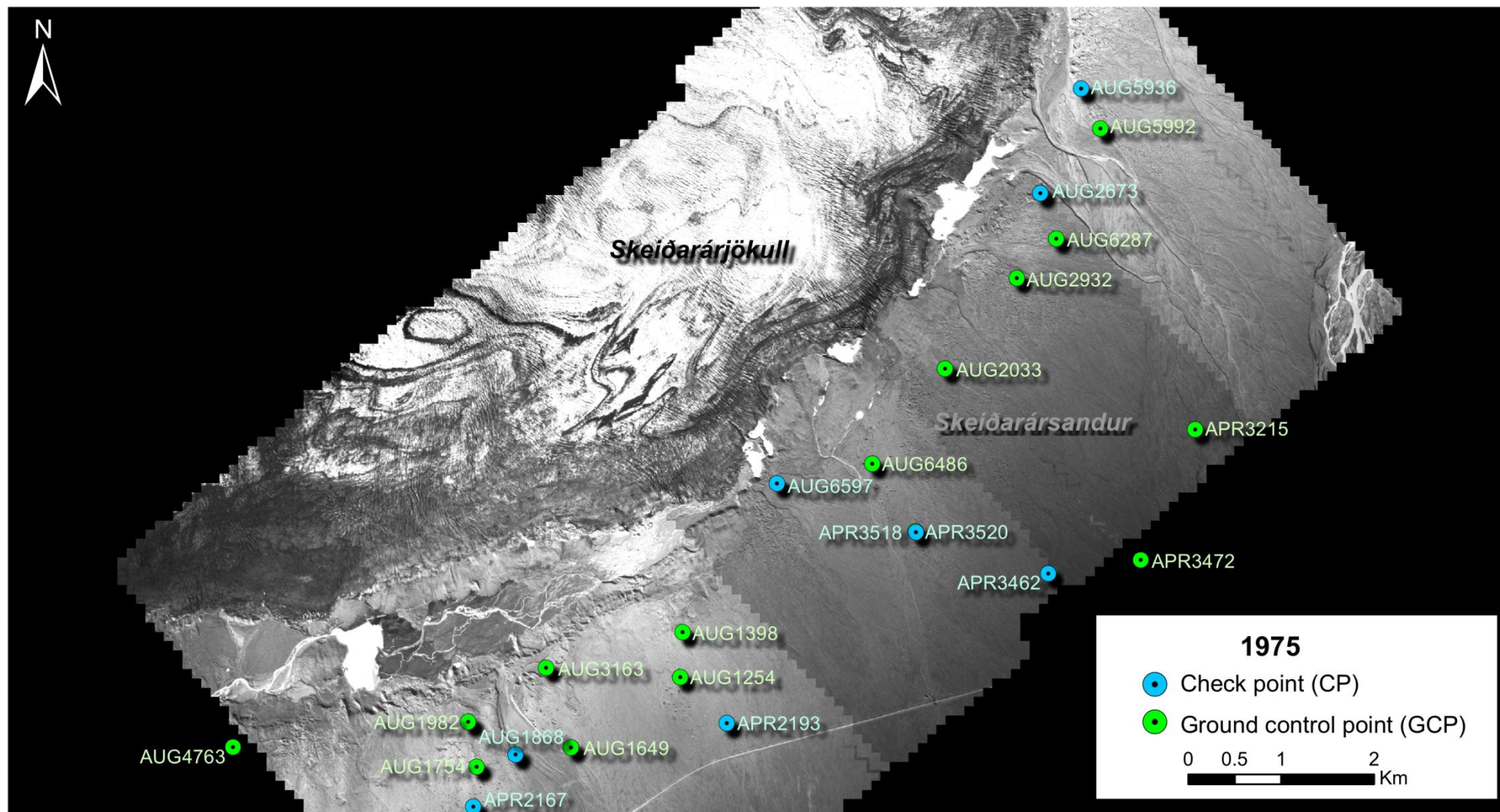


Figure B.4 1975 Ground control points and check points.



## 1986 COMPARISON OF CHECK POINT FILE TO DTM FILE

Point# Point ID Z Diff

1	AUG1254	2.2666
2	AUG1754	-1.7268
3	AUG5155	-0.2794
4	AUG5190	0.0001
5	AUG5248	0.5117
6	APR1899	1.5228
7	APR2193	3.1691
8	AUG0164	3.1006
9	AUG5274	-0.4809
10	AUG5275	-0.4774
11	AUG5148	2.2370
12	AUG4776	-1.8143
13	AUG0348	3.2628
14	AUG0528	3.2487

Number of Points= 14

ave Z diff = 1.0386, rms = 2.0769, std = 1.8665

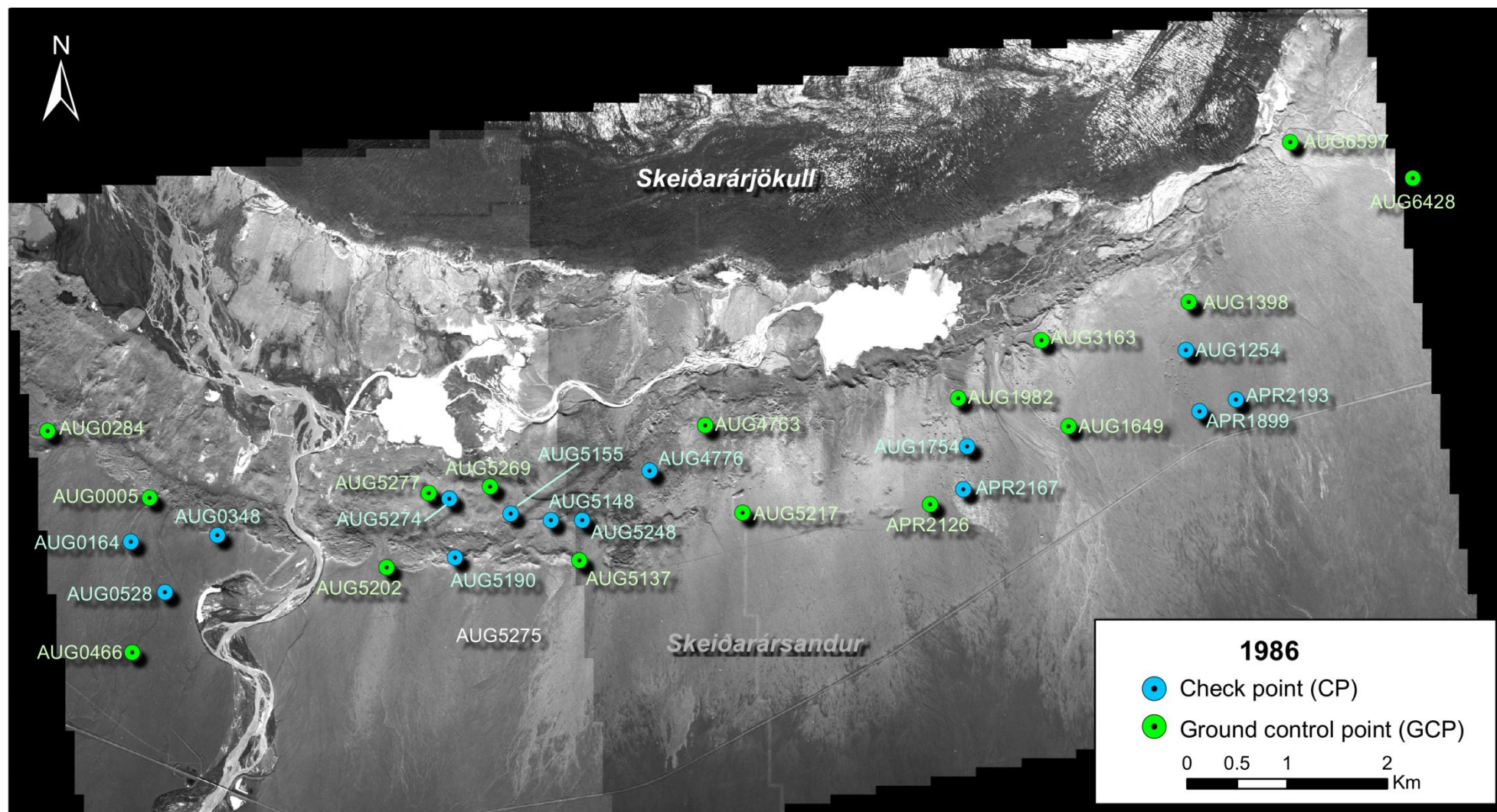


Figure B.5 1986 Ground control points and check points.

## 1992 COMPARISON OF CHECK POINT FILE TO DTM FILE

Point#	Point ID	Z Diff	X	Y	Z
1	AUG1868	1.5139	588247.1250	386249.6790	92.7190
2	AUG1982	-0.1928	587737.2220	386600.5380	109.4180
3	APR1709	-1.2267	586591.0240	385302.4720	83.9840
4	APR1899	-0.1942	590151.5680	386471.3280	84.5640
5	APR1909	-2.3368	589798.7720	386375.8580	86.3190
6	APR1948	-2.2966	586589.0330	385303.2500	83.1350
7	APR2167	-3.7909	587790.5800	385690.3060	84.8810
8	APR2180	1.6531	592298.6860	387275.6090	84.4380
9	APR2193	0.2009	590513.4840	386586.7650	84.7560
13	AUG0164	0.3044	579473.7030	385168.8690	77.6190
14	AUG5269	-3.8320	583059.9960	385718.6930	85.7240
15	AUG5274	-3.3093	582654.0900	385597.1650	84.8050
16	AUG5275	-3.3041	582654.0980	385597.2300	84.8070
17	AUG5148	-0.4859	583668.5190	385383.0490	85.4910
18	AUG4776	-0.6763	584652.6250	385879.2680	89.7270
19	AUG0348	-0.6734	580335.7090	385233.4800	99.4440
20	AUG0528	-2.3203	579814.2310	384659.9170	70.2720

Number of Points= 17

ave Z diff = -1.2334, rms = 2.0994, std = 1.7512



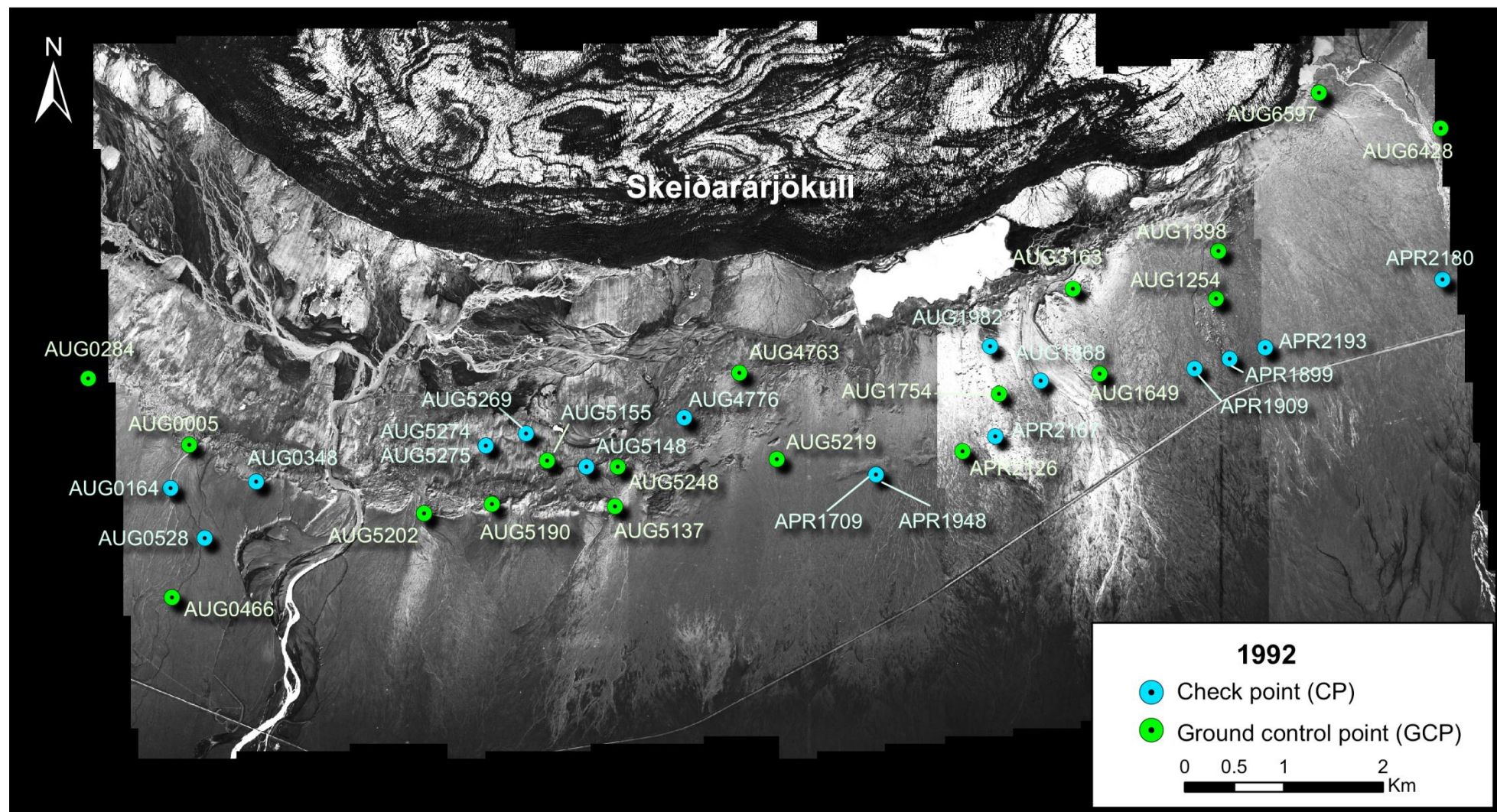


Figure B.6 1992 Ground control points and check points.

## 1997 COMPARISON OF CHECK POINT FILE TO DTM FILE

Point#	Point ID	Z Diff	X	Y	Z
1	AUG1254	1.0182	590016.1780	387084.3290	101.5260
2	AUG1868	1.8064	588247.1250	386249.6790	92.7190
3	AUG5877	2.1419	595425.0580	392225.6060	108.9660
4	AUG5994	3.8233	594533.9190	393000.4470	121.8270
5	AUG6003	1.8009	594336.3010	393395.9790	126.1560
6	AUG6486	-3.5214	592076.0680	389378.5900	104.6180
7	APR1899	-0.0310	590151.5680	386471.3280	84.5640
8	APR3139	2.2681	593905.1230	392273.6480	126.0260
9	APR3203	-0.3969	594985.1140	390878.5620	100.0930
10	APR3227	4.7539	592754.0640	386943.5180	78.5040
11	AUG5095	4.8091	585587.1810	385456.8370	93.2080
12	AUG5274	2.3439	582654.0900	385597.1650	84.8050
13	AUG4778	1.1140	584541.3750	385780.7710	87.0660
14	AUG4875	2.0445	584747.7200	386148.6080	95.4520
15	AUG6697	-1.3152	587566.2720	386852.2920	112.7700
16	APR0005	-0.0098	588290.9590	386917.1460	110.0300
17	APR0682	2.6051	575647.6390	391538.2360	103.6296
18	APR0740	2.1647	575921.5280	389428.4710	86.0718
19	APR1433	-5.6904	578057.7220	387152.7370	79.7553

Number of Points= 19

ave Z diff = 1.1436, rms = 2.7784, std = 2.6015



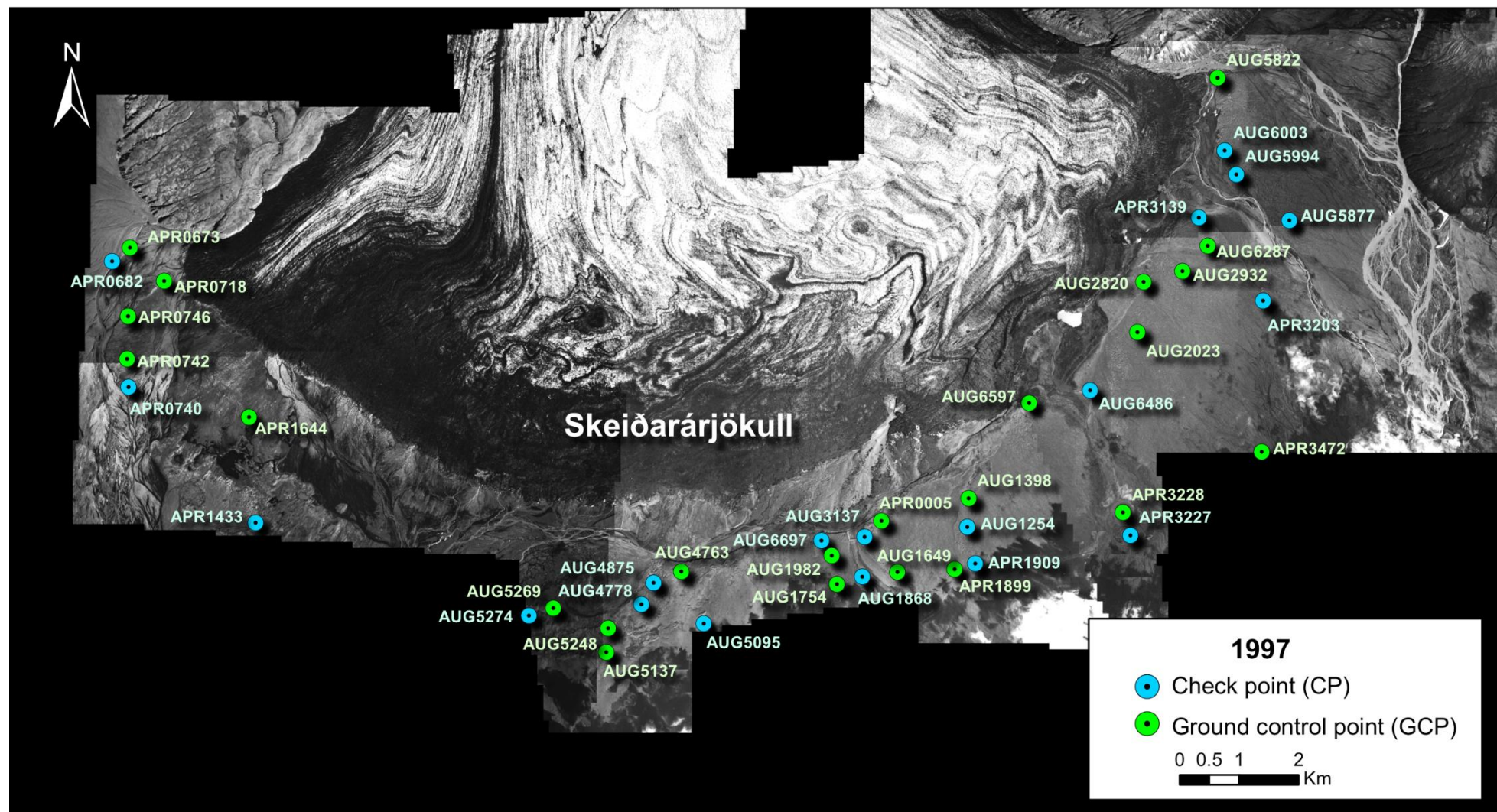


Figure B.7 1997 Ground control points and check points.



## 1997 vs 1997 Roads Authority

Point#	Point ID	Z Diff	X	Y	Z
1	AUG1254	0.9369	590016.1780	387084.3290	101.5260
2	AUG1868	4.9172	588247.1250	386249.6790	92.7190
3	AUG5877	-1.0998	595425.0580	392225.6060	108.9660
4	AUG5994	-0.5717	594533.9190	393000.4470	121.8270
5	AUG6003	1.0139	594336.3010	393395.9790	126.1560
6	AUG6486	-3.5906	592076.0680	389378.5900	104.6180
7	APR1899	-0.3528	590151.5680	386471.3280	84.5640
8	APR3139	0.5434	593905.1230	392273.6480	126.0260
9	APR3203	-0.8002	594985.1140	390878.5620	100.0930
10	APR3227	1.1027	592754.0640	386943.5180	78.5040
11	AUG5095	4.7121	585587.1810	385456.8370	93.2080
12	AUG5274	3.4040	582654.0900	385597.1650	84.8050
13	AUG4778	2.3894	584541.3750	385780.7710	87.0660
14	AUG4875	3.2019	584747.7200	386148.6080	95.4520
15	AUG6697	0.4850	587566.2720	386852.2920	112.7700
16	APR0005	1.8298	588290.9590	386917.1460	110.0300
17	APR0682	5.8238	575647.6390	391538.2360	103.6296
18	APR0740	2.8403	575921.5280	389428.4710	86.0718
19	APR1433	1.7187	578057.7220	387152.7370	79.7553

Number of Points= 19

ave Z diff = 1.5002, rms = 2.7248, std = 2.3369

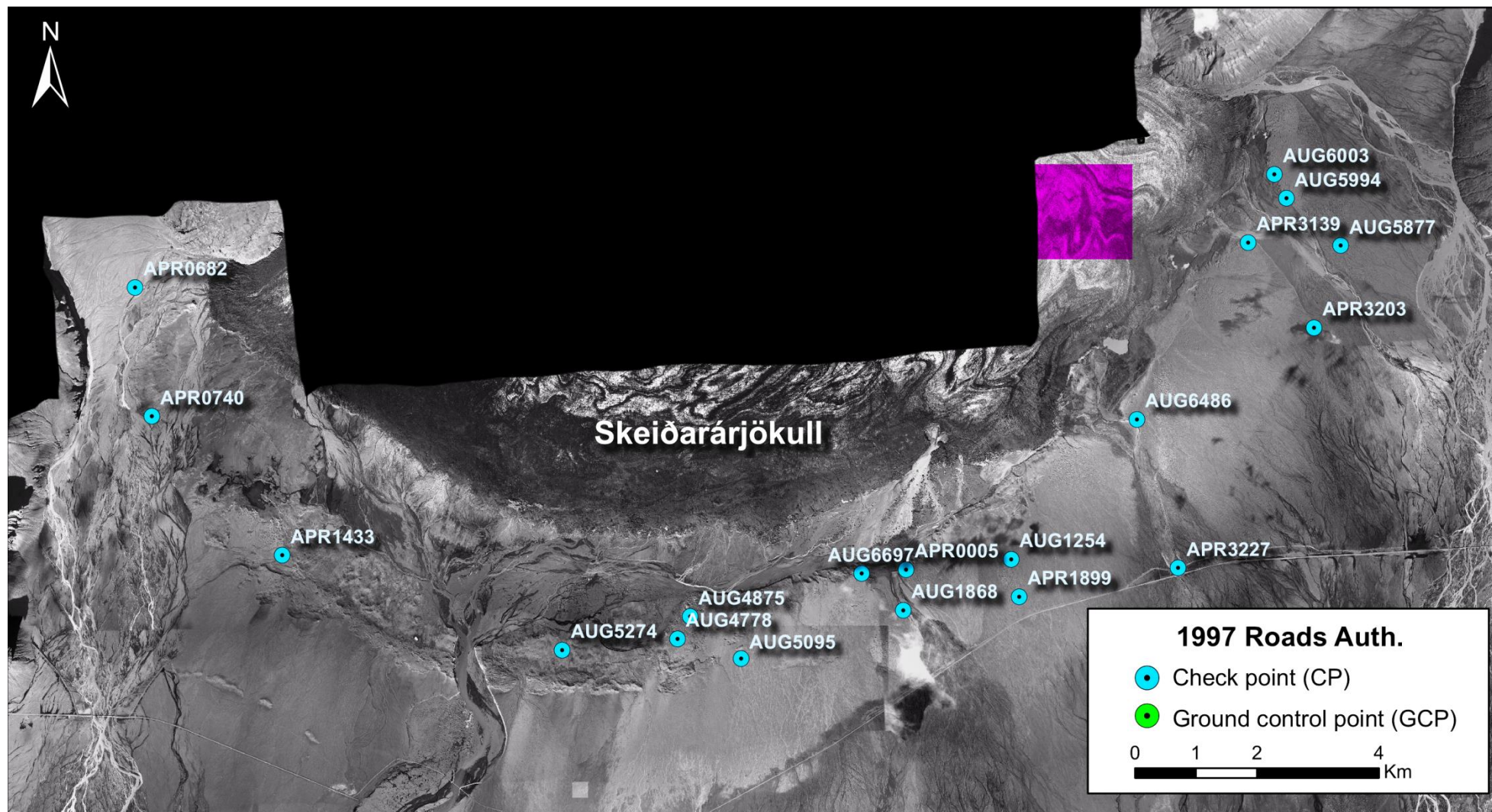


Figure B.8 1997 Check points vs 1997 Roads Authority 10m DEM.

## 1997 vs 2003 DEM

Point#	Point ID	Z Diff	X	Y	Z
1	AUG1254	-0.6997	590016.1780	387084.3290	101.5260
2	AUG1868	1.7079	588247.1250	386249.6790	92.7190
3	AUG5877	-2.8016	595425.0580	392225.6060	108.9660
4	AUG5994	-1.0434	594533.9190	393000.4470	121.8270
5	AUG6003	-0.2878	594336.3010	393395.9790	126.1560
6	AUG6486	-8.6951	592076.0680	389378.5900	104.6180
7	APR1899	-1.4286	590151.5680	386471.3280	84.5640
8	APR3139	0.2353	593905.1230	392273.6480	126.0260
9	APR3203	-3.0636	594985.1140	390878.5620	100.0930
10	APR3227	-1.9504	592754.0640	386943.5180	78.5040
11	AUG5095	3.2177	585587.1810	385456.8370	93.2080
12	AUG5274	1.6302	582654.0900	385597.1650	84.8050
13	AUG4778	0.2398	584541.3750	385780.7710	87.0660
14	AUG4875	-0.0001	584747.7200	386148.6080	95.4520
15	AUG6697	-2.4489	587566.2720	386852.2920	112.7700
16	APR0005	-1.1590	588290.9590	386917.1460	110.0300
19	APR1433	0.8658	578057.7220	387152.7370	79.7553

Number of Points= 17

ave Z diff = -0.9224, rms = 2.7059, std = 2.6221



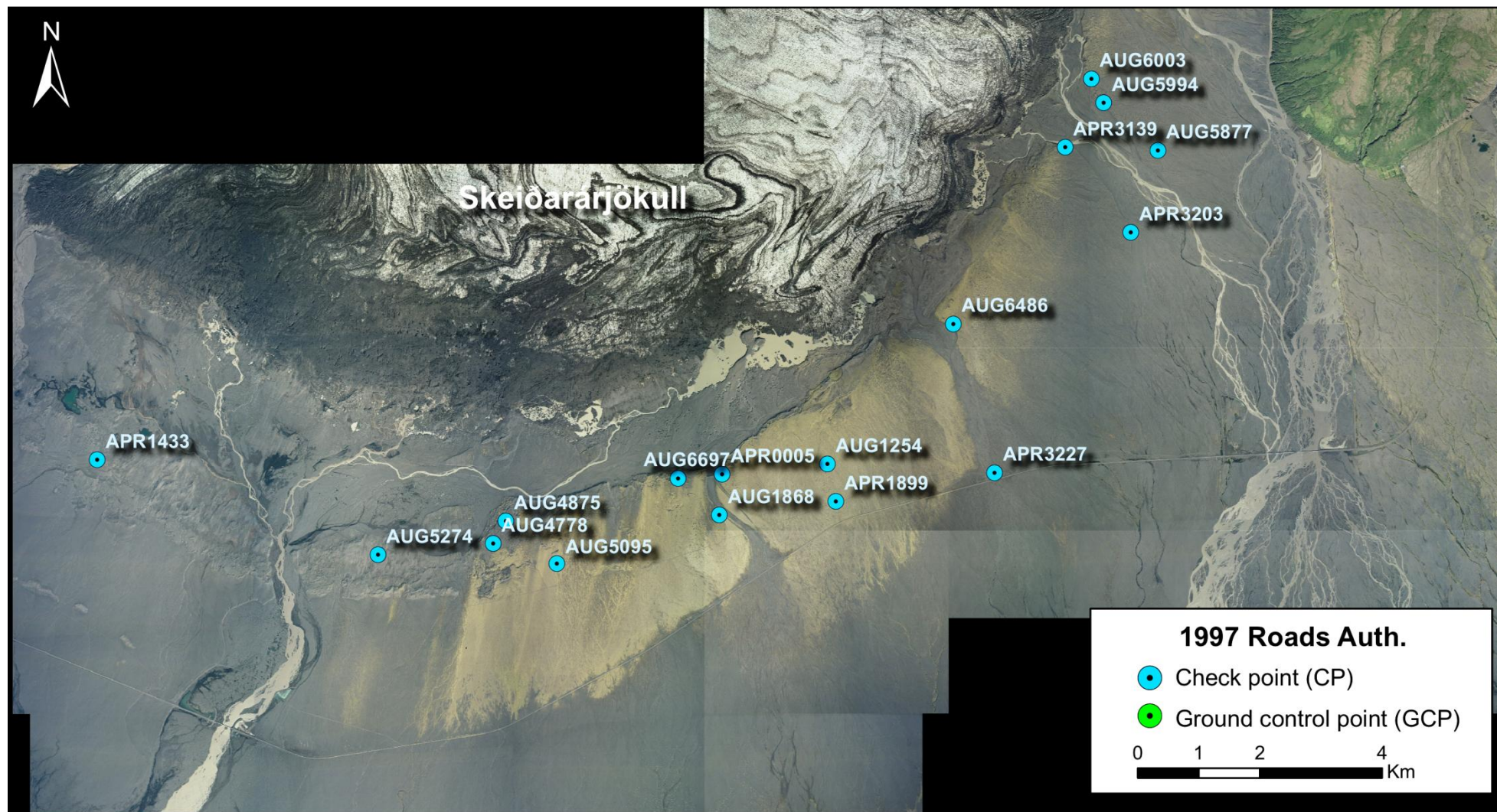


Figure B.9 1997 Check points vs 2003 Roads Authority 10m DEM.

## 2007 COMPARISON OF CHECK POINT FILE TO DTM FILE

Point# Point ID Z Diff X Y Z

1	AUG1412	3.0267	590021.9210	388046.6690	126.9500
2	AUG1634	0.7703	587375.7140	386958.6400	94.7690
3	AUG1710	0.3925	588662.7530	386612.8100	97.4530
4	AUG1731	0.3102	587997.5070	386283.1900	98.3730
5	AUG3955	2.2016	593299.0580	392643.8910	122.0890
6	AUG4748	0.4137	585001.3900	385656.0580	87.8480
7	AUG4770	-0.2368	584837.7020	386181.5200	95.6080
8	AUG4775	0.1230	584672.2620	385931.9060	90.8190
9	AUG4872	1.2839	584687.7160	386520.7030	80.0400
10	AUG4975	1.4655	585579.9750	386311.1380	103.5740
11	AUG5244	2.8741	585625.6620	385104.5970	84.6910
12	AUG5955	1.3910	595114.2880	392174.2540	109.0020
13	AUG6031	-0.3926	594227.8830	394051.5630	124.1780
14	AUG6254	-1.0190	592025.9610	390460.9030	124.1450
15	AUG6529	-1.5486	592028.1440	388695.7950	100.9790
16	AUG6652	0.2915	588543.9750	386211.4260	86.3090
17	AUG6831	0.6020	586548.8330	386710.1250	102.2240
18	AUG6940	-1.2114	585980.2920	385673.6770	92.8860
19	APR0514	-2.1758	588325.9760	388274.7470	93.7690
20	APR0612	-1.9479	589036.6920	387654.2940	118.5900
21	APR1909	0.3044	589798.7720	386375.8580	86.3190
22	APR2127	-0.2347	587454.0460	385549.8790	87.9170
23	APR2162	-1.3185	587761.2910	385654.5490	84.6740
24	APR2850	-3.8345	587812.4030	389460.2000	104.9680
25	APR3518	2.4070	592543.9680	388648.4250	99.7470

Number of Points= 25, ave Z diff = 0.157504, rms = 1.618673 std = 1.644211







**Appendix C. Locations of figures for Chapters 5, 6 and 7.**

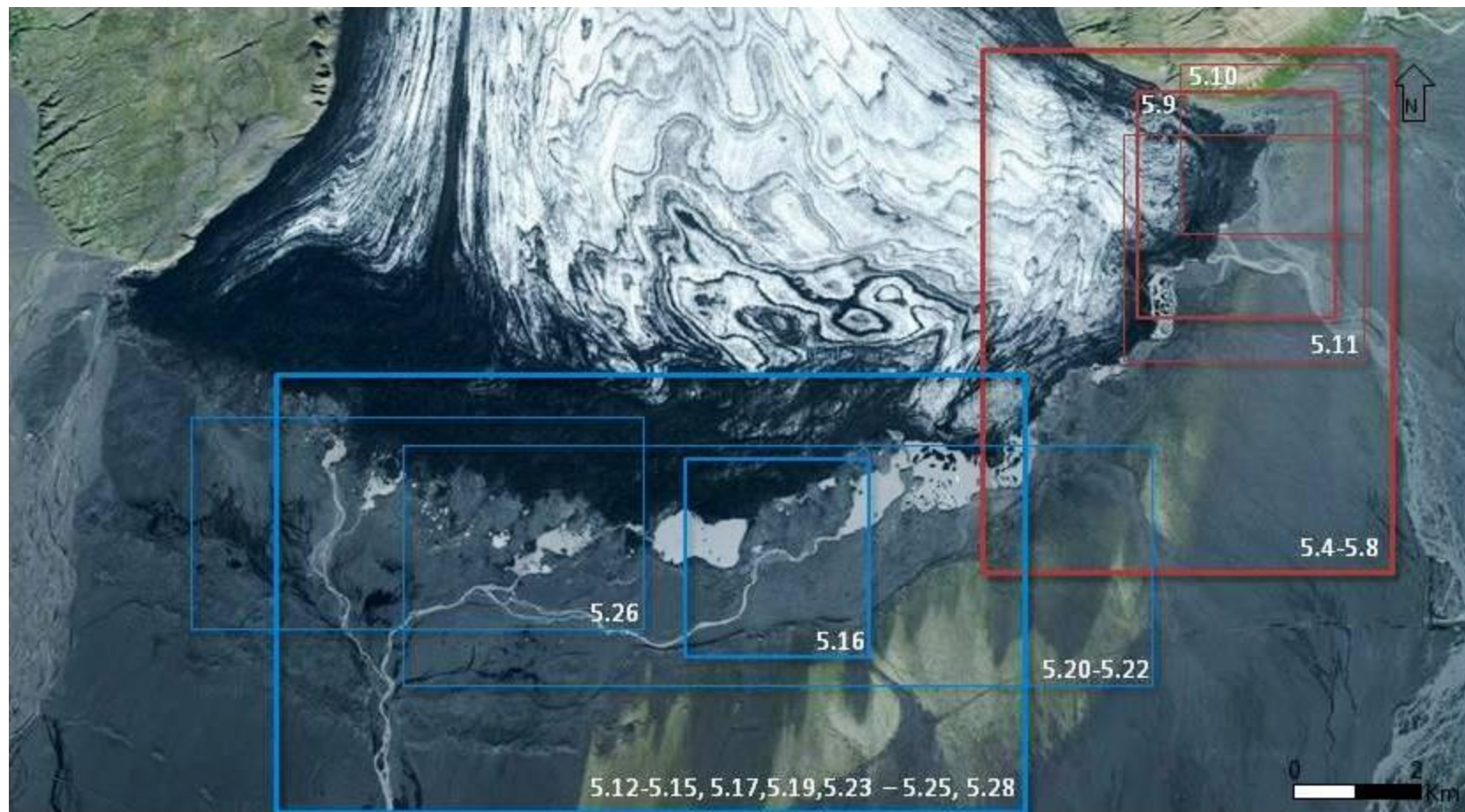


**Figure C.1 Location of Figures for Chapter 5 (East and Central areas) (Imagery basemap Google Earth 2010).**

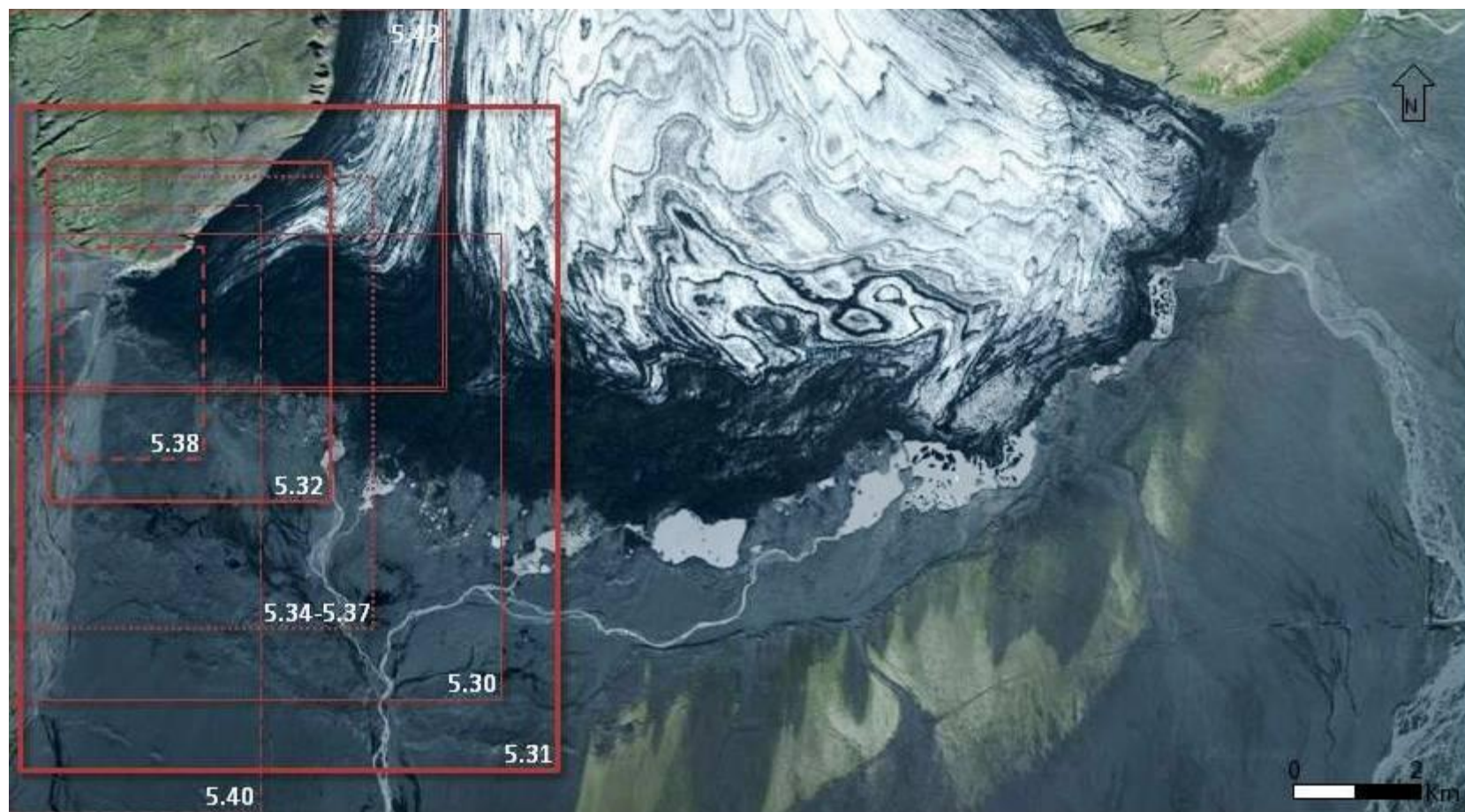


Figure C.2 Location of Figures for Chapter 5 (Western area) (Imagery basemap Google Earth 2010).



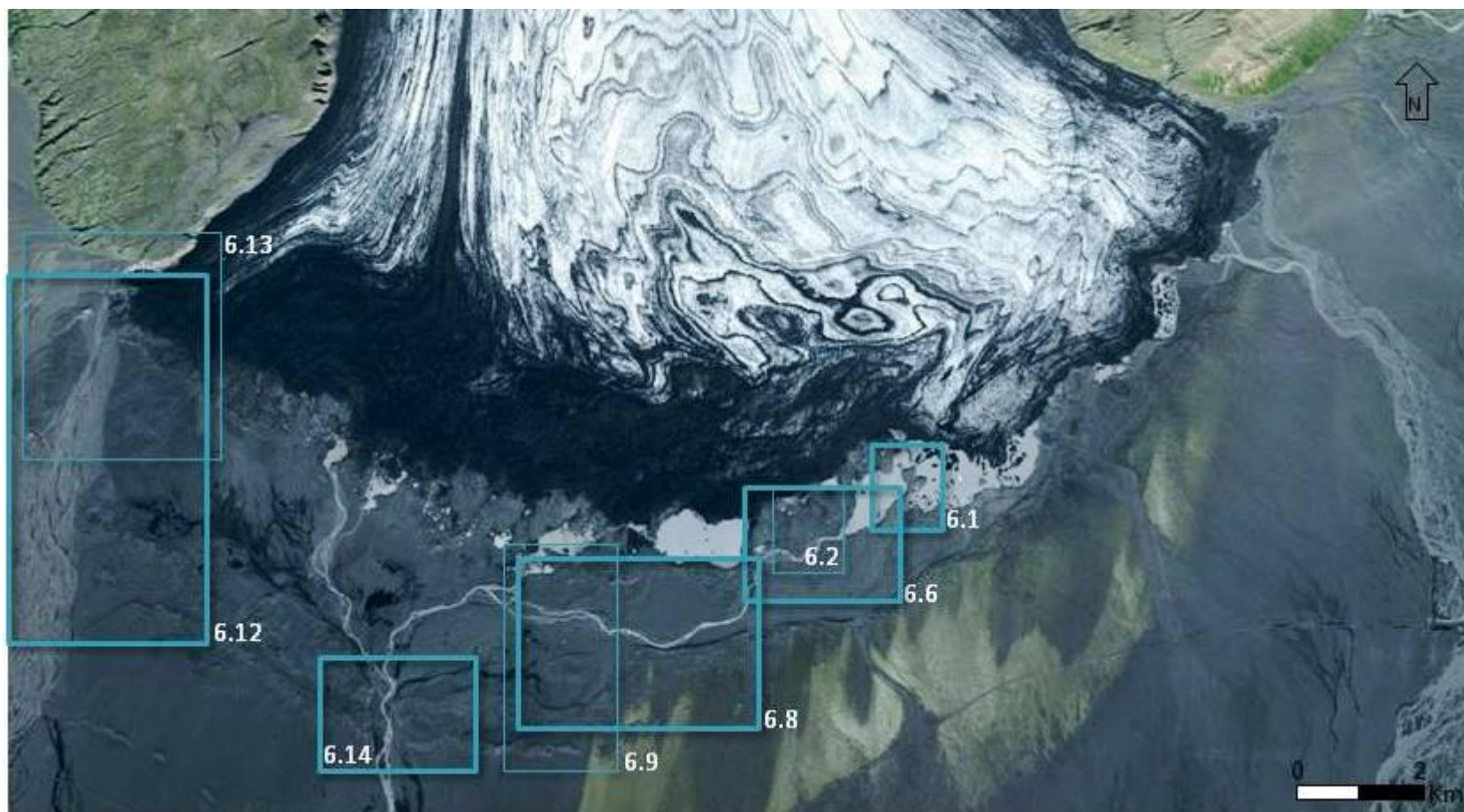


Figure C.3 Location of Figures for Chapter 6 (Imagery basemap Google Earth 2010).

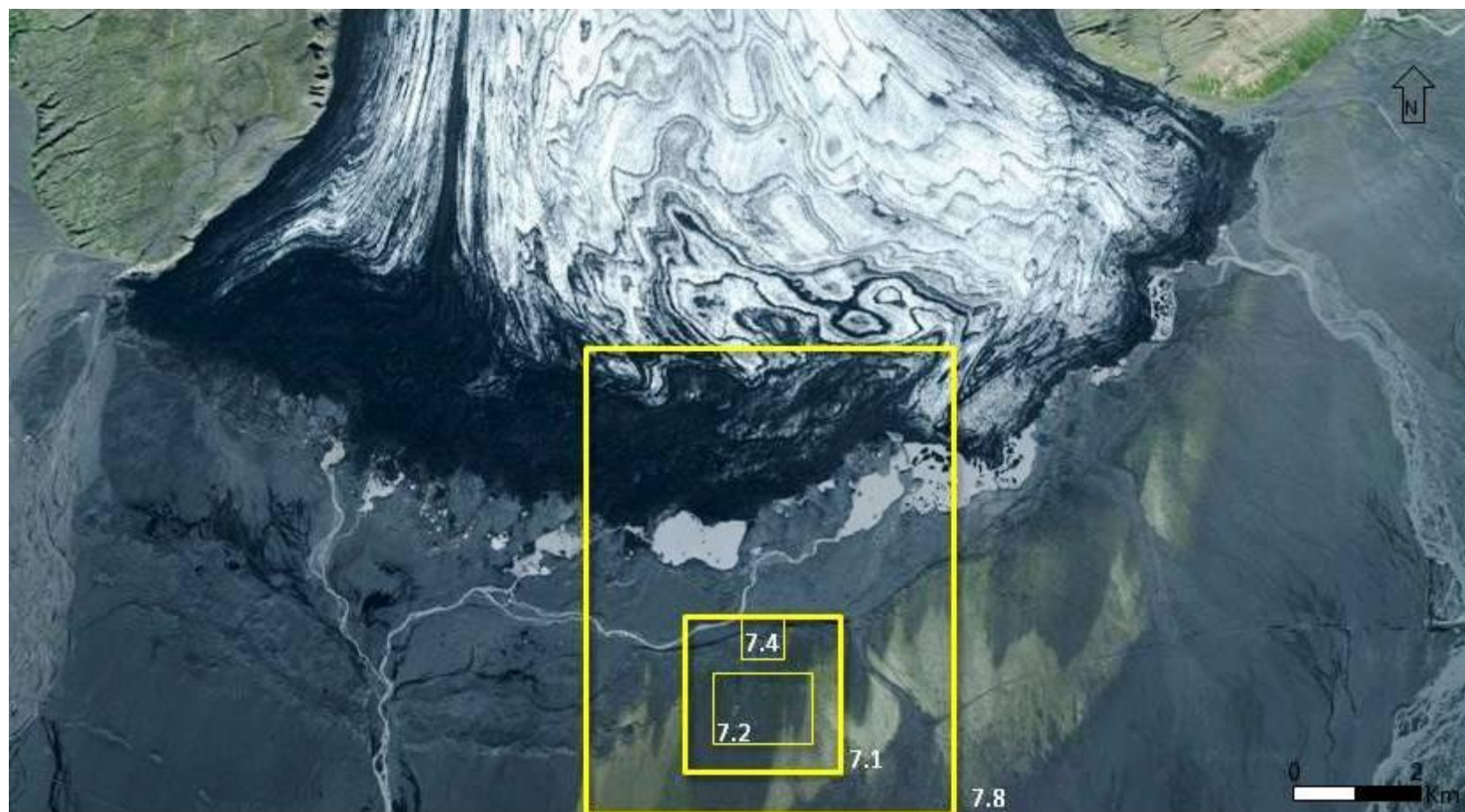


Figure C.4 Location of Figures for Chapter 7 (Imagery basemap Google Earth 2010).

## References

- Ahlmann, H. W. (1938) *Land of ice and fire*. London: K. Paul, Trench, Trubner and co. Ltd.
- Alley, R. B., Lawson, D. E., Evenson, E. B., and Strasser, J. C. (1998) 'Glaciohydraulic supercooling: a freeze-on mechanism to create stratified, debris-rich basal ice: II. Theory', *Journal of Glaciology*, 44, pp. 563-569.
- Anderson, M. G. and Calver, A. (1977) 'On the persistence of landscape features formed by a large flood', *Transactions of the Institute of British Geographers*, New Series, 2(2) pp. 243-254.
- Andre, M. F. (1990) 'Geomorphic impact of spring avalanches in Northwest Spitsbergen', *Permafrost and Periglacial Processes*, 1, pp. 97-110.
- Andrzejewski, L. and Molewski, P. (1999) 'Glaciodynamic and sedimentological conditions of glaciotectionic disturbances in selected marginal zones of glaciers in Iceland', *Quaternary Studies in Poland* (Special Issue), pp. 209-218.
- Arnborg, L. (1955) 'The development of frontal glacial lakes', *Geografiska Annaler*, 37(3-4), pp. 226-233.
- Astakhov, V. I. and Isayeva, L. L. (1988) 'The 'ice hill': an example of 'retarded glaciation' in Siberia', *Quaternary Science Reviews*, 7, pp. 29-40.
- Baily, B., Collier, P., Farres, P. and Inkpen, R. (2003) 'Comparative assessment of analytical and digital photogrammetric methods in the construction of DEMs and geomorphological forms', *Earth Surface Processes and Landforms*, 28, pp. 307-320.
- Baker, V. R. (1973) 'Paleohydrology and sedimentology of Lake Missoula flooding in Eastern Washington', *Geological Society of America. Special Paper*, (144).
- Baker, V. R. (ed.) (1984) 'Flood sedimentation in bedrock fluvial systems,' in *Sedimentology of Gravels and Conglomerates. Canadian Society of Petroleum Geologists. Memoir*. (10), pp. 87-98.
- Baker, V. R. and Kochel, R. C. (1988) 'Flood sedimentation in bedrock fluvial systems', in Baker, V. R. , Kochel, R. C. and Patton, P. C. (eds), *Flood geomorphology*. London: Wiley, pp. 123-137.
- Ballentyne, C. K. (2002) 'Paraglacial geomorphology', *Quaternary Science Reviews*, 21, pp. 1935-2017.
- Baltsavaia, E. P., Favey, E., Bauder, A. and Bosch, H. (2001) 'Digital surface modelling by airborne laser scaling and digital photogrammetry for glacier monitoring', *Photogrammetric Record*, 17(98), pp. 243-273.
- Benediktsson, I. O., Moller, P., Ingolfsson, O. and van der Meer, J. (2008) 'Instantaneous end moraine and sediment wedge formation during the 1890 glacier surge of Bruarjokull, Iceland', *Quaternary Science Reviews*, 27, pp. 209-234.
- Benn, D., Kirkbride, M. P., Owen, L. A. and Brazier, V. (2004) 'Glaciated valley landsystems', in Evans, D. J. (ed.) *Glacial Land Systems* London: Edward Arnold, pp. 372-406.
- Benn, D. I. and Evans, D. J. A. (1998) *Glaciers and glaciation*. London: Edward Arnold.
- Benn, D. I. and Evans, D. J. A. (2010) *Glaciers and glaciation*. London: Edward Arnold.
- Bennett, M.R., Huddart, D., and Waller, R.I. (2000) 'Glaciofluvial crevasse and conduit fills as indicators of supraglacial dewatering during a surge, Skeiðarárjökull, Iceland.' *Journal of Glaciology* 46, pp. 25-34.
- Betts, H. D., Trustrum, N. A. and Derose, R. C. (2003) 'Geomorphic changes in a complex gully system measured from sequential digital elevation models, and implications for management', *Earth Surface Processes and Landforms*, 28, pp. 1043-1058.

- Bjarnadóttir, L. R. (2007) 'The formation and geomorphological evolution of crevasse clast ridges through a surge cycle', *M.Sc. Study, Poster, University of Iceland*.
- Björnsson, H. (1974) 'Explanation of jökulhlaups from Grímsvötn, Vatnajökull, Iceland', *Jökull*, 24, pp. 1-26.
- Björnsson, H. (1975) 'Subglacial water reservoirs, jökulhlaups and volcanic eruptions', *Jökull*, 25, pp. 1-11.
- Björnsson, H. (1979) 'Nine glaciers in Iceland', *Jökull*, 29, pp. 74-80.
- Björnsson, H. (1992) 'Jökulhlaups in Iceland: prediction, characteristics and simulation', *Annals of Glaciology*, 16, pp. 95-106.
- Björnsson, H. (1997) *Grímsvatnahlaup Fyrr og Nu*. in Haraldsson, H. (ed.) *Vatnajökull: Gos og hlaup 1996*. Reykjavik: Vegagerdin, pp. 61-77.
- Björnsson, H. (1998) 'Hydrological characteristics of the drainage system beneath a surging glacier', *Nature*, 395, pp. 771-774.
- Björnsson, H. (ed.) (2009) *Jökulhlaups in Iceland: sources, release and drainage*. Cambridge University Press, pp. 50-62.
- Björnsson, H., Palsson, F. and Magnusson, E. (1999) 'Skeiðarárjökull: landslag of rennslisleidir vatns undir spordi', *Raunvísindastofnun Háskolans*, RH-11-99.
- Björnsson, H., Palsson, F., Sigurðsson, O. and Flowers, G. E.. (2003) 'Surges of glaciers in Iceland', *Annals of Glaciology*, 36, pp. 82-90.
- Blewett, W. L. and Winters, H. A. (1995) 'The importance of glaciofluvial features within Michigan's Port Huron Moraine', *Annals of the Association of American Geographers* 85(2), pp. 306-319.
- Bogacki, M. (1973) 'Geomorphological and geological analysis of the proglacial area of Skeiðarárjökull. Central, western and eastern sections', *Geographia Polonica*, 26, pp. 57-88.
- Boothroyd, J. C. and Ashley, G. M. (1975) 'Processes, bar morphology, and sedimentary structures on braided outwash fans, northeastern Gulf of Alaska', in Jopling, A. V. and McDonald, B. C. (eds), *Glaciofluvial and glaciolacustrine sedimentation*. SEPM Special Publication (23), pp. 193-222.
- Boothroyd, J. C. and Nummedal, D. (1978) 'Proglacial braided outwash: a model for humid alluvial-fan deposits', *Fluvial Sedimentology*, 5, pp. 641-688.
- Boulton, G. S. (1967) 'The development of a complex supraglacial moraine at the margin of Sorbreen, Ny Friesland, Vestspitsbergen', *Journal of Glaciology*, 6(47), pp. 717-735.
- Boulton, G. S. (1968) 'Flow tills and related deposits on some Vestspitsbergen glaciers', *Journal of Glaciology*, 7, pp. 391-412.
- Boulton, G. S. (1972) 'Modern Arctic glaciers as depositional models for former ice sheets', *Journal of the Geological Society of London*, 128, pp. 361-393.
- Boulton, G. S. (1976) 'The origin of glacially fluted surfaces: observations and theory', *Journal of Glaciology*, 17, pp. 287-309.
- Boulton, G. S. (1986) 'Push moraines and glacier contact fans in marine and terrestrial environments', *Sedimentology*, 33, pp. 677-698.
- Boulton, G. S. (1987) 'A theory of drumlin formation by subglacial sediment deformation'. in Menzies, J. and Rose, J. (eds), *Drumlin symposium: proceedings of the Drumlin Symposium, first International Conference on Geomorphology, Manchester, 16-18 September 1985*. Rotterdam: A. A. Balkema, pp. 25-80.
- Boulton, G. S. and Caban, P. E. (1995) 'Groundwater flow beneath ice sheets: part II. Its impact on glacier tectonic structures and moraine formation', *Quaternary Science Reviews*, 15, pp. 563-587.
- Boulton, G. S. and Eyles, N. (1979) 'Sedimentation by valley glaciers; a model and genetic classification', in Schluechter, C. (ed.) *INQUA symposium on genesis and*



- lithology of Quaternary deposits: Moraines and varves, origin, genesis, classification, Zurich.* Rotterdam: A. A. Balkema, pp. 11-23.
- Boulton, G.S., Jones, A.S., Clayton, K.M. and Kenning, M.J. (1977) 'A British ice-sheet model and patterns of glacial erosion and deposition in Britain' in Shotton, F. W. (ed.) *British Quaternary Studies, Recent Advances*, Oxford: Clarendon Press, pp. 213-246.
- Boyce, E. S., Motyka, R. J. and Truffer, M. (2007) 'Flotation and retreat of a lake-calving terminus, Mendenhall Glacier, southeast Alaska, USA', *Journal of Glaciology*, 53(181), pp. 211-224.
- Branney, M. J. (1995) 'Downsag and extension at calderas: new perspectives on collapse geometries from ice-melt, mining and volcanic subsidence', *Bulletin of Volcanology*, 57, pp. 303-318.
- Branney, M. J. and Gilbert, J. S. (1995) 'Ice-melt collapse pits and associated features in the 1991 lahar deposits of Volcan Hudson, Chile: criteria to distinguish eruption-induced glacier melt', *Bulletin of Volcanology*, 57, pp. 293-302.
- Brennand, T. A. (2000) 'Deglacial meltwater drainage and glacio-dynamics: Implications for esker genesis and meltwater regime', *Sedimentary Geology*, 91, pp. 9-55.
- Bretz, J. H., Smith, H. T. U. and Neff, G. E. (1956) 'Channeled Scabland of Washington: new data and interpretations', *Geological Society of America Bulletin*, 67, pp. 957-1049.
- Bridge, J. S. (1993) 'The interaction between channel geometry, water flow, sediment transport and deposition in braided rivers.' *Geological Society, London, Special Publications*, (75), pp. 13-72.
- Bristow, C. S. and Best, J. L. (1993) 'Braided rivers: perspectives and problems.' *Geological Society, London, Special Publications*, (75), pp. 1-11,
- Buckley, S. J., Mills, J. P. and Mitchell, H. L. (2004) 'Improving the accuracy of photogrammetric absolute orientation using surface matching', *XXth ISPRS Congress, Istanbul, Turkey. International Archives of the Photogrammetry, Remote Sensing and Spatial Information Services*, 34, part XXX, pp. 1-6.
- Burke, M. J., Woodward, J., Russell, A. J. and Fleisher, P. J. (2009) 'Structural controls on englacial esker sedimentation: Skeiðarárjökull, Iceland', *Annals of Glaciology*, 50, (51), pp. 85-92.
- Burke, M. J., Woodward, J., Russell, A. J., Fleisher, P. J. and Bailey, P. K. (2008) 'Controls on the sedimentary architecture of a single event englacial esker: Skeiðarárjökull, Iceland', *Quaternary Science Reviews*, 27, pp. 1829-1847.
- Burke, M. J., Woodward, J., Russell, A. J., Fleisher, P. J. and Bailey, P. K. (2010) 'The sedimentary architecture of outburst flood eskers: a comparison of ground-penetrating radar from Bering Glacier, Alaska and Skeiðarárjökull, Iceland', *GSA Bulletin*, 122(9-10), pp. 1637-1645.
- Carling, P. A. (1989) 'Hydrodynamic models of boulder berm deposition', *Geomorphology*, 2, pp. 319-340.
- Carling, P. A. (1996) 'Morphology, sedimentology, and paleohydraulic significance of large gravel dunes, Altai Mountains, Siberia', *Sedimentology*, 43, pp. 647-664.
- Carling, P. A. (1999) 'Subaqueous gravel dunes', *Journal of Sedimentary Research*, 69(3), pp. 534-545.
- Carrivick, J. L. (2004) *Characteristics and impacts of jökulhlaups (glacial outburst floods) from Kverkfjöl, Iceland*. Unpublished dissertation, Keele University.
- Carrivick, J. L. (2007) 'Modelling coupled hydraulics and sediment transport of a high-magnitude flood and associated landscape change', *Annals of Glaciology*, 45, pp. 143-154.

- Carrivick, J. L. (2007) 'Hydrodynamics and geomorphic work of jökulhlaups (glacial outburst floods) from Kverkfjöll volcano, Iceland', *Hydrological Processes*, 21(6), pp. 725-740.
- Cassidy, N. J., Knudsen, Ó., Rushmer, E. L., Van Dijk, T. A. G. P., Russell, A. J., Marren, P. M. and Fay, H. (2003) 'GPR derived architecture of November 1996 jökulhlaup deposits, Skeiðarársandur, Iceland', in Bristow, C. and Jol, H. M., (eds) *Ground Penetrating Radar in Sediments*, Geological Society, London, Special Publication, (211), pp. 153-166.
- Chandler, J. (1999) 'Effective application of automated digital photogrammetry for geomorphological research', *Earth Surface Processes and Landforms*, 24, pp. 51-63.
- Christian, C. S. and Steward, G. A. (1952) *General Report on Survey of Katherine-Darwin Region, 1946*. Land Research Series, 1, Melbourne: CSIRO.
- Christoffersen, P., Piotrowski, J. A. and Nicolaj, K. L. (2005) 'Basal processes beneath an Arctic glacier and their geomorphic imprint after a surge, Elisebreen, Svalbard', *Quaternary Research*, 64, pp. 125-137.
- Church, M. and Gilbert, R. (1975) 'Proglacial fluvial and lacustrine environments'. in Jopling, A. V. and McDonald, B. C. (eds), *Glaciofluvial and glaciolacustrine sedimentation*. SEPM Special Publication (23), pp. 22-100.
- Church, M. and Ryder, J. M. (1972) 'Paraglacial sedimentation: a consideration of fluvial processes conditioned by glaciation', *Geological Society of America Bulletin*, 83, pp. 3059-3071.
- Churski, Z. (1973) 'Hydrographic features of the proglacial area of Skeiðarárjökull', *Geographia Polonica*, 26, pp. 209-254.
- Clapperton, C. M. (1975) 'The debris content of surging glaciers in Svalbard Iceland', *Journal of Glaciology*, 14(72), pp. 395-406.
- Clarke, G. K. C., Collins, S. G. and Thomsson, D. E. (1984) 'Flow, thermal structure and subglacial conditions of a surge-type glacier', *Canadian Journal of Earth Sciences*, 21, pp. 232-240.
- Clayton, L. (1964) 'Karst topography on stagnant glaciers', *Journal of Glaciology*, 5, pp. 107-112.
- Clayton, L., Attig, J. W. and Mickelson, D. M. (1999) 'Tunnel channels formed in Wisconsin during the last glaciation', *Geological Society of America, Special Paper*, (337), pp. 69-82.
- Clayton, L., Mickelson, D. M. and Attig, J. W. (1985) 'Surging of the southwestern part of the Laurentide Ice Sheet', *Boreas*, 14, pp. 235-241.
- Clayton, L. and Moran, S. R. (1974) *A glacial process-form model*. Binghamton: State University of New York.
- Colman, S. M. (2002) 'Paleoclimate - a fresh look at glacial floods', *Science*, 296, (5571), pp. 1251-1252.
- Cooper, M. and Cross, P. (1988) 'Statistical concepts and their application in photogrammetry and surveying', *Photogrammetric Record*, 12(71), pp. 637-663.
- Croot, D. G. (1988) 'Morphological, structural and mechanical analysis of neoglacial ice-pushed ridges in Iceland'. in Croot, D. G. (ed.) *Glaciotectonics: forms and processes*. Rotterdam: A. A. Balkema, pp. 33-47.
- Deroose, R. C., Gomez, B., Marden, M. and Trustrum, N. A. (1998) 'Gully erosion in Mangatu Forest, New Zealand, estimated from digital elevation models', *Earth Surface Processes and Landforms*, 23, pp. 1045-1053.
- Dickson, J. and Head, J. W. (2006) 'Evidence for an Hesperian-aged South circum-Polar lake margin environment on Mars', *Planetary and Space Science*, 54, pp. 251-272.

- Dredge, L. A. and Cowan, W. R. (1989) 'Lithostratigraphic record on the Ontario Shield.', in Fulton, R. J., (ed) *Quaternary Geology of Canada and Greenland. Geology of Canada No. II*. Ottawa: Geological Survey of Canada, pp. 235-249.
- Driscoll, F. G., Jr. (1980) 'Wastage of the Klutlan ice-cored moraines, Yukon Territory, Canada', *Quaternary Research*, 14, pp. 31-49.
- Duller, R. (2007) *Depositional processes associated with volcanoclastic jökulhlaups, Mýrdalssandur, Iceland*. Unpublished dissertation, Keele University.
- Dykes, R. C., Brook, M. S. and Winkler, S. (2010) 'The contemporary retreat of Tasman Glacier, Southern Alps, New Zealand, and the evolution of Tasman proglacial lake since AD 2000', *Erdkunde*, 64(2), pp. 141-154.
- Evans, D. J. A. (2003) *Glacial landsystems*. London: Arnold.
- Evans, D. J. A. (2005) 'The glacier-marginal landsystems of Iceland' in: *Iceland - Modern Processes and Past Environments*. Oxford: Elsevier.
- Evans, D. J. A. (2011) 'Glacial landsystems of Satujökull, Iceland: A modern analogue for glacial landsystem overprinting by mountain icecaps', *Geomorphology*, 129, pp. 225-237.
- Evans, D. J. A., Lemmen, D. S. and Read, B. R. (1999) 'Glacial landsystems of the southwest Laurentide Ice Sheet: modern Icelandic analogues', *Journal of Quaternary Science*, 14, pp. 673-691.
- Evans, D. J. A. and Rea, B. R. (1999) 'Geomorphology and sedimentology of surging glaciers: a land-systems approach', *Annals of Glaciology*, 28, pp. 75-82.
- Evans, D. J. A. and Rea, B. R. (2003) 'Surging glacier landsystem'. in Evans, D. J. (ed.) *Glacial Land Systems* London: Edward Arnold, pp. 259-288.
- Evans, D. J. A. and Twigg, D. R. (2002) 'The active temperate glacial landsystem: A model based on Breiðamerkurjökull and Fjallsjökull, Iceland', *Quaternary Science Reviews*, 21(20-22), pp. 2143-2177.
- Evenson, E. B., Lawson, D. E., Strasser, J. C., Larson, G. J., Alley, R. B., Ensminger, S. L. and Stevenson, W. E. (1999) 'Field evidence for the recognition of glaciohydraulic supercooling', in Mickelson, D. M., and Attig, J. W. (eds) *Glacial processes: past and present*. Geological Society of America Special Paper (337), pp. 23-35.
- Everest, J. and Bradwell, T. (2003) 'Buried glacier ice in southern Iceland and its wider significance', *Geomorphology*, 52, pp. 347-358.
- Eyles, N. (1979) 'Facies of supraglacial sedimentation on Icelandic and Alpine temperate glaciers', *Canadian Journal of Earth Sciences*, 16, pp. 1341-1361.
- Eyles, N. (1983) *Glacial Geology*. Oxford: Pergamon.
- Fay, H. (2002) 'Formation of ice-block obstacle marks during the November 1996 glacier-outburst flood (jökulhlaup), Skeiðarársandur, southern Iceland', in Martini, I. P., Baker, V. R. and Garzonón, G. (eds) *Flood and Megaflood Processes and Deposits: Recent and Ancient Examples. International Association of Sedimentologists Special Publication (32)*, pp. 85-97.
- Fitzsimons, S. J. (1991) 'Supraglacial eskers in Antarctica', *Geomorphology*, 4, pp. 293-299.
- Fleisher, P. J. (1986) 'Dead-ice sinks and moats: environments of stagnant ice deposition', *Geology*, 14, pp. 39-42.
- Fleisher, P. J., Cadwell, D. H. and Muller, E. H. (1998) 'Tsivat Basin conduit system persists through two surges, Bearing Piedmont Glacier, Alaska', *GSA Bulletin*, 110(7), pp. 877-887.
- Fleisher, P. J., Cadwell, D. H., Tormey, B., Lissitschenko, P. and Dell, J. (1997) 'Post-surge changes and abundant frazil ice, eastern sector, Bering Glacier, Alaska', *Geological Society of America, Abstracts with Programs*, 29, p. 216.

- Flowers, G. E., Björnsson, H. and Pálsson, F. (2004) 'A coupled sheet-conduit mechanism for jökulhlaup propagation', *Geophysical Research Letters*, 31(L05401), pp. 1-4.
- Fountain, A. G. and Walder, J. S. (1998) 'Water flow in glaciers', *Reviews of Geophysics*, 36, pp. 299-328.
- Fountain, A. G., Walder, J. S., Anderson, S. P., Anderson, R. S., Trabant, D., Lindsay, D. and Cunico, M. (1999) 'The 1999 outburst of glacier-dammed Hidden Creek Lake' [abstract], *EOS (Transactions of the American Geophysical Union, 80(16), supplement)*, p. 426.
- Fowler, A.C., Murray, T., and Ng, F.S.L. (2001) 'Thermally controlled glacier surging', *Journal of Glaciology*, 47, pp. 527-538.
- French, H. M. and Harry, D. G. (1990) 'Observations on buried glacier ice and massive segregated ice, western Arctic coast, Canada', *Permafrost and Periglacial Processes* 1, pp. 31-43.
- Funk, M. and Rothlisberger, H. (1989) 'Forecasting the effects of a planned reservoir which will partially flood the tongue of Unteraargletscher in Switzerland', *Annals of Glaciology*, 13, pp. 76-81.
- Galon, R. (1973a) 'Geomorphological and geological analysis of the proglacial area of Skeiðarárjökull: central section', *Geographica Polonica*, 26, pp. 15-57.
- Galon, R. (1973b) 'A synthetic description of deposits and landforms observed on the proglacial area of Skeiðarárjökull, conclusions with regard to the age of the deposits and the way in which deglaciation is proceeding', *Geographia Polonica*, 26, pp. 139-150.
- Gilbert, R. and Scheifer, E. (2007) 'Reconstructing morphometric change in a proglacial landscape using historical aerial photography and automated DEM generation', *Geomorphology*, 88, pp. 167-187.
- Glasner, D. (2009) 'Karl Popper, critical rationalist – modern philosopher', *National Review*, 47(24), p. 46.
- Glasser, N. F. and Hambrey, M. H. (2002) 'Sedimentary facies and landform genesis at a temperate outlet glacier: Soler Glacier, North Patagonian Icefield', *Sedimentology*, 49, pp. 43-64.
- Gomez, B., Russell, A. J., Smith, L. C. and Knudsen, Ó. (2002) 'Erosion and deposition in the proglacial zone: the 1996 jökulhlaup on Skeiðarársandur, southeast Iceland', *IAHS-AISH Publication* (271), pp. 217-222.
- Gomez, B., Smith, N. D., Smith, L. C., Magilligan, F. J. and Mertes, L. A. K. (2000) 'Glacier outburst floods and outwash plain development: Skeiðarársandur, Iceland', *Terra Nova*, 12(3), pp. 126-131.
- Gooch, M. J., Chandler, J. H. and Stojic, M. (1999) 'Accuracy assessment of digital elevation models generated using the Erdas Imagine Orthomax digital photogrammetric system', *Photogrammetric Record*, 16(93), pp. 519-531.
- Gudmundsson, M. T., Björnsson, H. and Pálsson, F. (1995) 'Changes in jökulhlaup sizes in Grímsvötn, Vatnajökull, Iceland, 1934-91, deduced from in-situ measurements of subglacial lake volume', *Journal of Glaciology*, 41(138), pp. 263-272.
- Gudmundsson, M. T., Bonnel, A. and Gunnarsson, K. (2002) 'Seismic soundings of sediment thickness on Skeiðarársandur, SE-Iceland', *Jökull*, 51, pp. 53-64.
- Gudmundsson, M. T., Sigmundsson, F. and Björnsson, H. (1997) 'Ice-volcano interaction of the 1996 Gjalp subglacial eruption, Vatnajökull, Iceland', *Nature*, 389, pp. 954-957.
- Gudmundsson, M. T., Sigmundsson, F., Björnsson, H. and Hognadóttir, T. (2004) 'The 1996 eruption at Gjalp, Vatnajökull ice cap, Iceland: efficiency of heat transfer, ice deformation and subglacial water pressure', *Bulletin of Volcanology*, 66, pp. 46-65.

- Gustavason, T. C. and Boothroyd, J. C. (1987) 'A depositional model for outwash, sediment sources and hydrologic characteristics, Malaspina Glacier, Alaska: a modern analogue of the southeastern margin of the Laurentide Ice Sheet', *Geological Society of America Bulletin*, 99, pp. 187-200.
- Hambrey, M. J. (1984) 'Sedimentary processes and buried ice phenomena in the proglacial areas of Spitsbergen glaciers', *Journal of Glaciology*, 30(104), pp. 116-119.
- Hambrey, M. J. (1999) 'Debris entrainment and transfer in polythermal valley glaciers', *Journal of Glaciology*, 45, pp. 69-86.
- Harvey, E. (2005) *An integrated approach to landform genesis: case study of the Mueller Glacier*. Unpublished M.A. thesis, University of Otago, Dunedin.
- Henderson, E. (1819) *Iceland, or the journal of a residence in that island during the years 1814-1815*. Edinburgh: Waugh and Innes.
- Hjulström, F. (1952) 'The geomorphology of the alluvial outwash plains (sandurs) of Iceland and the mechanics of braided rivers', *Proceedings of the XVIIIth International Congress of the International Geographical Union, Washington*, pp. 337-342.
- Hooke, R. L. (1989) 'Englacial and subglacial hydrology: a qualitative review', *Arctic and Alpine Research*, 21, pp. 221-233.
- Hooke, R. L. and Jennings, C. E. (2006) 'On the formation of tunnel valleys of the southern Laurentide ice sheet', *Quaternary Science Reviews*, 25, pp. 1364-1372.
- Hooke, R. L. and Pohjola, V. A. (1994) 'Hydrology of a segment of a glacier situated in an overdeepening, Storglaciaren, Sweden', *Journal of Glaciology*, 40(134), pp. 140-148.
- Houmark-Nielsen, M., Hansen, L., Jorgensen, M. E. and Kronborg, C. (1994) 'Stratigraphy of a Late Pleistocene ice-cored moraine at Kap Herschell, Northeast Greenland', *Boreas* 23(4), pp. 505-512.
- Howarth, P. J. and Price, R. J. (1969) 'The proglacial lakes of Breiðamerkurjökull and Fjallsjökull, Iceland.', *Geographical Journal*, 135, pp. 573-581.
- Huddart, D. and Hambrey, M. H. (1996) 'Sedimentary and tectonic development of a high-Arctic thrust-moraine complex: Comfortlessbreen, Svalbard', *Boreas*, 25, pp. 227-243.
- Ives, J. D. (2007) *Skaftafell in Iceland: a thousand years of change*. Reykjavik: Ormstunga.
- Jewtuchowicz, S. (1971) 'The present-day marginal zone of Skeiðarárjökull', *Acta Geographica Lodzenia*, 27, pp. 43-52.
- Jewtuchowicz, S. (1973) 'The present-day marginal zone of Skeiðarárjökull', *Geographia Polonica*, 26, pp. 115-138.
- Johnson, M. D. (1999) 'Spooners Hills, northwest Wisconsin: High-relief hills carved by subglacial meltwater of the Superior Lobe', *Geological Society of America, Special Paper* (337), pp. 83-92.
- Johnson, P. G. (1971) 'Ice cored moraine formation and degradation, Donjek Glacier, Yukon Territory, Canada', *Geografiska Annaler, Series A, Physical Geography*, 53(3-4) pp. 198-202.
- Johnson, P. G. (1992) 'Stagnant glacier ice, St. Elias Mountains, Yukon', *Geografiska Annaler, Series A, Physical Geography* 74(1), pp. 13-19.
- Jonsson, J. (1955) 'On the formation of frontal glacial lakes', *Geografiska Annaler*, 37(3-4), pp. 229-233.
- Kamb, B. (1987) 'Glacier surge mechanism based on linked cavity configuration of the basal water conduit system', *Journal of Geophysical Research*, 92, pp. 9083-9100.

- Kamb, B., Raymond, C. F., Harrison, W. D., Englehardt, H., Echelmeyer, K. A., Humphrey, N., Brugman, M. M. and Pfeffer, T. (1985) 'Glacier surge mechanism: 1982-1983 surge of Variegated Glacier, Alaska', *Science*, 227(4686), pp. 469-479.
- Kerle, N. (2002) 'Volume estimation of the 1998 flank collapse at Casita volcano, Nicaragua: a comparison of photogrammetric and conventional techniques', *Earth Surface Processes and Landforms*, 27(7), pp. 759-772.
- Kirkbride, M. (1993) 'The temporal significance of transitions from melting to calving termini at glaciers in the central Southern Alps of New Zealand', *The Holocene*, 3, pp. 232-240.
- Kirkbride, M. and Spedding, N. (1996) 'The influence of englacial drainage on sediment-transport pathways and till texture of temperate valley glaciers', *Annals of Glaciology*, 22, pp. 160-166.
- Kirkbride, M. P. and Warren, C. R. (1999) 'Tasman Glacier, New Zealand: twentieth-century thinning and predicted calving retreat', *Global and Planetary Change*, 22, pp. 11-28.
- Kjaer, K. H., Larsen, E., van der Meer, J., Ingolfsson, O., Kruger, J., Benediktsson, I. O., Knudsen, C. G. and Schomacker, A. (2006) 'Subglacial decoupling at the sediment / bedrock interface: a new mechanism for rapid flowing ice', *Quaternary Science Reviews*, 25, pp. 2704-2712.
- Klimek, K. (1972) 'Present-day fluvial processes and relief of Skeiðarársandur plain (Iceland)', *Polska Academia Nauk Institut Geografi*, 94, pp. 129-139.
- Klimek, K. (1973) 'Geomorphological and geological analysis of the proglacial area of the Skeiðarárjökull: Extreme eastern and extreme western sections', *Geographica Polonica*, 26, pp. 89-113.
- Knudsen, O. (1995) 'Concertina eskers, Bruarjökull, Iceland: an indicator of surge-type behaviour', *Quaternary Science Reviews*, 14, pp. 487-493.
- Knudsen, O., Jóhannesson, H., Russell, A. J. and Haraldsson, H. (2001) 'Changes in the Gígjukvísl river channel during the November 1996 jökulhlaup, Skeiðarársandur, Iceland', *Jökull*, 50, pp. 19-32.
- Koteff, C. and Pessl, F. (1981) 'Systematic Ice Retreat in New England', *USGS Professional Paper* (1179).
- Kozarski, S. and Szupryczynski, J. (1973) 'Glacial forms and deposits', *Geographia Polonica*, 26, pp. 255-311.
- Krigström, A. (1962) 'Geomorphological studies of sandur plains and their braided rivers in Iceland', *Geografiska Annaler*, 44(3-4), pp. 328-346.
- Krüger, J. (1997) 'Development of minor outwash fans at Kotlujökull, Iceland', *Quaternary Science Reviews*, 16, pp. 649-659.
- Krüger, J. and Aber, J. S. (1999) 'Formation of supraglacial sediment accumulations on Kotlujökull, Iceland', *Journal of Glaciology*, 45, pp. 400-402.
- Krüger, J. and Kjær, K. (2000) 'De-icing progression of ice-cored moraines in a humid, subpolar climate, Kötlujökull, Iceland', *The Holocene* 10(6), pp. 737-747.
- Krüger, J. and Thomsen, H. H. (1984) 'Morphology, stratigraphy, and genesis of small drumlins in front of the glacier Myrdalsjökull, South Iceland', *Journal of Glaciology*, 30(104), p. 94-105.
- Lane, S. N., James, T. D. and Crowell, M. D. (2000) 'Application of digital photogrammetry to complex topography for geomorphological research', *Photogrammetric Record*, 16, (95), pp. 793-821.
- Lane, S. N., Richards, K. S. and Chandler, J. (1993) 'Developments in photogrammetry; the geomorphological potential', *Progress in Physical Geography*, 17(3), pp. 306-328.
- Lawson, D. E., Strasser, J. C., Evenson, E. B., Alley, R. B., Larson, G. J. and Arcone, S. A. (1998) 'Glaciohydraulic supercooling a freeze-on mechanism to create



- stratified, debris-rich basal ice: I. Field evidence', *Journal of Glaciology*, 44, pp. 547-562.
- Le Heron, D. P. and Etienne, J. L. (2005) 'A complex subglacial clastic dyke swarm, Sólheimajökull, southern Iceland', *Sedimentary Geology*, 181, pp. 25-37.
- Leick, A. (2004) *GPS Satellite Surveying 3<sup>rd</sup> edn*. Hoboken, NJ: John Wiley and Sons, Inc.
- Li, Z. (1988) 'On the measure of digital terrain model accuracy', *Photogrammetric Record*, 12(72), pp. 873-877.
- Lister, H. (1953) 'Report on glaciology at Breidamerkurjökull, 1951', *Jökull* 1, pp. 23-31.
- Lliboutry, L. A. (1981) 'The effect of the subglacial water pressure on the sliding velocity of a glacier in an idealized numerical model', *Journal of Glaciology*, 27, pp. 407-421.
- Magilligan, F. J., Smith, L. C., Smith, N. D., Finnegan, D., Garvin, J. B., Gomez, B. and Mertes, L. A. K. (2002) 'Geomorphic effectiveness, sandur development, and the pattern of landscape response during jökulhlaups: Skeiðarárjökull, southeastern Iceland', *Geomorphology*, 44(1-2), pp. 95-113.
- Maizels, J. (1979) 'Proglacial aggradation and changes in braided channel patterns during a period of glacial advance: an Alpine example', *Geografiska Annaler*, 61A, pp. 87-101.
- Maizels, J. K. (1977) 'Experiments on the origin of kettle-holes', *Journal of Glaciology*, 18, pp. 291-303.
- Maizels, J. K. (ed.) (1991) 'Origin and evolution of Holocene sandurs in areas of jökulhlaup drainage, South Iceland', in: Maizels, J. K. and Caseldine, C. (eds) *Environmental change in Iceland: past and present*. Dordrecht: Kluwer, pp. 267-300.
- Maizels, J. K. (1992) 'Boulder ring structures produced during jökulhlaup flows-origin and hydraulic significance', *Geografiska Annaler* 74A, pp. 21-33.
- Maizels, J. K. (1997) 'Jökulhlaup deposits in proglacial areas', *Quaternary Science Reviews*, 16(7), pp. 793-819.
- Maizels, J. K. and Russell, A. J. (1992) *Quaternary perspectives on jökulhlaup prediction*, in Gray, J. M. (ed.) *Applications of Quaternary Research*, Quaternary Proceedings, 2, pp. 133-153.
- Marren, P. M. (2002a) 'Fluvial-lacustrine interaction on Skeiðarársandur, Iceland: Implications for sandur evolution', *Sedimentary Geology*, 149(1-3), pp. 43-58.
- Marren, P. M. (2002b) 'Glacier margin fluctuations, Skaftafellsjökull, Iceland: Implications for sandur evolution', *Boreas*, 31(1), pp. 75-81.
- Marren, P. M. (2005) 'Magnitude and frequency in proglacial rivers: a geomorphological and sedimentological perspective', *Earth Science Reviews*, 70, pp. 203-251.
- McDonald, B. C. and Shilts, W. W. (1975) 'Interpretation of faults in glaciofluvial sediments' in Jopling, A. V. and McDonald, B. C. (eds), *Glaciofluvial and glaciolacustrine sedimentation*. SEPM Special Publication, (23) pp. 123-131.
- McGlone, C. J., Mikhail, E. M. and Mullen, R. (2004) *Manual of Photogrammetry*. Bethesda, MD: American Society for Photogrammetry and Remote Sensing.
- McKenzie, G. D. (1969) 'Observations on a collapsing kame terrace in Glacier Bay National Monument, south eastern Alaska', *Journal of Glaciology*, 8, pp. 413-425.
- Meier, M. and Post, A. S. (1969) 'What are glacier surges?' *Canadian Journal of Earth Science*, 6(4), pp. 807-817.
- Miall, A. D. (1977) 'A review of the braided river depositional environment', *Earth Science Reviews*, 13, pp. 1-62.
- Miall, A. D. (1985) 'Architectural-element analysis: a new method of facies analysis applied to fluvial deposits', *Earth Science Reviews*, 22, (261-308).

- Miller, P. E. (2007) 'A robust surface matching technique for coastal geohazard monitoring'. Unpublished dissertation, Newcastle University.
- Molewski, P., and A. Olszewski. (2000) 'Sedimentology of the deposits and their palaeomorphological significance in the Gígjukvísl River Gap, marginal zone of the Skeiðarárjökull, Iceland', *Polish Polar Studies, XXVII International Polar Symposium*, Torun, pp. 235-258.
- Mooers, H. D. (1990) 'A glacial-process model: the role of spatial and temporal variations in a glacier thermal regime', *Geological Society of America Bulletin*, 102, pp. 243-251.
- Munro-Stasiuk, M. J., Russell, A. J. and Arnold, B. (2008) 'A glacial hydrofracture origin for the Súla ridges, Skeiðarársandur, Iceland', *American Geophysical Union*, Fall Meeting 2008, abstract #C23B-08.
- Murray, T., Strozzi, T., Luckman, A., Jiskoot, H. And Christakos, P. (2003). Is there a single surge mechanism? Contrasts in dynamics between glacier surges in Svalbard and other regions', *Journal of Geophysical Research*, 108 (2237), 15 p.
- Nakawo, M. and Young, G. J. (1981) 'Field experiments to determine the effect of a debris layer on ablation of glacier ice', *Annals of Glaciology*, 2, pp. 85-91.
- Näslund, J. O. and Hassinen, S. (1996) 'Supraglacial sediment accumulations and large englacial water conduits at high elevations in Myrdalsjökull, Iceland', *Journal of Glaciology*, 42, pp. 190-192.
- Natel, E. and Fleisher, P. J. (1994) 'Pre-surge meltwater properties in ice-contact lakes, Eastern Piedmont Lobe, Bering Glacier, Alaska', *Geological Society of America, Abstracts with Programs*, 26, p. 65.
- Nicholson, L. and Benn, D. I. (2006) 'Calculating ice melt beneath a debris layer using meteorological data', *Journal of Glaciology* 52, (178), pp. 463-470.
- Nielson, N. (1937) *Vatnajökull: Baratta Elds og Isa*. Reykjavik: Mal og Menning.
- Nye, J. F. (1976) 'Water flow in glaciers: jökulhlaups, tunnels and veins', *Journal of Glaciology*, 17, pp. 181-207.
- O'Conner, J. E. (1993) 'Hydrology, hydraulics and geomorphology of the Bonneville Flood', *Geological Society of America, Special Paper*, (274).
- Olszewski, A. and Weckwerth, P. (1999) 'The morphogenesis of kettles in the Höfðabrekkujökull forefield, Mýrdalssandur, Iceland', *Jökull*, 47, pp. 71-88.
- Østrem, G. (1959) 'Ice melting under a thin layer of moraine and the existence of ice cores in moraine ridges', *Geografiska Annaler* 41, pp. 228-230.
- Østrem, G. (1961) 'A new approach to end moraine chronology', *Geografiska Annaler* 43, pp. 418-419.
- Pálsson, S., Zóphóníasson, S., Sigurðsson, O., Kristmannsdóttir, H. and Adalsteinsson, H. (1992) 'Skeiðarárhlaup og framhlaup Skeiðarárjökuls 1991', *Unnio fyrir Vegagero ríkisins*. Reykjavik: Orkustofnun.
- Piotrowski, J. A. (1997) 'Subglacial flow during the last glaciation in northwestern Germany', *Sedimentary Geology*, 111, pp. 217-224.
- Price, R. J. (1969) 'Moraines, sandar, kames and eskers near Breiðamerkurjökull, Iceland', *Transactions of the Institute of British Geographers*, (46), pp. 17-43.
- Price, R. J. and Howarth, P. J. (1970) 'The evolution of the drainage system (1904 - 1965) in front of Breiðamerkurjökull, Iceland', *Jökull*, 20, pp. 27-37.
- Raymond, C. F. (1987) 'How do glaciers surge?', *Journal of Geophysical Research*, 92, pp. 9121- 9134.
- Reid, T. D. and Brock, B. W. (2010) 'An energy-balance model for debris-covered glaciers including heat conduction through the debris layer', *Journal of Glaciology*, 56(199), pp. 903-915.

- Rijsdijk, K. F., Owen, G., Warren, W. P., McCarroll, D. and van der Meer, J. (1999) 'Clastic dykes in over-consolidated tills: evidence of subglacial hydrofracturing at Killiney Bay, eastern Ireland', *Sedimentary Geology*, 129, pp. 111-126.
- Rist, S. (1955) 'Skeiðarárhlaup 1954', *Jökull*, 5, pp. 30-35.
- Roberts, M. J. (2005) 'Jökulhlaups: a reassessment of floodwater flow through glaciers', *Reviews of Geophysics*, 41(1), pp. 1-21.
- Roberts, M. J., Palsson, F., Gudmundsson, M. T., Björnsson, H. and Tweed, F. S. (2005) 'Ice-water interactions during floods from Grænalón glacier-dammed lake, Iceland', *Annals of Glaciology*, 40, pp. 133-138.
- Roberts, M. J., Russell, A. J., Tweed, F. S. and Knudsen, Ó. (2000) 'Ice fracturing during jökulhlaups; implications for englacial floodwater routing and outlet development', *Earth Surface Processes and Landforms*, 25, pp. 1429-1446.
- Roberts, M. J., Russell, A. J., Tweed, F. S. and Knudsen, Ó. (2001) 'Controls on englacial sediment deposition during the November 1996 jökulhlaup, Skeiðarárjökull, Iceland.', *Earth Surface Processes and Landforms*, 26, pp. 935-952.
- Roberts, M. J., Tweed, F. S., Russell, A. J., Knudsen, C. G., Lawson, D. E., Larson, G. J., Evenson, E. B. and Björnsson, H. (2002) 'Glaciohydraulic supercooling in Iceland', *Geology*, 30, pp. 439-442.
- Roberts, M. J., Tweed, F. S., Russell, A. J., Knudsen, O. and Harris, T. D. (2003) 'Hydrologic and geomorphic effects of temporary ice-dammed lake formation during jökulhlaups', *Earth Surface Processes and Landforms*, 28, pp. 723-737.
- Roussel, E., Chenet, M., Grancher, D. and Jomelli, V. (2008) 'Processes and rates of post-Little Ice Age proximal sandur incision', *Geomorphologie: Relief, Processus, Environment*, 4, pp. 235-248.
- Rudoy, A. N. and Baker, V. R. (1993) 'Sedimentary effects of cataclysmic late Pleistocene glacial outburst flooding, Altay Mountains, Siberia', *Sedimentary Geology*, 85, pp. 53-62.
- Russell, A. J. (1993) 'Obstacle marks produced by flow around stranded ice blocks during a glacier outburst flood (jökulhlaup) in west Greenland', *Sedimentology*, 40, pp. 1091-1111.
- Russell, A. J., Fay, H., Harris, T., and Roberts, M. (2003) 'Preservation of jökulhlaups within subglacial sediments', in: *XVI INQUA Congress Abstracts with Programs*, p. 148.
- Russell, A. J., Fay, H., Marren, P. M., Tweed, F. S. and Knudsen, O. (2005) 'Icelandic jökulhlaup impacts', in *Caseldine, C. (ed.) Iceland: modern processes and past environments*. London: Elsevier, pp. 153-203.
- Russell, A. J., Gregory, A. R., Large, A. R. G., Fleisher, P. J. and Harris, T. D. (2007) 'Tunnel channel formation during the November 1996 jökulhlaup, Skeiðarárjökull, Iceland', *Annals of Glaciology*, 45, pp. 95-103.
- Russell, A. J., Knight, P. G. and Van Dijk, T. A. G. P. (2001a) 'Glacier surging as a control on the development of proglacial, fluvial landforms and deposits, Skeiðarársandur, Iceland', *Global and Planetary Change*, 28, (1-4), pp. 163-174.
- Russell, A. J. and Knudsen, --O-- (1999) 'Controls on the sedimentology of the November 1996 jökulhlaup deposits, Skeiðarársandur, Iceland', in Smith, N. D., Rogers, J. (eds) *Advances in fluvial sedimentology. International Association of Sedimentologists Special Publications* (28) pp. 315-329.
- Russell, A. J., Knudsen, C. G., Maizels, J. K. and Marren, P. M. (1999) 'Channel cross-sectional area changes and peak discharge calculations in the Gígjukvísl River during the November 1996 jökulhlaup, Skeiðarársandur, Iceland', *Jökull*, 47, pp. 45-57.
- Russell, A. J. and Knudsen, Ó. (2002) 'The effects of glacier-outburst flood flow dynamics on ice-contact deposits: November 1996 jökulhlaup, Skeiðarársandur,

- Iceland', in: Martini, I. P., Baker, V. R., and Garzon, G. (eds) *Flood and megaflood deposits: recent and ancient examples*. Oxford: Blackwell Science, pp. 67-83.
- Russell, A. J., Knudsen, O., Fay, H., Marren, P. M., Heinz, J. and Tronicke, J. (2001b) 'Morphology and sedimentology of a giant supraglacial, ice-walled jökulhlaup channel, Skeiðarárjökull, Iceland: implications for esker genesis', *Global and Planetary Change*, 28, pp. 193-216.
- Russell, A. J., Knudsen, Ó., Maizels, J. K. and Marren, P. M. (1999b) 'Channel cross-sectional area changes and peak discharge calculations in the Gígjukvísl river during the 1996 jökulhlaup, Skeiðarárjökull, Iceland', *Jökull*, 47, pp. 45-58.
- Russell, A. J., Roberts, M. J., Fay, H., Marren, P. M., Cassidy, N. J., Tweed, F. S. and Harris, T. (2006) 'Icelandic jökulhlaup impacts: implications for ice-sheet hydrology, sediment transfer and geomorphology', *Geomorphology*, 75, pp. 33-64.
- Sanford, A. R. (1959) 'Analytical and experimental study of simple geologic structures', *Geological Society of America Bulletin*, 70, pp. 19-52.
- Schenk, T. (1999) *Digital Photogrammetry*. TerraScience: Laurelville, Ohio: TerraScience.
- Schiefer, R. and Gilbert, R. (2007) 'Reconstructing morphometric change in a proglacial landscape using historical aerial photography and automated DEM generation', *Geomorphology*, 88, pp. 167-178.
- Schomacker, A. (2008) 'What controls dead-ice melting under different climate conditions? A discussion', *Earth-Science Reviews*, 90, pp. 103-113.
- Schomacker, A. and Kjær, K. H. (2008) 'Quantification of dead-ice melting in ice-cored moraines at the high-Arctic glacier Holmströmbreen, Svalbard', *Boreas*, 37, pp. 211-225.
- Schomacker, A., Kruger, J. and Kjaer, K. H. (2006) 'Ice-cored drumlins at the surge-type glacier Bruarjökull, Iceland: a transitional-state landform', *Journal of Quaternary Science*, 21(1), pp. 85-93.
- Sharp, M. J. (1985a) "'Crevasse-fill" ridges - a landform characteristic of surging glaciers?', *Geografiska Annaler*, 67A, pp. 213-220.
- Sharp, M. J. (1985b) 'Sedimentation and stratigraphy at Eyjabakkajökull - an Icelandic surging glacier', *Quaternary Research*, 24, pp. 268-284.
- Sharp, M. J. (1988) 'Surging glaciers: geomorphic effects', *Progress in Physical Geography*, 12, pp. 533-559.
- Sharp, R. P. (1949) 'Studies of superglacial debris on valley glaciers', *American Journal of Science*, 247, pp. 289-315.
- Shaw, J. (1983) 'Drumlin formation related to inverted melt-water erosional marks', *Journal of Glaciology*, 29, pp. 461-479.
- Shaw, J. and Kvill, D. (1989) 'Drumlins and catastrophic subglacial floods', *Sedimentary Geology*, 62, pp. 177-202.
- Shreve, R. L. (1972) 'Movement of water in glaciers', *Journal of Glaciology*, 11, pp. 205-214.
- Shreve, R. L. (1985) 'Esker characteristics in terms of glacier physics, Katahdin esker system, Maine', *Geological Society of America Bulletin*, 96, pp. 639-646.
- Sigurðsson, O. (1998) 'Glacier variations in Iceland 1930-1995: from the database of the Iceland Glaciological Society', *Jökull*, 45, pp. 3-25.
- Sigurðsson, O. (1998) 'Glacier variations in Iceland 1930-1995', *Jökull*, 45, pp. 3-25.
- Sigurðsson, O. (2005) 'Variations of termini of glaciers in Iceland in recent centuries and their connection with climate', *Developments in Quaternary Sciences*, 5, pp. 241-255.

- Sigurðsson, O., Jonsson, T. and Johannesson, T. (2007) 'Relation between glacier-termini variations and summer temperature in Iceland since 1930', *Annals of Glaciology*, 6, pp. 170-176.
- Sjogren, D. B., Gisher, T. G., Lawrence, D. T., Harry, M. J. and Munro-Stasiuk. (2002) 'Incipient tunnel channels', *Quaternary International*, 90, pp. 41-56.
- Smith, L. C., Alsdorf, D. E., Magilligan, F. J., Gomez, B., Mertes, L. A. K., Smith, N. D. and Garvin, J. B. (2000) 'Estimation of erosion, deposition, and net volumetric change caused by the 1996 Skeiðarársandur jökulhlaup, Iceland, from SAR interferometry', *Water Resources and Research*, 36, pp. 1583-1594.
- Smith, L. C., Sheng, Y., Magilligan, F.J., Smith, N.D., Gomez, B., Mertes, L.A.K., Krabill, W.B., and Garvin, J.B. (2006) 'Geomorphic impact and rapid subsequent recovery from the 1996 Skeiðarársandur jökulhlaup, Iceland, measured with multi-year airborne lidar', *Geomorphology*, 75, pp. 65-75.
- Smith, M. J. and Clark, J. S. (2005) 'Methods for the visualization of digital elevation models for landform mapping', *Earth Surface Processes and Landforms*, 30, pp. 885-900.
- Smith, M. J., Smith, D. G., Tragheim, D. G. and Holt, M. (1997) 'DEMs and ortho-images from aerial photographs', *Photogrammetric Record*, 15(90), pp. 945-950.
- Snorrason, Á., Jónsson, P., Pálsson, S., Árnason, O., Sigurðsson, S., Víkingsson, S., Sigurðsson, A. and Zóphóníasson, S. (eds.) (1997) "*Hlaupið Á Skeiðarársandi Haustið 1996 Útbreiðsla, Rennsli Og Aurburður*" Vatnajökull Gos Og Hlaup 1996, Vegagerðin, pp 79-137.
- Snorrason, A., Jonsson, P., Sigurðsson, O., Palsson, S., Arnason, S., Vikinsson, S. and Kaldal, I. (2002) 'November 1996 jökulhlaup on Skeiðarársandur outwash plain, Iceland', *International Association of Sedimentologists Special Publication SP-32*, pp. 55-65.
- Spedding, N. and Evans, D. J. A. (2002) 'Sediments and landforms at Kviarjökull, southeast Iceland: a reappraisal of the glaciated valley landsystem', *Sedimentary Geology*, 149, pp. 21-42.
- Stokes, C. R., Popvnin, V., Aleynikov, A., Gurney, S. D. and Shahgedanova, M. (2007) 'Recent glacier retreat in the Caucasus Mountains, Russia, and associated increase in supraglacial debris cover and supra-/proglacial lake development', *Annals of Glaciology*, 46, pp. 195-203.
- Teller, J. T. (1995) 'History and drainage of large ice-dammed lakes along the Laurentide Ice Sheet', *Quaternary International*, 28, pp. 83-92.
- Thompson, A. (1988) 'Historical development of the proglacial landforms of Svinafellsjökull and Skaftafellsjökull, southeast Iceland', *Jökull*, 38, pp. 17-31.
- Thorarinsson, S. (1939) 'The ice dammed lakes of Iceland with particular reference to their value as indicators of glacier oscillation', *Geografiska Annaler*, 21, pp. 216-242.
- Thorarinsson, S. (1943) 'Oscillations of the Iceland Glaciers in the last 250 years', *Geografiska Annaler*, 25, pp. 1-54.
- Thorarinsson, S. (1974) *Vötnin Strið: Saga Skeiðarárjlaupa og Grímsvatnagosa*. Reykjavík: Menningarsjods.
- Thorarinsson, S., Einarsson, T. and Kjartansson, G. (1959) 'On the geology and geomorphology of Iceland', *Geografiska Annaler*, 41A.
- Thorarinsson, S., Sæmundsson, K. and Williams, S. W. J. (1951) 'ERTS-1 image of Vatnajökull: analysis of glaciological, structural and volcanic features', *Jökull*, 23, pp. 7-17.
- Tweed, F. S., Roberts, M. J. and Russell, A. J. (2005) 'Hydrologic monitoring of supercooled meltwater from Icelandic glaciers', *Quaternary Science Reviews*, 24, pp. 2308-2318.

- Tweed, F. S. and Russell, A. J. (1999) 'Controls on the formation and sudden drainage of glacier-impounded lakes: implications for jökulhlaup characteristics', *Progress in Physical Geography*, 23, pp. 79-110.
- van der Meer, J. (1998) 'Fracture mechanics approach to penetration of bottom crevasses on glaciers', *Cold Regions Science and Technology*, 27(3), pp. 213-223.
- van der Veen, C. J. (1996) 'Tidewater calving glaciers', *Journal of Glaciology*, 42(141), pp. 375-385.
- van der Veen, C. J. (2002) 'Calving glaciers', *Progress in Physical Geography*, 26(1), pp. 96-122.
- van Dijk, T. A. G. P. (2002) *Glacier surges as a control on the development of proglacial fluvial landforms and deposits*. Unpublished dissertation, Keele University.
- van Dijk, T. A. G. P. and Sigurðsson, O. (2002) 'Surge-related floods at Skeiðarárjökull Glacier, Iceland: implications for ice-marginal outwash deposits', in: *Snorasson, A., Finnsdottir, H.P., Moss, M. (eds), The Extremes of the extremes: extraordinary floods, International Association of Hydrological Sciences IAHS-AISH Publication (271)*, pp. 193-198.
- Vogfjörð, K. S., Jakobsdottir, S. S. and Gudmundsson, G. B. (2005) 'Forecasting and monitoring a subglacial eruption in Iceland', *EOS (Transactions of the American Geophysical Union)*, 86(26), pp. 245-248.
- Wadell, H. (1935) 'Ice Floods and Volcanic Eruptions in Vatnajökull', *Geographical Review*, 25(1), pp. 131-136.
- Waitt, R. B. J. (1985) 'Case for periodic, colossal jökulhlaups from Pleistocene glacial Lake Missoula', *Geological Society of America Bulletin*, 96, pp. 1271-1286.
- Walder, J. S. (1986) 'Hydraulics of subglacial cavities', *Journal of Glaciology*, 32, pp. 439-445.
- Walder, J. S. and Costa, J. E. (1996) 'Outburst floods from glacier-dammed lakes: the effect of mode of drainage on flood magnitude', *Earth Surface Processes and Landforms*, 21, pp. 701-723.
- Walker, A. S. (1996) 'Analogue, analytical and digital photogrammetric workstations: practical investigations of performance', *Photogrammetric Record*, 15(85), pp. 17-25.
- Waller, R. I., Russell, A. J., Van Dijk, T. A. G. P. and Knudsen, O. (2001) 'Jökulhlaup related ice fracture and the supraglacial routing of water and sediment, Skeiðarárjökull, Iceland', *Geografiska Annaler*, 83, (Series A), pp. 433-449.
- Waller, R. I., van Dijk, T. A. G. P. and Knudsen, Ó. (2008) 'Subglacial bedforms and conditions associated with the 1991 surge, Skeiðarárjökull, Iceland', *Boreas*, 37, pp. 179-194.
- Walstra, J. (2006) *Historical aerial photographs and digital photogrammetry for landslide assessment*. Unpublished thesis. Loughborough University.
- Wangensteen, B., Gudmundsson, A., Eiken, T., Kaab, A., Farbrót, H. and Etzelmüller, B. (2006) 'Surface displacements and surface age estimates for creeping slope landforms in northern and eastern Iceland using digital photogrammetry', *Geomorphology*, 80, pp. 59-79.
- Warner, W. S., Graham, R. W. and Read, R. E. (1996) *Small format aerial photography*. Caithness, Scotland: Whittles Pub.
- Warren, C. and Aniya, M. (1999) 'The calving glaciers of southern South America', *Global and Planetary Change*, 22(1-4), pp. 59-77.
- Warren, C., Benn, D., Winchester, V. and Harrison, S. (2001) 'Buoyancy-driven lacustrine calving, Glaciar Nef, Chilean Patagonia', *Journal of Glaciology*, 47(156), pp. 135-146.



- Warburton, J. and Fenn, C. R. (1994) 'Unusual flood events from an Alpine glacier: observations and deductions on generating mechanism', *Journal of Glaciology*, 40, pp. 176-186.
- Williams, P. W. (1987) 'Geomorphic inheritance and the development of tower karst', *Earth Surface Processes and Landforms*, 12, pp. 453-465.
- Wisniewski, E., Andrzejewski, L., Molewski, P. (1997) 'Fluctuations of the snout of Skeiðarárjökull in Iceland in the last 100 years and some of their consequences in the central part of its forefield.', *Landform Analysis*, 1, pp. 73-78.
- Wojcik, G. (1973a) 'Glaciological studies on the Skeiðarárjökull', *Geographia Polonica*, 26, pp. 185-208.
- Wojcik, G. (1973b) 'The results of the meteorological investigations on the forefield of Skeiðarárjökull', *Geographia Polonica*, 26, pp. 157-183.
- Wolf, P. R. and Dewitt, B. A. (2000) *Elements of photogrammetry with applications in GIS*. New York: McGraw-Hill.
- Wolf, P. R. and Ghilani, C. D. (1997) *Adjustment computations, statistics and least squares in surveying and GIS*. New York: John Wiley and Sons.
- Wolman, G. M. and Miller, J. P. (1960) 'Magnitude and frequency of forces in geomorphic processes', *Journal of Geology*, 68, pp. 54-73.
- Woodward, J., Burke, M. J., Tinsley, R. and Russell, A. J. (2008) 'Investigating reworking of proglacial sediments using GPR: Skeiðarárjökull, Iceland', in Rodgers, C. D. F., Chignell, R. J. (eds), *Proceedings of the 12th International Conference on Ground Penetrating Radar*. Birmingham: University of Birmingham.
- Zielinski, T. and van Loon, A. J. (2002) 'Present-day sandurs are not representative of the geologic record', *Sedimentary Geology*, 152, pp. 1-5.